

University of Southampton Research Repository

Copyright © and Moral Rights for this thesis and, where applicable, any accompanying data are retained by the author and/or other copyright owners. A copy can be downloaded for personal non-commercial research or study, without prior permission or charge. This thesis and the accompanying data cannot be reproduced or quoted extensively from without first obtaining permission in writing from the copyright holder/s. The content of the thesis and accompanying research data (where applicable) must not be changed in any way or sold commercially in any format or medium without the formal permission of the copyright holder/s.

When referring to this thesis and any accompanying data, full bibliographic details must be given, e.g.

Thesis: Author (Year of Submission) "Full thesis title", University of Southampton, name of the University Faculty or School or Department, PhD Thesis, pagination.

Data: Author (Year) Title. URI [dataset]

University of Southampton

FACULTY OF MEDICINE

Institute of Developmental Sciences

**The effect of prenatal vitamin D supplementation
on DNA methylation: Investigation into biomarkers
and causal mechanisms of later bone health**

by

Nevena Krstic

Thesis for the degree of Doctor of Philosophy

October 2019

University of Southampton

Abstract

Faculty of Medicine

Institute of Developmental Sciences

Thesis for the degree of Doctor of Philosophy

The effect of prenatal vitamin D supplementation on DNA methylation: Investigation into biomarkers and causal mechanisms of later bone health

by Nevena Krstic

Osteoporosis is a systemic skeletal disease which affects the ageing population and results in an increased risk of developing fractures, for example at the wrist, hip and spine. Peak bone mass in early adulthood has been shown to predict the risk of developing osteoporosis in later life and studies have shown that the early life environment might influence the bone health trajectory, through epigenetic processes such as DNA methylation. DNA methylation can be measured in suitable candidate genes to potentially act as a biomarker for predicting bone health in later life, and to guide interventions aimed at improving the accrual of bone mass during growth.

Studies within the SWS cohort have identified two candidate biomarkers, *RXRA* and *CDKN2A*, of which DNA methylation has been shown to be associated with bone measures in later childhood. Whether DNA methylation is causally involved in bone outcomes is unknown therefore, randomised controlled trials provide an opportunity to investigate these associations further and to determine the possibility of a causal relationship. Within this thesis, DNA methylation of four genes, *RXRA*, *CDKN2A*, *Osterix* and *Runx2*, were measured within the MAVIDOS trial, a randomised, controlled, double blind study where pregnant mothers were recruited and received either 1000 IU/d cholecalciferol or placebo daily from 14 weeks gestation until delivery. Infants born during the winter months to cholecalciferol supplemented mothers had greater bone measures at birth compared to the placebo group. The results showed that infants born to cholecalciferol supplemented mothers had lower methylation of *RXRA* and *Osterix* CpG loci and higher methylation at *CDKN2A* CpG loci. Furthermore, DNA methylation of *Osterix* and *Runx2* was positively associated with bone measures at birth. Next, the functional importance of the *RXRA* CpGs of interest was investigated in osteosarcoma cell lines to provide a mechanistic insight into the interactions between vitamin D and *RXRA* methylation. The results showed that site directed mutagenesis upstream of the *RXRA* promoter impaired luciferase expression within osteosarcoma cell lines, both in the presence and absence of vitamin D supplementation. In humans, the measurement of DNA methylation in tissues central to the pathogenesis of osteoporosis is difficult, so DNA methylation of several key genes was measured in adult tibiae from mice exposed to a prenatal vitamin D deficient diet. The results showed that a prenatal vitamin D deficient diet altered tibial DNA methylation and suggests a link between prenatal vitamin D deficiency, mechanical loading and DNA methylation within tibiae.

These observations provide insight into candidate biomarkers of bone health that respond accordingly to a dietary intervention of maternal vitamin D supplementation within the MAVIDOS trial, and provide insight into the mechanisms and functional importance that altered DNA methylation of these genes could have on bone phenotype.

Table of Contents

Table of Contents	i
Table of Tables	ix
Table of Figures	xiii
Research Thesis: Declaration of Authorship	xvii
Acknowledgements	xix
Definitions and Abbreviations	xxi
Chapter 1 Introduction	1
1.1 Osteoporosis.....	3
1.1.1 Morbidity and Mortality.....	3
1.1.2 Diagnosis and Treatment	5
1.1.3 Pathways to osteoporosis	6
1.1.3.1 Peak bone mass.....	7
1.1.3.2 Accelerated loss of bone following peak bone mass	9
1.2 Bone formation	10
1.2.1 Osteoblast differentiation	14
1.2.1.1 Transcription factors	16
1.2.1.2 Signalling pathways	18
1.2.1.3 Systemic regulation	24
1.2.2 Osteoclasts	30
1.2.3 Bone remodelling	31
1.2.4 Genome wide association studies (GWAS)	33
1.2.5 Pathogenesis of osteoporosis	34
1.3 Developmental origins of health and disease (DOHaD)	36
1.3.1 Evidence for the developmental origins of osteoporosis	38
1.3.1.1 Human studies.....	38
1.3.1.2 Animal studies	40
1.3.2 Vitamin D status and bone health.....	41
1.3.2.1 Human studies.....	41

Table of Contents

1.3.2.2	Animal studies.....	44
1.4	Epigenetics.....	48
1.4.1	Epigenetic mechanisms.....	49
1.4.1.1	DNA methylation.....	49
1.4.1.2	Histone modifications.....	50
1.4.1.3	Micro RNAs.....	51
1.4.1.4	Long non-coding RNAs.....	52
1.4.2	Epigenetics and the early life environment.....	52
1.4.3	Vitamin D and epigenetics.....	54
1.4.4	Epigenetics and bone.....	55
1.5	Epigenetic biomarkers of later health.....	57
1.5.1	Epigenetic biomarkers of later bone health.....	59
1.5.1.1	<i>RXRA</i>	59
1.5.1.2	<i>CDKN2A</i>	61
1.6	Aims and Hypotheses.....	64
Chapter 2	Materials and Methods.....	69
2.1	Materials.....	71
2.2	Methods.....	74
2.2.1	Cohorts.....	74
2.2.1.1	MAVIDOS study.....	74
2.2.1.2	SPRING cohort.....	75
2.2.2	Genomic DNA extraction from umbilical cord.....	77
2.2.3	Genomic DNA extraction from placental tissue.....	78
2.2.3.1	Primary cytotrophoblast isolation from placental tissue.....	78
2.2.3.2	Placental fragment culture with vitamin D.....	79
2.2.4	Measuring DNA methylation.....	79
2.2.4.1	Bisulfite conversion of DNA.....	80
2.2.4.2	Polymerase chain reaction (PCR).....	80
2.2.4.3	Pyrosequencing.....	82

2.2.4.4	Primer validation	82
2.2.5	Cell culture	82
2.2.5.1	Human osteosarcoma cell lines.....	82
2.2.5.2	Human mesenchymal stem cells (MSCs) from umbilical cord	83
2.2.6	Supplementing human osteosarcoma cell lines with vitamin D.....	83
2.2.6.1	Culturing human osteosarcoma cell lines with vitamin D.....	83
2.2.6.2	Isolation of total RNA from osteosarcoma cell lines.....	83
2.2.6.3	Isolation of genomic DNA from osteosarcoma cell lines	85
2.2.7	Transfection of osteosarcoma cell lines with luciferase reporter constructs..	86
2.2.7.1	Cloning the <i>RXRA</i> promoter	86
2.2.7.2	Cloning the <i>RXRA</i> enhancer constructs.....	89
2.2.7.3	PCR mutagenesis of p <i>RXRA</i> promLuc and pMenhLuc(CpGs1-12).....	94
2.2.7.4	Agar plates and Luria broth media.....	95
2.2.7.5	Transformation.....	96
2.2.7.6	Minipreparation of plasmid DNA	96
2.2.7.7	Confirming the presence of plasmid DNA.....	96
2.2.7.8	Midipreparation of plasmid DNA	97
2.2.7.9	Preparation of glycerol stocks for long term storage	98
2.2.7.10	Transfection of plasmid DNA.....	98
2.2.8	Isolation of nuclear extract	100
2.2.9	Analysis of transcription factor binding by electrophoretic mobility shift assays	100
2.2.9.1	Annealing oligonucleotides	100
2.2.9.2	Electrophoretic mobility shift assay (EMSA)	102
2.2.10	Mouse animal model.....	103
2.2.10.1	Genomic DNA extraction from murine tibiae	104
2.2.11	Statistical Analyses	104
2.2.11.1	Statistical analysis of DNA methylation.....	104
2.2.11.2	Statistical analysis of luciferase expression data	106
2.2.11.3	Statistical analysis of real time PCR data.....	106

Chapter 3	Maternal vitamin D supplementation during pregnancy alters methylation of specific CpGs upstream of the <i>RXRA</i> promoter	109
3.1	Introduction	111
3.1.1	Hypothesis	112
3.1.2	Aims	112
3.1.3	Methods.....	112
3.2	Results.....	115
3.2.1	Characteristics of participants in the MAVIDOS trial.....	115
3.2.2	<i>RXRA</i> methylation was lower in the vitamin D supplemented group compared to the placebo group in the MAVIDOS trial.....	116
3.2.2.1	There were seasonal differences in maternal and neonatal characteristics in the MAVIDOS trial.....	118
3.2.3	Are there any associations between cord <i>RXRA</i> CpG methylation and bone outcomes at birth within the MAVIDOS trial?.....	123
3.2.4	Does vitamin D supplementation alter <i>RXRA</i> methylation in placenta?.....	127
3.2.4.1	Placenta from the MAVIDOS trial	127
3.2.4.2	Placenta from the SPRING study.....	131
3.2.4.3	<i>In vitro</i> treatment of placental fragments with 25(OH)D ₃ does not alter methylation of <i>RXRA</i>	132
3.2.4.4	<i>In vitro</i> treatment of cytotrophoblasts with 25(OH)D ₃ does not alter <i>RXRA</i> methylation	133
3.3	Discussion.....	134
Chapter 4	Maternal vitamin D supplementation during pregnancy alters <i>CDKN2A</i> DNA methylation at birth within the MAVIDOS trial	141
4.1	Introduction	143
4.1.1	Hypothesis	143
4.1.2	Aims	143
4.1.3	Methods.....	144
4.2	Results.....	145

4.2.1	<i>CDKN2A</i> methylation at birth was higher in the vitamin D supplemented group compared to the placebo group within the MAVIDOS trial.....	145
4.2.2	Infants born in autumn to vitamin D supplemented mothers had higher <i>CDKN2A</i> methylation at birth compared to the placebo group within the MAVIDOS trial.....	146
4.2.3	There were no significant associations between cord <i>CDKN2A</i> CpG methylation and neonatal bone measures within the MAVIDOS trial.....	148
4.3	Discussion	152
Chapter 5 Maternal vitamin D supplementation during pregnancy alters DNA methylation of transcription factors involved in osteoblast differentiation within the MAVIDOS trial		157
5.1	Introduction.....	159
5.1.1	Hypothesis.....	159
5.1.2	Aims.....	160
5.1.3	Methods	160
5.2	Results	162
5.2.1	Selection of the regions of interest upstream of the <i>Runx2</i> and <i>Osterix</i> transcriptional start sites	162
5.2.2	Investigation into <i>Runx2</i> CpG methylation as an epigenetic biomarker of bone health.....	162
5.2.2.1	Maternal cholecalciferol supplementation and season of birth are associated with altered <i>Runx2</i> CpG methylation at birth within the MAVIDOS trial.....	162
5.2.2.2	Amongst infants born in winter, <i>Runx2</i> CpG methylation at birth was associated with bone measures at birth	165
5.2.3	Investigation into <i>Osterix</i> CpG methylation as an epigenetic biomarker of bone health.....	169
5.2.3.1	There are seasonal differences in <i>Osterix</i> CpG methylation at birth between the two maternal treatment groups within the MAVIDOS trial.....	169

Table of Contents

5.2.3.2	Are there any associations between cord <i>Osterix</i> CpG methylation and bone outcomes at birth within the MAVIDOS trial?.....	172
5.3	Discussion.....	176
5.3.1	<i>Runx2</i> CpG methylation at birth results	176
5.3.2	<i>Osterix</i> CpG methylation at birth results	177
5.3.3	Conclusion.....	179
Chapter 6 Investigating the functional importance of the <i>RXRA</i> differentially methylated CpGs on <i>RXRA</i> promoter activity in osteosarcoma cell lines ..181		
6.1	Introduction	183
6.1.1	Hypothesis	184
6.1.2	Aims	184
6.2	Results.....	186
6.2.1	<i>In silico</i> analysis of the <i>RXRA</i> CpGs of interest.....	186
6.2.1.1	<i>In silico</i> analysis shows that the <i>RXRA</i> CpGs of interest lie within a DNase 1 hypersensitive region.....	186
6.2.1.2	The ENCODE database highlights histone mark enrichment across the <i>RXRA</i> DMR.....	186
6.2.1.3	MatInspector analysis propose several putative transcription factor binding sites over the <i>RXRA</i> CpGs of interest.....	188
6.2.2	Site directed mutagenesis of specific <i>RXRA</i> CpG sites alters <i>RXRA</i> promoter activity in osteosarcoma cells	190
6.2.3	The DMR upstream of <i>RXRA</i> acts as an enhancer region in osteosarcoma cell lines.....	192
6.2.3.1	The full <i>RXRA</i> enhancer region preferentially acts in the forward orientation upstream of the minimal promoter in osteosarcoma cell lines.....	192
6.2.3.2	Removal of <i>RXRA</i> CpGs 1-3 in the full <i>RXRA</i> enhancer luciferase construct increases luciferase expression in osteosarcoma cells.....	194
6.2.3.3	The <i>RXRA</i> minimal enhancer region increases luciferase expression in osteosarcoma cell lines	196

6.2.4	Short term <i>in vitro</i> vitamin D treatment in osteosarcoma cell lines alters <i>RXRA</i> gene expression, methylation and <i>RXRA</i> linked luciferase expression.....	200
6.2.4.1	Short term <i>in vitro</i> vitamin D treatment in osteosarcoma cells alters <i>RXRA</i> gene expression	200
6.2.4.2	Short term <i>in vitro</i> vitamin D treatment in osteosarcoma cells alters <i>RXRA</i> methylation.....	202
6.2.4.3	Vitamin D supplementation increases <i>RXRA</i> linked luciferase expression in Saos2 cells only.....	204
6.2.4.4	The minimal enhancer <i>RXRA</i> region responds to vitamin D treatment and site specific mutations prevent a luciferase response to vitamin D in osteosarcoma cell lines	206
6.2.5	Specific transcription factors bind across <i>RXRA</i> CpGs 4-5 in MG63 cells	207
6.2.5.1	EMSA show specific competitive binding in MG63 with <i>RXRA</i> CpGs 4-5	212
6.2.5.2	Treatment of osteosarcoma cell lines and MSCs with vitamin D does not alter transcription factor binding	214
6.3	Discussion.....	216
Chapter 7 A mouse model of vitamin D deficiency: maternal vitamin D deficiency and mechanical load effect on DNA methylation		225
7.1	Introduction.....	227
7.1.1	Hypothesis.....	228
7.1.2	Aims.....	228
7.1.3	Methods	229
7.2	Results	232
7.2.1	Selection of regions of potential differential methylation in the candidate genes of interest.....	232
7.2.2	Vitamin D deficiency during pregnancy is associated with altered offspring DNA methylation in tibial tissue	232
7.2.3	Mechanical loading is associated with altered tibial DNA methylation in mice exposed to a prenatal vitamin D deficient diet.....	234
7.2.4	DNA methylation is associated with tibial stiffness in 18 week old mice.....	236

Table of Contents

7.3 Discussion..... 237

Chapter 8 Final Discussion.....247

8.1 Final discussion 249

8.2 Summary of main findings 249

8.3 Discussion of main findings..... 252

8.3.1 DNA methylation of *RXRA* may be used as a predictive biomarker of later bone health 252

8.3.2 Maternal cholecalciferol supplementation is associated with altered methylation of *CDKN2A* and *Osterix* and methylation of *Runx2* and *Osterix* were associated with bone measures at birth within the MAVIDOS trial..... 254

8.3.3 A prenatal vitamin D deficient diet is associated with altered DNA methylation in tibiae from adult mice..... 257

8.4 Future work..... 258

8.5 Implications for human health..... 259

List of References261

Table of Tables

Table 2.1 Reagents used in experiments.....	71
Table 2.2 Pyrosequencing amplicons and sequencing primers used to measure DNA methylation and PCR conditions.	81
Table 2.3 Quantitect Primer Assays for qRT-PCR.....	85
Table 2.4 <i>RXRA</i> oligonucleotide sequences for EMSA probes.....	101
Table 2.5 Oligonucleotide sequences of transcription factors cocktails for EMSAs.....	102
Table 3.1 Baseline maternal and neonatal characteristics of the subset of randomly assigned pregnant women from the MAVIDOS trial included in the current analyses.....	116
Table 3.2 Differences in <i>RXRA</i> methylation between the treatment groups in the MAVIDOS trial.	117
Table 3.3 Baseline maternal and neonatal characteristics of subset of the randomly assigned pregnant women from the MAVIDOS trial included in the analyses, stratified by season of birth.	120
Table 3.4 Differences in <i>RXRA</i> methylation between treatment groups in the MAVIDO trial when stratified by season of birth.	121
Table 3.5 Associations between <i>RXRA</i> CpG methylation at birth and bone outcomes at birth.....	124
Table 3.6 Associations between <i>RXRA</i> CpG methylation at birth and bone outcomes at birth, when stratified by treatment group.....	125
Table 3.7 Associations between <i>RXRA</i> CpG methylation at birth and bone outcomes at birth in the MAVIDOS trial when stratified by season of birth.....	126
Table 3.8 Baseline maternal and neonatal characteristics of the present subset of randomly assigned pregnant women from the MAVIDOS trial from which placental data were included in the analyses.	128
Table 3.9 Correlation between <i>RXRA</i> methylation at birth in umbilical cord tissue compared to placental tissue from the MAVIDOS trial.....	129

Table 3.10 Differences in <i>RXRA</i> methylation between the treatment groups in the MAVIDOS trial in placenta.	130
Table 3.11 Differences in <i>RXRA</i> methylation in placenta between the treatment groups in the SPRING study.	131
Table 3.12 Differences in mean <i>RXRA</i> methylation between matched placental fragments treated with 20µM 25(OH)D₃, <i>in vitro</i>, for 8 hours.	132
Table 3.13 Differences in mean <i>RXRA</i> methylation between matched cytotrophoblasts treated with 20uM 25(OH)D₃, <i>in vitro</i>, for 24 hours.	133
Table 4.1 Differences in <i>CDKN2A</i> methylation between the treatment groups in the MAVIDOS trial.	145
Table 4.2 Differences in <i>CDKN2A</i> methylation between treatment groups in the MAVIDOS trial when stratified by season of birth.	147
Table 4.3 Associations between <i>CDKN2A</i> methylation at birth and bone outcomes at birth in the MAVIDOS trial.	149
Table 4.4 Associations between <i>CDKN2A</i> CpG methylation at birth and bone outcomes at birth in the MAVIDOS trial when stratified by treatment group.	150
Table 4.5 Associations between <i>CDKN2A</i> CpG methylation at birth and bone outcomes at birth in the MAVIDOS trial when stratified by season of birth.	151
Table 5.1 Differences in <i>Runx2</i> CpG methylation at birth between the treatment groups within the MAVIDOS trial.	163
Table 5.2 Differences in <i>Runx2</i> methylation between treatment groups in the MAVIDOS trial when stratified by season of birth.	164
Table 5.3 Associations between <i>Runx2</i> methylation at birth and bone outcomes at birth in the MAVIDOS trial.	166
Table 5.4 Associations between <i>Runx2</i> CpG methylation at birth and bone outcomes at birth in the MAVIDOS trial when stratified by treatment group.	167
Table 5.5 Associations between <i>Runx2</i> CpG methylation at birth and bone outcomes at birth in the MAVIDOS trial when stratified by season of birth.	168

Table 5.6 Differences in <i>Osterix</i> methylation between the treatment groups in the MAVIDOS trial.	169
Table 5.7 Differences in <i>Osterix</i> methylation between treatment groups in the MAVIDOS trial when stratified by season of birth.	171
Table 5.8 Associations between <i>Osterix</i> methylation at birth and bone outcomes at birth in the MAVIDOS trial.	173
Table 5.9 Associations between <i>Osterix</i> CpG methylation at birth and bone outcomes at birth in the MAVIDOS trial when stratified by treatment group.	174
Table 5.10 Associations between <i>Osterix</i> CpG methylation at birth and bone outcomes at birth in the MAVIDOS trial when stratified by season of birth.	175
Table 6.1 Summary of the <i>RXRA</i> CpG sites, current findings and their relation to the <i>RXRA</i> TSS.	184
Table 6.2 <i>RXRA</i> methylation of osteosarcoma cell lines treated with vitamin D.	203
Table 7.1 Associations between DNA methylation and stiffness or ultimate force.	236
Table 7.2 Trabecular, cortical and bone formation parameters of mouse tibiae²⁴⁵.	239

Table of Figures

Figure 1.1 Peak bone mass in men and women ²⁵	7
Figure 1.2 The main steps involved in intramembranous ossification ⁵⁰	11
Figure 1.3 The main steps in endochondral ossification ⁵⁰	12
Figure 1.4 Anatomy of a long bone ⁵⁵	13
Figure 1.5 Overview of osteoblast differentiation ⁶⁵	15
Figure 1.6 Overview of hedgehog signalling pathway.	18
Figure 1.7 Overview of Notch signalling pathway.	19
Figure 1.8 Overview of <i>WNT</i> signalling pathway.	20
Figure 1.9 Overview of BMP signalling pathway.....	22
Figure 1.10 Overview of FGF signalling pathway.	24
Figure 1.11 Overview of Vitamin D metabolism pathway.....	27
Figure 1.12 Overview of the actions of VDR and RXRA ¹⁵²	28
Figure 1.13 Metabolism of vitamin D and the biologic effects of 1,25(OH) ₂ D ₃ on calcium, phosphorus, and bone metabolism ¹⁵⁹	30
Figure 1.14 Overview of bone remodelling ¹⁶⁶	32
Figure 1.15 Pathogenesis of osteoporosis ¹⁸²	34
Figure 1.16 An overview to prenatal famine exposure during the Dutch Winter Famine from 1943-1947 and the disease risk in later adulthood ²¹¹	38
Figure 1.17 An overview of the main epigenetic modifications.....	48
Figure 1.18 DNA methylation of cytosine to 5-methylcytosine by DNMTs.	49
Figure 1.19 Overview of identifying <i>CDKN2A</i> CpG methylation as a candidate biomarker for adiposity in later childhood ³²²	63
Figure 1.20 Concept flow diagram.....	66
Figure 2.1 MAVIDOS trial study design.	75

Table of Figures

Figure 2.2 SPRING trial study design.	76
Figure 2.3 Map of the <i>RXRA</i> from geneART plasmid.	87
Figure 2.4 Map of the pGL4.17 basic luciferase plasmid.	88
Figure 2.5 Map of pGL4: <i>RXRA</i> (p <i>RXR</i> ApromLuc) luciferase reporter construct plasmid.	89
Figure 2.6 Schematic of the <i>RXRA</i> enhancer inserts, PCR primers and PCR conditions.	91
Figure 2.7 Schematic of enhancer region insets following digestion with restriction enzymes.	93
Figure 2.8 <i>RXRA</i> PCR mutagenesis primers and PCR cycling conditions.	95
Figure 3.1 The location of the <i>RXRA</i> CpGs of interest.	114
Figure 3.2 Significant differences in <i>RXRA</i> methylation at birth between the treatment groups in the MAVIDOS trial.	117
Figure 3.3 Significant differences in <i>RXRA</i> methylation at birth between the treatment groups in the MAVIDOS trial in infants born in summer and autumn.	122
Figure 3.4 Correlation between methylation at birth of <i>RXRA</i> CpG -2693 in cord compared to placenta in the MAVIDOS trial.	129
Figure 3.5 Pictogram representing pregnancy and UVB exposure during the year.	136
Figure 4.1 <i>CDKN2A</i> locus and the location of the DMR containing the 9 CpGs of interest.	144
Figure 4.2 Box whisker plots of <i>CDKN2A</i> CpG methylation at birth between the treatment groups within the MAVIDOS trial.	146
Figure 4.3 Box whisker plots of seasonal differences in <i>CDKN2A</i> CpG methylation at birth between the treatment groups within the MAVIDOS trial.	147
Figure 4.4 Schematic of <i>CDKN2A</i> and cell cycle progression.	153
Figure 5.1 Schematic of the <i>Runx2</i> and <i>Osterix</i> locus and the location of the CpGs of interest.	161
Figure 5.2 Box whisker plots of differences in <i>Osterix</i> CpG methylation at birth between the treatment groups within the MAVIDOS trial.	170
Figure 5.3 Box whisker plots of seasonal differences in <i>Osterix</i> CpG methylation at birth between the treatment groups within the MAVIDOS trial.	171
Figure 6.1 Histone marks and DNase 1 hypersensitive sites across <i>RXRA</i>	187

Figure 6.2 MatInspector analysis proposes several transcription factor binding sites across the <i>RXRA</i> CpGs of interest located in the differentially methylated region upstream of the <i>RXRA</i> promoter.....	189
Figure.6.3 The effect of mutated p <i>RXRA</i> promLuc on <i>RXRA</i> expression in osteosarcoma cells.	191
Figure 6.4 The effect of the orientation and positioning of the <i>RXRA</i> enhancer constructs in osteosarcoma cells.....	193
Figure 6.5 The effect of smaller fragments of the full <i>RXRA</i> enhancer region luciferase constructs in osteosarcoma cells.....	195
Figure 6.6 The effect of the minimal <i>RXRA</i> enhancer region luciferase constructs in osteosarcoma cells.....	197
Figure 6.7 The effect of mutating the minimal <i>RXRA</i> enhancer region luciferase constructs in osteosarcoma cell lines.....	199
Figure 6.8 Gene expression of osteosarcoma cell lines treated with vitamin D.....	201
Figure 6.9 Boxplots of <i>RXRA</i> CpG methylation in osteosarcoma cells following treatment with 10 nM 1,25(OH) ₂ D ₃	202
Figure 6.10 The effect of vitamin D treatment on <i>RXRA</i> expression following transfection with wildtype and mutated p <i>RXRA</i> promLuc constructs in osteosarcoma cells.	205
Figure 6.11 The effect vitamin D on the mutated minimal <i>RXRA</i> enhancer region luciferase constructs in osteosarcoma cell lines.....	207
Figure 6.12 Consensus DNA binding site motifs for nuclear receptors ³⁵⁷	208
Figure 6.13 Putative transcription factor binding across <i>RXRA</i> EMSA probes.....	210
Figure 6.14 EMSAs of <i>RXRA</i> CpG probes in Saos2, MG63 and MSCs.....	211
Figure 6.15 EMSAs of <i>RXRA</i> CpGs 4-5 in MG63 cells with combined and individual transcription factor binding.	213
Figure 6.16 EMSAs of hormone treated Saos2, MG63 and MSC cells.	215
Figure 6.17 Heat map representation of the magnitude of luciferase responses following transfection with the enhancer constructs.....	218
Figure 7.1 Location of the CpGs of interest with respect to the gene transcriptional start site.	230

Table of Figures

Figure 7.2 Tibial DNA methylation in mice fed a control diet and prenatal vitamin D deficient diet.	233
Figure 7.3 Tibial DNA methylation in the non-loaded and loaded tibiae of mice fed a control or prenatal vitamin D deficient diet.	235
Figure 7.4 Possible relationship linking prenatal vitamin D deficient diet with altered methylation and bone measures.	244
Figure 8.1 Summary of main findings.	251
Figure 8.2 Possible relationship between maternal cholecalciferol supplementation, altered <i>RXRA</i> methylation and improved bone measures.	254
Figure 8.3 Summary of main <i>CDKN2A</i>, <i>Runx2</i> and <i>Osterix</i> findings within the MAVIDOS trial.	256

Research Thesis: Declaration of Authorship

Print name: Nevena Krstic

Title of thesis: The effect of prenatal vitamin D supplementation on DNA methylation: Investigation into biomarkers and casual mechanisms of later bone health

I declare that this thesis and the work presented in it are my own and has been generated by me as the result of my own original research.

I confirm that:

1. This work was done wholly or mainly while in candidature for a research degree at this University;
2. Where any part of this thesis has previously been submitted for a degree or any other qualification at this University or any other institution, this has been clearly stated;
3. Where I have consulted the published work of others, this is always clearly attributed;
4. Where I have quoted from the work of others, the source is always given. With the exception of such quotations, this thesis is entirely my own work;
5. I have acknowledged all main sources of help;
6. Where the thesis is based on work done by myself jointly with others, I have made clear exactly what was done by others and what I have contributed myself;
7. Parts of this work have been published as:-

Krstic, N. *et al.* Gestational Vitamin D Supplementation Leads to Reduced Perinatal *RXRA* DNA Methylation: Results From the MAVIDOS Trial. *J. Bone Miner. Res.* **34**, 231–240 (2019).

Signature:

Date:

Acknowledgements

I firstly wanted to thank my Supervisors Professor Karen Lillycrop and Professor Nick Harvey for providing me with this opportunity and for helping me throughout my PhD. I would especially like to thank Karen, I really appreciate all that you have done for me, for helping with experiments and where to go next, for being so supportive and understanding over the last four years and for being so accommodating with my health. I would also like to thank Professor Graham Burdge for all of his help with my thesis and for always being available to listen if I needed help or just to talk to someone.

I would like to thank Dr Robert Murray or PostDoc Rob for all of his help over the last four years and for always being available to answer my million questions. You have been a very good teacher and I have really enjoyed listening to your wisdom and learning new techniques in the lab with you. I would like to thank Dr Nicola Irvine, also known as my partner in crime. I am so glad that you were there during the time of my PhD and thank you for always being there to support me and provide me with the latest gossip whenever needed. I would also like to thank Matt and Mark, for always making me laugh, for having the most random conversations and for being there to help with experiments. I would also like to thank everyone in the Epigen and DevEpi group for making me feel so welcome.

I would like to thank my family, especially my mum. Mum you are always there for me whenever I need you and I honestly do not know where I would be without you. Thank you for helping me all of these years and for always supporting me and encouraging me to with everything that I do. I would also like to thank my brothers, for putting up with me when I have been stressed and for taking me out for dinner and cake all of the time.

I would like to thank Roxanna for helping to keep me sane over the last two years, for being the best gym buddy and for always being up for Sprinkles, burger or pizza! I would also like to thank my friends back home, especially Ruth and Laura for always being there for me, to Femke and Freddie, for being amazing members of adventure squad, and to my Uni girls, especially Emily and Catherine, for always checking in on me.

Definitions and Abbreviations

Abbreviation	Full Term
°C	Degrees Centigrade
1,24,25(OH) ₂ D ₃	1,24,25-dihydroxyvitamin D ₃
1,25(OH) ₂ D ₃	1,25-dihydroxyvitamin D ₃
24,25(OH)D ₃	24,25-hydroxyvitamin D ₃
25(OH)D ₃	25-hydroxyvitamin D ₃
3DUS	Three dimensional ultrasound
ABC4A	ATP-binding cassette, sub family A member 4
ABCA1	ATP Binding Cassette Subfamily A Member 1
ALPL	Alkaline phosphatase
ANCR	Angelman Syndrome Chromosome Region
ANRIL	Antisense non-coding RNA in the INK4 locus
AP1	Activator protein 1
ATP	Adenosine triphosphate
BA	Bone area
BATMAN	Bayesian Tool for Methylation Analysis
BMC	Bone mineral content
BMD	Bone mineral density
BMI	Body mass index
BMP	Bone morphogenetic protein
BMUs	Basic multicellular units
bp	Base pair
BS	Bone Surface
BV	Bone Volume
C	Control
C/EBP α/β	CCAAT/enhancer binding protein alpha/beta
CaMos	Canadian Multicentre Osteoporosis Study
cAMP	Cyclic adenosine monophosphate
CCD	Cleidocranial dysplasia
CDK	Cyclin dependent kinase
CDKN2A	Cyclin dependent kinase inhibitor 2A
CFU-F	Fibroblast colony forming units
CFU-M	Monocyte colony forming units
CI	Confidence Interval
CO ₂	Carbon dioxide
Col11a2	Collagen type XI alpha 2 chain
Col2a1	Type II collagen alpha 1
COPD	Chronic obstructive pulmonary disease
CSMI	Cross-sectional moment of inertia
CTRB1	Chymotrypsinogen B1
CTX	C terminal cross linking telopeptide of type I collagen
CVD	Cardiovascular disease
CYP	Cytochrome P450
DAAM2	Dishevelled-associated activator of morphogenesis 2
DAP12	DNAX-activation protein 12
DBD	DNA binding Doman
DBP	Vitamin D binding protein
DC-STAMP	Dendrocyte Expressed Seven Transmembrane Protein
dH ₂ O	Distilled water

Definitions and Abbreviations

Abbreviation	Full Term
DKK1	Dickkopf WNT Signaling Pathway Inhibitor 1
DLL	Delta Like Canonical Notch Ligand
DMEM	Dulbecco modified eagle medium
DMR	Differentially methylated region
DNA	Deoxyribonucleic acid
DNMT	DNA methyltransferase
dNTPs	Deoxynucleotide
DOHaD	Developmental Origins of Health and Disease
DRD4	Dopamine receptor D4
E2F	Retinoblastoma-associated Protein 1
eBMD	Estimated bone mineral density
EDTA	Ethylenediaminetetraacetic acid
EGFL8	Epidermal Growth Factor-Like Protein 8
EMSA	Electrophoretic mobility shift assay
ENCODE	Encyclopedia of DNA elements
eNOS	Endothelial nitric oxide synthase
ESR1	Estrogen Receptor 1
EZH2	Enhancer Of Zeste 2 Polycomb Repressive Complex 2 Subunit
FBS	Fetal bovine serum
FcRγ	Fc receptor gamma chain
FGF	Fibroblast growth factor
FGFR	Fibroblast growth factor receptor
GH	Growth Hormone
GLI	Glioma-associated Oncogene
GNASAS	GNAS antisense RNA
GR	Glucocorticoid Receptor
GWAS	Genome wide association studies
H3K4Me1	Histone 3, lysine 4 methyl 1
H3K4Me3	Histone 3, lysine 4 methyl 3
HATs	Histone acetyltransferases
HDAC	Histone deacetylase
HES	Hairy and Enhancer of Spring
HEY	HES-related with YRPW motif
HF	High Fat
HIV	Human immunodeficiency virus
HMTs	Histone methyltransferases
HOXA10	Homeobox A10
HRT	Hormone replacement therapy
HSCs	Hematopoietic stem cells
IGF2	Insulin growth factor 2
IHH	Indian hedgehog
IL	Interleukin
INSIGF	Insulin induced gene
IQR	Interquartile Range
ITAM	Immunoreceptor tyrosine-based activation motif
JAG	Jagged
JNK	Jun N terminal kinase
Kb	Kilobases
KDM6a	Lysine demethylase 6A
LB	Lysogeny broth
LBD	Ligand Binding Domain

Abbreviation	Full Term
LCoR	Ligand-dependent Co-repressor
LEP	Leptin
lncRNAs	Long non-coding RNAs
LRP5/6	Lipoprotein receptor related protein 5/6
MAOA	Monoamine oxidase A
MAPK	Mitogen activated protein kinase
MAVIDOS	Maternal gestational vitamin D supplementation and osteoporosis study
MBD1-3	Methyl CpG binding domain proteins 1-3
M-CSF	Macrophage colony stimulating factor
MeCP2	Methyl CpG binding protein 2
MEG3	Maternally expressed gene 3
MEST	Mesoderm specific transcript
miRNAs	Micro RNAs
ml	Mililitre
MMP9	Matrix Metalloproteinase 9
mRNA	Messenger RNA
MSCs	Mesenchymal stem cells
mSin3	Mammalian Sin3 transcriptional corepressor
MTHFR	Methylenetetrahydrofolate Reductase
mTOR	Mammalian target of rapamycin
N4BP2	NEDD4 binding protein 2
N-cadherin	Neural cadherin
N-CAM	Neural cell adhesion molecule
NCoR	Nuclear Receptor Co-repressor 1
Nfatc1	Nuclear factor of activated T cells cytoplasmic 1
NF-κB	Nuclear factor kappa light chain enhancer of activated B cells
ng	Nanogram
NICD	Notch Intracellular Domain
nM	Nanomolar
NO66	Nucleolar protein 66
NTCs	Non template control
NTX	Procollagen type I N propeptide
NuRD	Nucleosome Remodelling Deacetylase
nVDRE	Negative vitamin D response element
OPG	Osteoprotegerin
OPPG	Osteoporosis Pseudoglioma Syndrome
PAH	Princess Anne Hospital
PAX1	Paired box 1
PBS	Phosphate buffered saline
PCR	Polymerase chain reaction
PDK4	Pyruvate Dehydrogenase Kinase 4
PEG10	Paternally expressed gene 10
PGC1α	Peroxisome proliferator activated receptor gamma coactivator 1 alpha
pH	Potential of hydrogen
PI3K	Phosphoinositide 3-kinase
PI3KCD	Phosphoinositide-3-kinase, catalytic, δ -polypeptide
PKA	Protein Kinase A
PKC	Protein Kinase C
PLC	Phospholipase C
PPAR	Peroxisome proliferator activated receptor
PTCH1	Patched homologue 1

Definitions and Abbreviations

Abbreviation	Full Term
PTH	Parathyroid hormone
PTHrP	Parathyroid hormone related protein
RA	Retinoic Acid
RANK	Receptor activation of NF-kB
RANKL	Ligand for RANK
Rb	Retinoblastoma
RISC	RNA Induced Silencing Complex
RNA	Ribonucleic acid
ROI	Region of Interest
rpm	Revolutions per minute
Runx2	Runt related transcription factor 2
RXRA	Retinoid x receptor alpha
Saos2	Sarcoma osteogenic
scBMC	Size corrected bone mineral content
SEM	Standard error of the mean
SERMs	Selective estrogen receptor modulators
SGCE	Sarcoglycan Epsilon
siRNA	Small Interfering RNA
SLC6A4	Sodium dependent serotonin transporter
SMO	Smoothened
SNPs	Single nucleotide polymorphisms
SOC	Super optimal broth with catabolite repression
SOD1	Superoxide Dismutase 1
SOST	Sclerostin
SOX9	Sex-determining region Y Box 9 protein
SPRING	Southampton Pregnancy Intervention for the Next Generation
SRY	Sex-determining region Y
STAT1	Signal transducer and activator of transcription 1
SUMOylation	Small ubiquitin like modifier proteins
SWS	Southampton Women's Survey
TAE	Tris base, acetic acid and EDTA
TBP	TATA box binding protein
TET	Ten eleven translocase
TFAM	Transcription factor A, mitochondrial
TNES	Tris, NaCl, EDTA, SDS
TNFR	Tumour necrosis factor receptor
TR	Thyroid Receptor
TRAcP	Tartrate-Resistant Acid Phosphatase
TRAF6	Tumour necrosis associated factor 6
TSPAN3	Tetraspanin 3
TSS	Transcriptional start site
TV	Trabecular Volume
UV	Ultraviolet
V	Volt
VDIR	VDR interacting repressor
VDR	Vitamin D receptor
VDREs	Vitamin D response elements
ZNF690	Zinc Finger Protein 690
µg	Microgram
µl	Microlitre
µM	Micromolar

Chapter 1 Introduction

1.1 Osteoporosis

Osteoporosis is a major non communicable disease that affects the ageing population. It is described as “a systemic skeletal disease characterised by low bone mass and micro architectural deterioration of bone tissue, with a consequent increase in bone fragility and susceptibility to fracture”¹. The incidence of osteoporosis is greater in postmenopausal women than men and in 2010 it was estimated that 22 million women and 5.5 million men in the EU had osteoporosis². Common sites of osteoporotic fracture include the wrist, spine and hip, with hip fractures being deemed the most serious osteoporotic fracture, accounting for a third of all osteoporotic fractures and nearly always resulting in hospitalisation³. The incidence rate for hip fracture increases exponentially with age in both men and women³, and the incidence rate is higher in women than men⁴. In 2010 in the EU it was estimated that there were 3.5 million new fractures including approximately 610,000 hip fractures, 520,000 vertebral fractures, 560,000 forearm fractures and 1,800,000 other fractures such as pelvis, rib, humerus, tibia, fibula, clavicle, scapula, sternum and other femoral fractures².

There are several factors which can contribute to an increased risk of fracture such as the early life environment, low bone mass, low body weight, heavy alcohol or tobacco use, corticosteroid use, protein-energy malnutrition, low calcium intake and inadequate levels of vitamin D⁵. Hereditary factors are also thought to play a role in fracture risk where a maternal history of hip fracture has been shown to double the risk of fracture in individuals⁶. Therefore, osteoporosis is now thought to be due to a combination of both environmental and genetic factors.

The economic cost associated with osteoporosis is great and in 2010 in the EU it was estimated that the cost of osteoporosis was 37 billion euros of which 66 % was attributed to treating incident fractures, 5 % was spent on pharmacological prevention and 29 % was spent on long term fracture care². Furthermore, hip fractures represented 54 % of the costs, 5 % was due to vertebral fractures, 1 % were due to forearm fractures and the remaining 39 % represented other fractures². Therefore, preventative measures need to be investigated earlier in the life course, which could delay the onset of developing osteoporosis. The identification of biomarkers which could be predictive of later osteoporosis risk would be beneficial in identifying at risk individuals, allowing for suitable interventions to delay disease progression.

1.1.1 Morbidity and Mortality

With advancing age, and in women a decrease in estrogen following menopause, there is an increase in bone loss and an increase in the prevalence of developing osteoporosis². Osteoporotic fractures are often defined as fractures arising from low energy trauma, such as a fall from standing

Chapter 1

height or less, or trauma that would not cause a fracture in an otherwise healthy individual. They often occur in individuals over the age of 50 who also present with low bone mineral density (BMD)².

Fragility fractures are a major cause of morbidity and the most common fractures occur at the wrist hip and spine⁷. Wrist fractures lead to acute pain and loss of function however, recovery is usually very good⁷. Whereas hip fractures cause acute pain, loss of function and nearly always result in hospitalisation. Furthermore, hip fracture recovery is slow, rehabilitation is often incomplete and many patients become permanently institutionalised in nursing homes⁷. Vertebral fractures may cause acute pain and loss of function but they can also present with no symptoms, they often recur and there is increasing disability associated with the increasing number of fractures⁷. Studies have shown that following a fracture there is increased likelihood of developing another fracture, especially within the first year and it is estimated that less than 20 % of fragility fracture patients receive therapy to reduce future fractures within the first year following a fracture⁸⁻¹⁰. Barton *et al.*, found that 38 % of patients in a retrospective cohort study had had another osteoporotic fracture within two years of the incident fracture and of those 74 % had one or more new vertebral fractures and 14 % had a hip or femur fracture¹¹.

Osteoporosis and the consequent fragility fractures are associated with increased mortality, except for fractures occurring at the wrist⁷. In the EU in 2010, it was estimated that the number of deaths causally related to fractures was 43,000⁷. In women it was estimated that 50 % of fracture related deaths were due to hip fractures, 28 % to clinical vertebral and 22 % to other fractures whereas in men these percentages were 47, 39 and 14 % respectively⁷. Following a hip fracture, most deaths occur within 3-6 months of the fracture and it has been shown that 20-30 % of deaths are causally related to the hip fracture itself⁷. A longitudinal population based study in Australia by Bliuc *et al.*, studied 614 patients above 60 who sustained a fracture between 1989 and 2007¹². The study found that women were nearly twice as likely to sustain a fracture compared to men, the mortality rate amongst fracture years was nearly double that of the mortality rate in the region, and that the mortality rate was higher in men than women¹². Von Friesendorff *et al.*, studied 1013 patients in Sweden who sustained a hip fracture between 1984-1985 and followed them up for 22 years¹³. The study found that the risk of death following a hip fracture was greatest within the first year, men were younger when they fractured their hip than women and mortality was higher in both men and women following a hip fracture at all time points across the 22 year follow up period¹³. Kanis *et al.*, studied 158,589 hospital admissions for patients with hip fractures between 1987 and 1996 and the overall mortality rate was 53 %¹⁴. Patients of all ages were at a greater risk of mortality within the first year of their hip fracture compared to the general population and an increase in age was associated with the proportion of deaths associated or causally related to hip fracture¹⁴. An

observational study in Canada on 504 patients with hip fractures by Papaioannou *et al.*, found that the overall 1 year mortality was 25.2 %, 5.2 % of the patients re-fractured their hip in the first year and 4.7 % fractured had a second vertebral, wrist or rib fracture¹⁵. The study found that dementia, respiratory disease and living in an institution at the time of fracture were associated with increased mortality¹⁵. Institutionalisation was associated with increasing age, trochanteric fracture and post-operative complications and individuals living in an institution prior to the fracture were more likely to be deceased at 12 months¹⁵.

1.1.2 Diagnosis and Treatment

Osteoporosis can be diagnosed by measuring an individual's BMD with a dual-energy X-ray absorptiometry (DXA) scan at the femoral neck or spine. Clinically, osteoporosis is defined as having a value for BMD which is 2.5 standard deviations or more below the young adult mean¹⁶. Whereas osteopenia, or low bone mass, is a value for BMD more than 1 standard deviation below the young adult mean but less than 2.5 standard deviations below this value¹⁶. The 10 year probability of a major fracture or hip fracture can be predicted using the computer based algorithm, FRAX¹⁷. The predicted fracture risk is calculated from age, sex, weight, height, body mass index (BMI), prior fragility fractures, parental history of hip fracture, current smoking habits, glucocorticoid use, alcohol consumption, and other secondary causes of osteoporosis such as rheumatoid arthritis, hyperthyroidism, primary hyperparathyroidism, diabetes, inflammatory bowel diseases, chronic obstructive pulmonary disease (COPD) and human immunodeficiency virus (HIV)¹⁸. Furthermore, measurements of femoral neck BMD can be optionally used to enhance the prediction¹⁷. Adachi *et al.*, have identified four risk factors which were independent predictors of two year low trauma non-vertebral fracture using participants from the population based prospective cohort CaMos (Canadian Multicentre Osteoporosis Study)¹⁹. The risk factors included the number of falls in the past year, low trauma fracture in the past year, poorer physical function/ performance and lower hip BMD¹⁹.

Post-menopausal women are at a greater risk of developing osteoporosis due to the decline in estrogen levels following menopause therefore, postmenopausal women are recommended to make a number of dietary and lifestyle changes to reduce the risk of fracture¹⁸. These include a daily calcium intake of 800-1200 mg, sufficient dietary protein ideally through dairy consumption, regular weight bearing exercise and in women with an increased risk of fracture, daily supplementation with 800 IU/d cholecalciferol is also advised¹⁸. Further treatment of osteoporosis involves hormone replacement therapy (HRT) and bisphosphonates which are drugs that inhibit bone resorption. Nevertheless, it has been shown that a high number of patients with osteoporosis remain untreated and the use of pharmacological interventions to prevent fractures has decreased in recent years^{2,7}.

It is estimated that there are 18.44 million women within the EU who are at a high risk for fracture and that 57 % of these women do not receive bone specific treatment⁷. Moreover, studies have shown that many fracture patients are undiagnosed with osteoporosis and therefore are not receiving the appropriate treatment to decrease the risk of following fractures. A retrospective cohort study by Barton *et al.*, investigated 2933 patients aged over 50 years who sustained a new vertebral fracture between 2008 and 2014 however, amongst the 2933 fracture patients only 27 % of patients were taking either supplements or pharmacological interventions prior to the fracture and within the first year following the fracture, only a further 10.7 % of patients started taking supplements or medication¹¹. Juby *et al.*, investigated hip fractures in 311 patients and found that only 6 % of patients were receiving HRT, bisphosphonates or calcitonin²⁰. Hajcsar *et al.*, studied 108 fracture patients in Canada and found that 32.4 % were prescribed calcium supplementation, 13 % were prescribed vitamin D supplementation, 7.4 % were taking bisphosphonates and 16 % of women were taking HRT²¹. Cree *et al.*, studied 449 hip fracture patients in Alberta between 1996-1997 and found there was low usage of anti-resorptive therapy with only 38 individuals taking medication consisting of hormones, bisphosphonates, calcitonin and/or activated vitamin D prior to their hip fracture²².

Therefore, this highlights the need for appropriate diagnosis of osteoporosis and targeted interventions to reduce the risk of a fragility fracture. Furthermore, appropriate treatment needs to be prescribed in patients following a fracture to decrease the likelihood of additional fractures.

1.1.3 Pathways to osteoporosis

Osteoporosis is thought to occur due to three main pathogenetic mechanisms. These are “1. Failure to achieve a skeleton of optimal strength during growth and development. 2. Excessive bone resorption resulting in loss of bone mass and disruption of architecture. 3. Failure to replace lost bone due to defects in bone formation.”²³. In humans, BMD increases during the growth period until it peaks in early adulthood, where it remains relatively stable through adult life before progressively declining with ageing²⁴ (**Figure 1.1**). It has been shown that the early life environment, both intra-uterine and in early childhood, can influence the magnitude of peak BMD in early adulthood, and therefore bone health in later life. Furthermore, it has been shown that the rate of bone loss in adulthood can contribute to the risk of developing osteoporosis. Therefore, it is thought that osteoporosis may result from a decreased peak bone mass in early adulthood, or through accelerated bone loss with ageing, or a combination of both⁵.

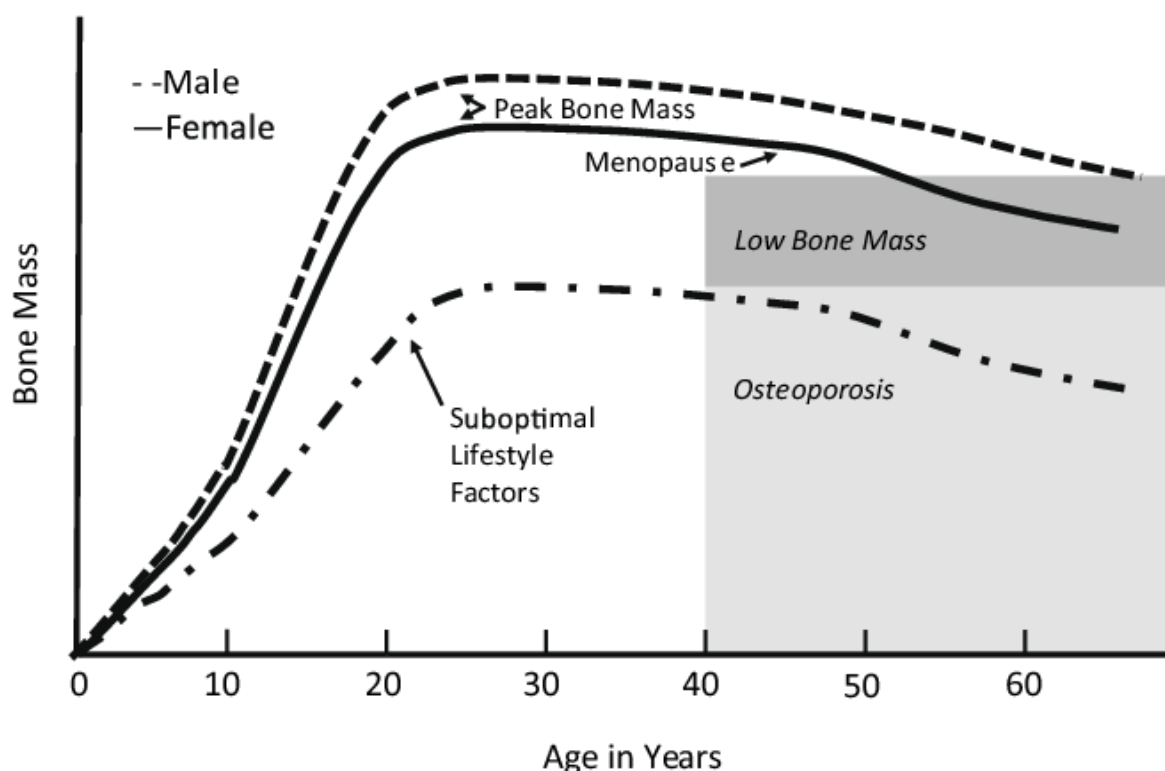


Figure 1.1 Peak bone mass in men and women²⁵.

1.1.3.1 Peak bone mass

Peak bone mass is the maximal BMD that is accrued during growth and development and peaks in early adulthood²⁶. A cross sectional study by Matkovic *et al.*, measured bone mass in 265 females aged 8-50 years and found that rapid cessation of accumulation of bone mass occurred by the average age of 18²⁷. However, some studies have shown that there is some bone gain following cessation of linear growth and that this can occur until the third decade of life. A longitudinal prospective study in healthy students at the University of Omaha by Recker *et al.*, found that in the third decade of life there was an increase per decade in forearm bone mineral content (BMC) and BMD (4.8 %), lumbar spine BMC (5.9 %) and BMD (6.8 %) and whole body BMC (12.5 %) and that the end of bone gain ranged between 28.3 to 29.5 years of age²⁸. Matkovic *et al.*, also found that between the ages of 18 and 50 in premenopausal women, BMD at most skeletal sites remained constant whereas BMD at the skull continued to increase with age whereas BMD at the hip region decreased with age²⁷.

It has been shown that peak bone mass can determine the risk of developing osteoporosis in later life. A computer simulation in bone remodelling using data from cross sectional studies within the Hologic database predicted that a 10 % increase in peak BMD delayed the development of osteoporosis by 13 years²⁹. There are a number of maternal factors which can influence peak bone

Chapter 1

mass including maternal calcium and vitamin D status during pregnancy, bone mass, fat distribution, BMI, levels of physical activity and smoking during pregnancy²⁹. Factors during childhood include nutrition, physical exercise and medication use and a study on the Raine cohort found that participation in organised sport during childhood and adolescence was positively associated with bone mass at age 20³⁰.

Studies have shown that body composition plays a role in determining BMD and that there is a positive correlation between both height and weight with BMD. Slemenda *et al.*, measured bone mass and anthropometric measurements of 342 female adult twins and found that frame size, muscularity and adiposity have independent effects on the skeleton³¹. Furthermore, shoulder width, subscapular skinfold thickness and calf circumference were strongly correlated with BMD at all skeletal sites including at the radius, femoral neck, Ward's triangle, trochanter and spine³¹. A study of Iranian children found that obese children had greater BMD than normal weight children however, lean mass and not fat mass was the most important predictor of BMD in both Iranian boys and girls³². Whereas a study in healthy school children found that both lean mass and fat mass correlated with BMC³³.

1.1.3.1.1 Heritability of peak bone mass

It has been estimated that between 40-80 % of the variance in BMD is attributable to genetic factors. To determine heritability, many studies investigated variance in BMD in monozygotic and dizygotic twins. Harris *et al.*, investigated heritability in 48 monozygotic and 49 dizygotic twin pairs and found that the genetic heritability for bone specific alkaline phosphatase, lumbar spine BMD and femoral neck BMD was 63 %, 77 % and 72 % respectively³⁴. Nguyen *et al.*, measured lean mass, fat mass and BMD in 57 monozygotic and 55 dizygotic twins from the Sydney Twin Study of Osteoporosis in Australia and found that in monozygotic and dizygotic twins, both lean mass and fat mass were positively correlated with BMD at all sites³⁵. Furthermore, they estimated that the heritability of lumbar spine, femoral neck and total body BMD were 78 %, 76 % and 79 % respectively³⁵. Seeman *et al.*, measured lean mass, fat mass, muscle strength and BMD in 56 monozygotic and 56 dizygotic female twin pairs and found that genetic factors accounted for 60-80 % variance in BMD depending on the site³⁶. A 10 % difference in lean mass was associated with 4 % difference in BMD at the lumbar spine and 7-10 % at the femoral sites, a 10 % difference in fat mass was associated with a 0.6 % difference in BMD at the lumbar spine and 1.2-1.9 % at the femoral sites and 10 % difference in muscle strength was associated with a 1.5-1.8 % difference in BMD at the femoral sites³⁶. Arden *et al.*, investigated the genetic component of muscle strength and lean body mass on BMD in 227 monozygotic and 126 dizygotic twin pairs and found that lean mass was correlated with grip strength and leg extensor strength and there was a weak correlation

between grip strength and leg extensor strength³⁷. Lean mass, grip strength and leg extensor strength were correlated with femoral neck, lumbar spine, ultra-distal forearm and whole body BMD and the three muscle variables explained between 8-18.5 % variance in site specific BMD³⁷. A cross sectional twin study in older women by Flicker *et al.*, investigated the influence of environmental and genetic factors on BMD³⁸. Multiple regression analyses identified lean mass and smoking as significant predictors of BMD and lean mass and fat mass were significant predictors of BMC³⁸. The study found that maternal and lifestyle factors such as age, body composition, tobacco use and alcohol consumption accounted for 20-33 % variation in BMD whereas, genetic heritability could explain 75 % total variance in BMD and 76 % variance in BMC³⁸.

Genetic heritability has also been measured within families. Krall *et al.*, measured BMD in 40 families, each with a postmenopausal mother, adult premenopausal daughter, adult son and the children's biological father and found that 46-62 % of the variance in BMD was hereditary³⁹. Having a family history of fracture has been shown to influence BMD and fracture risk. Kulak *et al.*, found that 71 % of the premenopausal women with either osteoporosis or low bone mass had a history of a fragility fracture or low BMD in a grandparent, parent or sibling⁴⁰. Furthermore, studies have shown that daughters born to mothers with osteoporosis have a higher risk of developing osteoporosis in later life. Seeman *et al.*, investigated bone mass in daughters of women with postmenopausal osteoporosis compared to daughters of women without postmenopausal osteoporosis and found that mothers with osteoporosis had lower BMC in the lumbar spine (33 %), femoral neck (23 %) and femoral midshaft (15 %) compared to normal postmenopausal women⁴¹. Furthermore, the daughters of mothers with osteoporosis had lower BMC in the lumbar spine (7 %), femoral neck (5 %) and femoral midshaft (3 %) compared to daughters of normal mothers⁴¹.

1.1.3.2 Accelerated loss of bone following peak bone mass

There are a number of factors that can affect bone loss such as ageing, sex steroid concentrations and medication use. Estrogen plays a role in bone metabolism in both men and women however, following menopause in women, estrogen levels decline. Kulak *et al.*, found that the primary cause of bone loss in post-menopausal women was estrogen deficiency⁴⁰ and Garnero *et al.*, have shown that following menopause, there is an increase in bone turnover which is responsible for the acceleration in the rate of bone loss⁴². The study found that following menopause, there is a 37-52 % increase in bone formation markers and a 79-97 % increase in bone resorption markers⁴². Bone formation can be assessed by serum Osteocalcin, serum bone specific alkaline phosphatase and serum C-propeptide of type I collagen⁴². Whereas bone resorption can be measured by urinary excretion of procollagen type I N propeptide (NTX) and C terminal cross linking telopeptide of type I collagen (CTX)⁴². Christiansen *et al.*, proposed that post-menopausal bone loss can be predicted

by measuring four parameters of bone turnover in blood and urine including serum alkaline phosphatase, fasting urinary calcium and hydroxyproline and plasma Osteocalcin⁴³. Furthermore, another study by Christiansen *et al.*, found that these urinary measures, as well as BMC measurements, could predict individuals who had a greater rate of bone loss⁴⁴. This would highlight those in need of suitable interventions to improve bone health outcomes⁴⁴. Prestwood *et al.*, have shown that estrogen replacement therapy in postmenopausal women decreases bone turnover⁴⁵ which was beneficial in preventing bone loss and the risk of fracture.

Kulak *et al.*, found that secondary causes of bone loss in both pre and post-menopausal women included glucocorticoid therapy, thyrotoxicosis, inflammatory bowel disease, anticonvulsant drugs, organ transplantation, premenopausal estrogen deficiency and cancer chemotherapy⁴⁰. Other factors which can influence BMD and bone loss include endocrine disorders such as growth hormone deficiency, hypogonadism, Turner's syndrome, hyperthyroidism, type 1 diabetes mellitus, nutritional disorders such as anorexia nervosa, inflammatory bowel disease, celiac disease, chronic diseases of childhood and adolescence such as chronic kidney disease and chronic liver disease, and medications such as glucocorticoids, drugs that decrease sex steroid levels and oral contraceptives²⁶.

1.2 Bone formation

Bone formation involves the transformation of pre-existing mesenchymal tissue into bone tissue⁴⁶. This typically occurs in the second month of pregnancy and involves two mechanisms: intramembranous ossification and endochondral ossification.

Intramembranous ossification involves the direct conversion of mesenchymal cells into osteoblasts⁴⁷ and this primarily occurs in the bones of the skull and the clavicle⁴⁸ (**Figure 1.2**). Osteoblasts are involved in the calcification of the bone matrix by secreting collagen proteoglycan matrix⁴⁶. However, osteoblasts can also be trapped in the calcified matrix and become osteocytes⁴⁶. There are a number of proteins and transcription factors involved in intramembranous ossification, such as bone morphogenetic proteins (BMPs)⁴⁶ that activate a transcription factor called Runt-related transcription factor 2 (*Runx2*) which plays a role in differentiating mesenchymal cells into osteoblasts⁴⁹ as well as activating genes for *Osteocalcin*, *Osteopontin* and other bone specific extracellular matrix proteins⁴⁶.

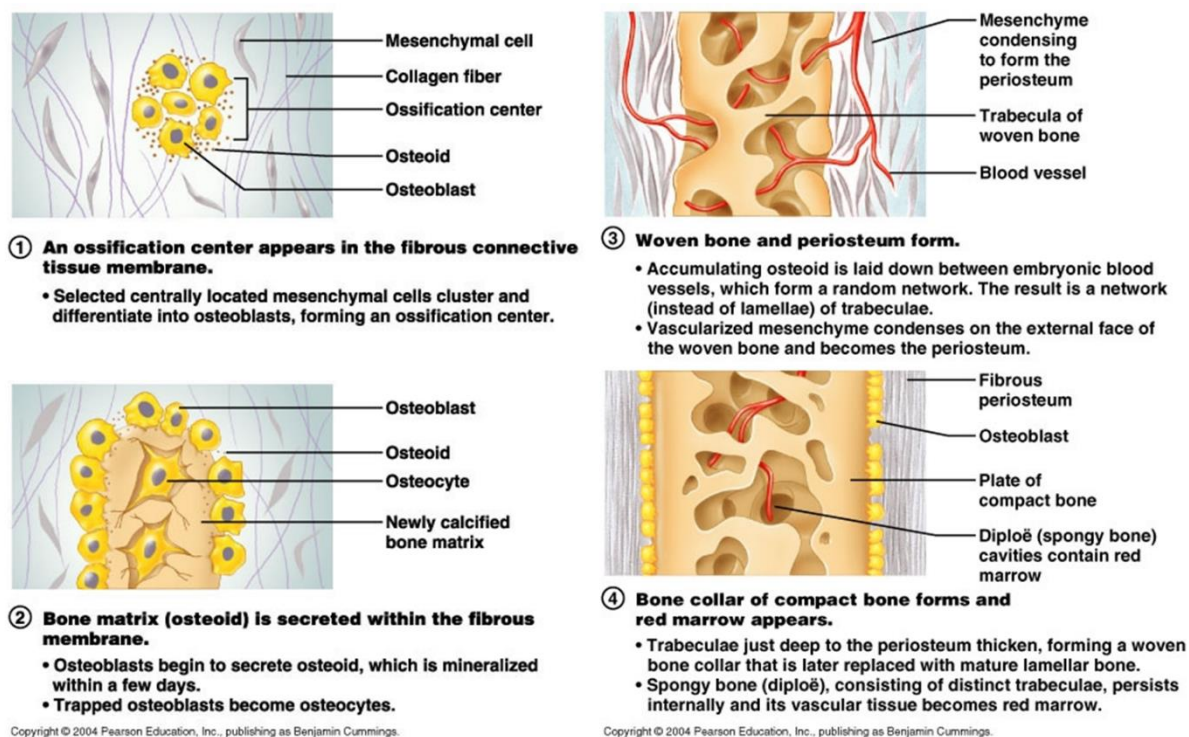
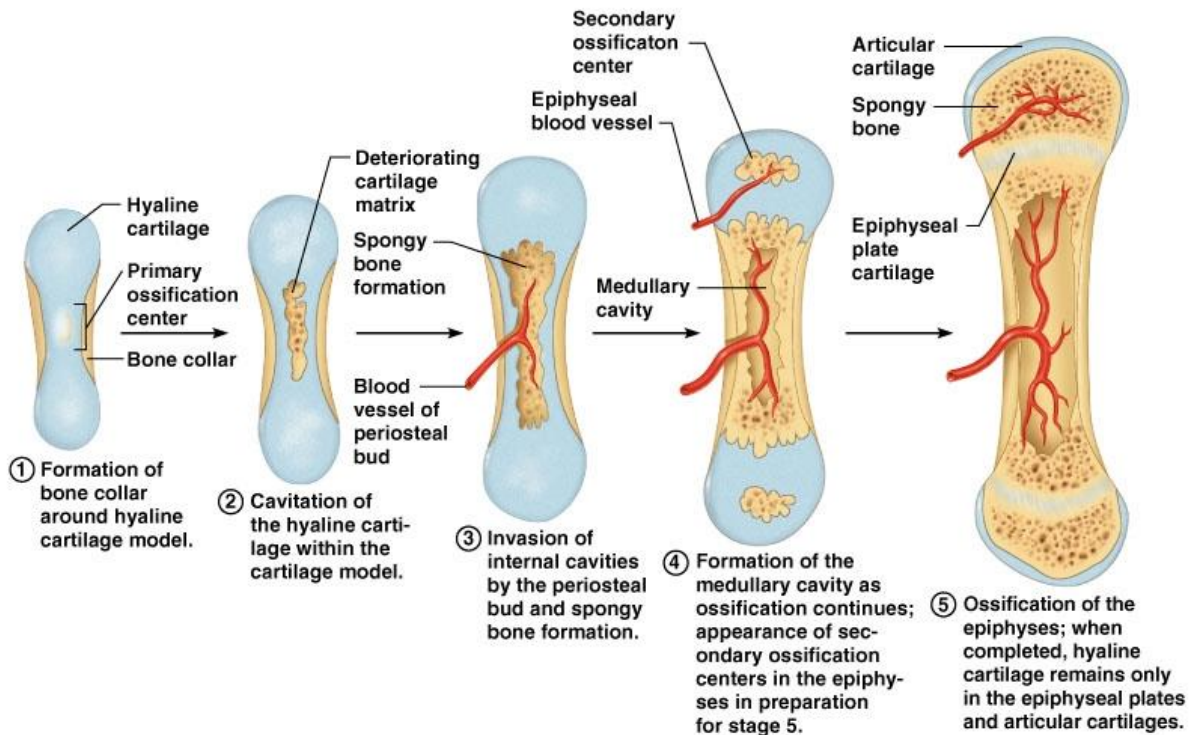


Figure 1.2 The main steps involved in intramembranous ossification⁵⁰.

Endochondral ossification involves aggregated mesenchymal cells forming cartilage tissue, which is later replaced by bone tissue, and this commonly occurs at the vertebral column, pelvis and limbs⁴⁶ (**Figure 1.3**). Firstly, mesodermal cells express two transcription factors, Paired box 1 (PAX1) and Scleraxis, which are thought to activate cartilage specific genes^{51,52} and result in mesenchymal cells committing to become cartilage cells⁴⁶. The committed mesenchymal cells condense into chondrocytes⁴⁶ and this process is thought to involve neural cadherin (N-cadherin), neural cell adhesion molecule (N-CAM)^{53,54} and Sex-determining region Y (SRY) box 9 protein (SOX9)⁴⁶. Next, the chondrocytes proliferate and secrete a cartilage specific extracellular matrix which becomes the hyaline cartilage model for the bone and is rich in type II collagen, the proteoglycan Aggrecan and other transcription factors^{46,47}. In the centre of the diaphysis, which is the central part of the bone, is the primary ossification centre which enlarges, spreading proximally and distally and osteoblasts surround the diaphysis and secrete osteoid to encase the cartilage in a bone collar⁵⁰. The chondrocytes stop dividing, increase their volume and become hypertrophic chondrocytes which produce collagen X and fibronectin which allow the matrix to be mineralised by calcium carbonate⁴⁶. During the third month of development, a periosteal bud invades the central cavity which contains a nutrient artery and vein, lymphatics, nerve fibres, red marrow elements, osteoblasts and osteoclasts⁵⁰. This triggers apoptosis of the hypertrophic chondrocytes and osteoblasts form spongy trabecular bone⁵⁰. As the primary ossification centre enlarges, osteoclasts break down the spongy bone and open up a medullary cavity in the centre of the shaft⁵⁰. Shortly

before or after birth, a secondary ossification centre appears in one or both epiphyses, which are either side of the diaphysis on the ends of the bones, and this is the location of the growth plate⁵⁰.



Copyright © 2004 Pearson Education, Inc., publishing as Benjamin Cummings.

Figure 1.3 The main steps in endochondral ossification⁵⁰.

In long bones, endochondral ossification starts in the centre and spreads outwards⁴⁶ forming the diaphysis (the midsection of bone) with epiphyses on either end⁵⁵ (**Figure 1.4**). The walls of the diaphysis are composed of dense, hard compact bone called cortical bone and the hollow region in the diaphysis is the medullary cavity filled with yellow marrow⁵⁵. The endosteum lines the medullary cavity and this is where bone growth, repair and remodelling occur⁵⁵. The periosteum covers the outer surface of bone and contains blood vessels, nerves and lymphatic vessels⁵⁵. Whereas in flat bones, such as from the cranium there is a layer of spongy bone lined on both sides by compact bone⁵⁵. The ends of long bones are called the epiphyses and are filled with spongy cancellous bone, called trabecular bone, and red marrow⁵⁵. The epiphysis meets the diaphysis at the metaphysis, which contains the epiphyseal growth plate consisting of a layer of hyaline cartilage in growing bones⁵⁵. The epiphyseal growth plates contain three regions including a region for chondrocyte proliferation, mature chondrocytes and hypertrophic chondrocytes^{46,56}. *Runx2* has an important role in the growth plate and drives proliferative chondrocytes to differentiate into hypertrophic chondrocytes⁴⁷. Cartilage forms on the epiphyseal side of the epiphyseal plate whereas on the diaphyseal side, cartilage is ossified and the diaphysis grows in length⁵⁵.

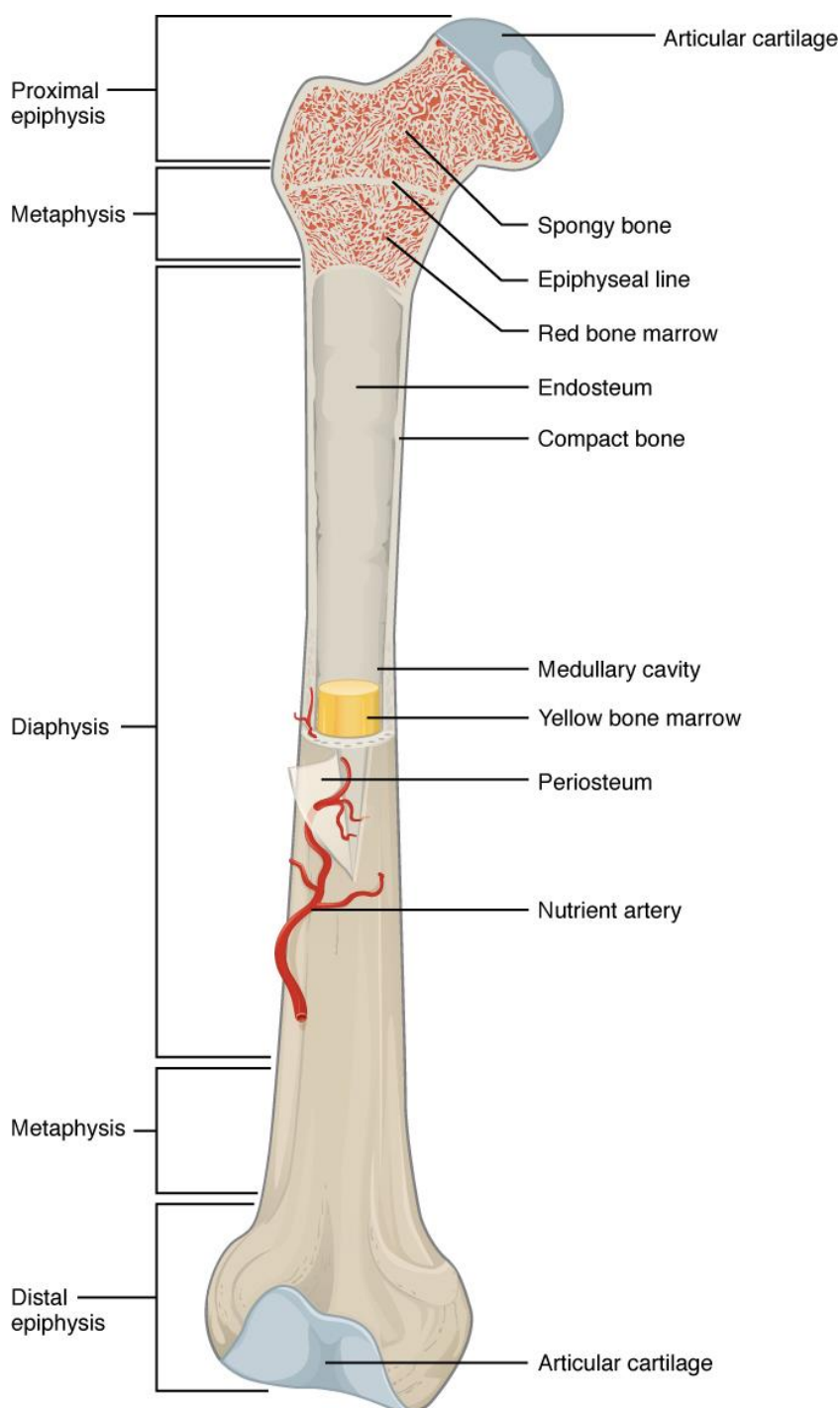


Figure 1.4 Anatomy of a long bone⁵⁵.

During bone growth, bones grow in diameter through modelling which involves resorption on one surface of a bone and deposition on another⁵⁵. By week 8 of gestation there is a complete cartilaginous scaffold with digits and joints present⁵⁷. Primary ossification centres form in the vertebrae and long bones between the 8th and 12th weeks and the bulk of skeletal mineralisation occurs in the 3rd trimester. At the 34th week of gestation, secondary ossification centres form in the femur which act as the growth plates, but the remaining epiphyses are cartilaginous until after birth. In early adulthood, bone growth stops and the hyaline cartilage is replaced by osseous tissue

and this becomes the epiphyseal line⁵⁵. In adults, bones undergo remodelling where old bone is resorbed on the same surface that osteoblasts lay new bone in replacement⁵⁵.

1.2.1 Osteoblast differentiation

Osteoblasts are cuboidal cells, derived from mesenchymal stem cells (MSCs), which have been shown to play a crucial role in bone formation. MSCs are pluripotent cells which have the ability to differentiate into adipocytes, chondrocytes, myoblasts and osteoblasts (**Figure 1.5**)⁵⁸. Osteogenesis is initiated by the transcription factors Runx2 and Osterix which result in the terminal osteoblast phenotype and calcification of the extracellular matrix⁵⁹. Osteoblasts deposit osteoid, which is uncalcified bone tissue that becomes bone tissue once mineralised. Osteoblasts synthesise several components of the bone matrix including alkaline phosphatase and Osteopontin in the early differentiation phase and Osteocalcin in the late differentiation phase^{59,60}. In osteoblastogenesis, MSCs differentiate into fibroblast colony forming units (CFU-F) before transcription factors induce their differentiation into pre-osteoblasts. Osteoblasts can undergo apoptosis, or terminally differentiate into lining cells or osteocytes in response to mechanical stimuli and growth factor receptor mediated signals^{61,62}. Osteocytes are the most abundant cell type embedded in bone matrix, they are able to sense mechanical stimuli via their dendritic processes and they secrete sclerostin (SOST) which negatively regulates osteoblast differentiation and plays a role in balancing bone formation and resorption⁶²⁻⁶⁴. There are a number of transcription factors and signalling pathways involved in osteoblast differentiation.

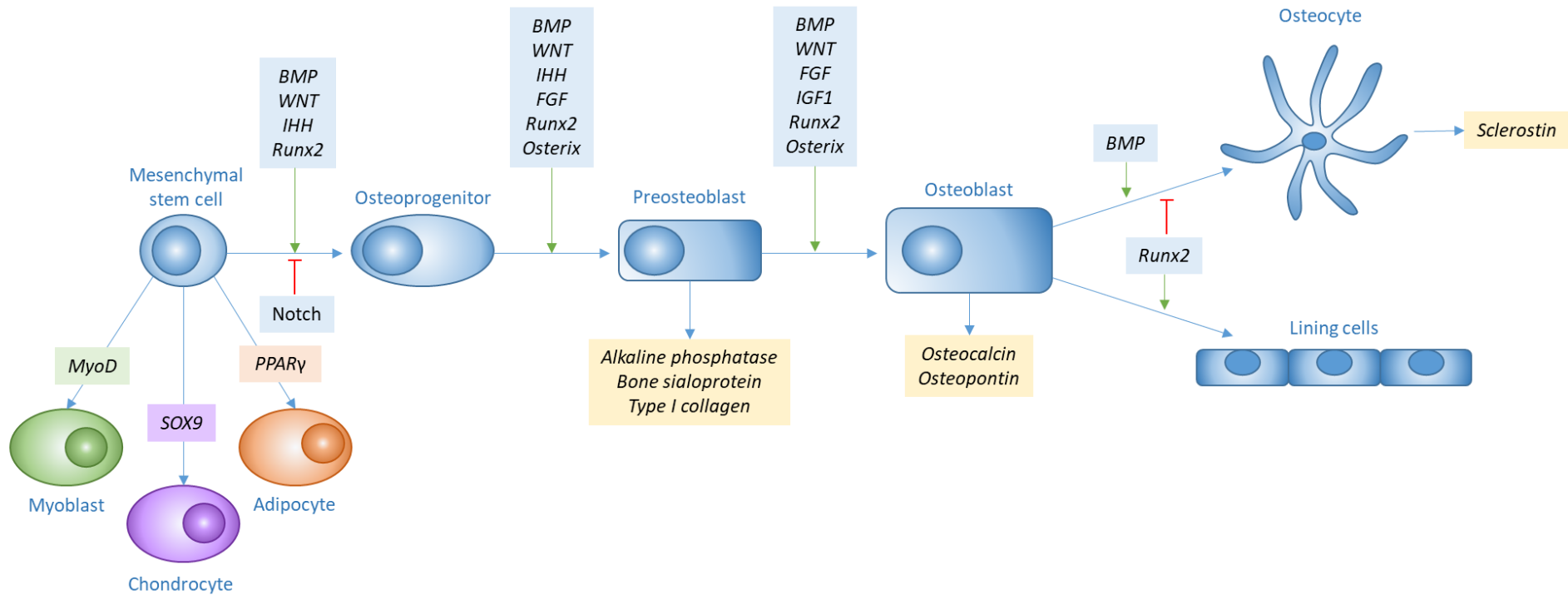


Figure 1.5 Overview of osteoblast differentiation⁶⁵.

MyoD = myogenic differentiation 1 protein, SOX9 = sex determining region Y-box 9, PPAR γ = peroxisome proliferator activated receptor gamma, BMP = bone morphogenetic protein, IHH = Indian hedgehog, Runx2 = runt related transcription factor 2, FGF = fibroblast growth factor, IGF1 = insulin growth factor 1.

1.2.1.1 Transcription factors

There are a number of transcription factors involved in osteoblast differentiation and in the formation of mineralised bone. These include Runx2, Osterix, SOX9 and β -catenin.

Runx2 is a member of the Runt containing transcription factor family and has been shown to have an important role in osteoblast differentiation and bone formation⁶⁶. Runx2 has been shown to regulate expression of osteoblastic marker genes such as Osteocalcin, Osteopontin and Type 1 collagen in osteoblasts⁶⁶⁻⁶⁹. Another role of Runx2 is to regulate Osterix, a zinc finger containing transcription factor, which plays a key role in regulating the differentiation of osteoblast progenitor cells to mature osteoblasts⁷⁰. Animal models have studied the effect of Runx2 on skeletal development and found that Runx2 plays an important role in both intramembranous and endochondral ossification^{66,71}. Studies in mice with a homozygous mutation in *Runx2* found that mice died after birth without breathing, had normal cartilage development however, their skeleton lacked ossification^{66,71}. Studies in humans with heterozygous mutations or deletions of *Runx2* develop cleidocranial dysplasia (CCD) which is an autosomal dominant disorder characterised by hypoplastic or absent clavicles, large fontanelles, dental anomalies and delayed skeletal development, which suggest a generalised defect in ossification^{72,73}.

Osterix is a transcription factor which is expressed in osteoblasts of all endochondral and membranous bones⁶⁷ and it has been shown to act downstream of Runx2⁷⁴. Studies have shown that Osterix activates the *Osteocalcin* and type I collagen genes^{67,74} and *Osterix* can be negatively regulated by nuclear factor activated T cells cytoplasmic 1 (Nfatc1) and nucleolar protein 66 (NO66). Nfatc1 is important for osteoclast differentiation and binds to DNA by forming a complex with Osterix. NO66 is a Jumonji C domain containing protein which inhibits *Osterix* mediated transcription through promoter histone modifications⁶⁰. Studies in *Osterix* null mice have found that there was no intramembranous or endochondral bone formation therefore, there was a lack of cortical or trabecular bone formation⁷⁴. In endochondral bone, mesenchymal cells, osteoclasts and blood vessels were shown to invade the mineralised cartilage matrix however, there was no bone matrix deposition and the mesenchymal cells could not differentiate into osteoblasts⁷⁴. The study found that there were normal expression levels of Runx2 in *Osterix* null mice, whereas in *Runx2* null mice, Osterix expression could not be detected, suggesting that Osterix acts downstream of Runx2⁷⁴. p53 plays an important role in regulating the cell cycle and it acts as a tumour suppressor and a study in *p53* null mice found that p53 negatively regulates Osterix and osteoblast differentiation⁷⁵. The *p53* null mice had high bone mass phenotype and Osterix expression was increased resulting in accelerated osteoblast differentiation⁷⁵.

β -catenin plays an important role in canonical WNT signalling⁷⁶ and it has been shown to have an essential role in osteoblast development. β -catenin plays a role in determining whether mesenchymal progenitors will differentiate into osteoblasts or chondrocytes^{76,77} and studies where *β -catenin* has been inactivated have found that there is ectopic formation of chondrocytes during both intramembranous and endochondral ossification⁷⁶. Furthermore, when *β -catenin* inactivated mesenchymal progenitors were cultured in osteoblastic conditions *in vitro*, there was chondrocyte differentiation⁷⁶. A study found that loss of mesenchymal *β -catenin* resulted in early osteoblast differentiation arrest and there were no mature osteoblasts present in endochondral and membranous bones⁷⁶.

SOX9 is a transcription factor of the SRY family of proteins which has an important role in chondrogenesis^{67,78}. SOX9 is expressed in all chondroprogenitors and chondrocytes except hypertrophic chondrocytes⁷⁹ and a study found that SOX9 prevents the conversion of proliferating chondrocytes into hypertrophic chondrocytes⁸⁰. Furthermore, SOX9 has been shown to be involved in the activation of chondrocyte specific marker genes such as type II collagen alpha 1 chain, (*Col2a1*), collagen type XI alpha 2 chain (*Col11a2*) and *Aggrecan*^{67,81-83} and to be involved in the regulation of β -catenin and Runx2 activity⁸⁴. Studies in mice have found that inactivation of *SOX9* in limb buds before mesenchymal condensation resulted in the absence of both cartilage and bone and that there was no Runx2 expression⁸⁰.

1.2.1.2 Signalling pathways

There are a number of signalling pathways involved in osteoblast differentiation including hedgehog signalling, notch signalling, WNT signalling, BMP signalling and fibroblast growth factor (FGF) signalling.

Hedgehog signalling is required for osteoblast differentiation during endochondral ossification⁸⁵. Indian hedgehog (IHH) is expressed by pre-hypertrophic and early hypertrophic chondrocytes within the endochondral cartilage primordium, the layer of dense irregular connective tissue which surrounds the cartilage of developing bone, and plays a role in coordinating the growth and differentiation of chondrocytes^{85,86}. IHH binds to the receptor Patched homologue 1 (*PTCH1*) and signals through the seven pass transmembrane protein smoothed (SMO) to regulate gene transcription⁷⁸ (**Figure 1.6**). This is done through both repression and activation of the Glioma-associated Oncogene (*GLI*) family of transcription factors⁸⁷. Studies in mice have shown that mice deficient in *IHH* lack osteoblasts within the endochondral skeleton although there is normal osteoblast formation in intramembranous skeleton^{78,86}. IHH has also been shown to signal to chondrocytes and adjacent perichondrial cells to promote osteoblast differentiation⁸⁶ and that absence of IHH signalling results in perichondrial progenitors failing to express Runx2⁸⁸.

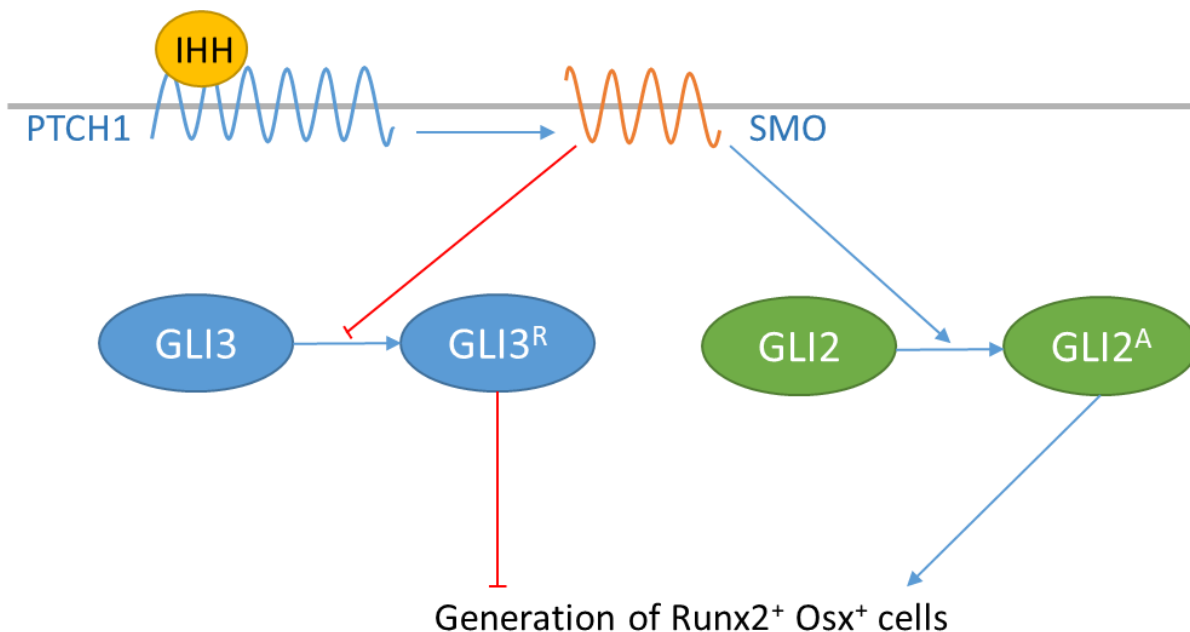


Figure 1.6 Overview of hedgehog signalling pathway.

Indian hedgehog (IHH) binds to the receptor Patched homologue 1 (PTCH1) which signals through smoothed (SMO) to regulate gene transcription. This results in the inhibition of the repressor GLI3 and transcription of the activator GLI2 transcription factors resulting in generation of mature osteoblasts⁷⁸.

Notch signalling is involved in inhibiting osteoblast differentiation and it has been shown to be involved in mediating communication between neighbouring cells through cell to cell contact⁷⁸. There are 4 Notch receptors (Notch 1-4) and the ligands are jagged 1 (JAG1), JAG2, Delta like canonical notch ligand 1 (DLL1), DLL3 and DLL4⁷⁸. Upon ligand binding, the receptor undergoes proteolytic cleavage by the γ -secretase complex which releases the Notch intracellular domain (NICD) from the plasma membrane⁸⁹ (**Figure 1.7**). The NICD translocates to the nucleus and activates transcription of target genes such as the *HES* (Hairy and Enhancer of Spring) and *HEY* (HES-related with YRPW motif) family of transcription factors which in turn control expression of other genes and inhibition of osteoblast differentiation⁹⁰. Studies in mice have found that Notch signalling suppresses osteoblast differentiation⁹¹.

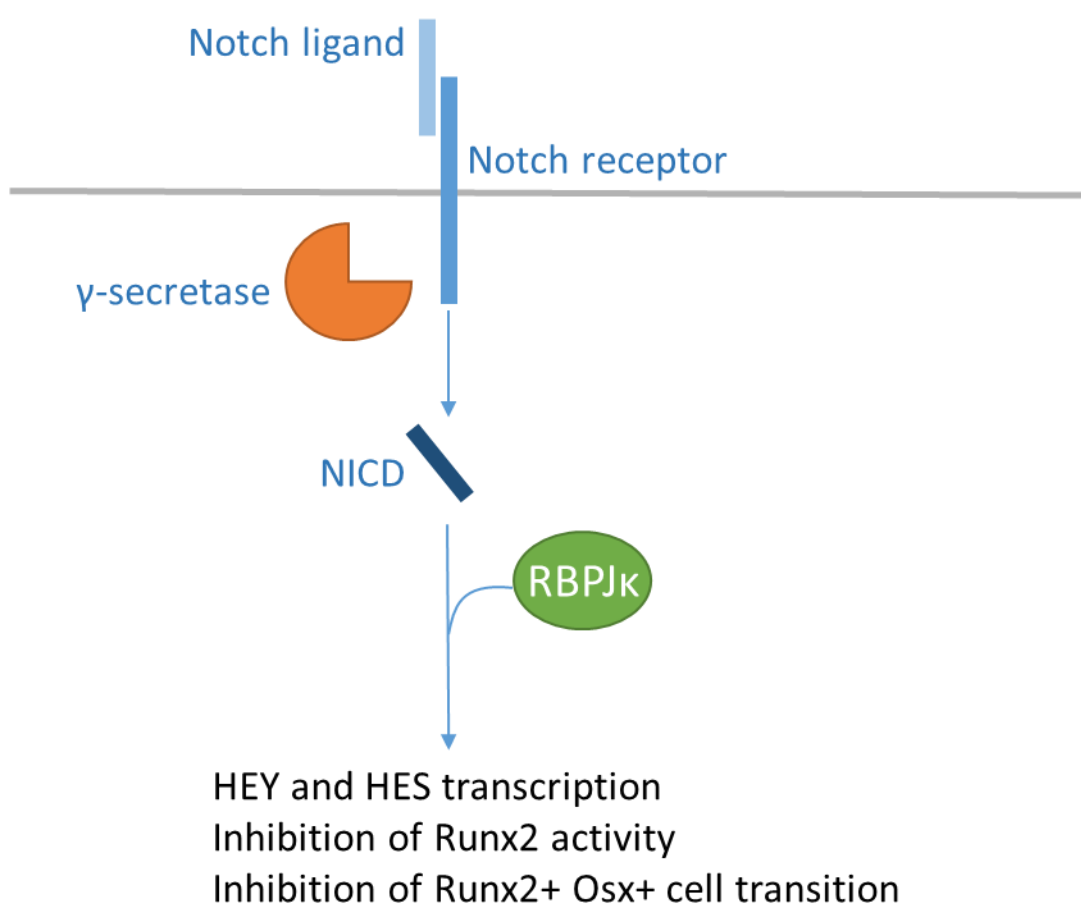


Figure 1.7 Overview of Notch signalling pathway.

The notch ligand binds to the receptor which undergoes proteolytic cleavage by γ -secretase releasing notch intracellular domain (NICD) from the plasma membrane where it translocates to the nucleus and activates transcription of HEY and HES transcription factors⁷⁸.

WNT signalling promotes osteoblast differentiation and there are three main pathways; the WNT- β -catenin pathway otherwise known as the canonical WNT pathway⁹², the non-canonical WNT-planar cell polarity pathway⁹³ and the WNT-calcium pathway⁹⁴ however, the exact mechanisms of the latter two remain to be determined. Canonical WNT signalling has been shown to repress commitment of MSCs to chondrogenic and adipogenic lineages and enhances commitment towards osteoblastic lineage⁹⁵. In the canonical pathway, WNT ligands bind to the dual receptor complex which is composed of frizzled and either LRP5 or LRP6⁹⁵ (**Figure 1.8**). This triggers phosphorylation of the LRP5/6 cytoplasmic tail allowing Axin to bind⁹². The recruitment of Axin inactivates the destruction complex which binds free β -catenin and which is important for the proteosomal degradation of β -catenin⁹². This triggers the inactivation of proteosomal degradation of β -catenin and results in accumulation in the cytoplasm followed by translocation into the nucleus and transcription of target genes⁹⁵. Mutations in the WNT co-receptor *LRP5* was found to alter bone mass and density, and a loss of function mutation was associated with low bone mass and osteoporosis pseudoglioma syndrome (OPPG) which is an autosomal recessive disorder and children have low bone mass and are prone to developing fractures and deformations⁹⁶. Whereas a gain of function mutation in *LRP5* was associated with high bone mass^{97,98}. A study found that Runx2 is a target of β -catenin and canonical WNT signalling⁹⁹.

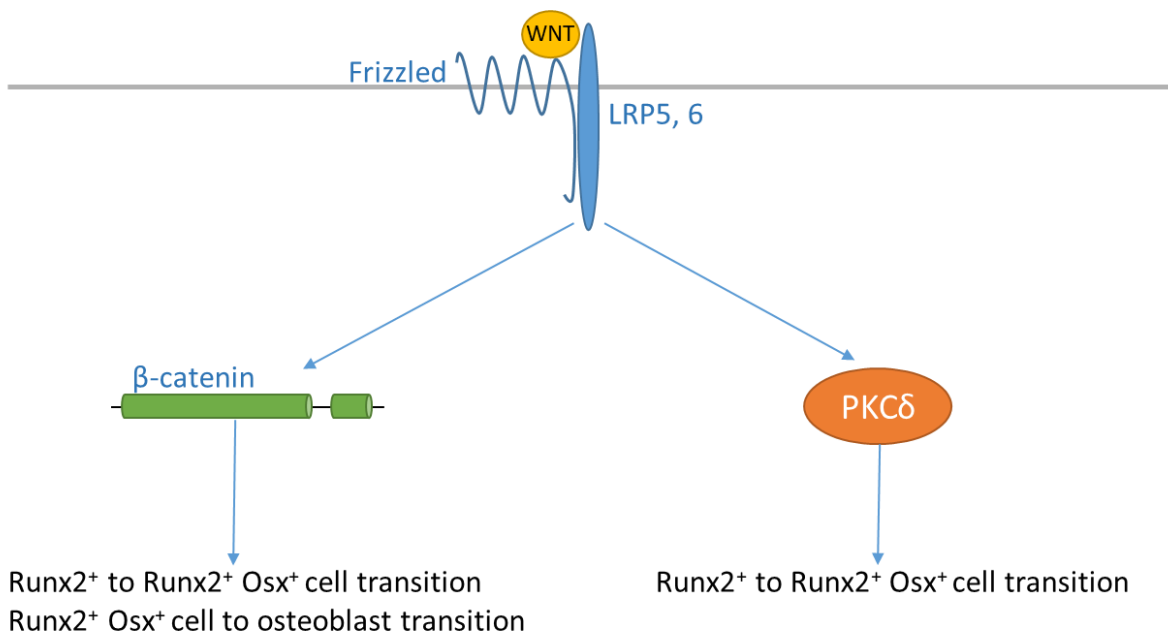


Figure 1.8 Overview of WNT signalling pathway.

WNT binds to the dual receptor composed of frizzled and either *LRP5* or *6*. This results in accumulation of β -catenin in the cytoplasm followed by translocation into the nucleus and transcription of target genes. WNT can also signal via *PKCδ* although the mechanism is unclear⁷⁸.

Osteoblast activity can be impaired through SOST which acts as a WNT signal antagonist and competitively binds to the LRP5/6 WNT co-receptor in osteoblasts, inhibiting WNT signalling^{74,100,101}. SOST is primarily secreted by osteocytes and the *SOST* promoter has been shown to be hypermethylated in osteoblasts and hypomethylated in osteoclasts¹⁰². Mutations in the *SOST* gene result in a lack of SOST expression which has been shown to be the cause of high bone mass in sclerosteosis and Van Buchem disease^{103,104}. Sclerosteosis is a skeletal disorder characterised by high bone mass due to increased osteoblast activity¹⁰¹ and loss of the *SOST* gene product, sclerostin. Van Buchem disease is an autosomal recessive skeletal dysplasia characterised by generalised bone overgrowth, especially in the skull and mandible¹⁰⁴. Sclerosteosis and Van Buchem are both very similar disorders and can be distinguished by the differences in hand malformations¹⁰⁴. In the non-canonical WNT pathway, WNT activates the G protein linked phosphatidylinositol signalling and protein kinase C delta (PKC δ)¹⁰⁵. *In vivo* studies have shown that WNT7b stimulates osteoblast differentiation through the PKC δ pathway¹⁰⁵.

The BMP family members belong to the transforming growth factor β superfamily and are expressed throughout limb development and have been shown to promote cartilage formation^{106,107}. The BMP pathway regulates mesenchymal cell differentiation during skeletal development, bone formation and bone homeostasis and there is also crosstalk between the BMP signalling pathway and other signalling pathways including WNT, Hedgehog, Notch, parathyroid hormone related protein (PTHrP) and FGF¹⁰⁸. There are two main pathways in BMP signalling; the SMAD dependent pathway and the SMAD independent pathway. In the SMAD dependent pathway, BMP2 or 4 bind to BMP type I and II receptors which are serine/threonine kinase receptors⁶⁶ (**Figure 1.9**). Ligand binding results in receptor phosphorylation followed by phosphorylation of SMAD1, 5 or 8, which can form a complex with their partner SMAD4. The complex translocates into the nucleus and regulates transcription of target genes⁶⁶ through the recruitment of transcription factors such as Runx2 and Osterix which play a role in osteoblast differentiation. In the non-SMAD dependent pathway, BMPs activate the p38 mitogen-activated protein kinase (MAPK) pathway¹⁰⁹ resulting in the phosphorylation of Runx2 and Osterix to promote their transcriptional activity¹⁰⁸. A study in mice found that loss of both *BMP2* and *BMP4* resulted in a severe impairment of osteogenesis shown by severely deformed limbs. *In vivo* studies have shown that BMPs can induce ectopic bone formation when implanted into soft tissue^{110,111}. A study found that BMP2 plays an important role in fracture repair and that mice lacking the ability to produce BMP2 do not resolve their fractures with time and that the earliest steps of fracture healing are blocked¹¹². SMAD4 plays an important role in maintaining the normal development of chondrocytes in the growth plate and mice with a mutant *SMAD4* gene in differentiated osteoblasts had lower bone mass up to 6 months

of age¹¹³. Proliferation and function of the mutant osteoblasts were significantly decreased and mice had reduced BMD, bone volume, bone formation rate and osteoblast numbers¹¹³.

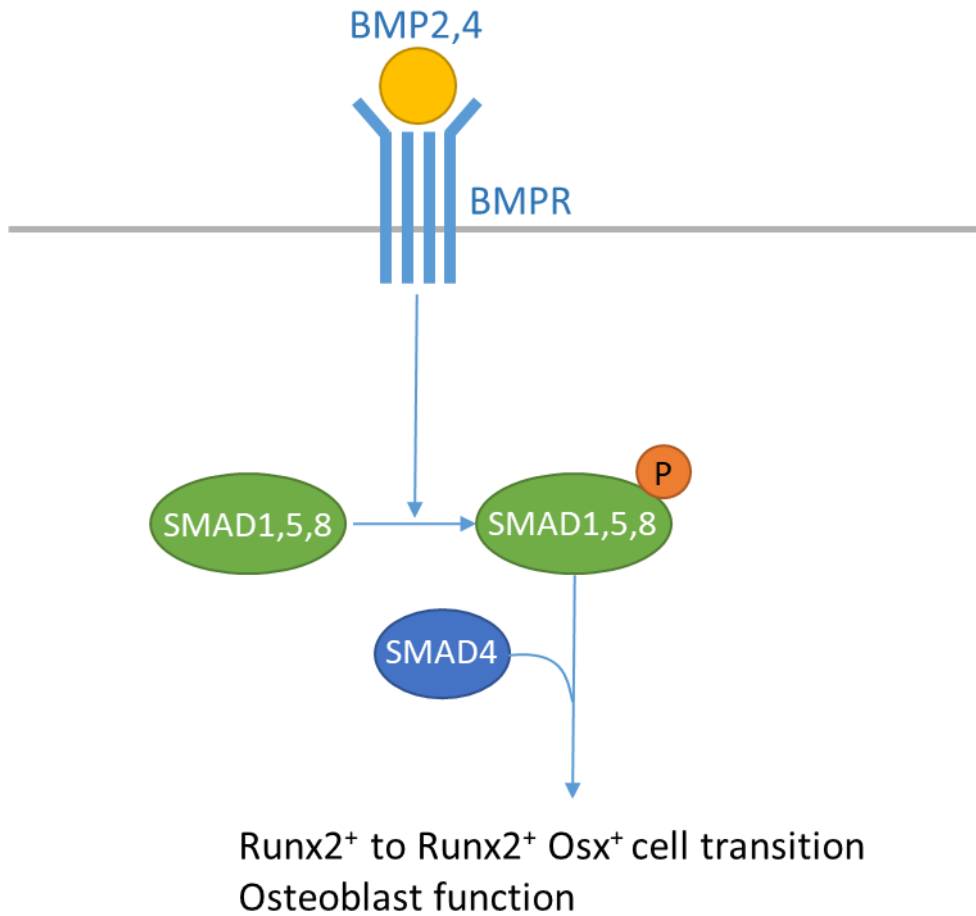


Figure 1.9 Overview of BMP signalling pathway.

BMP2 or 4 bind to the BMP receptor which results in phosphorylation of SMAD1, SMAD5 or SMAD8 which forms a complex with SMAD4 and regulates transcription of target genes⁷⁸.

There are a number of intracellular and extracellular antagonists which regulate BMP activity¹⁰⁹. Noggin is a glycoprotein which binds directly to BMPs and prevents them from interacting with their receptors^{109,114}. A study found that the use of noggin prevented mesenchymal condensation and inhibited cartilage formation^{106,114}. Noggin prevented mesenchymal cells from aggregating into prechondrogenic condensations and these cells persist in an undifferentiated state and chondroprogenitors were blocked from differentiating into chondrocytes¹⁰⁶.

FGFs are a large family of proteins containing 22 FGF polypeptides and 4 FGF receptors which have diverse roles in osteoblast lineage cells¹¹⁵. FGF signalling regulates pre-osteoblast proliferation and osteoblast differentiation, as well as the function of mature osteoblasts. However, the precise stages at which FGFs regulate proliferation and differentiation, and the intracellular signalling

cascades responsible for each function, are unknown. FGFs bind to cell surface Tyrosine kinase FGF receptors⁷⁸ resulting in the phosphorylation of a range of signalling proteins and the activation of multiple signalling pathways including MAPK, phosphoinositide 3-kinase (PI3K), signal transducer and activator of transcription 1 (STAT1) and PKC⁷⁸ (**Figure 1.10**). FGFs have been shown to positively regulate *Runx2* which plays an important role in osteoblast differentiation⁶⁶.

Genetic studies in mice have shown the importance of FGF signalling in osteoblast lineage cells, both during the *in utero* environment and postnatally. FGF2 is expressed in osteoblasts in bone and in growth plate chondrocytes¹¹⁵ and it is an important modulator of cartilage and bone growth and differentiation¹¹⁶. A study in mice lacking FGF2 found that there was a reduction in total bone mass in adulthood¹¹⁶. FGF18 is expressed in the perichondrium and periosteum of developing long bones, in developing joints and in osteogenic cells of the calvarium¹¹⁵ and it has been shown to regulate chondrocyte proliferation and differentiation by signalling through FGF receptor 3 (FGFR3)¹⁰⁶. A study found that FGF18 regulates cell proliferation and differentiation positively in osteogenesis and negatively in chondrogenesis¹⁰⁷. A study in *FGF18* null embryos found that there were defects in the formation of mature osteoblasts, although *Runx2* expression was normal^{117,118}. A study in mice lacking *FGFR3* showed that there was an increase in osteoblast number but a decrease in osteoid mineralisation¹¹⁵. Studies have shown that there is differential expression of the FGF receptors in the developing and mature skeleton¹¹⁹. FGFR1 and 2 are expressed in the developing growth plate in condensing mesenchymal cells which give rise to cartilage, and in the perichondrium and periosteum which are tissues that give rise to osteoblasts and cortical bone¹¹⁹. FGFR3 is expressed in proliferating chondrocytes and regulates cell growth and differentiation and it is expressed in differentiated osteoblasts where it regulates bone density and cortical thickness¹¹⁹.

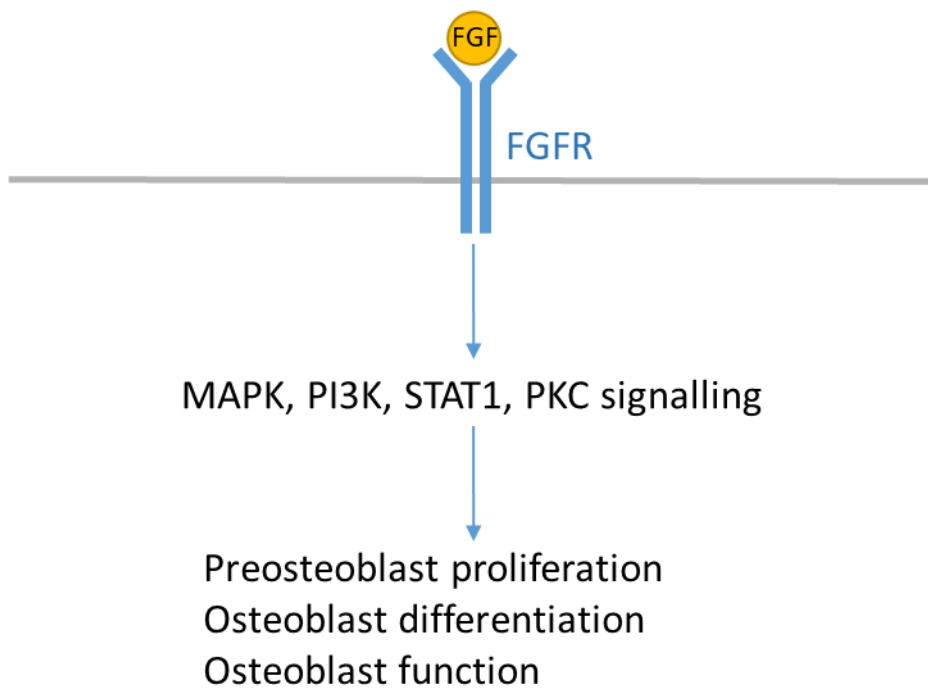


Figure 1.10 Overview of FGF signalling pathway.

FGF binds to the FGF receptor and signals via the MAPK, PI3K, STAT1 and PKC signalling pathways⁷⁸.

1.2.1.3 Systemic regulation

Bone formation is also regulated systemically and the three main systemic regulators of osteoblast differentiation are parathyroid hormone (PTH), insulin like growth factor 1 (IGF1) and $1,25(\text{OH})_2\text{D}_3$.

PTH plays an important role in maintaining whole body calcium homeostasis⁷⁸ and it has been shown to play a role in regulating bone formation and bone resorption. Studies have shown that continuous exposure to high concentrations of PTH, such as due to chronic renal disease and primary hyperparathyroidism¹²⁰, leads to progressive bone loss¹²¹. Whereas intermittently administered PTH increases bone mass, especially trabecular bone¹²¹. A study has shown that intermittent PTH administration had an anti-apoptotic effect on osteoblasts which resulted in increased osteoblast number, bone formation rate and bone mass in mice¹²². PTH and PTHrP bind to the PTH/PTHrP receptor which is a G-protein coupled receptor. This results in the activation of the cyclic adenosine monophosphate (cAMP) dependent protein kinase A (PKA) pathway and the Phospholipase C beta (PLC β)/PKC pathway¹²³. Low serum calcium levels trigger the release of PTH from the parathyroid gland, which signals to the bone, kidney and intestine to increase calcium levels⁷⁸. In bones, PTH stimulates bone resorption by osteoclasts, thereby releasing calcium from the bone minerals⁷⁸. The main target organs for PTH are the kidney where they increase proximal tubular resorption of calcium, phosphate excretion and $1,25(\text{OH})_2\text{D}_3$ formation¹²⁰. PTH can also act indirectly, as the increase in $1,25(\text{OH})_2\text{D}_3$ formation in the kidney increases intestinal calcium

absorption¹²⁰. PTH has been shown to regulate alkaline phosphatase, type I collagen, collagenase, Osteopontin, bone sialoprotein and 25(OH)D₃¹²³.

IGF1 is the most abundant growth factor in the bone matrix and it plays a role in maintaining bone mass in adulthood¹²⁴. The release of IGF1 in bone remodelling stimulates osteoblastic differentiation of recruited MSCs through the activation of mammalian target of rapamycin (mTOR) which maintains adequate bone microarchitecture and mass¹²⁴. *In vitro* studies have shown that IGF1 stimulates osteoblast proliferation, accelerates their differentiation and enhances bone matrix production and IGF1 has also been shown to play a role in bone resorption¹²⁵. IGF1 has been shown to play a role in postnatal growth through mediating growth hormone function¹²⁵. *In vivo* and *In vitro* studies have shown that IGF1 stimulates the proliferation of chondrocytes in the growth plate and has an important role in longitudinal bone growth and in the formation of trabecular bone¹²⁵. Signalling through IGF1 receptor (IGF1R) has been shown to promote cell proliferation and mediate anti apoptotic actions¹²⁵ and studies in *IGF1R* knockout (KO) mice in preosteoblastic cells showed lower bone mass and mineral deposition rates¹²⁴.

1,25(OH)₂D₃ is a fat soluble vitamin that plays a vital role in mineral homeostasis, calcium metabolism, maintaining skeletal integrity and tissue differentiation^{126,127}. 1,25(OH)₂D₃ binds to the vitamin D receptor (VDR) which dimerises with retinoid X receptor alpha (RXRA) and binds to vitamin D response elements (VDREs) in target genes. Studies have shown that there are VDREs in *Osteocalcin* and *Osteopontin* which play a role in mineralisation of the bone matrix¹²⁸. Furthermore, 1,25(OH)₂D₃ has been shown to downregulate PTH and PTHrP by binding to negative VDREs (nVDREs) in these genes¹²⁸. *In vitro* treatment with 1,25(OH)₂D₃ has been shown to inhibit osteoblast proliferation but induces osteoblast differentiation when given at the differentiation stage and protects osteoblastic cells from undergoing apoptosis¹²⁹. 1,25(OH)₂D₃ has also been shown to promote osteoclast differentiation and alters chondrocyte development¹²⁹. Studies have shown that 1,25(OH)₂D₃ affects the expression of several genes in osteoblasts, osteoclasts and chondrocytes which result in regulating cellular growth and differentiation of these cells¹²⁹. Studies in rat calvaria osteoblast cultures have shown that 1,25(OH)₂D₃ treatment of mature osteoblasts resulted in upregulation of osteoblast associated genes such as *Osteopontin* and *Osteocalcin*¹³⁰. In rodent osteoblastic cells, 1,25(OH)₂D₃ treatment downregulated Runx2 expression which is essential for osteoblast differentiation¹³¹. However, there were differing results in primary human osteoblasts. After treatment for 1 hour there was downregulation of Runx2 expression and after 48 hours there was upregulation of Runx2 expression¹³². 1,25(OH)₂D₃ has been shown to regulate expression of noncollagenous extracellular matrix proteins. *In vitro* studies in both humans and rats have shown that 1,25(OH)₂D₃ stimulates Osteocalcin expression^{133,134} whereas in mice, 1,25(OH)₂D₃ inhibits Osteocalcin expression¹³⁵. *In vitro* studies have shown that physiological concentrations of

1,25(OH)₂D₃ stimulate chondrocyte proliferation whereas high concentrations inhibit^{136,137}. 1,25(OH)₂D₃ was also shown to affect alkaline phosphatase expression, collagen production and matrix calcification which are all characteristics of chondrocyte differentiation^{138,139}. *In vitro* studies in MC3T3-E1 cells found that 1,25(OH)₂D₃ stimulates matrix mineralisation¹³⁰. In humans, a mutation in the 1 α -hydroxylase gene results in vitamin D dependency rickets type I, and patients have severe rickets despite normal dietary intakes of vitamin D and sufficient exposure to UV light¹²⁷. Vitamin D plays an important role in calcium metabolism, bone growth and cellular differentiation¹²⁷. There is currently debate as to whether vitamin D deficiency alters the rates of bone formation and resorption in both animals and humans¹⁴⁰. A study in vitamin D deficient rats found that the total osteoblastic matrix formation rate was 20 % less and the total osteoclastic bone resorption rate was 80 % more than in control rats¹⁴⁰.

1.2.1.3.1 Vitamin D pathway

Vitamin D is a fat soluble vitamin that plays a vital role in mineral homeostasis, calcium metabolism, maintaining skeletal integrity and tissue differentiation^{126,127}. It has been shown that in more severe cases, vitamin D deficiency can result in rickets in children and osteomalacia in adults¹⁴¹. There are two main sources of vitamin D; cholecalciferol derived from 7-dehydrocholesterol in skin which is broken down by UV radiation, or vitamin D from fortified dairy products and fish oils in the diet¹⁴²⁻¹⁴⁴. There are a number of factors that can influence vitamin D status, such as: dietary intake, climate, sun cream use¹⁴⁵, clothing¹⁴⁶, season and latitude¹⁴⁷.

Previtamin D₃ can be photosynthesised in skin upon exposure to solar ultraviolet radiation before undergoing isomerisation in a temperature dependent manner (**Figure 1.11**). This process can take three days to be completed before being transported into the body for general circulation¹⁴⁸. Cytochrome P450 (CYP) mixed function oxidase enzymes are involved in the metabolism of vitamin D₃¹⁴⁹. Firstly, vitamin D is transported to the liver by the vitamin D binding protein (DBP) where it is 25-hydroxylated at Carbon-25 by the enzyme CYP2R1 to the inactive form of vitamin D, 25-hydroxyvitamin D₃ (25(OH)D₃)¹⁴². Once the inactive form is bound to DBP, it is transported to the kidneys and filtered through the glomerulus, where megalin is involved in the endocytic internalisation of 25(OH)D₃ into the proximal renal tubule¹⁵⁰. Conversion to the active form of vitamin D, 1,25-dihydroxyvitamin D₃ (1,25(OH)₂D₃), is catalysed by the 1, α -hydroxylase CYP27B1 which hydroxylates Carbon 1 on the A ring of 25(OH)D₃^{127,141}. Both the inactive and active vitamin D forms can be 24-hydroxylated by CYP24A1 to create 24,25(OH)D₃ and 1,24,25(OH)₂D₃ respectively as part of a negative feedback loop to prevent the accumulation of toxic levels of vitamin D in the body^{126,142,143}.

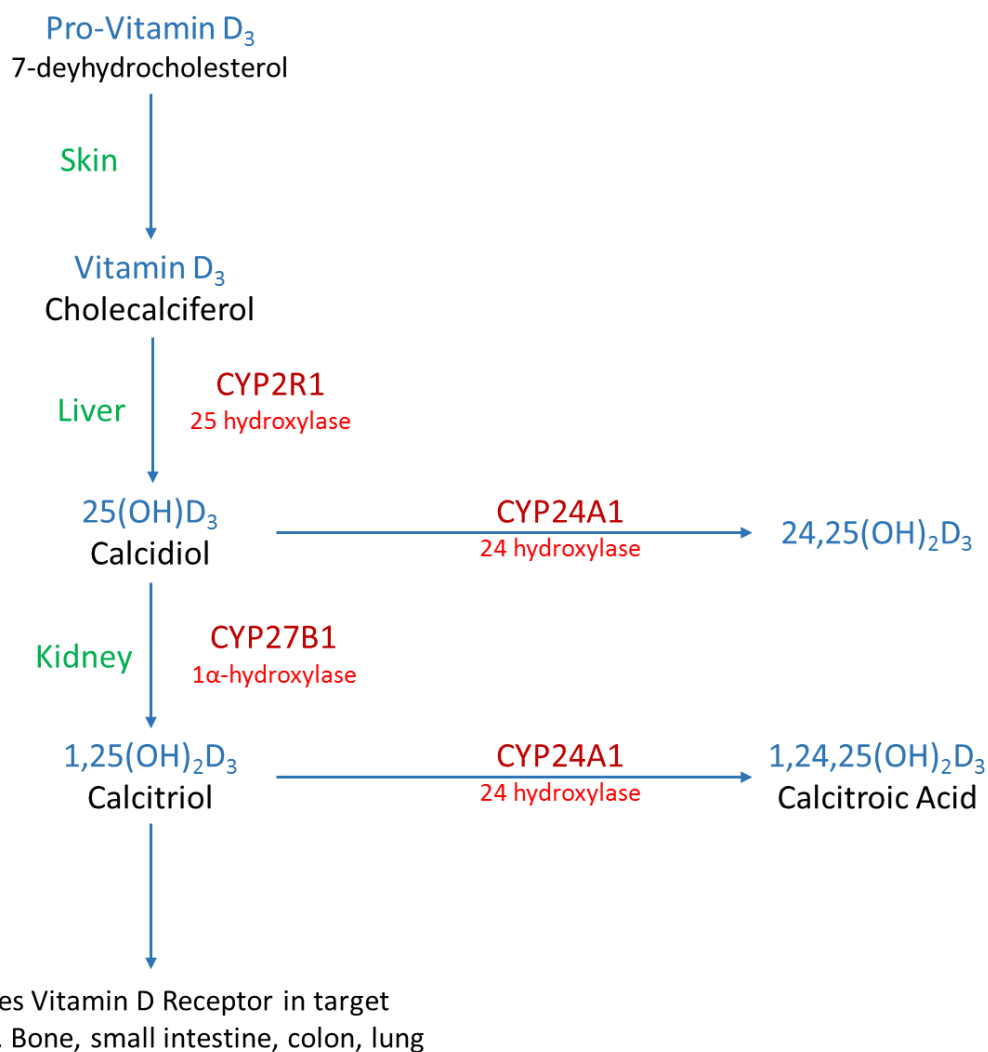


Figure 1.11 Overview of Vitamin D metabolism pathway.

Pro-vitamin D₃ is broken down in the skin by UV to Vitamin D₃. This is transported to the liver where CYP2R1 hydroxylates it to 25(OH)D₃, the inactive form of vitamin D. CYP27B1 hydroxylates 25(OH)D₃ to 1,25(OH)₂D₃, the active form of vitamin D, and it exerts its effects on a range of organs. Both 25(OH)D₃ and 1,25(OH)₂D₃ can be metabolised by CYP24A1¹⁴².

The active form of vitamin D acts as the ligand for the VDR, which forms a heterodimer with RXRA, before binding to VDREs in the genome and recruiting coregulatory complexes¹⁵¹ (**Figure 1.12**). The co-regulators recruited often have enzymatic properties including histone acetyltransferases (HATs), deacetylases (HDACs), methyl transferases (HMTs) and demethylases which can then either activate or suppress transcription. The VDR:RXRA complex can bind to VDREs in target genes such as *CYP24A1* and *Osteocalcin* and results in gene transcription or it can bind to nVDREs such as in *CYP27B1* and results in gene repression.

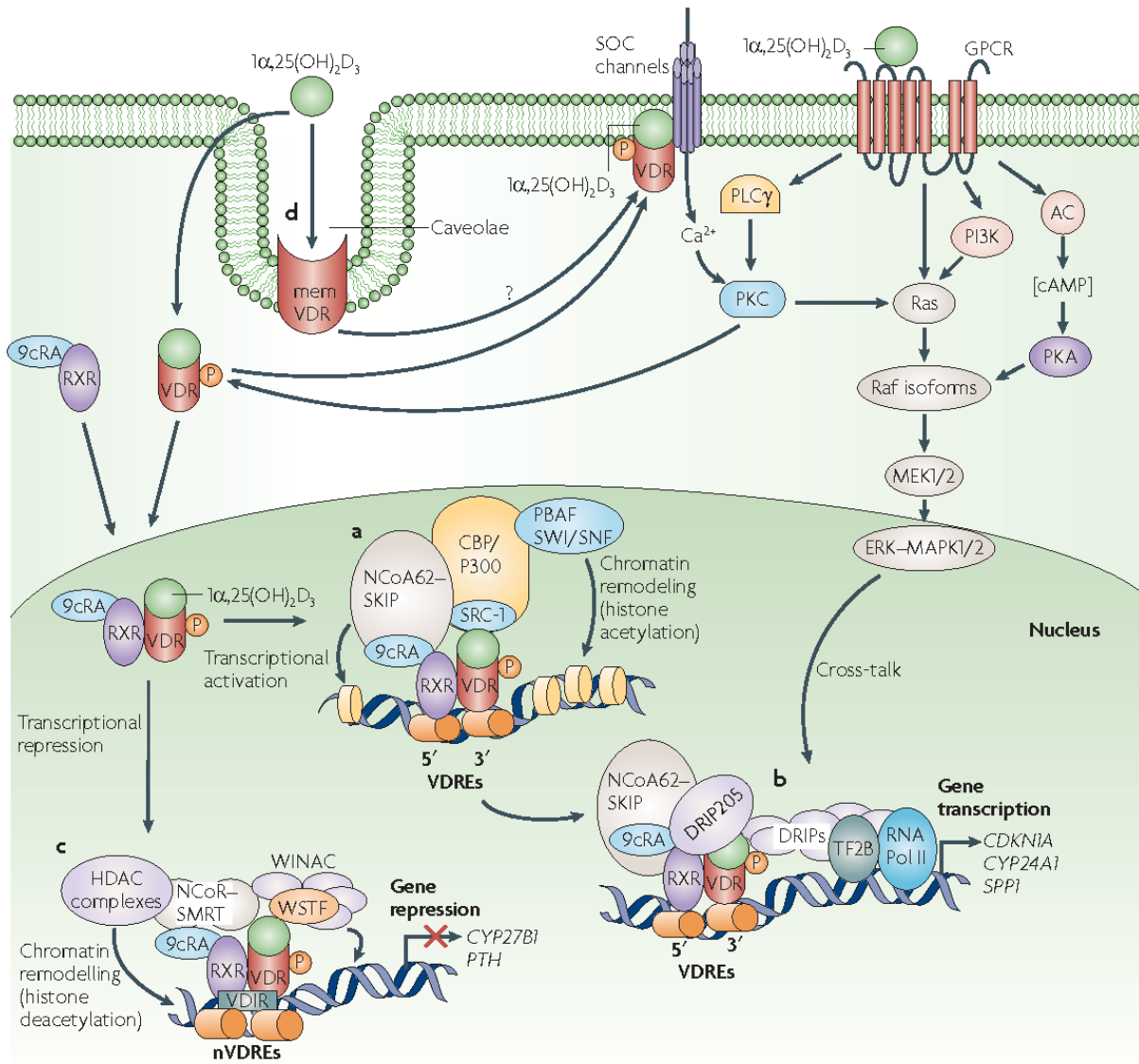


Figure 1.12 Overview of the actions of VDR and RXR¹⁵².

a) Histone acetylation, chromatin remodelling and transcriptional activation involves coactivators and histone acetyltransferases. b) Gene transcription involves binding of the vitamin D receptor-interacting protein 205 (DRIP205) to the VDR:RXR complex, binding of a mediator complex and bridging to transcription factor 2B (TF2B) and RNA polymerase II (RNA Pol II). This initiates transcription of genes such as *CDKN1A*, *CYP24A1* and *SPP1* (*Osteopontin*). c) Transcriptional repression involves the VDR:RXR heterodimer associating with VDR-interacting repressor (VDIR) bound to negative VDREs (nVDREs), dissociation of the HAT co-activator and recruitment of histone deacetylases and corepressors. This leads to gene repression of *CYP27B1* and *PTH*. d) Non genomic actions of 1,25(OH)₂D₃ are thought to include binding to cytosolic and membrane VDRs and are thought to activate the mitogen-activated protein kinase (MAPK) pathway. There is also thought to be cross talk with genomic VDR gene transcription. 9cRA – 9 cis retinoic acid, RXR – retinoid X receptor, VDR – vitamin D receptor, NCoA62-SKIP - nuclear coactivator-62 kDa-Ski-interacting protein, CBP-P300 - CREB binding protein p300, SRC-1 - steroid receptor coactivator-1, PBAF-SWI/SNF - polybromo- and SWI-2-related gene 1 associated factor, CDKN1A – cyclin dependent kinase inhibitor 1A, NCoR-SMRT – nuclear co-repressor complex, WINAC - ATP-dependent chromatin-remodelling complex, WSTF - Williams syndrome transcription factor, PLCγ – phospholipase C γ, PKC – protein kinase C, PI3K – phosphatidylinositol-3 kinase, AC- adenylate cyclase, PKA - protein kinase A.

The enzymes involved in vitamin D metabolism are tightly regulated by PTH, FGF23, dietary calcium and phosphate and by $1,25(\text{OH})_2\text{D}_3$ itself¹⁵³⁻¹⁵⁵ (**Figure 1.13**). PTH works closely with $1,25(\text{OH})_2\text{D}_3$ to tightly regulate serum calcium and phosphate levels in order to maintain skeletal mineralisation^{126,156}.

In the kidneys, CYP27B1 is involved in the $1,\alpha$ -hydroxylation of $25(\text{OH})\text{D}_3$ to $1,25(\text{OH})_2\text{D}_3$ ¹⁴¹. Production of CYP27B1 is stimulated by PTH and it is inhibited by FGF23 and $1,25(\text{OH})_2\text{D}_3$. An increase in calcium and phosphate ions act to suppress CYP27B1 directly but they can also suppress production indirectly. An increase in calcium ions can suppress PTH whereas an increase in phosphate ions can stimulate FGF23 production. CYP27B1 activity can be limited by $1,25(\text{OH})_2\text{D}_3$, which inhibits PTH and stimulates FGF23 production.

The 24-hydroxylase CYP24A1 catalyses both $25(\text{OH})\text{D}_3$ to $24,25(\text{OH})\text{D}_3$ and $1,25(\text{OH})_2\text{D}_3$ to $1,24,25(\text{OH})_2\text{D}_3$. CYP24A1 production is inhibited by PTH¹⁵⁷ and stimulated by FGF23¹⁵⁸ and the ions. $1,25(\text{OH})_2\text{D}_3$ strongly induces CYP24A1 production¹⁵⁷ which reduces the pool of available inactive vitamin D reducing the production of active vitamin D, and also stimulates the breakdown of active vitamin D into calcitric acid ($1,24,25(\text{OH})_2\text{D}_3$) controlling circulating levels of active vitamin D within the body¹⁴³.

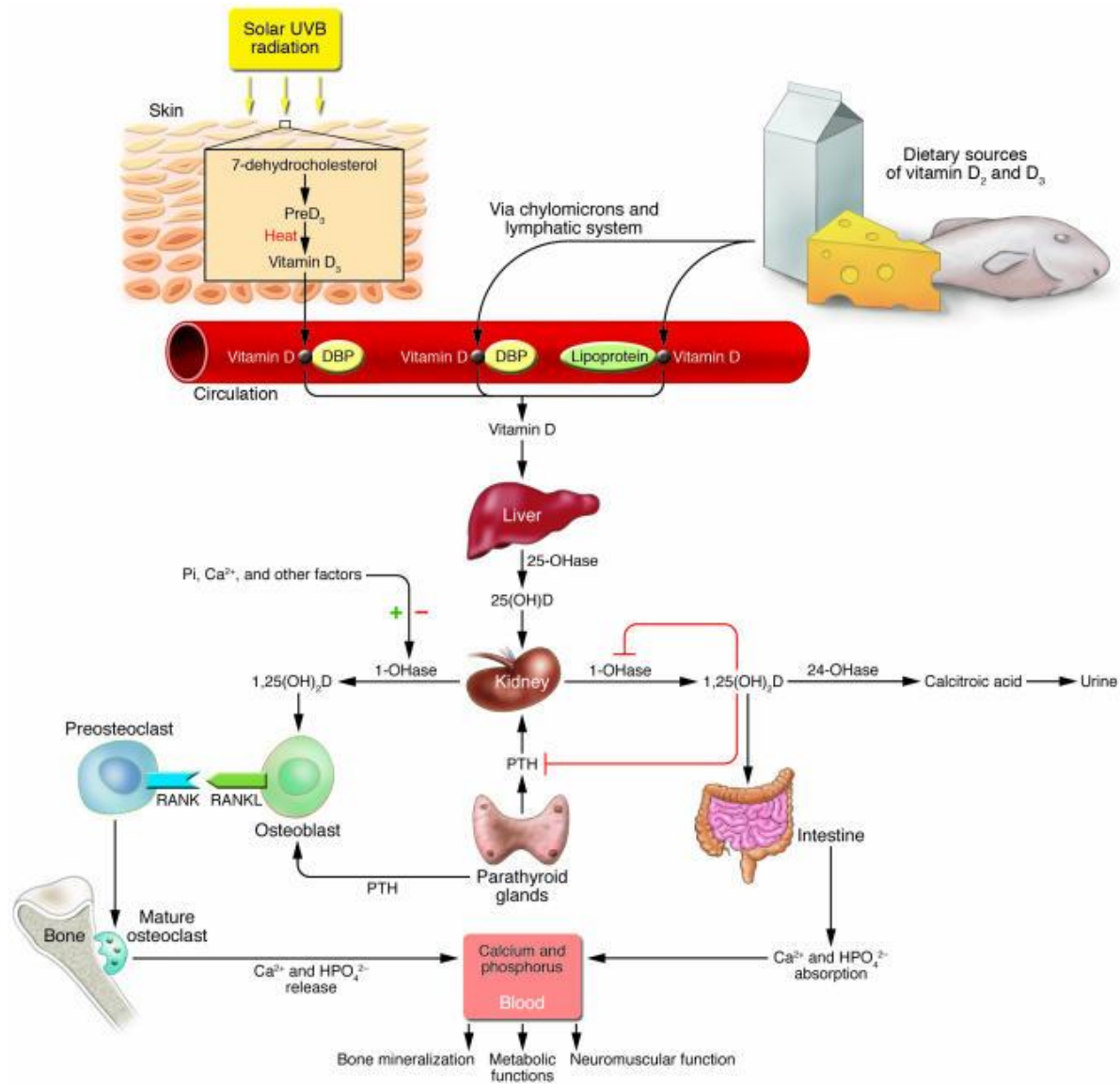


Figure 1.13 Metabolism of vitamin D and the biologic effects of 1,25(OH)₂D₃ on calcium, phosphorus, and bone metabolism¹⁵⁹..

1.2.2 Osteoclasts

Osteoclasts are large multinucleated cells from the hematopoietic lineage and their main role is to resorb and remodel bone^{65,160}. Macrophage colony stimulating factor (M-CSF) stimulates mononuclear precursor cells to initiate osteoclast differentiation⁶⁵. M-CSF is expressed by osteoblasts and stromal cells and it is required for both the proliferative and differentiation phase of osteoclast development¹⁶¹. This upregulates the expression of RANK (receptor activation of NF-κB (nuclear factor kappa light chain enhancer of activated B cells)) which is a transmembrane receptor expressed on the surface of preosteoclasts and mature osteoclasts¹⁶¹. The ligand for RANK (RANKL) is expressed in osteoblasts and stromal cells⁶⁵ and it is critical for osteoclastogenesis and bone resorption¹⁶¹. There are a number of different cell types which secrete RANKL to stimulate osteoclast differentiation from monocytes, including: osteoblasts, osteocytes, stromal cells, B and

T cells, synovial fibroblasts, hypertrophic chondrocytes and other osteoclasts^{160,162}. RANKL binds to RANK inducing trimerisation of the receptor leading to the recruitment of the adaptor protein tumour necrosis associated factor 6 (TRAF6). The recruitment of TRAF6 to the receptor complexes activates a number of intracellular signalling cascades including MAPK pathways such as Jun N terminal kinase (JNK), p38 and NF- κ B¹⁶³. There is co-stimulation with immunoreceptor tyrosine-based activation motif (ITAM) which contains the adapters DNAX-activation protein 12 (DAP12) and Fc receptor gamma chain (FcR γ)⁶⁵. Together these result in the activation of the transcription factors NF- κ B, activator protein 1 (AP1) and NFATc1⁶⁵ which are able to regulate expression of osteoclast genes such as dendrocyte expressed seven transmembrane protein (*DC-STAMP*), Tartrate-resistant acid phosphatase (*TRAcP*), *cathepsin K*, matrix metalloproteinase 9 (*MMP9*) and *β 3 integrin*⁶⁵.

Mature osteoblasts secrete the decoy receptor for RANKL, Osteoprotegerin, which is part of the tumour necrosis factor receptor (TNFR) superfamily and it is mainly involved in the inhibition of osteoclast activation and development by competitively binding to RANKL and inhibiting binding to RANK, inducing osteoclastogenesis^{62,162}. Osteoprotegerin has been shown to block osteoclast formation *in vitro* and bone resorption *in vivo* by binding to RANKL and preventing it from binding to RANK¹⁶¹. Together, RANK, RANKL and Osteoprotegerin comprise the RANKL-RANK-Osteoprotegerin system that is important in maintaining bone homeostasis^{164,165}.

1.2.3 Bone remodelling

Bone remodelling involves the coupling of bone formation and bone resorption and it is tightly controlled by steroid hormones, vitamin D, PTH, cytokines and growth factors. Osteoblasts and osteoclasts work together in bone remodelling units and these can occur on the surface of trabecular bone as irregular 'Howship lacunae' or in cortical bone as uniform cylindrical Haversian systems²³.

In bone remodelling there is resorption of bone on a particular surface by osteoclasts, followed by the formation of bone by osteoblasts¹⁶⁶ (**Figure 1.14**). During the resorption phase, activated osteoclasts resorb a discrete area of mineralised bone matrix, releasing growth factors from the matrix which activate osteoprogenitor cells which mature into osteoblasts and replace the resorbed bone¹⁶⁶. First, osteoclast progenitor cells are recruited to the bone matrix and proliferate and differentiate into osteoclasts¹⁶⁶. The lining osteoblasts remove the unmineralised osteoid layer on the bone surface using proteolytic enzymes such as MMPs, collagenase and gelatinase¹⁶⁶. This allows the osteoclasts to access the underlying mineralised bone¹⁶⁶. Osteoclasts are activated at the surface of the bone and resorb the bone by producing hydrogen ions and proteolytic enzymes

to degrade the mineralised matrix¹⁶⁶ after which the osteoclasts undergo apoptosis. Following bone resorption there is a reversal phase which lasts around 9 days¹⁶⁶. Osteoclasts disappear and osteoblast precursor cells migrate into the resorption lacuna where they proliferate and differentiate into osteoblasts¹⁶⁶. During the formation phase, osteoblasts deposit new bone matrix called osteoid which is unmineralised. Bone formation involves proliferation of primitive mesenchymal cells, differentiation into osteoblast precursor cells, maturation of osteoblasts, formation of matrix and then mineralisation¹⁶⁶. During the resting phase, osteoblasts at the bottom of the resorption cavity form the osteoid which begins to mineralise after 13 days and osteoblasts which are embedded in the osteoid mature into terminally differentiated osteocytes¹⁶⁶. Osteoblasts continue to form and mineralise osteoid with hydroxyapatite until the cavity is filled^{60,166} which can take 124-168 days in normal individuals¹⁶⁶. Any osteoblast cells which are lying on the surface of the newly formed bone are quiescent lining cells until they become activated¹⁶⁶. However, an imbalance, due to either too much bone resorption or inadequate bone formation, can result in decreased bone mass and strength leading to conditions such as osteoporosis⁵.

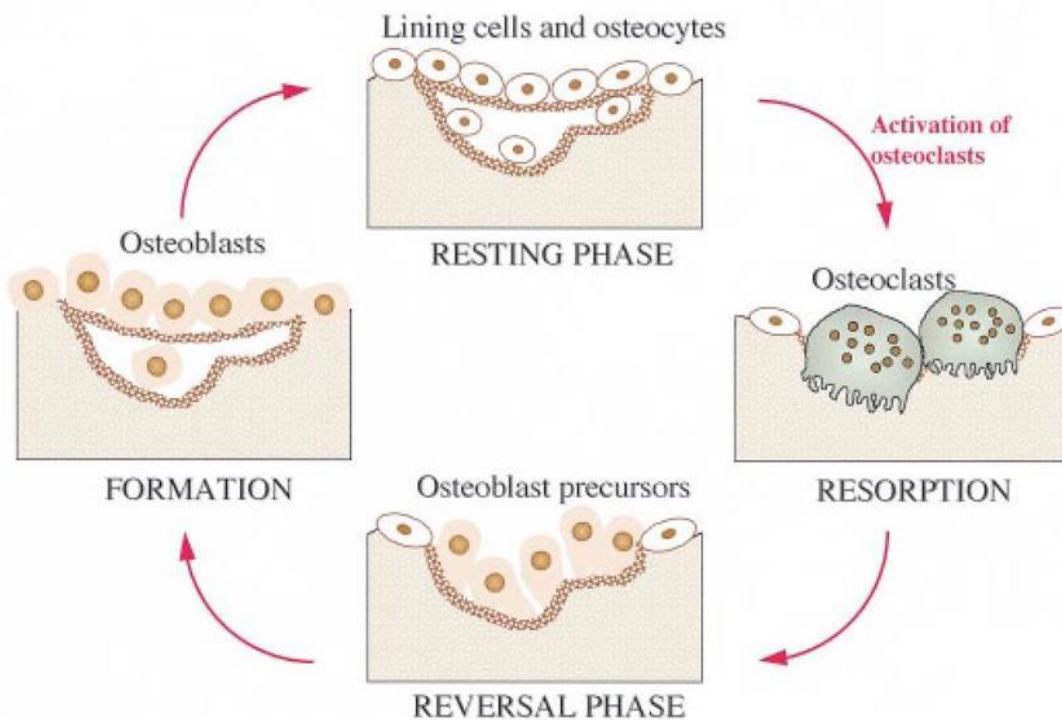


Figure 1.14 Overview of bone remodelling¹⁶⁶.

1.2.4 Genome wide association studies (GWAS)

Studies have shown that there are genetic factors that influence peak bone mass achieved in early adulthood or the rate of bone loss. These genetic factors, either alone or together with environmental factors (which are explained further in **Section 1.3**) may influence the likelihood of developing diseases such as osteoporosis in later life.

There have been a few genome-wide association studies (GWAS) studies which have identified single nucleotide polymorphisms (SNPs) within genes which are involved in the WNT, RANK-RANKL-Osteoprotegerin or endochondral ossification pathways¹⁶⁷. An initial GWAS was carried out in 2008 using data from the TwinsUK/ Rotterdam¹⁶⁸ and deCODE genetics studies¹⁶⁹ which identified SNPs in genes related to BMD including *Osteoprotegerin*, *LRP5*, *RANKL*, estrogen receptor 1 (*ESR1*) and *RANK*. Further GWAS studies have also identified SNPs in *Runx2*¹⁷⁰, *Osterix*¹⁷⁰⁻¹⁷³, *SOST*^{170,171} and *SOX9*¹⁷⁰. A GWAS study in the Framingham Heart Study examined genetic associations in bone mass using the Affymetric 100 k SNP GeneChip marker set¹⁷⁴. The study identified 40 SNPs which were found to be associated with several bone phenotypes and found that heritability estimates were 30-66 % for all the bone phenotypes¹⁷⁴. This study found that there were SNPs associated with methylenetetrahydrofolate reductase (*MTHFR*), *ESR1*, *LRP5*, *VDR*, *CYP19*, peroxisome proliferator activated receptor gamma (*PPAR γ*) and type I collagen¹⁷⁴. Other meta analyses have shown that SNPs within *ESR1*¹⁷⁵, *collagen type I alpha 1*¹⁷⁶, *MTHFR*¹⁷⁷ and *VDR*¹⁷⁸ explain a small percentage of the variation in BMD or fracture.

The first GWAS study in 400,000 individuals identified 515 loci which were associated with estimated BMD (eBMD)¹⁷⁹. The individual effects of each loci on eBMD were small however, when combined the loci explained ~20 % of variation in BMD¹⁷⁹. A second GWAS analysed fracture risk in UK BioBank participants and found that there were 13 loci which were associated with eBMD, which were also replicated in a cohort of individuals from 23andMe and in the initial GWAS study¹⁷⁹. Of these, a protein involved in *WNT/ β -catenin* signalling called dishevelled associated activator of morphogenesis 2 (*DAAM2*) was identified¹⁷⁹. Further studies found that *in vitro*, mutations in *DAAM2* reduces mineralisation in human osteoblasts¹⁷⁹. *DAAM2* KO mice had high cortical porosity and reduced bone strength¹⁷⁹. eBMD is predictive of fracture and has been shown to be highly heritable (50-80 %) ¹⁸⁰. From the eBMD GWAS, SNPs could be mapped to genes enriched for known bone density proteins which highlighted target genes of interest¹⁸⁰. Even though BMD is assessed by DXA in the clinical setting and used to predict fracture risk studies have shown that eBMD GWAS was able to identify 84 % of significant loci which were found in BMD GWAS studies¹⁸⁰.

1.2.5 Pathogenesis of osteoporosis

Osteoporosis involves the progressive loss of trabecular and cortical bone mass and micro-architectural deterioration of the skeleton leading to bone fragility and increased risk of fracture¹⁸¹. There are a number of factors which can contribute to the risk of developing an osteoporotic fracture including low peak bone mass, increased bone loss, ageing, hormonal factors, glucocorticoids, smoking, low physical activity, low intake of vitamin D and calcium, small body size and a personal or family history of fracture¹⁸² (**Figure 1.15**).

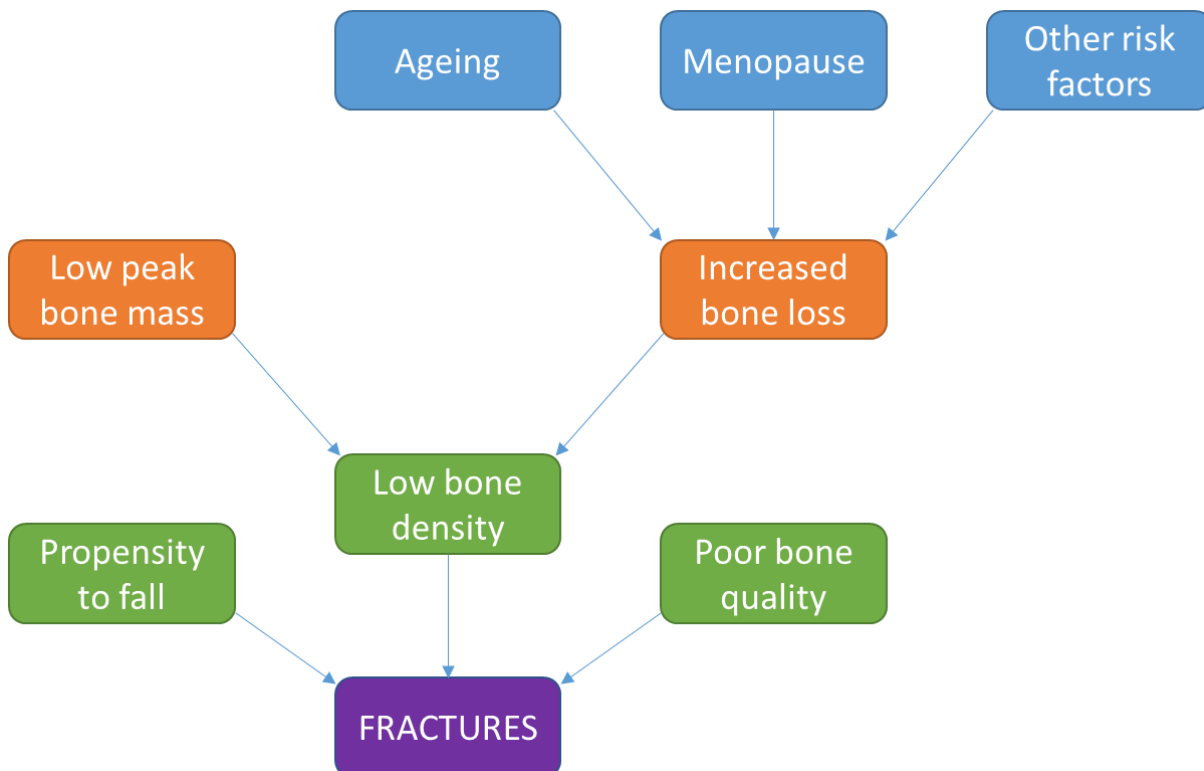


Figure 1.15 Pathogenesis of osteoporosis¹⁸².

There is complete regeneration of the adult skeleton every 10 years by bone remodelling¹⁸³ and bone loss occurs when the amount of bone formed during bone remodelling does not replace the bone that is removed by resorption¹⁸⁴. In both men and women, the amount of bone formed during each remodelling cycle decreases with age and new bone formation is less dense than old bone which can result in a decrease in wall thickness, especially in trabecular bone¹⁸¹. Bone resorption occurs faster than bone formation, therefore with an increase in bone remodelling there is transient bone mineral loss¹⁸¹. Both men and women begin to lose bone mass in their 40s however, in men this is a slow and steady decline whereas in women there is a sharper decline within the first 5-10 years following menopause due to the loss of estrogen¹⁸¹. Garnero *et al.*, found that during menopause there was a 37-52 % increase in bone formation and a 79-97 % increase in bone resorption marker levels⁴². In the first few years following menopause there is an increase in bone

formation and bone resorption which persists for up to 40 years post menopause⁴². Furthermore, women tend to accumulate less skeletal mass than men and often have smaller bones with a smaller diameter compared to men¹⁸¹.

Studies in bone marrow have shown that there is a decrease in osteoblastogenesis with increasing age¹⁸¹ and a study on MSCs from bone marrow have shown that the number of MSCs with osteogenic potential decreases with age¹⁸⁵. Using mouse models, studies have shown that there is a strong correlation between a decrease in the number of osteoblast progenitors, decreased bone formation and decreased bone mass¹⁸¹. Lips *et al.*, found that mean wall thickness in trabecular bone decreases with age and this correlates with a decrease in bone formation at the basic multicellular unit (BMU) level¹⁸⁶. Parfitt *et al.*, found that defective osteoblast recruitment contributes to the decrease in trabecular wall thickness¹⁸⁷. A mouse study found a link between low BMD and decreased osteoblastogenesis in the bone marrow as well as decreased osteoclast formation, bone formation and bone mass¹⁸⁴ however, other studies have shown that the resorption surface and number of osteoclasts remains constant with ageing^{186,188}. Studies incorporating tetracycline labelling have shown that there is a decrease in the calcification rate in cortical bone with ageing¹⁸⁶.

A lack of sex steroids has been shown to be associated with an increased rate in bone remodelling¹⁸¹ and in women this becomes apparent following menopause due to the decrease in estrogen levels. Studies in mice lacking the sex steroids have shown that there is upregulation in the formation of osteoblasts and osteoclasts^{189,190}. Loss of estrogen has been shown to lead to prolongation of the lifespan of osteoclasts and a shorter lifespan of osteoblasts and osteocytes¹⁸¹. Studies have shown that with loss of sex steroids, osteoclasts resorb deeper into the surface¹⁸¹.

Glucocorticoids are commonly prescribed for treating pulmonary, rheumatologic, autoimmune and gastrointestinal disease¹⁸³. Following glucocorticoid treatment, it is estimated that there is a rapid initial phase of approximately 12 % bone loss within the first few months followed by a slower rate of bone loss of around 2.5 % annually¹⁸³. Histological features of glucocorticoid induced osteoporosis include decreased bone formation rate, decreased trabecular wall thickness, increased bone resorption, a strong indication of decreased work output by osteoblasts and *in situ* death of portions of bone^{181,183}. Glucocorticoid excess has been shown to suppress osteoblastogenesis in bone marrow and promote apoptosis of osteoblasts and osteocytes¹⁸¹. In mice, glucocorticoid use has resulted in decreased BMD associated with a decrease in the number of osteoblasts and osteoclast progenitors in the bone marrow, as well as a decrease in mineral apposition and bone formation¹⁸³.

Medications and supplements often prescribed for the prevention and treatment of bone loss include estrogen replacement therapy, bisphosphonates, calcitonin, calcium and vitamin D¹⁸¹. The anti-resorptive agents, estrogen, bisphosphonates, selective estrogen receptor modulators (SERMs) and calcitonin act by decreasing osteoclast progenitor development and/or promoting apoptosis of mature osteoclasts which results in a decreased rate of bone remodelling¹⁸¹. A study found that treating women with HRT resulted in preservation of bone balance and there was a reduction in the resorptive activity at the BMU level however, there was no effect on osteoblastic matrix formation and there were no differences in osteoblastic activity over time¹⁹¹.

Vitamin D deficiency has been shown to cause secondary hyperparathyroidism, high bone turnover, bone loss, mineralisation defects and hip and other fractures¹⁹². Vitamin D is important for increasing the absorption of calcium and phosphate for the mineralisation of the skeleton¹⁹². A meta-analysis by Bischoff-Ferrari *et al.*, which included double blind randomised, controlled trials of vitamin D in elderly populations found that vitamin D appears to reduce the risk of falls by 20 % amongst older individuals with stable health that are ambulatory or institutionalised¹⁹³. Sambrook *et al.*, found that serum PTH concentrations were predictive of time to first fall in the frail elderly, independent of vitamin D status or measures of general health¹⁹⁴.

1.3 Developmental origins of health and disease (DOHaD)

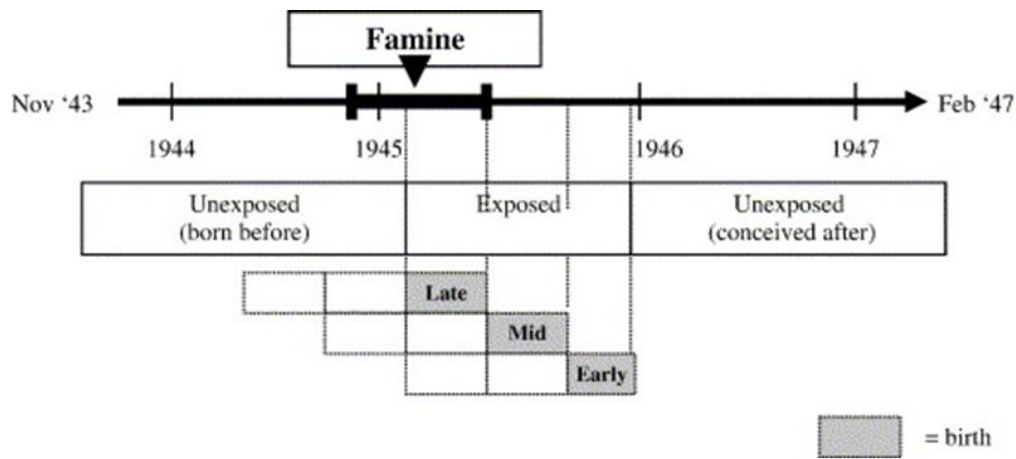
The early life environment has been shown to be important in determining disease risk in later life, and evidence to support this arises from the idea of developmental origins of health and disease (DOHaD). Barker *et al.*, found that with an increase in prosperity and an affluent diet there was an increase in ischemic heart disease in Britain, and mortality arising from ischemic heart disease was greater in less affluent areas of England and Wales. Therefore, Barker *et al.*, hypothesised that poorer living conditions during the early life environment and through childhood were associated with increased risk of mortality from ischemic heart disease in later adulthood. Barker *et al.*, found that the mortality from ischemic heart disease was strongly correlated with neonatal and post neonatal mortality. This provided evidence for the early life environment being associated with disease risk in later life¹⁹⁵.

This hypothesis was further investigated using individuals born in Hertfordshire between 1911-1948¹⁹⁶. In 1911 Ethel Margaret Burnside, who was Hertfordshire's first 'chief health visitor and lady inspector of midwives', assembled a team of midwives and nurses to keep detailed records during infancy¹⁹⁶. Data was recorded on birthweight, illnesses, development, method of infant feeding, and weight at 1 year of age¹⁹⁶. Since then, many studies have investigated health in later life of individuals still residing in Hertfordshire who had detailed records during birth and infancy. Studies

within the Hertfordshire cohort have shown associations between growth during the early life environment and during infancy with ischemic heart disease^{197,198}, cardiovascular disease (CVD)¹⁹⁹, diabetes²⁰⁰, adiposity²⁰¹, sarcopenia²⁰² and ageing²⁰³ in adulthood. Many studies found that smaller size at birth and at 1 year of age was associated with increased risk of developing these diseases in later life. This suggests that there was poorer nutrition during the early life environment and during early infancy which had an adverse effect in later life.

A number of studies have investigated the association of early life undernutrition on disease risk in later life using individuals who were exposed to the Dutch Hunger Famine around the periconceptual period. During the winter of 1944-1945 in The Netherlands there was famine which is referred to as the Dutch Hunger Winter²⁰⁴. During the war, nutrition was adequate up until October 1944 however, by November 26th 1944 rations had fallen below 1000 calories a day and by April 1945 rations were as low as 500 calories a day until food supplies were restored after liberation day on May 5th 1945²⁰⁴. Detailed food records were kept in The Netherlands which provides basis for experiments investigating the effect of early life famine exposure on disease risk in later life. The studies found that exposure to famine during the early life environment was associated with an increased risk of disease in adulthood, furthermore the timing of the exposure had differential effects on the disease risk²⁰⁵⁻²¹⁰ (**Figure 1.16**).

a)



b)

Exposure to Famine		
In late gestation	In mid gestation	In early gestation
Glucose intolerance	Glucose intolerance	Glucose intolerance
	Microalbuminuria	Atherogenic lipid profile
	Obstructive airways disease	Altered blood coagulation
		Obesity (women only)
		Stress sensitivity
		Coronary heart disease
		Breast cancer

Figure 1.16 An overview to prenatal famine exposure during the Dutch Winter Famine from 1943-1947 and the disease risk in later adulthood²¹¹.

To investigate the effect of the early life environment on offspring health, many studies have utilised animal models²¹²⁻²¹⁴ and investigated the effect of maternal nutrition during the early life environment on offspring disease risk in later life. The studies showed that a mismatch between the prenatal and postnatal environment can have detrimental effects on offspring including altered cardiovascular function, obesity and diabetes²¹²⁻²¹⁴. Therefore, these studies in both humans and animals suggest that the early life environment can have a detrimental effect on disease risk in later life and that the timing of the nutrient constraint has an effect on the risk of developing diseases in adulthood.

1.3.1 Evidence for the developmental origins of osteoporosis

1.3.1.1 Human studies

There is an abundance of evidence to suggest that the early life environment is associated with disease risk in later life, especially the risk of CVD, diabetes, obesity and cancer^{197,198,200,201,203}. There are also studies to suggest that the early life environment can influence BMD and the risk of developing osteoporosis.

Studies within the Hertfordshire cohort have shown associations between weight at birth and 1 year of age with bone measures in adulthood. Dennison *et al.*, measured bone area (BA), BMC and BMD in 498 men and 468 women aged 60-75 and born in Hertfordshire between 1931-1939 and found that in men and women, birthweight was associated with lumbar spine and proximal femur BA and BMC, and with proximal femur BMD in men only²¹⁵. In men and women, weight at 1 year was associated with lumbar spine and proximal femur BMC and in men there was an association with lumbar spine BMD²¹⁵. Oliver *et al.*, investigated the relationship between fetal and infant growth and bone strength in adulthood in 313 men and 318 women born in Hertfordshire between 1931-1939²¹⁶. The study found that there were sex specific differences in bone strength, but in both men and women, birthweight was positively correlated with radial length, radial total area, tibial length, tibial total area, tibial fracture load X and Y and tibial strength strain index²¹⁶. In men, birthweight was also positively correlated with radial cortical BA, and there was an inverse association with tibial trabecular density and weight at 1 year was positively correlated with radius length, radial fracture X and Y, and tibial length²¹⁶.

Twin studies have identified a link between birthweight and the risk of developing osteoporosis in adulthood. Antoniadou *et al.*, studied 4008 female twins and found that in monozygotic twins, but not dizygotic twins, birthweight was associated with BMC at the lumbar spine, femoral neck and forearm²¹⁷. The study also found that both monozygotic and dizygotic twins that weighed less than 2 kg at birth had lower BMD at the hip and forearm compared to twins with a birthweight greater than 2 kg²¹⁷. Other smaller studies have also shown associations between birthweight and bone measures in adulthood. Gale *et al.*, studied 143 men and women aged 70-75 in Sheffield and looked at the association between birthweight and adult body composition²¹⁸. In men, there was a positive association between birthweight and BA and BMC at the lumbar spine, femoral neck and whole body but not BMD²¹⁸. Whereas in women, birthweight was positively associated with BMC and BMD at the lumbar spine and femoral neck, and with whole body BA, BMC and BMD²¹⁸. Yarbrough *et al.*, studied 305 postmenopausal Caucasian women and found that birthweight was strongly associated with lumbar spine BMC even after adjustment for all covariates including age, BMI, alcohol use, exercise, current smoker, osteoarthritis, or use of estrogen replacement, calcium supplements, thyroid, thiazide or steroid medications²¹⁹.

Studies have shown that weight at 1 year of age, but not birthweight, was associated with peak bone mass. Cooper *et al.*, investigated associations between weight in infancy and bone mass in adult life in 189 women and 224 men aged 63-73 years who were born in Hertfordshire between 1920-1930²²⁰. In both men and women there were no associations between birthweight and BMC or BMD²²⁰. In men, increasing weight at 1 year was associated with lumbar spine BMC whereas in women, increasing weight at 1 year of age was associated with increasing BMC at the lumbar spine

Chapter 1

and femoral neck and women in the highest third of weight distribution at 1 year had 11 % higher lumbar spine BMC and 8 % higher femoral neck BMC than those in the lowest third²²⁰. Cooper *et al.*, studied 153 women born in Bath between 1968-1969 as part of a longitudinal study²²¹. The study found that there were no associations between birthweight and bone measures at the lumbar spine or femoral neck however, weight at 1 year of age was positively associated with BMC at the lumbar spine and femoral neck²²¹. A separate study by Cooper *et al.*, found that low childhood growth rate is a risk factor for later hip fracture in 3639 men and 3447 women born between 1924-1933 in Helsinki ²²². Some studies have shown that lifestyle choices in adulthood can influence the relationship between the early life environment and bone measures in adult life. A study by Moinuddin *et al.*, found that amongst males with low birthweight, those that were currently smoking in their adult life had lower femoral neck BMC and BMD²²³.

Therefore these studies highlight that growth during the early life environment and during infancy is associated with bone measures in later life and the risk of developing osteoporosis.

1.3.1.2 Animal studies

A number of animal studies have investigated the effect of the maternal diet during pregnancy and lactation on offspring skeletal health. A study by Oreffo *et al.*, investigated the effect of a maternal protein restricted diet in rats on offspring bone marrow stromal cells with respect to colony formation, proliferation and differentiation. Total colony number indicates the colony forming efficiency of MSCs and their proliferation potential and alkaline phosphatase activity which indicates osteogenic potential and differentiation²²⁴. The study found an association between maternal diet in pregnancy and osteoblast function in young offspring²²⁴. In control mice, total colony number, alkaline phosphatase number and alkaline phosphatase specific activity decreased from 8-16 weeks as mice reached skeletal maturity at 13 weeks²²⁴. Whereas in protein restricted mice, these parameters increased between 8 to 16 weeks suggesting delayed skeletal maturity with a delay in osteoblast activity²²⁴. Oreffo *et al.*, additionally cultured the bone marrow stromal cells with 10 nM 1,25(OH)₂D₃, 10 ng/ml IGF1 or 1 nm growth hormone (GH) and found that the addition of osteogenic growth factors were not sufficient to overcome the effects of a protein restricted maternal diet²²⁴.

Lanham *et al.*, studied the effect of a maternal protein restricted diet during pregnancy in female rats on offspring skeletal health and found that a maternal low protein diet alters the growth trajectory in female offspring and bone biochemistry in all offspring²²⁵. Lanham *et al.*, measured key osteogenic indicators including Osteocalcin, IGF1 and 25(OH)D₃ and found altered parameters amongst rats depending on the exposed diet²²⁵. At 4 weeks, Osteocalcin concentrations were higher in restricted offspring than control in males and females but there were no differences at other

time points which suggests increased osteoblast activity and increased bone formation²²⁵. Lanham *et al.*, also found that offspring born to protein restricted mothers had structurally weaker femoral heads and midshaft tibiae and stronger femoral necks and vertebrae than control rats at 75 weeks of age²²⁶. Female offspring had femoral heads with thinner, less dense trabeculae, femoral necks with closer packed trabeculae, vertebrae with thicker, denser trabeculae and midshaft tibiae with denser cortical bone²²⁶.

Lanham *et al.*, investigated the effect of a maternal protein restricted diet during the last trimester of pregnancy and the first 2 weeks of postnatal life on offspring skeletal health²²⁷. The study found that calorie restriction may alter bone size but not bone structure²²⁷. During the growth period, low protein piglets had lower mass and BMC and increased BMD which suggests accelerated bone development whereas at 3-5 months of age, there were no differences in femur mass, length, proximal femur or femoral midshaft parameters²²⁷.

Lanham *et al.*, investigated the effect of a maternal high fat diet during pregnancy and lactation in mice on offspring skeletal health. After weaning, offspring were fed either control (C) or high fat (HF) diet to create C/C, C/HF or HF/HF groups until 30 weeks of age²²⁸. The study found that a maternal HF diet during pregnancy increased bone marrow adiposity and altered bone structure in offspring including femur length, bone volume, trabecular spacing and midshaft cross sectional area²²⁸.

1.3.2 Vitamin D status and bone health

1.3.2.1 Human studies

Vitamin D deficiency in humans is associated with rickets in children and osteomalacia in adults. Rickets can occur through severe vitamin D and calcium deficiency and in the 19th century there was a surge in rickets due to inadequate UVB exposure. Rickets results in the failure to adequately mineralise bone and it presents as growth retardation, muscle weakness, skeletal deformities, hypocalcaemia, tetany and seizures¹⁵⁹. Diagnosis is through a radiograph of long bones which show cupping, splaying and fraying of the metaphysis²²⁹. Nowadays, rickets is less common amongst the population and this is thought to be due to sensible UVB exposure and fortification of dairy products with vitamin D.

There is currently debate within the literature as to whether vitamin D during pregnancy influences fetal skeletal development. Studies have shown that maternal 25(OH)D₃ concentrations positively correlate with cord 25(OH)D₃ concentrations, and that concentrations are lower in cord compared to the mother. Therefore, babies born to vitamin D deficient mothers have lower 25(OH)D₃

Chapter 1

concentrations. It is argued that these infants may be at a higher risk of developing rickets during infancy and adverse bone measures in later life. Conversely, some studies have shown that normal calcium and bone metabolism occur independently of vitamin D status and the VDR²³⁰.

There is evidence to suggest that maternal vitamin D status is associated with bone mineral accrual in the developing fetus. A prospective study by Mahon *et al.*, investigated fetal femoral development using participants from the Southampton Women's Survey (SWS) cohort²³¹. Pregnant women underwent high resolution three dimensional ultrasound (3DUS) imaging at 19 and 34 weeks gestation to measure the fetal thigh and the femoral splaying index was calculated by measuring the distal metaphyseal cross sectional area and dividing it by the fetal femur length. The study found that fetal femur length, distal cross sectional area and splaying index were similar in boys and girls at 19 and 34 weeks²³¹. However, at 19 and 34 weeks gestation, there was an inverse association with distal metaphyseal cross sectional area and splaying index which is analogous to splaying observed in rickets²³¹. In a cross sectional study with longitudinal follow up of 125 pregnant women, Viljakainen *et al.*, investigated associations between maternal vitamin D status and newborn bone outcomes²³². The study found that maternal vitamin D status affects bone mineral accrual during pregnancy and influences bone size²³². New-borns born to mothers with below median 25(OH)D₃ (42.6 nmol/L) had lower cord 25(OH)D₃ concentrations and lower tibial BMC and cross sectional area but there were no differences in gestational age, head circumference, birth length, weight or tibial BMD²³².

It has been argued that vitamin D does not play a role in fetal skeletal development. Brunvand *et al.*, investigated fetal growth in 30 Pakistani vitamin D deficient pregnant women and found that 29 of the 30 women had serum 25(OH)D₃ concentrations less than 30 nmol/L at delivery²³³. The study found no association between maternal serum 25(OH)D₃ and fetal growth and there were no associations between maternal serum 25(OH)D₃ or 1,25(OH)D₃ and crown-heel length or birthweight²³³.

There have been a few vitamin D intervention studies during pregnancy however, these have been small. Congdon *et al.*, studied vitamin D supplementation in vitamin D deficient Asian women. Cord blood was collected at delivery from 45 Asian women, 19 Asian women receiving 1000 IU/d vitamin D daily in the last trimester, and 12 white women as a control. The study found that 91 % of babies born to unsupplemented Asian mothers and 58 % babies born to supplemented Asian mothers had cord 25(OH)D₃ concentrations below 10 nmol/l²³⁴. However, despite a significant proportion of infants being born with very low 25(OH)D₃ concentrations, there were no differences in gestational age, birthweight, BMC or the proportion of infants born with craniotabes²³⁴. Amongst Asian babies, birthweight was significantly associated with BMC but there was no correlation between BMC and

cord 25(OH)D₃²³⁴. A larger scale vitamin D intervention study includes the maternal gestational vitamin D supplementation and offspring bone health (MAVIDOS) trial which was a double blind, randomised, placebo controlled trial which took place in Oxford, Sheffield and Southampton where pregnant mothers were supplemented with 1000 IU/d cholecalciferol or a placebo daily from 14 weeks gestation until delivery²³⁵. The study found that there were no significant differences in bone measures at birth between the two maternal treatment groups however, when the analyses were stratified by season of birth, infants born in the winter months to cholecalciferol supplemented mothers had greater BMC, BA and BMD at birth compared to the placebo group²³⁶.

Despite the lack of associations between maternal 25(OH)D₃ status during pregnancy and fetal skeletal development, some studies have found associations with bone measures in childhood. Brooke *et al.*, studied vitamin D deficient Asian women living in Britain where 59 were supplemented with 1000 IU/d ergocalciferol during the last trimester of pregnancy and 67 were the control²³⁷. At birth there were no differences in birthweight, crown-heel length, forearm length, triceps skinfold or head circumference²³⁷. The children were followed up at 3, 6, 9 and 12 months and at all four follow up visits, weight was significantly greater in the supplemented group compared to the control group and at 9 and 12 months, crown heel length was greater in the supplemented group compared to the control group²³⁸. A longitudinal study in Southampton by Javaid *et al.*, found that maternal vitamin D status during pregnancy was not associated with bone measures at birth however, there were associations with bone measures at 9 years of age²³⁹. In the study, 31 % mothers were regarded as vitamin D insufficient and 18 % as deficient in late pregnancy²³⁹. At 9 years of age there was a positive correlation between maternal 25(OH)D₃ and total body BMC, BA and BMD and lumbar BMC, and areal BMD at age 9²³⁹. There were no associations between maternal 25(OH)D₃ and height or lumbar BA at age 9²³⁹. Whole body BMC was significantly lower in children whose mothers were vitamin D deficient compared to vitamin D replete²³⁹. The study also found that UVB exposure during the third trimester of pregnancy had an effect on maternal serum 25(OH)D₃ status and bone measurements in childhood. Children whose third trimester fell during the summer months had greater BMC compared to children whose 3rd trimester fell in winter²³⁹.

Other studies have also shown that season can influence maternal serum 25(OH)D₃ status and associations with offspring bone size. An observational study by Morley *et al.*, investigated the relationship between maternal 25(OH)D₃ at 16 and 28 weeks gestation and offspring bone size²⁴⁰. The study found that mean maternal 25(OH)D₃ was lower in winter than in summer and infants born in winter had smaller knee-heel length than infants born in summer²⁴⁰. Infants born to mothers with a serum 25(OH)D₃ of less than 28 nmol/l in late gestation had a 0.7 week shorter mean

Chapter 1

gestation, lower mean knee-heel length, mid upper arm and calf circumferences compared to babies born to mothers with serum 25(OH)D₃ equal to or above 28 nmol/l²⁴⁰.

Therefore, these studies suggest that vitamin D during pregnancy may not affect fetal skeletal development however, the effects may be observed during infancy and childhood. This could perhaps be due to a lower demand for vitamin D during fetal skeletal development compared to the demand that is required during infancy and childhood. With a lower starting reserve of vitamin D at birth, the stores could be depleted quicker as demands increase resulting in adverse effects which could impede the bone density trajectory.

1.3.2.2 Animal studies

There have been a number of studies in animals which utilise a vitamin D deficient animal model to investigate skeletal development. Similar to studies in humans, there is conflict as to whether vitamin D affects fetal skeletal development, as most adverse effects are apparent during postnatal growth.

Miller *et al.*, used a vitamin D deficient rat model to investigate early skeletal development and found that there were changes to fetal skeletal mineralisation²⁴¹. Vitamin D deficient fetuses in late pregnancy had greater ratio of osteoid to mineralised tissue compared to the replete group and this was still apparent at 3 weeks post weaning²⁴¹. In fetuses, there were no differences in mineralised metaphyseal or epiphyseal tissue whereas from lactation day 14, vitamin D deficient pups had lower percentage of metaphyseal mineralised tissue but no differences in epiphyseal mineralised tissue²⁴¹. After weaning, growth plate thickness was higher and longitudinal bone growth rate was slower in deficient pups compared to replete pups²⁴¹.

Lanham *et al.*, investigated the effect of a maternal vitamin D deficient diet during pregnancy on rat offspring fetal skeletal development²⁴². At birth, vitamin D deficient pups had increased proximal femur bone surface (BS)/ bone volume (BV) and decreased proximal femur trabecular thickness and midshaft femur cross-sectional moment of inertia (CSMI), a biomechanical indicator of the structural distribution of bone mass from the neural bending axis. There were no differences in femur length, femur bone volume, proximal femur BV/ trabecular volume (TV), proximal femur trabecular spacing, midshaft femur diameter or midshaft femur wall thickness²⁴². At 140 days, vitamin D deficient offspring had increased proximal femur BS/BV, decreased proximal femur trabecular thickness and structural model index²⁴².

Other vitamin D deficient rat models have shown no effect on fetal skeletal development. Glazier *et al.*, found that a vitamin D deficient diet during pregnancy resulted in lower fetal 25(OH)D₃ and 1,25(OH)₂D₃ concentrations however, there was no effect on fetal skeletal development²⁴³.

Halloran *et al.*, found that a maternal vitamin D deficient diet did not affect fetal calcium concentrations or impair placental calcium transfer however, Halloran *et al.*, did not investigate fetal skeletal development²⁴⁴. Instead skeletal development from 2-6 weeks postpartum was investigated²⁴⁴. The study found that femur ash weight, percentage ash (ash weight/dry weight) and total femur calcium were lower in the deficient group during lactation, weaning and post weaning compared to the replete group²⁴⁴. At weaning, femur bone volume was lower in the vitamin D deficient group compared to the replete group however, there were no differences at lactation and weaning²⁴⁴. Whereas dry femur weight was lower in the vitamin D deficient group at weaning and post weaning²⁴⁴. Within the vitamin D deficient group, there was a decrease in bone volume at 6 weeks postpartum compared to the vitamin D replete group²⁴⁴.

Borg *et al.*, studied a vitamin D deficient mouse model in C57BL/6 female mice where mice were fed a vitamin D supplemented diet (1000 U/kg chow) or a vitamin D free diet (0 U/kg chow) during pregnancy and lactation²⁴⁵. Pups were weaned onto the vitamin D supplemented diet and underwent mechanical loading of their left tibia at 10 and 18 weeks of age²⁴⁵. The study found that offspring exposed to a prenatal vitamin D deficient diet had reduced bone strength and altered bone biomechanical properties compared to the control mice²⁴⁵. Offspring exposed to a prenatal vitamin D deficient diet had lower bone mass in the non-loaded limb, whereas in the loaded limb there was reduced bone mineral accrual following mechanical loading²⁴⁵. In both control mice and mice exposed to a prenatal vitamin D deficient diet, mechanical loading increased trabecular and cortical parameters²⁴⁵. In control mice, mechanical loading increased tibial stiffness and ultimate force required to fracture the tibia, whereas in mice exposed to a prenatal vitamin D deficient diet mechanical loading increased the ultimate force but there were no significant differences in tibial stiffness²⁴⁵. In 18 week old mice exposed to a prenatal vitamin D deficient diet, following mechanical loading there was a decrease in tibial stiffness and the ultimate force required to fracture the tibiae compared to control offspring²⁴⁵. The non-loaded limb of prenatal vitamin D deficient offspring had increased ratio of mineralisation surface to bone surface area however, there were no differences in the loaded limbs²⁴⁵. In both the loaded limb and non-loaded limb, a prenatal vitamin D deficient diet did not alter mineralisation apposition rate or the bone formation rate²⁴⁵. In the non-loaded limb cortical porosity was greater in offspring exposed to a prenatal vitamin D deficient diet and there were no differences in cortical and trabecular parameters²⁴⁵. Whereas in the loaded limb, cortical bone volume and the ratio of cortical bone volume to tissue volume were lower and cortical mineralisation area were higher in offspring exposed to a prenatal vitamin D deficient diet compared to control mice²⁴⁵. These findings suggest that a maternal vitamin D deficient diet during pregnancy and lactation has detrimental effects on the adult offspring skeleton. Furthermore, despite the beneficial effects of mechanical loading on bone strength, which

could be analogous to walking or participation in weight-bearing exercises in humans, an early life vitamin D deficient diet prevented the optimum response to loading compared to mice on a control diet.

1.3.2.2.1 Gene knockout studies in animals

There have been a number of knockout studies in animals which have targeted different components of the vitamin D pathway such as enzymes involved in vitamin D metabolism or catabolism. The studies have shown that vitamin D is not needed for fetal skeletal development and in animal models, adverse effects are not observed until weaning.

A number of studies have knocked out the *VDR* gene in mice. Kovacs *et al.*, generated a *VDR* wildtype (WT), heterozygous (+/-) and null model to show that the *VDR* is not required for fetal mineral homeostasis or for regulating placental calcium transfer²⁴⁶. The study found that fetal skeletal calcium and magnesium concentrations, and amniotic fluid calcium, phosphorous or PTH concentrations were similar in all three groups and that serum 1,25(OH)₂D₃ levels were similar in WT and *VDR* +/- mice and increased in *VDR* null fetuses²⁴⁶. The study found that the absence of *VDR* in the fetus does not alter skeletal mineral content, there were no gross abnormalities in fetal skeletons, the relative mineral distribution looked normal and the long bones in the appendicular skeleton were of normal length and morphology between the three groups²⁴⁶.

Kato *et al.*, found that adverse effects due to the absence of the *VDR* gene in offspring occurred after weaning²⁴⁷. The study found that from birth until weaning there were no differences in behaviour or growth rate between *VDR* WT, +/- or null mice however, after weaning *VDR* null showed marked growth retardation and the body weight at 10 weeks was about 50 % of WT and +/- littermates and the mice eventually developed rickets²⁴⁷. Histological analysis of *VDR* expressing tissues found that there were abnormalities in bone and skin but not in the intestine, kidney brain or spleen. From 7 weeks postpartum, null mice developed alopecia and poor whiskers and most had a flat face with a shorter nose. Furthermore, radiographic analysis of *VDR* null mice showed growth retardation with loss of bone density and there were typical features of advanced rickets in the tibia and fibula with widening of the epiphyseal growth plates, thinning of the cortex, fraying, cupping and widening of the metaphysis, and layers of cartilage were widened and lacked mineralisation²⁴⁷. There was an increase in the extent and width of osteoid seams in cancellous bone and the bone surfaces were lined with osteoblastic cells, although there were no differences in the number of osteoclasts²⁴⁷. Female 10 week old null mice had uterine hypoplasia but there were no abnormalities in male reproductive organs²⁴⁷. Therefore the study showed that *VDR* null mice were grossly similar to WT until weaning, after which mice developed rickets, hypocalcaemia, hypophosphatemia, alopecia and reproductive abnormalities. Nonetheless, studies have shown

that a rescue diet containing calcium and lactose can prevent some adverse changes observed in *VDR* null mice. Johnson *et al.*, fed WT, *VDR* +/- and *VDR* null mice a standard diet, medium calcium diet, high calcium diet, or a high calcium with lactose diet²⁴⁸. All of the nonstandard chow diets improved fertility of all mice to 100 %²⁴⁸. Furthermore, feeding a diet supplemented with calcium and/or lactose prevented hypocalcaemia in the *VDR* null mice²⁴⁸.

Mutation of the *CYP27B1* enzyme which is involved in metabolising the inactive form of vitamin D into the active form of 1,25(OH)₂D₃ resulted in adverse effects in mice. Dardenne *et al.*, used targeted ablation with a targeting vector for *CYP27B1* in mice which were interbred to produce *CYP27B1* +/- and null mice²⁴⁹. Similar to what was observed in *VDR* null mice, the mutation did not affect fetal skeletal development and adverse effects were observed after weaning where *CYP27B1* null mice exhibited growth retardation with decreased weight gain from 3-8 weeks of age and decreased femur length at 8 weeks²⁴⁹. Long bones from 3 week old pups were hypomineralised and the femurs presented evidence of rickets with impaired calcification of maturing cartilage, disorganisation of the columnar alignment of hypertrophic chondrocytes, increased growth plate width and accumulation of osteoid in trabecular bone²⁴⁹. At 8 weeks the effect of defective mineralisation was more profound, with more severe disorganisation in growth plate architecture, loss of columnar organisation in chondrocytes and marked osteomalacia with accumulation of osteoid in the femoral cortex²⁴⁹. A study by Panda *et al.*, in *CYP27B1* KO mice found that the bones in null mice exhibited histological features typical of rickets compared to WT mice at 4 weeks of age²⁵⁰. The hypertrophic zone was disorganised and wider, resulting in widening of the epiphyseal growth plates²⁵⁰, there was inadequate mineralisation of cartilage, the primary spongiosa and cortical bone and an increase in osteoid in both trabecular and cortical bone²⁵⁰. There was an increase in osteoblasts lining bone surfaces and greater trabecular BA in the primary spongiosa²⁵⁰. In cortical bone, type 1 collagen levels were normal and Osteocalcin was decreased, in bone osteoclast numbers and size were reduced and parathyroid glands were enlarged²⁵⁰. Ryan *et al.*, fed *CYP27B1* null mice a rescue diet with high calcium, phosphorous and lactose to normalise fertility²⁵¹. The study found that amongst *CYP27B1* null fetuses there were no differences in serum calcium, phosphorous, PTH, FGF23, 25(OH)D₃, 24,25(OH)₂D₃ and skeletal morphology and mineralisation patterns were similar to WT fetuses²⁵¹.

Therefore, these studies show that vitamin D is not essential for fetal skeletal development and adverse effects are observed after weaning. Furthermore, feeding dams a rescue diet is sufficient to prevent some of the adverse effects observed after weaning.

1.4 Epigenetics

Epigenetic modifications can influence gene expression without altering the DNA sequence²⁵². The three main epigenetic modifications include DNA methylation, histone modifications²⁵² and non-coding RNAs^{252–254} (**Figure 1.17**). It is known that skeletal size and BMD increase from early embryogenesis through the intrauterine and postnatal period before peaking in early adulthood. Furthermore, it has been shown that this bone growth trajectory is associated with the risk of developing osteoporosis in later life. Studies have shown that there are genetic factors which contribute to variance in BMD and fracture risk in later life however, studies have shown that SNPs play a small role in determining BMD. Therefore, it is thought that variance in BMD is also due to epigenetic modifications. Many studies have shown that the early life environment, including factors such as maternal nutrition, can influence epigenetic changes in the developing fetus and are associated with the risk of developing diseases in later life such as osteoporosis. It is thought that epigenetic changes may underlie the link between the maternal environment and bone development in the fetus and that this mechanism may also involve vitamin D although this is unclear. This link may provide insight into the pathogenesis of osteoporosis in later life²⁵⁵.

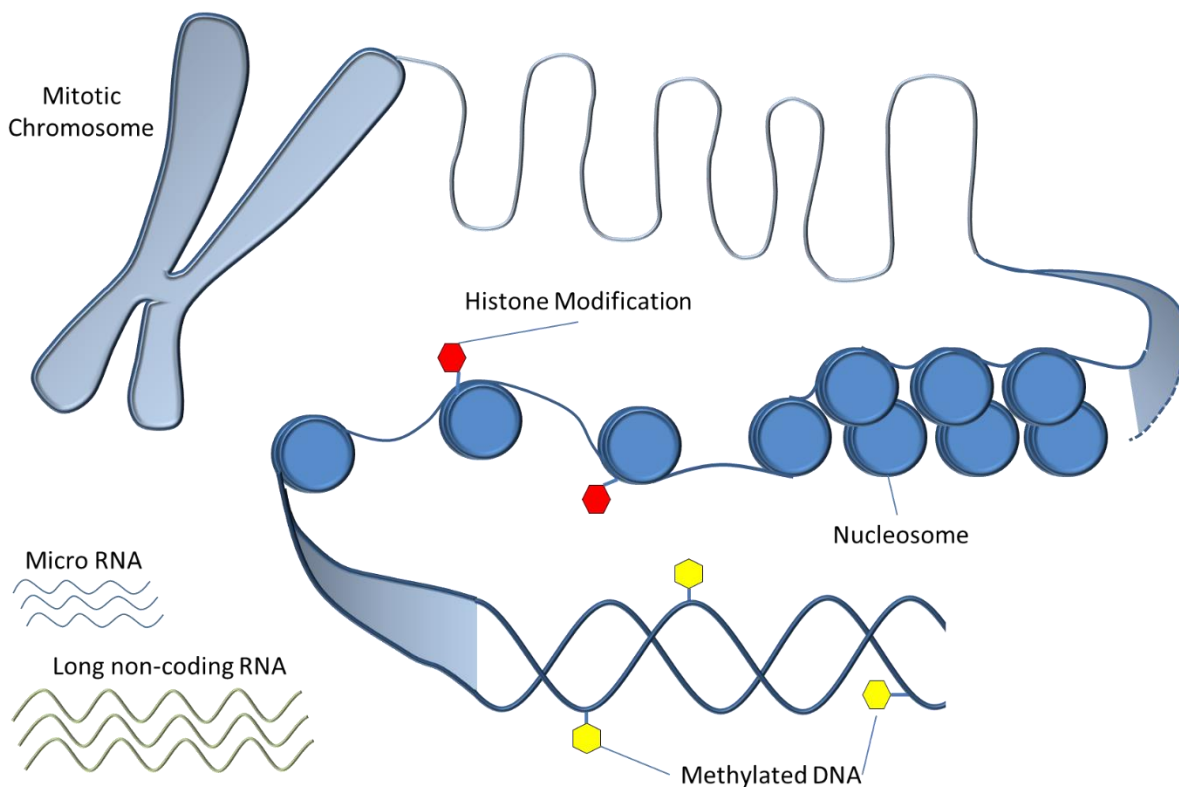


Figure 1.17 An overview of the main epigenetic modifications.

1.4.1 Epigenetic mechanisms

1.4.1.1 DNA methylation

DNA methylation is a stable epigenetic mark which involves the transfer of a methyl group to the 5' position of cytosine within CpG dinucleotides to create 5-methylcytosine (**Figure 1.18**)^{252,254,256}. This process involves a family of DNA methylase transferase enzymes (DNMTs) and S-adenosylmethionine (SAM) as a cofactor^{254,256}. It has been estimated that 70-80 % of all CpG dinucleotides within the human genome are methylated²⁵⁷ and that the remaining unmethylated CpGs are located in CpG islands. CpG islands are regions of DNA with a high number of CpGs and a GC content above 50 % and they are often located in the promoter regions of active or inducible genes²⁵⁸. Furthermore, methylation of CpG islands has been shown to be correlated with suppression of gene expression²⁵⁹⁻²⁶¹. CpG islands also have regions of lower CpG density which are termed 'shores'. These CpG shores have been shown to be associated with tissue specific methylation and transcriptional repression²⁵⁹.

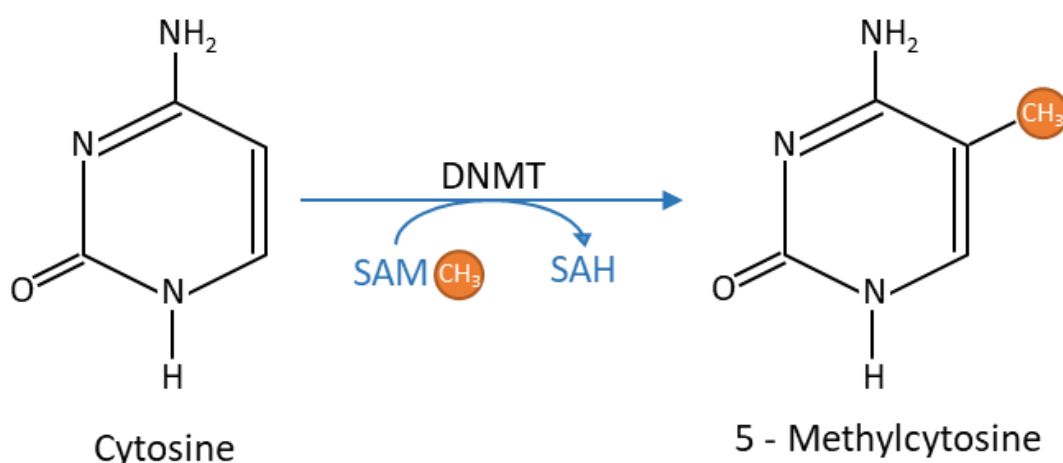


Figure 1.18 DNA methylation of cytosine to 5-methylcytosine by DNMTs.

SAM acts as a cofactor and provides the methyl group. DNMT - DNA methyl transferase, SAM - S-adenosylmethionine, SAH - S-adenosylhomocysteine.

There are three main DNMT enzymes: DNMT1, DNMT3a and DNMT3b. DNMT1 is involved in maintaining methylation patterns through replication cycles and there are three isoforms which are differentially expressed; DNMT1o is mainly expressed in oocytes and preimplantation embryos, DNMT1s is expressed in somatic cells and DNMT1p is expressed in pachytene spermatocytes^{262,263}. DNMT3a and DNMT3b are involved in *de novo* methylation²⁶⁴ prior to blastocyst implantation and the activity is coordinated by DNMT3L²⁶³. DNMT3L lacks enzymatic activity however, it has been shown to work in concordance with DNMT3a and DNMT3b to regulate methylation of maternally imprinted genes^{264,265}. There are a number of proteins involved in DNA methylation and these

Chapter 1

include methyl CpG binding protein 2 (MeCP2) and methyl CpG binding domain proteins 1-3 (MBD1-3). These DNA binding proteins can bind to methylated DNA in a methylation dependent manner and recruit transcriptional co-repressors and HDACs which remodel local chromatin and play a role in silencing gene transcription^{259,263,266}.

Patterns of DNA methylation are established in early life²⁶⁷ and they have an important role in silencing gene expression during development, and in the differentiation of individual tissues^{253,268}. The genome encodes imprinted genes where either the maternal or paternal allele needs to be silenced in the gamete prior to fertilisation to ensure their monoallelic expression²⁶⁷. Studies have shown that asymmetrical silencing is due to DNA methylation and this process is termed genomic imprinting^{269,270}. However, there are cases where DNA methylation fails to repress either the maternal or paternal allele resulting in biallelic expression of both parental genomes. This results in imprinting disorders such as Angelman, Beckwith Wiedemann and Prader- Willi syndrome^{271,272}.

The mechanism of DNA demethylation is not fully understood. There is evidence to suggest that DNA methylation marks can be removed by a family of Ten-eleven-ten translocase (TET) proteins. There are three types of TET proteins and they act as catalytic enzymes involved in DNA demethylation. The TET proteins also interact with proteins and complexes involved in histone modifications such as histone acetylation and methylation²⁷³. DNA demethylation involves a series of hydroxylation steps where firstly, 5-methylcytosine is hydroxylated to 5-hydroxymethylcytosine, before further hydroxylation to 5-formylcytosine and 5-carboxylcytosine²⁷³.

1.4.1.2 Histone modifications

DNA is packaged into chromatin which is wrapped around a nucleosome core. 146 bp of DNA is wrapped 1.65 times around the nucleosome core containing an octamer of 2 molecules each of histone proteins H2A, H2B, H3 and H4²⁵⁸. Nucleosomal DNA is further compacted by association with the linker histone H1 and other non-histone proteins^{258,274}. There are two types of chromatin, heterochromatin and euchromatin. Heterochromatin are condensed regions of the nucleus that do not decondense during interphase, are less susceptible to nuclease activity and contain few actively expressed genes. Whereas euchromatin decondenses upon exit of mitosis, is more open and accessible to nucleases and is rich in actively transcribing genes²⁵⁸.

The N-terminal tails of the histone proteins can be the target of post translational modifications such as acetylation, phosphorylation, methylation, sumoylation and ubiquitination²⁵⁸. Typically, histone acetylation and phosphorylation induce gene expression²⁵⁸ whereas histone methylation and deacetylation are associated with gene silencing. The lysine residues on histone tails can be acetylated by HATs and this a dynamic and reversible modification. It has been shown that the

acetylation of lysine residues in the tails of H3 and H4 results in the formation of bromodomains which associate with co activators such as TATA box binding protein (TBP), TBP associated factors, chromatin modifying enzymes and RNA polymerase II to promote gene expression²⁵⁸. Acetylation marks on histone tail lysine residues can be removed by HDACs and this is associated with gene silencing. To do this, HDACs interact with corepressor molecules such as nuclear receptor co-repressor 1 (NCoR), ligand-dependent co-repressor (LCoR), nucleosome remodelling deacetylase (NuRD) and the mammalian Sin3 transcriptional corepressor (mSin3) which aid in gene repression²⁵⁸. Histone methylation is deemed a more stable process than histone acetylation, it allows regulatory proteins to be recruited and it has been shown to be involved in the long term maintenance of expression status²⁵⁸. Lysine residues on histone tails can be mono, di or trimethylated whereas arginine residues are mono or dimethylated²⁵⁸. Furthermore, methylation of histone tails can either repress or activate transcription. Methylation of H3K9, H3K27, H3K79 and H4K20 are found to be associated with heterochromatin and gene silencing whereas methylation of H3K4 and H3K36 are associated with euchromatin and activated genes²⁵⁸.

There is evidence to suggest that DNA methylation and histone modifications work closely together to repress transcription²⁷⁵. Methylation of DNA is associated with the recruitment of DNMTs, methyl cytosine binding proteins, HDAC and HMTs which inhibit transcription factor binding by chromatin condensation and blocking the binding of the RNA polymerase complex^{275,276}.

1.4.1.3 Micro RNAs

MicroRNAs (miRNAs) are small single stranded non-coding RNAs that are around 22 nucleotides in length. miRNAs have been shown to target messenger RNAs (mRNAs) for cleavage resulting in translational repression²⁷⁷ and they have been shown to be linked to many cellular processes such as differentiation, growth and apoptosis²⁷⁸. miRNAs can be transcribed from intergenic regions of promoters or from an intronic part of a gene²⁷⁸. When intergenic, their expression is coordinated with other miRNAs as a cluster²⁷⁸ whereas when transcribed from an intronic region, they are often expressed from the same strand as their host gene²⁷⁸.

miRNAs are initially expressed as long transcripts which are processed in the nucleus to yield ~65 nucleotide RNA hairpin intermediates called pre-miRNAs²⁷⁹. This process involves an RNase III protein called 'Drosha' which excises the upper part of the primary miRNA hairpin to create the pre-miRNA intermediate²⁷⁹. The pre-miRNAs are exported out of the nucleus and into the cytoplasm by exportin-5²⁷⁹. In the cytoplasm the pre-miRNAs are processed by a RNase III protein called 'Dicer' to yield mature 22 nucleotide miRNAs²⁷⁹. The miRNA is then incorporated into the RNA induced silencing complex (*RISC*) to find appropriate mRNA targets²⁷⁹. miRNA needs to be

tightly regulated as aberrant regulation of miRNA expression or deficiency of miRNA biogenesis has been shown to be implicated in some cancers²⁸⁰.

1.4.1.4 Long non-coding RNAs

Long non-coding RNAs (lncRNAs) are mRNA like transcripts that range in length from 200 nucleotides to 100 kilobases (kb) which do not have an open reading frame²⁸¹. They have been shown to create repressive domains over large regions of the chromosome²⁵² and can mediate epigenetic changes by recruiting chromatin remodelling complexes to specific genomic loci²⁸². Furthermore, they have also been shown to be involved in developmental, tissue specific and disease processes such as X chromosome dosage compensation, germ cell development and embryogenesis, neural and immune cell development, kidney and testis development, B-cell neoplasia, lung cancer and prostate cancer²⁸³.

H19 is an example of a lncRNA which is involved in gene imprinting and it is expressed exclusively on the maternal allele however, loss of imprinting at the *H19* locus has been shown to result in high H19 expression in cancers of the oesophagus, colon, liver, bladder²⁸¹. Another lncRNA is antisense non-coding RNA in the *INK4* locus (*ANRIL*) which is transcribed by RNA pol II and processed into alternatively spliced isoforms. *ANRIL* is located on the *INK4b-ARF-INK4a* locus and has an important role in cell cycle control, cell senescence, stem cell renewal and apoptosis²⁸¹. SNPs within *ANRIL* have been shown to be associated with human diseases such as cancer and the locus is often deleted or hypermethylated in cancers such as leukaemia, melanoma, lung and bladder cancers²⁸¹.

1.4.2 Epigenetics and the early life environment

There is a growing body of evidence suggesting that the early life environment can influence the epigenome and the susceptibility to developing diseases in later life. Environmental cues during early development allow the fetus to adapt to the anticipated postnatal environment through epigenetic processes^{284,285}. These epigenetic modifications can induce phenotypic changes which have been shown to be associated with altered cardiovascular and metabolic homeostasis, growth and body composition, repair processes and longevity²⁸⁶. During evolution, the ability to adapt the phenotype to the prevailing environment provided a fitness advantage as environmental induction of different phenotypes from a single gene can occur quicker than mutations arising from evolution influenced by natural selection²⁶³. However, if the future environment is predicted incorrectly, this can result in a mismatch and an increased risk of developing diseases in later life. A mismatch can occur through poorer environmental conditions during pregnancy, or richer conditions in later life, or through both²⁸⁷. Poorer *in utero* conditions can be due to inaccurate nutritional cues from the mother or placenta during pregnancy²⁸⁸. It has also been shown that an unbalanced maternal diet

and body composition of the pregnant mother can result in poor oxygen supply, nutrients or an increased exposure to different hormones to the fetus resulting in poorer intrauterine conditions²⁶³. Whereas, a change in the later environment can be due to socioeconomic migration or through adapting to a more Western lifestyle where food is in abundance and levels of physical activity are low²⁸⁹.

There have been a number of studies on individuals who were exposed during their early life to the Dutch Hunger Winter in 1944-1945. These studies have shown that poor maternal nutrition during pregnancy, in this case undernutrition due to famine, can alter postnatal phenotype and increase the risk of developing diseases in later life. Furthermore, these studies found that the timing of exposure had a significant effect on disease progression in later life. Follow up studies in individuals who were exposed to the famine periconceptually and during late gestation measured DNA methylation in whole blood in 60 year old adults. Heijmans *et al.*, measured DNA methylation of insulin growth factor 2 (*IGF2*), which is a paternally imprinted gene that plays a key role in human growth and development, in 60 individuals who were exposed to famine and of their unexposed same sex siblings²⁹⁰. The study found that individuals who were periconceptionally exposed to the famine had lower methylation of the *IGF2* gene compared to their unexposed same sex siblings²⁹⁰. Nonetheless, there were no differences amongst individuals exposed during late gestation²⁹⁰. In another similar study, Tobi *et al.*, measured DNA methylation in 15 candidate genes which were shown to be related to metabolic disease and CVD²⁹¹. The study found that individuals exposed to famine during the periconceptional period had higher methylation in the *GNAS* antisense RNA (*GNASAS*), maternally expressed gene 3 (*MEG3*), interleukin 10 (*IL10*), ATP binding cassette subfamily A member 1 (*ABCA1*) and Leptin (*LEP*) proximal promoters and lower methylation in the insulin induced gene (*INSIGF*) promoter²⁹¹. Whereas individuals exposed to famine during late gestation had lower *GNASAS* promoter methylation compared to their unexposed same sex siblings and there were no significant differences in DNA methylation amongst the other genes²⁹¹. These studies suggest that the timing of constraint during early development is important and that it can influence which organ systems are affected²⁶⁹.

There have been a number of animal models which have been used to try and mimic human studies by altering maternal nutrition during pregnancy and weaning. One of the main animal studies that shows that the maternal diet during pregnancy can alter the phenotype of offspring can be seen in *agouti* mice^{292,293}. The methylation status of the *agouti* gene determine the phenotype in mice, where hypomethylation of the *agouti* gene promoter results in increased expression and mice develop a yellow coat and are obese whereas hypermethylation of the *agouti* gene promoter was associated with decreased expression and mice were of normal weight and with a brown coat^{292,293}. There have been studies where pregnant mice were fed a diet during pregnancy that was deficient

in methyl donors and cofactors including folic acid, betaine, choline and vitamin B12^{292–295}. The results showed that offspring were born with a yellow coat, had hypomethylation of the *agouti* gene promoter and increased prevalence of obesity and cancer^{292–295}. Lillycrop *et al.*, utilised a protein restricted rat model during pregnancy and measured methylation within the glucocorticoid receptor (*GR*) promoter of offspring²⁹⁶. The study found that maternal protein undernutrition during pregnancy resulted in hypomethylation of the *GR* promoter and upregulation of *GR* expression in offspring when compared to control rats²⁹⁶. Furthermore, the study found that expression of DNMT1 was also downregulated but there was no effect on hepatic DNMT3a or DNMT3b expression²⁹⁶. In another study by Lillycrop *et al.*, pregnant rats were fed a protein restricted diet together with either low folate or high folate²⁹⁷. DNA methylation of *PPARα* and *GR* were measured in pups 6 days after weaning and the study found that there was hypomethylation of *PPARα* and *GR* promoters and higher expression of both genes in protein restricted vs control pups²⁹⁷. However, the high folate diet was able to prevent these methylation and gene expression changes²⁹⁷. In a similar study by Lillycrop *et al.*, the effect of a maternal restricted diet during pregnancy on offspring health at 34 and 80 days after birth was investigated²⁹⁸. Methylation of the *PPARα* promoter was measured in liver tissue and the study found that offspring in the low folate protein restricted diet had lower mean *PPARα* methylation than control rats, whereas there was no difference between high folate protein restricted rats and the control²⁹⁸. Nonetheless, at individual CpG sites within the *PPARα* promoter, methylation was lower at specific individual CpG sites in the low folate protein restricted group, and higher at other CpG sites in the high folate protein restricted group compared to the control²⁹⁸. The study showed that prenatal nutrition induces differential changes in methylation of individual CpGs and these changes were observed in juvenile rats and were shown to persist into adulthood²⁹⁸.

1.4.3 Vitamin D and epigenetics

There is evidence to suggest that maternal vitamin D status during pregnancy is linked to altered epigenetic status of genes related to bone health in later life. A study in the SWS cohort by Harvey *et al.*, found that maternal free 25(OH)D₃ index was inversely associated with *RXRA* CpG methylation in umbilical cord tissue²⁹⁹. Furthermore, vitamin D deficiency during pregnancy has been shown to be associated with bone mineral accrual of the developing fetus.

Studies have shown that vitamin D regulates transcription of target genes, such as enzymes involved in the vitamin D pathway. Furthermore, the methylation status of these genes has been shown to differ in different tissue types and in either the presence or absence of 1,25(OH)₂D₃. 1,25(OH)₂D₃ binds to VDR and the VDR:RXRA dimer binds to VDREs in *CYP24A1* resulting in active transcription of the gene. The *CYP24A1* enzyme is involved in the 24-hydroxylation of both the

inactive and active forms of vitamin D however, the *CYP24A1* promoter has been shown to be differentially methylated in different tissue types³⁰⁰. In healthy kidney, skeletal muscle, whole blood, brain, skin fibroblasts and sperm the *CYP24A1* promoter is not methylated³⁰¹, in peripheral blood lymphocytes methylation was low around 5 %³⁰² whereas in placental tissue following delivery there was 56.6 % promoter methylation³⁰³. *CYP2R1* is an enzyme involved in the 25 hydroxylation of cholecalciferol to create 25(OH)D₃. A genome wide methylation scan found that the *CYP2R1* promoter was hypermethylated in individuals with severe vitamin D deficiency³⁰⁴ whereas in another study, following 12 months of vitamin D supplementation, post-menopausal women had hypomethylation of the *CYP2R1* promoter³⁰⁵.

Vitamin D has also been shown to be associated with epigenetic modifications in genes related to the WNT signalling pathway which plays an important role in osteoblast differentiation. A study in Canada measured promoter methylation of the WNT regulatory gene Dickkopf *WNT* signalling pathway inhibitor 1 (*DKK1*) and found that dietary vitamin D intake was inversely associated with methylation of *DKK1*³⁰⁶.

Some studies have found that 1,25(OH)₂D₃ is able to induce DNA demethylation however, the mechanism is unclear³⁰⁰ and it is unsure whether this is a passive process occurring over a few cycles of DNA replication or an active process occurring over 1-4 hours suggesting active demethylation³⁰⁷.

Vitamin D also has a role in gene silencing of *CYP27B1* which is the key enzyme involved in the 1 α hydroxylation of 25(OH)D₃ into the active form of vitamin D. This process involves deacetylation of histones and methylation of the gene promoter and exon regions³⁰⁰. *CYP27B1* has a nVDRE which can be bound by the VDR:RXRA dimer. In the absence of 1,25(OH)₂D₃, the VDR-interacting repressor (VDIR) is bound to the nVDRE and recruits histone acetyltransferases to induce *CYP27B1* transcription³⁰⁰. However, when 1,25(OH)₂D₃ is present, VDIR acts as a scaffold to recruit HDAC2, DNMT1 and DNMT3b resulting in repression of *CYP27B1* transcription³⁰⁰.

Together, these studies provide evidence that there is some interaction between vitamin D and epigenetic modifications of target genes.

1.4.4 Epigenetics and bone

Studies have shown that epigenetic changes can affect genes related to osteoblasts and osteoclasts, which can affect bone formation and subsequent bone health.

DNA methylation has been shown to play a role in key genes involved in mineralisation of the bone matrix. Delgado-Calle *et al.*, measured DNA methylation and expression of alkaline phosphatase in human cells of the osteoblastic lineage and found that methylation patterns varied amongst tissues

Chapter 1

and cell types¹⁰². The study found that in MG63 cells, alkaline phosphatase expression was low and DNA methylation was high whereas in human osteoblasts, alkaline phosphatase gene expression was high and DNA methylation was low¹⁰². The study found that microdissected osteocytes did not express alkaline phosphatase and their CpG island was highly methylated and lining osteoblasts had intermediate levels of methylation around 58 %¹⁰². Villagra *et al.*, investigated methylation of *Osteocalcin*, which is induced by osteoblasts in the late stages of differentiation, in rat osteosarcoma cells and found that during osteoblast differentiation there was chromatin remodelling of the *Osteocalcin* gene resulting in an increase in Osteocalcin expression³⁰⁸. Furthermore, this increase in transcription and expression was associated with reduced methylation of the *Osteocalcin* gene³⁰⁸.

Histone modifications have been shown to play a role in regulating transcription of key genes involved in bone matrix mineralisation and in determining the MSC lineage into either osteoblasts or adipocytes. Hassan *et al.*, investigated the transcription factor Homeobox A10 (HOXA10) and its effect on chromatin remodelling and histone modifications in osteoblastic cells. The study found that *BMP2* induces HOXA10 which activates *Runx2* and other osteoblastic genes such as *alkaline phosphatase*, *Osteocalcin* and *bone sialoproteins*³⁰⁹. *In vitro* studies using small interfering RNA (siRNA) knockdown showed that HOXA10 mediates chromatin hyperacetylation and H3K4 methylation of these genes resulting in chromatin remodelling and gene transcription³⁰⁹. Hemming *et al.*, investigated the role of two histone modifying proteins, enhancer of Zeste 2 polycomb repressive complex 2 subunit (EZH2) and lysine demethylase 6A (KDM6a), and their role in MSC differentiation³¹⁰. EZH2 is a methyltransferase which trimethylates histone 3 lysine 27 resulting in gene silencing whereas the methyl groups can be removed by KDM6a resulting in gene transcription³¹⁰. Within the study, EZH2 was overexpressed in human bone marrow derived MSCs which promoted adipogenesis and inhibited osteogenic differentiation. Whereas overexpression of KDM6a inhibited adipogenesis and promoted osteogenic differentiation *in vitro*³¹⁰. Conversely, inhibition of either EZH2 or *KDM6a* had the opposite effect on adipogenesis and osteogenesis. Therefore, the study found that trimethylation of H3K27 by EZH2 or demethylation of H3K27me3 by KDM6a could dictate MSC lineage determination³¹⁰.

Both osteoblasts and adipocytes are derived from MSCs and studies have shown that miRNAs can influence lineage differentiation in MSCs⁵⁹. Huang *et al.*, found that miRNA22 regulates adipogenic and osteogenic differentiation in human adipose tissue derived MSCs³¹¹. The study found that there was a decrease in miRNA22 during adipogenic differentiation and an increase during osteogenic differentiation³¹¹. Furthermore, following overexpression of miRNA22 there was repression of adipogenic differentiation and promotion of osteogenic differentiation³¹¹. miRNA22 was also found to target HDAC6, which is a corepressor of *Runx2*³¹¹, and that silencing endogenous HDAC6

expression enhanced osteogenesis but repressed adipogenesis³¹¹. Li *et al.*, showed that miRNAs play a role in osteogenesis, either enhancing or impeding osteogenic differentiation⁵⁹. They found that miRNA17p and miRNA106a were post transcriptional regulators of osteogenic and adipogenic differentiation and directly targeted BMP2⁵⁹.

Studies have shown that lncRNAs play a role in osteoblast differentiation. Zuo *et al.*, induced osteoblast differentiation in murine MSCs with BMP2. Following this, an Arraystar microarray looked at the expression of lncRNAs between the BMP2 and untreated group. The study found that there were 116 differentially expressed lncRNAs between the BMP2 and untreated group, of which 59 were upregulated and 57 were downregulated in the BMP2 treated group³¹². Zhu *et al.*, found that the lncRNA Angelman syndrome chromosome region (ANCR) plays a role in osteoblast differentiation and that ANCR- siRNA blocks of the expression of endogenous ANCR in human fetal osteoblastic hFOB1.19 cells and results in osteoblast differentiation whereas ANCR overexpression inhibits osteoblast differentiation³¹³. The study also showed that ANCR is associated with EZH2 which results in inhibition of *Runx2* and osteoblast differentiation³¹³.

1.5 Epigenetic biomarkers of later health

A biomarker is described as “a characteristic that can be objectively measured and evaluated as an indicator of a physiological as well as a pathological process or pharmacological response to a therapeutic intervention”³¹⁴. Studies have shown that the early life environment can alter the epigenome and predict the disease risk in later life. Therefore, it would be useful to be able to detect these marks in early life which would allow for suitable interventions to increase the chances of a better health outcome.

DNA methylation is an example of a relatively stable, heritable epigenetic mark which can be easily measured in patient samples at a single locus or at multiple genomic regions to predict disease risk in later life. Clarke-Harris *et al.*, have shown that some epigenetic marks are stable during early childhood. DNA methylation was measured within the Peroxisome proliferator-activated receptor gamma coactivator 1-alpha (*PGC1α*) promoter and the results showed that methylation of these CpG sites were maintained in males from 5-14 years of age³¹⁵. Conversely, some studies have shown that methylation marks can be dynamically regulated, such as following acute bursts of physical exercise. Barrès *et al.*, measured DNA methylation in skeletal muscle biopsies from healthy sedentary men and women. The study found that following exercise there was decreased whole genome methylation and decreased methylation within the *PGC1α*, pyruvate dehydrogenase kinase 4 (*PDK4*) and *PPARγ* promoters which was associated with increased expression of these genes³¹⁶. Similarly, Wong *et al.*, measured DNA methylation in monozygotic and dizygotic twins in

buccal cell samples between the ages of 5 and 10 years and found that DNA methylation was highly dynamic in a range of genes including Dopamine Receptor D4 (*DRD4*), Monoamine oxidase A (*MAOA*) and Sodium-dependent serotonin transporter (*SLC6A4*)³¹⁷. It can be argued that a suitable biomarker should be stable throughout the life course and genes which can be dynamically regulated should be excluded. However, the biomarker does not need to be associated with the outcome at the point that you measure the biomarker in order to be used as risk prediction. For example, if a biomarker measured at birth is predictive of adult bone health, it is not required that the same biomarker is measured during adulthood and the associations should persist.

Ideally, a biomarker would be measured in human tissues central to the pathogenesis of the disease however, in most cases this is not possible. A suitable epigenetic biomarker would be measured in easily accessible tissues although this poses a problem as epigenetic marks can be tissue specific³⁰³. Woodfine *et al.*, measured DNA methylation of imprinted genes in human adult brain, breast, colon, heart, kidney, liver, placenta, testis and blood and found that DNA methylation was stable in germ line differentially methylated regions (DMRs) and paternally methylated somatic DMRs however, there was greater variance in maternally methylated somatic DMRs³¹⁸. Lu *et al.*, measured DNA methylation of 5 genes and found that methylation values were stable and similar in 24 cell lines from 13 human tissue types³¹⁹. The genes measured were NEDD4 binding protein 2 (*N4BP2*), epidermal growth factor-like protein 8 (*EGFL8*), chymotrypsinogen B1 (*CTRB1*), tetraspanin 3 (*TSPAN3*) and zing finger protein 690 (*ZNF690*) and the human tissue types included cell lines derived from brain, breast, lung and colon³¹⁹. Murphy *et al.*, measured DNA methylation in adrenal gland, brain, eye, gonad, heart, intestine, kidney, liver, spleen, lung, muscle, pancreas, thymus, placenta and umbilical cord and found that methylation of *H19*, mesoderm specific transcript (*MEST*), sarcoglycan epsilon (*SGCE*)/ paternally expressed gene 10 (*PEG10*) were similar across all of these tissues but there was some variation in DNA methylation of other genes³²⁰.

Conversely, studies have shown that DNA methylation of proxy tissues such as umbilical cord tissue can be predictive of later health outcomes, despite the lack of using a tissue central to the pathogenesis of the disease being investigated. Godfrey *et al.*, measured *RXRA* DNA methylation in umbilical cord tissue and found a strong association with adiposity in later childhood³²¹ and methylation of this CpG explained over 25 % of the variance in the age and sex adjusted fat mass data²⁵². Lillycrop *et al.*, measured DNA methylation of cyclin dependent kinase inhibitor 2A (*CDKN2A*) in umbilical cord tissue and found an inverse association with adiposity measures in later childhood, as well as being consistently associated with cardiovascular disease³²². Clarke-Harris *et al.*, measured DNA methylation of the *PGC1 α* promoter in blood from children between the ages of 5 to 14 years and found that methylation of these loci were stable and that DNA methylation at four loci was able to predict adiposity during childhood up to 14 years of age independent of sex,

age and the onset of puberty³¹⁵. Therefore, these studies suggest that detection of these epigenetic marks at birth, even in peripheral tissues, can be used to predict future disease risk.

1.5.1 Epigenetic biomarkers of later bone health

The early life environment has been shown to alter DNA methylation which has been shown to be associated with disease risk in later life. Therefore, in this thesis, we are interested in identifying suitable candidate biomarkers which respond to an early life intervention and can be used to predict bone health in later life. Amongst the current literature, studies within the SWS and Princess Anne Hospital (PAH) cohort have investigated DNA methylation in umbilical cord of candidate biomarkers and have found associations with bone health in childhood^{299,323}. These candidate biomarkers include DNA methylation of specific CpGs upstream of the *RXRA* promoter and within the first intron of *CDKN2A*^{299,323}. Initially, these candidate biomarkers were chosen with respect to associations with adiposity in later childhood^{321,322} however, given that adipose cells and osteoblastic cells are both derived from MSCs and that body fat mass and lean mass have been shown to be predictive of BMD, this led to further investigation with respect to bone health.

1.5.1.1 *RXRA*

RXRA belongs to the nuclear receptor superfamily containing ligand activated transcription factors^{324,325}. There are 3 isoforms of *RXRA*: α , β and γ and they are all activated by 9-cis retinoic acid (RA)^{324,325}. *RXRA* is able to form homodimers and heterodimers with other steroid hormones such as VDR, thyroid receptor (TR)³²⁶, PPAR³²⁷ etc. and therefore, *RXRA* plays an important role in a number of different signalling pathways, such as in fetal development and the epigenetic regulation of vitamin D activation³²⁸. *RXRA* binds to response elements in target genes and the binding site depends on the *RXRA* partner. RXRs have 5 distinct regions including the ligand binding domain (LBD) and the DNA binding domain (DBD) which is responsible for recognising core motifs on response elements³²⁹. Most of the binding sites contain a direct repeat of two consensus core motifs of AGGTCA with a spacer varying from 1 to 5 base pairs (DR1-5)³³⁰. Heterodimerisation with VDR requires 3 base pairs between the core motifs (DR3) whereas for the TR there are 4 base pairs (DR4). Upon ligand binding, *RXRA* and VDR dimerise and bind to VDREs in target genes^{331,332}. Binding to positive VDREs such as those present in *CYP24A1* result in gene transcription whereas binding to nVDREs, such as in *CYP27B1*, results in gene repression¹⁵². Staal *et al.*, have shown that the *RXRA*:VDR heterodimer binds to VDREs in *Osteocalcin* and *Osteopontin* which encode major non-collagenous proteins that contribute to bone formation and resorption³³³. MAFB is a corepressor of several osteoclastic transcription factors and studies have shown that MAFB expression is downregulated during osteoclastogenesis³³⁴. Menéndez-Gutiérrez *et al.*, used a hematopoietic

Chapter 1

specific *RXR* deficient mouse model to show that *RXR* is involved in osteoclast proliferation, differentiation and activation through controlling regulation of the transcription factor MAFB in osteoclast progenitor cells³³⁵. The study found that mice had larger, non-resorbing osteoclasts and increased bone mass in male mice and that under basal physiological conditions, MAFB is a target of the *RXR* homodimer in osteoclast progenitor cells³³⁵.

Studies within the SWS and PAH cohort initially identified DNA methylation of *RXRA* as a candidate biomarker of adiposity measures in later childhood³²¹ however, due to the common precursor between adipocytes and osteoblasts, it was further investigated with respect to bone measures in childhood²⁹⁹. 15 randomly selected umbilical cords from the PAH study underwent methylation specific chromatin precipitation followed by hybridisation to an oligomer microarray of 24,134 human genes and of these genes, a panel of 78 were selected and analyses identified 5 candidate genes which showed evidence of correlation between overall gene methylation status and DXA measurements of adiposity at age 9³²¹. These 5 candidate genes included *RXRA*, endothelial nitric oxide (*eNOS*), superoxide dismutase-1 (*SOD1*), interleukin-8 (*IL8*) and phosphoinositide-3-kinase, catalytic, δ -polypeptide (*PI3KCD*)³²¹. The results showed that within the PAH study, methylation of cord *RXRA* and *eNOS* were positively associated with childhood fat mass and percentage fat mass³²¹. Whereas in the SWS cohort, cord *RXRA* methylation was positively associated with childhood fat mass and percentage fat mass but there were no significant associations with *eNOS*³²¹. Next, Harvey *et al.*, investigated associations between *RXRA* CpG methylation in umbilical cord with bone measures at 4 years of age within the SWS cohort²⁹⁹. The study found that that there was an inverse association between *RXRA* methylation in umbilical cord tissue and scBMC at age 4 however, there were no associations with BA, BMC or BMD at age 4²⁹⁹. The study also found that there was an inverse association between maternal free vitamin D index in late gestation, which is the ratio of serum 25(OH)D₃ to vitamin D binding protein concentrations, with *RXRA* methylation in umbilical cord tissue²⁹⁹. Harvey *et al.*, sought to replicate these findings in a second cohort, using participants from the PAH study however, there were no significant associations between *RXRA* methylation in umbilical cord tissue and bone measures at age 9²⁹⁹.

Therefore, *RXRA* has been shown to play an important role in pathways related to vitamin D as well as other signalling pathways depending on the dimerisation partner. Furthermore, studies have identified DNA methylation of *RXRA* in umbilical cord tissue as a candidate biomarker for later health with regards to adiposity and bone mass in childhood^{299,321}.

1.5.1.2 CDKN2A

CDKN2A is a gene which encodes two tumour suppressor proteins, p14^{ARF} and p16^{INK4a}, and the long non coding RNA ANRIL³²². Both p16^{INK4a} and p14^{ARF} play a role in cellular senescence and ageing^{322,336,337}. p16^{INK4a} is negatively regulated by ANRIL and inhibits cyclin dependent kinase 4 (CDK4) and CDK6 activity which have been shown to regulate the retinoblastoma (Rb)-retinoblastoma-associated protein 1 (E2F) axis and cell cycle progression^{322,338–341}. The Rb tumour suppressor protein regulates cell proliferation by binding to transcription factors such as E2Fs and preventing genes required for S phase from being transcribed^{338,339}. Phosphorylation of Rb at late G1 phase by CDK4/6 results in the release of these transcription factors that are needed for cell cycle progression and entry into S phase^{338,339}. p16^{INK4a} inhibits CDK4/6 from phosphorylating retinoblastoma family members which promotes binding of E2F and results in a G1 cell cycle arrest³³⁶. MDM2 is a proto-oncogene involved in the rapid degradation of the tumour suppressor protein, p53, maintaining low concentrations and allowing cell cycle progression. p14^{ARF} has been shown to bind to and inactivate MDM2 which results in the accumulation of p53 and cell cycle arrest^{322,336,342,343}.

SNPs within *ANRIL* have been shown to be associated with cardiovascular disease, diabetes and frailty³⁴⁴. Cheng *et al.*, found that ANRIL was upregulated in osteosarcoma tissues and promoted the proliferation of metastasis of osteosarcoma cells and *in vitro* knockdown studies of *ANRIL* found that there was reduced osteosarcoma cell proliferation, invasion and migration³⁴⁵. As *CDKN2A* encodes tumour suppressor proteins, studies have shown that the *CDKN2A* locus has been deleted in a range of tumours including melanoma, pancreatic adenocarcinoma, glioblastoma and bladder carcinoma³³⁶. A study on giant cell tumour of bone, which is a type of benign bone tumour, found that there was downregulation of *CDKN2A* expression and an increase in *CDKN2A* promoter methylation compared to normal bone tissue³⁴⁶. Mohseny *et al.*, found that there is genomic loss of *CDKN2A* in osteosarcoma³⁴⁷ and Nielsen *et al.*, found that some osteosarcoma patients, with mutations in the *Rb* gene and inactivation of the Rb protein, also had loss of p16^{INK4a} expression and some had homozygous *CDKN2A* deletions³⁴⁸.

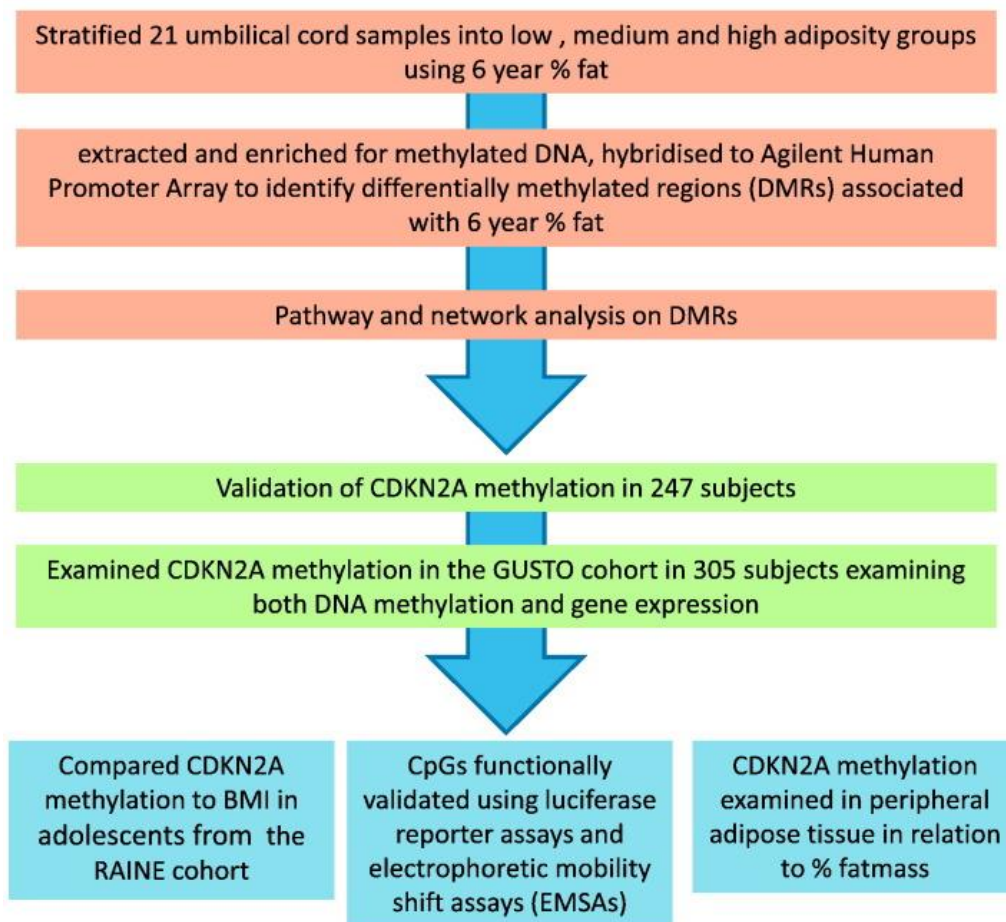
Similar to *RXRA*, DNA methylation of *CDKN2A* was first investigated with respect to adiposity in later childhood³²². Lillycrop *et al.*, quantified DNA methylation levels from 21 umbilical cords from children within the SWS cohort using the Agilent Human Promoter Whole-Genome ChIP-on-chip array and a basic overview can be seen in **Figure 1.19**³²². The umbilical cords were selected to represent children at age 6 with percentage fat measurements between the 5th and 95th percentiles³²². Data from the whole genome methylation array was analysed using BATMAN (Bayesian Tool for Methylation Analysis) which identified 93 differentially methylated regions³²².

Chapter 1

Following this, gene pathway analysis identified DNA replication and repair as the top pathway which was enriched amongst 41 of the 93 identified DMRs³²². Within this pathway were DMRs associated with *CDKN2A* therefore, Lillycrop *et al.*, investigated associations between DNA methylation of *CDKN2A* in umbilical cord with childhood adiposity³²². Within the SWS cohort, there was an inverse association between *CDKN2A* methylation in umbilical cord tissue and total fat mass and percentage fat mass at 4 and 6 years of age³²² however, there were no associations between *CDKN2A* methylation in umbilical cord tissue and adiposity measurements taken at birth³²². Next, due to the common lineage of adipocytes and osteoblasts, *CDKN2A* methylation in umbilical cord tissue was investigated with respect to bone measures in childhood using participants from the SWS cohort³²³. The study found that there was an inverse association between *CDKN2A* methylation in umbilical cord tissue and BA, BMC and BMD at 4 and 6 years of age³²³.

Therefore, DNA methylation of these CpG sites in umbilical cord could be used as a biomarker which is predictive of bone outcomes in later childhood. This would help to identify individuals at risk of potentially not achieving their peak bone mineral density in early adulthood, which has been shown to be causally related to fracture risk in later adulthood³⁴⁹, allowing for suitable interventions during early childhood which could have a beneficial impact on the peak bone mineral density trajectory. This would help to aid in the delay of onset of osteoporosis, which is associated with morbidity and mortality in the ageing population⁷.

(A)



(B)

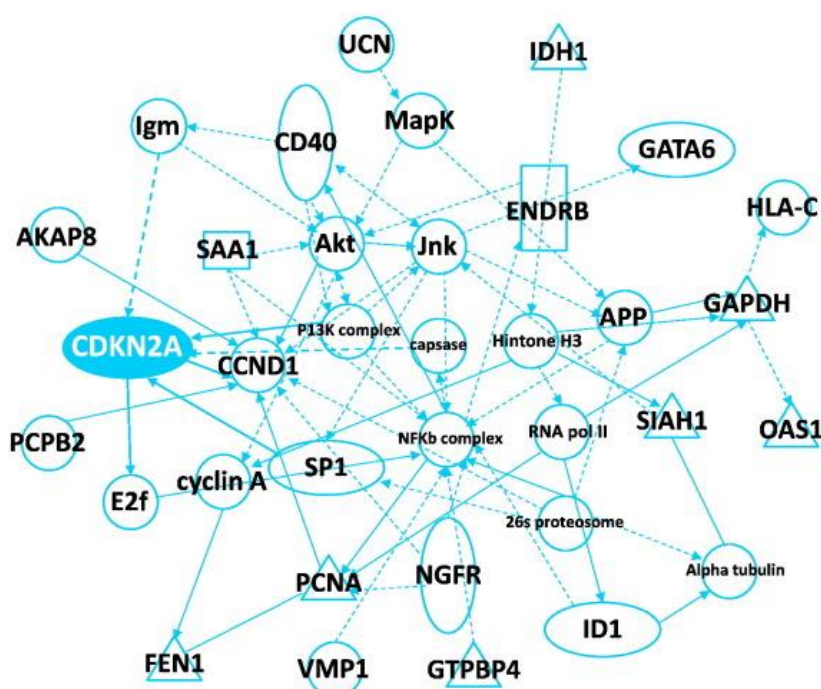


Figure 1.19 Overview of identifying *CDKN2A* CpG methylation as a candidate biomarker for adiposity in later childhood³²².

1.6 Aims and Hypotheses

Osteoporosis is a major burden to the ageing population, not only due to the morbidity and mortality associated, but also due to the high economic cost to the healthcare system². There are a number of factors which can increase the risk of developing osteoporosis and one of the main considerations is the magnitude of peak bone mass in early adulthood, where an increase in peak bone mass has been shown to delay the onset of osteoporosis²⁹. There are a number of factors which can influence peak bone mass and we are particularly interested in maternal nutrition during the early life environment. There are conflicting studies on whether maternal vitamin D status is associated with fetal skeletal development, nonetheless studies have shown correlation between maternal vitamin D status during pregnancy and bone measures in childhood²³⁹. The early life environment has been shown to induce alterations to DNA methylation which influence phenotypes such as bone outcomes in later life²⁵². There is also mounting evidence to suggest that epigenetic marks can be detected during early infancy and can act as a biomarker to identify individuals with an increased risk of developing diseases such as osteoporosis in later life^{299,323}. This would identify suitable interventions, either during the early life environment or during early infancy in these at-risk individuals, with the hope to improve future health outcomes. Causality is not required for risk prediction and whether these methylation changes are causally involved in the aetiology of osteoporosis and bone development, or whether they are simply a marker of bone health is currently unknown. If a biomarker is causally involved, interventions could be designed to target changes to DNA methylation which would subsequently alter bone outcomes. Whereas if DNA methylation is a marker of bone health, interventions could target bone health to be the primary outcome and DNA methylation could be measured to either predict future disease risk, or to be reflective of the current bone state. Studies within the SWS cohort have independently identified inverse associations between DNA methylation at birth, within *RXRA*²⁹⁹ and *CDKN2A*³²³, and bone measures in later childhood. Randomised controlled trials, such as the MAVIDOS trial which has been shown to improve bone outcomes amongst infants born in the winter months, allow investigation into the relationship between DNA methylation, the early life environment and bone health. Furthermore, this could help to provide an insight into disease progression in adulthood and the risk of developing osteoporosis in later life.

A concept flow diagram can be seen in **Figure 1.20**. We hypothesised that maternal vitamin D supplementation during pregnancy will be causally linked to decreased DNA methylation of candidate genes which will be inversely associated with bone measures at birth and in later life. To test this, within **Chapters 3-5**, DNA methylation of candidate genes will be measured in umbilical cord and placental tissue using participants from the MAVIDOS trial where mothers were supplemented with 1000 IU/d cholecalciferol or placebo during pregnancy, and bone measures

were recorded at birth. We hypothesised that maternal vitamin D supplementation during pregnancy will be associated with decreased methylation of *RXRA*, *CDKN2A*, *Runx2* and *Osterix* in umbilical cord tissue and this will be inversely associated with bone measures recorded at birth. In **Chapter 3** we hypothesise that there will be similar findings with respect to *RXRA* methylation in placental tissue. Within **Chapter 6**, we investigated the functional importance of the *RXRA* CpGs of interest to determine whether there were any causal mechanisms involved between vitamin D treatment, DNA methylation and *RXRA* promoter activity within two osteosarcoma cell lines. We hypothesised that individual CpGs upstream of the *RXRA* promoter are functionally important for *RXRA* expression and to the response to vitamin D supplementation. Within **Chapter 7**, we wanted to investigate whether a maternal vitamin D deficient diet in pregnant mice resulted in altered DNA methylation in tibiae from adult offspring. Furthermore, we wanted to investigate the effect of mechanical loading on DNA methylation with respect to maternal vitamin D intake which could be analogous to walking or exercise in humans. We hypothesised that a maternal vitamin D deficient diet during pregnancy would be linked to increased *RXRA*, *VDR*, *Runx2* and *Osterix* methylation in adult tibiae and that mechanical loading would decrease DNA methylation of these candidate genes.

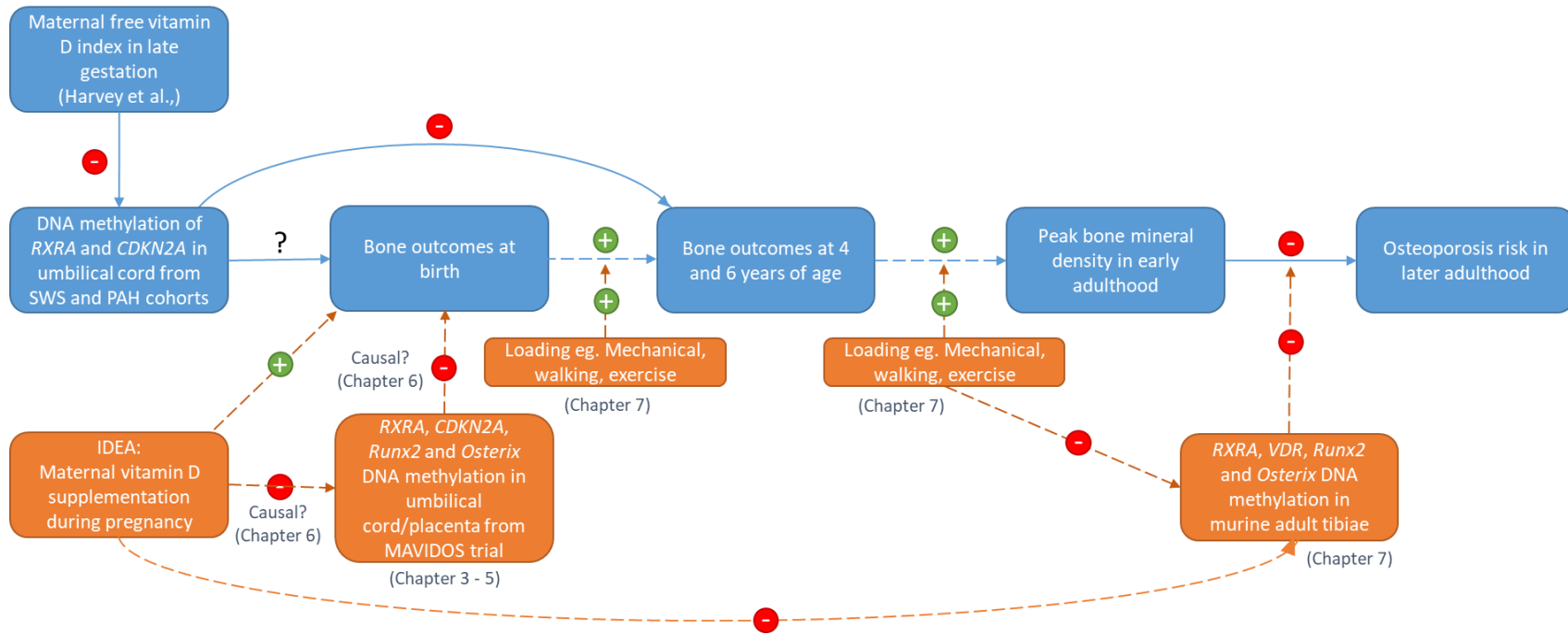


Figure 1.20 Concept flow diagram.

The specific aims of my project are:

Chapters 3 - 5:

1. Determine whether maternal vitamin D supplementation alters DNA methylation of *RXRA*, *CDKN2A*, *Runx2* and *Osterix* in umbilical cord tissue within the MAVIDOS trial
2. Determine associations between *RXRA*, *CDKN2A*, *Runx2* and *Osterix* methylation at birth in umbilical cord tissue, and bone measures at birth within in the MAVIDOS trial
3. Determine whether vitamin D supplementation is linked to altered *RXRA* methylation in placental tissue (**Chapter 3** only)

Chapter 6:

1. Determine the functional importance of the identified *RXRA* CpG dinucleotides that are predictive of bone measures in childhood on *RXRA* promoter activity in osteosarcoma cell lines, and to investigate whether it is part of a causal pathway
2. Identify specific transcription factor binding across the *RXRA* CpGs of interest

Chapter 7:

1. Determine whether a maternal vitamin D deficient diet is linked to altered DNA methylation of *RXRA*, *VDR*, *Runx2* and *Osterix* in adult tibiae
2. Determine whether mechanical loading is linked to altered DNA methylation of *RXRA*, *VDR*, *Runx2* and *Osterix* in adult tibiae

Chapter 2 Materials and Methods

2.1 Materials

Table 2.1 Reagents used in experiments.

Reagent	Details
10x Tris-Borate-EDTA Buffer (TBE)	Fisher Scientific, #T/P050/15
1 α ,25-dihydroxyvitamin D ₃	Enzo Life Sciences, #BML-DM200-0050
3,3',5-Triiodo-L-thyronine sodium salt (T3)	Sigma, #T6397
4-(2-Hydroxyethyl)-1-Piperazineethanesulfonic Acid (HEPES)	Sigma Aldrich, #H4034
40% Acrylamide Solution	Fisher Scientific, #BPE1402-1
Agar	Fisher Scientific, #BP1423
Agarose	Melford, #MB1200
Ammonium Persulfate (APS)	Fisher Scientific, #BPE179-25
Ampicillin	Sigma Aldrich, #A9393
Antarctic Phosphatase	New England Biolabs, #M0289S
ATP, [γ - ³² P]	Perkin Elmer, #BLU002A250UC
BCA Protein Assay Kit	Fisher Scientific, #23227
BlueJuice Gel Loading Buffer 10X	Invitrogen, #10816015
Carestream® Kodak® autoradiography GBX developer/replenisher	Sigma-Aldrich, #P7042
Carestream® Kodak® processing chemicals for autoradiography films GBX fixer/replenisher	Sigma-Aldrich, #P7167
Chloroform	Fisher Scientific, #10102190
CL-XPosure™ Film	Thermo Scientific, #34088
CpG Methyltransferase (M.SssI)	New England Biolabs, #MO226S
CpGenome Universal Methylated DNA	Millipore, #S7821
Deoxynucleotide Triphosphates (dNTPs)	Promega, #U1420
Dithiothreitol (DTT)	Melford, #MB1015
DNase 1 Amplification Grade Kit	Sigma Aldrich, #AMPD1
DNase and RNase free water, DEPC treated	Fisher Scientific, #BPE561-1
Dual-Luciferase® Reporter Assay System	Promega, #E1910
Dulbecco's Modified Eagle Medium (DMEM)	PAA, #E15-843
Dulbecco's Modified Eagle Medium (DMEM)/ Ham's F-12	Gibco, #11320-074
EpiTect Control DNA (1000) Unmethylated human control DNA	Qiagen, #59665
Ethanol 99%+	Fisher Scientific, #E/0600/05

Chapter 2

Reagent	Details
Ethylenediaminetetraacetic Acid Disodium Salt (EDTA)	Sigma Aldrich, #03690
EZ DNA methylation gold kit (2x96)	Cambridge Bioscience, #D5007
FastDigest AseI (VspI)	Fisher Scientific, #FD0914
FastDigest BsaI (Eco31I)	Fisher Scientific, #FD0294
FastDigest DpnI	Fisher Scientific, #FD1704
FastDigest HindIII	Fisher Scientific, #FD0504
FastDigest KpnI	Fisher Scientific, #FD0524
FastDigest SphI (PaeI)	Fisher Scientific, #FD0604
FastDigest XhoI	Fisher Scientific, #FD0694
Fetal Bovine Serum	PAA, #A15-151
Ficoll 400	Sigma-Aldrich, #F9378
FuGENE 6 Transfection Reagent	Promega, #E2691
Gelatin	Fisher Scientific, #G1393
GelRed Nucleic Acid Stain 10,000X	Cambridge Bioscience, #BT41003
GeneJet Plasmid Midiprep Kit	Fisher Scientific, #K0481
GeneJET Plasmid Miniprep Kit	Fisher Scientific, #10242490
GenElute Mammalian Genomic DNA Miniprep Kit	MERCK, #G1N350
Glycerol	Sigma Aldrich, #G6279
HotStarTaq DNA Polymerase	Qiagen, #203205
Human Osteosarcoma SaoS-2 Cell Line	Cell Lines Service, #36025
Hyaluronidase	Sigma Aldrich, #H3506
Igepal CA-630	Sigma Aldrich, #I8896
illustra™ MicroSpin™ G-50 Columns	GE Healthcare, #27-5330-01
Isopropanol	Fisher Scientific, #11398461
JM109 Competent cells	Promega, #L2001
Leupeptin Hemisulfate Salt	Sigma Aldrich, #L5793
L-Glutamine	Sigma-Aldrich, #G7513
Lipofectamine 3000	Life Technologies, #L3000008
Luria Bertani Broth (LB)	Sigma Aldrich, #L3022
Mesenchymal Stem Cells from human umbilical cord	ATCC, #PCS-500-010
MG63 cells	Cell Lines Service, #300441
M-MLV Reverse Transcriptase Kit	Promega, #M1701
Monarch PCR and DNA Cleanup Kit	New England Biolabs, #T1030S
Opti-MEM Medium	Invitrogen, #31985062
Penicillin-Streptomycin	PAA, #P11-010
pGL4.17 Vector	Promega, #E6721
pGL4.23 Vector	Promega, #E8411
Phenol	Life Technologies, #15509-037
Phenylmethanesulfonyl Fluoride (PMSF)	Sigma Aldrich, #P7626
Phosphate Buffered Saline (PBS) Tablets	Fisher Scientific, #12821680

Reagent	Details
Phusion High Fidelity Polymerase	New England Biolabs, #MO531S
Poly(deoxyinosinic-deoxycytidylic) Acid	
Sodium Salt (Poly DIDC)	Sigma Aldrich, #P4929
Potassium Chloride (KCl)	Sigma Aldrich, #P9541
pRL-CMV Vector	Promega, #E2261
Promega Human Genomic DNA	Promega, #G3041
Proteinase K	Qiagen, #19131
PyroMark Annealing Buffer	Qiagen, #979009
PyroMark Binding Buffer	Qiagen, #979006
PyroMark Gold Q96 Reagents	Qiagen, #972804
PyroMark Wash Buffer	Qiagen, #979008
QIAmp DNA Mini Kit	Qiagen, 51304
Quantitect Primer Assay CYP24A1	Qiagen, #QT00015428
Quantitect Primer Assay GAPDH	Qiagen, #QT00079247
Quantitect Primer Assay Osterix	Qiagen, #QT00213514
Quantitect Primer Assay Runx2	Qiagen, #QT00020517
Quantitect Primer Assay RXRA	Qiagen, #QT00005726
Quantitect Primer Assay VDR	Qiagen, #QT01010170
QuantiTect SYBR Green PCR Mastermix	Qiagen, #204143
Quick Blunting Kit	New England Biolabs, #E1201S
Quick Ligation™ Kit	New England Biolabs, #M2200S
Random Nonamers	Sigma Aldrich, #R7647
RNase A	Qiagen, #19101
Roche DNA	Sigma, #11691112001
SequalPrep Long PCR Kit with dNTPs	Fisher Scientific, #A10498
SOC media	Sigma, #S1797
Sodium Acetate Solution	Sigma Aldrich, #S8388
Sodium Chloride	Sigma Aldrich, #S3014
Sodium Hydroxide (NaOH)	Sigma Aldrich, #S5881
Streptavidin Sepharose Beads	Fisher Scientific, #GZ17511301
T4 Polynucleotide Kinase (100u)	Promega UK, #M4101
Tetramethylethylenediamine (TEMED)	Sigma Aldrich, #T7024
Tri Reagent	Sigma Aldrich, # T9424
Tris Base	Sigma Aldrich, #T6791
Tris-acetate-EDTA (TAE) solution 50X	Fisher Scientific, #BPE1332-1
Trypsin EDTA	PAA, #L11-004
Whatman Chromatography Paper	Fisher Scientific, #11939197
Zymoclean Gel DNA Recovery Kit	Cambridge Bioscience, #D4001

2.2 Methods

2.2.1 Cohorts

2.2.1.1 MAVIDOS study

The MAVIDOS (Maternal Vitamin D Osteoporosis Study) trial is a randomised, double blind, placebo controlled trial which took place at three trial centres in Southampton, Sheffield and Oxford²³⁵. The study was approved by the Southampton and South West Hampshire Research Ethics Committee (ISRCTN82927713, registered on 11th April 2008). Pregnant women were recruited when attending their 12 week ultrasound scans and were randomly assigned at 14 weeks gestation to 1000 IU/day of cholecalciferol or a placebo until delivery. Prior to randomisation, screening blood tests determined maternal serum 25(OH)D₃ levels and calcium levels. Pregnant women aged over 18 years, with a singleton pregnancy less than 17 weeks gestation, with serum 25(OH)D₃ levels between 25-100 nmol/L and calcium levels below 2.75 mmol/L were eligible to enrol in the study. Interviewer led questionnaires at 14 and 34 weeks gestation assessed parity, baseline demographics, smoking, alcohol intake, calcium and vitamin D dietary intake, exercise, health, sunlight exposure and medication. Anthropometric measures including height, weight, grip strength and skinfold thicknesses at triceps, biceps, subscapular and suprailiac sites were measured. Maternal blood samples were obtained for measurement of 25(OH)D₃, vitamin D binding protein, calcium, bone specific alkaline phosphatase and albumin. Pregnant women underwent a high resolution 3D ultrasound scan and an NHS anomaly scan between 18-21 weeks gestation and a further growth and 3D ultrasound scan was repeated at 34 weeks gestation. At birth, venous cord blood and umbilical cord and placental tissue were collected. At birth, neonatal anthropometric indices were measured including length, weight, skinfold thickness, head circumference and abdominal circumference. Neonates underwent a DXA scan to assess bone density within 14 days of birth using a densitometer [Hologic Discovery instrument using paediatric software (Hologic Inc., Bedford, MA, USA)]. The DXA scan measured whole body and lumbar spine bone area, bone mineral content and bone mineral density. Children underwent yearly follow up assessments and repeat DXA measurements were taken at 4 years of age.

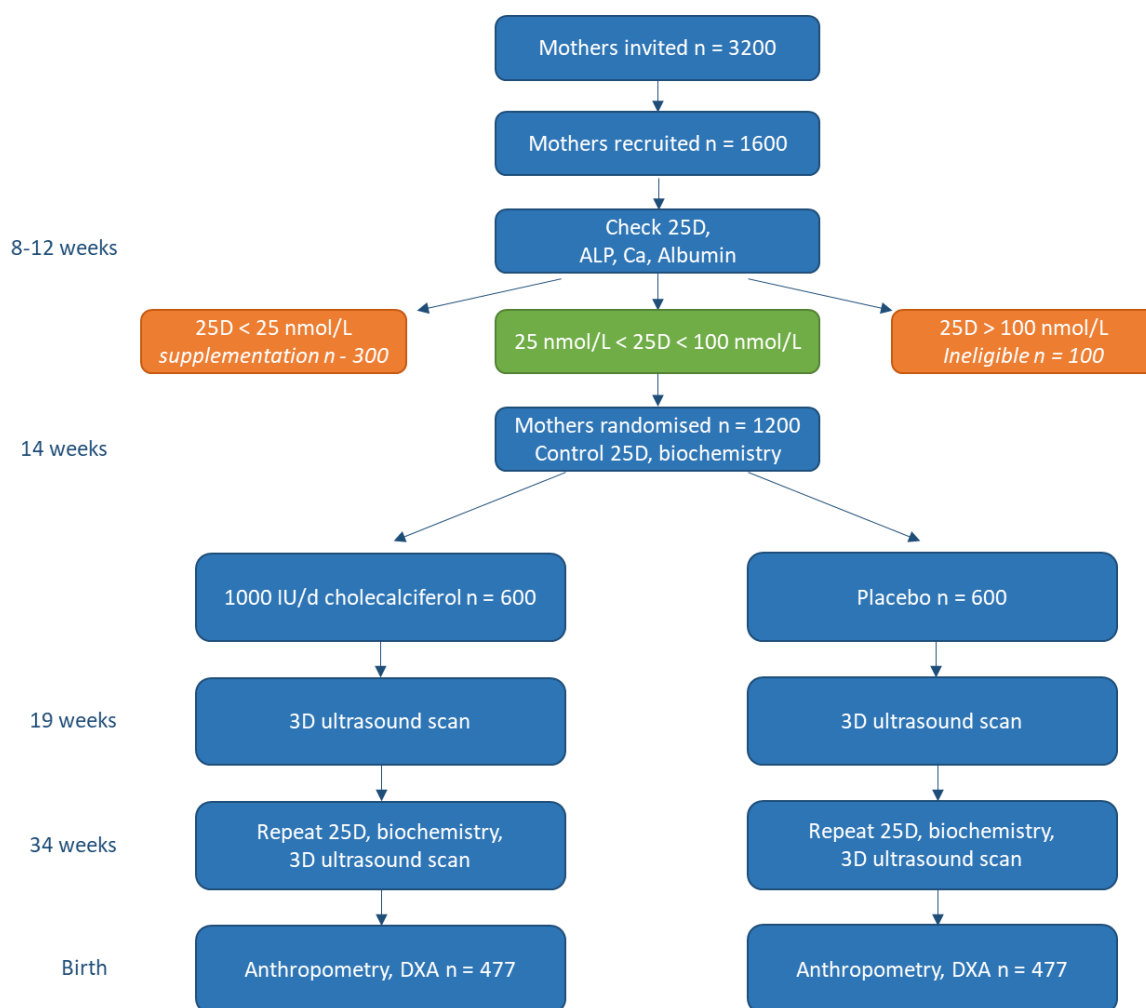


Figure 2.1 MAVIDOS trial study design.

2.2.1.2 SPRING cohort

The SPRING (Southampton Pregnancy Intervention for the Next Generation) study is an ongoing randomised control trial using a two-by-two factorial design which aimed to investigate two interventions during pregnancy: behaviour change through Healthy Conversation Skills and vitamin D supplementation. The SPRING study received approval from the MHRA, Southampton and South West Hampshire Research Ethics Committee, University Hospital Southampton R and D (sponsor) and the UHS Data Protection Office (ISRCTN07227232, registered on 13 September 2013). Pregnant women in Southampton aged over 18, with a singleton pregnancy and less than 17 weeks gestation were recruited between 8 and 12 weeks gestation and randomised into one of four groups: Healthy Conversation Skills support plus 1000 IU/d vitamin D supplementation; Healthy Conversation Skills support plus placebo; usual care plus 1000 IU/d vitamin D; usual care plus placebo. A trial summary can be seen in **Figure 2.2**. Interviewer led questionnaires at 14 weeks gestation assessed parity, baseline demographic features, diet and diet assessment using a 20 item food frequency questionnaire, sunlight exposure, smoking and alcohol consumption, general health, medication, psychological health and wellbeing, self-efficacy and food involvement. Maternal anthropometric

Chapter 2

measurements including height, weight, grip strength and skinfold thicknesses at biceps, triceps, subscapular and supriliac sites were measured and venous blood samples were taken at 14 and 34 weeks gestation. At 18-21 weeks pregnant women had a NHS fetal anomaly scan and a high resolution 3D ultrasound scan which were repeated at 34 weeks gestation. At 34 weeks gestation and 1 month postnatally, interviewer led questionnaires assessed dietary and supplementary vitamin D intake, smoking, alcohol, exercise, medications, health, wellbeing and self-efficacy. At delivery, venous umbilical cord blood and placental and umbilical cord tissue were collected. After delivery, a paediatrician assessed the infant hips to exclude congenital hip dislocation and the baby's length, weight, skinfolds and abdominal circumference were measured. Neonates underwent a DXA scan to assess bone density within 14 days of birth using a densitometer [Hologic Discovery instrument using paediatric software (Hologic Inc., Bedford, MA, USA)]. The DXA scan measured whole body and lumbar spine bone area, bone mineral content and bone mineral density.

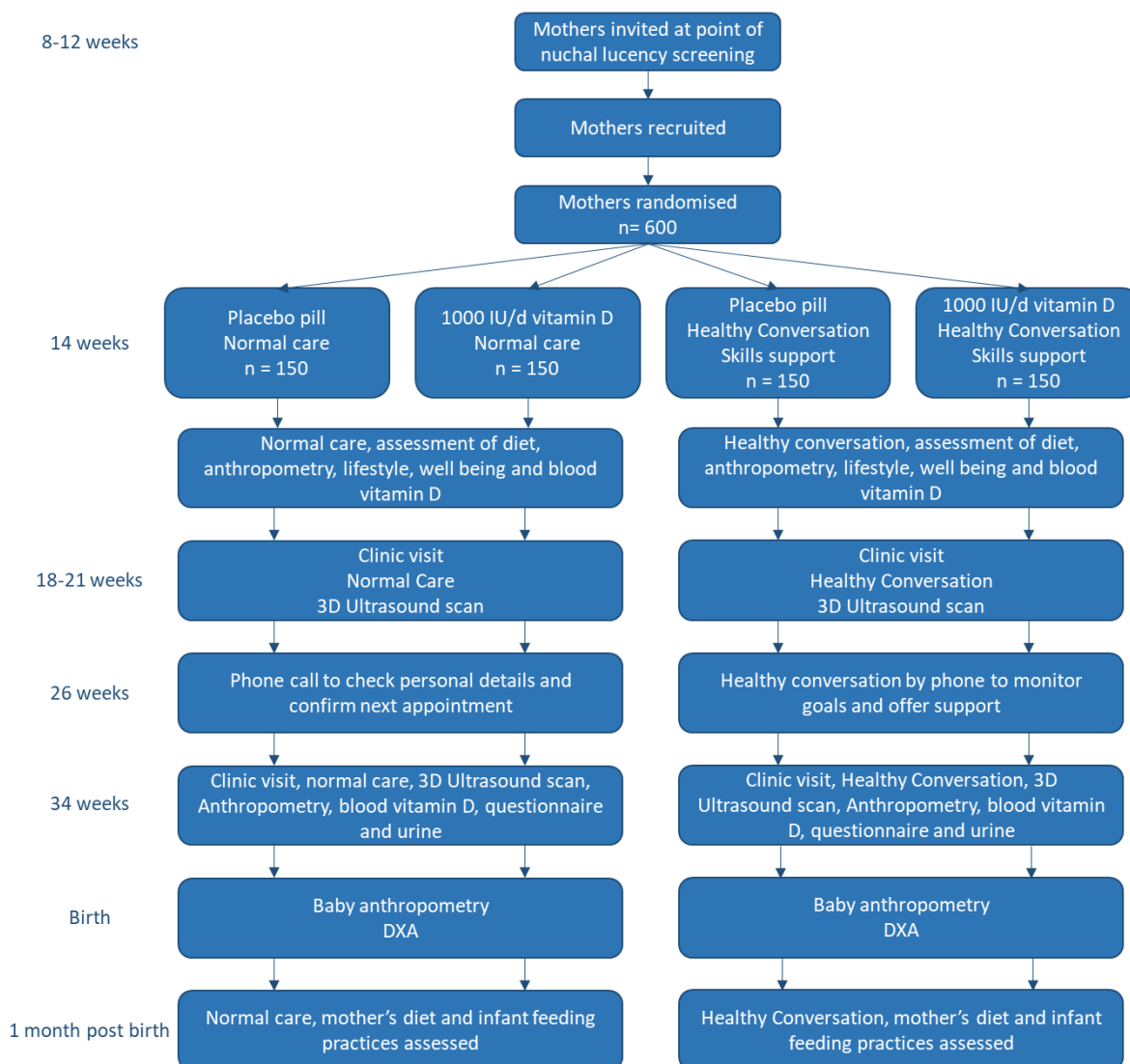


Figure 2.2 SPRING trial study design.

2.2.2 Genomic DNA extraction from umbilical cord

Genomic DNA was extracted from human umbilical cords (n = 449) from the MAVIDOS study. Prior to DNA extraction, cords were collected and stored at -80 °C. Cord tissue was pulverised using liquid nitrogen and stored at -80 °C until use. Previously, Dr Eloise Cook extracted DNA from 150 cords. DNA was extracted from the remaining 300 cords. Briefly, 500 µl of hyaluronidase solution (10-11 U/ml in PBS), (Sigma, #H3506), was added to 500 mg of crushed umbilical cord in a Dispomix tube. The cord was pulse spun briefly at room temperature and incubated at 37 °C for 30 minutes whilst shaking at 150 rpm. Following incubation, 500 µl TNES solution was added and the tissue was homogenised using Xiril Dispomix Homogeniser using the following programme:

5 seconds at + 4,000 rpm
3 seconds off
5 seconds at – 4,000 rpm
3 seconds off
5 seconds at + 4,000 rpm
3 seconds off
5 seconds at – 4,000 rpm

Samples were pulse spun at room temperature, 5 µl Proteinase K (20 mg/ml, Qiagen, #19131) was added and the samples were incubated overnight at 55 °C. After 16 hours, lysate was transferred to a new 2.2 ml Eppendorf and 500 µl 2.6 M NaCl (Sigma Aldrich, #S3014) was added. The samples were shaken vigorously for 15 seconds before centrifugation at 12,000 rpm for 20 minutes at room temperature. The supernatant was split equally between two new Eppendorf's and an equal volume of ice cold 100 % ethanol (Fisher Scientific, #E/0600/05) was added. The samples were gently inverted five times and precipitated DNA was spooled into a new Eppendorf containing 500 µl water and 5 µl RNase A (10 mg/ml), (Qiagen, #19101) prior to incubation at 37 °C for 1 hour. Following incubation, 500 µl of phenol/chloroform solution (Life Technologies, #15509-037 / Fisher Scientific, #10102190) was added to the samples. The tubes were gently inverted five times before centrifugation at 12,000 rpm for 5 minutes at room temperature. The aqueous upper phase was transferred to a new Eppendorf, an equal volume of phenol/chloroform mixture (Life Technologies, #15509-037 / Fisher Scientific, #10102190) was added and samples were centrifuged for a further 5 minutes at 12,000 rpm. The aqueous upper phase was transferred to a new Eppendorf and DNA was precipitated with the addition of 1/10th of the volume 3 M NaAc pH 5.2 (Sigma Aldrich, #S88388) and twice the volume ice cold 100 % ethanol (Fisher Scientific, #E/0600/05). Precipitated DNA was spooled to a new Eppendorf containing 500 µl dH₂O. Samples were stored at 4 °C for short

term use and at -20 °C for longer term storage. DNA concentrations were determined using the Nanodrop Spectrophotometer.

2.2.3 Genomic DNA extraction from placental tissue

Collection of placental tissue and DNA extractions were performed by Dr Brogan Ashley, University of Southampton. Placental tissue samples were taken at random from SPRING and MAVIDOS placentas, the tissue was snap frozen in liquid nitrogen and stored at -80 °C. Term placentas were collected from the Princess Anne Hospital, Southampton, within 30 minutes of delivery which were used for the isolation of primary cytotrophoblasts as briefly described in **section 2.2.3.1.**, and placental fragments were treated with vitamin D as briefly described in **section 2.2.3.2** prior to storage at -80 °C.

Dr Ashley extracted DNA from placental tissue using the DNeasy Blood and Tissue Kit (Qiagen, #69504) as per manufacturer's instructions. Briefly, 18-35 mg of crushed, frozen tissue or 9×10^6 cells were thawed at room temperature and 180 µl of Buffer ATL was added prior to thorough vortexing. Next, 20 µl of proteinase K was added, mixed thoroughly by vortexing and incubated at 65 °C for 1-3 hours until complete lysis. Following lysis, samples were vortexed for 15 seconds, 200 µl of Buffer AL was added and the sample was vortexed to mix. 200 µl of 100 % ethanol (Fisher Scientific, #E/0600/05) was added prior to thorough vortexing. The sample was loaded onto the DNeasy spin column placed in a 2 ml collection tube. Next, the sample was centrifuged at 8,000 rpm for 1 minute, the flow through and collection tube discarded and the spin column was transferred to a new collection tube. 500 µl Buffer AW1 was added to the spin column prior to centrifugation at 8,000 rpm for 1 minute. The collection tube containing the flow through was discarded and the spin column was placed in a new collection tube. 500 µl Buffer AW2 was added to the spin column and centrifuged at 14,000 rpm for 3 minutes, the collection tube and flow through was discarded and the spin column was placed in a new collection tube. DNA was eluted in 200 µl Buffer AE (10 mM Tris-Cl, 0.5 mM EDTA, pH 9.0), following incubation at room temperature for 1 minute and centrifugation at 8,000 rpm for 1 minute. The elution step was repeated into a fresh collection tube. Eluted DNA was stored at -20 °C until use.

2.2.3.1 Primary cytotrophoblast isolation from placental tissue

Dr Ashley isolated primary cytotrophoblasts from placentas obtained within 30 minutes of delivery from healthy, term, consenting patients which delivered at Princess Anne Hospital, Southampton. Cytotrophoblasts are undifferentiated stem cells within trophoblasts, which form the outer layer of a blastocyst, and can differentiate into syncytiotrophoblasts which are a continuous, specialised layer of epithelial cells³⁵⁰. Briefly, the fetal side of the placenta was cut into 2 cm³ pieces and washed

three times in sterile 0.9 % saline. The chorionic plate and underlying 3 mm of tissue, decidua and underlying 3 mm of tissue and vessels, blood clots and gritty tissue were removed. The remaining placental tissue was digested three times with Hanks balanced salt solution (HBSS, Thermo Fisher Scientific, # 24020117), DNase (Sigma-Aldrich, #AMPD1) and Trypsin (PAA, #L11-004) at 37 °C for 30 minutes whilst shaking at 80 rpm. Following the first and second digest a proportion of the top layer of supernatant was transferred to a sterile flask. Following the third digestion, the flask contents were strained through gauze, and then through wire mesh (50 µm² hole, 0.036 mm wire) into a sterile beaker. The supernatant following digestion and the strained flask contents were added to new-born calf serum (NCS, Thermo Fisher Scientific, #16010167) and erythrocytes were pelleted, with a thin pale layer containing cytotrophoblasts and supernatant. The supernatant was removed and pellets washed in warm DMEM (PAA, #E15-843). Next the cell suspension was pipetted onto a Percoll gradient and cells were collected from the 35-55 % region. Following further wash and centrifugation steps, the primary cytotrophoblasts were seeded at a density of 3 x 10⁶ cells per well in 6 well plates in 2 ml of culture media containing DMEM/Ham's F-12 (Gibco, #11320-074), 10 % FBS (PAA, #A15-151), 10,000 IU penicillin (PAA, #P11-010)/ 10 mg/ml streptomycin (PAA, #P11-010) and 300 mmol/l L-glutamine (Sigma-Aldrich, #G7513). Culture media was replaced every 24 hours after an initial 18 hours, and after 66 hours 25(OH)D₃ or a control was added to make a final concentration of 20 µM. At 90 hours, the media was removed and the cells were washed in warm PBS (Fisher Scientific, #12821680) prior to scraping the cells into the appropriate medium for DNA extraction.

2.2.3.2 Placental fragment culture with vitamin D

Dr Ashley removed 3 x 10 mg villous tissue fragments from the maternal side of the placenta and incubated the fragments in Tyrode's buffer (135 mmol/l NaCl (Sigma Aldrich, #S3014), 10 mmol/l HEPES (Thermo Fisher Scientific, # 15630106), 5.6 mmol/l D-Glucose (Sigma-Aldrich, # G8270), 5 mmol/l KCl (Sigma Aldrich, #P9541), 1.8 mmol/l CaCl₂.2(H₂O) (Sigma-Aldrich, # C7902) and pH to 7.4 with NaOH (Sigma Aldrich, #S5881)) and 20 µM 25(OH)D₃ dissolved in ethanol (Fisher Scientific, #E/0600/05) and 0.7 mmol/l BSA, or an ethanol (Fisher Scientific, #E/0600/05) and BSA control at 37 °C for 8 hours. Following incubation, the buffer was removed, fragments washed in fresh Tyrode's buffer and fragments were snap frozen on dry ice and stored at -80 °C until use.

2.2.4 Measuring DNA methylation

DNA methylation was measured in DNA extracted from human umbilical cord (**Chapters 3-5**), human placental tissue (**Chapter 3**), human osteosarcoma cell lines (**Chapter 6**) and murine tibiae (**Chapter 7**) using the methods described below.

2.2.4.1 Bisulfite conversion of DNA

DNA was bisulfite converted using the EZ DNA methylation Gold bisulfite conversion kit (Zymo research, #D5007) as per manufacturer's instructions. Briefly, 130 μ l CT conversion reagent was added to 1 μ g of DNA (50 ng/ μ l) prior to incubation in a thermal cycler for 10 minutes at 98 °C, 2.5 hours at 64 °C and incubation at 4 °C for up to 20 hours. Following incubation, 600 μ l Binding Buffer was added to a spin column plate with a collection plate. The incubated DNA samples were transferred to the binding buffer prior to centrifugation at 10,000 rpm for 30 seconds and the flow through was discarded. Next, 100 μ l Wash Buffer was added to the spin column, centrifuged for 30 seconds at 10,000 rpm and the flow through discarded. 200 μ l Desulphonation Buffer was added to the columns prior to incubation at room temperature for 15 minutes and centrifugation at 13,000 rpm for 30 seconds. The flow through was discarded and 200 μ l wash buffer was added to the column before centrifugation at 13,000 rpm for 30 seconds. The wash step was repeated. Next, the spin plate was placed over an elution plate, 30 μ l elution buffer was added to the wells before incubation at room temperature for 2 minutes and centrifugation at 1,000 rpm for 30 seconds. 4 μ l aliquots were prepared and stored at -20 °C for PCR use.

2.2.4.2 Polymerase chain reaction (PCR)

Following bisulfite conversion, converted DNA was amplified with Hotstar Taq (Qiagen, #203205) and PCR primers of interest, with the reverse primer containing a biotin tag, as per manufacturer's instructions (**Table 2.2A**). Briefly, a master mix containing 5 μ l buffer, 1 μ l forward primer (10 μ M), 1 μ l reverse primer (10 μ M), 1 μ l dNTPs (10 μ M, Promega, #U1420), 0.25 μ l Hotstar Taq (Qiagen, #203205) and 39.75 μ l water was added to 2 μ l bisulfite converted DNA (4 μ l of cord DNA). The samples underwent thermal cycling using the conditions in **Table 2.2** Error! Reference source not found. Alongside the DNA samples of interest, internal controls were also amplified. Each PCR plate additionally had three Promega DNA controls (Promega, #G3041), three Roche controls (Promega, #11691112001), 0 % methylated control (Qiagen, #59655), 100 % methylated control (Millipore, #S7821) and four non-template controls (NTCs) containing the master mix and water. Following PCR amplification, 5 μ l of a selection of samples including the NTCs were visualised on a 0.8 % agarose gel (Melford, #MB1200) for 20 minutes at 120 V to determine successful amplification and to rule out possible contamination. PCR plates were stored at 4 °C until use.

Table 2.2 Pyrosequencing amplicons and sequencing primers used to measure DNA methylation and PCR conditions.

A

Pyrosequencing Amplicons and Sequencing Primers			
Gene	Amplicon	Sequencing Primer	
Human RXRA	RXRA 0-5 60°C	F: TGGGAAGGTTGAAGGTTTTAGAA R: AACACAAAACCTAAATATAAACCCAAATCT	RXRA 0-3 GTTATTTTTGTTTTAGAGAT RXRA 4-5 AGAAGGGTTTTTTGTTTTAA
	RXRA 6-7 60°C	F: GGAAGGTTGGGTTGAAGTGT R: ACCCACATAAAAATCTATCTACATATACC	RXRA 6 GTTGTGGTGTGGGA RXRA 7 GTGTTTGAAGGTTATTTTTAATAG
	RXRA 8-12 60°C	F: TGGGATTATTGGTTTTGAGTTAGGT R: CCCACTATTAATAAACCTCAAACACTT	RXRA 8-11 CCCAACCTCCCACC RXRA 12 CCTACTACTCCTCTCT
Human CDKN2A	CDKN2A 3-1 57.6°C	F: TTTATTTTTTTGGAAGGTGGGAGAGG R: TTTTTCTCCCAACCTCCC	CDKN2A 1 GGAGGTTGGGGAGAA CDKN2A 3-2 TGGGAGAGGGTGATT
	CDKN2A 9-4 57.6°C	F: GGTGTAAAATTTTTTAAGAAGTAAGTG R: CTCCTTAAAAAATTATTACTAACCATCT	CDKN2A 7-4 GATTTTGTAGTATTTTAGGA CDKN2A 9-8 AGAAGTAAGTGTGTGTTTT
Human Runx2	Runx2 1-9 60°C	F: TTTTAGGGTGGGAGAGTAAG R: CCACTCCCTCCTACAATTAC	Runx2 1-3 GTGGGAGAGTAAGA Runx2 4-9 AGATTGTTTTAGTTGGG
Human Osterix	Osterix 1-9 57°C	F: GAGGGGTTTAGGGTTAGTTAGTAGG R: ACTTCTCCAAACTACATCCAACTCTTC	Osx 1-2 s GTTAGTAGGGGTGT Osx 3-4 s AAGTTAGTTTTTGAGTTTTGAT Osx 6-9 s TGAGAGATTGGTAGGT
Mouse RXRA	RXRA A 1-4 60°C	F: GGTGTGAGGGGTAGAATTA R: CCCACAAAACCTTCTCAATCC	RXRA A 1 s GAGATTATAAGTTTTATTTAGGGA RXRA A 2-3 s TTTTTTTAAATTTTTGGGTTATT RXRA A 4 s TGAAATTTGGGTTGTAGAT
	RXRA B 1-6 57°C	F: AGAGGGGTTTATTAAGTTTATAGGT R: AATTTCTCTATATAACCCTAACATCCT	RXRA B 1-2 s TTTTAAGATAAAAAAGAAAGT RXRA B 3-4 s TTTTTTTGTAAAAAGTAATAGT RXRA B 5-6 s TGGTGGTATAAGTTTTTAATATTAG
Mouse Runx2	Runx2 24-28 57°C	F: ATGGAGTGGTGGTAATTAATAGT R: ATAACTTACTTTCATTACCCCTCATT	Runx2 25-24S GGGAGGAGAATAAATATTTTT Runx2 26 S GGGAGTTTTTATTGAAATATG Runx2 27 S GGTTTTAAGATAGGATTTTTATA Runx2 28 S AGTGGTGGTAATTAATAGTA
Mouse Osterix	Osterix 8-18 54°C	F: GTTTTTATGTGGGTAGTAGAGAGT R: ATCCAATCCTACAATCCTACTCTTAA	Osx 11-8 S AGTAGTAGTAGTAGTAATAGA Osx 17 S GTTTTAGTTTTTTGTGTGAG Osx 19-18 S ATGTGGGTAGTAGAGAGTA
Mouse VDR	VDR 1-6 57°C	F: TGTTATATTATTAATTTGTAGGGGGTAG R: CCTCATAAAAACCACTTACTTACTCT	VDR 1-2 S TTTAGTTAAGTGGAGATAAAATTAG VDR 3-5 S AGTGAGTTTTGGGTG VDR 6 S AAGATTTTGTAGAGAGGTA
	VDR 8-10 60°C	F: GGTGTGGTTTTGTTAAGAATATTAAAG R: CACTCCAAATTTCTAACTAACCTTAA	VDR 8 S AGTTAAGTGATTATTGGTAATAT VDR 9 S GGTGTATAGTAATTTTGTGTAT VDR 10 S AGGATTTGGAATTGTAATG

B

Cycling Conditions		
Temperature (°C)	Time	Cycles
95	5 mins	1
95	30 sec	
Variable	30 sec	45
72	1 min	
72	10 min	1
4	∞	

A) The forward and reverse PCR primer for each amplicon, the CpGs the amplicon covers and the optimal temperature for the PCR primers. Sequencing primers and the CpGs they cover within each amplicon. *RXRA* = retinoid X receptor alpha, *CDKN2A* = cyclin dependent kinase inhibitor 2A, *Runx2* = runt-related transcription factor 2, *VDR* = vitamin D receptor. B) The thermal cycler conditions.

2.2.4.3 Pyrosequencing

DNA methylation was measured using the PyroMark pyrosequencer as per manufacturer's instructions following amplification with PCR primers. Briefly, 10 µl PCR product was used for measurement of all of the genes except for human *RXRA* CpGs 1-5 and human *CDKN2A* CpGs 1-3 where 20 µl PCR product was used. A master mix containing 30 µl water, 30 µl Binding Buffer (Qiagen, #979006) and 2 µl Streptavidin beads (Fisher Scientific, #GZ17511301) were added to the PCR product. The samples were immediately placed on a shaker for 5 minutes prior to being passed through the PyroMark workstation following manufacturer's instructions. The PCR product bound to streptavidin beads were released into 0.5 µl sequencing primer (10 µM) and 11.5 µl annealing buffer (Qiagen, #979009) prior to incubation at 80 °C for 2 minutes and incubation at room temperature for 5 minutes. The annealed samples were loaded onto the pyrosequencer and DNA methylation of specific CpGs within the different genes was measured.

2.2.4.4 Primer validation

PCR and pyrosequencing primers for *RXRA* CpGs -1-5 and 8-12 and *CDKN2A* CpGs 1-9 were previously designed and validated by Dr Robert Murray and Dr Rebecca Clarke-Harris, University of Southampton. The remaining PCR and pyrosequencing primers were validated before use. To do this, DNA from random samples were pooled together, bisulfite converted as described in **section 2.2.4.1** and amplified with PCR primers using a temperature gradient of 45 °C, 48 °C, 51 °C, 54 °C, 57 °C and 60 °C. 5 µl of PCR product was visualised on a 0.8 % agarose gel (Melford, #MB1200) for 20 minutes at 120 V. Amplified product underwent pyrosequencing as described in **section 2.2.4.3** and a temperature which yielded a strong band on the agarose gel and a good signal strength and pass rate on the pyrosequencer was chosen as the optimal temperature for the PCR primers.

2.2.5 Cell culture

2.2.5.1 Human osteosarcoma cell lines

The human osteosarcoma cell lines, Saos2 (Cell Lines Service, #36025) and MG63 (Cell Lines Service, #300441), were cultured in Dulbecco's Modified Eagle's Medium (DMEM) Ham's F-12 (Gibco, #11320-074) supplemented with 5 % fetal bovine serum (FBS) (PAA, A15-151), 2 mM L-glutamine (Sigma-Aldrich, #G7513) and 1 % penicillin streptomycin (PAA, #P11-010) in 75 cm² tissue culture flasks. Cells were maintained at 37 °C in an atmosphere of 5 % CO₂ and were subcultured when 80 % confluent using 0.25 % trypsin EDTA (PAA, #L11-004).

2.2.5.2 Human mesenchymal stem cells (MSCs) from umbilical cord

Human mesenchymal stem cells (MSCs) from umbilical cord (ATCC) were grown to 80 % confluence on 10 % gelatin (Fisher Scientific, #G1393) coated 175 cm² flasks in DMEM (PAA, #E15-843) supplemented with 15 % FBS (PAA, #A15-151), 2 mM L-glutamine (Sigma-Aldrich, #G7513) and 1 % penicillin streptomycin (PAA, #P11-010). Cells were maintained at 37 °C in an atmosphere of 5 % CO₂ and were subcultured when 80 % confluent using 0.25 % trypsin EDTA (PAA, #L11-004).

2.2.6 Supplementing human osteosarcoma cell lines with vitamin D

2.2.6.1 Culturing human osteosarcoma cell lines with vitamin D

1,25(OH)₂D₃ (Enzo Life Sciences, #BML-DM200-0050) was dissolved in 100 % ethanol (Fisher Scientific, #E/0600/05) to make a final ethanol concentration in the cells of 0.01 %. Physiological plasma concentrations of 1,25(OH)₂D₃ have been measured at 185 pmol/L (0.185 nM)³⁵¹ however, many *in vitro* studies use a supraphysiological concentration of 1,25(OH)₂D₃ between 1 and 1000 nM³⁵²⁻³⁵⁵. A dose response in both human osteosarcoma cell lines (data not shown) found that the lowest concentration of 1,25(OH)₂D₃ (Enzo Life Sciences, #BML-DM200-0050) that was able to elicit a luciferase response following transfection with the *RXRA* promoter luciferase construct was 10 nM, therefore a concentration of 10 nM 1,25(OH)₂D₃ was used in all of the *in vitro* experiments. Saos2 cells and MG63 cells were seeded at 450,000 cells and 225,000 cells respectively per well in a 6 well plate in 3 ml of DMEM/Ham's F-12 media (Gibco, #11320-074) supplemented with 5 % FBS (PAA, #A15-151), 2 mM L-glutamine (Sigma-Aldrich, #G7513) and 1 % penicillin streptomycin (PAA, #P11-010) at 37 °C and an atmosphere of 5 % CO₂. The cells were seeded in duplicates of 6, and wells were seeded for both DNA and RNA extractions from osteosarcoma cell lines. After 30 hours, each well was treated with 10 nM 1,25(OH)₂D₃ (Enzo Life Sciences, #BML-DM200-0050) or with 100 % ethanol (Fisher Scientific, #E/0600/05). 24 hours after initial seeding, the media was discarded from the wells and washed with warm PBS (Fisher Scientific, #12821680). 500 µl of TriReagent (Sigma Aldrich, #T9424) was added to the wells intended for RNA extraction and the plates were stored at -80 °C until use. Osteosarcoma cells intended for DNA extractions were removed from the wells using 0.25 % Trypsin EDTA (PAA, #L11-004), inactivated with media, centrifuged for 10 minutes at 3,000 g and the supernatant was removed. Cell pellets were snap frozen on dry ice and stored at -80 °C until use.

2.2.6.2 Isolation of total RNA from osteosarcoma cell lines

Total RNA was extracted from osteosarcoma cell lines using TriReagent (Sigma Aldrich, # T9424). The 6 well plates containing osteosarcoma cells in TriReagent were defrosted at room temperature.

Chapter 2

Cells were scraped from the bottom of each well using a plate scraper. The cells in TriReagent were transferred to sterile Eppendorf's, 100 μ l chloroform (Fisher Scientific, #10102190) was added, and the samples were vortexed and incubated at room temperature for 2 minutes. Next, the samples were centrifuged at 13,000 rpm at 4 °C for 10 minutes and the aqueous upper phase was transferred to a sterile Eppendorf containing 250 μ l isopropanol (Fisher Scientific, #11398461). The sample was vortexed prior to centrifugation at 13,000 rpm at 4 °C for 10 minutes and the supernatant was discarded. 250 μ l 70 % ethanol (Fisher Scientific, #E/0600/05) was carefully added and the pellet prior to centrifugation at 13,000 rpm at 4 °C for 5 minutes. The supernatant was removed and the pellet was dried at room temperature for 10 minutes. The RNA pellet was resuspended in 50 μ l water and the concentration of total RNA was determine using the Nanodrop spectrophotometer as per manufacturer's instructions. Samples with a 260/230 ratio of less than 1.8 underwent a further chloroform wash step to remove any phenol or chloroform contaminants. Briefly, 50 μ l water was added to the affected samples before addition of 100 μ l chloroform (Fisher Scientific, #10102190). The sample was vortexed for 10 seconds and centrifuged at 13,000 rpm for 5 minutes at 4 °C. The upper phase was transferred to a sterile Eppendorf prior to addition of 400 μ l 100 % ethanol (Fisher Scientific, #E/0600/05) and 20 μ l 3 M NaAC pH 5.2 (Sigma Aldrich, #S8388) and incubation at -20 °C overnight. The following day, the sample was centrifuged for 30 minutes at 13,000 rpm at 4 °C and the supernatant was removed. 500 μ l 70 % ethanol (Fisher Scientific, #E/0600/05) was carefully added prior to centrifugation at 13,000 rpm at 4 °C for 5 minutes. Next, the supernatant was removed and the RNA pellet was resuspended in 50 μ l water. The RNA concentration was determine using the Nanodrop spectrophotometer and the RNA samples were stored at -80 °C until use.

2.2.6.2.1 DNase treatment and cDNA synthesis

Extracted total RNA from osteosarcoma cell lines underwent DNase 1 treatment prior to cDNA synthesis. Briefly, 1 μ l each of DNase 1 buffer and enzyme (Sigma Aldrich, #AMPD1) were added to 8 μ l of RNA (125 ng/ μ l) prior to incubation at room temperature for 15 minutes. Following incubation, 1 μ l of Stop Solution was added to each sample between incubation at 70 °C for 10 minutes and incubation on ice until use. Next, 1 μ l of 10 mM DNTP mix (Promega, #U1420) and 1 μ l Random Nonamers (Sigma Aldrich, #R7647) were added to each well prior to incubation at 70 °C for 10 minutes. A master mix containing 4 μ l of M-MLV Reverse Transcriptase Buffer (10X), 1 μ l M-MLV Reverse Transcriptase (Promega, #M1701) and 5 μ l of nuclease free water was added to each sample prior to incubation at room temperature for 10 minutes, 37 °C for 1 hour and 90 °C for 10 minutes to generate cDNA.

2.2.6.2.2 Real time PCR using cDNA from osteosarcoma cell lines

Quantitative real time PCR (qRT-PCR) of 6 different genes (**Table 2.3**) were measured in duplicate using a LightCycler 480 Real-Time PCR System (Roche). The quantitect primers were reconstituted to 100 μ M in 1.1 ml RNase free water (Fisher Scientific, #BPE561-1) and stored at -20 °C until use. First, 25 ng cDNA (6.25 ng/ μ l) was aliquoted in duplicate into each well prior to addition of 5 μ l 2X SYBR Green master mix (Qiagen, #204143) and 1 μ l quantitect primer mix (forward and reverse). The qRT-PCR assay was loaded onto the LightCycler and the PCR conditions involved a holding stage of 95 °C for 2 minutes followed by 40 cyclers of primer denaturation at 95 °C for 30 seconds, annealing at 55 °C for 60 seconds and elongation at 72 °C for 60 seconds. A melt curve step involved 95 °C for 15 seconds, 60 °C for 60 seconds and 95 °C for 15 seconds.

Table 2.3 Quantitect Primer Assays for qRT-PCR

Gene	Primer	Reference	Product Size (bp)
RXRA		QT00005726	134
VDR		QT01010170	128
CYP24A1		QT00015428	119
Osterix		QT00213514	120
Runx2		QT00020517	101
GAPDH		QT00079247	95

Quantitect primers obtained from Qiagen. A standard annealing temperature of 55C was used. *RXRA* = retinoid X receptor alpha, *VDR* = vitamin D receptor, *CYP24A1* = cytochrome P450 family 24 subfamily A member 1, *Runx2* = runt-related transcription factor 2, *GAPDH* = glyceraldehyde-3-phosphate dehydrogenase.

2.2.6.3 Isolation of genomic DNA from osteosarcoma cell lines

Genomic DNA was extracted from osteosarcoma cell lines using the GenElute Mammalian Genomic DNA Miniprep Kit (Sigma Aldrich, #G1N350) as per manufacturer's instructions. Briefly, the previously prepared osteosarcoma cell pellets were thawed slightly before resuspension in 200 μ l Resuspension Solution. Next, 20 μ l of RNase A solution was added prior to incubation at room temperature for 2 minutes. Cells were lysed using 20 μ l of proteinase K and 200 μ l of Lysis Solution C, vortexed for 15 seconds and incubated at 70 °C for 10 minutes. The GenElute binding columns were prepared with the addition of 500 μ l Column Preparation Solution, centrifugation at 12,000 g for 1 minute and the flow through was discarded. 200 μ l of ethanol (Fisher Scientific, #E/0600/05) was added to the cell lysate, vortexed for 10 seconds and the lysate was transferred to the pre-prepared binding column. The column was centrifuged at 6,500 g for 1 minute and the column was transferred to a new collection tube. Next, 500 μ l of Wash Buffer was added to the column before

centrifugation at 6,500 g for 1 minute. The column was transferred to a new collection tube, 500 µl of Wash Buffer was added and the sample was centrifuged at 6,500 g for 3 minutes and the column was transferred to a new collection tube. The DNA was eluted three times into 3 fresh Eppendorf's. For each elution, 50 µl was added to the binding column before incubation for 5 minutes at room temperature and centrifugation at 6,500 g for 1 minute. The DNA concentration was determined using the Nanodrop Spectrophotometer and DNA was stored at 4 °C for short term use and -20 °C for long term storage.

2.2.6.3.1 Measurement of *RXRA* DNA methylation in osteosarcoma cell lines

DNA methylation of *RXRA* was measured as previously described in sections. Briefly, 500 ng of DNA from Saos2 and MG63 cells was bisulfite converted using the bisulfite conversion kit (**Section 2.2.4.1**). 2 µl of bisulfite converted DNA was used in each PCR reaction (**Section 2.2.4.2**) and *RXRA* methylation was measured by pyrosequencing (**Section 2.2.4.3**).

2.2.7 Transfection of osteosarcoma cell lines with luciferase reporter constructs

2.2.7.1 Cloning the *RXRA* promoter

2.2.7.1.1 Excising the *RXRA* promoter from the *RXRA* GeneART plasmid

A custom plasmid construct was previously designed by Dr Robert Murray and generated using GeneART gene synthesis by Thermo Fisher Scientific (**Figure 2.3**). The custom plasmid contains an *RXRA* promoter insert ranging from -2680 bp to +86 bp with respect to the *RXRA* transcriptional start site. 2 µg of the *RXRA* GeneART construct was digested overnight at 37 °C with restriction enzymes: XhoI (Fisher Scientific, #FD0694), HindIII (Fisher Scientific, #FD0504) and AseI (Fisher Scientific, #FD0914) generating four fragments of 2766 bp, 1235 bp, 1123 bp and 10 bp. The digested *RXRA* GeneART plasmids were loaded onto a 0.8 % agarose gel (Melford, #MB1200) and visualised after 40 minutes at 120 V. The largest band corresponding to the *RXRA* insert (2766 bp) was excised out of the gel using a sterile knife under UV conditions and the plasmid DNA fragment was purified using a Zymoclean Gel DNA Recovery Kit (Cambridge Bioscience, #D4001) as per manufacturer's instructions. Briefly, the excised gel was weighed and three times the volume of ADB was added to the gel and incubated at 50 °C for 10 minutes until fully dissolved. The melted agarose solution was transferred to a Zymo spin column in a collection tube before centrifugation for 30 seconds at 10,000 g and the flow through was discarded. 200 µl of wash buffer was added to the column before centrifugation for 30 seconds at 10,000 g and the flow through was discarded. The wash step was repeated and 10 µl of elution buffer was added directly to the column matrix and underwent centrifugation for 60 seconds at 10,000 g.

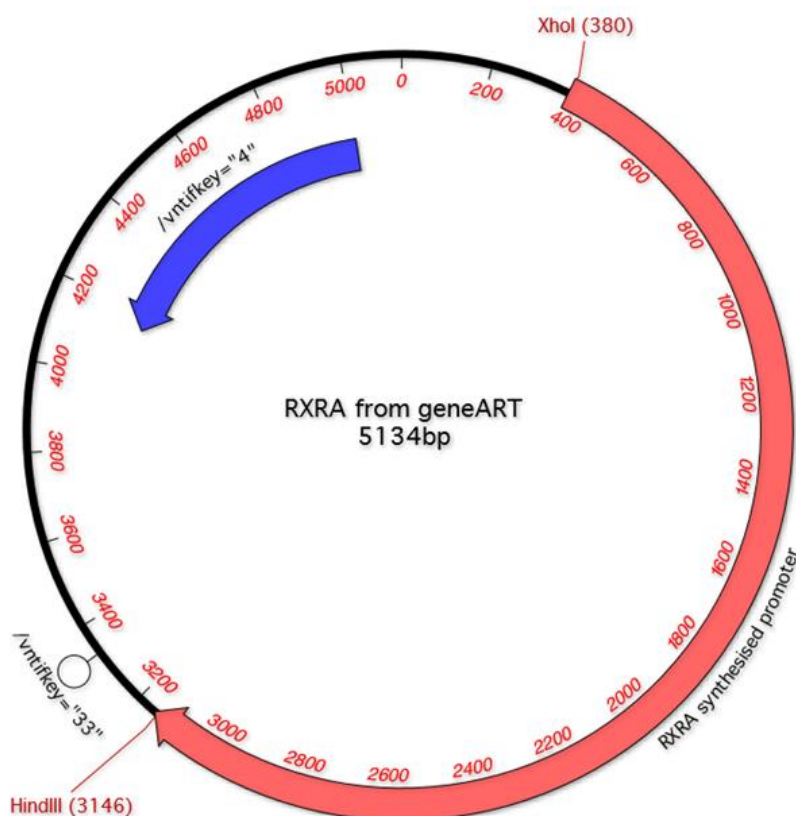


Figure 2.3 Map of the *RXRA* from geneART plasmid.

The restriction enzyme sites for XhoI and HindIII are shown. The *RXRA* synthesised promoter ranges from -2680 bp to +86 bp with respect to the transcriptional start site (TSS).

2.2.7.1.2 Digestion and Antarctic Phosphatase treatment of pGL4.17

The promoter-less luciferase reporter construct pGL4.17 basic (Promega, #E6721) was used for the cloning of the *RXRA* promoter (**Figure 2.4**). 500 ng of pGL4.17 was digested overnight at 37 °C with two restriction enzymes, XhoI (Fisher Scientific, #FD0694) and HindIII (Fisher Scientific, #FD0504), which produced two fragments of 5567 bp and 32 bp. The digested pGL4.17 plasmids were loaded onto a 0.8 % agarose gel (Melford, #MB1200) and visualised after 40 minutes at 120 V. The largest band (5567 bp) was excised out of the gel using a sterile knife under UV conditions and purified using a Zymoclean Gel DNA Recovery Kit (Cambridge Bioscience, #D4001) as per manufacturer's instructions. Following gel purification, the cut pGL4.17 vector was dephosphorylated on its 5' end using Antarctic Phosphatase (New England Biolabs, #M0289S) as per manufacturer's instructions. Briefly, 500 ng of purified pGL4.17 was incubated for 1 hour at 37 °C with 1 µl 10X Antarctic Phosphatase Reaction buffer, 1 µl (5 units) of Antarctic Phosphatase and water to make a final volume of 10 µl. Following incubation, the reaction was heat inactivated at 65 °C for 5 minutes.

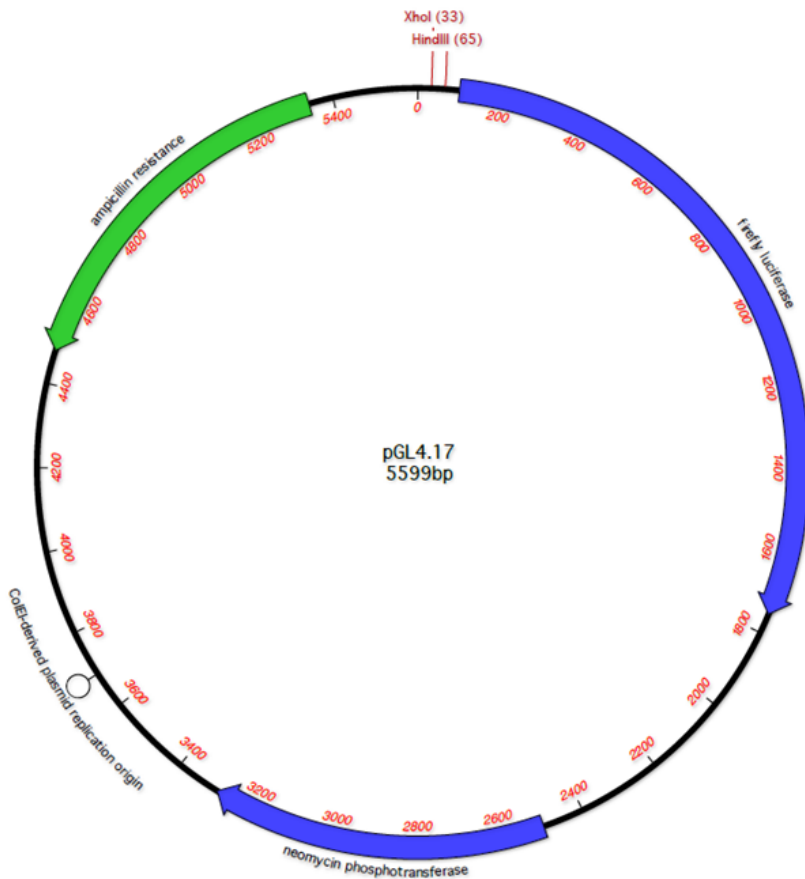


Figure 2.4 Map of the pGL4.17 basic luciferase plasmid.

The plasmid was obtained from Promega. The restriction enzyme sites for Xho1 and HindIII are shown.

2.2.7.1.3 Ligation of the *RXRA* promoter into pGL4.17 plasmid

A 3-fold molar mass excess of the *RXRA* insert was ligated to 50 ng of the Antarctic phosphatase treated pGL4.17 vector using the Quick Ligation Kit (New England Biolabs, #M2200S) as per manufacturer's instructions to create the pGL4:*RXRA* luciferase reporter construct (p*RXRA*promLuc) (**Figure 2.5**). A 3-fold molar mass excess was calculated using the equation below:

$$\frac{[\text{ng vector} \times \text{size of insert (in Kb)}]}{\text{size of vector (in Kb)}}$$

Antarctic Phosphatase treated pGL4.17 was also ligated to water instead of the *RXRA* insert as a negative control. Briefly, the vector and insert were combined with 10 μl Quick Ligase Reaction Buffer (2X), 1 μl Quick Ligase and water to make a final volume of 20 μl were gently mixed and incubated at room temperature for 5 minutes. Following incubation, the reaction was chilled on ice until required for the transformation.

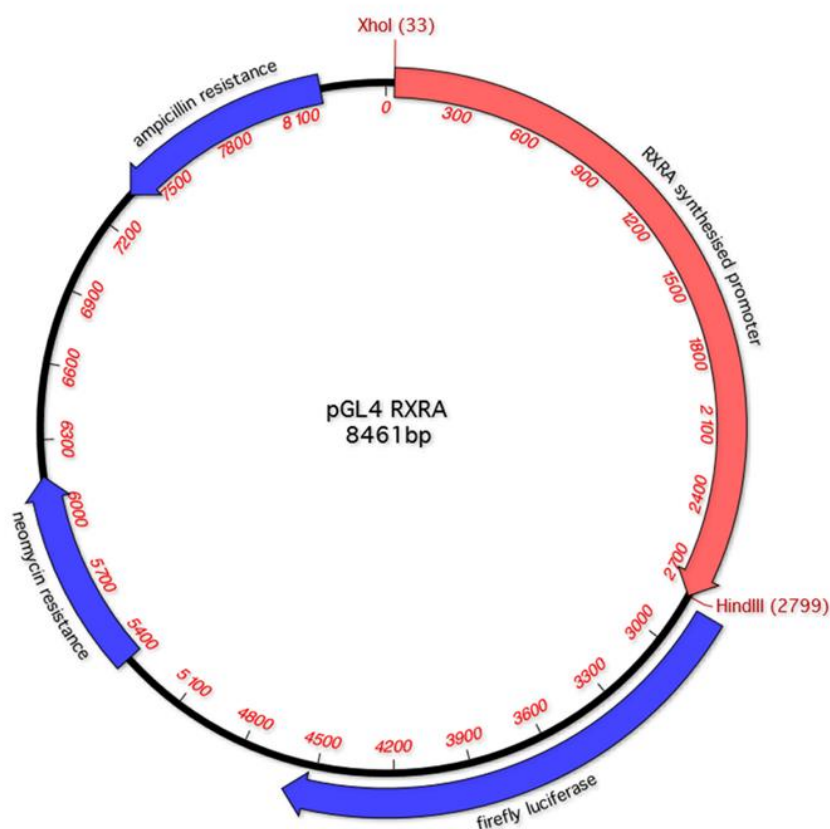


Figure 2.5 Map of pGL4:RXRA (pRXRApromLuc) luciferase reporter construct plasmid.

The *RXRA* promoter (-2680 bp to +86 bp with respect to the *RXRA* transcriptional start site) was ligated to pGL4.17 basic.

2.2.7.2 Cloning the *RXRA* enhancer constructs

2.2.7.2.1 PCR amplification of genomic DNA to make the enhancer inserts

Genomic DNA containing the *RXRA* CpGs of interest was amplified using PCR. Primers were designed using Primer-BLAST and the restriction enzyme sites for KpnI (GGTACC) and HindIII (AAGCTT) as well as flanking base pairs (GCC) were added to the primer sequences (**Figure 2.6B**). Three inserts containing the core *RXRA* CpGs were amplified by PCR to create the full enhancer region (pFenhLuc(CpGs1-12)), the 5' truncated full enhancer region (p5'truncFenhLuc(CpGs1-12)) and the minimal enhancer region (pMenhLuc(CpGs1-12)) (**Figure 2.6A**). Genomic DNA was amplified using the Phusion High Fidelity Polymerase (New England Biolabs, #MO531S) as per manufacturer's instructions. Briefly, 2.5 μ l each of forward and reverse primer (10 μ M), 25 μ l Phusion Master Mix (2X) and 50 ng genomic DNA in a 50 μ l reaction were combined and underwent thermal cycling using the conditions in **Figure 2.6C**. PCR primers were optimised using a temperature gradient of 59 $^{\circ}$ C, 62 $^{\circ}$ C, 65 $^{\circ}$ C, 68 $^{\circ}$ C and 70 $^{\circ}$ C, with and without 1.5 μ l DMSO, and PCR product was visualised on a 0.8 % agarose gel (Melford, #MB1200) for 20 minutes at 120 V. Temperatures of 65 $^{\circ}$ C were chosen for pFenhLuc(CpGs1-12) primers and 68 $^{\circ}$ C for

Chapter 2

p5'truncFenhLuc(CpGs1-12) and pMenhLuc(CpGs1-12) primers without DMSO. Next, five 50 μ l reactions were amplified for each primer pair, the five reactions were combined and purified using the Monarch PCR and DNA Cleanup Kit (New England Biolabs, #T1030S) as per manufacturer's instructions. Briefly, the PCR reaction was transferred to the spin column in a collection tube before centrifugation at 13,000 rpm for 1 minute and the flow through was discarded. 200 μ l DNA Wash Buffer was added prior to centrifugation at 13,000 rpm for 1 minute and the flow through was discarded. The wash step was repeated. The column was transferred to a new 1.5 ml Eppendorf, 10 μ l DNA Elution Buffer was added prior to incubation at room temperature for 1 minute and centrifugation at 13,000 rpm for 1 minute. The elution step was repeated into a new 1.5 ml Eppendorf. The DNA concentration was determined using the nanodrop spectrophotometer. Next, the purified PCR product was digested with KpnI (Fisher Scientific, #FD0524) and HindIII (Fisher Scientific, #FD0504) restriction enzymes for 1 hour at 37 °C and the digested PCR product was passed through the Monarch PCR and DNA Cleanup Kit (New England Biolabs, #T1030S). Purified, digested enhancer inserts were stored at 4 °C until use.

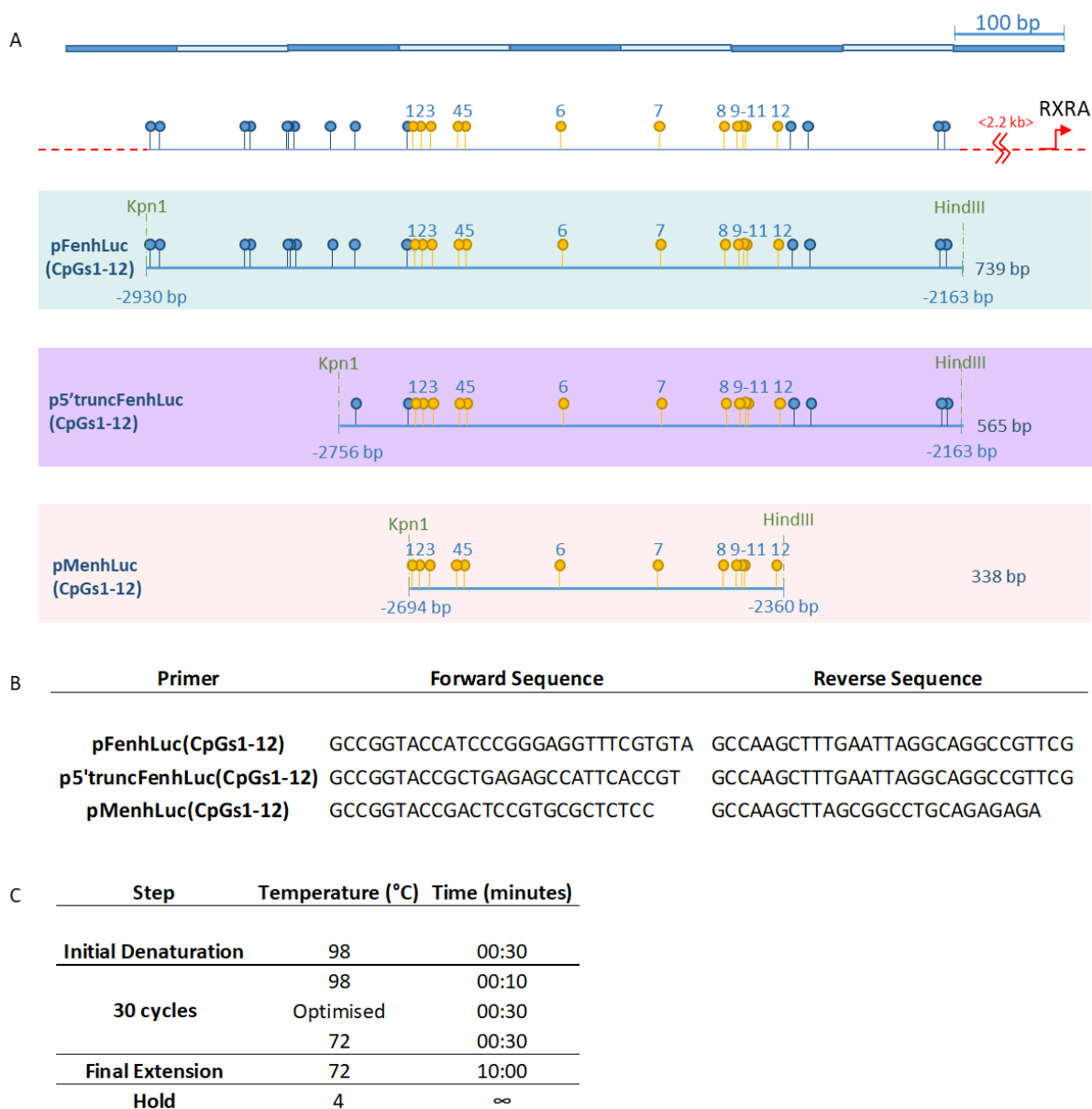


Figure 2.6 Schematic of the *RXRA* enhancer inserts, PCR primers and PCR conditions.

A) Overview of the *RXRA* inserts for the full enhancer region (FenhLuc(CpGs1-12)), 5' truncated full enhancer region (5'truncFenhLuc(CpGs1-12)) and the minimal enhancer region (MenhLuc(CpGs1-12)). Core *RXRA* CpGs of interest are highlighted in yellow and flanking CpGs are highlighted in blue. B) The PCR primers used to amplify genomic DNA. C) The PCR cycling conditions. An optimal temperature of 65 °C was used for FenhLuc(CpGs1-12) and 68 °C for 5'truncFenhLuc(CpGs1-12) and MenhLuc(CpGs1-12).

2.2.7.2.2 Ligation of the enhancer inserts into pGL4.23 plasmid

The luciferase reporter vector pGL4.23 (Promega, #E8411), which has a minimal promoter upstream of the luciferase gene and is designed for the insertion of response elements of interest, was used for the cloning of the *RXRA* CpGs of interest without the presence of the *RXRA* promoter. 500 ng of pGL4.23 was digested overnight at 37 °C with KpnI (Fisher Scientific, #FD0524) and HindIII (Fisher Scientific, #FD0504) restriction enzymes which produced two fragments of 4236 bp and 47 bp. The digested pGL4.23 plasmids were visualised on a 0.8 % agarose gel (Melford, #MB1200) for 20 minutes at 120 V and the larger band (4236 bp) was excised out of the gel using a sterile knife under UV conditions. Next, the digested pGL4.23 DNA was recovered using the Zymoclean Gel DNA Recovery Kit (Cambridge Bioscience, #D4001) as previously described (**section 2.2.7.1.2**) and 250 ng of recovered DNA was treated with Antarctic Phosphatase (New England Biolabs, #M0289S) as previously described (**section 2.2.7.1.2**). A 3-fold molar mass excess of each enhancer insert was ligated to 50 ng of Antarctic Phosphatase treated pGL4.23 vector using the Quick Ligation Kit (NEB) as described in **section 2.2.7.1.3**.

2.2.7.2.3 Digestion of pFenhLuc(CpGs1-12) and pMenhLuc(CpGs1-12) to make additional luciferase constructs

Luciferase plasmids containing the full and minimal enhancer region inserts were each digested with restriction enzymes to create four further enhancer constructs with differing core CpGs (**Figure 2.7**). pFenhLuc(CpGs1-12) and pMenhLuc(CpGs1-12) were digested with restriction enzymes for 1 hour at 37 °C before visualisation on a 0.8 % agarose gel (Melford, #MB1200), excision of the heavier band and purification as described previously. pFenhLuc(CpGs1-12)/ pMenhLuc(CpGs1-12) were digested with HindIII (Fisher Scientific, #FD0504) and SphI (Fisher Scientific, #FD0604) to create pFenhLuc(CpGs1-6)/ pMenhLuc(CpGs1-6), digestion with HindIII (Fisher Scientific, #FD0504) and BsaI (Fisher Scientific, #FD0294) to create pFenhLuc(CpGs1-3)/ pMenhLuc(CpGs1-3), digestion with KpnI (Fisher Scientific, #FD0524) and SphI (Fisher Scientific, #FD0604) to create pFenhLuc(CpGs7-12)/ pFenhLuc(CpGs7-12) and digestion with KpnI (Fisher Scientific, #FD0524) and BsaI (Fisher Scientific, #FD0294) to create pFenhLuc(CpGs4-12)/ pMenhLuc(CpGs4-12). Next, the digested constructs were blunt end treated using the Quick Blunting Kit (New England Biolabs, #E1201S) as per manufacturer's instructions. Briefly, 250 ng digested plasmid was added to 2.5 µl Blunting Buffer (10X), 2.5 µl 1 mM dNTP mix (Promega, #U1420), 1 µl Blunt Enzyme mix and water to make a final volume of 25 µl. The reaction was incubated at room temperature for 15 minutes prior to heat inactivation at 70 °C for 10 minutes. The blunt end treated plasmids were ligated using the Quick Ligation Kit (New England Biolabs, #M2200S) and chilled on ice until transformation.

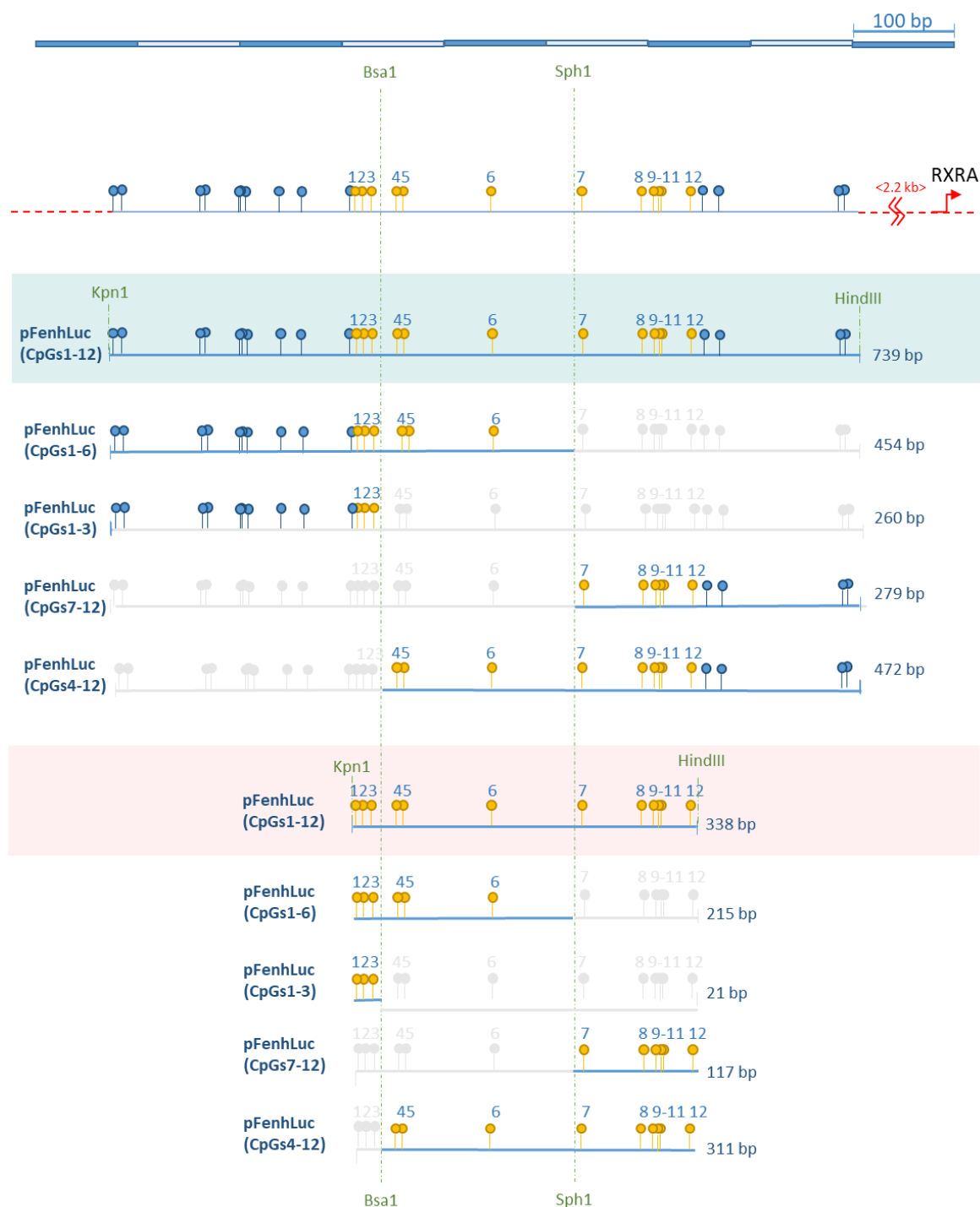


Figure 2.7 Schematic of enhancer region insets following digestion with restriction enzymes.

The full enhancer region plasmid (pFenhLuc(CpGs1-12)) and minimal enhancer region plasmid (pMenhLuc(CpGs1-12)) were digested with a combination of restriction enzymes prior to blunt end treating and ligation to generate additional enhancer plasmids. pFenhLuc(CpGs1-12)/ pMenhLuc(CpGs1-12) were digested with HindIII and Sph1 to create pFenhLuc(CpGs1-6)/ pMenhLuc(CpGs1-6), digestion with HindIII and Bsa1 to create pFenhLuc(CpGs1-3)/ pMenhLuc(CpGs1-3), digestion with Kpn1 and Sph1 to create pFenhLuc(CpGs7-12)/ pMenhLuc(CpGs7-12) and digestion with Kpn1 and Bsa1 to create pFenhLuc(CpGs4-12)/ pMenhLuc(CpGs4-12). The core *RXRA* CpGs are highlighted in yellow and the flanking CpGs are highlighted in blue.

2.2.7.3 PCR mutagenesis of pRXRApromLuc and pMenhLuc(CpGs1-12)

Site directed mutagenesis mutated *RXRA* CpGs 4, 5, 6, 8 and 12 in the luciferase construct containing the *RXRA* promoter (pRXRApromLuc) and in the construct containing the minimal *RXRA* enhancer region (pMenhLuc(CpGs1-12)) to TpG using Sequa prep PCR mutagenesis (Fisher Scientific, #A10498) as per manufacturer's instructions. The PCR primers were designed using http://www.bioinformatics.org/primerx/cgi-bin/DNA_1.cgi and can be seen in **Figure 2.8A**. Briefly, 50 ng of plasmid DNA (pRXRApromLuc or pMenhLuc(CpGs1-12)) was combined with 2 µl buffer, 0.4 µl DMSO, 1 or 2 µl enhancer A or B, 0.36 µl polymerase, 10 µl of 10 mM forward and reverse primer and water to make a final volume of 20 µl. The PCR set up can be seen in **Figure 2.8B**. Following PCR mutagenesis, 5 µl of the PCR reaction was visualised on a 0.8 % agarose gel (Melford, #MB1200) for 20 minutes at 120 V. The remaining PCR product was digested with 1 µl of the restriction enzyme DpnI (Fisher Scientific, #FD1704) to remove residual template plasmid DNA for 2 hours at 37 °C. Following DpnI digestion, 5 µl of digested PCR product was visualised on a 0.8 % agarose gel (Melford, #MB1200) for 20 minutes at 120 V. After comparison of the PCR products, both pre and post digestion, samples with a remaining PCR band were transformed as described in **section 2.2.7.5**. However 1 µl PCR product was transformed into 10 µl JM109 cells (Promega, #L2001), 50 µl of SOC media (Sigma, #S1797) was added and a single agar plate was inoculated with all of the transformed JM109 cells and media.

A

PCR Mutagenesis Primers		
Primer	Forward Sequence	Reverse Sequence
RXRA mut. 4 A	GCAGGGGATGATGCCTTCCGGTGTTTCTTAGG	CCTAAGAAACACCGGAAGGCATCATCCCCTGC
RXRA mut. 4 B	GTCTCTAGAGCAGGGGATGATGCCTTCCGGTG	CACCGGAAGGCATCATCCCCTGCTCTAGAGAC
RXRA mut. 4 C	GCAGGGGATGATGCCTTCCGGTGTTTCTTAGG	CCTAAGAAACACCGGAAGGCATCATCCCCTGC
RXRA mut. 5 A	GAGCAGGGGATGACGCCTTCTGGTGTTCCTTAG	CTAAGAAACACCAGAAGGCATCATCCCCTGCTC
RXRA mut. 5 B	GATGACGCCTTCTGGTGTTCCTTAGGAACAGAGG	CCTCTGTTCTAAGAAACACCAGAAGGCATCATC
RXRA mut. 5 C	GATGACGCCTTCTGGTGTTCCTTAGGAACAGAGG	CCTCTGTTCTAAGAAACACCAGAAGGCATCATC
RXRA mut. 6	GTCTGCATGTGCCTCCCTGACTCCAGGCCAACAG	CTGTTGGTGCCTGGAGTCAGGGAGGCACATGCAGAC
RXRA mut. 8	CACCATTGCCTGGTGTGCTCCTGACCTG	CAGGTGAGGACACACCAGGCAATGGTG
RXRA mut. 12	CTTCTCTGCAGGCTGCTGCTCAGCCGGC	GCCGGCTGAGCAGCAGCCTGCAGAGAGAAG

B

PCR Mutagenesis Thermal Cyclers Conditions		
Cycles	Temperature (°C)	Time (minutes)
x1	94	02:00
	94	00:10
x10	Gradient	00:30
	68	06:10
x8	94	00:10
	Gradient	00:30
	68 (Auto Delta Step)	06:10
x1	72	00:00
	4	∞

Figure 2.8 RXRA PCR mutagenesis primers and PCR cycling conditions.

A) Forward and reverse primer sequences for PCR mutagenesis for a mutation of CpG to TpG in the 5' to 3' orientation. Three different primers have been used for mutating *RXRA* CpGs 4 and 5. *RXRA* = retinoid X receptor alpha. B) PCR thermal cycling conditions for PCR mutagenesis. A gradient of 67 °C, 69 °C and 72 °C was used. The 'Auto Delta Step' on the thermal cycler added an extra 20 seconds to this stage every cycle.

2.2.7.4 Agar plates and Luria broth media

To make the agar plates, 10 g Luria Broth powder (Sigma Aldrich, #L3022) and 7.5 g of Agar powder (Fisher Scientific, #BP1423) were resuspended in 500 ml water and autoclaved on a standard cycle. Next, when the melted agar solution had cooled to the point it was touchable by hand, 500 µg Ampicillin (Sigma Aldrich, #A9393) was added to make a final concentration of 100 µg/ml. The agar solution was poured into twenty 10 cm dishes and were incubated at room temperature for 20 minutes. Once set, the plates were stored inverted at 4 °C for up to one month. To make the Luria Broth media, 10 g Luria Broth powder (Sigma Aldrich, #L3022) was resuspended in 500 ml water and autoclaved on a standard cycle. Once cool, 500 µg Ampicillin (Sigma Aldrich, #A9393) was added to make a final concentration of 100 µg/µl and the media was stored at 4 °C for up to one month.

2.2.7.5 Transformation

Plasmid DNA was transformed into competent *E. coli* JM109 cells (Promega, #L2001) as per manufacturer's instructions. Briefly, JM109 cells were thawed on ice. 25 ng of ligated plasmid DNA was added to 50 µl of thawed JM109 cells and were gently mixed by flicking. Next, the reaction was incubated on ice for 10 minutes, at 42 °C for 45 seconds and on ice for a further 2 minutes. Following the heat shock cycle, 100 µl SOC media (Sigma, #S1797, 20 g/l Tryptone, 5 g/l yeast extract, 4.8 g/l MgSO₄, 3.603 g/l dextrose, 0.5 g/l NaCl, 0.186 g/l KCl) was added and the reaction was incubated at 37 °C for 1 hour whilst shaking at 225 rpm. Following incubation, 3 agar plates were inoculated with 10 µl, 50 µl and 100 µl of the transformed JM109 cells. Following transformation into JM109 cells with a positive or negative control, 2 agar plates were inoculated with 10 µl or 100 µl of the reaction.

2.2.7.6 Minipreparation of plasmid DNA

Plasmid DNA was extracted from JM109 bacterial culture using the GeneJet Plasmid Miniprep Kit Protocol A (Fisher Scientific, #10242490) as per manufacturer's instructions. Single colonies were scraped with a sterile tip, placed into 5 ml Luria Broth media and incubated overnight at 37 °C whilst shaking at 225 rpm to make bacterial culture. 16 hours later, 2 ml of bacterial culture was transferred to a 2.2 ml Eppendorf and pelleted at 8,000 rpm for 5 minutes. The supernatant was discarded and the pellet resuspended in 250 µl Resuspension Solution by vortexing. Next, 250 µl Lysis Solution was added and the Eppendorf's were gently inverted 4-6 times until the solution became viscous and slightly clear. Following lysis, 350 µl Neutralisation Solution was added and immediately inverted 4-6 times before centrifugation at 8,000 rpm for 5 minutes. The supernatant was transferred to a GeneJET spin column, centrifuged for 1 minute at 8,000 rpm and the flow through was discarded. 500 µl Wash Solution was added to the sample, centrifuged for 30-60 seconds and the flow through discarded. The wash step was repeated, and the spin column was further centrifuged for 1 minute to remove any residual wash solution. The spin column was placed in a new 1.5 ml Eppendorf, 50 µl elution Buffer was added and incubated at room temperature for 2 minutes before centrifugation at 8,000 rpm for 2 minutes. The purified plasmid DNA was stored at 4 °C for short term use.

2.2.7.7 Confirming the presence of plasmid DNA

Following transformation of plasmid DNA and minipreparation, the correct plasmids and any incorrect mutations were confirmed following restriction enzyme digests and through sequencing plasmid DNA. Suitable restriction enzymes were selected using the online tool <http://nc2.neb.com/NEBcutter2/>. The plasmid DNA sequence was uploaded onto the website and

possible restriction enzyme digestion sites were given as well as the DNA fragment sizes that are to be expected following digestion with the selected enzymes. FastDigest restriction enzymes were ordered from Thermo Fisher Scientific. Typically, 250 ng plasmid DNA (from minipreparation or control plasmid DNA) was incubated at 37 °C for 1 hour with 1 µl of each FastDigest restriction enzyme, 1 µl buffer (10X) and water to make a final volume of 10 µl. Following incubation, the digested plasmid DNA was visualised on a 1 % agarose gel (Melford, #MB1200) for 1 hour at 120 V. Plasmids which appeared to be the correct size were sent for Sanger sequencing (GATC Biotech) to confirm. Upon completion of sequencing, multiple sequence alignment (<https://www.ebi.ac.uk/Tools/msa/clustalo/>) compared the plasmid DNA sequence of interest against the expected sequence and any mutations were highlighted.

2.2.7.8 Midipreparation of plasmid DNA

Plasmid DNA from JM109 bacterial culture was purified on a greater scale for use in transfections using the GeneJET Plasmid Midiprep Kit (Fisher Scientific, #K0481) as per manufacturer's instructions. Prior to midipreparation, single colonies were scraped with a sterile tip, placed into 5 ml Luria Broth media and left to incubate at 37 °C overnight whilst shaking at 225 rpm to make bacterial culture. 16 hours later the bacterial culture was incubated at 4 °C. 8 hours later, 150 µl of bacterial culture was added to 100 ml of Luria Broth media before incubation overnight at 37 °C whilst shaking at 225 rpm. 16 hours later, the cloudy bacterial culture was transferred to two 50 ml falcon tubes underwent centrifugation at 5,000 g for 10 minutes. The supernatant was discarded and the pellet could either be stored at -80 °C until use or plasmid DNA could be extracted using the Midiprep Kit. Briefly, the bacterial cell pellet was resuspended in 2 ml Resuspension Solution by vortexing. Following resuspension, 2 ml of Lysis solution was added and inverted gently 4-6 times prior to incubation at room temperature for 3 minutes. Following the incubation, 2 ml of Neutralisation Solution was added and immediately inverted 5-8 times. Next, 0.5 ml Endotoxin Binding Reagent was added and immediately inverted 5-8 times prior to incubation at room temperature for 5 minutes. Following incubation, 3 ml 96 % ethanol (Fisher Scientific, #E/0600/05) was added and immediately inverted 5-6 times before centrifugation for 40 minutes at 4,000 g. After centrifugation, the supernatant was transferred to a 15 ml falcon tube, 3 ml 96 % ethanol (Fisher Scientific, #E/0600/05) was added and immediately inverted 5-6 times. The sample was passed through the supplied columns by centrifugation for 3 minutes at 2,000 g and the flow through discarded. Next, 4 ml Wash Solution I was added, underwent centrifugation for 2 minutes at 3,000 g and the flow through discarded. 4 ml of Wash Solution II was added, underwent centrifugation for 2 minutes at 3,000 g and the flow through discarded and this wash step was repeated. After discarding the flow through, the sample was centrifuged for a further 5 minutes at 3,000 g to remove residual wash solution. The column was transferred to a new 15 ml collection

Chapter 2

tube, 0.35 ml Elution Buffer was added prior to incubation at room temperature for 2 minutes and centrifugation at 3,000 g for 5 minutes. The purified plasmid DNA was stored at 4 °C until use.

2.2.7.9 Preparation of glycerol stocks for long term storage

Glycerol stocks of the plasmid DNA were prepared for long term storage. 30 % glycerol (Sigma Aldrich, #G6279) was sterilised on a standard autoclave cycle. 350 µl of the JM109 bacterial culture containing plasmid DNA of interest used for minipreparations was combined with 350 µl sterile glycerol in 1.5 ml screw cap tubes. Next, the bacterial glycerol mixture was vortexed and snap frozen on dry ice before storage at -80 °C.

2.2.7.10 Transfection of plasmid DNA

2.2.7.10.1 Preparing plasmid DNA for tissue culture

Plasmid DNA was sterilised before transfection into osteosarcoma cell lines. Water was added to 100 µg of pRXRApromLuc wildtype and mutated DNA plasmids and pGL4.17 to make a final volume of 150 µl, or to 50 µg of the RXRA enhancer constructs and pGL4.23 to make a final volume of 300 µl. Twice the volume of ethanol (Fisher Scientific, #E/0600/05) and 1/10 the volume of sodium acetate (Sigma Aldrich, #S8388) was added to the diluted plasmid DNA before incubation at -20 °C overnight. Next, the sample was centrifuged for 30 minutes at 13,000 rpm. In a sterile hood, the supernatant was discarded. The pellet was washed in 100 µl 70 % ethanol (Fisher Scientific, #E/0600/05) which was discarded and the pellet was left to air dry at room temperature for 10 minutes. Next, the plasmid DNA pellet was resuspended in 100 µl sterile water. The concentration of plasmid DNA was determined using a Nanodrop spectrophotometer and the plasmid DNA was further diluted to a concentration of approximately 200 ng/µl. The sterile plasmid DNA was stored at 4 °C.

2.2.7.10.2 Transfection into Saos2 cells with Fugene 6

Saos2 cells were seeded at 100,000 cells per well in a 24 well plate and 6 wells were plate for each luciferase construct. Cells were grown in 1 ml of DMEM/Ham's F-12 media (Gibco, #11320-074) supplemented with 5 % FBS (PAA, #A15-151), 2 mM L-glutamine (Sigma-Aldrich, #G7513) and 1 % penicillin streptomycin (PAA, #P11-010) at 37 °C and an atmosphere of 5 % CO₂. 24 hours later, Saos2 cells were transfected with plasmid DNA using Fugene 6 (Promega, #E2691) as per manufacturer's instructions. First, Opti-MEM (Invitrogen, #31985062) and Fugene 6 were warmed to room temperature. Fugene 6 was vortexed immediately prior to use and 3 µl was added to Opti-MEM (Invitrogen, #31985062) before incubation at room temperature for 5 minutes. 492.5 ng of plasmid DNA and 7.5 ng of CMV renilla (Promega, #E2261) were added to Opti-MEM and fugene 6

to make a final volume of 25 μ l per well. The DNA lipid complex was incubated at room temperature for 15 minutes and 25 μ l of the reaction was added to each well.

2.2.7.10.3 Transfection into MG63 cells with Lipofectamine 3000

MG63 cells were seeded at 50,000 cells per well in a 24 well plate and 6 wells were plated for each luciferase construct. Cells were grown in 1 ml of DMEM/Ham's F-12 (Gibco, #11320-074) media supplemented with 5 % FBS (PAA, #A15-151), 2 mM L-glutamine (Sigma-Aldrich, #G7513) and 1 % penicillin streptomycin (PAA, #P11-010) at 37 °C and an atmosphere of 5 % CO₂. 24 hours later, MG63 cells were transfected with plasmid DNA using Lipofectamine 3000 (Life Technologies, #L3000008) as per manufacturer's instructions. First, 25 μ l of Opti-MEM (Invitrogen, #31985062) was combined with 0.75 μ l Lipofectamine 3000 reagent. In a separate Eppendorf, 25 μ l of Opti-MEM (Invitrogen, #31985062) was combined with 492.5 ng plasmid DNA, 7.5 ng CMV Renilla (Promega, #E2261) as the internal control and 0.75 μ l P3000 reagent. The diluted plasmid DNA solution was added to the diluted Lipofectamine solution before incubation at room temperature for 10-15 minutes. Following incubation, 50 μ l of the DNA lipid complex was added to each well.

2.2.7.10.4 Treating transfected osteosarcoma cells with vitamin D

1,25(OH)₂D₃ was obtained from Enzo Life Sciences (#BML-DM200-0050) and was reconstituted in filtered 100 % ethanol (Fisher Scientific, #E/0600/05). Six hours post transfection with plasmid DNA, the human osteosarcoma cell lines were treated with 10 nM 1,25(OH)₂D₃ or with filtered 100 % ethanol (Fisher Scientific, #E/0600/05) for a total of 18 hours. The final ethanol concentration in the osteosarcoma cell lines was 0.01%.

2.2.7.10.5 Preparing cells for the dual luciferase assay

The osteosarcoma cells were lysed 24 hours post transfection. First, the media was removed and the cells were washed in warm PBS (Fisher Scientific, #12821680). Once the residual liquid had been removed 150 μ l of 1x passive lysis buffer (Promega, #E1910) was added to each well and the transfection plates were frozen at -80 °C. The 24 well plates were freeze thawed twice to ensure complete cell lysis. The cell lysate was thoroughly pipetted up and down before 30 μ l was transferred to an opaque 96 well plate so that luciferase expression could be measured on the Glomax machine (Promega). The dual luciferase assay program was loaded onto the Glomax machine, the injectors were primed with 500 μ l Luciferase Assay Reagent II and 500 μ l Stop and Glo reagent (Promega, #E1910) according to manufacturer's instructions. 100 μ l Luciferase Reagent II was added to each well, luciferase expression was measured, 100 μ l of Stop and Glo reagent was added to each well and CMV renilla expression was measured. Upon completion of the luciferase assay, firefly luciferase expression was normalised to CMV renilla expression.

2.2.8 Isolation of nuclear extract

Nuclear extracts were prepared from human osteosarcoma cell pellets (Saos2 and MG63) and from MSCs from human umbilical cord (ATCC, #PCS-500-010). Cell pellets were resuspended in 800 μ l of ice cold lysis buffer containing 10 mM HEPES (Sigma Aldrich, #H4034), 10 mM KCl (Sigma Aldrich, #P9541), 0.1 mM EDTA (Sigma Aldrich, #03690), 1 mM DTT (Melford, #MB1015), 0.5 mM PMSF (Sigma Aldrich, #P7626) and 0.025 mM leupeptin (Sigma Aldrich, #L5793), vortexed until re-suspended and incubated on ice for 10 minutes. Next, 50 μ l of 10 % NP-40 (Sigma Aldrich, #I8896) was added, samples were vortexed for 10 seconds and transferred to a chilled 1.5 ml Eppendorf. The sample was centrifuged at 13,000 rpm for 30 seconds at 4 °C and the supernatant was discarded. The cell pellet containing nuclei was resuspended in ice cold nuclear extraction buffer containing 20 mM HEPES (Sigma Aldrich, #H4034), 0.4 M NaCl (Sigma Aldrich, #S3014), 1 mM EDTA (Sigma Aldrich, #03690), 1 mM DTT (Melford, #MB1015) and 0.5 mM PMSF (Sigma Aldrich, #P7626) and vortexing. Typically, 30 μ l of nuclear extraction buffer is used for 6×10^6 cells however, extra can be used if required. The samples were incubated on ice for at least an hour or until full resuspension. Once resuspended, the samples were centrifuged at 13,000 rpm at 4 °C for 5 minutes to pellet nuclear debris. The protein concentration of the nuclear extracts was determined using the Pierce BCA Protein Assay Kit (Fisher Scientific, #23227) according to manufactures instructions. Nuclear extracts were aliquoted to prevent multiple freeze thaw cycles and were snap frozen in dry ice and stored at -80 °C until use.

2.2.9 Analysis of transcription factor binding by electrophoretic mobility shift assays

2.2.9.1 Annealing oligonucleotides

Complementary single stranded oligonucleotides (100 μ M) for the *RXRA* CpGs of interest (**Table 2.4**) were annealed in two different concentrations: 1 pmol/ μ l (100x) for radioactive probe labelling and 5 pmol/ μ l (500x) for competitor concentrations. 5 μ l (100x) or 25 μ l (500x) each of forward and reverse single stranded oligonucleotide sequences were combined with annealing buffer containing 10 mM Tris (Sigma Aldrich, #T6791), 1 mM EDTA (Sigma Aldrich, #03690) and 50 mM NaCl (Sigma Aldrich, #S3014) in a total volume of 1 ml. Next, the samples were placed in a water bath, which was preheated at 100 °C, and slowly cooled to room temperature overnight. Once cool, the annealed oligonucleotides were aliquoted and stored at -20 °C until use.

Table 2.4 RXRA oligonucleotide sequences for EMSA probes.

EMSA Oligonucleotide Sequences		
Oligonucleotide	Forward Sequence	Reverse Sequence
RXRA CpGs 1-3	CTCCGGACTCCGTGCGCTCTCCACGTGGTCTCTAG	CTAGAGACCACGTGGAGAGCGCACGGAGTCCGGAG
RXRA CpGs 4-5	AGAGCAGGGGATGACGCCTCCGGTGTTCCTTAGG	CCTAAGAAACACCGGAAGGCGTCATCCCCTGCTCT
RXRA CpG 8	TCCCACCATTGCCTGGCGTGTCTGACCTGCCGTC	GACGGCAGGTCAGGACACGCCAGGCAATGGTGGGA
RXRA CpG 12	CCTTCTCTCTGCAGGCCGCTGCTCAGCCGCCCTG	CAGGGCCGGCTGAGCAGCGCCTGCAGAGAGAAGG

Forward and reverse sequences are in the 5' to 3' orientation. EMSA = electrophoretic mobility shift assay, RXRA = retinoid X receptor alpha.

2.2.9.1.1 Annealing transcription factor cocktails

Complementary single stranded oligonucleotides (100 μ M) for individual transcription factors were annealed (Table 2.5). 25 μ l of the forward and reverse oligonucleotide were combined with 50 μ l annealing buffer composed of 20 mM Tris (Sigma Aldrich, #T6791), 2 mM EDTA (Sigma Aldrich, #03690) and 100 mM NaCl (Sigma Aldrich, #S3014). Next, the samples were placed in a water bath which had been preheated to 100 $^{\circ}$ C, and left to cool to room temperature overnight. Once the individual transcription factors were annealed, ten different transcription factors were combined to make a transcription factor cocktail.

Table 2.5 Oligonucleotide sequences of transcription factors cocktails for EMSAs.

Cocktail 1	AP1	CGTTGATGACTCAGCCGGAA	Cocktail 5	RAR	AGGGTAGGGTTACCCGAAAGTTCACCTC
	AP2a	GATCGAACTGACCCGCCGCGCCCGT		RXR	AGCTTCAGGTCAGAGGTCAGAGAGCT
	AR	GAAGTCTGGTACAGGGTGTCTTTTGG		SIE	GTGCATTTCCCCTAAATCTTGTCTACA
	Brn3	CACAGCTCATTAACGCGC		Smad	GTCTAGACCA
	CBP	AGACCGTACGTGATTGGTTAATCTCTT		Smad3+4	TCGAGAGCCAGACAAAAAGCCAGACATTTAGCCAGACAC
	CDP	ACCCAATGATTATTAGCCAATTTCTGA		Smuc	GGATCCCCCAACACCTGCTGCCTGA
	CEBP	TGCAGATTGCGCAATCTGCA		Sp1	ATTTCGATCGGGCGGGGGCGAGC
	cMyb	TACAGGCATAACGGTTCCGTAGTGA		SRE	GGATGTCATATTTAGGACATCT
	CREB	AGAGATTGCCTGACGTCAGAGAGCTAG		Stat1	CATGTTATGCATATTTCTGTAAAGTG
	CTCF	GGCGGCCCGCTAGGGGTCTCTCT		Stat3	GATCCTTCTGGGAATTCCTAGATC
Cocktail 2	E2F1	ATTTAAGTTTTCGGCCCTTTCTCAA	Cocktail 6	Stat4	GAGCCTGATTTCCCAGAAATGATGAGC
	Egr	GGATCCAGCGGGGGGAGCGGGGGCGA		Stat5	AGATTTCTAGGAATTCATCC
	ER	GGATCTAGGTCACTGTGACCCCGGATC		Stat56	GTATTTCCCAGAAAAGGAAC
	Ets	GGGCTGCTTGAGGAAGTATAAGAAT		Tbet	AATTTACACCTAGGTGTGAAATF
	Ets1	GATCTCGAGCAGGAAGTTTCA		TFE3	GATCTGGTCATGTGGCAAGGC
	FAST1	TGTGTATTCA		TFEB	CACGTG
	GAS	AAGTACTTTCAGTTTCATATTACTCTA		TFIID	GCAGAGCATATAAAATGAGGTAGGA
	GATA	CACTTGATAACAGAAAGTGATAACTCT		TGIF	CCTCGCTTGACAGGCAGAGT
	Gfi1	TAAATCACTGC		TR	AGCTTCAGGTCACAGGAGGTGAGAG
	GR	AGAGGATCTGTACAGGATGTTCTAGAT		USF1	CACCCGGTCCAGTGGCCTACACC
Cocktail 3	HIF1a	TCGTACGTGACCACACTCACCTC	Cocktail 7	VDR	AGCTTCAGGTCAGGAGGTGAGAGAGC
	Sox2	CATTGTG		YY1	CGCTCCCGGCCATCTTGGCGGCTGGT
	HNF4	CTCAGCTGTACTTTGGTACAACATA		ZEB	GATCTGGCCAAAGGTGACAGGATC
	IRF1	GGAAGCGAAAATGAAATGACT		HNF1	GTTAATGATTAAC
	MEF1	GATCCCCCAACACCTGCTGCCTGA		ARP1	AGGTGACCTTTGCCCA
	MEF2	GATCGCTCTAAAAATAACCCGTGCG		NFY	ATCAGCCAATCAGAGC
	MIBP1	TCTTTTCCCA		HNF3	GCCCATGTGTTGTTTTAAGCC
	MycMax	GGAAGCAGACCACGTGGTCTGCTTCC		BARP	TCACCTCAAGTTCAAGTTATT
	NF1	TTTTGGATTGAAGCCAATATGATAA		SREBP1	TTTGAAAATCACCCTGCAAACTC
	NFE2	TGGGAACCTGTGCTGAGTCACTGGAG		HSF1	GATCTCGGCTGGAATATTTCCCAGCTGGCAGCCGA
Cocktail 4	NFATc	CGCCCAAGAGGAAAATTTGTTTCATA	Cocktail 8	NRF1	YGCAGYCGGCR
	NFkB	AGTTGAGGGGACTTTCCCAGGC		PAX3	GATCCTGAGTCTAATTTGGATCCTGAGTCTAATTG
	NR5A2	GATCAACGACCCGACCTTGAG		Mash1	CCCAACACCTGCTGCCTGAGCC
	OCT1	TGTCGAATGCAAATCACTAGAA		Maf	GGCAGTCCCGACTCGGCACGAT
	p53	TACAGAACATGTCTAAGCATGCTGGGG		MyoD	TCCAACGTGACCAACTGAC
	Pax5	GAATGGGGCACTGAGGCGTGACCACCG		Oct4	GCCGAATTTGCATATTTGCATGGCTG
	Pbx1	CTCCAATTAGTGCATCAATCAATTCTG		GABPA	ACTTCCGGT
	Pit1	TGTCTTCTGAATATGAATAAGAAAATA		NR4a2	AAAGGTCAC
	PPAR	AGGTCAAAGGTCA		TCF4	ACANNTGT
	PR	GATCCGTACAGGATGTTCTAGTACA		Zic	CTAGAACTACCTCCTCTTTTAGAACTATG

Each cocktail contained 10 transcription factors.

2.2.9.2 Electrophoretic mobility shift assay (EMSA)

The *RXRA* probes were radioactively labelled by combining 2 µl of 100x annealed probe, 5 µl of 10x T4 PNK buffer, 1 µl T4 PNK enzyme (Promega UK, #M4101), 40 µl water and 2 µl of γ-32P ATP (Perkin Elmer, #BLU002A250UC). Next, the sample was incubated for 30 minutes at 37 °C, 50 µl of water was added and the sample was passed through a microspin G-25 column (GE Healthcare, #27-5330-01) as per manufacturer's instructions. Following purification, 2 µl of radiolabelled probe was used per reaction and the probe was stored in a safe container at -20 °C until use.

Prior to loading the radioactive material the 5 % polyacrylamide gels, composed of polyacrylamide (Fisher Scientific, #BPE1402-1), 10X TBE (Fisher Scientific, #T/P050/15), 10 % APS (Fisher Scientific, #BPE179-25) and TEMED (Sigma Aldrich, #T7024), were pre run for 1 hour at 100 V.

All EMSAs were run in duplicate as an experimental control. Samples were prepared by combining 10 µl Parker buffer (8 % Ficoll (Sigma-Aldrich, #F9378), 20 mM HEPES pH 7.9 (Sigma Aldrich, #H4034), 50 mM KCl (Sigma Aldrich, #P9541), 1 mM EDTA (Sigma Aldrich, #03690) and 0.5 mM

dithiothreitol [DTT] (Melford, #MB1015)), 1 μ l poly di dc (Sigma Aldrich, #P4929), 5 μ g nuclear extract, 2 μ l of 500x competitor (eg. Specific, non-specific, transcription factor cocktail or individual transcription factor) and water to make a final volume of 22 μ l. Two controls were run on each gel with the probe alone (P) without any nuclear extract, and a probe and extract only (P+E) without any 500x competitor. Next, the reaction was incubated in the fridge for 10 minutes, 2 μ l of radioactive probe was added, mixed and pulse spun before incubation at room temperature for 10 minutes. 20 μ l of the prepared sample was loaded onto the pre-run 5 % polyacrylamide gels and were ran at 100 V for 1 hour. The radiolabelled gels were blotted and cross linked using Whatman chromatography paper (Fisher Scientific, #11939197) and a semi dry blotter for 45 minutes at 80 °C. The dried gel was placed against film (Thermo Scientific, #34088) for exposure overnight at -80 °C. 24 hours later the films were exposed using developer (Sigma-Aldrich, #P7042) and fixer (Sigma-Aldrich, #P7167).

2.2.10 Mouse animal model

The animal model was designed by Dr Steph Borg, University of Sheffield, as part of a collaboration and animal work was carried out as per regulations under the Animals (Scientific Procedures) Act 1986. C57/BL6 mice were placed on a standard diet containing 1000 units/kg Vitamin D or a vitamin D free diet(0 units/kg) based on the AIN93G diet from 4 weeks of age prior to mating at 10 weeks of age. Litters remained on the maternal diet until weaning at 3 weeks of age and the postnatal diet refers to diet from weaning. The experimental design consisted of 4 groups: antenatal and postnatal replete; antenatal replete postnatal deplete; antenatal and postnatal deplete; antenatal deplete and postnatal replete. At 8 weeks the mice underwent mechanical loading *in vivo* of their left tibia 3 times per week for 2 weeks. Briefly, a 10.5 N load was superimposed onto a 0.5 N preload at a rate of 160, 000 N/s as a peak load of 11 N has been shown to induce an osteogenic response in female C57BL/6 mice³⁵⁶. The left tibiae underwent 40 trapezoidal waveform load cycles with a 0.2 s hold at 11 N followed by a 10 s interval between each cycle. Following loading, half of the mice were culled and tibiae preserved and the remaining mice underwent further loading of their left tibia at 16 weeks for 2 weeks prior to being culled and the tibiae preserved. All of the tibiae underwent 3 point bending using the Bose Electroforce 3200 mechanical testing machine with a 450 N load cell. Briefly, a preload of 0.5 N was applied to tibiae before compressing at a constant force of 0.25 N/s until failure. Tibial stiffness (N/mm) was calculated from the linear elastic region of the force displacement curve and the break force was recorded as the load at failure. After cervical dislocation, plasma 25(OH)D₃ concentrations were measured from dried blood spots collected by cardiac puncture. Control dams had 25(OH)D₃ concentrations of 96.1 \pm 10.9 nM and deficient dams had concentrations of 0.9 \pm 0.2 nM. At 18 weeks of age, plasma 25(OH)D₃

concentrations were 79.2 ± 13.3 nM and 58.8 ± 8.9 nM in control and deficient mice respectively. DNA was extracted from tibia from mice that were 18 weeks old that were antenatal and postnatal replete and antenatal deplete and postnatal replete.

2.2.10.1 Genomic DNA extraction from murine tibiae

Mouse tibiae for DNA extraction and measurement of DNA methylation were provided by Dr Borg, University of Sheffield. An overview of Dr Borg's animal model can be seen in **section** Error! eference source not found.. Mouse tibiae were pulverised using liquid nitrogen and stored at -80 °C until use. DNA was extracted using the DNeasy Blood and Tissue kit (Qiagen, #69504) and a user defined protocol. Briefly, 360 μ l Buffer ATL and 30 μ l Proteinase K were added to 10 mg of crushed tibia, mixed by vortexing and incubated at 56 °C for 1 hour. Following incubation, the sample was vortexed for 15 seconds, 400 μ l Buffer AL was added and the sample vortexed to mix thoroughly. Next, 400 μ l 100 % ethanol (Fisher Scientific, #E/0600/05) was added and mixed by vortexing. Next, the sample was transferred to the DNeasy Minispin column before centrifugation at 6,000 g for 1 minute and the flow through discarded. The column was transferred to a new collection tube, 500 μ l Buffer AW1 was added, the sample was centrifuged at 6,000 g for 1 minute and the collection tube and flow through was discarded. The column was transferred to a new collection tube, 500 μ l Buffer AW2 was added, the sample was centrifuged at 20,000 g for 3 minutes and the collection tube and flow through was discarded. The column was transferred to a new Eppendorf, 50 μ l buffer AE was added before incubation at room temperature for 1 minute and centrifugation at 6,000 g for 1 minute. The column was eluted 3 times into fresh Eppendorf's. DNA was stored at 4 °C for short term use and at -20 °C for longer term storage.

2.2.11 Statistical Analyses

2.2.11.1 Statistical analysis of DNA methylation

DNA methylation data were exported from the pyrosequencer and imported into Microsoft Excel. Any samples that did not pass the internal bisulfite control or with an inadequate peak height were excluded. Statistical tests were carried out in IBM SPSS Statistics 24. Normal distribution was determined using a histogram and data for individual CpGs were transformed as appropriate to achieve normality as mentioned in each respective results chapter. A box whisker plot was used to determine outliers and 'extreme' outliers where the data were more than 3 times greater than the interquartile range were excluded. Data were plotted as mean and 95% confidence intervals and a p value of less than 0.05 was accepted as statistically significant.

2.2.11.1.1 Statistical analysis of DNA methylation measured in umbilical cord tissue

RXRA, *CDKN2A*, *Runx2* and *Osterix* DNA methylation in umbilical cord tissue was investigated in **Chapters 3-5**. Independent t-tests compared methylation at individual CpG sites between the cholecalciferol supplemented group and the placebo group within the MAVIDOS trial. The data were stratified by season of birth, and independent t-tests compared DNA methylation at birth between the treatment groups. The basic model for linear regression analyses involved adjustment for sex, gestational age, treatment allocation and season of birth. Linear regression analyses identified associations between CpG methylation at birth and bone measures at birth. The data were further stratified by treatment group and separately by season of birth and linear regression analyses identified any associations between CpG methylation at birth and bone measures at birth. Data were plotted as mean and 95 % confidence intervals and a p value of less than 0.05 was accepted as statistically significant.

2.2.11.1.2 Statistical analysis of DNA methylation measured in placental tissues

RXRA DNA methylation in placental tissue was investigated in **Chapter 3**. Independent t-tests compared *RXRA* CpG methylation between the cholecalciferol supplemented group and the placebo group within the MAVIDOS trial. The SPRING study is currently blinded therefore, the two treatment groups were coined 'group A' or 'group B' however, it is not yet known as to which is the vitamin D or placebo group. Independent t-tests compared *RXRA* methylation at birth between the two blinded treatment groups within the SPRING study. Matched paired t-tests compared *RXRA* methylation between the vitamin D treated placental fragments and cytotrophoblasts and their respective controls. Data were plotted as mean and 95 % confidence intervals and a p value of less than 0.05 was accepted as statistically significant. Post hoc power calculations were used to determine the sample size required to obtain a power of 0.8.

2.2.11.1.3 Statistical analysis of methylation data from osteosarcoma cell lines

RXRA DNA methylation was investigated in Saos2 and MG63 cell lines in **Chapter 6**. *RXRA* methylation data were exported from the PyroMark pyrosequencing software and imported into Microsoft Excel. Any samples that did not pass the internal bisulfite control or with an inadequate peak height were excluded. Normality was assessed using histograms and the data did not undergo any transformations to achieve normality. Methylation data were imported into SPSS and independent t-tests compared *RXRA* methylation between the vitamin D treated and control cells extracted from Saos2 and MG63 cells. Data were plotted as mean \pm SEM and a p value of less than 0.05 was accepted as statistically significant.

2.2.11.1.4 Statistical analysis of DNA methylation measured in murine tibiae

RXRA, *VDR*, *Runx2* and *Osterix* DNA methylation was investigated in murine tibiae in **Chapter 7**. Independent t-tests compared CpG methylation between the control and prenatal vitamin D deficient tibiae in both the non-loaded and loaded tibiae, as well as between the non-loaded and loaded tibiae in each of the two treatment groups. A p value of less than 0.05 was accepted as statistically significant.

2.2.11.2 Statistical analysis of luciferase expression data

Luciferase expression was investigated in Saos2 and MG63 cell lines in **Chapter 6**. Following the dual luciferase assay, luciferase expression data were exported into Excel. Luciferase expression data were normalised to the CMV renilla expression data. Next, luciferase expression data of the control luciferase construct was set at 100 % and the remaining luciferase constructs in the same experiment were normalised to the control. Normality was assessed using histograms and the data were deemed normally distributed. Following this, data were imported into GraphPad Prizm v7.03 and an independent t-test with Welch's correction, which is designed for samples with unequal variance but the assumption of normality is maintained, compared normalised expression data of the control luciferase plasmid and each individual plasmid of interest. Data were presented on the same graph for visual representation despite luciferase expression of only two plasmids being compared at one time. Data were plotted as mean \pm SEM and a p value of less than 0.05 was accepted as statistically significant.

2.2.11.3 Statistical analysis of real time PCR data

Gene expression of *RXRA* (Qiagen, #QT00005726), *CYP24A1* (Qiagen, #QT00015428), *VDR* (Qiagen, #QT01010170), *Runx2* (Qiagen, #QT00020517), *Osterix* (Qiagen, #QT00213514) and the internal control *GAPDH* (Qiagen, #QT00079247) were investigated in Saos2 and MG63 cell lines in **Chapter 6**. Real time PCR data were analysed using the delta CT method using GraphPad Prizm v7.03. Briefly, the average Ct values of samples run in duplicate was taken and samples with a standard deviation of greater than 1 were excluded. RNA expression of *RXRA*, *VDR*, *CYP24A1*, *Osterix* and *Runx2* were normalised to RNA expression of *GAPDH*. Real time expression for Saos2 cells and MG63 cells were calculated separately. For each gene, the sample with the highest Ct value was identified and the ddCT value was obtained using the equation below:

$$= \text{LOG}(\text{POWER}(2, -((X1 - Y1) - (X2 - Y2))))$$

Where X1 is the Ct value of sample you are calculating and Y1 is the corresponding *GAPDH* Ct value for that sample. X2 corresponds to the highest Ct value for that gene and Y2 is the corresponding

GAPDH Ct value for that sample. The ddCT values were imported into GraphPad Prizm v.7.03 and normality was assessed using histograms. Independent t-test with Welch's correction compared normalised real time data between the vitamin D treatment and the ethanol control for each gene. Data were plotted as mean \pm SEM and a p value of less than 0.05 was accepted as statistically significant.

Chapter 3 Maternal vitamin D supplementation during pregnancy alters methylation of specific CpGs upstream of the *RXRA* promoter

3.1 Introduction

Bone mass and skeletal strength increase from birth and through childhood before peaking in early adulthood, followed by a decline with ageing²⁴. It has been shown that peak bone mass and the subsequent rate of bone loss that follows may be predictive of later osteoporosis risk⁵. The early life environment has been suggested to influence early bone accrual through the altered epigenetic regulation of genes. Consistent with this paradigm, the methylation status of a number of CpG loci at birth have been shown to be predictive of later bone health. For instance, within the Southampton Women's Survey (SWS) cohort, methylation of CpG loci upstream of the *RXRA* promoter in umbilical cord were shown to be inversely correlated with size corrected bone mineral content (scBMC) at 4 years of age²⁹⁹. The *RXRA* gene is located on chromosome 9 and encodes the retinoid X receptor which is part of the nuclear receptor family. RXRA forms a heterodimer with the VDR as well as other nuclear receptors such as the thyroid receptor and constitutive androstane receptor. Upon ligand binding, VDR heterodimerises with RXRA and binds to VDREs in proximal promoters and regulatory regions of target genes where they induce a range of effects^{60,357}.

The identification of suitable biomarkers at birth which are predictive of later bone health would provide valuable insight into the bone growth trajectory through childhood. This would allow the identification of individuals at a higher risk of developing diseases such as osteoporosis and could aid in the development of targeted interventions. Such marks may also provide an immediate outcome measure to evaluate early life interventions during pregnancy that can modify the bone trajectory. Due to tissue specific DNA methylation patterns, measurement of DNA methylation in a tissue that is central to the pathogenesis of osteoporosis, such as bone tissue, would be ideal however, this is not feasible. Therefore, proxy tissues which are easily accessible and are often discarded after delivery are used instead, such as the umbilical cord and placenta. Studies within the SWS cohort have shown that it is possible to detect methylation changes in peripheral tissues, such as umbilical cord tissue, which are predictive of altered phenotype in childhood and have the potential to be utilised as biomarkers of later bone health^{299,323}. The placenta plays a vital role in the normal growth and development of the fetus and is involved in the exchange of nutrients and waste between the maternal and fetal circulatory systems³⁵⁸. Furthermore, the placenta plays an important role in the intrauterine environment³⁵⁸ which has been shown to be associated with phenotype and disease progression in later life¹⁹⁵. Therefore, it would be interesting to determine DNA methylation changes in placental tissue as well as umbilical cord tissue.

The MAVIDOS trial investigated the effect of maternal cholecalciferol supplementation from 14 weeks gestation until delivery in a double blind, randomised, placebo controlled trial which took place in Southampton, Sheffield and Oxford. Initial results from the MAVIDOS trial found that there

were no significant differences in bone measures at birth between the two maternal treatment groups. However, when the analyses were stratified by season of birth, infants born in the winter months to cholecalciferol supplemented mothers had greater whole body bone mineral content (BMC), bone area (BA), and scBMC compared to placebo born infants³⁵⁹.

The MAVIDOS trial provides an ideal opportunity to investigate the use of *RXRA* methylation as a predictive biomarker of later bone health, which has been initially investigated using participants from the SWS cohort²⁹⁹. To investigate this further, associations between maternal vitamin D supplementation, bone measures at birth and DNA methylation of *RXRA* will be investigated in umbilical cord tissue as well as in placental tissue.

3.1.1 Hypothesis

We hypothesise that maternal cholecalciferol supplementation is associated with decreased *RXRA* CpG methylation in both umbilical cord and placental tissue, and that *RXRA* methylation in umbilical cord tissue is inversely associated with bone measures at birth within the MAVIDOS trial.

3.1.2 Aims

1. To determine whether maternal vitamin D supplementation during pregnancy alters *RXRA* CpG methylation in umbilical cord tissue
2. To determine whether umbilical cord *RXRA* CpG methylation is associated with bone measures at birth within the MAVIDOS trial
3. To determine whether maternal vitamin D supplementation during pregnancy alters *RXRA* CpG methylation in placental tissue

3.1.3 Methods

DNA methylation upstream of the *RXRA* promoter (**Figure 3.1**) was measured in DNA samples extracted from the umbilical cord of n=449 infants from the MAVIDOS trial. Pregnant mothers received either 1000 IU/d cholecalciferol or a placebo daily from 14 weeks of gestation until delivery as part of a double blind, randomised, placebo controlled trial which took place in Southampton, Oxford and Sheffield. Umbilical cords were collected at birth from mothers giving birth in Southampton, DNA was extracted and DNA methylation of 13 CpG sites 2.3 kb upstream of the *RXRA* promoter were measured using bisulfite pyrosequencing as described in **Material and Methods 2.2.4.1**. Methylation data at some of the *RXRA* CpG sites were not normally distributed and underwent transformations to achieve normality prior to statistical analyses being carried out.

The nature of individual transformations can be seen in results tables and figure legends where appropriate.

To determine whether maternal cholecalciferol supplementation during pregnancy altered *RXRA* CpG methylation at birth in cord tissue, independent t-tests compared *RXRA* methylation at birth between the 1000 IU/d cholecalciferol supplemented group and the placebo group within the MAVIDOS trial firstly within the whole subset of participants ($n = 449$, **Section 3.2.2**) and secondly when the participants were stratified by season of birth (**Section 3.2.2.1**). The seasons were defined as winter (December to February), spring (March to May), summer (June to August) and autumn (September to November). Associations between *RXRA* CpG methylation in umbilical cord tissue and bone measures at birth were assessed by linear regression analyses adjusted for sex, gestational age, treatment and season of birth. The data were further stratified by treatment allocation and season of birth prior to analyses (**Section 3.2.3**).

Prior to measurement of *RXRA* methylation in placental tissues, Dr Brogan Ashley, University of Southampton, collected placentas and extracted DNA as described in **Materials and Methods 2.2.3 and 2.2.4**. Whole placentas were collected from the MAVIDOS trial and the SPRING (Southampton Pregnancy Intervention for the Next Generation) study. The SPRING study is a randomised control trial in Southampton which recruits pregnant women randomly assigned to receive either 1000 IU/d cholecalciferol supplementation or a placebo from 14 weeks gestation until delivery. The participants were further randomised to receive a healthy conversation skill support or the usual care. The SPRING study is currently ongoing, the supplementation groups are blinded and therefore 'dummy' group assignments of *A* and *B* have been assigned. Furthermore, data on maternal and neonatal characteristics between the maternal treatment groups are not yet available, therefore the baseline characteristics between the two treatment groups could not be assessed. Independent t-tests compared *RXRA* CpG methylation in placental tissue between the two treatment groups amongst participants from the MAVIDOS (**Section 3.2.4.1**) and SPRING studies (**Section 0**). In addition, to determine whether short term *in vitro* exposure alters *RXRA* DNA methylation, placental fragments and cytotrophoblasts obtained from control placentas from the Princess Anne Hospital (PAH) were treated with 20 μM 25(OH) D_3 dissolved in ethanol and BSA or an ethanol and BSA control for 8 and 24 hours respectively prior to DNA extraction and *RXRA* DNA methylation pyrosequencing. Paired t-tests were used to compare *RXRA* CpG methylation between the matched pairs of placental fragments (**Section 0**) and primary cytotrophoblasts (**Section 0**) treatment with 25(OH) D_3 *in vitro*.

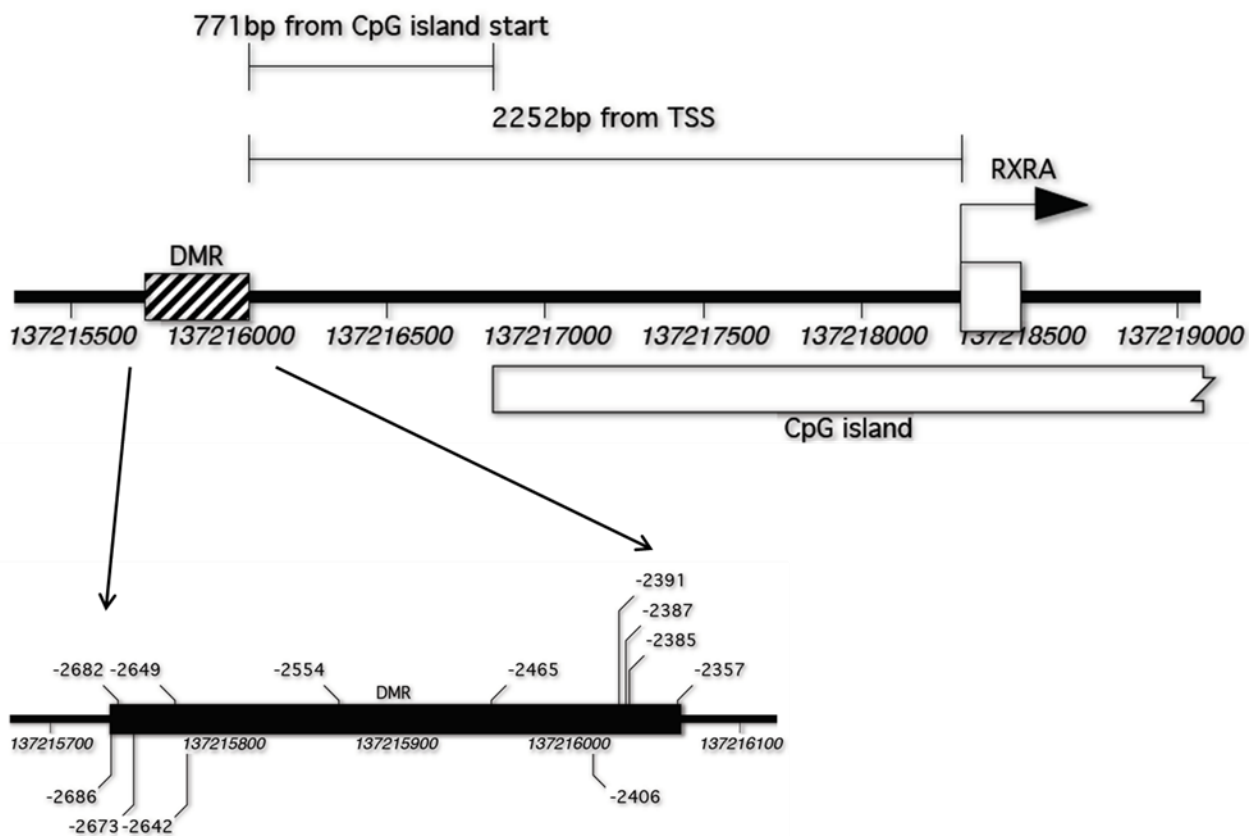


Figure 3.1 The location of the *RXRA* CpGs of interest.

The *RXRA* CpGs of interest are located within the differentially methylated region (DMR) which is located 2252 bp upstream of the transcriptional start site (TSS) of the *RXRA* gene. CpG Island is defined as stretches of DNA with a CG ratio of more than 0.6.

3.2 Results

3.2.1 Characteristics of participants in the MAVIDOS trial

Participants in the MAVIDOS trial were randomly assigned into the cholecalciferol supplemented or placebo arm of the trial at 14 weeks gestation. Within the overall MAVIDOS population (n = 1134), which includes participants from Southampton, Sheffield and Oxford, there were no significant differences in maternal or neonatal characteristics between the two maternal treatment groups. Within the samples analysed here (n = 449), DNA was extracted from a subset of individuals whose umbilical cords were available following delivery at Southampton. Firstly, we wanted to determine whether there were any differences in maternal and neonatal characteristics between the treatment groups amongst these 449 umbilical cords (

Table 3.1), which may differ to the published MAVIDOS findings (n = 1134). There were no significant differences between the maternal treatment groups with respect to women's age, BMI and skinfold thickness and a similar proportion were nulliparous and current smokers. The baseline maternal serum 25(OH)D₃ concentrations at 14 weeks was similar between the two groups whereas at 34 weeks gestation, those in the cholecalciferol supplemented group had greater serum 25(OH)D₃ compared to the placebo group (p = 0.001). Amongst the neonates, there were no significant differences in the proportion of males and females, and gestational age and birthweight were similar between the maternal treatment groups. Neonatal DXA measurements were available for 375 neonates (189 born to mothers randomised to cholecalciferol, and 186 born to placebo). There were no significant differences in age or bone and adiposity measures taken at the neonatal DXA scan within 14 days of delivery between the cholecalciferol and placebo groups. These findings are similar to what has been shown in the published MAVIDOS trial results which take into account infants from Southampton, Sheffield and Oxford³⁵⁹.

Table 3.1 Baseline maternal and neonatal characteristics of the subset of randomly assigned pregnant women from the MAVIDOS trial included in the current analyses.

	Cholecalciferol (n = 221)	Placebo (n = 228)	p
Womens Age (years)	30.8 (5.1)	30.9 (5.2)	0.834
Womens BMI (Kg/m²)^a	24.9 (22.4-28.7)	25.6 (23.0-29.7)	0.148
Sum of skinfold thickness (mm)	87.72 (28.21)	87.23 (26.76)	0.865
25(OH)D 14 weeks (nmol/L)	44.2 (15.2)	45.0 (16.2)	0.636
25(OH)D 34 weeks (nmol/L)	66.3 (19.8)	42.7 (20.0)	0.001*
Nulliparous (%)	42.9	45.8	0.545
Current Smoker (%)	5.7	7.4	0.473
Males (%)	58.0	49.1	0.062
Gestational Age (weeks)	40.2 (1.3)	40.1 (1.3)	0.704
Birthweight (g)	3575.9 (490.7)	3547.9 (483.2)	0.543
Age at neonatal DXA scan (days)^a	6 (1-10)	6 (1-11)	0.654
BMC (g)	61.9 (10.7)	61.2 (10.7)	0.540
BA (cm²)	303.2 (33.2)	299.6 (36.2)	0.315
BMD (g/cm²)	0.2 (0.0)	0.2 (0.0)	0.868
scBMC (g)	59.7 (4.6)	59.7 (4.8)	0.997
Total Body Fat Mass (g)^a	336.4 (216.7,536.1)	375.0 (253.5,505.8)	0.180
Total Body Lean Mass (g)	3077.8 (414.3)	3045.3 (444.5)	0.465
Percentage Fat Mass (%)^a	9.5 (6.5,14.5)	10.6 (7.7,13.7)	0.128
Percentage Lean Mass (%)	86.2 (8.1)	86.2 (6.9)	0.987
Weight at neonatal DXA scan (g)	3586.4 (495.2)	3543.4 (520.1)	0.413

Values are mean (standard deviation), median (IQR) or %. Percentages calculated accounting for missing variables. Independent t-tests compared the cholecalciferol supplemented to placebo group. ^aData were not normally distributed so a Mann-Whitney test was used instead. The proportion of males within each treatment group was calculated using a chi-test.

3.2.2 *RXRA* methylation was lower in the vitamin D supplemented group compared to the placebo group in the MAVIDOS trial

The results showed that new-born infants from the cholecalciferol supplemented group had significantly lower methylation at CpGs -2686 ($p = 0.025$, mean difference = -2 %, 95 % CI: -3.78, -0.26), -2682 ($p = 0.022$, mean difference = -1.7 %, 95 % CI: -3.16, -0.25), -2673 ($p = 0.027$, mean difference = -1.9 %, 95 % CI: -3.59, -0.22), -2649 ($p = 0.043$, mean difference = -1.7 %, 95 % CI: -3.28, -0.05) and -2642 ($p = 0.020$, mean difference = -2.0 %, 95 % CI: -3.64, -0.03) compared to the placebo group (Table 3.2 and Figure 3.2).

Table 3.2 Differences in *RXRA* methylation between the treatment groups in the MAVIDOS trial.

<i>RXRA</i> CpG	n	Mean difference (%)	(95 % CI)	p
-2693	441	-1.8	(-3.801, 0.116)	0.065
-2686	447	-2.0	(-3.776, -0.255)	0.025*
-2682	450	-1.7	(-3.158, -0.252)	0.022*
-2673	452	-1.9	(-3.587, -0.219)	0.027*
-2649	446	-1.7	(-3.277, -0.053)	0.043*
-2642	449	-2.0	(-3.636, -0.311)	0.020*
-2554	443	-0.8	(-1.949, 0.321)	0.159
-2465	430	-0.2	(-1.424, 0.936)	0.685
-2406	452	-0.8	(-1.987, 0.339)	0.165
-2391	450	-0.8	(-2.335, 0.652)	0.269
-2387	449	-0.7	(-2.057, 0.639)	0.302
-2385	448	-0.6	(-2.049, 0.886)	0.437
-2357	449	-0.5	(-1.739, 0.652)	0.372

Independent t-tests compared *RXRA* methylation between the cholecalciferol supplemented and placebo group within the MAVIDOS trial.

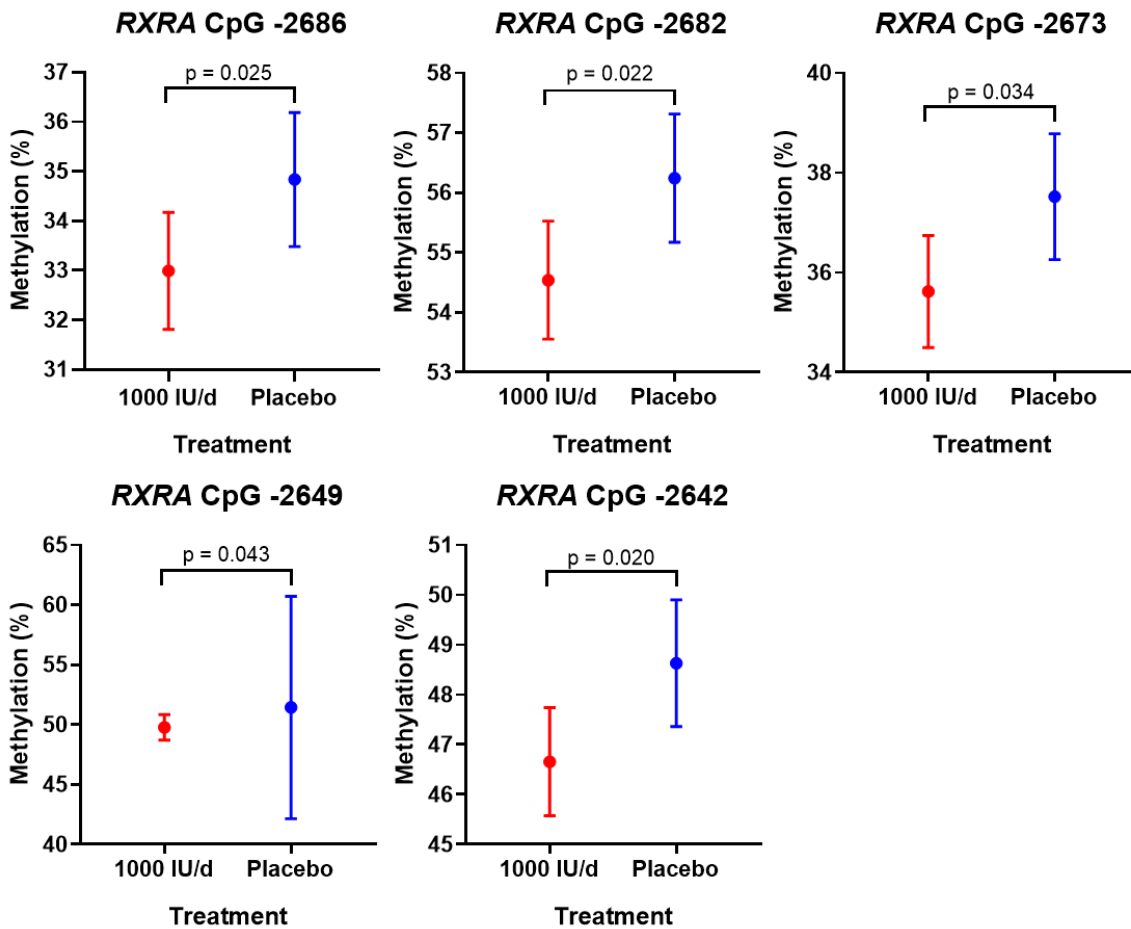


Figure 3.2 Significant differences in *RXRA* methylation at birth between the treatment groups in the MAVIDOS trial.

Independent t-tests compared *RXRA* methylation between the cholecalciferol supplemented and placebo group within the MAVIDOS trial. Graphs represent mean and 95 % confidence intervals.

3.2.2.1 There were seasonal differences in maternal and neonatal characteristics in the MAVIDOS trial

The baseline maternal and neonatal characteristics between the maternal cholecalciferol supplemented and placebo group, according to season of birth, were examined amongst the 449 participants from Southampton (**Table 3.3**). The seasons were defined as winter (December to February), spring (March to May), summer (June to August) and autumn (September to November). The results showed that across all four seasons, there were no significant differences in maternal age, BMI, or the proportion of nulliparous or smoking mothers between the two treatment groups. Furthermore, across all four seasons, there were no significant differences in maternal serum 25(OH)D₃ concentrations at 14 weeks gestation whereas maternal serum 25(OH)D₃ concentrations at 34 weeks gestation were greater in cholecalciferol supplemented mothers compared to placebo supplemented mothers ($p = 0.001$). Amongst infants born in winter, those in the maternal cholecalciferol supplementation group had greater birthweight ($p = 0.029$), BMC ($p = 0.014$), BA ($p = 0.049$), BMD ($p = 0.041$), total body fat mass ($p = 0.020$), percentage fat mass ($p = 0.032$) and weight at the neonatal DXA scan ($p = 0.016$) when compared to the placebo group. However, in the remaining seasons, there were no significant differences in neonatal characteristics between the maternal treatment groups. The findings within this subset of the MAVIDOS trial are mostly similar to the overall MAVIDOS findings²³⁶, however there are some differences. Within this subset, amongst infants born in winter there were no significant differences in scBMC and there were additional significant differences observed in percentage fat mass and weight at the time of the neonatal DXA scan between the treatment groups.

To determine whether there were seasonal differences in *RXRA* CpG methylation between the maternal treatment groups, the analyses were stratified by season of birth and independent t-tests compared *RXRA* methylation between the maternal cholecalciferol supplemented group and the placebo group within the MAVIDOS trial (**Table 3.4 and Figure 3.3**). Amongst infants born in the winter months, there were no significant differences in methylation at birth between the two treatment groups however, there was a trend towards an increase in CpG -2554 methylation although this did not reach statistical significance ($p = 0.056$, mean difference = 2.8 %, 95 % CI: -0.07, 5.69). Amongst Infants born in the spring months, there were no significant differences in *RXRA* CpG methylation at birth between the two treatment groups. Amongst infants born in the summer months, those in the cholecalciferol supplemented group had significantly lower methylation at CpGs -2693 ($p = 0.018$, mean difference = -4.2 %, 95 % CI: -7.66, -0.72), -2686 ($p = 0.047$, mean difference = -3.0 %, 95 % CI: -5.943, -0.04), -2673 ($p = 0.039$, mean difference = -3.0 %, 95 % CI: -5.88, -0.16) and -2642 ($p = 0.022$, mean difference = -3.2 %, 95 % CI: -5.87, -0.48) compared to the placebo group. Amongst infants born in the autumn months, those in the cholecalciferol

Chapter 3

supplemented group had significantly lower methylation at CpGs -2682 ($p = 0.015$, mean difference = -3.7 %, 95 % CI: -6.60, -0.74), -2673 ($p = 0.043$, mean difference = -3.5 %, 95 % CI: -6.90, -0.10) - 2649 ($p = 0.029$, mean difference = -3.8 %, 95 % CI: -7.13, -0.39), -2642 ($p = 0.033$, mean difference = -4.0 %, 95 % CI: -7.62, -0.33), -2406 ($p = 0.024$, mean difference = -2.7 %, 95 % CI: -5.09, -0.37), - 2387 ($p = 0.025$, mean difference = -2.9 %, 95 % CI: -5.48, -0.37), -2385 ($p = 0.022$, mean difference = -3.4 %, 95 % CI: -6.27, -0.50) and -2357 ($p = 0.018$, mean difference = -2.8 %, 95 % CI: -4.98, -6.13) compared to the placebo group.

Table 3.3 Baseline maternal and neonatal characteristics of subset of the randomly assigned pregnant women from the MAVIDOS trial included in the analyses, stratified by season of birth.

	Winter			Spring			Summer			Autumn		
	Cholecalciferol (n = 44)	Placebo (n = 41)	p	Cholecalciferol (n = 50)	Placebo (n = 63)	p	Cholecalciferol (n = 64)	Placebo (n = 63)	p	Cholecalciferol (n = 63)	Placebo (n = 61)	p
Womens Age (years)	30.5 (5.9)	30.5 (5.0)	0.987	29.5 (4.9)	30.9 (5.2)	0.132	31.5 (4.4)	30.7 (5.4)	0.370	31.3 (5.1)	31.3 (5.3)	0.991
Womens BMI (Kg/m ²) ^a	25.3 (22.6,29.5)	23.6 (22.5,29.5)	0.463	24.7 (22.2,29.9)	25.0 (22.6,28.6)	0.995	24.0 (22.4,28.1)	26.3 (23.5,29.7)	0.063	25.4 (22.2,29.9)	26.8 (23.2,30.5)	0.097
Sum of skinfold thickness (mm)	90.8 (29.4)	78.2 (29.5)	0.100	92.8 (30.8)	84.8 (29.8)	0.195	84.0 (25.5)	92.7 (24.1)	0.064	85.6 (28.0)	89.7 (22.6)	0.429
25(OH)D 14 weeks (nmol/L)	48.9 (15.1)	54.5 (15.5)	0.095	46.6 (14.9)	41.7 (14.6)	0.087	40.1 (15.6)	40.1 (14.8)	0.982	43.4 (14.4)	46.9 (16.9)	0.219
25(OH)D 34 weeks (nmol/L)	56.9 (19.0)	31.9 (15.3)	0.001*	64.9 (21.1)	31.4 (18.3)	0.001*	71.3 (19.8)	48.9 (17.5)	0.001*	68.8 (17.1)	55.1 (17.0)	0.001*
Nulliparous (%)	52.3	53.7	0.898	44.0	47.6	0.775	37.5	33.3	0.671	34.9	42.6	0.224
Current Smoker (%)	4.5	7.3	0.606	10.0	9.5	0.904	3.1	4.8	0.622	4.8	6.6	0.603
Males (%)	54.5	46.3	0.450	46.0	54.0	0.400	65.6	50.8	0.090	60.3	42.6	0.051
Gestational Age (weeks)	40.4 (1.2)	39.9 (1.3)	0.058	40.1 (1.5)	40.1 (1.4)	0.881	40.2 (1.3)	40.3 (1.2)	0.914	40.0 (1.2)	40.2 (1.4)	0.368
Birthweight (g)	3603.6 (369.8)	3399.3 (472.7)	0.029*	3620.2 (613.8)	3535.6 (551.2)	0.443	3532.7 (477.6)	3674.7 (442.9)	0.085	3565.4 (475.4)	3529.6 (430.5)	0.661
Age at neonatal DXA scan (days) ^a	1 (1,9)	7 (1,9)	0.083	7 (2,11.5)	6 (1,11)	0.320	6 (1,9)	3 (1,11)	0.971	6 (1,9)	7 (1,10.5)	0.654
BMC (g)	62.7 (8.1)	56.9 (10.2)	0.014*	63.3 (13.1)	60.4 (12.2)	0.267	60.8 (10.6)	63.1 (10.1)	0.255	61.5 (10.7)	62.5 (9.4)	0.614
BA (cm ²)	302.1 (27.9)	286.6 (33.5)	0.049*	309.8 (40.3)	296.6 (39.2)	0.110	300.5 (31.1)	308.1 (35.0)	0.234	301.9 (33.0)	301.3 (34.2)	0.935
BMD (g/cm ²)	0.2 (0.0)	0.2 (0.0)	0.041*	0.2 (0.0)	0.2 (0.0)	0.903	0.2 (0.0)	0.2 (0.0)	0.393	0.2 (0.0)	0.2 (0.0)	0.239
scBMC (g)	60.5 (5.9)	59.7 (4.8)	0.607	60.0 (3.9)	59.5 (4.4)	0.584	59.1 (4.3)	58.6 (4.5)	0.626	59.6 (4.7)	60.8 (5.5)	0.266
Total Body Fat Mass (g) ^a	397.0 (271.4,515.7)	299.4 (162.0,377.6)	0.020*	354.7 (242.9,624.1)	432.6 (273.0,722.2)	0.392	308.2 (197.6,524.8)	393.9 (248.1,480.4)	0.243	301.7 (221.3,529.3)	378.9 (293.7,486.8)	0.180
Total Body Lean Mass (g)	3075.7 (467.5)	2940.8 (415.7)	0.237	3115.4 (436.1)	2956.2 (513.4)	0.113	3063.0 (388.8)	3204.8 (360.2)	0.052	3066.5 (394.5)	3040.8 (422.6)	0.746
Percentage Fat Mass (%) ^a	10.3 (7.7,14.0)	8.9 (5.4,11.3)	0.032*	9.2 (7.1,16.3)	11.1 (8.1,20.0)	0.229	8.9 (5.9,13.4)	10.7 (7.4,12.4)	0.250	9.2 (6.5,14.0)	10.8 (9.1,13.7)	0.128
Percentage Lean Mass (%)	85.6 (7.4)	88.9 (6.1)	0.058	85.8 (8.6)	84.0 (8.5)	0.331	86.8 (8.4)	87.4 (5.0)	0.667	86.4 (8.0)	86.1 (6.5)	0.830
Weight at neonatal DXA scan (g)	3587.5 (417.1)	3312.9 (464.4)	0.016*	3667.7793 ()	3533.5 (588.9)	0.281	3546.0 (467.6)	3686.1 (508.7)	0.137	3567.2 (476.7)	3536.7 (446.5)	0.734

Values are mean (standard deviation), median (interquartile range [IQR]) or %. Percentages calculated accounting for missing variables. Independent t-tests compared the cholecalciferol supplemented to placebo group. ^aData were not normally distributed so a Mann-Whitney test was used instead. The proportion of males within each treatment group was calculated using a chi-test. Seasons are defined as winter (December to February), spring (March to May), summer (June to August) and autumn (September to November).

Table 3.4 Differences in *RXRA* methylation between treatment groups in the MAVIDO trial when stratified by season of birth.

<i>RXRA</i> CpG	Winter				Spring				Summer				Autumn			
	n	Mean diff. (%)	(95 % CI)	p	n	Mean diff. (%)	(95 % CI)	p	n	Mean diff. (%)	(95 % CI)	p	n	Mean diff. (%)	(95 % CI)	p
-2693	84	1.0	(-4.178, 6.198)	0.700	109	0.0	(-3.947, 3.849)	0.980	121	-4.2	(-7.659, -0.719)	0.018*	121	-2.9	(-6.696, 0.853)	0.128
-2686	85	-0.6	(-4.821, 3.680)	0.790	111	-0.4	(-4.017, 3.264)	0.838	124	-3.0	(-5.943, -0.038)	0.047*	121	-3.5	(-7.258, 0.242)	0.066
-2682	84	0.5	(-3.329, 4.244)	0.811	111	-0.1	(-3.758, 2.244)	0.618	125	-2.0	(-4.346, 0.381)	0.099	124	-3.7	(-6.596, -0.735)	0.015*
-2673	85	0.6	(-3.611, 4.730)	0.790	111	-0.6	(-4.159, 2.963)	0.740	126	-3.0	(-5.879, -0.162)	0.039*	124	-3.5	(-6.901, -0.104)	0.043*
-2649	84	0.3	(-3.757, 4.450)	0.867	109	-0.5	(-3.645, 2.734)	0.778	126	-2.0	(-4.732, 0.745)	0.152	122	-3.8	(-7.129, -0.386)	0.029*
-2642	84	0.7	(-3.388, 4.758)	0.739	110	-0.3	(-3.546, 3.030)	0.877	126	-3.2	(-5.872, -0.475)	0.022*	123	-4.0	(-7.622, -0.334)	0.033*
-2554	84	2.8	(-0.071, 5.691)	0.056	108	-1.1	(-3.261, 0.989)	0.292	124	-1.7	(-3.754, 0.311)	0.096	121	-2.1	(-1.354, 0.162)	0.069
-2465	83	2.1	(-0.622, 4.794)	0.128	106	0.3	(-1.895, 2.585)	0.761	118	-0.9	(-2.885, 1.108)	0.380	117	-1.9	(-4.491, 0.738)	0.158
-2406	85	1.3	(-1.574, 4.176)	0.371	113	-0.4	(-2.772, 1.901)	0.713	126	-0.7	(-2.750, 1.272)	0.468	124	-2.7	(-5.089, -0.372)	0.024*
-2391	85	1.7	(-2.074, 5.453)	0.374	113	-0.3	(-3.336, 2.689)	0.832	124	-1.0	(-3.558, 1.526)	0.430	124	-2.9	(-5.955, 0.190)	0.066
-2387	85	2.0	(-1.529, 5.564)	0.261	113	0.1	(-2.717, 2.828)	0.969	123	-0.9	(-3.271, 1.430)	0.440	124	-2.9	(-5.475, -0.369)	0.025*
-2385	85	2.2	(-1.332, 6.423)	0.195	113	1.0	(-1.778, 3.876)	0.464	123	-1.4	(-3.938, 1.177)	0.287	123	-3.4	(-6.269, -0.500)	0.022*
-2357	85	0.8	(-2.063, 3.649)	0.582	111	1.8	(-0.895, 4.399)	0.192	126	-1.3	(-3.323, 0.765)	0.218	123	-2.8	(-4.979, -6.132)	0.013*

Independent t-tests compared *RXRA* methylation between the cholecalciferol supplemented and placebo group within the MAVIDOS trial.

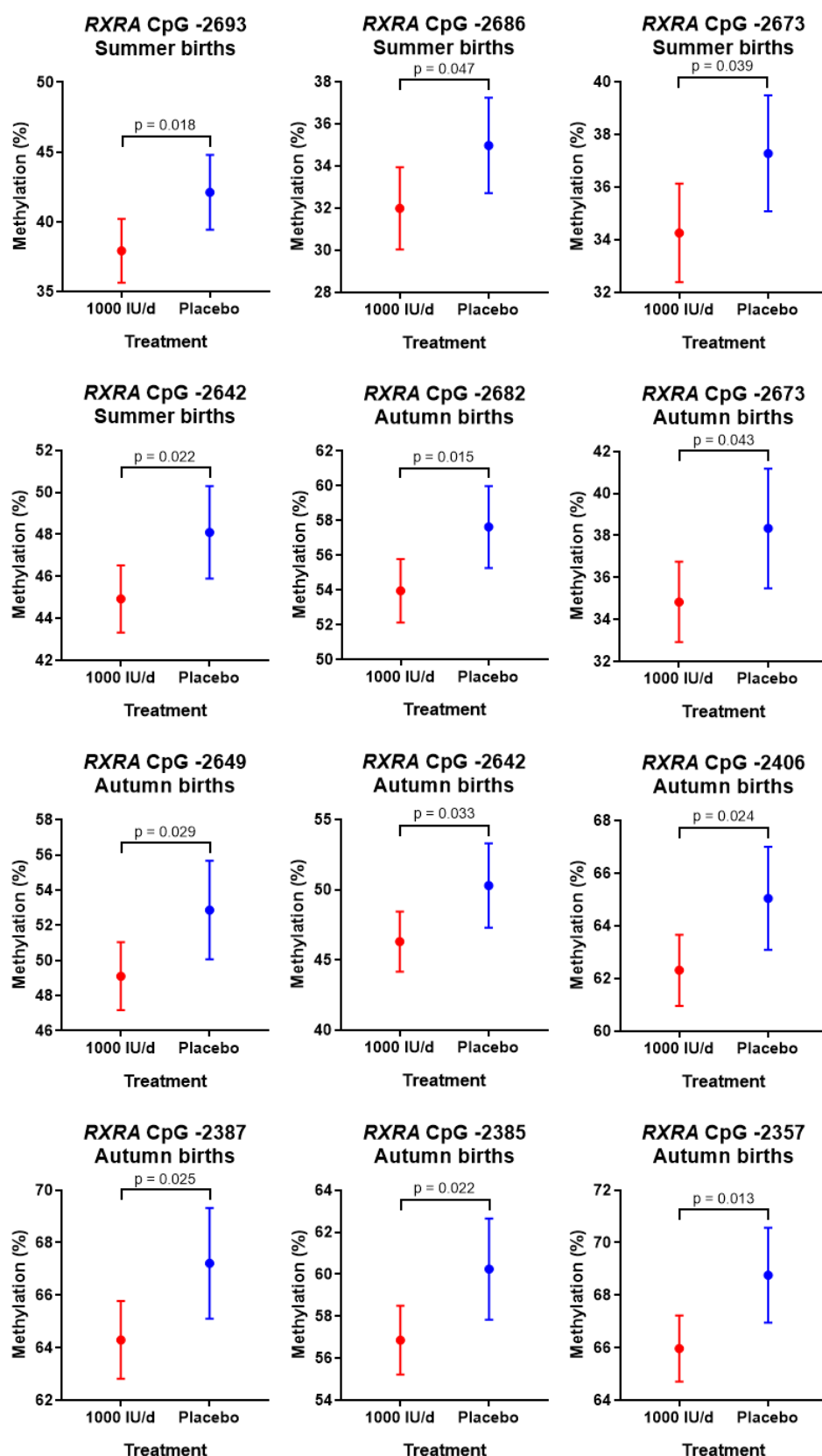


Figure 3.3 Significant differences in *RXRA* methylation at birth between the treatment groups in the MAVIDOS trial in infants born in summer and autumn.

Independent t-tests compared *RXRA* methylation between the cholecalciferol supplemented and placebo group within the MAVIDOS trial. Graphs represent mean and 95 % confidence intervals.

3.2.3 Are there any associations between cord *RXRA* CpG methylation and bone outcomes at birth within the MAVIDOS trial?

We have shown that *RXRA* CpG methylation is altered by maternal vitamin D supplementation during pregnancy and season of delivery. Therefore, the linear regression analyses were adjusted for sex, gestational age, treatment allocation and season of birth. The results showed that there were no significant associations between cord *RXRA* CpG methylation and BMC, BA, BMD or scBMC at birth when adjusted for sex, gestational age, treatment allocation and season of birth (**Table 3.5**).

In the cholecalciferol group, *RXRA* CpG -2554 methylation was inversely associated with BMC at birth ($b = -0.248$ (95 % CI: -0.497, 0.000) $p = 0.050$) when adjusted for sex, gestational age and season of birth. However, there were no significant associations between methylation and BA, BMD or scBMC at birth. Within the placebo group there were no significant associations between *RXRA* CpG methylation at birth and BMC, BA, BMD or scBMC at birth (**Table 3.6**).

Amongst infants born in the winter and spring months there were no significant associations between *RXRA* methylation and BMC, BA, BMD or scBMC at birth when adjusted for sex, gestational age and treatment allocation. Amongst infants born in the summer months, there was an inverse association between *RXRA* CpG -2385 methylation at birth and BA at birth ($b = -0.928$ (95 % CI: -1.815, -0.060) $p = 0.037$). However, there were no significant associations between methylation and BMC, BMD or scBMC at birth. Amongst infants born in the autumn months, there was a positive association between *RXRA* CpG -2465 methylation at birth and BA at birth ($b = 0.909$ (95 % CI: 0.053, 1.764) $p = 0.038$) and there were no significant associations between methylation and BMC, BMD or scBMC at birth (**Table 3.7**).

Table 3.5 Associations between *RXRA* CpG methylation at birth and bone outcomes at birth.

<i>RXRA</i> CpG	Total BMC			Total BA			Total BMD			Total scBMC		
	n	B (95 % CI)	p	n	B (95 % CI)	p	n	B (95 % CI)	p	n	B (95 % CI)	p
-2693	363	0.008 (-0.085, 0.101)	0.868	363	-0.023 (-0.336, 0.290)	0.887	363	5.01x10 ⁻⁵ (-1.22x10 ⁻⁴ , 2.23x10 ⁻⁴)	0.887	308	0.011 (-0.040, 0.063)	0.667
-2686	368	0.019 (-0.081, 0.119)	0.706	368	0.078 (-0.260, 0.416)	0.649	368	1.21x10 ⁻⁵ (-1.73x10 ⁻⁴ , 1.97x10 ⁻⁴)	0.649	312	-0.004 (-0.059, 0.051)	0.880
-2682	372	0.001 (-0.123, 0.126)	0.982	372	0.021 (-0.400, 0.441)	0.923	372	-7.04x10 ⁻⁵ (-2.36x10 ⁻⁴ , 2.22x10 ⁻⁴)	0.923	316	0.000 (-0.068, 0.068)	0.999
-2673	372	0.020 (-0.087, 0.126)	0.715	372	0.064 (-0.296, 0.424)	0.727	372	2.47x10 ⁻⁵ (-1.71x10 ⁻⁴ , 2.21x10 ⁻⁴)	0.727	316	0.004 (-0.054, 0.062)	0.897
-2649	366	0.027 (-0.086, 0.140)	0.639	366	0.095 (-0.289, 0.479)	0.628	366	2.59x10 ⁻⁵ (-1.82x10 ⁻⁴ , 2.34x10 ⁻⁴)	0.807	311	-0.001 (-0.063, 0.062)	0.982
-2642	368	0.048 (-0.062, 0.158)	0.391	368	0.137 (-0.236, 0.509)	0.471	368	6.25x10 ⁻⁵ (-1.40x10 ⁻⁴ , 2.65x10 ⁻⁴)	0.545	312	0.013 (-0.048, 0.074)	0.680
-2554	363	-0.081 (-0.245, 0.084)	0.335	363	-0.170 (-0.726, 0.386)	0.548	363	-1.81x10 ⁻⁴ (-4.83x10 ⁻⁴ , 1.21x10 ⁻⁴)	0.239	307	0.005 (-0.088, 0.098)	0.916
-2465	355	-0.040 (-0.205, 0.124)	0.629	355	0.084 (-0.474, 0.642)	0.767	355	-2.11x10 ⁻⁴ (-5.13x10 ⁻⁴ , 9.16x10 ⁻⁵)	0.171	303	-0.042 (-0.133, 0.049)	0.363
-2406	373	-0.001 (-0.158, 0.155)	0.986	373	-0.038 (-0.566, 0.490)	0.888	373	-2.99x10 ⁻⁶ (-2.91x10 ⁻⁴ , 2.85x10 ⁻⁴)	0.984	318	0.020 (-0.065, 0.104)	0.647
-2391	371	0.001 (-0.120, 0.122)	0.991	371	-0.004 (-0.413, 0.404)	0.983	371	-6.90x10 ⁻⁸ (-2.23x10 ⁻⁴ , 2.22x10 ⁻⁴)	1.000	316	0.008 (-0.058, 0.073)	0.818
-2387	370	-0.004 (-0.138, 0.131)	0.956	370	-0.006 (-0.460, 0.449)	0.981	370	-1.03x10 ⁻⁵ (-2.58x10 ⁻⁴ , 2.38x10 ⁻⁴)	0.935	315	0.016 (-0.057, 0.089)	0.665
-2385	369	-0.015 (-0.139, 0.110)	0.818	369	0.002 (-0.418, 0.423)	0.992	369	-5.77x10 ⁻⁵ (-2.88x10 ⁻⁴ , 1.72x10 ⁻⁴)	0.622	315	0.004 (-0.065, 0.072)	0.919
-2357	371	-0.021 (-0.173, 0.130)	0.783	371	-0.022 (-0.535, 0.491)	0.932	371	-6.51x10 ⁻⁵ (-3.45x10 ⁻⁴ , 2.14x10 ⁻⁴)	0.647	315	0.002 (-0.082, 0.085)	0.969

Linear regression analyses adjusted for sex, treatment group and season of birth. BMC = bone mineral content, BA = bone area, BMD = bone mineral density and scBMC = size corrected bone mineral content. Neonatal DXA measurements were taken within 14 days of birth.

Table 3.6 Associations between *RXRA* CpG methylation at birth and bone outcomes at birth, when stratified by treatment group.

CHOLECALCIFEROL												
<i>RXRA</i> CpG	Total BMC			Total BA			Total BMD			Total scBMC		
	n	B (95 % CI)	p	n	B (95 % CI)	p	n	B (95 % CI)	p	n	B (95 % CI)	p
-2693	182	-0.046 (-0.196, 0.105)	0.550	182	-0.196 (-0.679, 0.288)	0.425	182	-8.78x10 ⁻⁵ (-2.59x10 ⁻² , 2.58x10 ⁻²)	0.995	150	-0.010 (-0.092, 0.073)	0.816
-2686	193	-0.023 (-0.189, 0.143)	0.785	183	-0.136 (-0.670, 0.397)	0.615	183	3.34x10 ⁻³ (-2.09x10 ⁻² , 2.76x10 ⁻²)	0.818	150	-0.001 (-0.089, 0.087)	0.985
-2682	187	-0.057 (-0.256, 0.143)	0.577	187	-0.225 (-0.868, 0.417)	0.490	187	-1.64x10 ⁻⁵ (-3.77x10 ⁻⁴ , 3.44x10 ⁻⁴)	0.929	154	0.015 (-0.089, 0.120)	0.772
-2673	187	-0.035 (-0.211, 0.141)	0.695	187	-0.152 (-0.718, 0.414)	0.596	187	-9.51x10 ⁻⁴ (-2.86x10 ⁻² , 2.67x10 ⁻²)	0.988	154	0.008 (-0.085, 0.102)	0.862
-2649	183	-0.025 (-0.212, 0.163)	0.796	183	-0.160 (-0.768, 0.448)	0.604	183	4.30x10 ⁻⁵ (-2.95x10 ⁻⁴ , 3.81x10 ⁻⁴)	0.802	151	0.017 (-0.082, 0.117)	0.733
-2642	184	0.014 (-0.176, 0.203)	0.887	184	0.020 (-0.592, 0.632)	0.949	184	3.47x10 ⁻⁵ (-3.08x10 ⁻⁴ , 3.77x10 ⁻⁴)	0.842	151	0.005 (-0.097, 0.107)	0.923
-2554	184	-0.248 (-0.497, 0.000)	0.050*	184	-0.679 (-1.484, 0.127)	0.098	184	-4.05x10 ⁻⁴ (-8.59x10 ⁻⁴ , 4.87x10 ⁻⁵)	0.080	151	0.047 (-0.090, 0.184)	0.498
-2465	177	-0.070 (-0.322, 0.183)	0.586	177	0.071 (-0.749, 0.890)	0.865	177	-3.13x10 ⁻⁴ (-7.62x10 ⁻⁴ , 1.35x10 ⁻⁴)	0.170	148	-0.055 (-0.189, 0.080)	0.425
-2406	187	-0.057 (-0.308, 0.195)	0.657	187	-0.056 (-0.867, 0.755)	0.892	187	-1.71x10 ⁻⁴ (-6.24x10 ⁻⁴ , 2.81x10 ⁻⁴)	0.456	155	-0.044 (-0.173, 0.086)	0.507
-2391	187	0.006 (-0.186, 0.199)	0.948	187	0.070 (-0.550, 0.691)	0.823	187	-2.71x10 ⁻⁵ (-3.73x10 ⁻⁴ , 3.19x10 ⁻⁴)	0.878	155	-0.013 (-0.113, 0.087)	0.796
-2387	186	-0.046 (-0.258, 0.167)	0.672	186	-0.096 (-0.781, 0.589)	0.782	186	-8.46x10 ⁻⁵ (-4.69x10 ⁻⁴ , 3.00x10 ⁻⁴)	0.665	154	-0.010 (-0.120, 0.100)	0.860
-2385	185	-0.126 (-0.318, 0.066)	0.196	185	-0.287 (-0.905, 0.331)	0.361	185	-2.32x10 ⁻⁴ (-5.79x10 ⁻⁴ , 1.16x10 ⁻⁴)	0.190	154	-0.047 (-0.150, 0.055)	0.364
-2357	187	-0.175 (-0.428, 0.078)	0.174	187	-0.467 (-1.283, 0.349)	0.261	187	-2.69x10 ⁻⁴ (-7.26x10 ⁻⁴ , 1.87x10 ⁻⁴)	0.246	154	-0.046 (-0.180, 0.088)	0.501

PLACEBO												
<i>RXRA</i> CpG	Total BMC			Total BA			Total BMD			Total scBMC		
	n	B (95 % CI)	p	n	B (95 % CI)	p	n	B (95 % CI)	p	n	B (95 % CI)	p
-2693	180	0.033 (-0.084, 0.150)	0.575	180	0.055 (-0.359, 0.469)	0.794	180	7.71x10 ⁻³ (-1.44x10 ⁻² , 2.98x10 ⁻²)	0.527	157	0.023 (-0.046, 0.092)	0.506
-2686	184	0.038 (-0.086, 0.161)	0.550	184	0.186 (-0.254, 0.625)	0.406	184	-9.77x10 ⁻⁴ (-2.11x10 ⁻² , 1.92x10 ⁻²)	0.901	161	-0.006 (-0.079, 0.066)	0.863
-2682	184	0.029 (-0.128, 0.187)	0.713	184	0.155 (-0.405, 0.715)	0.585	184	-2.26x10 ⁻⁵ (-3.20x10 ⁻⁴ , 2.75x10 ⁻⁴)	0.881	161	-0.012 (-0.104, 0.080)	0.800
-2673	184	0.042 (-0.090, 0.174)	0.530	184	0.149 (-0.322, 0.620)	0.533	184	2.67x10 ⁻³ (-2.02x10 ⁻² , 2.55x10 ⁻²)	0.831	161	0.003 (-0.074, 0.080)	0.942
-2649	182	0.051 (-0.089, 0.191)	0.474	182	0.226 (-0.273, 0.725)	0.372	182	1.97x10 ⁻⁶ (-2.64x10 ⁻⁴ , 2.68x10 ⁻⁴)	0.988	159	-0.011 (-0.094, 0.072)	0.794
-2642	183	0.052 (-0.081, 0.186)	0.439	183	0.151 (-0.323, 0.626)	0.530	183	5.85x10 ⁻⁵ (-1.94x10 ⁻⁴ , 3.11x10 ⁻⁴)	0.648	160	0.017 (-0.062, 0.096)	0.678
-2554	178	0.040 (-0.177, 0.258)	0.715	178	0.213 (-0.559, 0.984)	0.587	178	-3.76x10 ⁻⁵ (-4.44x10 ⁻⁴ , 3.69x10 ⁻⁴)	0.855	155	-0.034 (-0.164, 0.095)	0.600
-2465	177	-0.035 (-0.252, 0.183)	0.753	177	0.025 (-0.746, 0.796)	0.950	177	-1.47x10 ⁻⁴ (-5.61x10 ⁻⁴ , 2.66x10 ⁻⁴)	0.483	154	-0.030 (-0.157, 0.096)	0.636
-2406	185	0.015 (-0.182, 0.212)	0.879	185	-0.096 (-0.798, 0.605)	0.786	185	8.27x10 ⁻⁵ (-2.92x10 ⁻⁴ , 4.57x10 ⁻⁴)	0.663	162	0.061 (-0.053, 0.176)	0.292
-2391	183	-0.012 (-0.166, 0.142)	0.878	183	-0.094 (-0.641, 0.453)	0.734	183	9.31x10 ⁻⁶ (-2.82x10 ⁻⁴ , 3.01x10 ⁻⁴)	0.950	160	0.022 (-0.066, 0.111)	0.618
-2387	183	0.013 (-0.159, 0.186)	0.879	183	0.018 (-0.596, 0.632)	0.953	183	1.96x10 ⁻⁵ (-3.08x10 ⁻⁴ , 3.47x10 ⁻⁴)	0.906	160	0.033 (-0.068, 0.134)	0.517
-2385	183	0.056 (-0.107, 0.220)	0.497	183	0.163 (-0.418, 0.744)	0.580	183	5.81x10 ⁻⁵ (-2.52x10 ⁻⁴ , 3.68x10 ⁻⁴)	0.712	160	0.041 (-0.054, 0.136)	0.400
-2357	183	0.056 (-0.130, 0.243)	0.552	183	0.212 (-0.454, 0.878)	0.530	183	2.55x10 ⁻⁵ (-3.29x10 ⁻⁴ , 3.80x10 ⁻⁴)	0.887	160	0.024 (-0.086, 0.133)	0.669

Linear regression analyses adjusted for sex and season of birth. BMC = bone mineral content, BA = bone area, BMD = bone mineral density and scBMC = size corrected bone mineral content.

Neonatal DXA measurements were taken within 14 days of birth.

Table 3.7 Associations between *RXRA* CpG methylation at birth and bone outcomes at birth in the MAVIDOS trial when stratified by season of birth.

		WINTER														
		Total BMC			Total BA			Total BMD			Total scBMC					
<i>RXRA</i>	CpG	n	B (95 % CI)	p	n	B (95 % CI)	p	n	B (95 % CI)	p	n	B (95 % CI)	p			
-2693	63	0.013	(-0.170, 0.195)	0.890	63	-0.171	(-0.798, 0.456)	0.587	63	1.70x10 ⁻⁴	(-2.26x10 ⁻⁴ , 5.66x10 ⁻⁴)	0.394	49	0.040	(-0.093, 0.173)	0.551
-2686	63	0.039	(-0.167, 0.244)	0.708	63	-0.007	(-0.715, 0.702)	0.985	63	1.41x10 ⁻⁴	(-3.06x10 ⁻⁴ , 5.89x10 ⁻⁴)	0.529	49	0.026	(-0.121, 0.174)	0.721
-2682	63	-0.007	(-0.254, 0.241)	0.957	63	-0.112	(-0.963, 0.740)	0.794	63	5.08x10 ⁻⁵	(-4.89x10 ⁻⁴ , 5.91x10 ⁻⁴)	0.851	49	0.040	(-0.140, 0.219)	0.657
-2673	63	0.028	(-0.196, 0.253)	0.802	63	-0.130	(-0.903, 0.644)	0.739	63	1.90x10 ⁻⁴	(-2.98x10 ⁻⁴ , 6.78x10 ⁻⁴)	0.439	49	0.063	(-0.098, 0.223)	0.435
-2649	62	0.025	(-0.214, 0.263)	0.836	62	-0.104	(-0.927, 0.719)	0.801	62	1.57x10 ⁻⁴	(-3.62x10 ⁻⁴ , 6.76x10 ⁻⁴)	0.548	48	0.066	(-0.106, 0.239)	0.444
-2642	62	0.028	(-0.210, 0.266)	0.813	62	0.033	(-0.790, 0.855)	0.937	62	6.71x10 ⁻⁵	(-4.53x10 ⁻⁴ , 5.87x10 ⁻⁴)	0.797	48	0.049	(-0.125, 0.223)	0.571
-2554	62	-0.124	(-0.438, 0.189)	0.431	62	-0.164	(-1.252, 0.924)	0.764	62	-3.50x10 ⁻⁴	(-1.03x10 ⁻³ , 3.34x10 ⁻⁴)	0.310	48	0.006	(-0.229, 0.242)	0.956
-2465	62	-0.032	(-0.380, 0.316)	0.854	62	-0.040	(-1.235, 1.155)	0.947	62	-9.48x10 ⁻⁵	(-8.55x10 ⁻⁴ , 6.66x10 ⁻⁴)	0.804	49	0.029	(-0.233, 0.290)	0.827
-2406	63	-0.021	(-0.343, 0.302)	0.897	63	0.122	(-0.989, 1.233)	0.827	63	-1.96x10 ⁻⁴	(-8.99x10 ⁻⁴ , 5.07x10 ⁻⁴)	0.579	49	0.012	(-0.221, 0.245)	0.918
-2391	63	-0.024	(-0.274, 0.226)	0.851	63	0.125	(-0.736, 0.986)	0.772	63	-1.94x10 ⁻⁴	(-7.38x10 ⁻⁴ , 3.49x10 ⁻⁴)	0.477	49	-0.008	(-0.188, 0.173)	0.931
-2387	63	-0.038	(-0.303, 0.227)	0.775	63	0.035	(-0.879, 0.949)	0.940	63	-1.84x10 ⁻⁴	(-7.61x10 ⁻⁴ , 3.93x10 ⁻⁴)	0.526	49	0.000	(-0.190, 0.190)	0.999
-2385	63	-0.056	(-0.293, 0.181)	0.638	63	0.050	(-0.770, 0.869)	0.904	63	-2.53x10 ⁻⁴	(-7.68x10 ⁻⁴ , 2.62x10 ⁻⁴)	0.330	49	-0.010	(-0.185, 0.166)	0.913
-2357	63	0.000	(-0.325, 0.326)	0.998	63	0.226	(-0.893, 1.345)	0.688	63	-2.02x10 ⁻⁴	(-9.11x10 ⁻⁴ , 5.06x10 ⁻⁴)	0.570	49	-0.022	(-0.250, 0.206)	0.844
		SPRING														
		Total BMC			Total BA			Total BMD			Total scBMC					
<i>RXRA</i>	CpG	n	B (95 % CI)	p	n	B (95 % CI)	p	n	B (95 % CI)	p	n	B (95 % CI)	p			
-2693	91	-0.001	(-0.204, 0.202)	0.992	91	-0.009	(-0.725, 0.708)	0.981	91	1.24x10 ⁻⁵	(-3.03x10 ⁻⁴ , 3.28x10 ⁻⁴)	0.938	78	0.045	(-0.045, 0.135)	0.321
-2686	93	0.046	(-0.166, 0.258)	0.667	93	0.218	(-0.531, 0.968)	0.564	93	1.27x10 ⁻⁵	(-3.18x10 ⁻⁴ , 3.43x10 ⁻⁴)	0.940	80	0.028	(-0.070, 0.126)	0.573
-2682	93	-0.045	(-0.309, 0.220)	0.738	93	-0.147	(-1.082, 0.788)	0.755	93	-3.83x10 ⁻⁵	(-4.50x10 ⁻⁴ , 3.73x10 ⁻⁴)	0.854	80	0.035	(-0.082, 0.151)	0.553
-2673	93	0.040	(-0.175, 0.256)	0.712	93	0.112	(-0.649, 0.874)	0.770	93	5.68x10 ⁻⁵	(-2.79x10 ⁻⁴ , 3.92x10 ⁻⁴)	0.737	80	0.041	(-0.054, 0.137)	0.393
-2649	91	0.082	(-0.172, 0.336)	0.521	91	0.192	(-0.711, 1.095)	0.674	91	1.49x10 ⁻⁴	(-2.47x10 ⁻⁴ , 5.45x10 ⁻⁴)	0.456	78	0.064	(-0.050, 0.177)	0.266
-2642	92	0.023	(-0.219, 0.265)	0.849	92	0.003	(-0.858, 0.864)	0.994	92	6.51x10 ⁻⁵	(-3.12x10 ⁻⁴ , 4.42x10 ⁻⁴)	0.732	79	0.072	(-0.036, 0.180)	0.190
-2554	90	-0.257	(-0.635, 0.122)	0.181	90	-0.782	(-2.131, 0.568)	0.253	90	-3.15x10 ⁻⁴	(-9.10x10 ⁻⁴ , 2.80x10 ⁻⁴)	0.295	77	0.009	(-0.165, 0.182)	0.921
-2465	90	-0.285	(-0.655, 0.084)	0.129	90	-0.724	(-2.029, 0.581)	0.273	90	-5.08x10 ⁻⁴	(-1.09x10 ⁻³ , 7.42x10 ⁻⁴)	0.086	78	0.035	(-0.125, 0.195)	0.662
-2406	95	-0.138	(-0.475, 0.198)	0.416	95	-0.396	(-1.586, 0.795)	0.511	95	-2.04x10 ⁻⁴	(-7.31x10 ⁻⁴ , 3.23x10 ⁻⁴)	0.444	82	0.046	(-0.103, 0.195)	0.540
-2391	95	-0.072	(-0.319, 0.175)	0.562	95	-0.396	(-1.265, 0.473)	0.368	95	2.88x10 ⁻⁵	(-3.58x10 ⁻⁴ , 4.16x10 ⁻⁴)	0.883	82	0.091	(-0.014, 0.195)	0.088
-2387	95	-0.032	(-0.302, 0.238)	0.816	95	-0.120	(-1.075, 0.834)	0.803	95	-7.80x10 ⁻⁵	(-4.31x10 ⁻⁴ , 4.15x10 ⁻⁴)	0.971	82	0.079	(-0.038, 0.197)	0.184
-2385	95	-0.052	(-0.322, 0.219)	0.706	95	-0.097	(-1.054, 0.859)	0.840	95	-1.02x10 ⁻⁴	(-5.25x10 ⁻⁴ , 3.22x10 ⁻⁴)	0.635	82	0.043	(-0.077, 0.163)	0.479
-2357	94	0.020	(-0.273, 0.312)	0.895	94	0.012	(-1.026, 1.049)	0.982	94	2.70x10 ⁻⁵	(-4.26x10 ⁻⁴ , 4.80x10 ⁻⁴)	0.906	81	0.060	(-0.072, 0.192)	0.367
		SUMMER														
		Total BMC			Total BA			Total BMD			Total scBMC					
<i>RXRA</i>	CpG	n	B (95 % CI)	p	n	B (95 % CI)	p	n	B (95 % CI)	p	n	B (95 % CI)	p			
-2693	104	-0.029	(-0.230, 0.172)	0.776	104	-0.411	(-1.052, 0.231)	0.207	104	1.71x10 ⁻⁴	(-1.74x10 ⁻⁴ , 5.55x10 ⁻⁴)	1.038	93	0.010	(-0.095, 0.115)	0.849
-2686	107	-0.034	(-0.267, 0.199)	0.771	107	-0.429	(-1.183, 0.326)	0.263	107	1.75x10 ⁻⁴	(-2.42x10 ⁻⁴ , 5.92x10 ⁻⁴)	0.832	95	-0.003	(-0.118, 0.111)	0.952
-2682	108	-0.038	(-0.327, 0.251)	0.794	108	-0.526	(-1.463, 0.412)	0.269	108	2.34x10 ⁻⁴	(-2.88x10 ⁻⁴ , 7.56x10 ⁻⁴)	0.888	96	0.012	(-0.131, 0.155)	0.865
-2673	108	-0.011	(-0.252, 0.230)	0.929	108	-0.357	(-1.141, 0.427)	0.369	108	2.01x10 ⁻⁴	(-2.34x10 ⁻⁴ , 6.37x10 ⁻⁴)	0.916	96	0.004	(-0.113, 0.122)	0.943
-2649	107	-0.054	(-0.303, 0.194)	0.665	107	-0.449	(-1.257, 0.359)	0.273	107	1.31x10 ⁻⁴	(-3.21x10 ⁻⁴ , 5.83x10 ⁻⁴)	0.567	95	-0.025	(-0.148, 0.099)	0.694
-2642	107	-0.071	(-0.333, 0.191)	0.592	107	-0.554	(-1.402, 0.294)	0.198	107	1.45x10 ⁻⁴	(-3.30x10 ⁻⁴ , 6.21x10 ⁻⁴)	0.545	95	-0.023	(-0.156, 0.110)	0.733
-2554	106	-0.111	(-0.444, 0.223)	0.512	106	-0.809	(-1.886, 0.268)	0.140	106	1.42x10 ⁻⁴	(-4.62x10 ⁻⁴ , 7.45x10 ⁻⁴)	0.642	94	0.124	(-0.055, 0.303)	0.172
-2465	100	-0.142	(-0.528, 0.243)	0.466	100	-0.774	(-2.026, 0.477)	0.222	100	7.21x10 ⁻⁵	(-6.28x10 ⁻⁴ , 7.72x10 ⁻⁴)	0.838	89	-0.039	(-0.229, 0.151)	0.681
-2406	107	-0.130	(-0.462, 0.203)	0.441	107	-0.912	(-1.989, 0.165)	0.096	107	1.37x10 ⁻⁴	(-4.66x10 ⁻⁴ , 7.40x10 ⁻⁴)	0.654	96	0.008	(-0.155, 0.171)	0.922
-2391	105	-0.111	(-0.391, 0.169)	0.434	105	-0.730	(-1.636, 0.176)	0.113	105	1.10x10 ⁻⁴	(-3.96x10 ⁻⁴ , 6.17x10 ⁻⁴)	0.667	94	-0.005	(-0.142, 0.132)	0.940
-2387	104	-0.140	(-0.436, 0.156)	0.349	104	-0.928	(-1.881, 0.026)	0.056	104	1.59x10 ⁻⁴	(-3.83x10 ⁻⁴ , 7.01x10 ⁻⁴)	0.561	93	0.031	(-0.113, 0.175)	0.670
-2385	104	-0.171	(-0.444, 0.101)	0.215	104	-0.937	(-1.815, -0.060)	0.037*	104	4.76x10 ⁻⁵	(-4.53x10 ⁻⁴ , 5.49x10 ⁻⁴)	0.851	93	0.013	(-0.122, 0.149)	0.846
-2357	107	-0.134	(-0.458, 0.190)	0.415	107	-0.621	(-1.679, 0.436)	0.247	107	-1.14x10 ⁻⁴	(-6.05x10 ⁻⁴ , 5.83x10 ⁻⁴)	0.970	95	-0.028	(-0.190, 0.134)	0.733
		AUTUMN														
		Total BMC			Total BA			Total BMD			Total scBMC					
<i>RXRA</i>	CpG	n	B (95 % CI)	p	n	B (95 % CI)	p	n	B (95 % CI)	p	n	B (95 % CI)	p			
-2693	102	0.039	(-0.126, 0.205)	0.639	102	0.335	(-0.214, 0.884)	0.229	102	-2.59x10 ⁻⁵	(-4.37x10 ⁻⁴ , 2.40x10 ⁻⁴)	0.566	85	-0.029	(-0.134, 0.076)	0.586
-2686	102	0.011	(-0.153, 0.175)	0.896	102	0.296	(-0.249, 0.841)	0.284	102	-2.59x10 ⁻⁴	(-5.10x10 ⁻⁴ , 1.58x10 ⁻⁴)	0.299	85	-0.045	(-0.149, 0.058)	0.386
-2682	105	0.066	(-0.147, 0.280)	0.538	105	0.569	(-0.133, 1.271)	0.111	105	-2.59x10 ⁻⁴	(-5.94x10 ⁻⁴ , 2.57x10 ⁻⁴)	0.433	88	-0.072	(-0.206, 0.062)	0.287
-2673	105	0.007	(-0.181, 0.195)	0.939	105	0.375	(-0.246, 0.995)	0.234	105	-2.59x10 ⁻⁴	(-5.98x10 ⁻⁴ , 1.47x10 ⁻⁴)	0.233	88	-0.072	(-0.189, 0.046)	0.227
-2649	103	0.040	(-0.146, 0.226)	0.673	103	0.462	(-0.159, 1.082)	0.143	103	-2.59x10 ⁻⁴	(-5.61x10 ⁻⁴ , 1.78x10 ⁻⁴)	0.306	87	-0.074	(-0.193, 0.046)	0.224
-2642	104	0.109	(-0.068, 0.285)	0.224	104	0.546	(-0.034, 1.126)	0.065	104	-2.59x10 ⁻⁵	(-3.70x10 ⁻⁴ , 3.40x10 ⁻⁴)	0.933	87	-0.038	(-0.151, 0.074)	0.499
-2554	102	0.076	(-0.222, 0.375)	0.614	102	0.730	(-0.250, 1.710)	0.143	102	-2.59x10 ⁻⁴	(-8.77x10 ⁻⁴ , 3.03x10 ⁻⁴)	0.337	85	-0.086	(-0.273, 0.101)	0.362
-2465	100	0.112	(-0.145, 0.370)	0.389	100	0.909	(0.053, 1.764)	0.038*	100	-2.59x10 ⁻⁴	(-7.75x10 ⁻⁴ , 2.44x10 ⁻⁴)	0.303	84	-0.103	(-0.270, 0.064)	0.223
-2406	105	0.207	(-0.061, 0.475)	0.129	105	0.741	(-0.149, 1.631)	0.102	105	7.71x10 ⁻⁴	(-3.63x10 ⁻⁴ , 7.18x10 ⁻⁴)	0.517	88	0.024	(-0.145, 0.194)	0.777
-2391	105	0.105	(-0.099, 0.309)	0.307	105	0.586	(-0.086, 1.258)	0.087	105	-2.59x10 ⁻⁵	(-4.43x10 ⁻⁴ , 3.76x10 ⁻⁴)	0.873	88	-0.047	(-0.177, 0.083)	0.473
-2387	105	0.122	(-0.124, 0.368)	0.328	105	0.705	(-0.107, 1.516)	0.088	105	-2.59x10 ⁻⁵	(-5.62x10 ⁻⁴ , 4.26x10 ⁻⁴)	0.785	88	-0.060	(-0.218, 0.099)	0.456
-2385	104	0.114	(-0.108, 0.336)	0.312	104	0.562	(-0.170, -1.294)	0.131	104	7.71x10 ⁻⁷	(-4.47x10 ⁻⁴ , 4.49x10 ⁻⁴)	0.997	88	-0.022	(-0.165, 0.120)	0.757
-2357	104	0.029	(-0.272, 0.330)	0.849	104	0.237	(-0.761, 1.236)	0.638	104	-2.59x10 ⁻⁵	(-6.51x10					

3.2.4 Does vitamin D supplementation alter *RXRA* methylation in placenta?

3.2.4.1 Placenta from the MAVIDOS trial

3.2.4.1.1 Cohort characteristics

First we wanted to determine whether the maternal and neonatal characteristics were representative of the published MAVIDOS findings from across all three test centres (**Table 3.8**). Amongst these 73 participants, there were no significant differences in maternal age, BMI, skinfold thickness or the proportion of nulliparous women and women that were currently smoking. There were no significant differences in maternal serum 25(OH)D₃ concentrations at 14 weeks gestation whereas at 34 weeks gestation, maternal serum 25(OH)D₃ concentrations were significantly higher in the cholecalciferol group compared to the placebo group ($p = 0.001$). There were no significant differences in neonatal characteristics between the cholecalciferol supplemented group and the placebo group including the proportion of males to females, gestational age and birthweight. Neonatal DXA measurements, which were taken within 14 days of birth, were available for 57 neonates (27 born to mothers randomised to cholecalciferol, and 29 born to placebo). There were no differences in age of the neonate at the time of the DXA scan, BMC, BA, BMD, scBMC, total fat mass, % fat mass, total lean mass, % lean mass or weight at the neonatal DXA scan between the cholecalciferol supplemented and placebo group. Therefore, these baseline characteristics are similar to what has been seen in the overall MAVIDOS trial population³⁵⁹.

Table 3.8 Baseline maternal and neonatal characteristics of the present subset of randomly assigned pregnant women from the MAVIDOS trial from which placental data were included in the analyses.

	Cholecalciferol (n = 33)	Placebo (n = 40)	p
Womens Age (years)	32.1 (5.2)	31.8 (5.0)	0.750
Womens BMI (Kg/m²)	26.2 (5.5)	28.6 (4.9)	0.058
Sum of skinfold thickness (mm)^a	72.3 (55.0,108.4)	89.7 (77.0,116.6)	0.098
25(OH)D 14 weeks (nmol/L)	48.9 (17.9)	48.2 (18.8)	0.864
25(OH)D 34 weeks (nmol/L)	74.8 (18.2)	44.9 (20.4)	0.001*
Nulliparous (%)	45.5	42.5	0.800
Current Smoker (%)	3.0	7.5	0.404
Males (%)	48.5	52.5	0.442
Gestational Age (weeks)	40.4 (1.0)	40.0 (1.6)	0.162
Birthweight (g)	3573.3 (465.3)	3535.8 (448.2)	0.727
Age at neonatal DXA scan (days)^a	2.5 (1.0,9.8)	4.0 (1.0,11.0)	0.567
BMC (g)	62.6 (10.7)	60.8 (11.2)	0.547
BA (cm²)	305.7 (29.9)	297.4 (36.5)	0.358
BMD (g/cm²)	0.2 (0.0)	0.2 (0.0)	0.940
scBMC (g)	59.7 (5.2)	60.5 (4.4)	0.566
Total Body Fat Mass (g)^a	344.9 (240.9,429.6)	294.4 (150.6,451.1)	0.176
Total Body Lean Mass (g)	3144.2 (304.2)	3107.8 (405.3)	0.707
Percentage Fat Mass (%)^a	9.5 (7.9,11.9)	8.2 (5.0,11.0)	0.181
Percentage Lean Mass (%)	88.3 (3.5)	89.3 (5.6)	0.444
Weight at neonatal DXA scan (g)	3569.5 (411.4)	3494.4 (498.7)	0.543

Values are mean (standard deviation, median (interquartile range [IQR]) or %. Percentages calculated accounting for missing variables. Independent t-tests compared the cholecalciferol supplemented to the placebo group. ^aData were not normally distributed so a Mann-Whitney test was used instead. The proportion of males, nulliparous women and current smokers within each treatment group were calculated using a chi-test.

3.2.4.1.2 Does *RXRA* methylation in cord correlate with *RXRA* methylation in placenta in the MAVIDOS trial?

Within the MAVIDOS trial, there was an overlap of 45 participants which had *RXRA* methylation measurements in both umbilical cord and placenta. To determine any correlation in *RXRA* CpG methylation between cord and placental tissues, Spearman's correlation test was used (**Table 3.9 and Figure 3.4**). Some methylation values for CpGs in either one tissue type or both failed due to internal controls which resulted in the exclusion of that matched pair and differing sample numbers available at each *RXRA* CpG site. There was a significant positive correlation of *RXRA* CpG -2693 in umbilical cord and placental tissue ($p = 0.007$, $\rho = 0.510$). There were no significant correlations between cord and placental methylation at the remaining CpG sites.

Table 3.9 Correlation between *RXRA* methylation at birth in umbilical cord tissue compared to placental tissue from the MAVIDOS trial.

CpG	n	Correlation Coefficient	p
-2693	27	0.510	0.007*
-2686	28	0.291	0.133
-2682	29	0.159	0.410
-2673	29	0.242	0.205
-2649	35	0.305	0.075
-2642	35	-0.062	0.725
-2554	40	-0.215	0.184
-2465	40	0.214	0.186
-2406	44	0.051	0.745
-2391	43	0.152	0.331
-2387	39	0.079	0.631
-2385	38	0.036	0.830
-2357	44	0.261	0.087

Non parametric Spearman's correlation compared *RXRA* methylation in cord and placenta.

Correlation between *RXRA* CpG -2693 methylation at birth in cord compared to placenta from the MAVIDOS trial

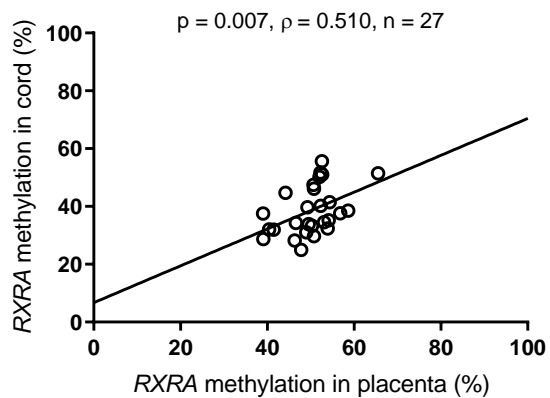


Figure 3.4 Correlation between methylation at birth of *RXRA* CpG -2693 in cord compared to placenta in the MAVIDOS trial.

3.2.4.1.3 Maternal vitamin D supplementation during pregnancy alters *RXRA* methylation at birth in placenta within the MAVIDOS trial

To determine whether cholecalciferol supplementation during pregnancy altered *RXRA* CpG methylation in placental tissue, independent t-tests compared *RXRA* methylation at birth between 1000 IU/d cholecalciferol supplemented group and the placebo group within the MAVIDOS trial (Table 3.10). The results showed that infants born to cholecalciferol supplemented mothers had higher *RXRA* CpG -2554 methylation in placental tissue, compared to the placebo group ($p = 0.033$). There were no significant differences in placental methylation between the maternal treatment groups at the remaining *RXRA* CpG sites.

Table 3.10 Differences in *RXRA* methylation between the treatment groups in the MAVIDOS trial in placenta.

<i>RXRA</i> CpG	n	Mean difference (%)	95 % CI	p
-2693	49	-0.382	(-4.070, 3.306)	0.836
-2686	49	0.169	(-3.519, 3.858)	0.927
-2682 (squared)	49	96.351	(-289.998, 482.700)	0.618
-2673 (inverse)	50	0.000	(-0.004, 0.003)	0.845
-2649 (squared)	57	174.608	(-230.391, 579.607)	0.391
-2642	57	2.106	(-0.776, 4.987)	0.149
-2554 (squared)	68	473.966	(39.347, 908.585)	0.033*
-2465	69	1.649	(-0.316, 3.614)	0.099
-2406	68	1.576	(-1.523, 4.674)	0.314
-2391	68	-0.244	(-2.669, 2.181)	0.842
-2387	62	-0.309	(-3.091, 2.472)	0.825
-2385 (log)	62	-0.002	(-0.041, 0.037)	0.921
-2357 (inverse)	68	0.000	(-0.002, 0.002)	0.806

Independent t-tests compared *RXRA* methylation in placental tissue between the cholecalciferol supplemented and placebo group within the MAVIDOS trial. *RXRA* CpGs -2682, -2673, -2649, -2554, -2385 and -2357 were not normally distributed so underwent transformation to achieve normality prior to analyses.

3.2.4.2 Placenta from the SPRING study

3.2.4.2.1 Maternal supplementation is not associated with altered *RXRA* methylation in placental tissue within the SPRING study

To determine whether the vitamin D intervention alters *RXRA* methylation in placenta from the SPRING study, independent t-tests compared *RXRA* CpG methylation between the maternal treatment groups (**Table 3.11**). There was no evidence of significant differences in *RXRA* CpG methylation between the cholecalciferol supplemented and placebo group.

Table 3.11 Differences in *RXRA* methylation in placenta between the treatment groups in the SPRING study.

<i>RXRA</i> CpG	n	Mean difference (%)	95 % CI	p
-2693	78	-0.113	(-3.184, 2.957)	0.942
-2686	80	0.214	(-2.142, 2.570)	0.857
-2682 (squared)	80	-65.775	(-421.405, 289.856)	0.714
-2673	80	-1.037	(-3.407, 1.333)	0.386
-2649	67	2.298	(-1.131, 5.272)	0.185
-2642	69	1.408	(-1.870, 4.686)	0.394
-2554	91	0.442	(-2.222, 3.106)	0.742
-2465	94	0.714	(-1.107, 2.535)	0.438
-2406	93	1.218	(-1.499, 3.935)	0.376
-2391	92	-0.130	(-2.193, 1.933)	0.901
-2387	88	-0.069	(-2.210, 2.071)	0.949
-2385 (squared)	87	95.881	(-73.256, 265.017)	0.263
-2357	92	0.984	(-1.095, 3.063)	0.349

Independent t-tests compared *RXRA* methylation in placental tissue between the *A* and *B* group within the SPRING study. *RXRA* CpGs -2682 and -2385 were square transformed prior to analyses.

3.2.4.3 *In vitro* treatment of placental fragments with 25(OH)D₃ does not alter methylation of *RXRA*

Having shown that maternal cholecalciferol supplementation during pregnancy is associated with altered *RXRA* methylation in placental tissue from the MAVIDOS trial, we examined whether short term *in vitro* exposure of placental fragments to 25(OH)D₃ altered *RXRA* CpG methylation. Matched placental fragments from 8 placentas were treated with 20 μM 25(OH)D₃ or a BSA and ethanol control for 8 hours and paired t-tests were used to compare *RXRA* CpG methylation between the matched pairs. The results showed that there were no significant differences in *RXRA* CpG methylation between the treatment groups (Table 3.12).

Table 3.12 Differences in mean *RXRA* methylation between matched placental fragments treated with 20μM 25(OH)D₃, *in vitro*, for 8 hours.

<i>RXRA</i> CpG	n	Average mean difference	95 % CI	p
-2693	8	2.330	(-1.107, 5.767)	0.153
-2686	8	-0.354	(-3.130, 2.422)	0.772
-2682	8	2.446	(-0.983, 5.875)	0.135
-2673	8	0.173	(-4.135, 4.480)	0.927
-2649	8	2.313	(-1.745, 6.370)	0.220
-2642	8	1.144	(3.801, 6.089)	0.601
-2554	8	0.723	(-5.559, 7.004)	0.793
-2465	6	1.098	(-1.198, 3.394)	0.274
-2406	8	1.734	(-3.630, 7.097)	0.470
-2391 (squared)	8	80.049	(-198.992, 359.090)	0.519
-2387	8	1.996	(-3.468, 7.461)	0.416
-2385	8	2.011	(-3.185, 7.208)	0.391
-2357 (log)	8	0.022	(-0.032, 0.076)	0.369

Matched paired t-tests between the 25(OH)D₃ and BSA ethanol control.

3.2.4.4 *In vitro* treatment of cytotrophoblasts with 25(OH)D₃ does not alter *RXRA* methylation

Dr Ashley cultured primary cytotrophoblasts from 8 term placentas with 20 μM 25(OH)D₃ or a BSA and ethanol control for 24 hours. Paired t-tests were used to compare *RXRA* CpG methylation between the matched pairs however there were no significant differences between the treatment groups (Table 3.13).

Table 3.13 Differences in mean *RXRA* methylation between matched cytotrophoblasts treated with 20uM 25(OH)D₃, *in vitro*, for 24 hours.

<i>RXRA</i> CpG	n	Average mean difference	95 % CI	p
-2693	6	-0.600	(-14.948, 13.748)	0.919
-2686 (log)	6	0.000	(-0.197, 0.196)	0.997
-2682 (squared)	6	-642.398	(-3529.132, 2244.336)	0.592
-2673	6	4.135	(-7.945, 16.215)	0.419
-2649	5	6.834	(-9.558, 23.226)	0.311
-2642	5	4.628	(-11.894, 21.150)	0.480
-2554 (log)	8	0.065	(-0.078, 0.208)	0.318
-2465 (log)	6	0.063	(0.099, 0.224)	0.365
-2406	7	1.953	(3.740, 7.646)	0.433
-2391	7	2.737	(-2.022, 7.496)	0.209
-2387 (log)	7	0.076	(-0.033, 0.185)	0.137
-2385 (log)	7	0.090	(-0.007, 0.187)	0.065
-2357 (log)	8	0.065	(-0.054, 0.183)	0.237

Matched paired t-tests between the 25(OH)D₃ and BSA ethanol control.

3.3 Discussion

The early life environment has been shown to influence epigenetic markers, such as DNA methylation, which have been shown to be associated with disease risk in later life. Within the MAVIDOS trial, we have shown that maternal cholecalciferol supplementation during pregnancy is associated with altered *RXRA* CpG methylation in umbilical cord tissue. This suggests that the early life environment, with respect to vitamin D supplementation, is associated with altered DNA methylation which may alter gene expression and phenotype. Infants born in the winter months to cholecalciferol supplemented mothers had greater neonatal bone measures than the placebo group however, these phenotypic changes were not reflected in DNA methylation changes amongst infants born in the winter months. This could be due to altered methylation of *RXRA* not being part of the causal pathway between maternal vitamin D supplementation and altered bone outcomes, or the lack of findings may be due to the small sample size when the analyses were stratified by season of birth. Studies within the SWS cohort have identified inverse associations between *RXRA* methylation in umbilical cord tissue and bone measures at 4 and 6 years of age²⁹⁹. Within the MAVIDOS trial, there are no significant associations between *RXRA* methylation in umbilical cord tissue and bone measures at birth however, it would be interesting to determine any associations at 4 and 6 years of age. These findings provide insight into the use of *RXRA* methylation as a biomarker for bone measures at birth and childhood which could help to identify suitable interventions during the early life environment and could highlight at risk individuals in need of targeted interventions in early infancy to prevent adverse bone outcomes, such as osteoporosis, in later life.

Within the MAVIDOS trial, there were no significant associations between *RXRA* methylation at birth in umbilical cord and neonatal bone measures at birth with intervention as a covariate however, it would be interesting to determine associations at 4 and 6 years of age and to determine whether the direction of association is similar to that seen in the SWS cohort²⁹⁹. Infants born to cholecalciferol supplemented mothers had lower cord methylation at *RXRA* CpGs -2686, -2682, -2673, -2649 and -2642 compared to the placebo group which suggests that the early life vitamin D intervention alters *RXRA* CpG methylation. The functional importance of this region has been investigated in **Chapter 6** which showed that mutation of these CpGs of interest has a negative effect on *RXRA* promoter activity, suggesting that DNA methylation within this region is associated with decreased gene expression. Following maternal cholecalciferol supplementation, the decrease in *RXRA* methylation is likely linked to an increase in *RXRA* gene expression which could result in increased heterodimerisation with VDR and binding to VDREs in target genes, such as in *Osteocalcin* which is involved in mineralisation of the bone matrix, leading to bone formation and improved bone health. The differences in methylation are small, around 1.9 % so it is unsure how functionally

significant this change would be. Arguably, altered methylation in a small percentage of cell types could alter gene expression and have a significant impact on downstream targets and processes which could result in altered phenotype. Tobi *et al.*, measured DNA methylation amongst individuals periconceptionally exposed to the Dutch Hunger Winter and their unexposed sibling and found within-pair differences of 2 – 8 % which were linked to altered phenotype in adulthood³⁶⁰.

The MAVIDOS trial found that infants born in the winter months to cholecalciferol supplemented mothers had improved bone measures at birth compared to the placebo group²³⁶ however, there were no differences in cord *RXRA* CpG methylation between the treatment groups amongst infants born in the winter months. Instead, there were significant differences in *RXRA* methylation between the treatment groups amongst infants born in the summer and autumn months. This suggests that the phenotypic changes observed amongst infants born in the winter months are not reflected in altered methylation of these *RXRA* CpGs of interest. It would be interesting to determine whether there are significant differences between the treatment groups within each season in bone measures in later childhood. It is possible that there is altered methylation at other CpG loci upstream of the *RXRA* promoter which could be investigated further through bisulfite pyrosequencing. Conversely, altered *RXRA* methylation may not lie on the causal pathway related to altered bone outcomes and DNA methylation of other genes could be investigated. Nonetheless, the lack of associations could be due to the small sample size when analyses are stratified by season of birth and expansion of MAVIDOS samples from the Sheffield and Oxford trial centres could show significant results. A study which examined fetal and neonatal proximal femoral metaphyses found that the relative amount of bone and cartilage was higher in the third trimester compared to the second trimester and that osteoid thickness increases with gestational age³⁶¹. This would suggest that the demand for vitamin D would be greatest in the third trimester suggesting that this may be an important exposure period with respect to fetal skeletal development. It is thought that UVB exposure resulting in vitamin D synthesis in the skin is the major determinant of maternal serum 25(OH)D₃ concentrations rather than through diet or supplements²³². Mothers that give birth in winter are exposed to the least amount of sunshine in the second and third trimesters (**Figure 3.5**), so vitamin D supplementation is especially important amongst these women that are due to give birth in the winter months, and this can be shown by the improved bone measures amongst infants born in winter to cholecalciferol supplemented mothers²³⁶. Furthermore, maternal 25(OH)D₃ status at 34 weeks gestation amongst women that delivered in the winter months was 54.5 nmol/L in cholecalciferol supplemented mothers and 31.9 nmol/L in placebo mothers (**Table 3.3**). As maternal vitamin D status positively correlates with cord vitamin D status, this suggests that infants born in winter to placebo mothers had a lower starting reserve of vitamin D, which could influence fetal skeletal development as well as development in early infancy which could be associated with

decreased peak bone mass and increased risk of developing osteoporosis in later adulthood. With the significant differences amongst the winter months with maternal vitamin D status during late pregnancy as well as the differences in neonatal bone measures at birth between the treatment groups, if on the causal pathway you would expect to see altered DNA methylation amongst winter births rather than in the other seasons. However, there was altered *RXRA* CpG methylation amongst infants born in the summer and autumn months. Furthermore, maternal vitamin D status in both the treatment groups amongst women that delivered in summer and autumn was significantly higher than in the winter months which is likely due to greater sunshine exposure due to the spring and summer months during late pregnancy in both groups and the additional supplementation in the cholecalciferol supplemented group. Altered methylation in response to maternal cholecalciferol supplementation amongst infants born in the summer and autumn months could be part of a feedback loop due to the increased availability of vitamin D. With an increase in available $1,25(\text{OH})_2\text{D}_3$ to bind to VDR, there could be greater demand for RXRA to heterodimerise and bind to VDREs in target genes, therefore there is greater RXRA gene expression which is accompanied by lower *RXRA* methylation.

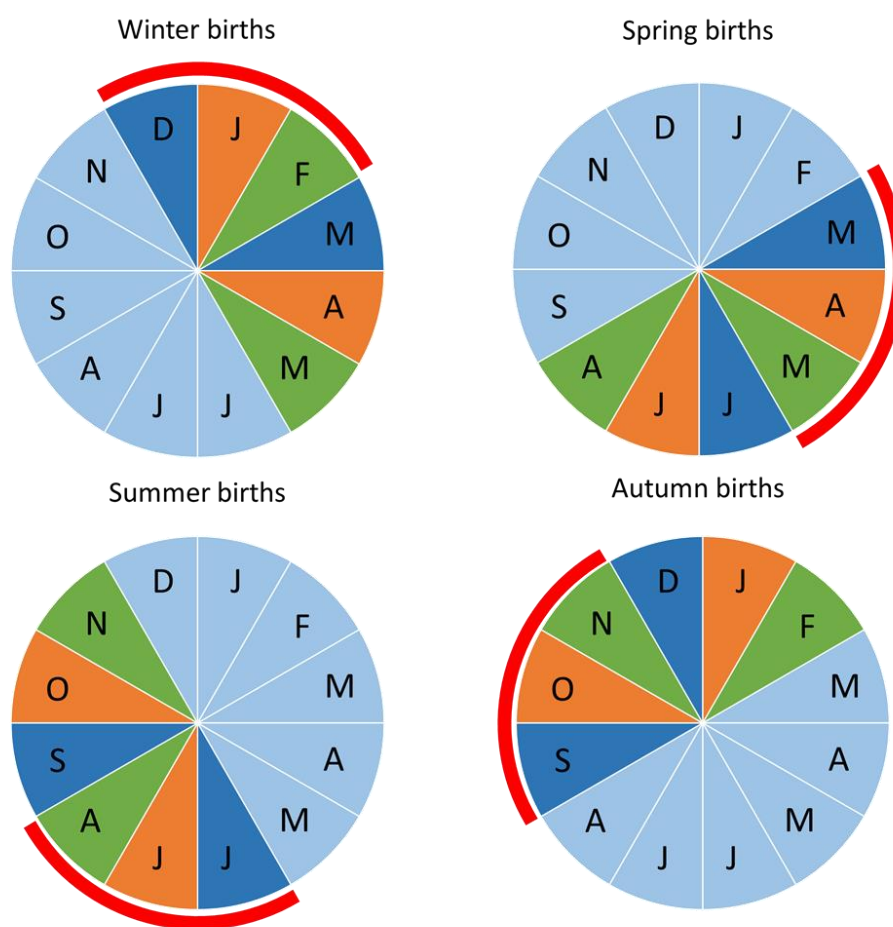


Figure 3.5 Pictogram representing pregnancy and UVB exposure during the year.

The segments represent the months of the year (from January to December). Red denotes the month of birth. The corresponding colours of dark blue, orange and green represent the associated month of conception.

The results suggest that there is an interaction between vitamin D supplementation during pregnancy, season of birth, the methylation status of *RXRA* and bone measures at birth, however the exact mechanism is unknown and it is unclear whether this is part of a causal or indirect pathway. Beckett *et al.*, found that plasma 25(OH)D₃ positively correlates with *VDR* methylation and negatively correlates with methylation of *CYP2R1* and *CYP24A1*³⁶². Methylation marks in the promoter region are often repressive, therefore the results by Beckett *et al.*, would suggest that following an increase in plasma 25(OH)D₃ concentrations there is downregulation of *VDR* expression and upregulation of *CYP2R1* and *CYP24A1* expression. If this results in a decrease in available *VDR* present in the cell, this would result in a smaller proportion of 1,25(OH)₂D₃ being able to bind and a decreased need for available *RXRA* to bind to liganded *VDR*. This suggests that there is an alternative mechanism such as through binding to membrane bound *VDR* or by binding to G-protein coupled receptors however the mechanisms are unclear¹⁵². It has been hypothesised that 1,25(OH)₂D₃ can bind to cytosolic and membrane bound *VDR* and G-protein coupled receptors on the cell surface resulting in phosphorylation and activation of PKC leading to the activation of the MAPK-ERK1 and 2 signalling pathways¹⁵². Furthermore, it is thought that there is cross talk between the non-genomic and genomic *VDR* pathways resulting in gene transcription of key genes such as *Osteocalcin*, which is involved in bone mineralisation^{152,363}. Within the MAVIDOS trial, infants born to cholecalciferol supplemented mothers had lower *RXRA* methylation in umbilical cord tissue compared to the placebo group. This suggests that there may be an increase in *RXRA* gene expression which could result in increased heterodimerisation with other partners such as the thyroid hormone receptor which has been shown to play a role in regulating bone turnover and bone mineral density³⁶⁴.

Within this chapter, we investigated *RXRA* CpG methylation in a range of placental tissues however the sample size was much smaller compared to the number of available umbilical cords. In the MAVIDOS trial, there was a positive correlation in methylation of *RXRA* CpG -2693 between placental and umbilical cord tissue which suggests that there are some similarities between the tissue types. Conversely, there was no correlation at the remaining CpG sites, which may be due to tissue specific methylation differences or due to the small sample size. A study has reported that there is no correlation between global methylation of different genes in umbilical cord and placenta, and that mean methylation was significantly higher in cord tissue³⁶⁵. Whereas amongst these samples, methylation was higher in placental tissue than umbilical cord. Furthermore, within the MAVIDOS trial, in placental tissue, cholecalciferol supplementation during pregnancy was linked to higher *RXRA* CpG -2554 methylation compared to the placebo group, whereas in umbilical cord tissue, there was lower *RXRA* methylation. In the SPRING study there were no significant differences in *RXRA* CpG methylation between the treatment groups. It is possible that a methylation difference

cannot be seen due to the low sample size ($n=94$) and therefore the analysis is underpowered. A power calculation based on methylation of *RXRA* CpG -2649 suggested that a sample size of 146 is needed to obtain a power of 0.8 whereas the current sample size is 67. Furthermore, as the SPRING study is currently blinded, it is possible that the maternal baseline characteristics and neonatal outcomes are significantly different in this subset of the population which could result in a biased dataset. *RXRA* methylation from placental *in vitro* studies with 25(OH)D₃ showed no difference in *RXRA* methylation, however, this could be due to only having an 8 hour exposure in the fragments and 24 hours in cytotrophoblasts. Perhaps this exposure was too brief to illicit a significant effect on *RXRA* methylation. Conversely, due to the small sample number the study is currently powered at 0.29 and a sample size of 33 for placental fragments and 221 for placental cytotrophoblasts rather than 8 is needed to detect significance. The lack of associations in placental tissue could be due to tissue specific methylation differences. Epithelial, mesenchymal and hematopoietic stem cells can be isolated from umbilical cord and placental tissue^{366–369}. However, there could be differing proportions of each stem cell which can influence *RXRA* methylation measurements in a heterogeneous population. Wu *et al.*, found that the proliferation potential of mesenchymal stem cells from umbilical cord is greater than MSCs from placental tissue³⁷⁰. There are also differences in secretion patterns of growth factors and cytokines including hepatocyte growth factor (*HGF*), *IGF1*, prostaglandin E2 (*PGE2*) and vascular endothelial growth factor (*VCAM1*)³⁷⁰. Placental tissue also contain cytotrophoblasts which are absent in umbilical cord tissue.

There were some limitations to the experiments. Firstly, DNA methylation would ideally be measured in a tissue central to the pathogenesis of osteoporosis, such as bone tissue, however this is not feasible. Studies within the SWS cohort have found that *RXRA* methylation within umbilical cord tissue is predictive of bone measures in childhood²⁹⁹ so DNA methylation was investigated in umbilical cord tissue as well as preliminary investigation into placental tissue. Second, umbilical cord tissue is a heterogeneous tissue and therefore, associations should be adjusted for cell type due to cell type specific methylation patterns. 850k arrays have been carried out on the majority of the MAVIDOS samples, however the cell type composition data is not available yet. Third, the MAVIDOS trial was mainly on a Caucasian population therefore, these results may not represent the wider general public. To overcome this, associations should be investigated in other randomised controlled trials and cohorts. Fourth, multiple tests have been performed, driven by the a priori hypothesis. However, the analyses were not corrected for multiple testing as it was thought that adjustment for Bonferroni correction would be overly conservative.

In conclusion, maternal cholecalciferol supplementation during pregnancy was associated with altered *RXRA* methylation in umbilical cord tissue which suggests that *RXRA* methylation can be used as a biomarker for early life interventions which may alter bone health in later life. Despite

Chapter 3

the lack of associations between *RXRA* CpG methylation at birth and neonatal bone measures at birth, follow up studies will determine associations at 4 and 6 years of age to determine whether there is a similar association as observed in the SWS cohort²⁹⁹. Next, it would be interesting to determine the effect of maternal cholecalciferol supplementation during pregnancy on *CDKN2A* methylation (**Chapter 4**), which has been previously shown to be inversely associated with bone measures in childhood within the SWS cohort³²³. These *RXRA* findings suggest that DNA methylation may not lie on the causal pathway with altered bone outcomes at birth however, causality is not required for risk prediction. It is possible that altered *RXRA* methylation is simply a marker that can be used to predict bone measures in later childhood, and the mechanisms underlying this will be investigated further in **Chapter 6**.

**Chapter 4 Maternal vitamin D supplementation during
pregnancy alters *CDKN2A* DNA methylation at birth
within the MAVIDOS trial**

4.1 Introduction

Studies within the SWS have shown that *RXRA* CpG methylation in umbilical cord tissue is inversely associated with scBMC in later childhood²⁹⁹ and within **Chapter 3** we have shown that maternal vitamin D supplementation during pregnancy is linked to altered *RXRA* methylation in umbilical cord tissue however, there are no associations between *RXRA* methylation and bone measures at birth. A second candidate epigenetic biomarker, *CDKN2A*, has been identified within the SWS cohort and DNA methylation of *CDKN2A* in umbilical cord tissue was shown to be inversely associated with bone outcomes at 4 and 6 years of age³²³. As physiological measures in the MAVIDOS are ongoing, and the 4 or 6 year time points are not yet available, associations between *CDKN2A* methylation at birth and bone measures at birth were investigated.

The *CDKN2A* gene locus encodes the long non-coding RNA, ANRIL, as well as two cell cycle inhibitors, p14^{ARF} and p16^{INK4a} (**Figure 4.1**). Both cell cycle inhibitors have been shown to function as tumour suppressors and are involved in cellular senescence and ageing. P16^{INK4a} is an inhibitor of CDK4 and CDK6, with CDK6 playing a role in osteoblast differentiation³⁷¹. P14^{ARF} has been shown to activate the p53 tumour suppressor gene and has also been shown to have apoptotic properties^{322,323}. The *CDKN2A* CpGs of interest are located within a Differentially Methylation Region (DMR) within the first intron of the *CDKN2A* gene and within the promoter region of *ANRIL*.

The MAVIDOS trial, a vitamin D intervention trial during pregnancy, has shown that infants born in the winter months to cholecalciferol supplemented mothers had greater neonatal bone measures compared to infants born to placebo supplemented mothers²³⁶. This trial offers the opportunity to investigate whether maternal vitamin D supplementation is linked to altered *CDKN2A* methylation and whether *CDKN2A* methylation is associated with bone measures at birth.

4.1.1 Hypothesis

We hypothesise that maternal cholecalciferol supplementation during pregnancy is associated with decreased *CDKN2A* methylation in umbilical cord tissue and *CDKN2A* methylation is inversely associated with bone measures at birth within the MAVIDOS trial.

4.1.2 Aims

1. To determine whether maternal vitamin D supplementation during pregnancy alters *CDKN2A* DNA methylation in umbilical cord tissue within the MAVIDOS trial
2. To determine whether *CDKN2A* DMR methylation in umbilical cord tissue is associated with bone measures at birth within the MAVIDOS trial

4.1.3 Methods

DNA methylation of 9 CpG sites within the first intron of the *CDKN2A* gene, and within the promoter region of *ANRIL* (**Figure 4.1**) were measured in DNA samples extracted from the umbilical cord of 449 infants from the MAVIDOS trial. Full materials and methods for this chapter are described in **Sections 2.2.2, 2.2.4** and Error! Reference source not found.. Briefly, pregnant mothers received 000 IU/d cholecalciferol or a placebo daily from 14 weeks of gestation until delivery as part of a double blind, randomised, placebo controlled trial which took place in Southampton, Oxford and Sheffield. Umbilical cords were collected at birth from 449 mothers who gave birth in Southampton. DNA was extracted from these umbilical cords and DNA methylation of individual CpG sites at the *CDKN2A* DMR were measured by bisulfite pyrosequencing using primers as described by Lillycrop *et al.*, 2017³²² which can be seen in **materials and methods section 2.2.4.3**.

Statistical tests were carried out in IBM SPSS Statistics 24 and histograms were used to confirm normality. To determine if maternal vitamin D supplementation influences *CDKN2A* DNA methylation independent t-tests were used to compare *CDKN2A* CpG methylation at birth between the 1000 IU/d cholecalciferol supplemented group and the placebo group (**Section 4.2.1**). Data were further stratified by season of birth and Independent t-tests were used to compare *CDKN2A* methylation at birth between the 1000 IU/d cholecalciferol supplemented group and the placebo group (**Section 4.2.2**). To determine whether *CDKN2A* methylation in umbilical cord tissue was associated with bone measures at birth, linear regression analyses were adjusted for sex, gestational age, treatment allocation and season of birth (**Section 4.2.3**). Furthermore, data were stratified by treatment allocation and also by season of birth prior to linear regression analyses (**Section 4.2.3**).

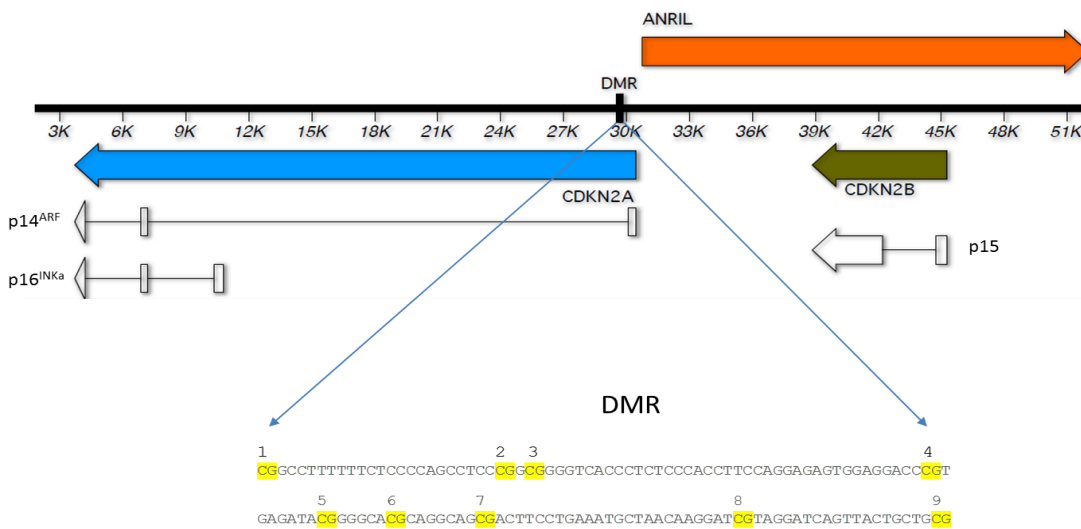


Figure 4.1 *CDKN2A* locus and the location of the DMR containing the 9 CpGs of interest.

The location of the CpG loci in relation to the gene body of *ANRIL*, *CDKN2A* and *CDKN2B*. The transcript of *CDKN2B*, *p15*, and the main transcripts of *CDKN2A*, *p14^{ARF}* and *p16^{INKa}*, have also been shown.

4.2 Results

4.2.1 *CDKN2A* methylation at birth was higher in the vitamin D supplemented group compared to the placebo group within the MAVIDOS trial

The results showed that new-born infants from the cholecalciferol supplemented group had higher cord CpG 9 methylation compared to the placebo group ($p = 0.050$, mean difference = 2.0 %, 95 % CI: < 0.01, 4.02) (**Table 4.1 and Figure 4.2**). There was a trend towards higher CpG 5 methylation in the cholecalciferol supplemented group compared to the placebo group however this did not reach statistical significance ($p = 0.056$, mean difference = 1.8 %, 95 % CI: -0.05, 3.72). There were no significant differences at the remaining CpG sites between the two maternal treatment groups.

Table 4.1 Differences in *CDKN2A* methylation between the treatment groups in the MAVIDOS trial.

<i>CDKN2A</i> CpG	n	Mean diff. (%)	(95 % CI)	p
1	372	1.7	(-0.786, 4.279)	0.176
2	372	1.1	(-1.242, 3.508)	0.349
3	427	0.7	(-1.402, 2.893)	0.495
4	427	1.1	(-0.801, 3.019)	0.254
5	429	1.8	(-0.045, 3.716)	0.056
6	429	1.3	(-0.694, 3.360)	0.197
7	399	1.4	(-0.496, 3.360)	0.145
8	427	1.5	(-0.534, 3.451)	0.151
9	417	2.0	(0.004, 4.023)	0.050*

Independent t-tests compared *CDKN2A* methylation between the cholecalciferol supplemented and placebo group within the MAVIDOS trial.

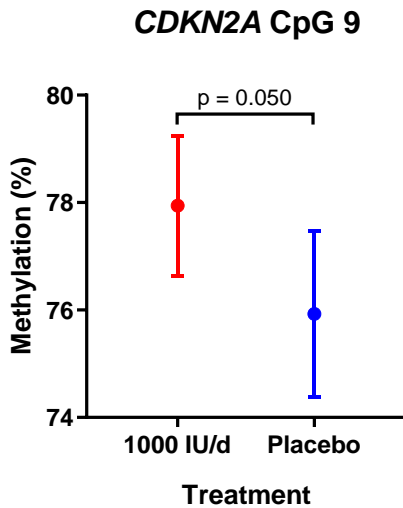


Figure 4.2 Box whisker plots of *CDKN2A* CpG methylation at birth between the treatment groups within the MAVIDOS trial.

Independent t-tests comparing *CDKN2A* CpG methylation at birth between the two maternal treatment groups. Graphs represent mean and 95 % confidence intervals.

4.2.2 Infants born in autumn to vitamin D supplemented mothers had higher *CDKN2A* methylation at birth compared to the placebo group within the MAVIDOS trial

Amongst infants born in the autumn months, those in the cholecalciferol supplemented group had significantly higher methylation at birth at CpGs 5 ($p = 0.015$, mean difference = 4.5 %, 95 % CI: 0.90, 8.03), 6 ($p = 0.049$, mean difference = 4.0 %, 95 % CI: 0.02, 7.90) and 7 ($p = 0.041$, mean difference = 3.9 %, 95 % CI: -0.42, 8.25) compared to the placebo group (**Table 4.2 and Figure 4.3**). Amongst infants born in the winter, spring and summer months, there were no significant differences in DNA methylation at birth.

Table 4.2 Differences in *CDKN2A* methylation between treatment groups in the MAVIDOS trial when stratified by season of birth.

<i>CDKN2A</i> CpG	Winter				Spring				Summer				Autumn			
	n	Mean diff. (%)	(95 % CI)	p	n	Mean diff. (%)	(95 % CI)	p	n	Mean diff. (%)	(95 % CI)	p	n	Mean diff. (%)	(95 % CI)	p
1	72	1.4	(-4.658, 7.467)	0.645	94	-1.7	(-6.496, 3.093)	0.483	101	3.0	(-2.009, 7.921)	0.240	101	3.9	(-1.323, 9.145)	0.141
2	72	-0.7	(-6.815, 5.353)	0.812	94	-3.2	(-7.598, 1.155)	0.147	101	4.1	(-0.487, 8.660)	0.079	101	3.7	(-0.823, 8.147)	0.109
3	83	-2.2	(-8.049, 3.555)	0.443	107	-2.6	(-6.567, 1.354)	0.195	113	3.0	(-1.046, 6.992)	0.146	120	3.5	(-0.453, 7.544)	0.082
4	83	-2.6	(-7.230, 1.955)	0.256	107	-1.3	(-4.912, 2.320)	0.479	113	3.0	(-0.555, 6.486)	0.098	120	3.7	(-0.310, 7.610)	0.070
5	83	-2.1	(-6.490, 2.339)	0.352	107	0.6	(-3.124, 4.366)	0.743	114	2.8	(-0.984, 6.512)	0.147	121	4.5	(0.896, 8.037)	0.015*
6	83	-2.8	(-8.211, 2.597)	0.304	107	-1.1	(-4.834, 2.730)	0.582	114	3.5	(-0.251, 7.228)	0.067	121	4.0	(0.022, 7.901)	0.049*
7	73	-2.0	(-6.960, 2.966)	0.426	100	-0.1	(-3.748, 3.476)	0.941	110	2.3	(-1.263, 5.956)	0.200	112	4.0	(0.167, 7.801)	0.041*
8	77	-2.0	(-7.242, 3.275)	0.455	105	-0.4	(-4.165, 3.274)	0.813	112	3.2	(-0.477, 6.848)	0.088	119	3.3	(-0.704, 7.285)	0.106
9	76	-0.6	(-5.421, 4.174)	0.797	107	0.4	(-3.293, 4.129)	0.824	112	3.1	(-0.594, 6.802)	0.099	118	3.9	(-0.420, 8.248)	0.076

Independent t-tests compared *CDKN2A* methylation between the cholecalciferol supplemented and placebo group within the MAVIDOS trial. Seasons are defined as winter (December to February), spring (March to May), summer (June to August) and winter (September to November).

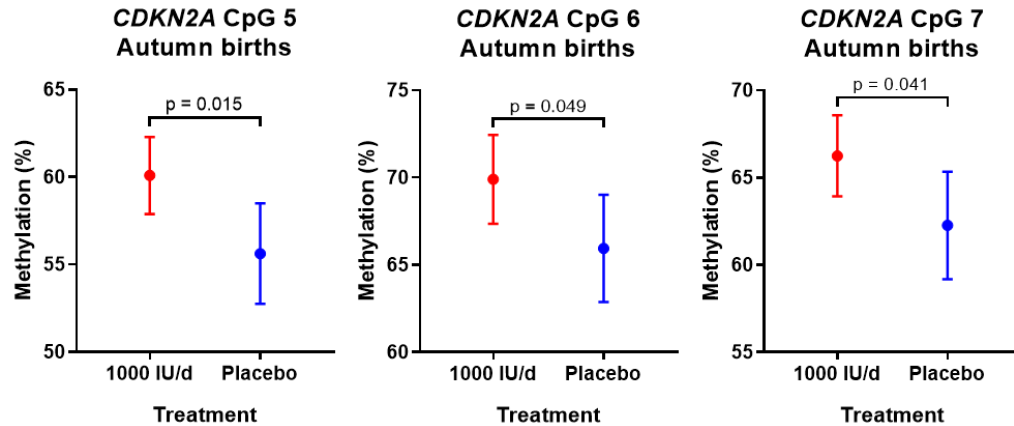


Figure 4.3 Box whisker plots of seasonal differences in *CDKN2A* CpG methylation at birth between the treatment groups within the MAVIDOS trial.

Independent t-tests comparing *CDKN2A* CpG methylation at birth between the two maternal treatment groups. Graphs represent mean and 95 % confidence intervals.

4.2.3 There were no significant associations between cord *CDKN2A* CpG methylation and neonatal bone measures within the MAVIDOS trial

No significant associations were observed between *CDKN2A* DMR methylation with BMC, BA, BMD or scBMC at birth, adjusting for sex, gestational age, treatment group and season of birth (**Table 4.3**). The data were stratified by intervention group to examine if there were within-group effects on bone mass however, no significant associations were seen when linear regression analyses were adjusted for sex, gestational age and season of birth (**Table 4.4**). Stratification of the analyses by season of birth also did not identify any significant associations between *CDKN2A* methylation at birth and bone measures at birth when linear regression analyses were adjusted for sex, gestational age and treatment allocation (**Table 4.5**).

Table 4.3 Associations between *CDKN2A* methylation at birth and bone outcomes at birth in the MAVIDOS trial.

<i>CDKN2A</i> CpG	Total BMC			Total BA			Total BMD			Total scBMC		
	n	B (95 % CI)	p	n	B (95 % CI)	p	n	B (95 % CI)	p	n	B (95 % CI)	p
1	299	0.012 (-0.072, 0.096)	0.785	299	-0.028 (-0.314, 0.258)	0.848	299	6.60×10^{-5} (- 8.67×10^{-5} , 2.19×10^{-4})	0.396	253	0.016 (-0.029, 0.062)	0.485
2	299	0.006 (-0.071, 0.084)	0.871	299	-0.008 (-0.270, 0.253)	0.949	299	2.77×10^{-5} (- 1.17×10^{-4} , 1.72×10^{-4})	0.706	253	0.005 (-0.038, 0.048)	0.819
3	352	0.014 (-0.071, 0.100)	0.743	352	0.046 (-0.241, 0.334)	0.752	352	1.48×10^{-5} (- 1.44×10^{-4} , 1.74×10^{-4})	0.854	302	-0.005 (-0.052, 0.042)	0.832
4	352	-0.036 (-0.142, 0.070)	0.501	352	-0.105 (-0.470, 0.261)	0.574	352	-5.45×10^{-5} (- 2.43×10^{-4} , 1.34×10^{-4})	0.569	302	-0.004 (-0.060, 0.052)	0.883
5	354	-0.031 (-0.133, 0.071)	0.551	354	-0.066 (-0.415, 0.283)	0.710	354	-6.96×10^{-5} (- 2.57×10^{-4} , 1.18×10^{-4})	0.465	303	-0.015 (-0.071, 0.042)	0.613
6	354	-0.006 (-0.104, 0.091)	0.903	354	0.028 (-0.303, 0.359)	0.869	354	-5.48×10^{-5} (- 2.33×10^{-4} , 1.23×10^{-4})	0.546	303	-0.018 (-0.072, 0.036)	0.513
7	329	-0.026 (-0.125, 0.073)	0.603	329	-0.017 (-0.353, 0.319)	0.922	329	-9.00×10^{-5} (- 2.69×10^{-4} , 8.91×10^{-5})	0.324	278	-0.024 (-0.078, 0.031)	0.393
8	343	-0.023 (-0.120, 0.075)	0.645	343	-0.044 (-0.376, 0.288)	0.793	343	-5.14×10^{-5} (- 2.28×10^{-4} , 1.25×10^{-4})	0.566	292	-0.023 (-0.076, 0.029)	0.386
9	344	-0.033 (-0.125, 0.058)	0.475	344	-0.053 (-0.364, 0.257)	0.737	344	-7.11×10^{-5} (- 2.37×10^{-4} , 9.52×10^{-5})	0.401	292	-0.014 (-0.063, 0.035)	0.568

Linear regression analyses adjusted for sex, gestational age, treatment group and season of birth. BMC = bone mineral content, BA = bone area, BMD = bone mineral density and scBMC = size corrected bone mineral content. Neonatal DXA measurements were taken within 14 days of birth.

Table 4.4 Associations between *CDKN2A* CpG methylation at birth and bone outcomes at birth in the MAVIDOS trial when stratified by treatment group.

CHOLECALCIFEROL													
		Total BMC			Total BA			Total BMD			Total scBMC		
<i>CDKN2A</i>	CpG	n	B (95 % CI)	p	n	B (95 % CI)	p	n	B (95 % CI)	p	n	B (95 % CI)	p
	1	149	0.068 (-0.064, 0.200)	0.313	149	0.157 (-0.262, 0.577)	0.459	149	1.40x10 ⁻⁴ (-9.98x10 ⁻⁵ , 3.80x10 ⁻⁴)	0.250	122	0.028 (-0.040, 0.095)	0.419
	2	149	0.054 (-0.064, 0.173)	0.366	149	0.194 (-0.186, 0.574)	0.315	149	5.56x10 ⁻⁴ (-1.60x10 ⁻⁴ , 2.71x10 ⁻⁴)	0.611	122	-0.010 (-0.072, 0.052)	0.753
	3	177	0.038 (-0.097, 0.173)	0.583	177	0.241 (-0.191, 0.673)	0.272	177	-3.22x10 ⁻⁵ (-2.77x10 ⁻⁴ , 2.13x10 ⁻⁴)	0.796	147	-0.037 (-0.107, 0.033)	0.294
	4	177	0.031 (-0.130, 0.192)	0.706	177	0.169 (-0.360, 0.697)	0.529	177	-2.54x10 ⁻⁵ (-3.14x10 ⁻⁴ , 2.63x10 ⁻⁴)	0.863	147	-0.026 (-0.111, 0.059)	0.539
	5	177	0.048 (-0.107, 0.203)	0.543	177	0.209 (-0.295, 0.712)	0.415	177	-3.55x10 ⁻⁶ (-2.87x10 ⁻⁴ , 2.80x10 ⁻⁴)	0.980	147	-0.023 (-0.107, 0.061)	0.589
	6	177	0.044 (-0.112, 0.201)	0.579	177	0.238 (-0.266, 0.743)	0.352	177	-3.59x10 ⁻⁵ (-3.19x10 ⁻⁴ , 2.47x10 ⁻⁴)	0.802	147	-0.043 (-0.127, 0.041)	0.309
	7	165	0.067 (-0.088, 0.222)	0.393	165	0.296 (-0.204, 0.795)	0.244	165	-2.22x10 ⁻⁶ (-2.82x10 ⁻⁴ , 2.77x10 ⁻⁴)	0.988	135	-0.027 (-0.111, 0.058)	0.537
	8	172	0.035 (-0.124, 0.194)	0.666	172	0.142 (-0.370, 0.653)	0.585	172	9.44x10 ⁻⁷ (-2.85x10 ⁻⁴ , 2.87x10 ⁻⁴)	0.995	142	-0.030 (-0.114, 0.053)	0.476
	9	174	0.040 (-0.115, 0.194)	0.615	174	0.254 (-0.242, 0.751)	0.314	174	-3.68x10 ⁻⁵ (-3.15x10 ⁻⁴ , 2.41x10 ⁻⁴)	0.794	143	-0.018 (-0.097, 0.062)	0.659
PLACEBO													
		Total BMC			Total BA			Total BMD			Total scBMC		
<i>CDKN2A</i>	CpG	n	B (95 % CI)	p	n	B (95 % CI)	p	n	B (95 % CI)	p	n	B (95 % CI)	p
	1	149	-0.022 (-0.130, 0.087)	0.691	149	-0.129 (-0.526, 0.268)	0.522	149	1.65x10 ⁻⁵ (-1.81x10 ⁻⁴ , 2.14x10 ⁻⁴)	0.869	130	0.005 (-0.059, 0.068)	0.883
	2	149	-0.017 (-0.121, 0.087)	0.743	149	-0.130 (-0.496, 0.235)	0.482	149	3.27x10 ⁻⁵ (-1.66x10 ⁻⁴ , 2.31x10 ⁻⁴)	0.746	130	0.020 (-0.042, 0.081)	0.527
	3	174	0.018 (-0.093, 0.130)	0.747	174	-0.045 (-0.439, 0.349)	0.823	174	9.12x10 ⁻⁵ (-1.22x10 ⁻⁴ , 3.04x10 ⁻⁴)	0.399	154	0.024 (-0.043, 0.090)	0.483
	4	174	-0.077 (-0.220, 0.066)	0.287	174	-0.287 (-0.805, 0.231)	0.276	174	-5.05x10 ⁻⁵ (-3.04x10 ⁻⁴ , 2.03x10 ⁻⁴)	0.694	154	0.014 (-0.064, 0.092)	0.730
	5	176	-0.082 (-0.219, 0.056)	0.243	176	-0.243 (-0.736, 0.250)	0.332	176	-1.01x10 ⁻⁴ (-3.55x10 ⁻⁴ , 1.54x10 ⁻⁴)	0.435	155	-0.009 (-0.088, 0.071)	0.830
	6	176	-0.023 (-0.148, 0.103)	0.724	176	-0.073 (-0.525, 0.378)	0.749	176	-3.31x10 ⁻⁵ (-2.68x10 ⁻⁴ , 2.02x10 ⁻⁴)	0.781	155	0.000 (-0.072, 0.073)	0.990
	7	163	-0.086 (-0.214, 0.042)	0.184	163	-0.217 (-0.678, 0.243)	0.353	163	-1.40x10 ⁻⁴ (-3.76x10 ⁻⁴ , 9.56x10 ⁻⁵)	0.242	142	-0.023 (-0.096, 0.050)	0.538
	8	170	-0.051 (-0.173, 0.072)	0.415	170	-0.137 (-0.581, 0.306)	0.542	170	-6.73x10 ⁻⁵ (-2.91x10 ⁻⁴ , 1.57x10 ⁻⁴)	0.554	149	-0.019 (-0.089, 0.050)	0.588
	9	169	-0.070 (-0.182, 0.042)	0.218	169	-0.220 (-0.623, 0.183)	0.282	169	-7.50x10 ⁻⁵ (-2.82x10 ⁻⁴ , 1.32x10 ⁻⁴)	0.476	148	-0.012 (-0.076, 0.052)	0.721

Linear regression analyses adjusted for sex, gestational age and season of birth. BMC = bone mineral content, BA = bone area, BMD = bone mineral density and scBMC = size corrected bone mineral content. Neonatal DXA measurements were taken within 14 days of birth.

Table 4.5 Associations between *CDKN2A* CpG methylation at birth and bone outcomes at birth in the MAVIDOS trial when stratified by season of birth.

WINTER												
CDKN2A CpG	Total BMC			Total BA			Total BMD			Total scBMC		
	n	B (95 % CI)	p	n	B (95 % CI)	p	n	B (95 % CI)	p	n	B (95 % CI)	p
1	51	0.011 (-0.172, 0.194)	0.902	51	0.149 (-0.524, 0.822)	0.659	51	-5.04x10 ⁻⁵ (-4.42x10 ⁻⁴ , 3.41x10 ⁻⁴)	0.797	41	-0.013 (-0.153, 0.127)	0.852
2	51	0.020 (-0.133, 0.172)	0.798	51	0.165 (-0.376, 0.706)	0.545	51	-5.25x10 ⁻⁵ (-3.92x10 ⁻⁴ , 2.87x10 ⁻⁴)	0.758	41	-0.008 (-0.124, 0.108)	0.891
3	61	-0.013 (-0.169, 0.143)	0.869	51	0.114 (-0.440, 0.667)	0.683	61	-1.28x10 ⁻⁴ (-4.72x10 ⁻⁴ , 2.17x10 ⁻⁴)	0.462	49	-0.020 (-0.139, 0.100)	0.743
4	61	-0.126 (-0.380, 0.127)	0.321	61	-0.150 (-0.997, 0.697)	0.723	61	-3.41x10 ⁻⁴ (-8.66x10 ⁻⁴ , 1.85x10 ⁻⁴)	0.199	49	-0.068 (-0.239, 0.103)	0.427
5	61	-0.086 (-0.340, 0.168)	0.499	61	-0.211 (-1.062, 0.640)	0.621	61	-1.54x10 ⁻⁴ (-6.85x10 ⁻⁴ , 3.77x10 ⁻⁴)	0.563	49	-0.006 (-0.189, 0.176)	0.944
6	61	-0.030 (-0.246, 0.185)	0.780	61	0.004 (-0.718, 0.726)	0.991	61	-1.12x10 ⁻⁴ (-5.62x10 ⁻⁴ , 3.38x10 ⁻⁴)	0.619	49	-0.026 (-0.179, 0.126)	0.729
7	54	-0.055 (-0.271, 0.162)	0.615	54	-0.037 (-0.764, 0.691)	0.920	54	-1.71x10 ⁻⁴ (-6.23x10 ⁻⁴ , 2.81x10 ⁻⁴)	0.451	43	-0.044 (-0.198, 0.110)	0.567
8	36	-0.077 (-0.309, 0.155)	0.509	56	-0.043 (-0.833, 0.746)	0.912	56	-2.51x10 ⁻⁴ (-7.21x10 ⁻⁴ , 2.18x10 ⁻⁴)	0.287	45	-0.070 (-0.224, 0.083)	0.361
9	56	-0.019 (-0.219, 0.181)	0.850	56	-0.051 (-0.721, 0.618)	0.879	56	-3.25x10 ⁻⁵ (-4.58x10 ⁻⁴ , 3.93x10 ⁻⁴)	0.879	45	-0.002 (-0.147, 0.143)	0.978
SPRING												
CDKN2A CpG	Total BMC			Total BA			Total BMD			Total scBMC		
	n	B (95 % CI)	p	n	B (95 % CI)	p	n	B (95 % CI)	p	n	B (95 % CI)	p
1	77	-0.083 (-0.280, 0.114)	0.405	77	-0.386 (-1.057, 0.285)	0.256	77	-3.35x10 ⁻⁶ (-3.03x10 ⁻⁴ , 3.09x10 ⁻⁴)	0.983	65	-0.006 (-0.093, 0.082)	0.900
2	77	-0.090 (-0.266, 0.085)	0.307	77	-0.364 (-0.983, 0.255)	0.246	77	-6.66x10 ⁻⁵ (-3.41x10 ⁻⁴ , 2.07x10 ⁻⁴)	0.630	65	-0.045 (-0.126, 0.035)	0.267
3	90	-0.084 (-0.279, 0.112)	0.398	90	-0.308 (-1.002, 0.385)	0.380	90	-7.06x10 ⁻⁵ (-3.76x10 ⁻⁴ , 2.35x10 ⁻⁴)	0.647	78	-0.035 (-0.122, 0.051)	0.420
4	90	-0.118 (-0.370, 0.133)	0.353	90	-0.404 (-1.311, 0.503)	0.378	90	-1.65x10 ⁻⁴ (-5.46x10 ⁻⁴ , 2.16x10 ⁻⁴)	0.391	78	-0.086 (-0.198, 0.026)	0.128
5	90	-0.023 (-0.241, 0.196)	0.837	90	-0.243 (-1.025, 0.540)	0.539	90	-5.70x10 ⁻⁵ (-2.84x10 ⁻⁴ , 3.98x10 ⁻⁴)	0.740	78	-0.029 (-0.129, 0.071)	0.568
6	90	-0.068 (-0.286, 0.150)	0.535	90	-0.258 (-1.027, 0.511)	0.507	90	-8.86x10 ⁻⁵ (-4.27x10 ⁻⁴ , 2.50x10 ⁻⁴)	0.604	78	-0.058 (-0.154, 0.039)	0.236
7	82	-0.016 (-0.236, 0.204)	0.885	82	-0.165 (-0.941, 0.611)	0.674	82	-5.09x10 ⁻⁶ (-3.46x10 ⁻⁴ , 3.36x10 ⁻⁴)	0.976	70	-0.036 (-0.135, 0.062)	0.465
8	87	-0.109 (-0.327, 0.110)	0.325	87	-0.447 (-1.223, 0.329)	0.255	87	-8.64x10 ⁻⁵ (-4.23x10 ⁻⁴ , 2.50x10 ⁻⁴)	0.611	75	-0.046 (-0.144, 0.052)	0.351
9	89	-0.133 (-0.353, 0.088)	0.235	89	-0.457 (-1.244, 0.329)	0.251	89	-1.46x10 ⁻⁴ (-4.82x10 ⁻⁴ , 1.91x10 ⁻⁴)	0.392	76	-0.020 (-0.114, 0.074)	0.671
SUMMER												
CDKN2A CpG	Total BMC			Total BA			Total BMD			Total scBMC		
	n	B (95 % CI)	p	n	B (95 % CI)	p	n	B (95 % CI)	p	n	B (95 % CI)	p
1	83	0.021 (-0.142, 0.184)	0.795	83	0.050 (-0.483, 0.583)	0.852	83	-4.91x10 ⁻⁵ (-2.54x10 ⁻⁴ , 3.52x10 ⁻⁴)	0.748	74	0.062 (-0.018, 0.141)	0.126
2	83	0.052 (-0.108, 0.211)	0.524	83	0.369 (-0.134, 0.872)	0.148	83	-5.13x10 ⁻⁵ (-3.42x10 ⁻⁴ , 2.39x10 ⁻⁴)	0.726	74	-0.001 (-0.076, 0.074)	0.972
3	95	0.078 (-0.110, 0.265)	0.412	95	0.392 (-0.201, 0.984)	0.193	95	-3.12x10 ⁻⁵ (-3.09x10 ⁻⁴ , 3.71x10 ⁻⁴)	0.856	86	0.009 (-0.079, 0.097)	0.839
4	95	-0.045 (-0.273, 0.184)	0.700	95	0.200 (-0.562, 0.962)	0.603	95	-2.51x10 ⁻⁴ (-6.62x10 ⁻⁴ , 1.59x10 ⁻⁴)	0.227	86	-0.004 (-0.117, 0.109)	0.941
5	96	-0.040 (-0.247, 0.167)	0.701	96	0.248 (-0.436, 0.933)	0.473	96	-2.93x10 ⁻⁴ (-6.65x10 ⁻⁴ , 7.92x10 ⁻⁵)	0.121	86	-0.024 (-0.126, 0.078)	0.648
6	96	-0.002 (-0.213, 0.209)	0.987	96	0.331 (-0.366, 1.027)	0.348	96	-2.02x10 ⁻⁴ (-5.84x10 ⁻⁴ , 1.79x10 ⁻⁴)	0.295	86	-0.007 (-0.111, 0.098)	0.900
7	93	-0.079 (-0.286, 0.128)	0.449	93	0.147 (-0.541, 0.836)	0.672	93	-3.29x10 ⁻⁴ (-6.93x10 ⁻⁴ , 3.40x10 ⁻⁵)	0.075	82	-0.035 (-0.138, 0.068)	0.506
8	95	0.030 (-0.167, 0.227)	0.766	95	0.476 (-0.173, 1.125)	0.148	95	-1.98x10 ⁻⁴ (-5.49x10 ⁻⁴ , 1.53x10 ⁻⁴)	0.266	84	-0.046 (-0.141, 0.050)	0.346
9	95	-0.017 (-0.205, 0.172)	0.862	95	0.300 (-0.322, 0.923)	0.340	95	-2.19x10 ⁻⁴ (-5.53x10 ⁻⁴ , 1.15x10 ⁻⁴)	0.196	84	-0.026 (-0.116, 0.065)	0.575
AUTUMN												
CDKN2A CpG	Total BMC			Total BA			Total BMD			Total scBMC		
	n	B (95 % CI)	p	n	B (95 % CI)	p	n	B (95 % CI)	p	n	B (95 % CI)	p
1	85	0.060 (-0.089, 0.209)	0.425	85	0.102 (-0.411, 0.614)	0.695	85	1.38x10 ⁻⁴ (-1.45x10 ⁻⁴ , 4.21x10 ⁻⁴)	0.335	70	-0.002 (-0.089, 0.086)	0.969
2	85	0.053 (-0.092, 0.198)	0.471	85	-0.101 (-0.580, 0.378)	0.677	85	2.42x10 ⁻⁴ (-4.58x10 ⁻⁵ , 5.30x10 ⁻⁴)	0.098	70	0.055 (-0.036, 0.147)	0.234
3	103	0.079 (-0.079, 0.237)	0.325	103	0.059 (-0.468, 0.585)	0.825	103	2.04x10 ⁻⁴ (-1.13x10 ⁻⁴ , 5.21x10 ⁻⁴)	0.205	86	0.031 (-0.070, 0.131)	0.548
4	103	0.064 (-0.100, 0.228)	0.440	103	-0.035 (-0.597, 0.528)	0.902	103	2.50x10 ⁻⁴ (-5.01x10 ⁻⁵ , 5.51x10 ⁻⁴)	0.101	86	0.052 (-0.043, 0.147)	0.275
5	104	0.001 (-0.178, 0.179)	0.995	104	-0.070 (-0.664, 0.523)	0.814	104	5.01x10 ⁻⁵ (-3.04x10 ⁻⁴ , 4.04x10 ⁻⁴)	0.780	87	-0.005 (-0.118, 0.107)	0.925
6	104	0.075 (-0.088, 0.237)	0.364	104	0.109 (-0.434, 0.653)	0.690	104	1.50x10 ⁻⁴ (-1.81x10 ⁻⁴ , 4.81x10 ⁻⁴)	0.371	87	0.012 (-0.094, 0.117)	0.824
7	97	0.033 (-0.137, 0.203)	0.701	97	0.011 (-0.559, 0.580)	0.971	97	9.12x10 ⁻⁵ (-2.47x10 ⁻⁴ , 4.30x10 ⁻⁴)	0.594	80	0.007 (-0.100, 0.113)	0.900
8	102	0.035 (-0.129, 0.199)	0.672	102	-0.114 (-0.660, 0.433)	0.681	102	1.92x10 ⁻⁴ (-1.32x10 ⁻⁴ , 5.16x10 ⁻⁴)	0.242	85	0.033 (-0.071, 0.137)	0.529
9	101	0.000 (-0.151, 0.151)	0.996	101	-0.090 (-0.593, 0.414)	0.725	101	6.13x10 ⁻⁵ (-2.39x10 ⁻⁴ , 3.62x10 ⁻⁴)	0.686	84	-0.003 (-0.098, 0.091)	0.944

Linear regression analyses adjusted for sex, gestational age and treatment group. BMC = bone mineral content, BA = bone area, BMD = bone mineral density and scBMC = size corrected bone mineral content. Neonatal DXA measurements were taken within 14 days of birth. Seasons are defined as winter (December to February), spring (March to May), summer (June to August) and autumn (September to November).

4.3 Discussion

Maternal vitamin D status has been linked to fetal skeletal development^{231,232,236} and studies within the SWS cohort have identified CpG methylation of *CDKN2A* as a candidate biomarker that is predictive of bone health in childhood³²³. Within the MAVIDOS trial, a vitamin D intervention trial during pregnancy, infants born to cholecalciferol supplemented mothers had higher cord *CDKN2A* CpG methylation compared to the placebo group and there were seasonal differences in cord *CDKN2A* CpG methylation between the two treatment groups. There were no significant associations between *CDKN2A* CpG methylation at birth and bone measures at birth however, it would be interesting to investigate associations with bone measurements made during childhood as this data becomes available.

The early life environment is thought to influence the epigenome, with these changes associated with disease risk in later life³⁷². Within the MAVIDOS trial, infants born to cholecalciferol supplemented mothers had higher *CDKN2A* CpG 9 methylation at birth compared to the placebo group. The *CDKN2A* DMR is located 625 bp downstream of the *CDKN2A* transcriptional start site, within the first intron. *CDKN2A* plays an important role in progression through the cell cycle by encoding p16^{INK4a} which inhibits the action of CDK4/6 (Error! Reference source not found.). During cell cycle arrest and cell differentiation, retinoblastoma (Rb) is bound to E2F and prevents cell cycle progression. Moreover, Rb has been shown to act as a transcriptional coactivator of *Runx2*, which plays an important role in osteoblast differentiation³⁷¹. Phosphorylation of Rb by CDK4/6 results in the disassociation of Rb and E2F allowing cell cycle progression and cellular proliferation.

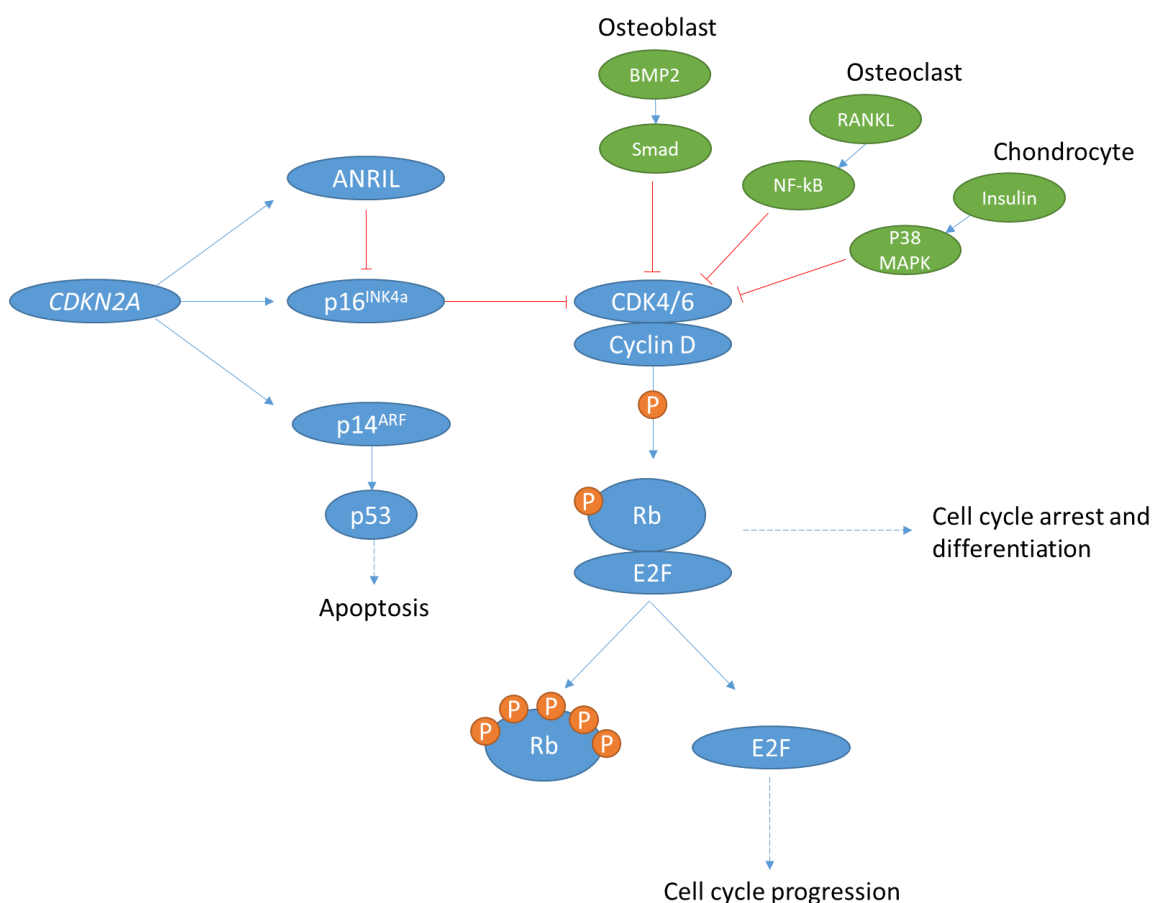


Figure 4.4 Schematic of *CDKN2A* and cell cycle progression.

Adapted from VanArsdale et al³⁷³ and Ogosawara et al³⁷¹. *CDKN2A* = cyclin dependent kinase inhibitor 2A, ANRIL = antisense non-coding RNA in the *INK4* locus, CDK4/6 = cyclin dependent kinase 4/6, Rb = retinoblastoma, BMP2 = bone morphogenetic protein 2, RANKL = receptor activator of nuclear factor kappa-B ligand, NF-kB = nuclear factor kappa-light-chain-enhancer of activated B cells, MAPK = mitogen activated protein kinases.

An increase in vitamin D during the early life environment could be linked with an increase in *CDKN2A* methylation and a decrease in *CDKN2A* expression, resulting in decreased production of p14^{ARF} and p16^{INK4a}. Attenuated expression of p16^{INK4a} would result in decreased inhibition of CDK4/6, which would result in phosphorylation of Rb, cell cycle progression and cell proliferation. This could result in an increase in proliferation of osteoblasts, osteoclasts and chondrocytes precursor cells. As part of a compensatory mechanism, signalling pathways related to these cells may inhibit CDK6 expression and result in differentiation of these cell types which can have a positive effect on bone formation and remodelling and decrease the risk of developing osteoporosis. Vitamin D supplementation during the early life environment could be linked to

increased proliferation and differentiation of key cells involved in maintaining healthy bones and optimal bone mineral density.

The CpGs of interest are located within the *ANRIL* promoter, and functional work by Lillycrop *et al.*, has shown that alteration of individual CpG dinucleotides within this DMR decreases promoter expression in a liposarcoma cell line³²². This demonstrates the direct functional importance of these CpG sites on local gene expression, and, if DNA methylation of these CpG sites were to have a similar effect to the findings by Lillycrop *et al.*³²² then an increase in methylation of these CpG loci within the *ANRIL* promoter would be coupled with a decrease in *ANRIL* expression and a decrease in inhibition of p16^{INK4a}. This would allow inhibition of CDK4/6 resulting in cell cycle arrest and differentiation and maintenance of the balance between cell proliferation and cell differentiation. Furthermore, signalling pathways related to osteoblasts, osteoclasts and chondrocytes have been shown to downregulate CDK6 expression resulting in cell cycle arrest and differentiation of cells into osteoblasts, osteoclasts and chondrocytes³⁷¹. It is also possible that DNA methylation of *CDKN2A* may not lie on the causal pathways, but rather acts as a biomarker for pre-natal vitamin D exposure. For instance, an increase in vitamin D could have downstream effects which result in an increase in differentiation of osteoblasts, osteoclasts and chondrocytes. Coupled with an increase in differentiation there is reciprocal downregulation of CDK6 through their respective signalling pathways therefore, the need for a CDK6 inhibitor decreases and this is consolidated through increased *CDKN2A* methylation.

Within the MAVIDOS trial, infants born in autumn to cholecalciferol supplemented mothers had higher methylation at *CDKN2A* CpGs 5-7 compared to the placebo group but there were no significant differences amongst infants born in the winter, spring or summer months. Mothers that give birth during autumn have increased sunlight in the second and third trimesters leading to increased vitamin D synthesis in the skin. Together with maternal vitamin D supplementation, this would result in increased maternal serum 25(OH)D₃ during pregnancy and increased transfer across the placenta to the developing fetus. It is possible that this increased transfer across the placenta, due to both supplementation and increased sunlight exposure, could result in an increase in *CDKN2A* methylation which is not observed in other months. This suggests that *CDKN2A* methylation at birth is influenced by maternal vitamin D supplementation and seasonal UVB exposure and supports the use of *CDKN2A* as a biomarker for early life vitamin D intervention studies.

Studies within the SWS cohort have shown an inverse association between methylation at birth of *CDKN2A* CpG clusters 3, 4-7, and 8-9 and bone measures at 4 and 6 years of age³²³. However, within the MAVIDOS trial, we did not find that *CDKN2A* CpG methylation at birth was associated with bone

measures at birth with intervention as a factor. It would be interesting to determine whether there are any associations at 4 and 6 years of age. Despite the differences in *CDKN2A* methylation between the maternal treatment groups, and increased bone measures amongst infants born in winter to cholecalciferol supplemented mothers²³⁶, there were no significant associations between *CDKN2A* methylation and neonatal bone measures within each treatment group, or within each season of birth. This could be due to a lack of power associated with a lower sample number. *CDKN2A* methylation at birth may reflect the setting of the bone trajectory such that differences may become apparent during later childhood. Within the MAVIDOS trial we have shown that infants born to cholecalciferol supplemented mothers had higher *CDKN2A* methylation at birth compared to the placebo group. This would suggest a negative impact of maternal vitamin D supplementation on bone measures in later childhood as an increase in *CDKN2A* methylation within the cholecalciferol supplemented group would be linked to a decrease in bone health in childhood. It would be interesting to determine whether there are any associations in later childhood and if so, the direction of the significant associations.

There are limitations to these experiments. First, DNA methylation was measured in umbilical cord tissue rather than a tissue central to the pathogenesis of osteoporosis, such as bone tissue, however this is not feasible. DNA methylation patterns can be tissue specific and a study found that DNA methylation differed in hematopoietic stem cells derived from cord blood, peripheral blood and bone marrow³⁷⁴. However, studies within the SWS cohort have found DNA methylation in umbilical cord tissue to be predictive of later bone health. To investigate this further, DNA methylation could be measured in additional tissue types such as cord blood or placental tissue. Second, umbilical cord tissue is a heterogeneous cell population and different samples may have been made up of differing composition of cell types. To overcome this, individual samples should be corrected for cell type composition however, these data are not yet unavailable.

In conclusion, within the MAVIDOS trial, maternal cholecalciferol supplementation during pregnancy and season of birth were shown to influence methylation of the *CDKN2A* DMR at birth compared to the placebo group. This suggests that there is a link between maternal vitamin D status, season of birth and *CDKN2A* methylation at birth, however this needs to be investigated further. Studies within the SWS cohort have found an inverse association between *CDKN2A* CpG methylation at birth and bone measures at 4 and 6 years of age³²³. Within the MAVIDOS trial, there were no significant associations between *CDKN2A* methylation at birth and bone measures at birth with intervention as a covariate however, it would be interesting to determine any associations at 4 and 6 years of age when this data becomes available. If methylation of *CDKN2A* is predictive of bone measures in childhood, and maternal vitamin D supplementation is linked to altered DNA methylation, this may highlight a suitable intervention during pregnancy which could improve bone

Chapter 4

measures during childhood and may play a role in delaying the onset of osteoporosis in later life. In **Chapter 3** and **Chapter 4**, the use of *RXR α* and *CDKN2A* as candidate biomarkers have been assessed within the MAVIDOS trial and the results showed that there is altered DNA methylation in response to maternal cholecalciferol supplementation nonetheless, there are no associations between DNA methylation and bone measures made at birth. To further investigate whether there is a link between maternal cholecalciferol supplementation, DNA methylation and fetal skeletal development, DNA methylation of two transcription factors directly involved in bone formation were investigated in **Chapter 5**.

Chapter 5 Maternal vitamin D supplementation during pregnancy alters DNA methylation of transcription factors involved in osteoblast differentiation within the MAVIDOS trial

5.1 Introduction

Studies within the Southampton Women's Survey (SWS) cohort have identified two candidate biomarkers, DNA methylation of *RXRA*³²¹ and *CDKN2A*³²³, which have been shown to be inversely related to bone health in later childhood. Within the previous two chapters we have shown that maternal vitamin D supplementation is linked to decreased *RXRA* methylation and increased *CDKN2A* methylation in umbilical cord tissue. Nonetheless, methylation of both genes were not associated with bone measures at birth with intervention as a covariate. To identify further epigenetic biomarkers, DNA methylation of *Runx2* and *Osterix*, which are two transcription factors directly involved in osteoblast differentiation and play a pivotal role in bone development³⁷⁵, were investigated.

Runx2 is involved in bone formation and chondrocyte maturation³⁷⁶ and has been shown to act upstream of *Osterix*⁷⁴ which plays a key role in regulating the differentiation of osteoblast progenitor cells to mature osteoblasts⁷⁰. *In vitro* studies in mesenchymal stem cells (MSCs) have shown that during osteoblast differentiation there is upregulation of *Runx2* and *Osterix* expression³⁷⁷. Vitamin D as well as other cytokines, growth factors and hormones have been shown to be involved in the regulation of *Runx2* gene expression and protein function^{49,378}. Studies in mice have provided evidence on the importance of *Runx2* and *Osterix* in bone formation and both *Runx2* and *Osterix* null mice have shown that both the intramembranous and endochondral ossification pathways were affected^{66,74}.

In this chapter, we will determine whether maternal cholecalciferol supplementation during pregnancy alters DNA methylation within the promoters of *Runx2* and *Osterix*. Furthermore, we will explore whether DNA methylation of *Runx2* and *Osterix* is associated with bone measures at birth and provide insight into their potential use as a biomarker.

5.1.1 Hypothesis

We hypothesise that maternal cholecalciferol supplementation during pregnancy will be associated with decreased methylation of individual CpG loci upstream of the *Runx2* and *Osterix* transcriptional start site (TSS) in umbilical cord tissue and that methylation of these two transcription factors, which are associated with osteoblast differentiation, will be inversely associated with bone measures at birth.

5.1.2 Aims

1. To determine whether maternal vitamin D supplementation during pregnancy alters *Runx2* and *Osterix* CpG methylation at birth in umbilical cord within the MAVIDOS trial
2. To determine whether CpG methylation at birth of *Runx2* and *Osterix* is associated with bone measures at birth within the MAVIDOS trial

5.1.3 Methods

DNA methylation of CpG sites upstream of the *Runx2* and *Osterix* TSS (**Figure 5.1**) was measured in DNA samples extracted from the umbilical cord of 449 infants from the MAVIDOS trial. Full materials and methods for this chapter are described in **Sections 2.2.2, 2.2.4 and Error! Reference source not found.** Briefly, pregnant mothers received either 1000 IU/d cholecalciferol or a placebo daily from 14 weeks of gestation up until birth as part of a double blind, randomised, placebo controlled trial which took place in Southampton, Oxford and Sheffield. Umbilical cords were collected at birth from 449 mothers which delivered their baby in Southampton. DNA was extracted from these umbilical cords and DNA methylation of individual CpG sites within these genes of interest were measured using bisulfite pyrosequencing. Primers were designed within the promoter region of each gene, in CpG shores where methylation is often associated with tissue specific methylation and transcriptional repression²⁵⁹.

Statistical tests were carried out in IBM SPSS Statistics 24 and histograms were used to confirm normality. To determine whether maternal cholecalciferol supplementation during pregnancy alters *Runx2* CpG methylation in umbilical cord, independent t-tests compared *Runx2* CpG methylation at birth between the 1000 IU/d cholecalciferol supplemented group and the placebo group using the data as a whole, and when stratified by season of birth (**Section 5.2.2.1**). Similar analyses using *Osterix* DNA methylation data can be seen in **Section 5.2.3.1**. To determine whether there were any associations between *Runx2* methylation in umbilical cord tissue and bone measures at birth linear regression analyses were adjusted for sex, gestational age, treatment allocation and season of birth. To determine whether there were associations within each treatment group, or within each season, the data were stratified by treatment allocation or season of birth respectively prior to linear regression analyses (**Section 5.2.2.2**). Similar analyses using *Osterix* methylation data can be seen in **Section 5.2.3.2**.

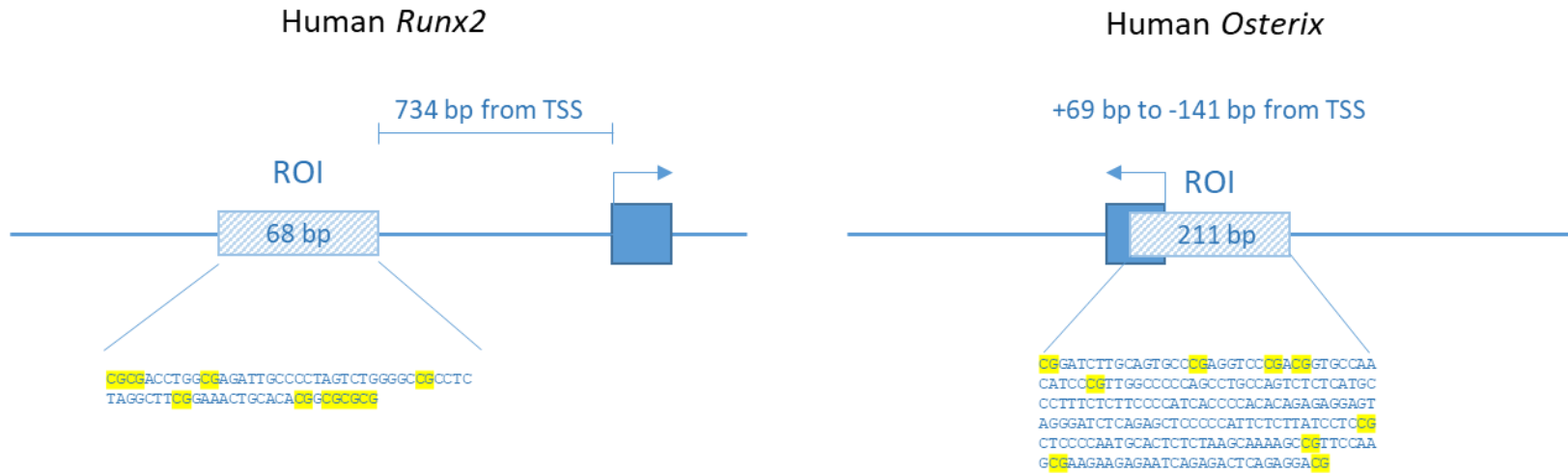


Figure 5.1 Schematic of the *Runx2* and *Osterix* locus and the location of the CpGs of interest.

Figure not to scale. ROI = region of interest, TSS = transcriptional start site. CpGs of interest are highlighted in yellow.

5.2 Results

5.2.1 Selection of the regions of interest upstream of the *Runx2* and *Osterix* transcriptional start sites

Regions of interest were manually selected based on *in silico* evidence compiled from www.ensembl.org and genome.ucsc.edu. For both genes, the transcriptional start site, promoter region, location of CpG islands and DNase 1 hypersensitive regions were mapped onto the respective genomic DNA sequences. This provided regions to avoid, such as CpG islands where CpG loci are often unmethylated in expressed genes, and provided regions of interest such as CpG shores where methylation is often associated with tissue specific methylation and transcriptional repression²⁵⁹, and DNase 1 hypersensitive sites which are thought to have a regulatory role in gene transcription. Therefore, primers were designed within the promoter region of both genes based on these parameters.

5.2.2 Investigation into *Runx2* CpG methylation as an epigenetic biomarker of bone health

5.2.2.1 Maternal cholecalciferol supplementation and season of birth are associated with altered *Runx2* CpG methylation at birth within the MAVIDOS trial

The results showed that there were no significant differences in *Runx2* methylation at birth between the two maternal treatment groups (**Table 5.1**).

Amongst all four seasons, there were no significant differences in *Runx2* methylation at birth between the two maternal treatment groups (**Table 5.2**).

Table 5.1 Differences in *Runx2* CpG methylation at birth between the treatment groups within the MAVIDOS trial.

<i>Runx2</i> CpG	n	Mean difference (%)	(95 % CI)	p
1	210	-0.1	(-0.321, 0.193)	0.623
2	205	0.0	(-0.215, 0.243)	0.904
3	279	0.1	(-0.114, 0.387)	0.285
4	281	0.2	(-0.046, 0.423)	0.114
5	258	0.0	(-0.172, 0.232)	0.772
6	158	0.0	(-0.231, 0.140)	0.626
7	95	-0.1	(-0.274, 0.065)	0.222
8	145	0.0	(-0.181, 0.127)	0.726
9	104	0.0	(-0.237, 0.165)	0.725

Independent t-tests compared *Runx2* methylation between the cholecalciferol supplemented and placebo group within the MAVIDOS trial.

Table 5.2 Differences in *Runx2* methylation between treatment groups in the MAVIDOS trial when stratified by season of birth.

<i>Runx2</i> CpG	Winter				Spring				Summer				Autumn			
	n	Mean diff. (%)	(95 % CI)	p	n	Mean diff. (%)	(95 % CI)	p	n	Mean diff. (%)	(95 % CI)	p	n	Mean diff. (%)	(95 % CI)	p
1	28	-0.3	(-1.218, 0.617)	0.506	42	-0.4	(-1.018, 0.170)	0.157	54	0.4	(-0.090, 0.916)	0.105	83	-0.2	(-0.549, 0.218)	0.394
2	47	0.1	(-0.476, 0.637)	0.771	52	-0.1	(-0.630, 0.355)	0.577	60	0.0	(-0.299, 0.374)	0.825	44	0.1	(-0.507, 0.621)	0.839
3	51	0.2	(-0.308, 0.747)	0.407	66	-0.1	(-0.549, 0.431)	0.810	78	0.2	(-0.276, 0.730)	0.372	83	0.2	(-0.307, 0.643)	0.484
4	47	0.5	(-0.119, 1.086)	0.112	69	0.0	(-0.422, 0.522)	0.834	83	0.0	(-0.455, 0.396)	0.890	78	0.3	(-0.119, 0.811)	0.142
5	43	0.0	(-0.522, 0.425)	0.839	61	0.0	(-0.463, 0.396)	0.876	75	0.2	(-0.159, 0.592)	0.255	76	-0.1	(-0.468, 0.312)	0.692
6	23	0.3	(-0.174, 0.707)	0.222	32	-0.1	(-0.472, 0.314)	0.685	46	0.1	(-0.213, 0.492)	0.430	54	-0.3	(-0.668, 0.035)	0.077
7	11	-0.2	(-0.621, 0.232)	0.330	25	0.1	(-0.066, 0.254)	0.236	25	0.0	(-0.303, 0.215)	0.728	34	-0.3	(-0.698, 0.086)	0.122
8	31	-0.3	(-0.595, 0.053)	0.097	43	0.1	(-0.225, 0.503)	0.445	40	-0.1	(-0.369, 0.195)	0.538	28	0.1	(-0.139, 0.412)	0.318
9	20	0.0	(-0.391, 0.387)	0.992	18	0.2	(-0.802, 1.234)	0.623	33	0.0	(-0.423, 0.332)	0.808	31	-0.2	(-0.563, 0.256)	0.443

Independent t-tests compared *Runx2* methylation between the cholecalciferol supplemented and placebo group within the MAVIDOS trial. Seasons are defined as winter (December to February), spring (March to May), summer (June to August) and winter (September to November).

5.2.2.2 Amongst infants born in winter, *Runx2* CpG methylation at birth was associated with bone measures at birth

The results showed that CpG 4 methylation was positively associated with BMC ($b = 1.290$ (95 % CI: 0.13, 2.45), $p = 0.030$) and BMD at birth ($b = 0.002$, (95 % CI: 0.000, 0.004), $p = 0.043$) when linear regressions were adjusted for sex, gestational age, treatment allocation and season of birth (**Table 5.3**). Methylation at CpG 6 was inversely associated with BMD at birth ($b = -0.005$ (95 % CI: -0.010, 0.000), $p = 0.046$) and methylation at CpG 9 was positively associated with BMC at birth ($b = 4.077$ (95 % CI: 0.13, 8.02), $p = 0.043$) and inversely associated with BMD at birth ($b = 14.343$ (95 % CI: 1.44, 27.25), $p = 0.030$). There were no significant associations between *Runx2* methylation at birth and scBMC at birth (**Table 5.3**).

Within the placebo group methylation at CpG 6 was inversely associated with BMC at birth ($b = -3.871$, (95 % CI: -6.86, -0.88), $p = 0.012$) and BMD at birth ($b = -0.008$ (95 % CI: -0.015, -0.001), $p = 0.026$) (**Table 5.4**). There was a positive association between CpG 9 methylation and BA at birth ($b = 17.091$ (95 % CI: 0.58, 33.60), $p = 0.043$) and there were no significant associations between *Runx2* methylation at birth and scBMC at birth when linear regression analyses were adjusted for sex, gestational age and season of birth. Within the cholecalciferol supplemented group, there were no significant associations between *Runx2* methylation at birth and BMC, BA, BMD or scBMC at birth. There was a trend towards a positive association between CpG 4 and BMD at birth however this did not reach statistical significance ($b = 0.003$ (95 % CI: 0.000, 0.005), $p = 0.058$) (**Table 5.4**).

Amongst infants born in the winter months there was a positive association between CpG 9 methylation and BMD at birth ($b = 0.025$ (95 % CI: 0.000, 0.049), $p = 0.047$) however there were no significant associations between *Runx2* methylation at birth and BMC, BA or scBMC at birth when adjusted for sex, gestational age and treatment allocation (**Table 5.5**). Amongst infants born in the spring months, methylation of CpG 4 was positively associated with BMC ($b = 2.459$ (95 % CI: 0.08, 4.84), $p = 0.043$) and BMD at birth ($b = 0.004$ (95 % CI: 0.000, 0.008), $p = 0.042$) and methylation of CpG 9 was positively associated with BA at birth ($b = 26.529$ (95 % CI: 3.81, 49.25), $p = 0.026$). There were no significant associations between *Runx2* methylation at birth and scBMC at birth. Amongst infants born in the summer months, CpG 1 methylation was inversely associated with BMD at birth ($b = -0.007$ (95 % CI: -0.014, -0.001), $p = 0.021$) whereas CpG 2 methylation was positively associated with BMD at birth ($b = 8.28 \times 10^{-3}$ (95 % CI: 2.85×10^{-4} , 1.63×10^{-3}), $p = 0.043$). There were no significant associations between *Runx2* methylation at birth and BMC, BA or scBMC at birth (**Table 5.5**).

Table 5.3 Associations between *Runx2* methylation at birth and bone outcomes at birth in the MAVIDOS trial.

<i>Runx2</i> CpG	Total BMC			Total BA			Total BMD			Total scBMC		
	n	B (95 % CI)	p	n	B (95 % CI)	p	n	B (95 % CI)	p	n	B (95 % CI)	p
1	178	-0.566 (-1.900, 0.768)	0.404	178	0.510 (-4.032, 5.052)	0.825	178	-2.24x10 ⁻³ (-4.92x10 ⁻³ , 4.46x10 ⁻⁴)	0.102	154	-0.537 (-1.345, 0.271)	0.191
2	164	0.845 (-0.984, 2.675)	0.363	134	1.896 (-4.441, 8.232)	0.555	164	1.13x10 ⁻³ (-2.18x10 ⁻³ , 4.50x10 ⁻³)	0.494	135	0.579 (-0.404, 1.562)	0.246
3	239	-0.252 (-1.374, 0.870)	0.658	239	-1.134 (-4.854, 2.586)	0.549	239	-7.13x10 ⁻⁵ (-2.20x10 ⁻³ , 2.06x10 ⁻³)	0.947	200	-0.061 (-0.701, 0.579)	0.851
4	238	1.290 (0.126, 2.453)	0.030*	238	2.549 (-1.353, 6.451)	0.199	238	2.26x10 ⁻³ (7.60x10 ⁻⁵ , 4.45x10 ⁻³)	0.043*	202	0.462 (-0.199, 1.123)	0.170
5	218	-1.184 (-2.710, 0.342)	0.128	218	-3.458 (-8.720, 1.805)	0.197	218	-1.81x10 ⁻³ (-4.59x10 ⁻³ , 9.77x10 ⁻⁴)	0.202	186	-0.196 (-1.017, 0.625)	0.638
6	135	-2.145 (-4.730, 0.439)	0.103	135	-2.950 (-11.796, 5.897)	0.511	135	-4.92x10 ⁻³ (-9.73x10 ⁻³ , -9.93x10 ⁻⁵)	0.046*	116	-0.774 (-2.225, 0.677)	0.293
7	81	1.801 (-3.226, 6.827)	0.478	81	9.822 (-6.641, 26.286)	0.238	81	-5.12x10 ⁻⁴ (-1.02x10 ⁻² , 9.14x10 ⁻³)	0.916	68	-1.344 (-4.185, 1.496)	0.348
8	120	-0.432 (-4.246, 3.382)	0.823	120	1.136 (-11.990, 14.262)	0.864	120	-2.26x10 ⁻³ (-8.67x10 ⁻³ , 4.16x10 ⁻³)	0.487	95	0.225 (-1.699, 2.149)	0.817
9	87	4.077 (0.133, 8.020)	0.043*	87	14.343 (1.436, 27.249)	0.030*	87	3.94x10 ⁻³ (-3.25x10 ⁻³ , 1.11x10 ⁻²)	0.278	76	-0.306 (-2.360, 1.748)	0.767

Linear regression analyses adjusted for sex, gestational age, treatment group and season of birth. BMC = bone mineral content, BA = bone area, BMD = bone mineral density and scBMC = size corrected bone mineral content. Neonatal DXA measurements were taken within 14 days of birth.

Table 5.4 Associations between *Runx2* CpG methylation at birth and bone outcomes at birth in the MAVIDOS trial when stratified by treatment group.

CHOLECALCIFEROL												
<i>Runx2</i> CpG	Total BMC			Total BA			Total BMD			Total scBMC		
	n	B (95 % CI)	p	n	B (95 % CI)	p	n	B (95 % CI)	p	n	B (95 % CI)	p
1	86	-0.179 (-2.025, 1.666)	0.847	86	2.737 (-3.373, 8.846)	0.375	86	-2.72x10 ⁻³ (-6.10x10 ⁻³ , 6.53x10 ⁻⁴)	0.112	74	-0.845 (-1.867, 0.177)	0.104
2	93	1.520 (-1.216, 4.255)	0.273	93	5.953 (-2.777, 14.683)	0.179	93	1.09x10 ⁻³ (-3.88x10 ⁻³ , 6.07x10 ⁻³)	0.663	74	0.177 (-1.290, 1.643)	0.811
3	112	0.228 (-1.368, 1.824)	0.778	112	0.180 (-4.986, 5.347)	0.945	112	5.71x10 ⁻⁴ (-2.44x10 ⁻³ , 3.58x10 ⁻³)	0.708	92	-0.426 (-1.331, 0.478)	0.351
4	121	1.416 (-0.178, 3.010)	0.081	121	2.544 (-2.647, 7.735)	0.334	121	2.65x10 ⁻³ (-8.88x10 ⁻³ , 5.39x10 ⁻³)	0.058	100	0.572 (-0.244, 1.387)	0.167
5	109	-1.765 (-4.207, 0.678)	0.155	109	-6.207 (-14.237, 1.824)	0.128	109	-0.56x10 ⁻³ (-5.69x10 ⁻⁵ , 2.56x10 ⁻³)	0.455	91	-0.255 (-1.427, 0.917)	0.666
6	71	-1.264 (-5.606, 3.078)	0.563	71	-2.376 (-16.364, 11.612)	0.736	71	-2.97x10 ⁻³ (-9.90x10 ⁻³ , 3.96x10 ⁻³)	0.396	60	-0.169 (-2.276, 1.938)	0.873
7	39	-2.469 (-14.148, 9.210)	0.670	39	-2.241 (-41.849, 37.367)	0.909	39	-4.48x10 ⁻³ (-2.36x10 ⁻² , 1.46x10 ⁻²)	0.637	32	-4.129 (-9.850, 1.591)	0.150
8	62	0.966 (-4.536, 6.468)	0.727	62	4.606 (-14.016, 23.227)	0.622	62	-8.84x10 ⁻⁵ (-9.15x10 ⁻³ , 8.97x10 ⁻³)	0.984	46	0.282 (-2.411, 2.974)	0.834
9	42	3.586 (-2.789, 9.960)	0.262	42	8.328 (-11.998, 28.654)	0.412	42	6.81x10 ⁻³ (-5.01x10 ⁻³ , 1.86x10 ⁻²)	0.251	36	0.704 (-2.743, 4.150)	0.680

PLACEBO												
<i>Runx2</i> CpG	Total BMC			Total BA			Total BMD			Total scBMC		
	n	B (95 % CI)	p	n	B (95 % CI)	p	n	B (95 % CI)	p	n	B (95 % CI)	p
1	91	-0.854 (-2.856, 1.147)	0.399	91	-1.237 (-8.286, 5.812)	0.728	91	-1.71x10 ⁻³ (-6.04x10 ⁻³ , 2.62x10 ⁻³)	0.434	79	-0.263 (-1.585, 1.060)	0.694
2	70	0.137 (-2.350, 2.624)	0.913	70	-1.452 (-11.061, 8.156)	0.764	70	8.60x10 ⁻⁴ (-3.65x10 ⁻³ , 5.37x10 ⁻³)	0.705	60	0.841 (-0.535, 2.216)	0.226
3	126	-0.624 (-2.190, 0.941)	0.431	126	-2.106 (-7.466, 3.253)	0.438	126	-5.85x10 ⁻⁴ (-3.58x10 ⁻³ , 2.41x10 ⁻³)	0.700	107	0.221 (-0.694, 1.137)	0.633
4	116	1.127 (-0.610, 2.865)	0.201	116	2.674 (-3.486, 8.834)	0.392	116	4.67x10 ⁻³ (-1.97x10 ⁻³ , 5.32x10 ⁻³)	0.365	101	0.299 (-0.816, 1.415)	0.595
5	108	-0.650 (-2.577, 1.277)	0.505	108	-0.507 (-7.620, 6.605)	0.888	108	-2.16x10 ⁻³ (-6.07x10 ⁻³ , 1.75x10 ⁻³)	0.276	94	-0.176 (-1.381, 1.029)	0.772
6	63	-3.871 (-6.860, -0.881)	0.012*	63	-6.411 (-18.093, 5.271)	0.277	63	-8.05x10 ⁻³ (-1.51x10 ⁻² , -9.77x10 ⁻⁴)	0.026*	55	-1.164 (-3.327, 0.998)	0.285
7	41	2.572 (-2.542, 7.686)	0.315	41	13.471 (-2.655, 29.598)	0.099	41	-1.32x10 ⁻³ (-1.30x10 ⁻² , 1.04x10 ⁻²)	0.820	35	-1.118 (-4.376, 2.140)	0.489
8	57	-1.452 (-7.112, 4.207)	0.609	57	-2.574 (-23.086, 17.937)	0.802	57	-3.03x10 ⁻³ (-1.27x10 ⁻² , 6.66x10 ⁻³)	0.533	48	-0.129 (-3.356, 3.098)	0.936
9	44	3.580 (-1.336, 8.496)	0.149	44	17.091 (0.583, 33.599)	0.043*	44	2.04x10 ⁻⁴ (-8.81x10 ⁻³ , 9.22x10 ⁻³)	0.964	39	-1.218 (-3.846, 1.411)	0.353

Linear regression analyses adjusted for sex, gestational age and season of birth. BMC = bone mineral content, BA = bone area, BMD = bone mineral density and scBMC = size corrected bone mineral content. Neonatal DXA measurements were taken within 14 days of birth.

Table 5.5 Associations between *Runx2* CpG methylation at birth and bone outcomes at birth in the MAVIDOS trial when stratified by season of birth.

WINTER												
Total BMC				Total BA			Total BMD			Total scBMC		
<i>Runx2</i> CpG	n	B (95 % CI)	p	n	B (95 % CI)	p	n	B (95 % CI)	p	n	B (95 % CI)	p
1	24	0.167 (-2.531, 2.865)	0.898	24	1.225 (-7.517, 9.967)	0.773	24	-3.54x10 ⁻⁴ (-7.26x10 ⁻³ , 6.55x10 ⁻³)	0.916	20	-0.241 (-2.659, 2.176)	0.835
2	33	0.208 (-3.797, 4.213)	0.916	33	-3.319 (-18.675, 12.037)	0.662	33	2.94x10 ⁻³ (-5.67x10 ⁻³ , 1.15x10 ⁻²)	0.491	24	1.315 (-2.001, 4.630)	0.418
3	42	0.914 (-1.968, 3.797)	0.525	42	4.561 (-4.642, 13.763)	0.322	42	-2.90x10 ⁻⁴ (-6.89x10 ⁻³ , 6.31x10 ⁻³)	0.930	32	-0.898 (-2.858, 1.062)	0.356
4	37	0.525 (-2.206, 3.256)	0.698	37	-1.980 (-10.046, 6.086)	0.621	37	2.86x10 ⁻³ (-3.67x10 ⁻³ , 9.40x10 ⁻³)	0.379	28	2.062 (-0.378, 4.502)	0.094
5	33	-2.384 (-6.693, 1.924)	0.267	33	-2.933 (-16.616, 10.749)	0.664	33	-6.23x10 ⁻³ (-1.57x10 ⁻² , 3.22x10 ⁻³)	0.188	25	-1.712 (-5.323, 1.899)	0.335
6	19	-4.476 (-11.311, 2.359)	0.183	19	-10.554 (-32.074, 10.966)	0.312	19	-8.43x10 ⁻³ (-2.31x10 ⁻² , 6.23x10 ⁻³)	0.239	14	-0.114 (-5.469, 5.240)	0.963
7	4	5.263 (-43.436, 53.962)	0.754	7	-9.769 (-193.122, 173.585)	0.876	7	2.64x10 ⁻² (-8.31x10 ⁻² , 1.36x10 ⁻¹)	0.499	4	18.163 (18.163, 18.163)	0.999
8	23	-1.770 (-12.068, 8.527)	0.723	23	-18.909 (-50.717, 12.899)	0.229	23	7.63x10 ⁻³ (-1.41x10 ⁻² , 2.93x10 ⁻²)	0.471	16	4.947 (-2.510, 12.403)	0.174
9	16	7.952 (-3.247, 19.151)	0.148	16	5.492 (-36.315, 47.298)	0.780	16	2.46x10 ⁻² (4.16x10 ⁻³ , 4.88x10 ⁻²)	0.047*	12	6.220 (-3.762, 16.202)	0.189

SPRING												
Total BMC				Total BA			Total BMD			Total scBMC		
<i>Runx2</i> CpG	n	B (95 % CI)	p	n	B (95 % CI)	p	n	B (95 % CI)	p	n	B (95 % CI)	p
1	36	-2.066 (-5.118, 0.986)	0.178	36	-8.115 (-17.301, 1.071)	0.081	36	-1.72x10 ⁻³ (-7.72x10 ⁻³ , 4.28x10 ⁻³)	0.563	35	0.010 (-1.564, 1.583)	0.990
2	43	0.544 (-3.145, 4.233)	0.767	43	6.886 (-5.568, 19.339)	0.270	43	-3.30x10 ⁻³ (-8.48x10 ⁻³ , 2.24x10 ⁻³)	0.235	37	-0.348 (-1.755, 1.059)	0.618
3	55	-1.042 (-3.822, 1.739)	0.455	55	-2.269 (-11.603, 7.064)	0.628	55	-2.31x10 ⁻³ (-6.75x10 ⁻³ , 2.14x10 ⁻³)	0.303	48	-0.352 (-1.555, 0.851)	0.558
4	60	2.459 (0.080, 4.839)	0.043*	60	6.333 (-2.204, 14.871)	0.143	60	3.90x10 ⁻³ (1.37x10 ⁻⁴ , 7.67x10 ⁻³)	0.042*	50	0.564 (-0.564, 1.692)	0.320
5	52	-1.913 (-5.078, 1.252)	0.230	52	-4.509 (-16.813, 7.796)	0.465	52	-3.69x10 ⁻³ (-8.76x10 ⁻³ , 1.39x10 ⁻³)	0.150	45	-0.277 (-1.903, 1.350)	0.733
6	24	1.826 (-5.641, 9.292)	0.616	24	7.469 (-21.258, 36.197)	0.594	24	5.93x10 ⁻⁴ (-1.25x10 ⁻² , 1.37x10 ⁻²)	0.926	22	0.332 (-4.481, 5.146)	0.886
7	20	17.841 (-7.215, 42.897)	0.151	20	56.102 (-40.468, 152.672)	0.236	20	1.69x10 ⁻² (-2.86x10 ⁻² , 6.23x10 ⁻²)	0.443	17	1.153 (-14.011, 16.317)	0.872
8	37	0.496 (-5.173, 6.165)	0.860	37	5.876 (-14.193, 25.944)	0.555	37	-2.23x10 ⁻³ (-1.07x10 ⁻² , 6.29x10 ⁻³)	0.598	29	-0.906 (-3.663, 1.852)	0.505
9	16	6.904 (-0.445, 14.253)	0.063	16	26.529 (3.814, 49.245)	0.026*	16	4.66x10 ⁻³ (-8.93x10 ⁻³ , 1.82x10 ⁻²)	0.470	15	-0.409 (-3.459, 2.640)	0.773

SUMMER												
Total BMC				Total BA			Total BMD			Total scBMC		
<i>Runx2</i> CpG	n	B (95 % CI)	p	n	B (95 % CI)	p	n	B (95 % CI)	p	n	B (95 % CI)	p
1	46	-2.227 (-5.701, 1.247)	0.203	46	0.019 (-12.144, 12.182)	0.998	46	-7.33x10 ⁻³ (-1.35x10 ⁻² , -1.15x10 ⁻³)	0.021*	39	-1.320 (-3.205, 0.564)	0.164
2	49	3.310 (-0.951, 7.570)	0.125	49	2.844 (-10.620, 16.308)	0.673	49	8.28x10 ⁻³ (2.85x10 ⁻⁴ , 1.63x10 ⁻²)	0.043*	44	1.966 (-0.198, 4.130)	0.074
3	68	-1.492 (-3.749, 0.765)	0.191	68	-3.649 (-11.108, 3.809)	0.332	68	-2.28x10 ⁻³ (-6.27x10 ⁻³ , 1.71x10 ⁻³)	0.258	60	-0.468 (-1.590, 0.653)	0.406
4	72	1.892 (-0.509, 4.293)	0.120	72	4.614 (-3.380, 12.609)	0.253	72	2.44x10 ⁻³ (-1.89x10 ⁻³ , 6.76x10 ⁻³)	0.265	66	0.337 (-0.751, 1.425)	0.538
5	65	0.719 (-2.354, 3.793)	0.641	65	0.079 (-10.219, 10.378)	0.988	65	1.65x10 ⁻³ (-3.81x10 ⁻³ , 7.11x10 ⁻³)	0.548	59	0.740 (-0.577, 2.057)	0.265
6	42	-2.450 (-7.869, 2.968)	0.366	42	-9.369 (-26.559, 7.821)	0.277	42	-2.27x10 ⁻³ (-1.29x10 ⁻² , 8.40x10 ⁻³)	0.669	37	0.503 (-2.164, 3.170)	0.704
7	21	-2.452 (-17.333, 12.428)	0.732	21	17.677 (-29.346, 64.701)	0.439	21	-1.86x10 ⁻² (-5.17x10 ⁻² , 1.44x10 ⁻²)	0.251	20	-5.880 (-15.163, 3.404)	0.198
8	33	-3.039 (-12.883, 6.805)	0.533	33	-9.948 (-40.836, 20.940)	0.515	33	-4.06x10 ⁻³ (-1.99x10 ⁻² , 1.18x10 ⁻²)	0.604	28	0.398 (-4.032, 4.827)	0.855
9	27	2.111 (-5.100, 9.323)	0.551	27	12.305 (-10.327, 34.938)	0.272	27	-1.87x10 ⁻³ (-1.48x10 ⁻² , 1.11x10 ⁻²)	0.767	24	-1.424 (-5.341, 2.492)	0.457

AUTUMN												
Total BMC				Total BA			Total BMD			Total scBMC		
<i>Runx2</i> CpG	n	B (95 % CI)	p	n	B (95 % CI)	p	n	B (95 % CI)	p	n	B (95 % CI)	p
1	69	0.835 (-1.320, 2.990)	0.442	69	7.238 (-0.399, 14.875)	0.063	69	-1.98x10 ⁻³ (-6.59x10 ⁻³ , 2.64x10 ⁻³)	0.396	57	-1.249 (-2.806, 0.309)	0.114
2	36	1.307 (-2.204, 4.818)	0.454	36	3.751 (-8.834, 16.337)	0.548	36	1.90x10 ⁻³ (-4.51x10 ⁻³ , 8.31x10 ⁻³)	0.550	27	0.371 (-1.776, 2.518)	0.724
3	71	1.913 (0.308, 3.518)	0.020*	71	2.814 (-2.889, 8.518)	0.328	71	4.57x10 ⁻³ (1.06x10 ⁻³ , 8.07x10 ⁻³)	0.011*	57	0.927 (-0.328, 2.183)	0.144
4	66	0.517 (-1.664, 2.698)	0.637	66	1.324 (-5.745, 8.394)	0.709	66	5.63x10 ⁻⁴ (-3.77x10 ⁻³ , 4.90x10 ⁻³)	0.796	55	-0.107 (-1.473, 1.258)	0.875
5	65	-2.176 (-4.858, 0.506)	0.110	65	-6.380 (-15.296, 2.537)	0.158	65	-2.75x10 ⁻³ (-7.84x10 ⁻³ , 2.34x10 ⁻³)	0.285	54	-0.524 (-2.120, 1.072)	0.513
6	47	-3.198 (-7.527, 1.131)	0.144	47	-2.246 (-17.013, 12.520)	0.760	47	-8.26x10 ⁻³ (-1.60x10 ⁻² , -5.23x10 ⁻⁴)	0.037*	40	-1.999 (-4.404, 0.406)	0.100
7	30	1.292 (-5.801, 8.385)	0.711	30	7.360 (-14.429, 29.149)	0.494	30	-8.64x10 ⁻⁴ (-1.30x10 ⁻² , 1.13x10 ⁻²)	0.885	24	-1.289 (-4.310, 1.732)	0.384
8	24	2.849 (-11.157, 16.856)	0.676	24	1.313 (-44.981, 47.607)	0.953	24	8.26x10 ⁻³ (-1.51x10 ⁻² , 3.17x10 ⁻²)	0.470	19	2.969 (-3.234, 9.171)	0.324
9	25	2.553 (-6.448, 11.555)	0.562	25	9.018 (-18.158, 36.195)	0.498	25	3.04x10 ⁻³ (-1.17x10 ⁻² , 1.78x10 ⁻²)	0.672	22	-0.976 (-4.487, 2.536)	0.567

Linear regression analyses adjusted for sex, gestational age and treatment group. BMC = bone mineral content, BA = bone area, BMD = bone mineral density and scBMC = size corrected bone mineral content. Neonatal DXA measurements were taken within 14 days of birth. Seasons are defined as winter (December to February), spring (March to May), summer (June to August) and autumn (September to November).

5.2.3 Investigation into *Osterix* CpG methylation as an epigenetic biomarker of bone health

5.2.3.1 There are seasonal differences in *Osterix* CpG methylation at birth between the two maternal treatment groups within the MAVIDOS trial

The results showed that infants born to cholecalciferol supplemented mothers had lower methylation at CpG 6 compared to the placebo group ($p = 0.027$, mean difference = 0.3%, 95 % CI: -0.52, 0.30). There were no significant differences in methylation at the remaining CpG sites (**Table 5.6** and **Figure 5.2**).

Amongst infants born in the spring months, those born to cholecalciferol supplemented mothers had lower methylation at CpGs 3 ($p = 0.040$, mean difference = 0.9 %, 95 % CI: -1.66, -0.04) and 6 ($p = 0.011$, mean difference = 0.7 %, 95 % CI: -1.17, -0.16) compared to the placebo group (**Table 5.7** and **Figure 5.3**). Amongst infants born in the winter, summer or autumn months there were no significant differences in *Osterix* methylation at birth between the two maternal treatment groups.

Table 5.6 Differences in *Osterix* methylation between the treatment groups in the MAVIDOS trial.

<i>Osterix</i> CpG	n	Mean difference (%)	(95 % CI)	p
1	139	0.1	(-0.224, 0.470)	0.485
2	264	-0.1	(-0.461, 0.181)	0.391
3	301	0.0	(-0.436, 0.340)	0.809
4	178	0.0	(-0.243, 0.254)	0.964
6	316	-0.3	(-0.521, -0.031)	0.027*
7	291	0.1	(-0.151, 0.301)	0.516
8	86	0.0	(-0.371, 0.374)	0.992
9	155	-0.1	(-0.338, 0.208)	0.640

Independent t-tests compared *Osterix* methylation between the cholecalciferol supplemented and placebo group within the MAVIDOS trial.

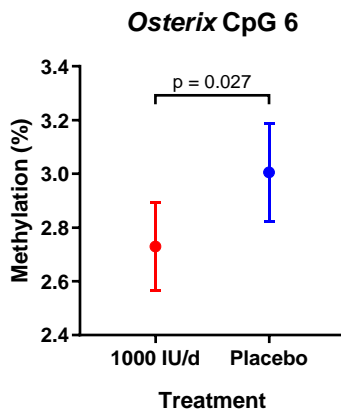


Figure 5.2 Box whisker plots of differences in *Osterix* CpG methylation at birth between the treatment groups within the MAVIDOS trial.

Independent t-tests comparing *Osterix* CpG methylation at birth between the treatment groups. Graphs represent mean and 95 % confidence intervals.

Table 5.7 Differences in *Osterix* methylation between treatment groups in the MAVIDOS trial when stratified by season of birth.

<i>Osterix</i> CpG	Winter				Spring				Summer				Autumn			
	n	Mean diff. (%)	(95 % CI)	p	n	Mean diff. (%)	(95 % CI)	p	n	Mean diff. (%)	(95 % CI)	p	n	Mean diff. (%)	(95 % CI)	p
1	25	0.4	(-0.537, 1.411)	0.362	23	-0.3	(-1.231, 0.568)	0.452	34	0.0	(-0.508, 0.546)	0.941	57	0.1	(-0.406, 0.705)	0.592
2	48	-0.3	(-1.182, 0.512)	0.430	68	-0.3	(-0.979, 0.343)	0.341	75	-0.3	(-0.808, 0.263)	0.313	72	0.4	(-0.281, 1.014)	0.262
3	55	0.1	(-0.804, 0.922)	0.891	74	-0.8	(-1.661, -0.039)	0.040*	85	0.7	(-0.066, 1.409)	0.074	83	-0.1	(-0.811, 0.672)	0.852
4	36	-0.7	(-1.505, 0.066)	0.070	39	0.4	(-0.060, 0.884)	0.085	56	0.2	(-0.242, 0.645)	0.367	47	-0.1	(-0.543, 0.351)	0.667
6	60	-0.2	(-0.756, 0.330)	0.435	76	-0.7	(-1.171, -0.159)	0.011*	92	0.0	(-0.511, 0.504)	0.989	85	-0.2	(-0.653, 0.244)	0.368
7	55	0.2	(-0.409, 0.803)	0.517	65	0.1	(-0.392, 0.531)	0.765	87	0.2	(-0.296, 0.600)	0.502	84	-0.1	(-0.454, 0.311)	0.710
8	16	-1.1	(-3.774, 1.542)	0.313	20	-0.1	(-0.625, 0.502)	0.822	35	0.3	(-0.384, 0.887)	0.426	13	0.2	(-0.404, 0.817)	0.472
9	28	0.3	(-0.241, 0.882)	0.252	41	-0.5	(-1.081, 0.111)	0.108	41	0.0	(-0.637, 0.645)	0.990	43	0.0	(-0.409, 0.446)	0.932

Independent t-tests compared *Osterix* methylation between the cholecalciferol supplemented and placebo group within the MAVIDOS trial. Seasons are defined as winter (December to February), spring (March to May), summer (June to August) and winter (September to November).

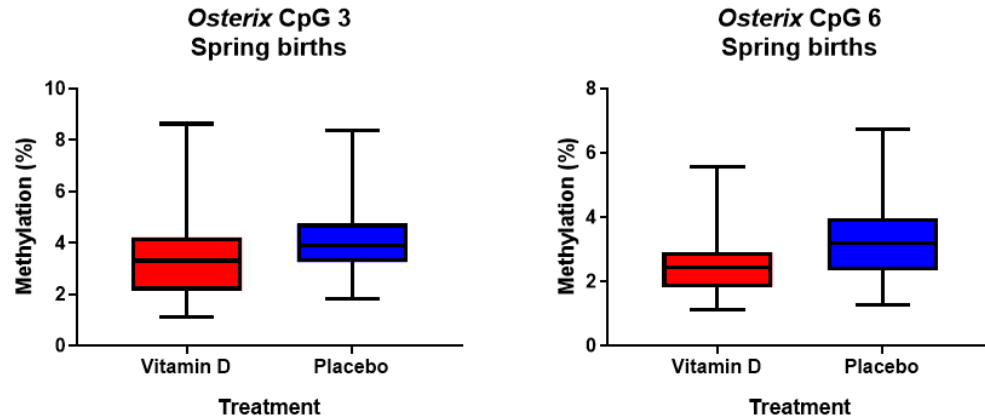


Figure 5.3 Box whisker plots of seasonal differences in *Osterix* CpG methylation at birth between the treatment groups within the MAVIDOS trial.

Independent t-tests comparing *Osterix* CpG methylation at birth between the treatment groups. Graphs represent mean and 95 % confidence intervals.

5.2.3.2 Are there any associations between cord *Osterix* CpG methylation and bone outcomes at birth within the MAVIDOS trial?

The results showed that there was a positive association between *Osterix* CpG 6 methylation at birth and BMC at birth when adjusted for sex, gestational age, treatment allocation and season of birth ($b = 1.189$ (95 % CI: 0.04, 2.34), $p = 0.042$). There were no significant associations between *Osterix* CpG methylation at birth and BA, BMD or scBMC at birth (**Table 5.8**).

Within the placebo group there were inverse associations between *Osterix* CpG 9 methylation and BMC at birth ($b = -3.951$ (95 % CI: -6.98, -0.93), $p = 0.011$) and BA at birth ($b = -17.509$ (95 % CI: -27.34, -7.68), $p = 0.001$) when the linear regression analyses were adjusted for sex, gestational age and season of birth, and there were no significant associations between methylation and BMD or scBMC. Within the cholecalciferol supplemented group there were no significant associations between methylation at birth and BMC, BA, BMD or scBMC at birth (**Table 5.9**).

Amongst infants born in the winter months there was an inverse association between CpG 3 methylation and BMD ($b = -0.005$ (95 % CI: -0.008, -0.001), $p = 0.024$) however there were no significant associations between *Osterix* methylation at birth and BMC, BA or scBMC (**Table 5.10**). Amongst infants born in the spring months there was a positive association between CpG 7 methylation and BMC at birth ($b = 3.648$ (95 % CI: 0.88, 6.42), $p = 0.011$) and BA at birth ($b = 13.459$ (95 % CI: 4.28, 22.64), $p = 0.005$). There were no significant associations between methylation and BMD and scBMC, although there was a trend towards an inverse association between *Osterix* CpG 9 methylation and scBMC however this did not reach statistical significance ($b = -1.496$ (95 % CI: -3.02, 0.03), $p = 0.054$). Amongst infants born in the summer months there was an inverse association between BA at birth and methylation at CpGs 2 ($b = -7.201$ (95 % CI: -13.775, -0.626), $p = 0.032$) and 9 ($b = -14.340$ (95 % CI: -23.02, 5.66), $p = 0.002$) however there were no significant associations between methylation at birth and BMC, BMD or scBMC at birth. Amongst infants born in the autumn months there was a positive association between CpG 7 methylation and BMD at birth ($b = 0.006$ (95 % CI: 0.001, 0.011), $p = 0.022$) and scBMC at birth ($b = 2.376$ (95 % CI: 0.85, 3.90), $p = 0.003$) however there were no associations between methylation at birth and BMC or BA at birth (**Table 5.10**).

Table 5.8 Associations between *Osterix* methylation at birth and bone outcomes at birth in the MAVIDOS trial.

<i>Osterix</i> CpG	Total BMC			Total BA			Total BMD			Total scBMC		
	n	B (95 % CI)	p	n	B (95 % CI)	p	n	B (95 % CI)	p	n	B (95 % CI)	p
1	111	-0.195 (-1.788, 1.398)	0.808	111	-2.097 (-7.704, 3.509)	0.460	111	1.05×10^{-3} (-0.002, 0.004)	0.488	93	0.039 (-0.840, 0.919)	0.930
2	218	-0.051 (-0.986, 0.884)	0.915	218	-1.289 (-4.504, 1.927)	0.430	218	6.60×10^{-4} (-0.001, 0.002)	0.456	183	-0.003 (-0.543, 0.538)	0.993
3	250	0.012 (-0.706, 0.730)	0.974	250	0.564 (-1.905, 3.032)	0.653	250	-4.34×10^{-4} (-0.002, 0.001)	0.514	208	-0.153 (-0.561, 0.255)	0.461
4	142	-0.366 (-2.236, 1.504)	0.700	142	0.895 (-5.343, 7.133)	0.777	142	-1.63×10^{-3} (-0.005, 0.002)	0.347	118	-0.455 (-1.546, 0.636)	0.410
6	263	0.562 (-0.518, 1.643)	0.306	263	1.351 (-2.349, 5.050)	0.473	263	8.52×10^{-4} (-0.001, 0.003)	0.380	218	0.094 (-0.505, 0.693)	0.758
7	249	1.189 (0.041, 2.336)	0.042*	249	3.115 (-0.779, 7.008)	0.116	249	1.58×10^{-3} (-0.001, 0.004)	0.143	211	0.389 (-0.267, 1.044)	0.244
8	68	0.003 (-2.723, 2.728)	0.998	68	2.963 (-6.274, 12.199)	0.524	68	-2.14×10^{-3} (-0.007, 0.003)	0.424	54	-0.384 (-1.718, 0.949)	0.565
9	126	-0.831 (-2.863, 1.200)	0.419	126	-3.901 (-10.872, 3.071)	0.270	126	-1.14×10^{-3} (-0.004, 0.004)	0.995	108	0.410 (-0.733, 1.553)	0.478

Linear regression analyses adjusted for sex, treatment group and season of birth. BMC = bone mineral content, BA = bone area, BMD = bone mineral density and scBMC = size corrected bone mineral content. Neonatal DXA measurements were taken within 14 days of birth.

Table 5.10 Associations between *Osterix* CpG methylation at birth and bone outcomes at birth in the MAVIDOS trial when stratified by season of birth.

WINTER												
Osterix												
CpG	Total BMC			Total BA			Total BMD			Total scBMC		
	n	B (95 % CI)	p	n	B (95 % CI)	p	n	B (95 % CI)	p	n	B (95 % CI)	p
1	13	0.491 (-5.261, 6.334)	0.853	13	-0.569 (-21.091, 19.954)	0.951	13	2.22x10 ⁻³ (-0.006, 0.010)	0.532	9	0.213 (-1.954, 2.380)	0.811
2	32	0.203 (-1.261, 2.493)	0.857	32	-0.785 (-9.215, 7.644)	0.850	32	1.63x10 ⁻³ (-0.004, 0.007)	0.524	24	-0.610 (-2.708, 1.487)	0.551
3	43	-1.495 (-9.261, 0.485)	0.135	43	-1.029 (-8.101, 6.042)	0.770	43	-4.56x10 ⁻³ (-0.008, -0.001)	0.024*	30	-1.148 (-2.528, 0.232)	0.099
4	26	-0.825 (-7.261, 2.713)	0.633	26	-3.343 (-15.003, 8.317)	0.558	26	1.27x10 ⁻⁵ (-0.008, 0.008)	0.997	19	-0.298 (-3.411, 2.814)	0.841
6	47	-0.993 (-3.261, 1.684)	0.458	47	-0.080 (-9.143, 8.982)	0.986	47	-3.48x10 ⁻³ (-0.009, 0.002)	0.187	33	-1.580 (-3.878, 0.718)	0.170
7	42	-0.313 (-1.261, 1.980)	0.784	42	-2.899 (-10.996, 5.198)	0.473	42	1.25x10 ⁻³ (-0.003, 0.006)	0.583	31	0.116 (-1.612, 1.844)	0.891
8	13	0.948 (-8.261, 7.491)	0.751	13	5.171 (-14.954, 25.296)	0.575	13	-4.28x10 ⁻⁴ (-0.011, 0.010)	0.930	9	-0.202 (-2.978, 2.573)	0.859
9	21	-1.877 (-4.261, 3.339)	0.458	21	-12.375 (-30.781, 6.031)	0.174	21	2.14x10 ⁻³ (-0.007, 0.012)	0.642	15	-0.519 (-6.666, 5.628)	0.856

SPRING												
Osterix												
CpG	Total BMC			Total BA			Total BMD			Total scBMC		
	n	B (95 % CI)	p	n	B (95 % CI)	p	n	B (95 % CI)	p	n	B (95 % CI)	p
1	20	-1.999 (-6.362, 2.364)	0.346	20	-7.580 (-19.867, 4.708)	0.209	20	-1.12x10 ⁻³ (-0.008, 0.006)	0.746	18	0.130 (-1.751, 2.012)	0.884
2	61	0.175 (-1.896, 2.246)	0.866	61	-2.687 (-9.791, 4.416)	0.452	61	1.91x10 ⁻³ (-0.001, 0.005)	0.234	51	0.613 (-0.265, 1.492)	0.167
3	63	1.209 (-0.418, 2.836)	0.142	63	4.109 (-1.611, 9.830)	0.156	63	1.01x10 ⁻³ (-0.001, 0.003)	0.400	55	0.034 (-0.602, 0.671)	0.914
4	31	2.266 (-3.642, 8.174)	0.438	31	6.127 (-12.708, 24.962)	0.510	31	2.39x10 ⁻³ (-0.006, 0.011)	0.574	27	0.712 (-1.280, 2.704)	0.467
6	64	1.189 (-1.421, 3.799)	0.366	64	2.570 (-6.592, 11.732)	0.577	64	1.93x10 ⁻³ (-0.002, 0.006)	0.327	55	0.257 (-0.746, 1.261)	0.609
7	56	3.648 (0.880, 6.417)	0.011*	56	13.459 (4.281, 22.636)	0.005*	56	2.29x10 ⁻³ (-0.002, 0.007)	0.304	49	0.097 (-1.094, 1.289)	0.870
8	13	4.970 (-6.895, 16.835)	0.368	13	20.149 (-20.794, 61.091)	0.294	13	3.70x10 ⁻³ (-0.015, 0.022)	0.664	10	-2.571 (-6.214, 1.072)	0.135
9	33	1.943 (-2.650, 6.536)	0.394	33	11.211 (-5.758, 28.180)	0.187	33	-1.31x10 ⁻³ (-0.007, 0.005)	0.659	28	-1.496 (-3.022, 0.031)	0.054

SUMMER												
Osterix												
CpG	Total BMC			Total BA			Total BMD			Total scBMC		
	n	B (95 % CI)	p	n	B (95 % CI)	p	n	B (95 % CI)	p	n	B (95 % CI)	p
1	29	2.143 (-1.645, 5.930)	0.255	29	1.672 (-10.985, 14.330)	0.788	29	5.56x10 ⁻³ (-0.002, 0.013)	0.157	26	0.718 (-1.523, 2.959)	0.513
2	63	-1.325 (-3.284, 0.635)	0.181	63	-7.201 (-13.775, -0.626)	0.032*	63	8.50x10 ⁻⁴ (-0.003, 0.005)	0.653	58	0.540 (-0.456, 1.536)	0.282
3	70	-0.599 (-1.927, 0.729)	0.371	70	-1.133 (-5.699, 3.432)	0.622	70	-1.31x10 ⁻³ (-0.004, 0.001)	0.261	62	-0.266 (-0.952, 0.421)	0.442
4	46	-0.538 (-4.689, 3.614)	0.795	46	0.561 (-13.079, 14.200)	0.934	46	-1.88x10 ⁻³ (-0.009, 0.005)	0.595	40	0.019 (-2.055, 2.093)	0.985
6	79	0.421 (-1.528, 2.369)	0.668	79	0.210 (-6.399, 6.819)	0.950	79	1.14x10 ⁻³ (-0.002, 0.005)	0.520	69	0.190 (-0.862, 1.242)	0.719
7	79	0.014 (-1.939, 1.966)	0.989	79	0.543 (-5.798, 6.885)	0.865	79	-8.81x10 ⁻⁴ (-0.005, 0.003)	0.642	70	-0.328 (-1.377, 0.722)	0.535
8	30	-2.578 (-8.237, 3.082)	0.358	30	-4.645 (-23.625, 14.336)	0.619	30	-6.66x10 ⁻³ (-0.019, 0.006)	0.281	24	-0.362 (-4.037, 3.314)	0.839
9	37	-2.778 (-5.679, 0.123)	0.060	37	-14.340 (-23.017, -5.663)	0.002*	37	8.57x10 ⁻⁴ (-0.006, 0.008)	0.805	33	1.015 (-0.806, 2.835)	0.264

AUTUMN												
Osterix												
CpG	Total BMC			Total BA			Total BMD			Total scBMC		
	n	B (95 % CI)	p	n	B (95 % CI)	p	n	B (95 % CI)	p	n	B (95 % CI)	p
1	46	0.069 (2.166, 2.303)	0.951	46	0.679 (-7.748, 9.105)	0.872	46	4.44x10 ⁻⁴ (-0.004, 0.005)	0.850	37	-0.606 (-2.248, 1.036)	0.458
2	59	0.041 (-1.624, 1.705)	0.961	59	1.701 (-3.918, 7.320)	0.547	59	-1.06x10 ⁻³ (-0.004, 0.002)	0.533	47	-0.348 (-1.510, 0.815)	0.550
3	71	0.282 (-0.937, 1.500)	0.646	71	0.890 (-3.220, 5.000)	0.667	71	5.64x10 ⁻⁴ (-0.002, 0.003)	0.672	58	-0.175 (-1.068, 0.719)	0.697
4	36	1.319 (-1.637, 2.480)	0.453	36	10.821 (-1.611, 23.253)	0.086	36	-2.20x10 ⁻³ (-0.011, 0.006)	0.604	28	-2.266 (-5.040, 0.509)	0.105
6	70	0.421 (-1.637, 2.480)	0.684	70	1.281 (-5.618, 8.179)	0.712	70	7.81x10 ⁻⁴ (-0.003, 0.005)	0.687	58	0.053 (-1.197, 1.303)	0.932
7	69	2.218 (-0.312, 4.748)	0.085	69	2.038 (-6.768, 10.844)	0.646	69	5.79x10 ⁻³ (0.001, 0.011)	0.022*	58	2.376 (0.847, 3.904)	0.003*
8	9	-0.305 (-11.492, 10.883)	0.947	9	3.634 (-40.086, 47.355)	0.839	9	-3.37x10 ⁻³ (-0.015, 0.009)	0.502	8	-0.694 (-5.771, 4.383)	0.724
9	32	-2.115 (-7.756, 3.525)	0.449	32	-3.712 (-20.010, 12.586)	0.644	32	-3.77x10 ⁻³ (-0.014, 0.007)	0.476	29	-0.834 (-3.845, 2.177)	0.573

Linear regression analyses adjusted for sex, gestational age and treatment group. BMC = bone mineral content, BA = bone area, BMD = bone mineral density and scBMC = size corrected bone mineral content. Neonatal DXA measurements were taken within 14 days of birth. Seasons are defined as winter (December to February), spring (March to May), summer (June to August) and autumn (September to November).

5.3 Discussion

The early life environment has been shown to alter the epigenome²⁹⁰ and to be associated with the risk of developing diseases such as osteoporosis in later life²¹⁷. There is evidence to suggest that vitamin D plays an important role in bone metabolism²³¹ and that the early life environment can influence the bone growth trajectory and peak bone mineral density in adulthood²²¹. Epigenetic biomarkers, such as the measurement of *RXRA* and *CDKN2A* DNA methylation^{299,323}, are being investigated and utilised to predict bone health in later life and to investigate this further, DNA methylation of two transcription factors which are important in osteoblast differentiation and play a pivotal role in bone development were investigated³⁷⁵. Within the MAVIDOS trial, maternal cholecalciferol supplementation during pregnancy altered *Osterix* CpG methylation at birth and there were seasonal differences in methylation, however there were no differences in *Runx2* methylation between the two maternal treatment groups. Furthermore, methylation of both *Runx2* and *Osterix* were shown to be associated with bone measures at birth within the MAVIDOS trial and it would be interesting to determine associations in later childhood.

5.3.1 *Runx2* CpG methylation at birth results

Within the MAVIDOS trial, there were no significant differences in *Runx2* methylation at birth between the two maternal treatment groups, or when the analyses were stratified by season of birth. This suggests that maternal cholecalciferol supplementation during pregnancy does not alter DNA methylation of these CpG sites. However, within the MAVIDOS trial there was a significant positive association between *Runx2* methylation and bone measures at birth with intervention as a covariate suggesting that there is a link between *Runx2* methylation and bone measures at birth. *Runx2* is involved in differentiation into osteoblasts and plays a vital role in bone formation therefore, we hypothesised that methylation of *Runx2* would be associated with bone measures at birth. The lack of associations between maternal cholecalciferol supplementation and altered *Runx2* methylation, which would likely be linked to altered *Runx2* gene expression, could be part of a compensatory mechanism that protects the developing fetus from detrimental effects on bone formation that could arise due to vitamin D deficiency during pregnancy.

The *Runx2* CpGs of interest are located within the promoter region upstream of the *Runx2* transcriptional start site and methylation within the promoter region is often associated with gene repression. We have shown that maternal cholecalciferol supplementation during pregnancy is not associated with altered methylation of these CpG loci however, further sequencing of the *Runx2* promoter could identify differentially methylated CpG loci which could be associated with altered transcription factor binding or gene expression in response to maternal cholecalciferol

supplementation. It would be difficult to determine the effect of maternal vitamin D supplementation at the molecular level, due to differences between *in vivo* and *in vitro* supplementation. *In vitro* treatment of primary human osteoblasts with $1,25(\text{OH})_2\text{D}_3$ for 1 hour resulted in downregulation of Runx2 expression whereas treatment for 48 hours resulted in upregulation of Runx2 expression¹³². *In vitro* studies in rodent osteoblastic cells have shown that vitamin D supplementation downregulates Runx2 gene expression¹³¹ therefore, you would expect a decrease in differentiation of MSCs into osteoblasts and a decrease in the synthesis of Osteocalcin, Osteopontin and other proteins involved in mineralising the matrix, which would have a detrimental effect on bone health. Conversely, studies in rat calvaria osteoblast cultures have shown that $1,25(\text{OH})_2\text{D}_3$ treatment of mature osteoblasts resulted in upregulation of osteoblast associated genes such as *osteopontin* and *osteocalcin*¹³⁰. In order to maintain skeletal homeostasis it may be beneficial for Runx2 gene expression to remain unaltered. The positive associations between *Runx2* methylation and bone measures at birth provide supporting evidence to the use of these *Runx2* CpGs as a biomarker of bone health. It is possible that methylation of these CpG loci is not part of the causal pathway between vitamin D, DNA methylation and bone outcomes however, maternal cholecalciferol supplementation may improve bone strength through methylation of other genes, which alters gene expression and phenotype, and DNA methylation of *Runx2* is simply a marker of the altered bone state and has the potential to be used to predict individuals at risk of developing osteoporosis in later life.

5.3.2 *Osterix* CpG methylation at birth results

Within the MAVIDOS trial, infants born to the cholecalciferol supplemented group had lower *Osterix* CpG 6 methylation compared to the placebo group, which suggests that there is a link between maternal vitamin D supplementation and *Osterix* methylation. DNA methylation within the promoter region of a gene is often associated with gene repression and a decrease in gene expression therefore, lower methylation is likely associated with increased gene expression. This could result in differentiation of osteoprogenitor cells into mature osteoblasts resulting in an increase in bone formation. Conversely, the methylation difference measured is very small so it is unsure how functionally significant this will be. Further sequencing of this region upstream of the TSS could identify differentially methylated CpG loci which could be investigated further. Furthermore, the functional significance of the CpGs of interest could be investigated by site directed mutagenesis in a luciferase reporter system to determine the effect that altered methylation has on *Osterix* promoter activity.

The results showed that there was a positive association between methylation of CpG 7 and BMC at birth with intervention as a covariate, which is not in the direction that you would expect. If

maternal vitamin D supplementation has a beneficial effect on skeletal development, and it is linked to decreased *Osterix* DNA methylation in umbilical cord tissue, then you would expect an inverse association between *Osterix* DNA methylation and bone measures at birth. The *Osterix* CpGs of interest are located within the promoter region upstream of the TSS which is often associated with gene repression. The positive association suggests that with increasing *Osterix* methylation, and most likely a decrease in *Osterix* gene expression, there is an increase in BMC at birth. However, if methylation is associated with downregulation of *Osterix* expression, this could result in fewer osteoprogenitor cells being stimulated to differentiate into mature osteoblasts and osteocytes which become embedded in the bone matrix, which could have a detrimental effect on bone formation rather than a positive effect which results in improved BMC. There may be a compensatory mechanism involved such as an increase in proliferation which ultimately leads to an increase in BMC. Conversely, altered methylation may prevent the binding of a repressive transcription factor. We have shown that infants born to cholecalciferol supplemented mothers had lower *Osterix* CpG 6 methylation, albeit at an alternate CpG site, so a positive association would suggest lower methylation is associated with lower BMC which implies that maternal cholecalciferol supplementation during pregnancy has adverse effects on skeletal development. It would be interesting to determine whether there are associations with bone measures in later childhood, and the direction of the association. The differences in CpG behaviour could be due to the small sample size and the small differences in methylation. *Osterix* CpGs 6 and 7 are closely located to each other, with a difference of 31 bp, so you would expect both CpGs to have a similar methylation profile. Nonetheless, they may be co-regulated by other transcription factors or there may be an activator, repressor or insulator within this 31 bp region which may explain the different results. This could be investigated using transcription factor software such as MatInspector or through functional *in vitro* studies with luciferase reporter assays.

When the analyses were stratified by treatment allocation, there were no significant associations within the cholecalciferol supplemented group between *Osterix* methylation and bone measures at birth however, within the placebo group there was a significant inverse association between *Osterix* CpG 9 and BMC and BA at birth. Moreover, this is a different CpG site and the association is in the opposite orientation. It is possible that the functional importance of individual CpGs differs and has differing biological effects. *Osterix* CpG 9 is located 68 bp away from CpG 6, so the difference in direction of associations could be due to the presence of an activator or repressor within this genomic region. The *Osterix* CpGs of interest lie within a DNase 1 hypersensitive site which act as regulatory regions. This suggests that this may be an open chromatin region which is easily accessible by transcriptional machinery and transcription factors. Furthermore, the presence of nearby insulators or enhancers can contribute to the complex mechanism. There may be an

interaction between vitamin D and bone formation, such as differences in osteoblast proliferation or differentiation or through one of the many signalling pathways involved in osteoblast differentiation, and altered bone health. It would be interesting to determine associations in later childhood investigate whether there is a positive association with intervention as a cofactor and the relationship between associations within each individual intervention group.

When the analyses were stratified by season of birth, infants born in the spring months to cholecalciferol supplemented mothers had lower methylation at birth of *Osterix* CpGs 6 and 9 compared to the placebo group. The MAVIDOS trial showed improved BMC, BA and BMD in infants born in winter to cholecalciferol supplemented mothers, however these phenotypic changes were not reflected in DNA methylation of *Osterix* as there were no associations between *Osterix* CpG methylation and bone measures amongst babies born in winter. Furthermore, there were inverse associations between *Osterix* CpG methylation at birth and bone measures amongst infants born in the winter and summer months, whereas there were positive associations amongst the spring and autumn months. Furthermore, associations were significant amongst differing CpG sites which further supports the complex relationship between maternal cholecalciferol supplementation, UVB exposure, DNA methylation and infant bone measures.

5.3.3 Conclusion

There are limitations to these experiments, such as the use of umbilical cord tissue, tissue specific methylation and multiple testing, which have already been addressed in Chapters 4 and 5. DNA methylation of *Osterix* and *Runx2* was measured within the CpG shores and within putative DNase1 hypersensitive sites. Unfortunately, methylation values were very low (~5 %) which suggests that altered methylation of this region only affects a small amount of cells and tissues so may not be functionally important to altered phenotype. Future work would involve measuring methylation of CpGs further upstream of their respective promoters to identify differentially methylated regions. Fourth, the sample number for individual CpG sites were low due to samples failing internal controls, as well as samples being unmethylated at individual CpG sites. Furthermore, the low spread in DNA methylation would make finding a correlation very difficult. Conversely, a genome-wide array, such as an EPIC array, would be used to identify suitable differentially methylated regions upstream of the two gene promoters. Currently, 400 of the MAVIDOS samples have undergone genome-wide analysis using the EPIC array but the results are currently unavailable and could not be investigated within this thesis but this can be investigated further as results become available. Another limitation is that, as these two genes play an important role in osteoblast differentiation and bone development, it is unlikely that they would be expressed in umbilical cord tissue. Nonetheless, umbilical cord tissue contains Wharton's jelly which contains mesenchymal

stem cells that can differentiate into osteoblasts. The findings may reflect the capacity to differentiate into osteoblasts and with further investigation could potentially be used to predict the bone health trajectory in an individual.

In conclusion, maternal cholecalciferol supplementation during pregnancy was linked to altered *Osterix* CpG methylation at birth but not *Runx2* methylation at birth, whereas methylation of CpG loci within both genes were shown to be associated with bone measures at birth with intervention as a covariate. It would be interesting to determine associations in later childhood as these measurements become available. The DNA methylation profile of individual *Osterix* CpG loci differed and associations with bone measures at birth were in opposite directions. This suggests that the relationship is complex and there is not a clear mechanism. As these CpG sites are located within a DNase 1 hypersensitive site which are often regulatory regions, there could be recruitment of specific transcription factors or histone modifiers or there could be insulators or enhancers nearby to modulate the effects. In **Chapter 6**, the functional importance of the *RXRA* CpG loci of interest is investigated. Due to time constraints, this could not be applied to the *Osterix* and *Runx2* CpGs of interest however, there is scope to investigate this in the future. DNA methylation of *Runx2* and *Osterix* could be investigated further through bisulfite pyrosequencing to identify differentially methylated regions upstream of the respective TSS. This could identify novel biomarkers which could be used in combination with *RXRA* and *CDKN2A* to predict bone measures in later childhood and identify individuals that require suitable interventions during early infancy to prevent the risk of developing osteoporosis in later life.

**Chapter 6 Investigating the functional importance of
the *RXRA* differentially methylated CpGs on *RXRA*
promoter activity in osteosarcoma cell lines**

6.1 Introduction

DNA methylation at CpG sites within the *RXRA* region have been shown to be associated with scBMC in later childhood²⁹⁹, and we have shown in the MAVIDOS trial that maternal vitamin D supplementation during pregnancy is associated with altered *RXRA* methylation in umbilical cord tissue. The MAVIDOS trial found that infants born in winter to cholecalciferol supplemented mothers had greater bone measures compared to the placebo group²³⁶. We hypothesise a potential mechanistic link between *RXRA* methylation, vitamin D supplementation during the early life period, and later bone mineral content and density.

The functional relevance of the *CDKN2A* CpGs of interest, which were explored in Chapter 4, have been previously investigated by Lillycrop *et al.*, which showed that site directed mutagenesis of the CpGs of interest had a negative effect on ANRIL promoter activity and p14^{ARF} expression³²². Furthermore, analysis by electrophoretic mobility shift assays (EMSAs) found specific transcription factor binding across the *CDKN2A* CpGs of interest and that the methylation state of individual CpG loci altered transcription factor binding³²². The functional relevance of individual CpG loci on promoter activity of *RXRA*, *Runx2* and *Osterix* has not been investigated however, due to time constraints, only the CpGs of interest upstream of the *RXRA* were investigated further.

The *RXRA* gene is located on chromosome 9 and encodes for the retinoid X receptor which is part of the nuclear receptor family and the *RXRA* CpGs of interest lie within a differentially methylated region (DMR) 2.3 kb upstream of the *RXRA* transcriptional start site (TSS) (**Table 6.1**). *RXRA* forms a heterodimer with the vitamin D receptor (VDR) as well as other nuclear receptors such as the thyroid receptor (TR) and Constitutive Androstane Receptor (CAR). Upon ligand binding, VDR heterodimerises with *RXRA* and binds to vitamin D response elements (VDREs) in proximal promoters and regulatory regions of target genes where they induce changes in gene expression^{60,357}. We have shown that there is altered DNA methylation of this region in umbilical cord tissue in response to maternal cholecalciferol supplementation but it is unknown whether this region is associated with altered *RXRA* transcription which could affect phenotype. Causality is not required for risk prediction however, it could aid in the effectiveness and precision of targeted interventions, either during the early life environment or during early childhood which could promote peak bone mineral density in early adulthood.

To determine whether the differentially methylated CpGs influence *RXRA* transcription, functional investigation, including the use of luciferase reporter constructs and transcription factor binding, were investigated in two well-characterised osteosarcoma cell lines, Saos2 and MG63, to allow investigation into cells which have a direct effect on bone development, and transcription factor binding was additionally investigated in mesenchymal stem cells (MSCs) from umbilical cord tissue.

RXRA CpG	Distance upstream of TSS	Harvey et al., scBMC	MAVIDOS vitamin D vs placebo
1	2686		lower methylation
2	2682		lower methylation
3	2673		lower methylation
4	2649	Inverse	lower methylation
5	2642	Inverse	lower methylation
6	2554	Inverse	
7	2465		
8	2406	Inverse	
9	2391		
10	2387		
11	2385		
12	2357	Inverse	

Table 6.1 Summary of the *RXRA* CpG sites, current findings and their relation to the *RXRA* TSS.

RXRA = retinoid X receptor alpha, TSS = transcriptional start site. Associations between methylation and scBMC by Harvey et al.,²⁹⁹. Within the MAVIDOS trial, infants born to cholecalciferol supplemented mothers had lower methylation at *RXRA* CpGs 1-5.

6.1.1 Hypothesis

The DMR containing the *RXRA* CpGs of interest has a regulatory role on *RXRA* gene transcription and expression.

6.1.2 Aims

1. To determine whether individual *RXRA* CpGs upstream of the *RXRA* TSS alter *RXRA* promoter activity in osteosarcoma cell lines. This will be investigated by PCR mutagenesis in a luciferase reporter construct.
2. To determine whether the genomic region containing the *RXRA* CpGs of interest act as an enhancer or regulatory region and whether vitamin D treatment alters luciferase expression of this region. This will be investigated through cloning of the DMR into a luciferase reporter construct and through excision of genomic regions using established molecular cloning techniques.
3. To determine whether vitamin D treatment alters *RXRA* gene expression and *RXRA* CpG methylation in osteosarcoma cell lines. This will be investigated by culturing two osteosarcoma cell lines with 10 nM 1,25(OH)₂D₃ prior to RNA and DNA extraction.
4. To determine whether specific transcription factors bind over the *RXRA* CpGs of interest in osteosarcoma cell lines and mesenchymal stem cells (MSCs). This will be investigated both

in silico, using MatInspector software, and through radiolabelled electrophoretic mobility shift assays (EMSAs) to determine specific transcription factor binding.

6.2 Results

6.2.1 *In silico* analysis of the *RXRA* CpGs of interest

The *RXRA* CpGs of interest are located in a DMR 2.3 kb upstream of the transcriptional start site of the *RXRA* gene. To determine whether this region might be functionally important in modulating the level of *RXRA* transcription, *in silico* sequence analysis of this region was carried out using the ENCODE database.

6.2.1.1 *In silico* analysis shows that the *RXRA* CpGs of interest lie within a DNase 1 hypersensitive region

The ENCODE database has mapped DNase 1 hypersensitive peak clusters from 95 cell types across the *RXRA* DMR (**Figure 6.1**). DNase I hypersensitive sites are located in regulatory regions such as promoters, enhancers and insulators³⁷⁹. They have an open chromatin structure, devoid of nucleosomes, which make these regions highly susceptible to cleavage by DNase I endonucleases. Analysis of the *RXRA* promoter region identified several regions of DNase I hypersensitivity including a region spanning 770 bp (-2779 bp to -2010 bp with respect to the *RXRA* TSS) which encompasses the *RXRA* DMR (-2686 bp to -2357 bp).

6.2.1.2 The ENCODE database highlights histone mark enrichment across the *RXRA* DMR

To determine whether this region was also enriched in histone marks characteristic of specific regulatory elements, the ChIP-seq tracks on the ENCODE database were also examined (**Figure 6.1**). There was a large enrichment of H3K4Me1, which typically mark active or primed enhancers^{380,381} and they have been shown to protect regulatory regions from *de novo* DNA methylation³⁸², approximately 250 bp downstream of the DMR and a smaller peak across the DMR containing the *RXRA* CpGs of interest. There were two similarly sized peaks of H3K4Me3, which is often found at regions flanking the promoter³⁸¹ of actively transcribed genes³⁸³, approximately 700 bp upstream of the *RXRA* TSS and 600 bp downstream of the *RXRA* TSS, but no peak across the DMR. There was also enrichment of H3K27ac, which are often associated with active enhancers, across the same regions marked by H3K4me3, but there was no peak of H3K27ac across the DMR.

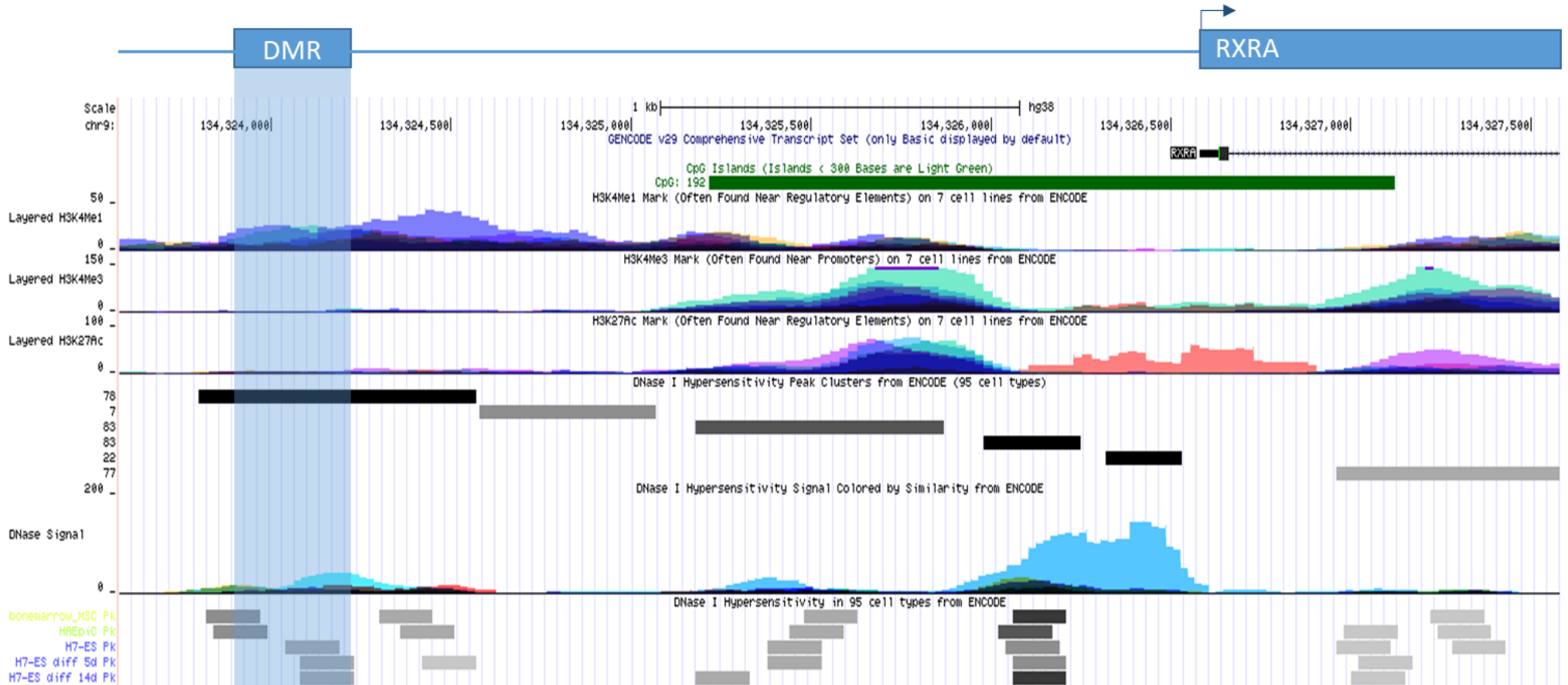


Figure 6.1 Histone marks and DNase 1 hypersensitive sites across *RXRA*.

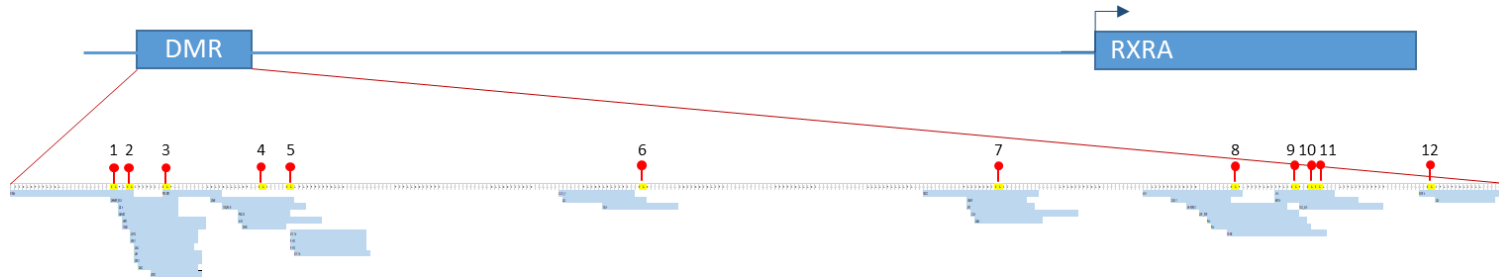
Data collected from the ENCODE project across a region 3 kb upstream of the *RXRA* transcriptional start site and 1 kb downstream of the *RXRA* transcriptional start site. The DMR region with the *RXRA* CpGs of interest has been highlighted in blue. Adapted from University of California Santa Cruz (UCSC) genome browser, date accessed 01.08.2019.

6.2.1.3 MatInspector analysis propose several putative transcription factor binding sites over the *RXRA* CpGs of interest

Having shown that the region containing the *RXRA* CpGs of interest contains histone enrichment of H3K4Me1 which is consistent with enhancer activity, although lacks enrichment of H3K27Ac which suggests that this region may be part of a primed enhancer rather than an active enhancer, MatInspector analyses were used to identify putative response element binding sites of transcription factors that could have a regulatory role in *RXRA* gene expression. First, potential transcription factor binding sites located directly over the *RXRA* CpGs of interest were examined (**Figure 6.2**). There was a predicted TWIST binding site over *RXRA* CpGs 2 and 3 of which heterodimerisation has been shown to be required for osteoblast differentiation; an ELK1 binding site over *RXRA* CpGs 3 and 4 which is a target of the Ras Raf MAPK signalling pathway, a CTCF insulator binding site over *RXRA* CpG 7 which mark insulators, a binding site for the RXRA:CAR heterodimer over *RXRA* CpG 8 and a predictive binding site for large Maf homodimers at *RXRA* CpG 12, which have been shown to play a key role in terminal differentiation of many tissues including bone³⁸⁴.

Potential transcription factor binding over the DMR containing the *RXRA* CpGs of interest was investigated. In the genomic region between *RXRA* CpGs 5 (-2642) and 6 (-2554), MatInspector analyses identified putative binding sites for glucocorticoid receptor (GR) which forms a homodimer with *RXRA* and has been found to bind to DNase1 hypersensitive sites³⁸⁵ (-2632 bp), a repressive binding site for GR (-2602 bp), a CTCF binding site (-2638), and a binding site for SOX9 which has been shown to play a role in chondrocyte differentiation and skeletal development (-2633 bp). In the genomic region between *RXRA* CpGs 6 (-2554) and 7 (-2465) there were additional binding sites for GR (-2516 bp) and CTCF (-2471 bp). In the genomic region between *RXRA* CpGs 7 (-2465) and 8 (-2406) there were predicted binding sites for thyroid hormone receptor beta (THRB) (-2452 bp) and *RXRA* (-2456 bp).

MatInspector analyses did not find any potential RXR:VDR binding sites within the DMR containing the *RXRA* CpGs of interest, however there were predicted binding sites closer to the *RXRA* TSS (-1975 bp, -1330 bp, -1254 bp, -923 bp, -822 bp, -738 bp and -240 bp).



1	2	3	4	5	6	7	8	9	10	11	12	Transcription Factor	More Information
												NRSE	Neural-restrictive-silencer-element
												CHREBP_MLX	Carbohydrate response element binding protein (CHREBP) and Max-like protein X (Mlx) bind as heterodimers to glucose-responsive promoters
												DICE	Downstream Immunoglobulin Control Element, interacting factor: BEN (also termed Mus-TRD1 and VBSCR11)
												GMEB2	Glucocorticoid modulatory element binding protein 2
												XBP1	X-box-binding protein 1
												TWIST	TWIST homolog of drosophila
												CMYC	Myelocytomatosis oncogene (c-myc proto-oncogene)
												ARNT	AhR nuclear translocator homodimers
												DEC2	Basic helix-loop-helix protein known as Dec2, Sharp1 or BHLHE41
												USF	Upstream stimulating factor
												ARNT	AhR nuclear translocator homodimers
												DEC1	Basic helix-loop-helix protein known as Dec1, Stra13, Sharp2 or BHLHE40
												ZBTB7	Zinc finger and BTB domain containing 7, Proto-oncogene FBI-1, Pokemon (secondary DNA binding preference)
												CREB	cAMP-responsive element binding protein
												TAX CREB	Tax/CREB complex
												PROX 1	Prospero homeobox protein 1, dimeric binding site
												ELK1	Elk-1
												WHN	Winged helix protein, involved in hair keratinization and thymus epithelium differentiation
												STAT6	STAT6: signal transducer and activator of transcription 6
												RFX1	X-box-binding protein RFX1
												RFX1	X-box-binding protein RFX1
												STAT6	STAT6: signal transducer and activator of transcription 6
												OCT3_4	POU domain, class 5, transcription factor 1
												SCX	Tendon-specific bHLH transcription factor scleraxis
												KLF	Kidney-enriched kruppel-like factor, KLF15
												ZBED4	Zinc finger, BED-type containing 4; GC-box binding sites
												SP1	Stimulating protein 1, ubiquitous zinc finger transcription factor
												CTCF	Insulator protein CTCF (CCCTC-binding factor)
												QLIS3	QLIS family zinc finger 3, Gli-similar 3
												PAX5	B-cell-specific activator protein
												ACAAT	Avian C-type LTR CCAAT box
												AHRARNT	Aryl hydrocarbon receptor / Arnt heterodimers
												CAR_RXR	Constitutive androstane receptor / retinoid X receptor heterodimer, DR4 sites
												P53	Tumor suppressor p53
												P53	Tumor suppressor p53
												ZF5	ZF5 POZ domain zinc finger, zinc finger protein 161 (secondary DNA binding preference)
												HMTF	Human motif ten element
												TAL1_E2A	T-cell acute lymphocytic leukemia 1, SCL
												MARE	Binding sites for homodimers of large Maf-proteins
												ZIC3	Zinc finger protein of the cerebellum (Zic3)

Figure 6.2 MatInspector analysis proposes several transcription factor binding sites across the *RXRA* CpGs of interest located in the differentially methylated region upstream of the *RXRA* promoter.

6.2.2 Site directed mutagenesis of specific *RXRA* CpG sites alters *RXRA* promoter activity in osteosarcoma cells

As the *in silico* analysis of the *RXRA* promoter suggested that the DMR may be located within an important regulatory region, the role of individual CpGs within the DMR on *RXRA* promoter activity was assessed. To do this, the *RXRA* promoter (-2680 bp to +86 bp) containing the core *RXRA* CpGs 3-12 was cloned upstream of the reporter gene luciferase in the vector, pGL4.17 basic, to create p*RXRAPromLuc* (**Figure.6.3A**). To investigate the functional importance of the CpGs, which have been shown to be predictive of later scBMC, *RXRA* CpGs 6, 8 and 12 were mutated individually (CpG to TpG) to create a series of constructs: p*RXRAPromLuc*-mutCpG6, -mutCpG8 and -mutCpG12 respectively. Unfortunately, CpGs 4 and 5 could not be successfully mutated within the *RXRA* promoter luciferase construct due to sequence constraints. Following mutagenesis, the wildtype and mutated *RXRA* promoter luciferase constructs were individually transfected into the human Saos2 and MG63 osteosarcoma cell lines. Firefly luciferase expression was measured to assess the effects of mutagenesis of the individual CpG sites within the DMR on *RXRA* promoter activity (**Figure.6.3B**).

In Saos2 cells, there was a significant decrease in luciferase expression following mutation of CpG 6 by 17 % ($p = 0.038$), a decrease of 45 % following mutation of CpG 8 ($p < 0.001$) and a decrease of 42 % following mutation of CpG 12 ($p < 0.001$) compared to wildtype p*RXRAPromLuc* luciferase expression. Similar results were seen in MG63 cells, with a significant decrease in luciferase expression following mutation of CpG 6 by 42 % ($p = 0.001$), a decrease of 32 % following mutation of CpG 8 ($p = 0.007$), and a decrease of 57 % following mutation of CpG 12 ($p < 0.001$) compared to wildtype p*RXRAPromLuc* expression (**Figure.6.3B**).

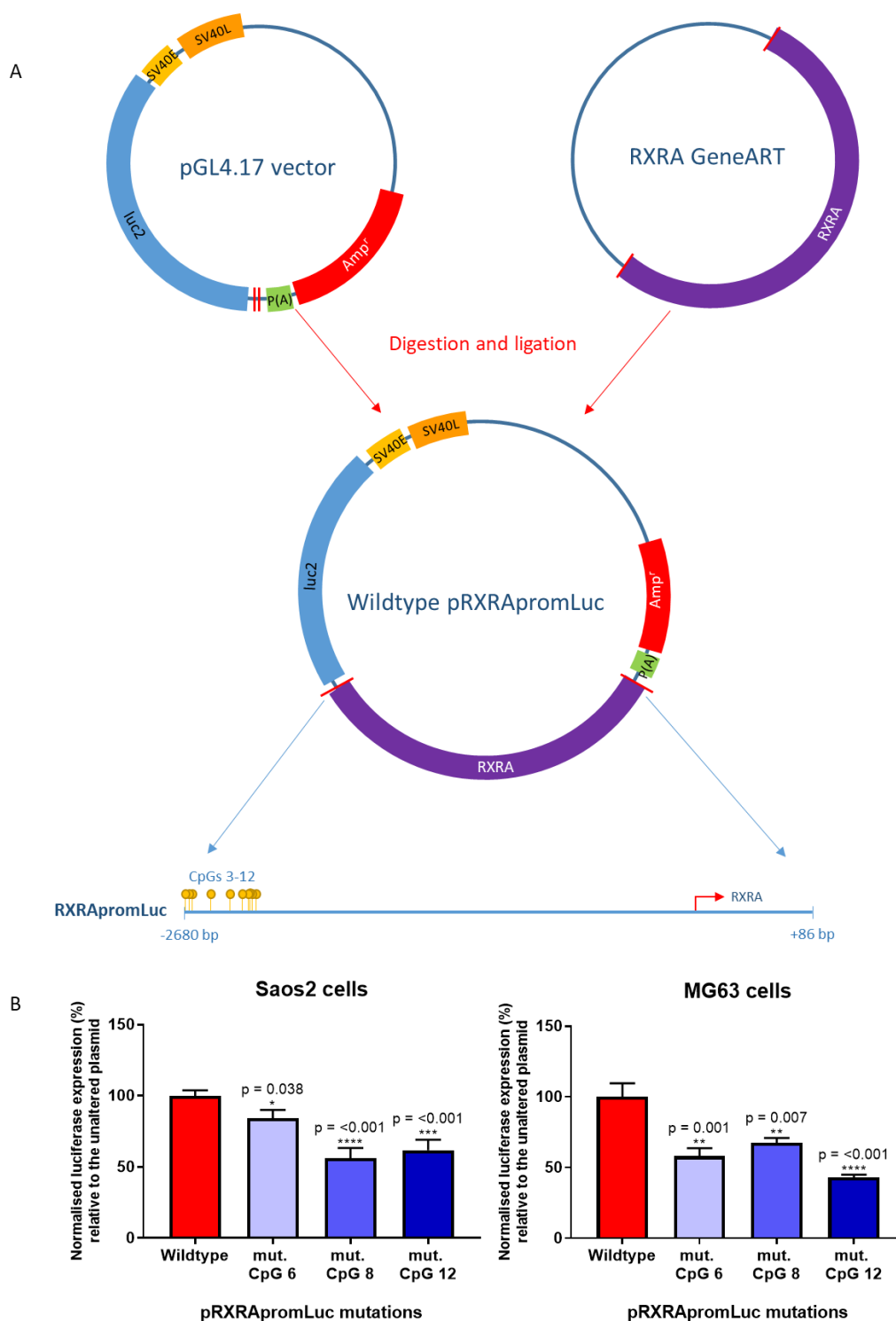


Figure.6.3 The effect of mutated pRXRApromLuc on RXRA expression in osteosarcoma cells.

A) The *RXRA* promoter insert (-2682 bp to +86 bp from *RXRA* TSS) was ligated upstream of the luciferase promoter in pGL4.17 to create wildtype pRXRApromLuc. Core *RXRA* CpGs of interest are highlighted in yellow and *RXRA* CpGs 6, 8 and 12 were mutated from CpG to TpG via PCR mutagenesis. SV40L = SV40 late poly(A) signal, SV40E = SV40 early enhancer/promoter, luc2 = luciferase reporter gene, p(A) = synthetic poly(A) signal, Amp^r = synthetic b-lactamase coding region. B) The wildtype and mutated pRXRApromLuc constructs were transfected into Saos2 cells using Fugene 6 or into MG63 cells using Lipofectamine 3000 for 24 hours. Firefly luciferase expression was normalised to CMV renilla expression and error bars show SEM. Independent t-tests with Welch's correction have been used, comparing the mutated constructs to wildtype, which has been set at 100 %. The average of two independent experiments have been used and each experiment consists of 6 replicates.

6.2.3 The DMR upstream of *RXRA* acts as an enhancer region in osteosarcoma cell lines.

6.2.3.1 The full *RXRA* enhancer region preferentially acts in the forward orientation upstream of the minimal promoter in osteosarcoma cell lines.

As site directed mutagenesis of the CpGs within the DMR led to a decrease in *RXRA* promoter activity, suggesting that these sequences are important for *RXRA* expression, and *in silico* analysis of the *RXRA* DMR suggested it may act as an enhancer, the *RXRA* DMR was cloned upstream of a heterologous weak promoter in the reporter vector pGL4.23 (**Figure 6.4A**). PCR was used to amplify the region -2930 bp to -2163 bp with respect to the *RXRA* TSS to create a full enhancer insert abbreviated to FenhLuc(CpGs1-12). This 739 bp region contains the 12 core *RXRA* CpGs of interest as well as additional flanking CpGs. The pGL4.23 plasmid contains a multiple cloning sequence 12 bp upstream of the minimal promoter, and an additional cloning region 1953 bp downstream of the minimal promoter. To investigate whether this region acts as an enhancer which can work when placed upstream, or downstream or in either orientation the FenhLuc(CpGs1-12) DNA insert was ligated upstream of the promoter in the forward orientation, upstream of the promoter in the reverse orientation, as well as in the forward orientation downstream of the minimal promoter. The three luciferase plasmids were individually transfected into osteosarcoma cells and luciferase expression was measured (**Figure 6.4B**) together with pGL4.23.

In Saos2 cells, ligation of the insert in the forward orientation upstream of the minimal promoter resulted in a significant ($p = 0.007$) 14 fold increase in luciferase expression compared to the control vector pGL4.23. Ligation of the insert in the reverse orientation upstream of the minimal promoter resulted in a significant 2.5 fold increase in luciferase expression ($p = 0.006$), while there was a 2 fold increase in luciferase expression when the insert was cloned in the forward orientation downstream of the minimal promoter ($p = 0.042$) compared to the control vector.

In MG63 cells there was an 18 fold increase in luciferase expression following ligation of the insert in the forward orientation upstream of the minimal promoter ($p < 0.001$), a 2.2 fold increase when ligated in the reverse orientation upstream of the minimal promoter ($p < 0.001$), and a decrease in luciferase expression by 30 % when ligated in the forward orientation downstream of the minimal promoter compared to the control vector ($p = 0.009$).

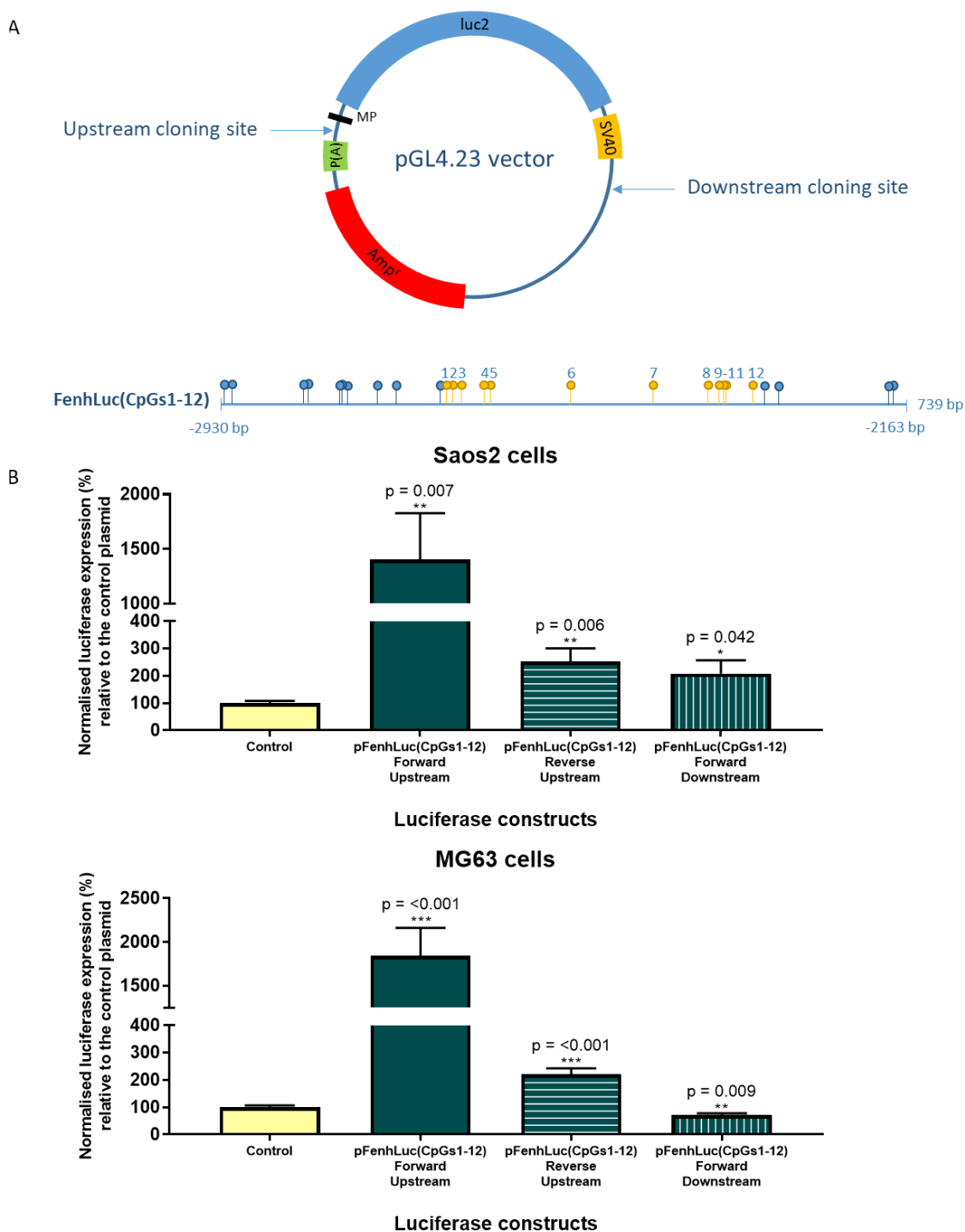


Figure 6.4 The effect of the orientation and positioning of the *RXRA* enhancer constructs in osteosarcoma cells.

A) The full *RXRA* enhancer region insert (FenhLuc(CpGs1-12)) was ligated in the forward orientation upstream of the minimal promoter, in the reverse orientation upstream of the minimal promoter and in the forward orientation downstream of the minimal promoter of pGL4.23. *RXRA* CpGs of interest are highlighted in yellow and additional CpGs are highlighted in blue. Amp^r = synthetic b-lactamase coding region, P(A) = synthetic poly(A) region, MP = minimal promoter, luc2 = luciferase reporter gene, SV40 = SV40 late poly(A) region. B) Saos2 cells transfected with Fugene 6 and MG63 cells transfected with Lipofectamine 3000 for 24 hours. Firefly luciferase expression was normalised to CMV renilla expression and error bars show SEM. Independent t-tests with Welch's correction compared luciferase expression between individual enhancer constructs and pGL4.23 (control, which has been set at 100 %). The average of two independent experiments have been used and each experiment consists of 6 replicates.

6.2.3.2 Removal of *RXRA* CpGs 1-3 in the full *RXRA* enhancer luciferase construct increases luciferase expression in osteosarcoma cells

Having shown that the *RXRA* enhancer region induced changes in luciferase reporter activity, we wanted to determine which of the CpGs sites within the enhancer region are important for its activity. The full *RXRA* enhancer region luciferase construct pFenhLuc(CpGs1-12), with the insert in the forward orientation upstream of the minimal promoter, was restricted into different fragments to create new constructs containing different portions of the full 739 bp region. Four additional constructs containing a subset of the CpGs: pFenhLuc(CpGs1-6), pFenhLuc(CpGs1-3), pFenhLuc(CpGs7-12) and pFenhLuc(CpGs4-12) were made. The core *RXRA* CpGs within each construct are depicted in parentheses and a schematic can be seen in **Figure 6.5A**. An additional enhancer region was amplified where the 5' region of the full enhancer region insert (-2930 bp to -2163 bp) was truncated and cloned into pGL4.23 to produce p5'truncFenhLuc(CpGs1-12) which spanned the region of -2756 bp to -2163 bp with respect to the *RXRA* TSS. The luciferase constructs were transfected into human osteosarcoma cell lines and luciferase expression was measured (**Figure 6.5B**).

In Saos2 cells, transfection with pFenhLuc(CpGs1-12) resulted in a 12 fold increase in luciferase expression compared to the control vector ($p = 0.001$), a 3.4 fold increase with pFenhLuc(CpGs1-6) ($p = 0.007$), a 4.6 fold increase with pFenhLuc(CpGs1-3) ($p = 0.029$), a 20 fold increase with pFenhLuc(CpGs7-12) ($p = 0.017$), a 46 fold increase with pFenhLuc(CpGs4-12) ($p = 0.012$) and a 3.3 fold increase with p5'truncFenhLuc(CpGs1-12) ($p = 0.007$) compared to the control vector (**Figure 6.5B**).

Similar results were observed in MG63 cells. Transfection of pFenhLuc(CpGs1-12) resulted in a 15.3 fold increase in luciferase expression compared to the control vector ($p < 0.001$), a 3.3 fold increase pFenhLuc(CpGs1-6) ($p = 0.001$), a 1.8 fold increase with pFenhLuc(CpGs1-3) ($p = 0.002$), a 32 fold increase with pFenhLuc(CpGs7-12) ($p = 0.019$), a 139 fold increase with pFenhLuc(CpGs4-12) ($p = 0.003$) and a 7 fold increase with p5'truncFenhLuc(CpGs1-12) ($p < 0.001$) compared to the control vector (**Figure 6.5B**).

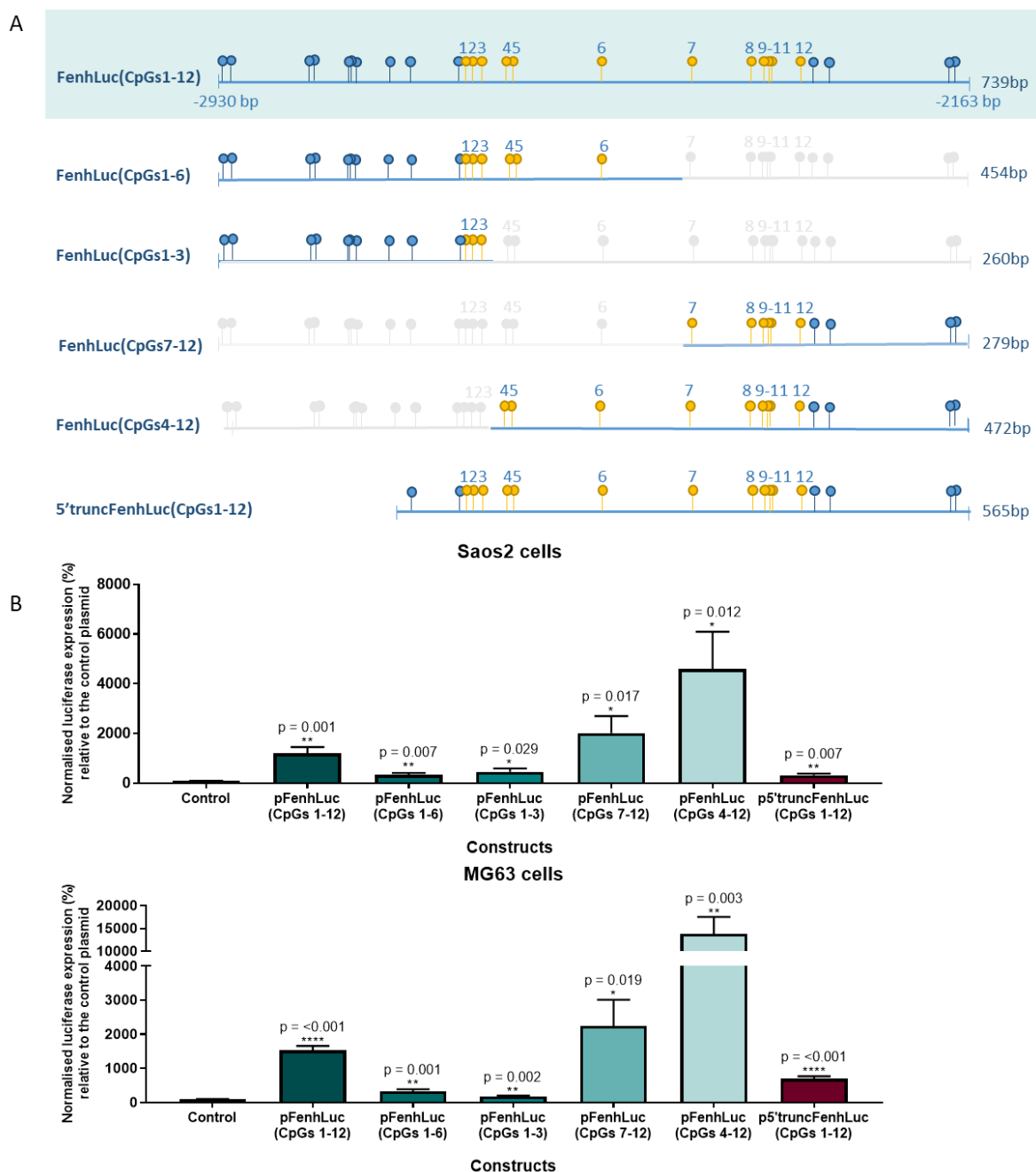


Figure 6.5 The effect of smaller fragments of the full *RXRA* enhancer region luciferase constructs in osteosarcoma cells.

A) The Full enhancer region insert was ligated in the forward orientation upstream of the luciferase promoter in pGL4.23 to create pFenhLuc(CpGs1-12). *RXRA* CpGs of interest are highlighted in yellow and additional CpGs are highlighted in blue. Further digestion of pFenhLuc(CpGs1-12) resulted in constructs containing specific core *RXRA* CpGs (1-3, 1-6, 7-12 and 4-12). A 5' truncated full enhancer region insert was also ligated upstream of the luciferase promoter in pGL4.23 to create p5'truncFenhLuc(CpGs 1-12). B) Saos2 cells transfected with Fugene 6 and MG63 cells transfected with Lipofectamine 3000 for 24 hours. Firefly luciferase expression was normalised to CMV renilla expression and error bars show SEM. Independent t-tests with Welch's correction compared luciferase expression between individual enhancer constructs and pGL4.23 (control, which has been set at 100 %). The average of two independent experiments have been used and each experiment consists of 6 replicates.

6.2.3.3 The *RXRA* minimal enhancer region increases luciferase expression in osteosarcoma cell lines

Deletion of the 5' region containing 10 flanking CpGs and the first three core *RXRA* CpGs of the full enhancer region construct (pFenhLuc(CpGs4-12)) dramatically increased luciferase expression following transfection into both human osteosarcoma cell lines. To investigate this further, a truncated *RXRA* enhancer region containing only the 12 core *RXRA* CpGs that lacked additional flanking CpGs was amplified by PCR and cloned into pGL4.23 to create the minimal enhancer region luciferase construct (pMenhLuc(CpGs1-12)) (**Figure 6.6A**). pMenhLuc(CpGs1-12) was further digested with the same combination of restriction enzymes used previously to create four additional minimal enhancer region luciferase constructs. The luciferase constructs were transfected into osteosarcoma cell lines and luciferase expression was measured (**Figure 6.6B**).

In Saos2 cells, there was a 14 fold increase in luciferase expression following transfection with pFenhLuc(CpGs1-12) ($p = 0.039$) and a 2 fold increase with p5'truncFenhLuc(CpGs1-12) ($p = 0.010$) compared to the control vector. Whereas following transfection with pMenhLuc(CpGs1-12), which contains the core *RXRA* CpGs and no additional flanking CpGs, there was a significant 116 fold ($p = 0.002$) increase in luciferase expression compared to the control vector. Similar results were seen in MG63 cells, with a 13 fold increase in expression following transfection with pFenhLuc(CpGs1-12) ($p = 0.001$), a 5 fold increase with p5'truncFenhLuc(CpGs1-12) ($p = 0.001$) and an 89 fold increase with pMenhLuc(CpGs1-12) compared to the control vector ($p = 0.001$).

Deletion analysis of the minimal enhancer region showed a complex relationship between the CpGs, with an overall similar pattern in both cell types however some cell type specific differences were also exhibited for some constructs. In Saos2 cells, overall luciferase expression was greater than in MG63 cells. Removal of the first 6 core *RXRA* CpGs (pMenhLuc(CpGs7-12)) increases luciferase expression to a similar magnitude (124 fold, $p = 0.014$) as the wildtype pMenhLuc(CpGs1-12) (116 fold), whereas transfection with the first 6 core *RXRA* CpGs (pMenhLuc(CpGs1-6)) results in a greatly reduced response in luciferase expression (7.8 fold, $p = 0.004$). Both transfection with only the first 3 core *RXRA* CpGs (pMenhLuc(CpGs1-3)) or with the removal of the first 3 core *RXRA* CpGs (pMenhLuc(CpGs4-12)) resulted in a similar increase in luciferase expression (64.4 fold, $p = 0.012$ and 75.5 fold, $p = 0.018$ respectively). In MG63 cells, the additional constructs derived from pMenhLuc(CpGs1-12) did not increase luciferase expression to the same magnitude as the wildtype pMenhLuc(CpGs1-12) (89 fold). There was a 4.3 fold increase in luciferase expression following transfection with pMenhLuc(CpGs1-6) ($p = 0.008$), a 12.5 fold increase with pMenhLuc(CpGs1-3) ($p < 0.001$), a 23.4 fold increase with pMenhLuc(CpGs7-12) ($p < 0.001$) and a 36 fold increase in luciferase expression following transfection with pMenhLuc(CpGs4-12) ($p = 0.002$).

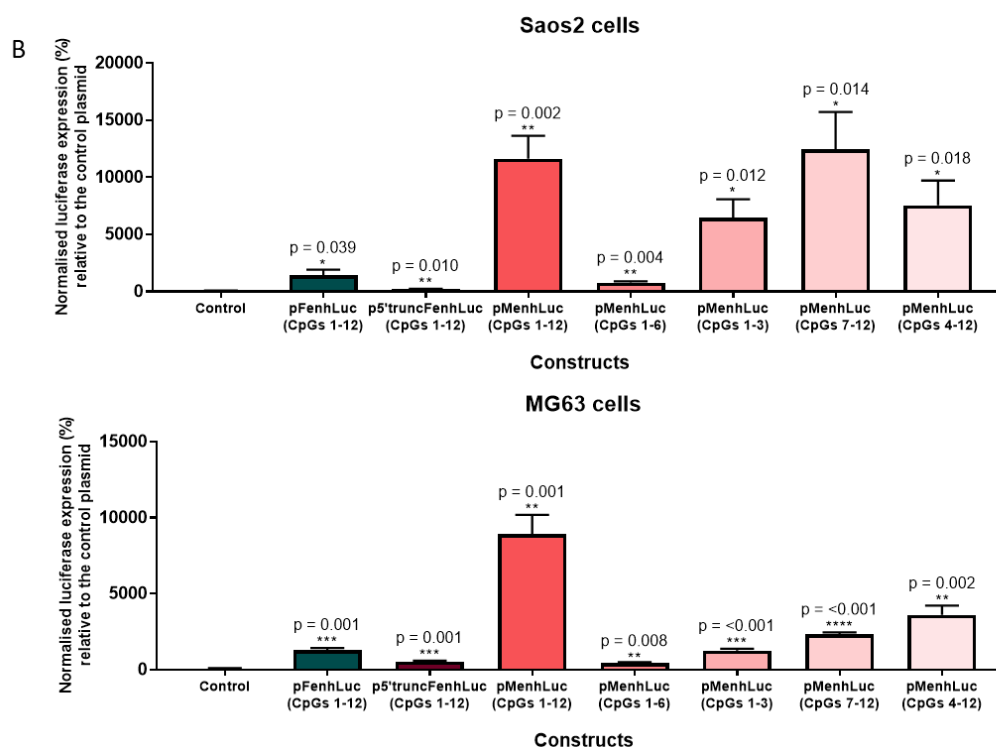
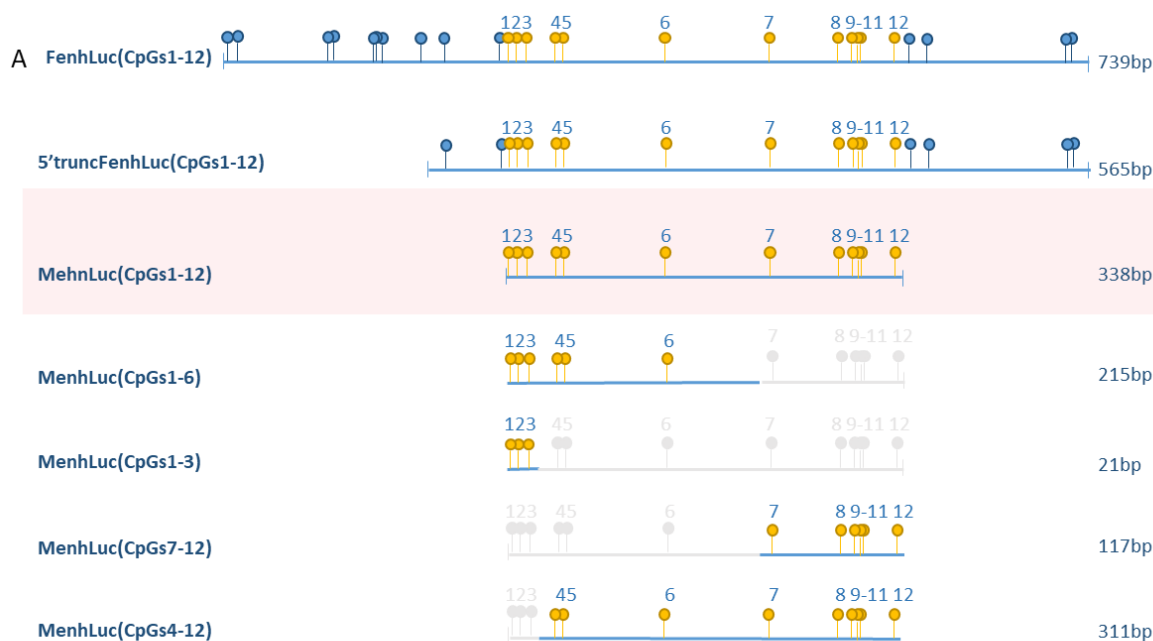


Figure 6.6 The effect of the minimal *RXRA* enhancer region luciferase constructs in osteosarcoma cells.

A) The Full enhancer region insert (FenhLuc(CpGs 1-12)), 5' truncated full enhancer region insert (5'truncFenhLuc(CpGs 1-12)) and the minimal enhancer region insert (MehnLuc(CpGs 1-12)) were ligated in the forward orientation upstream of the luciferase promoter in pGL4.23. *RXRA* CpGs of interest are highlighted in yellow and additional CpGs are highlighted in blue. Further digestion of pMehnLuc(CpGs 1-12) resulted in constructs containing specific core *RXRA* CpGs (1-3, 1-6, 7-12 and 4-12). B) Saos2 cells transfected with Fugene 6 and MG63 cells transfected with Lipofectamine 3000 for 24 hours. Firefly luciferase expression was normalised to CMV renilla expression and error bars show SEM. Independent t-tests with Welch's correction compared luciferase expression between individual enhancer constructs and pGL4.23 (control, which has been set at 100 %). The experiment consists of 6 replicates.

6.2.3.3.1 *RXRA* CpG mutations within the minimal enhancer region decrease luciferase expression in osteosarcoma cell lines

We have shown that transfection of the minimal enhancer region containing the core *RXRA* CpGs (pMenhLuc(CpGs1-12)) results in a large increase in luciferase expression. To establish what contribution the CpGs of interest make to the magnitude of luciferase expression, the effect of mutating *RXRA* CpGs which have been shown to be predictive of scBMC in the SWS cohort was investigated. The luciferase constructs were transfected into human osteosarcoma cell lines and luciferase expression was measured (**Figure 6.7**).

In Saos2 cells, there was a significant decrease in luciferase expression following transfection with mutated *RXRA* CpG 5 by 48 % ($p = 0.005$) and a decrease of 49 % following mutation of CpG 6 ($p = 0.006$) compared to the wildtype minimal enhancer region construct (pMenhLuc(CpGs1-12)). There were no significant differences in luciferase expression following mutation of *RXRA* CpGs 4, 8 or 12. In MG63 cells, there was a significant decrease in luciferase expression following transfection with mutated *RXRA* CpG 4 by 51 % ($p = 0.001$), a decrease of 80 % following mutation of CpG 5 ($p < 0.001$), a decrease of 31 % following mutation of CpG 6 ($p = 0.044$) and a decrease of 33 % following mutation of CpG 8 ($p = 0.032$) compared to the wildtype construct (pMenhLuc(CpGs1-12)). There were no significant differences in luciferase expression following mutation of *RXRA* CpG 12 compared to the wildtype construct (pMenhLuc(CpGs1-12)).

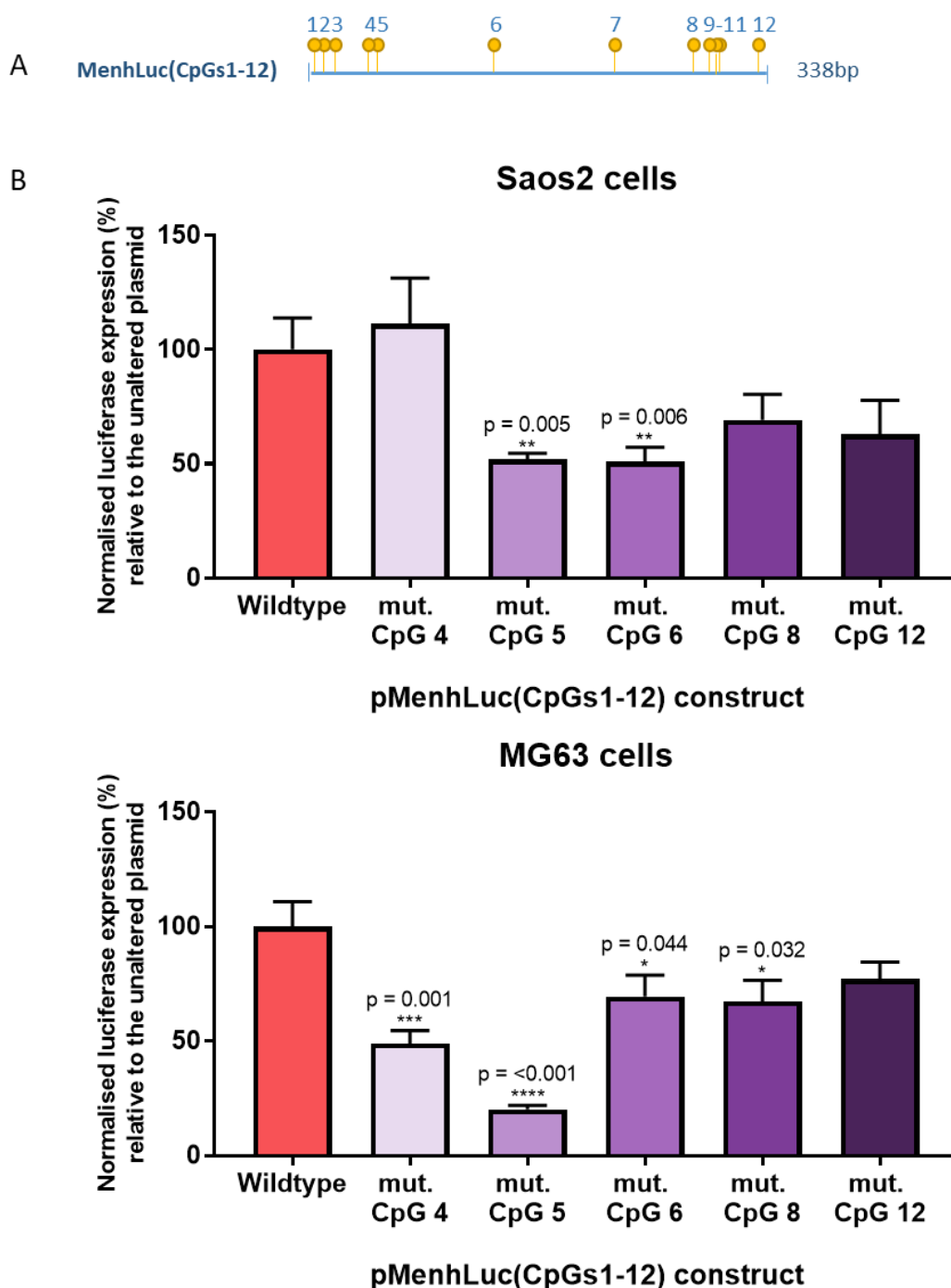


Figure 6.7 The effect of mutating the minimal *RXRA* enhancer region luciferase constructs in osteosarcoma cell lines.

A) The minimal enhancer region insert was ligated in the forward orientation upstream of the luciferase promoter in pGL4.23 to create pMenhLuc(CpGs 1-12). *RXRA* CpGs of interest are highlighted in yellow and additional CpGs are highlighted in blue. *RXRA* CpGs 4, 5, 6, 8 and 12 were mutated from CpG to TpG via PCR mutagenesis in construct pMenhLuc(CpGs 1-12). B) Saos2 cells transfected with Fugene 6 and MG63 cells transfected with Lipofectamine 3000 for 24 hours. Firefly luciferase expression was normalised to CMV renilla expression and error bars show SEM. Independent t-tests with Welch's correction compared luciferase expression between individual enhancer constructs and wildtype pMenhLuc(CpGs1-12) (which has been set at 100%). The average of two independent experiments have been used and each experiment consists of 6 replicates.

6.2.4 Short term *in vitro* vitamin D treatment in osteosarcoma cell lines alters *RXRA* gene expression, methylation and *RXRA* linked luciferase expression

6.2.4.1 Short term *in vitro* vitamin D treatment in osteosarcoma cells alters *RXRA* gene expression

Vitamin D supplementation during pregnancy is associated with altered *RXRA* methylation in umbilical cord within the MAVIDOS trial (**109Chapter 3**), therefore we investigated the effect of vitamin D treatment in two osteosarcoma cell lines on *RXRA* gene expression.

Gene expression in Saos2 and MG63 cell lines after treatment with $1,25(\text{OH})_2\text{D}_3$ was measured. Saos2 and MG63 cells are both derived from patients with osteosarcoma and share some osteoblastic properties, although the overall phenotypic profiles of both cells have been shown to be different. Both cell lines have been shown to express $1,25(\text{OH})_2\text{D}_3$ receptors^{386,387}. To represent the conditions that occur during luciferase transfections, where cells are transfected 24 hours after seeding and lysed 48 hours after seeding, the human osteosarcoma cell lines were treated with 10 nM $1,25(\text{OH})_2\text{D}_3$ 30 hours post the initial seeding, for a total of 18 hours prior to harvest. Following RNA extraction, gene expression of *RXRA*, *VDR*, *CYP24A1*, *Runx2* and *Osterix* was measured by qRT-PCR (**Figure 6.8**).

The *CYP24A1* enzyme is involved in the breakdown of both the inactive and active forms of vitamin D, and acts as a marker for *VDR* activation due to the presence of a VDRE within its promoter. Following treatment of Saos2 and MG63 cells with 10 nM $1,25(\text{OH})_2\text{D}_3$ there was up-regulation of *CYP24A1* gene expression (both $p = 0.0001$). In Saos2 cells, *Osterix* expression was down-regulated following treatment with $1,25(\text{OH})_2\text{D}_3$ ($p = 0.009$) and there were no significant differences in expression of *RXRA*, *VDR* or *Runx2* following vitamin D treatment. In MG63 cells, following $1,25(\text{OH})_2\text{D}_3$ treatment there was downregulation of *RXRA* expression ($p = 0.005$) and upregulation of *VDR* expression ($p = 0.022$) but there were no significant differences in *Osterix* or *Runx2* expression.

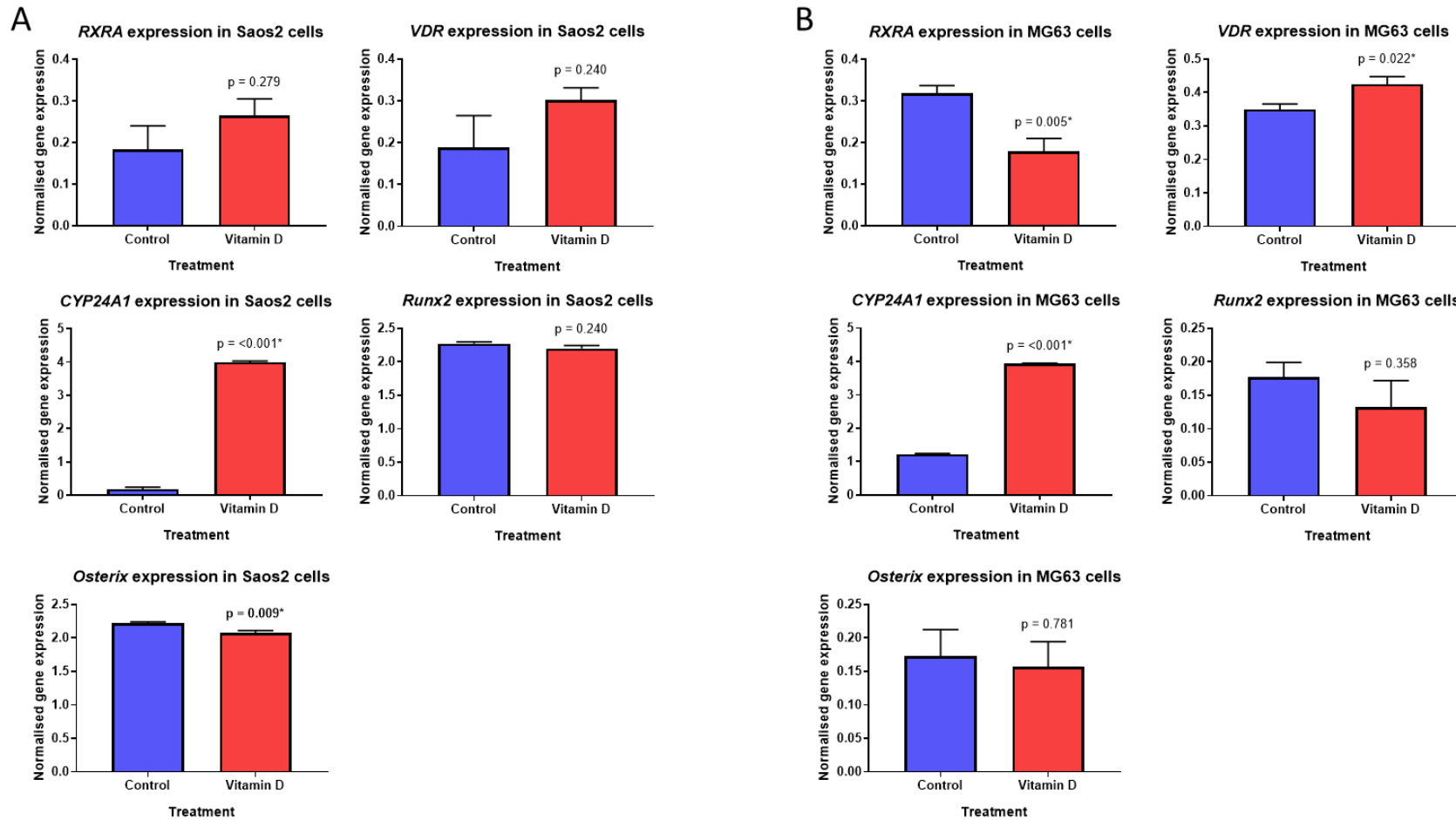


Figure 6.8 Gene expression of osteosarcoma cell lines treated with vitamin D.

Saos2 (A) and MG63 (B) cells treated with 10 nM $1,25(\text{OH})_2\text{D}_3$ or ethanol control for 18 hours. Gene expression was normalised using $\Delta\Delta\text{Ct}$. Independent t-tests with Welch's correction compared differences between the vitamin D treatment and control, error bars show SEM. *RXRA* = retinoid X receptor alpha, *VDR* = vitamin D receptor.

6.2.4.2 Short term in vitro vitamin D treatment in osteosarcoma cells alters *RXRA* methylation

Having shown that vitamin D treatment of human osteosarcoma MG63 cells down-regulated *RXRA* expression and did not significantly alter *RXRA* expression in Saos2 cells, DNA methylation of the *RXRA* CpGs of interest was examined in both cell types (**Figure 6.9 and Table 6.2**). *RXRA* CpG methylation in Saos2 cells varied across the region, with methylation of CpG -1 at around 9 % and methylation of CpG 12 at around 70 %, whereas in MG63 cells, methylation at CpG -1 was around 90 % and methylation at CpG 12 was around 80 %. In Saos2 cells, vitamin D treatment induced increased methylation of *RXRA* CpG 8 ($p = 0.049$, mean difference = 2.3 %, 95 % CI: -4.65, -0.02), and in MG63 cells there was significantly increased methylation of both *RXRA* CpGs 1 ($p = 0.003$, mean difference = 3.3 %, 95 % CI: -5.24, -1.41) and 12 ($p = 0.010$, mean difference = 2.1 %, 95 % CI: -3.52, -0.61).

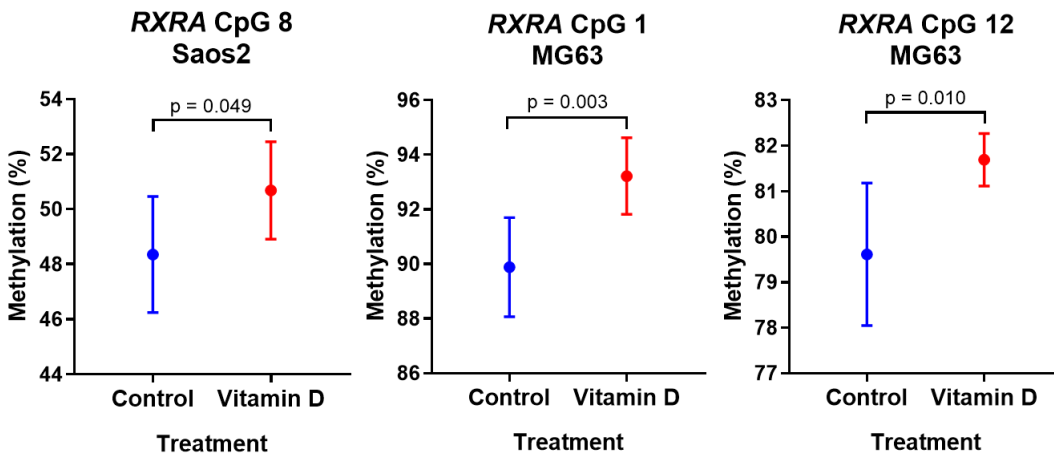


Figure 6.9 Boxplots of *RXRA* CpG methylation in osteosarcoma cells following treatment with 10 nM 1,25(OH)₂D₃.

Saos2 and MG63 cells treated with 10 nM 1,25(OH)₂D₃ or ethanol control for 18 hours. Independent t-tests compared % methylation between the vitamin D treated and control treated osteosarcoma cells. Graphs shows mean and 95 % confidence intervals. *RXRA* = retinoid X receptor alpha.

Table 6.2 *RXRA* methylation of osteosarcoma cell lines treated with vitamin D.

<i>RXRA</i> CpG	Saos2					MG63				
	n	Mean (%)	Mean diff. (%)	(95% CI)	p	n	Mean (%)	Mean diff. (%)	(95% CI)	p
-1	12	9.0	1.9	(-2.895, 6.679)	0.399	11	92.7	-2.7	(-6.304, 0.951)	0.129
1	12	9.8	1.2	(-3.981, 6.409)	0.615	11	91.7	-3.3	(-5.240, -1.41)	0.003 *
2	12	26.8	-0.1	(-4.815, 4.639)	0.968	11	94.2	-1.4	(-3.341, 0.441)	0.118
3	12	8.5	3.5	(-2.533, 9.619)	0.223	11	81.9	-0.8	(-2.395, 0.861)	0.316
4	12	21.9	-1.1	(-4.408, 2.119)	0.451	11	93.9	-1.2	(-3.339, 0.881)	0.222
5	12	22.6	0.1	(-3.108, 3.349)	0.937	11	90.9	-0.3	(-3.795, 3.111)	0.828
8	11	49.6	-2.3	(-4.647, 0.019)	0.049*	10	88.2	-2.3	(-4.777, 0.161)	0.064
9	11	39.2	-1.3	(-3.660, 1.159)	0.269	10	73.1	-2.7	(-6.919, 1.471)	0.173
10	11	66.1	-0.8	(-3.121, 1.529)	0.456	10	87.1	-0.8	(-3.462, 1.941)	0.534
11	11	51.6	0.0	(-3.416, 2.679)	0.789	10	76.7	-0.9	(-3.270, 1.421)	0.393
12	12	70.4	-2.6	(-6.606, 1.439)	0.183	12	80.7	-2.1	(-3.521, -0.61)	0.010*

Saos2 and MG63 cells treated with 10 nM 1,25(OH)₂D₃ or ethanol control for 18 hours. Independent t-tests compared % methylation between the vitamin D treated and control treated osteosarcoma cells.

6.2.4.3 Vitamin D supplementation increases *RXRA* linked luciferase expression in Saos2 cells only

Analysis of putative binding sites using MatInspector identified seven potential RXR:VDR binding sites within the *RXRA* promoter luciferase construct (p*RXRA*promLuc) although not over the DMR of interest and additional binding sites of nuclear receptors over the DMR. Treatment with 10 nM 1,25(OH)₂D₃ following transfection of the *RXRA* promoter luciferase construct into osteosarcoma cell lines could potentially stimulate luciferase expression. To test this, following transfection of p*RXRA*promLuc into Saos2 and MG63 cells, the cells were treated with 10 nM 1,25(OH)₂D₃ or the vehicle control for 18 hours and luciferase expression was measured. In Saos2 cells there was a significant 1.8 fold increase in luciferase expression following vitamin D treatment ($p = 0.002$) whereas there was no significant response in MG63 cells (**Figure 6.10**).

Having previously shown that site directed mutagenesis of *RXRA* CpGs 6, 8 and 12 within the p*RXRA*promLuc construct significantly decreased luciferase expression compared to wildtype p*RXRA*promLuc expression in both cell lines, we tested the response of these altered DNA constructs to vitamin D supplementation. There was a significant 2.9 fold increase in luciferase expression following transfection with mutated *RXRA* CpG 6 (p*RXRA*prom-mutCpG6, $p < 0.001$), a 2.4 fold increase with CpG 8 (p*RXRA*promLuc-mutCpG8, $p < 0.001$) and a 3 fold increase with CpG 12 (p*RXRA*prom-mutCpG12, $p = 0.001$) compared to their respective vehicle controls. There were no significant differences in MG63 cells. To compare the level of response to vitamin D supplementation in the altered DNA constructs in comparison to the level of response in the wildtype construct, independent t-tests with Welch's correction were used to compare luciferase expression of the vitamin D treated mutated promoter constructs (p*RXRA*promLuc- mutated CpGs 6, 8 and 12) against the vitamin D treated wildtype promoter construct (p*RXRA*promLuc) (data not shown). In Saos2 cells treated with vitamin D there was a significant decrease in luciferase expression with mutated *RXRA* CpG 8 ($p = 0.001$) compared to wildtype p*RXRA*promLuc, however; there were no significant differences in luciferase expression following mutation of *RXRA* CpG 6 or CpG 12 compared to the wildtype construct (p*RXRA*promLuc). In MG63 cells treated with vitamin D there was a significant decrease in luciferase expression following transfection with mutated *RXRA* CpG 6 ($p = 0.009$), CpG 8 ($p = 0.008$) and CpG 12 ($p = 0.001$) compared to the wildtype control (p*RXRA*promLuc).

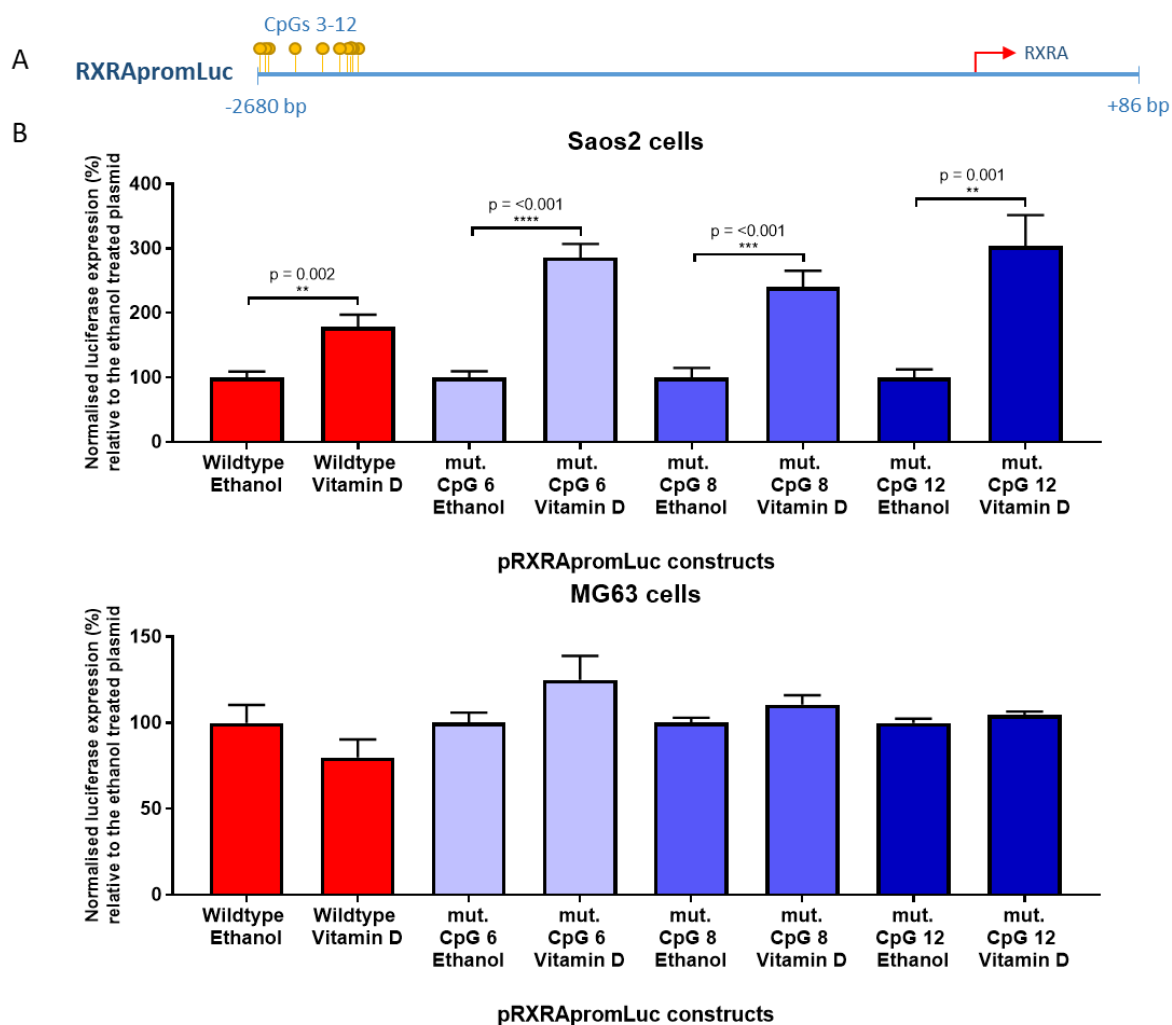


Figure 6.10 The effect of vitamin D treatment on *RXRA* expression following transfection with wildtype and mutated p*RXRA*promLuc constructs in osteosarcoma cells.

A) The *RXRA* promoter insert (-2682 bp to +86 bp from *RXRA* TSS) was ligated upstream of the luciferase promoter in pGL4.17 to create wildtype p*RXRA*promLuc. Core *RXRA* CpGs of interest are highlighted in yellow and *RXRA* CpGs 6, 8 and 12 were mutated from CpG to TpG via PCR mutagenesis. B) Saos2 cells were transfected with Fugene 6 and MG63 cells transfected with Lipofectamine 3000 for 24 hours. 6 hours post transfection, osteosarcoma cells were treated with 10 nM 1,25(OH)₂D₃ or an ethanol control for 18 hours. Firefly luciferase expression was normalised to CMV renilla expression and error bars show SEM. The ethanol controls have been set at 100 % and ethanol vitamin D treated construct has been adjusted to the ethanol control. Independent t-tests with Welch's correction compared luciferase expression between the ethanol and vitamin D treated luciferase reporter constructs. The average of two independent experiments have been used and each experiment consists of 6 replicates.

6.2.4.4 The minimal enhancer *RXRA* region responds to vitamin D treatment and site specific mutations prevent a luciferase response to vitamin D in osteosarcoma cell lines

Having shown that the vitamin D supplementation induced a response in luciferase expression from the p*RXRA*promLuc construct in Saos2 cells, the smaller pMenhLuc(CpGs1-12) DNA construct was tested in response to 10 nM vitamin D or the vehicle control for 18 hours and luciferase expression was measured (**Figure 6.11**). In Saos2 cells there was a significant decrease in luciferase expression following transfection with vitamin D treated pMenhLuc(CpGs 1-12) ($p = 0.03$) whereas in MG63 cells there was a significant increase in luciferase expression ($p = 0.026$). Site directed mutagenesis of CpGs 4, 5, 6, 8 and 12 to TpG altered the response to vitamin D treatment. In both human osteosarcoma cell lines, mutations at these *RXRA* CpG sites within pMenhLuc(CpGs 1-12) prevented a response to vitamin D treatment compared to the vehicle control.

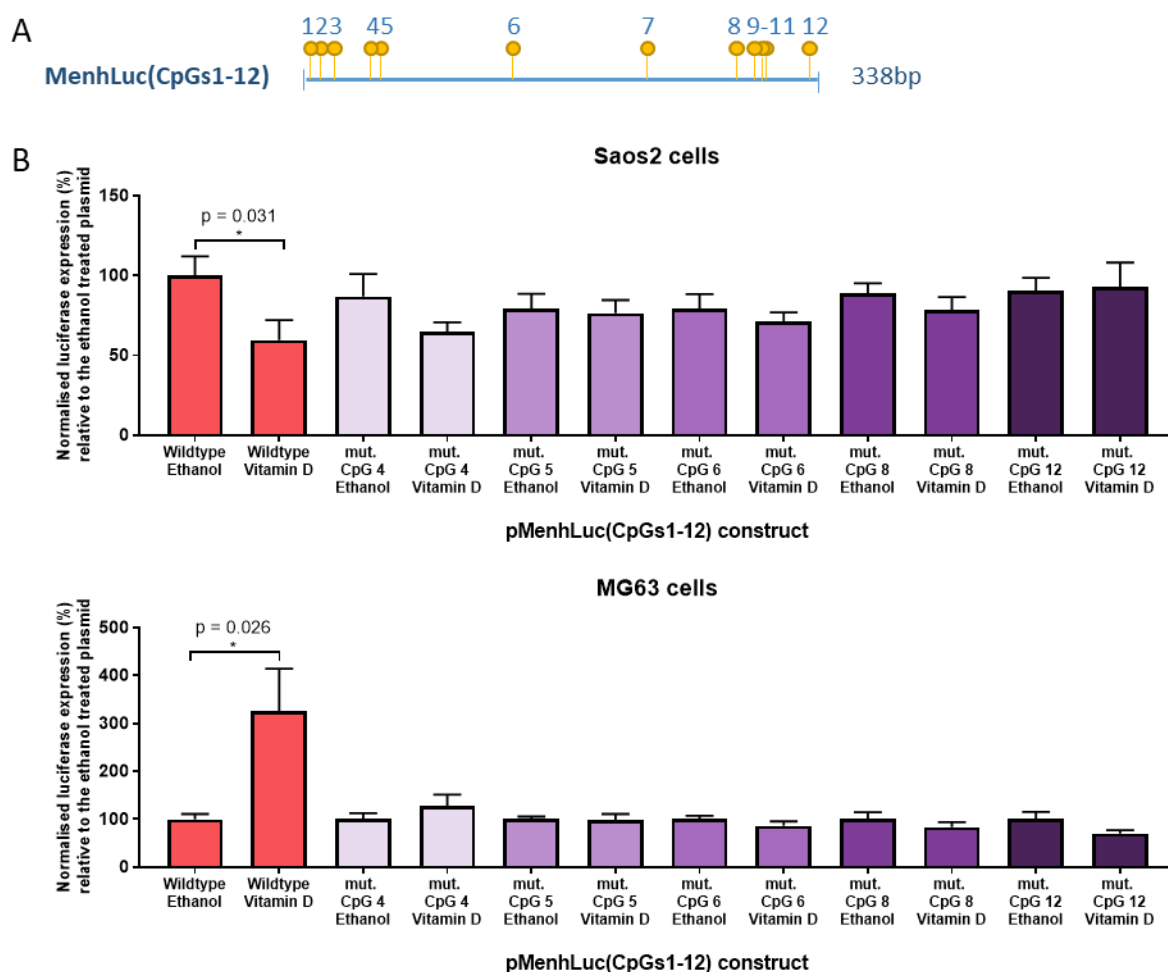


Figure 6.11 The effect vitamin D on the mutated minimal *RXRA* enhancer region luciferase constructs in osteosarcoma cell lines.

A) The minimal *RXRA* enhancer region insert (pMenhLuc(CpGs1-12)) were ligated in the forward orientation upstream of the luciferase promoter in pGL4.23. *RXRA* CpGs of interest are highlighted in yellow and additional CpGs are highlighted in blue. *RXRA* CpGs 6, 8 and 12 were mutated from CpG to TpG via PCR mutagenesis in pMenhLuc(CpGs1-12). B) Saos2 cells transfected with Fugene 6 and MG63 cells transfected with Lipofectamine 3000 for 24 hours. 6 hours post transfection, osteosarcoma cells were treated with 10 nM 1,25(OH)₂D₃ or ethanol control for 18 hours. Firefly luciferase expression was normalised to CMV renilla expression and error bars show SEM. Luciferase expression of each ethanol control has been set at 100 % and the vitamin D constructs have been normalised to their respective ethanol control. An independent t-test has been used on each ethanol and vitamin D pair. The experiment consists of 6 replicates.

6.2.5 Specific transcription factors bind across *RXRA* CpGs 4-5 in MG63 cells

To investigate specific transcription factor binding across the *RXRA* CpGs of interest, radiolabelled electrophoretic mobility shift assays (EMSAs) were used. MatInspector analyses identified putative nuclear factor binding sites over the *RXRA* CpGs of interest, such as the binding site for GR near to

CpG 5 and the binding site for CAR over CpG 8 (**Figure 6.13**). The binding site for GR consists of a symmetric consensus hexameric half site separated by 3 linker base pairs (**Figure 6.12**) which is also similar for the progesterone receptor (PR), androgen receptor (AR) and mineralocorticoid receptor (MR)³⁵⁷. The binding site for CAR is similar to that of the thyroid receptor (TR) therefore we hypothesised that these nuclear receptors may bind to the radiolabelled probes.

Symmetric sites

→ ←
AGACCA n TGTCT

n = 3		GR – GR PR – PR AR – AR MR – MR
-------	--	--

Direct repeats

→ →
AGGTCA n AGGTCA

n = 1	RXR-	RXR RAR PPAR COUP
n = 2	RXR-	PPAR RevErb – RevErb
n = 3	RXR-	VDR VDR – VDR
n = 4	RXR-	TR LXR CAR
n = 5	RXR-	RAR NGFI-B

Figure 6.12 Consensus DNA binding site motifs for nuclear receptors³⁵⁷.

GR = glucocorticoid receptor, PR = progesterone receptor, AR = androgen receptor, MR = mineralocorticoid receptor, RAR = retinoid alpha receptor, PPAR = peroxisome proliferator activated receptor, COUP = chicken ovalbumin upstream promoter, VDR = vitamin D receptor, TR = thyroid receptor, LXR = liver X receptor, CAR = constitutive androstane receptor, NGFI-B = nerve growth factor induced receptor.

Four radiolabelled probes were designed across *RXRA* CpGs 1-3, 4-5, 8 and 12 and putative binding sites from MatInspector analysis can be seen in **Figure 6.13**. To investigate whether specific transcription factors bind across the *RXRA* CpG sites of interest nuclear extracts were made from Saos2 cells, MG63 cells and MSCs from umbilical cord. Radioactive probes against *RXRA* CpGs 1-3, 4-5, 8-11 and 12 were used to investigate whether there was any specific transcription factor binding. Initial EMSAs were carried out in duplicate consisting of 4 lanes including the probe alone, the probe plus nuclear extract, non-specific binding where the nuclear extract was incubated with

a non-specific oligonucleotide sequence that does not match the probe sequence of interest and the 4th lane was used to investigate specific binding (cold competitor), where the nuclear extract was incubated with the non-radioactive oligonucleotide sequence that matches the probe of interest. It is expected that the band pattern produced from probe plus extract (lane 2) and non-specific competitor (lane 3) are similar, whereas if there is specific binding it is expected that the cold competitor would bind to the nuclear extract during the incubation prior to the addition of the radioactive labelled probe and there would be no band present.

Transcription factor binding varied between the three cell types for each of the 4 probes (**Figure 6.14**). Across *RXRA* CpGs 1-3, transcription factor binding was weaker in MG63 cells and MSCs compared to in Saos2 cells. In both Saos2 cells and MSCs there were no specific transcription factors bound that could be competed out with a specific *RXRA* CpGs 1-3 cold competitor.

Across *RXRA* CpGs 4-5, in Saos2 cells band 4 was competed out by unradiolabelled competitor. Bands 5 and 6 were fainter following incubation with the non-specific competitor and competed out by unradiolabelled competitor. In MG63 cells, bands 2 - 6 were fainter following incubation with the unradiolabelled competitor. In MSCs, the intensity of bands looked similar across the gel which suggests non-specific binding.

Across *RXRA* CpG 8, there was non-specific binding in Saos2 and MSCs. In MG63 cells, bands 2 and 5 were fainter following incubation with both the non-specific and specific competitor compared to probe and extract alone, however this suggests non-specific binding across this region.

Across *RXRA* CpG 12, binding was very faint in MSCs. In Saos2 cells, bands 4 and 5 were fainter following specific and nonspecific competition, however this suggests non-specific binding. In MG63 cells, the 5th band was fainter following cold competition with a specific competitor which suggests some specific binding that can be partially outcompeted.

Chapter 6

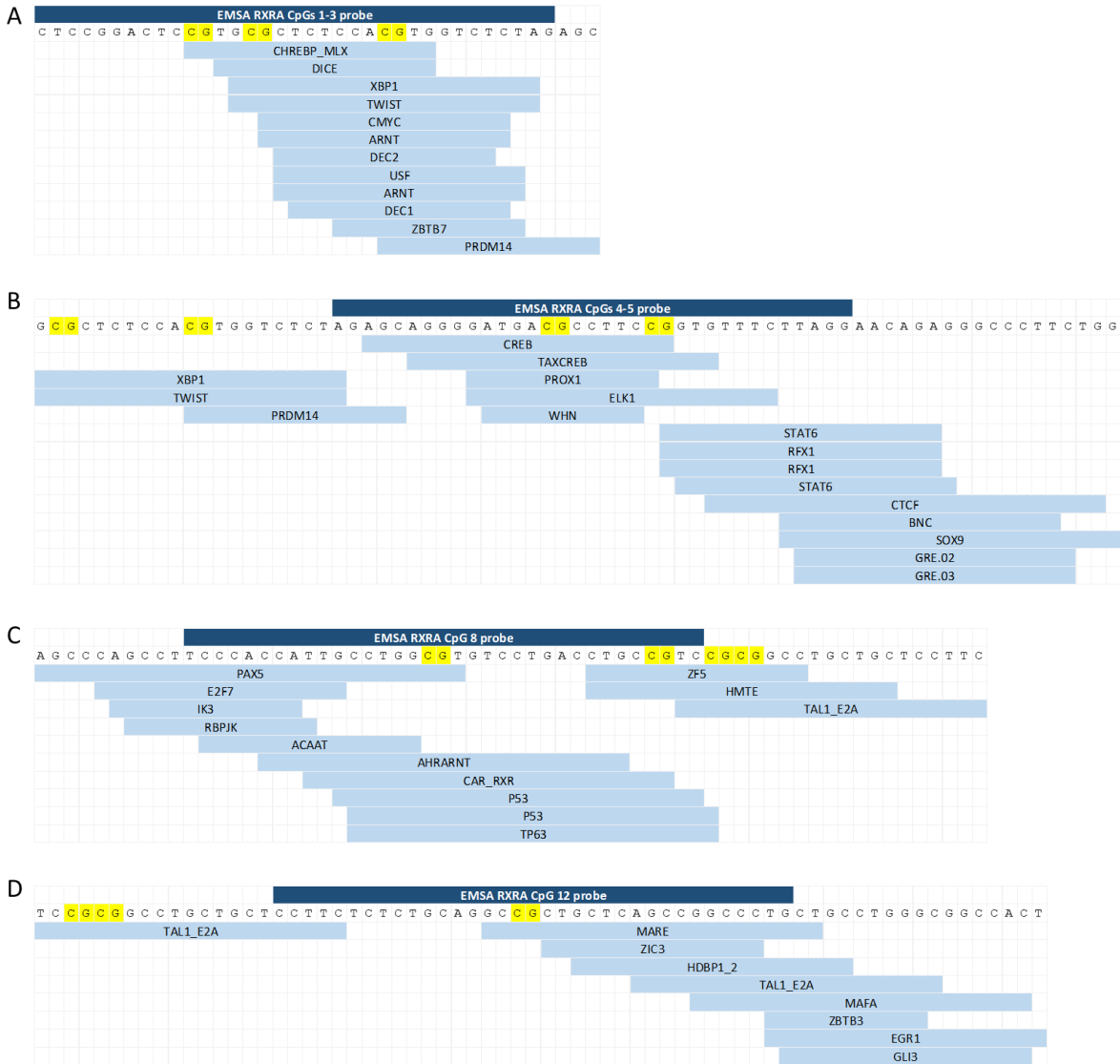


Figure 6.13 Putative transcription factor binding across *RXRA* EMSA probes.

EMSA = electrophoretic mobility shift assay. MatInspector proposes several putative transcription factor binding sites over the *RXRA* probes used in EMSAs. Highlighted CpGs are the *RXRA* CpGs of interest. A) Putative transcription factor binding sites over *RXRA* CpGs 1-3. B) Putative transcription factor binding sites over *RXRA* CpGs 4-5. *RXRA* CpGs 2 and 3 have also been highlighted. C) Putative transcription factor binding sites over *RXRA* CpG 8. *RXRA* CpGs 9, 10 and 11 have also been highlighted. D) Putative transcription factor binding sites over *RXRA* CpG 12. *RXRA* CpGs 10 and 11 have also been highlighted.

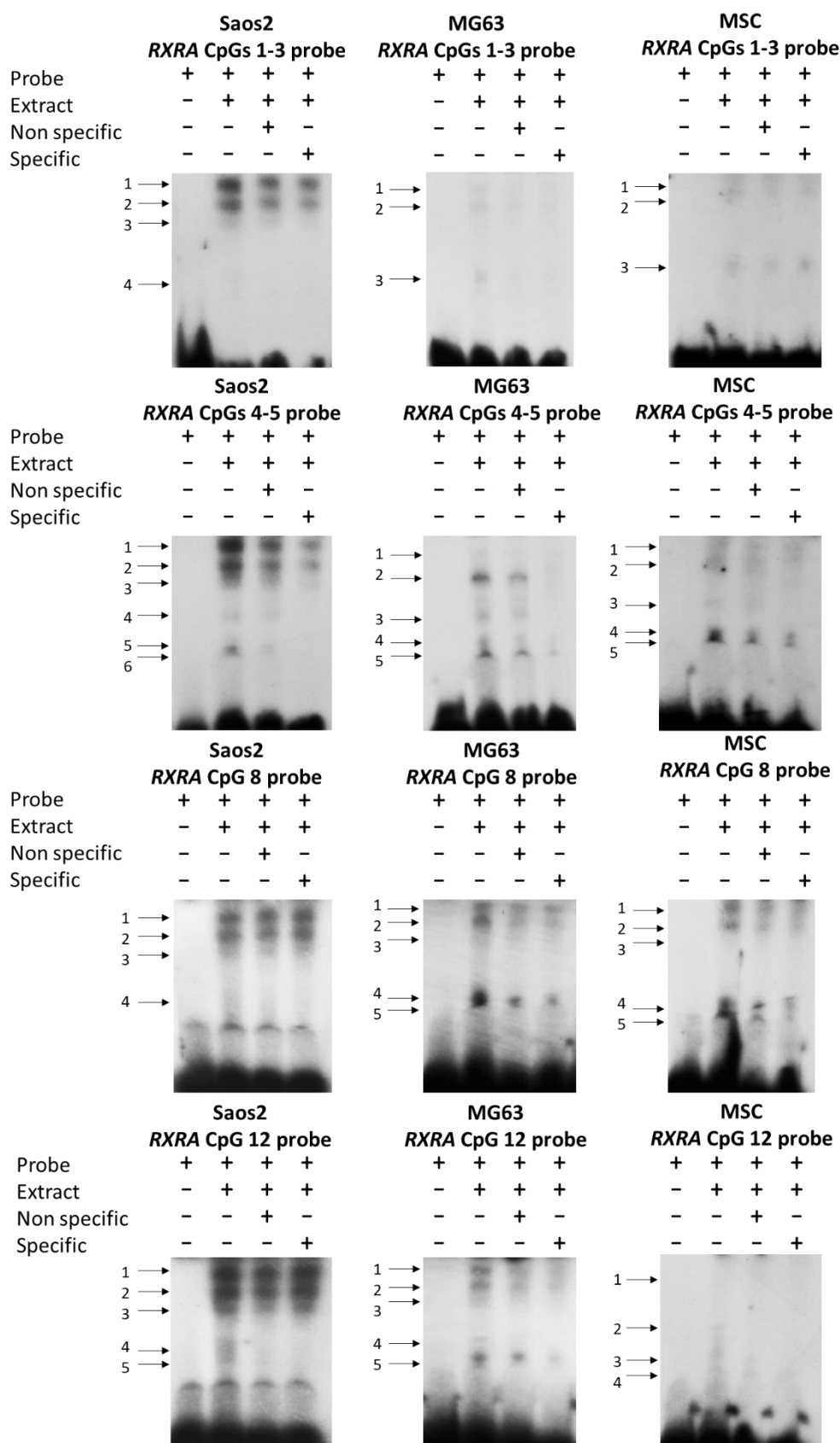


Figure 6.14 EMSAs of *RXRA* CpG probes in Saos2, MG63 and MSCs.

Electrophoretic mobility shift assay. A radiolabelled probe across *RXRA* CpGs 1-3, 4-5, 8 and 12 has been used. Non-specific and specific samples used a 500x cold competitor prior to addition of radiolabelled probe. MSCs = mesenchymal stem cells from umbilical cord. The arrows point to the location of the bands. The experiment was performed in duplicate and the trace is a representative of both.

6.2.5.1 EMSAs show specific competitive binding in MG63 with *RXRA* CpGs 4-5

A cocktail mix of known oligonucleotides was investigated against the *RXRA* CpG 4-5 radiolabelled probe in MG63 cells to determine whether there was any specific transcription factor binding. Eight transcription factor cocktail mixes, each with ten known transcription factor sequences were incubated with the nuclear extract prior to the addition of the radiolabelled probe (see **Materials and Methods 2.2.9**). MatInspector analysis identified putative binding sites for CREB *and* CTCF, of which the oligonucleotide sequences are present in transcription factor mix 1, GR which is in mix 2, and STAT6 which is in transcription factor mix 6 (**Figure 6.13**). Addition of transcription factor mix 2 resulted in competition of all 3 bands (**Figure 6.15A**). There was reduced binding of radiolabelled probe to band 3 after competition with transcription factor mixes 7 and 8 and some reduction in binding in response to transcription factor mixes 1 and 5 when compared to the probe plus extract lane. Transcription factor mixes 3, 4 and 6 did not show any competition.

A second EMSA was carried out which separated out the 2nd cocktail mix into individual transcription factor oligonucleotides (**Figure 6.15B**). At the same time, a concentration gradient of the 2nd transcription factor cocktail mix was also investigated to determine what concentration of competitor is needed to outcompete the probe. The results show that the 4th band was lighter with the addition of glucocorticoid receptor oligonucleotide and the upper bands disappeared. The concentration gradient showed that cold competition of the radiolabelled probe is efficient with a concentration of 350x the competitor.

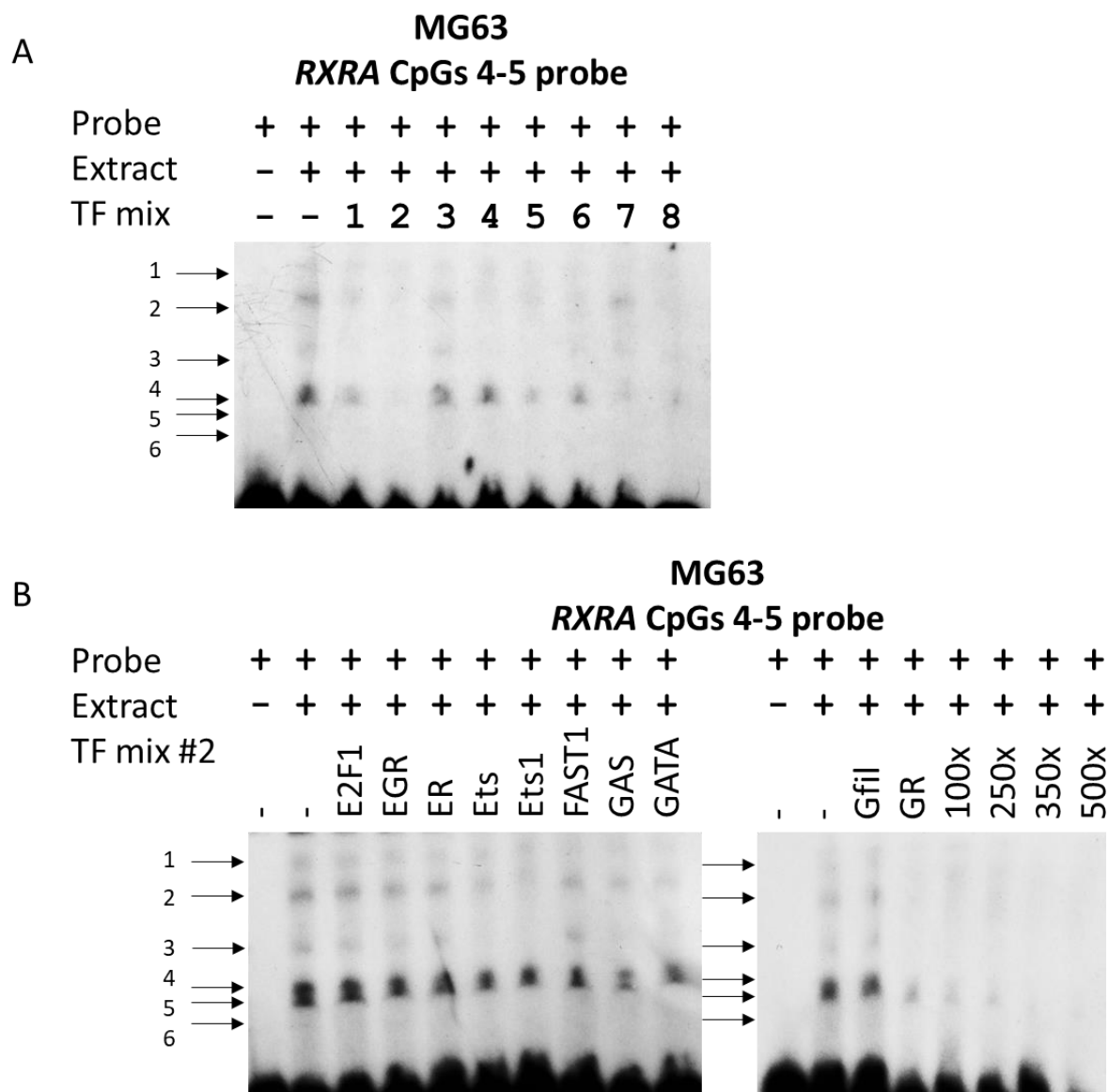


Figure 6.15 EMSAs of *RXRA* CpGs 4-5 in MG63 cells with combined and individual transcription factor binding.

Electrophoresis mobility shift assay. A radiolabelled probe across *RXRA* CpGs 4-5 has been used. The arrows point to the location of the bands. The experiment was performed in duplicate and the trace is a representative of both. A) Transcription factor cocktail binding across *RXRA* CpGs 4-5 in MG63 cells. Individual components of cocktail mix can be seen in [section 2.2.9.1.1](#). B) Individual binding of transcription factor cocktail mix number 2 across *RXRA* CpGs 4-5. EGR = early growth response, ER = estrogen receptor, Ets = ETS proto oncogene, Ets1 = ETS proto oncogene 1, FAST1 = Forkhead box protein 1, GAS = interferon gamma activated sequence, Gfil = growth factor independence 1, GR = glucocorticoid receptor, 100-500x concentration of transcription factor cocktail mix 2 used as a cold competitor prior to addition of radiolabelled probe.

6.2.5.2 Treatment of osteosarcoma cell lines and MSCs with vitamin D does not alter transcription factor binding

To investigate whether *in vitro* treatment with vitamin D or triiodothyronine (T3) altered transcription factor binding over the *RXRA* CpGs of interest, Saos2, MG63 and MSCs were cultured with either: 10 nM 1,25(OH)₂D₃, ethanol control, or 10 nM T3 and the vehicle NaOH control for 18 hours prior to cell pelleting and nuclear extraction. Treated nuclear cell extracts as well as untreated cell extracts were then used for radiolabelled EMSAs with four different *RXRA* probes to examine potential transcription factor binding (**Figure 6.16**).

Across *RXRA* CpGs 1-3, binding was stronger in Saos2 cells compared to MG63 and MSCs. In Saos2 cells, binding was similar in untreated and ethanol treated cells whereas vitamin D, T3 and the NaOH treated cells had an additional band (band 3). In MG63 cells, binding was very weak and cells treated with T3 and NaOH did not have this band. In MSCs, all three bands were darker using nuclear extracts from cells treated with vitamin D and NaOH.

Across *RXRA* CpGs 4-5, in Saos2 cells, treatment with T3 and NaOH resulted in a 3rd band and bands 4-6 were darker than the remaining nuclear extracts. In MG63 cells, bands 3, 5 and 6 were darker in untreated, vitamin D and T3 treated cells and band 4 was darker in untreated and vitamin D treated cells. In MSCs, band 5 was the darkest following treatment with NaOH, fainter in vitamin D and T3 treated cells and very faint with untreated and ethanol treated cells.

Across *RXRA* CpG 8, in Saos2 cells, there was a 3rd band present in untreated, T3 and NaOH treated cells which was absent in vitamin D and ethanol treated cells. In MG63 cells, binding was stronger in untreated cells, fainter in vitamin D, ethanol and T3 cells and very faint in NaOH treated cells. In MSCs, the first 2 bands were of similar intensity in untreated and NaOH treated cells compared to vitamin D, ethanol and T3 treated cells. The 3rd band was fainter in ethanol treated cells compared to the remaining cells.

Across *RXRA* CpG 12, in Saos2 cells, the 3rd band was weaker in vitamin D treated cells and less visible in untreated and ethanol treated cells compared to T3 and NaOH treated cells. T3 and NaOH cells had an additional 4th band. The 5th and 6th bands were stronger in vitamin D and T3 treated cells compared to the other cells which were very faint. In MG63 cells, the 3rd and 4th bands were of similar intensity in untreated and ethanol treated cells and very faint in the remaining nuclear extracts. In MSCs, the 3rd band was stronger in vitamin D and NaOH treated cells and absent in the remaining nuclear extracts.

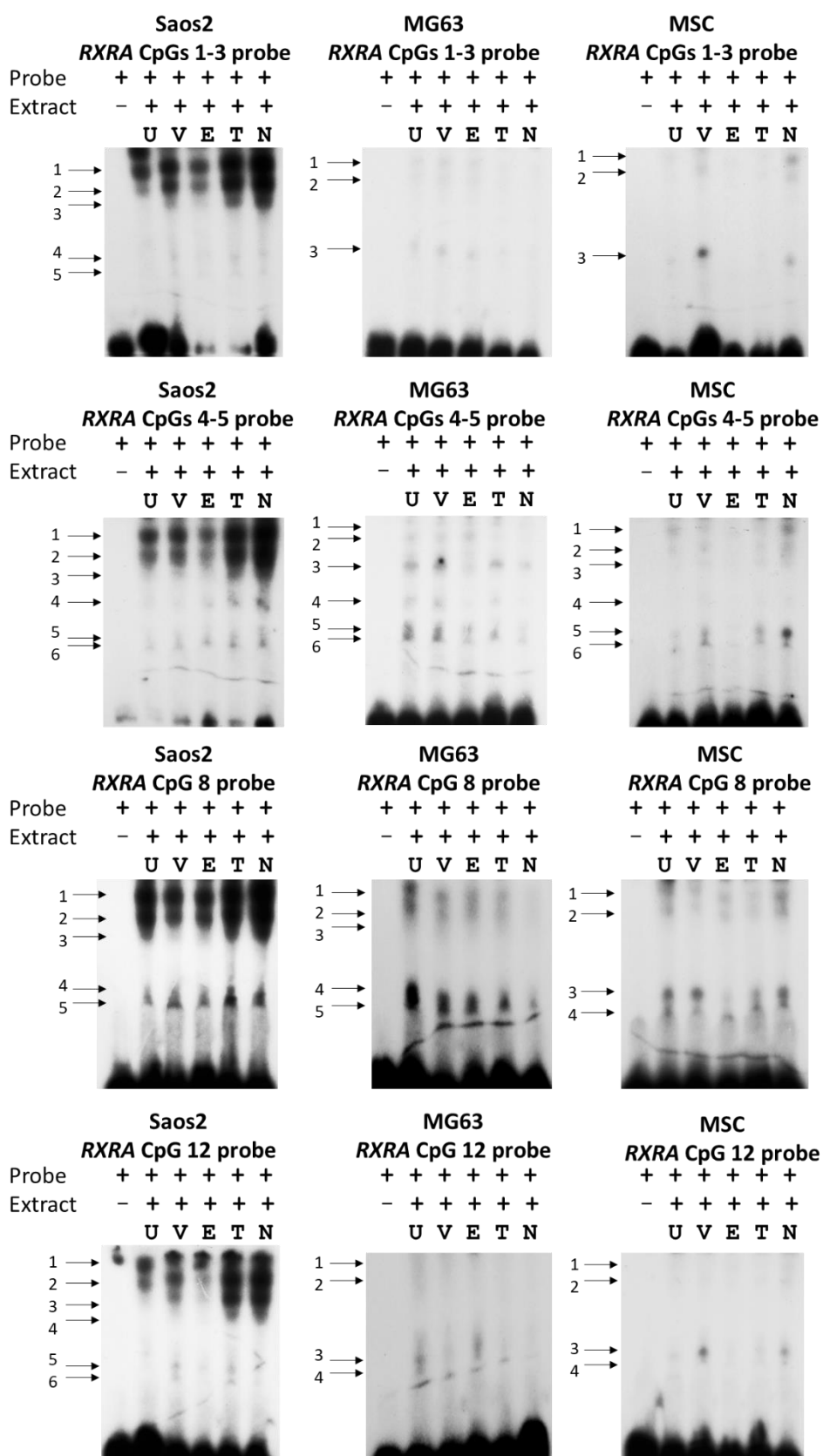


Figure 6.16 EMSAs of hormone treated Saos2, MG63 and MSC cells.

Electrophoretic mobility shift assay. Prior to nuclear extraction cells were untreated (U), treated with 10 nM 1,25(OH)₂D₃ (V), the vehicle ethanol control (E), 10 nM T₃ (T) or the NaOH vehicle control (N) for 18 hours.

6.3 Discussion

DNA methylation of specific CpGs upstream of the *RXRA* promoter have been shown to be inversely associated with scBMC in childhood²⁹⁹ and in **Chapter 3** we have shown that maternal cholecalciferol supplementation during pregnancy was associated with altered methylation of *RXRA* CpGs 1-5. However, it is unclear whether this region is functionally important for *RXRA* gene transcription and/or whether there is a causal link between this region and impaired bone health. Within this chapter we have shown that the *RXRA* CpGs of interest regulate promoter activity of the *RXRA* gene, which we have demonstrated through site directed mutagenesis in a luciferase construct. We have shown that the *RXRA* region of interest acts as an enhancer and that mutagenesis of specific loci within the enhancer region has a negative role on the enhancer activity. Furthermore, we have shown that specific transcription factors bind to this region of interest, which could suggest that altered methylation arising from early life interventions could alter transcription factor binding and expression of target genes although this needs to be investigated further.

Site directed mutagenesis of *RXRA* CpGs 6, 8 and 12, of which methylation has been shown to be associated with bone measures in childhood²⁹⁹ significantly decreased *RXRA* promoter activity in the luciferase promoter construct *pRXRApromLuc*. Due to the lack of technology available, the individual CpG sites could not be individually methylated however, with future advancement in CRISP-cas9 technology this could be investigated further. These findings are similar to what Lillycrop *et al.*, have shown, where site directed mutagenesis of individual CpG loci decreased ANRIL promoter activity and p14^{ARF} expression in liposarcoma cell lines³²². Zou *et al.*, have shown that hypermethylation of the *XAF1* promoter resulted in decreased gene expression, and that site directed mutagenesis of the same CpG loci decreased luciferase promoter activity³⁸⁸. We have shown that alterations to the genomic sequence are important however, as we have not methylated the CpG site we can only speculate that there would be similar findings between mutation and methylation of CpG loci. Methylation is often associated with gene repression, so a decrease in promoter activity following mutation of individual CpG loci would suggest that following methylation of these CpG loci, this would be accompanied by decreased *RXRA* promoter activity and *RXRA* gene expression. Within the MAVIDOS trial we have shown that maternal cholecalciferol supplementation during pregnancy is linked to lower *RXRA* methylation in umbilical cord tissue and amongst infants born in the winter months there are improved bone measures at birth. Using luciferase constructs we have shown that mutation of these CpG loci is linked to decreased promoter activity, so if the mutation is representative of methylation, lower methylation would likely be associated with upregulation of *RXRA* gene expression. An increase in *RXRA* activity could be associated with increased binding to VDR and binding to VDREs in target genes such as *Osteocalcin*, which is involved in mineralisation of the bone matrix. Therefore, these findings

suggest that altered methylation of these individual CpG loci, which we have shown through site directed mutagenesis, alters *RXRA* promoter activity and *RXRA* gene expression.

Having shown that mutation of individual *RXRA* CpG loci is linked to altered *RXRA* promoter activity, we investigated whether this region had regulatory properties. *In silico* analyses identified enrichment for DNase 1 hypersensitive sites across the DMR containing the *RXRA* CpGs of interest. DNase 1 hypersensitive sites are often associated with regulatory regions due to the open chromatin structure. The region of interest also showed enrichment for H3K4me3 although lacked H3K27Ac enrichment, of which both marks are often associated with active enhancers. Active enhancers are often enriched for H3K4Me1, H3K27Ac and actively transcribing RNA Pol II whereas primed enhancers are marked by H3K4Me1 and depletion of H3K4Me3 and H3K27Ac^{380,389–391}. The lack of H3K27Ac marks suggest that this region of interest may be part of a primed enhancer rather than an active enhancer. Furthermore, it is possible that this region has differing effects amongst different cell types which could result in altered transcription within different tissues. Enhancers are regions of DNA which have been shown to stimulate tissue specific transcription of target genes, independent of their orientation, upstream or downstream of the gene and potentially several kilobases distant from the target promoter³⁹². To investigate this further, the region of interest was cloned upstream of a minimal reporter vector, which is often used to test enhancers and regulatory regions of interest. Cloning of this region, without the presence of the *RXRA* promoter, significantly increased luciferase expression in both osteosarcoma cell lines. Furthermore, as enhancers are able to act in any orientation, the region was ligated in both the forward and reverse orientations upstream of the minimal promoter as well as downstream of the minimal promoter in the forward orientation. The results showed that the enhancer region can alter luciferase expression in any orientation, albeit with preference in the forward orientation upstream of the promoter. The *RXRA* promoter is located downstream of this region of interest, providing supporting evidence that this region has an enhancing effect on the *RXRA* promoter.

Maternal cholecalciferol supplementation during pregnancy has been shown to be associated with altered methylation of *RXRA* CpGs 1-5. Often, neighbouring CpG loci will be in a similar methylation state, nonetheless methylation of different CpG loci may have a greater influence on gene transcription. Excision of the genomic region containing either core *RXRA* CpG loci of interest, or flanking CpGs had a differential effect on luciferase expression and there were some cell type specific differences between the two human osteosarcoma cell lines, which could be due to altered transcription factor binding within each cell line. In Saos2 cells, transfection with pMenhLuc(CpGs7-12) resulted in the greatest increase in luciferase expression (124-fold) followed by a 116-fold increase following transfection with pMenhLuc(CpGs1-12) (**Figure 6.17**). This suggests that within the minimal enhancer construct, the genomic region containing core *RXRA* CpGs 1-6 has a small

regulatory effect on luciferase expression. This also suggests that the flanking region at the 3' end which is absent in the minimal enhancer construct and present in the full enhancer construct has negatively regulates luciferase expression. This can be seen by the 20-fold increase in luciferase expression following transfection with pFenhLuc(CpGs7-12) as opposed to the 124-fold increase following transfection with pMenhLuc(CpGs1-12).

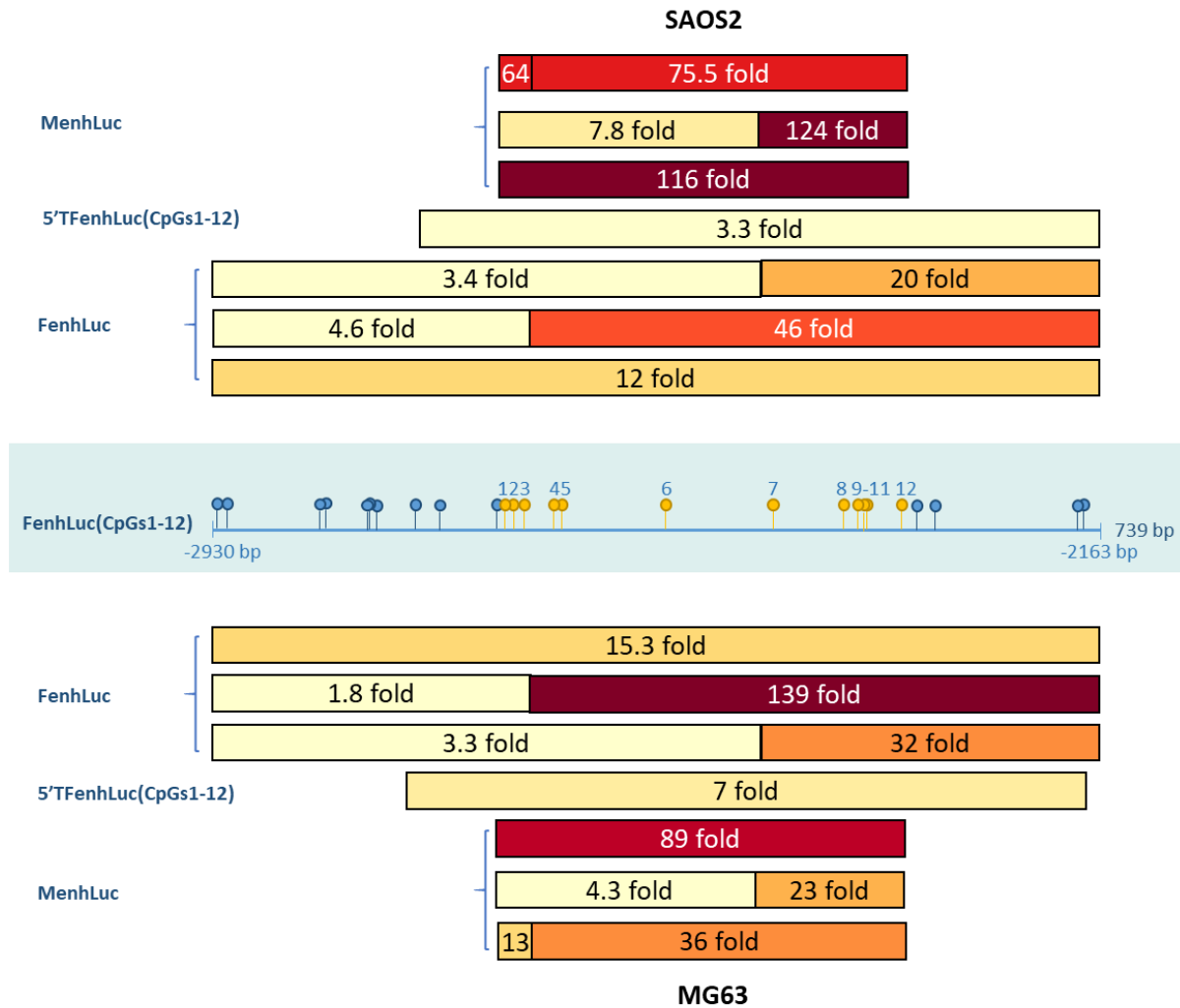


Figure 6.17 Heat map representation of the magnitude of luciferase responses following transfection with the enhancer constructs.

By truncating the 5' end of pFenhLuc(CpGs1-12) removing the first 8 flanking CpGs luciferase expression was diminished compared to pFenhLuc(CpGs1-12) nonetheless expression was 3.3 fold greater than pGL4.23. This suggests that this region containing 8 additional CpGs promote gene expression, and that by removing them expression diminishes. Whereas removal of all of the 5' flanking CpGs and core *RXRA* CpGs 1-3 results in a 46-fold increase in luciferase expression suggesting that something negative binds in the region across the core *RXRA* CpGs of interest 1-3 as well as the 2 additional 5' flanking CpGs immediately upstream. By removing the 3' end of pFenhLuc(CpGs1-12), both pFenhLuc(CpGs1-6) and pFenhLuc(CpGs1-3) increased luciferase

expression compared to pGL4.23 with a 3.4 fold increase and 4.6 fold increase respectively, resulting in similar expression levels as p5'truncenhLuc(CpGs1-12). Similar results could be seen in MG63 cells however there were some differences. In MG63 cells the greatest luciferase response (139-fold) was observed following transfection with pFenhLuc(CpGs3-12) followed by an 89-fold increase following transfection with pMenhLuc(CpGs1-12). This could be due to altered transcription factor binding within both cell types which have a different regulatory effect on luciferase activity. This suggests that altered methylation of these core *RXRA* CpGs of interest in different cell types would have differing effects on gene transcription.

Mutation of *RXRA* CpGs 5 and 6 within the minimal enhancer luciferase construct (pMenhLuc(CpGs1-12) significantly decreased luciferase expression in both osteosarcoma cell lines, and mutations of CpGs 4 and 8 additionally decreased luciferase expression in MG63 cells only. In this chapter we have shown that site directed mutagenesis of these core *RXRA* CpGs of interest decreases *RXRA* promoter activity in the p*RXRA*promLuc construct, and decreases the enhancing activity of the minimal enhancer construct (pMenhLuc(CpGs1-12). This suggests that altered methylation at these CpG loci alters the enhancing potential of this region, resulting in decreased *RXRA* promoter activity and *RXRA* gene expression. This could be through altered transcription factor binding, altered chromatin structure or through altered histone modifications and interactions. EMSAs identified specific GR binding across the probe for *RXRA* CpGs 4 and 5, and MatInspector analyses identify a putative GR binding site over *RXRA* CpG 5. Furthermore, GR binding has been shown to mark enhancer regions, providing supporting evidence that altered methylation of this region of interest can affect the enhancer properties of this region and alter the transcription potential. Transcription factor binding across this region could be investigated further by using an antibody against GR to exhibit a supershift. Furthermore, methylated probes could be used in EMSAs to determine whether the presence of a methyl group alters transcription factor binding, especially of GR. Interestingly, McDowell *et al.*, found that following *in vitro* glucocorticoid exposure there was induction of GR binding to pre-established enhancers within minutes³⁹³. This provides supporting evidence that this region of interest has enhancer properties. Furthermore, the study found that the strength and persistence of GR binding had a regulatory effect on enhancer activation resulting in altered transcription factor binding and histone modifications and changes to gene expression³⁹³. This could be investigated further by treating osteosarcoma cell lines with dexamethasone and measurement of DNA methylation of the *RXRA* CpGs of interest as well as changes to endogenous gene expression. Furthermore, following transfection with the minimal luciferase enhancer (pMenhLuc(CpGs1-12) and mutations of CpGs 4 and 5 the effect of dexamethasone treatment on luciferase expression could be determined. It is possible that altered methylation at these CpG loci could prevent GR from binding, preventing heterodimerisation with

RXRA and/or altering the enhancer activity of this region which has an impact on *RXRA* promoter activity. Conversely, excess glucocorticoid use can result in glucocorticoid induced osteoporosis³⁹⁴ and glucocorticoid treatment has been shown to inhibit osteoblast differentiation and reduces the pool of preosteoblastic cells that can differentiate into osteoblasts³⁹⁴. Steineger *et al.*, found that dexamethasone treatment upregulates *RXRA* gene expression and mRNA concentrations³⁹⁵. Despite the adverse effects of excess glucocorticoid use, GR binding can increase *RXRA* expression resulting in an increase in dimerization with VDR as well as other nuclear receptors such as TR. MatInspector analyses identified putative CAR binding sites over *RXRA* CpG 8 however, the EMSAs found non-specific binding. The binding site for CAR is similar to that of the TR as both bind to the consensus sequence AGGTCA n = 4 AGGTCA. This is similar to the VDR binding site which has a linker of n = 3 and studies have shown that VDR can bind as a homodimer to hexameric half repeats. It would be interesting to investigate nuclear receptor binding over the *RXRA* DMR and to investigate the effect that the presence of a methyl group will have. This could provide insight into the dimerisations and pathways that are involved depending on the methylation state.

To investigate the relationship between vitamin D, DNA methylation and bone outcomes it would be preferential to investigate in bone tissue or bone marrow rather than a proxy tissue such as umbilical cord. Furthermore, it would be interesting to measure gene expression within the cord tissue as well as DNA methylation however, due to the time sensitive nature of RNA this was not possible within the SWS cohort and MAVIDOS trials. *In vitro* experiments provide the means to investigate the effect of vitamin D treatment on DNA methylation and gene expression although there are limitations. The results showed that following 1,25(OH)₂D₃ treatment there was an increase in *RXRA* methylation at specific loci within both osteosarcoma cell lines. This is the opposite of what has been observed in the MAVIDOS trial, where maternal cholecalciferol supplementation was associated with lower *RXRA* methylation. The differences in results could be due to cell type specific methylation differences as osteosarcoma cell lines have osteoblastic properties whereas Wharton's jelly in umbilical cord tissue is a source of MSCs which have the potential to differentiate into osteoblasts. To investigate this further, DNA methylation of these *RXRA* CpG loci could be measured in MSCs from umbilical cord tissue following vitamin D treatment. Furthermore, a time course experiment could be performed where MSCs are cultured under osteogenic conditions to induce osteoblast differentiation and DNA methylation and gene expression could be measured at set time points along the differentiation pathway. This would help to provide insight into any effects that vitamin D treatment and *RXRA* methylation have on osteoblast differentiation. Gene expression of *RXRA* as well as of key genes involved in mineralisation of the bone matrix could also be measured to determine any changes that could impact bone formation.

To determine the effect that vitamin D treatment has on endogenous gene expression in human osteosarcoma cell lines, gene expression of CYP24A1, RXRA, VDR, Osterix and Runx2 was measured. Following 10 nM $1,25(\text{OH})_2\text{D}_3$ there was upregulation of CYP24A1 gene expression, which is a key enzyme involved in the catabolism of both the inactive and active forms of vitamin D and is often used to test VDR induction due to the presence of a VDRE, confirming the response in both cell types to vitamin D treatment. In MG63 cells, there was downregulation of RXRA expression and upregulation of VDR expression however, there were no significant differences in Saos2 cells. This suggests that in MG63 cells, in response to vitamin D treatment there is likely an increase in VDR transcription which could result in increased binding to the $1,25(\text{OH})_2\text{D}_3$ ligand, which could be part of a compensatory mechanism to reduce the amount of unbound $1,25(\text{OH})_2\text{D}_3$ and prevent non-genomic actions such as through interaction with G-protein coupled receptors and activation of MAPK pathways. With an increase in available $1,25(\text{OH})_2\text{D}_3$ bound to VDR, you would expect an increase in RXRA resulting in heterodimerisation and binding to VDREs in target genes. Nonetheless, the results showed downregulation of RXRA, which could act as the rate limiting step to regulate heterodimerisation with VDR and binding to target genes. The lack of significance in RXRA and VDR expression in Saos2 cells further highlights the cell line specific responses of both cell types. Conversely, this could be due to the aberrant changes to cell lines following immortalisation. Cell type specific changes to VDR expression have been shown in other cell lines in response to $1,25(\text{OH})_2\text{D}_3$ treatment. In a HIMeg cell line, derived from chronic granulocytic leukaemia, there was downregulation of VDR mRNA in a time dependent manner following treatment with 10 nM $1,25(\text{OH})_2\text{D}_3$ over a 24 hour exposure period however, there was no effect seen in a human osteosarcoma cell line, HOS-8603³⁹⁶. Gene expression of two transcription factors, Osterix and Runx2, were measured. Following vitamin D treatment Osterix expression was downregulated in Saos2 cells but not in MG63 cells. Osterix has been shown to act downstream of Runx2 and is involved in differentiation into mature osteoblasts and osteocytes. Saos2 cells have phenotypic features of mature osteoblasts which could explain why Osterix expression is altered in this cell line compared to in MG63 cells. Downregulation of Osterix expression would suggest a decrease in differentiation into mature osteoblasts and osteocytes which can be embedded in the bone matrix. The lack of associations could be due to the *in vitro* conditions and alternate results may be observed in MSCs or *in vivo*. In both osteosarcoma cell lines, there were no changes to Runx2 gene expression. This suggests that vitamin D treatment does not alter Runx2 gene expression. If there is a link between vitamin D treatment and bone formation, this suggests that it occurs independently of Runx2 gene expression, at least in osteosarcoma cell lines. Conversely, a study by Prideaux *et al.*, found that Runx2 expression was high in Saos2 cells and that expression decreased over time in mineralising conditions³⁹⁷ therefore you would expect Runx2 downregulation following

vitamin D treatment although the lack of significant effect could be due to the short period of exposure.

RXRA forms a heterodimer with VDR and binds to VDREs in target genes. Using the *RXRA* promoter luciferase construct (p*RXRA*promLuc) we have shown that there is an increase in *RXRA* promoter expression following vitamin D treatment in osteosarcoma cell lines. This suggests that in response to vitamin D, there is upregulation of *RXRA* promoter activity which could be linked with an increase in *RXRA* available to dimerise with VDR and bind to response elements in target genes. Another possibility is the presence of a VDRE within the p*RXRA*promLuc construct. MatInspector analyses identified putative VDREs upstream of the *RXRA* promoter but not over the DMR containing the *RXRA* CpGs of interest. This could be investigated further through *in vitro* gelshift assays or by reporter gene and chromatin immuno-precipitation (ChIP) assays. We have shown that site directed mutagenesis of *RXRA* CpG loci within the *RXRA* promoter luciferase construct (p*RXRA*promLuc) significantly decreases *RXRA* promoter activity and there is altered induction to vitamin D treatment at each CpG loci. There is still an increase in luciferase expression despite the mutation, however the magnitude is significantly lower than wildtype p*RXRA*promLuc levels following vitamin D treatment. This could be due to mutations of the CpG loci altering enhancer activity which negatively impacts *RXRA* promoter activity. Conversely, if there is a VDRE present within this promoter, this could be activated by the cell lines endogenous activity where following vitamin D treatment there is increased binding to VDREs in target genes, such as a putative binding site in the *RXRA* promoter luciferase construct. This could be investigated further by mutating the putative VDREs with and without the presence of mutated *RXRA* CpG loci and measurement of luciferase expression with and without vitamin D treatment.

Overall, there were some limitations to these experiments. Firstly, Saos2 and MG63 cells were used rather than primary cells which would have given a more accurate insight into the functional relevance of these CpGs. Both cell lines share some osteoblastic properties³⁹⁸ however, there are some differences: Saos2 cells are adherent epithelial cells derived from an 11 year old Caucasian female with osteosarcoma, while MG63 cells are adherent, fibroblast cells cultured from the osteosarcoma of a 14 year old Caucasian male. Furthermore, Saos2 cells have been shown to have a mature osteoblastic phenotype with positive markers for ALP, Osteocalcin, Bone Sialoprotein, decorin and collagen 1 and 3³⁹⁹ whereas MG63 cells were shown to have both immature and mature osteoblastic features³⁹⁹ and they were also positive for ALP however at a lower level than in Saos2 cells³⁹⁹. However, primary mesenchymal stem cells can be difficult to obtain and maintain as a pure population whereas cell lines can provide a pure population of cells, allowing a constituent sample and reproducible results. Investigation into these two human osteosarcoma cell lines could provide insight into the effect that altered *RXRA* methylation could have on osteoblastic cells with features

of immature osteoblasts and mature osteoblasts which could affect altered gene transcription of genes associated with mineralising the bone matrix, in turn impacting bone health. This provides the basis for preliminary results which can be further investigated in primary cell lines. Second, experimental replicates should be done in triplicate, however due to time constraints some experiments were only replicated twice. Third, preferentially the *RXRA* CpG sites would be methylated rather than mutated however there are limitations in technology and therefore it would be difficult to successfully methylate a specific CpG without eliciting methylation elsewhere in the DNA sequence. Several studies have tried methylation editing approaches however, these often involve methylation of the whole plasmid or the promoter region rather than just one specific CpG. Future work could involve utilising the CRISPR-Cas9 based tool to methylate individual CpGs. To provide insight as to whether methylation altered luciferase expression of the full *RXRA* luciferase construct, pFenhLuc(CpGs1-12) and the control vector were methylated with M.SssI (data not shown). When methylated, luciferase expression of both constructs significantly increased compared to their respective unmethylated control. However, the increase in luciferase expression was significantly lower in methylated pFenhLuc(CpGs1-12) compared to methylated pGL4.23. This suggests that methylation of the 739 bp insert in pFenhLuc(CpGs1-12) repressed luciferase expression. There are many limitations to this experiment. Firstly, a CpG free vector was not used and there were CpGs present in the gene body of the construct which often has a positive effect, nonetheless, both pGL4.23 and pFenhLuc(CpGs1-12) were methylated so any differences in expression were due to the insert in pFenhLuc(CpGs1-12). Secondly, following enzyme restriction digestion of methylated pFenhLuc(CpGs1-12) and confirmation with pyrosequencing the plasmids did not undergo complete methylation which is a common disadvantage of this technique.

In conclusion, mutation of specific CpG loci alters the enhancer properties of the DMR upstream of the *RXRA* promoter, which has a negative impact on *RXRA* promoter activity and likely *RXRA* expression. This may be due to altered transcription factor binding although this needs to be investigated further. The results suggest that there is a putative VDRE upstream of the promoter, so in response to vitamin D treatment there is increased transcription of *RXRA* which could be part of a positive feedback loop. This could result in increased heterodimerisation with VDR and binding to VDREs such as in the *Osteocalcin* gene. Maternal cholecalciferol supplementation during pregnancy may lower methylation of these *RXRA* CpG loci, which promotes the enhancer properties of this region on *RXRA* promoter activity. Furthermore, there may be increased binding to VDREs upstream of *RXRA*. Combined, the increase in *RXRA* promoter activity increases available *RXRA* which can dimerise with VDR as well as other nuclear receptors of which can also have a positive impact on bone health. Together these findings provide insight into the functional relevance of this

Chapter 6

region containing the *RXRA* CpGs of interest on *RXRA* promoter activity and provides insight into the possible mechanistic link related to altered bone measures in later childhood.

**Chapter 7 A mouse model of vitamin D deficiency:
maternal vitamin D deficiency and mechanical load
effect on DNA methylation**

7.1 Introduction

Within this thesis we have shown that maternal vitamin D supplementation is linked to altered *RXRA* and *CDKN2A* methylation in umbilical cord tissue however there were no significant associations between methylation of these two genes and bone measures at birth. Whereas studies within the SWS have shown that methylation of these two genes were inversely associated with bone measures during childhood^{299,323}. This suggests that there may be an external stimulus between these two time points, such as learning to walk, which could be responsible to the altered phenotype and associations that are observed. To investigate this further, we utilised a vitamin D deficient mouse model by Borg *et al.*, which found that mechanical loading improved bone measures but there was a reduced response in mice exposed to a prenatal vitamin D deficient diet²⁴⁵.

Borg *et al.*, fed C57BL6 mice a standard vitamin D diet containing 1000 IU/kg chow or a vitamin D deficient diet (0 IU/kg chow) during pregnancy and weaning²⁴⁵. At postnatal weeks 8 and 16, the left tibia of offspring mice underwent two weeks of mechanical loading and mice were culled at 18 weeks of age. Both the loaded and non-loaded tibias were removed and underwent biomechanical testing of bone stiffness and the ultimate force needed to result in fracture through 3 point bending test. Borg *et al.*, found that mechanical loading of tibiae increased cortical and trabecular parameters as well as bone strength however, tibiae from control mice responded more effectively to mechanical loading compared to mice exposed to prenatal vitamin D deficiency²⁴⁵

Animal models are an attractive means to study the question of how the early life environment affects offspring development and disease progression due to the ability to precisely control diet and the environmental conditions. Furthermore, tissues central to the pathogenesis of the disease of interest can be investigated further, rather than using blood or proxy tissues such as in human studies. Vitamin D studies in mice have provided valuable insight into offspring skeletal development. Studies in vitamin D receptor (*VDR*) knockout mice have shown that vitamin D does not appear to affect fetal skeletal development nonetheless, after weaning *VDR* knockout mice develop severe rickets and osteomalacia^{400,401}. There have been a small number of vitamin D deficient mouse models to investigate the effects of vitamin D deficiency on the skeletal system. In these studies lean mice were fed a standard diet with 1000 IU/kg chow vitamin D and the deficient mice were fed a diet completely lacking in Vitamin D or with concentrations of 125 IU/kg chow^{402,403}. The studies found conflicting evidence, Seldeen *et al.*, fed lean and obese mice a low (125 IU/kg), standard (1000 IU/kg) or high (4000 IU/kg) vitamin D diet from 24 weeks of age and after 24 weeks there were no significant differences in BMD between the low and standard vitamin D groups⁴⁰³. Whereas in adult male C57BL6 mice, after 8 months of a vitamin D deficient diet (125 IU/kg) there

was a significant decrease in bone density compared to the control mice⁴⁰². Furthermore, studies have shown that vitamin D deficiency in mice can be achieved after 3 weeks on a deficient diet and it took a further 3 weeks on a standard diet for serum 25(OH)D₃ concentrations to normalise⁴⁰⁴.

In collaboration with Dr Steph Borg, University of Sheffield, we investigated whether maternal vitamin D deficiency during pregnancy in mice altered DNA methylation in tibiae from 18 week old offspring. DNA methylation was measured in 4 genes, *RXRA*, *VDR*, *Runx2* and *Osterix*, which have been shown to play an important role in the vitamin D pathway and/ or are directly involved in osteoblast differentiation. Upon ligand binding, VDR heterodimerises with RXRA and together they bind to vitamin D response elements (VDREs) in target genes to regulate transcription. Furthermore, CpG methylation of *RXRA* has been shown to be predictive of bone health in later childhood in humans²⁹⁹. DNA methylation of two transcription factors involved in osteoblast differentiation, *Runx2* and *Osterix*, were also measured. We have shown that maternal cholecalciferol supplementation during pregnancy is linked to altered *Osterix* methylation in umbilical cord tissue and methylation of both genes were shown to be associated with bone measures at birth. *Runx2* has been shown to induce differentiation of MSCs into immature osteoblasts whereas *Osterix* is involved in the differentiation of pre-osteoblasts into mature osteoblasts and osteocytes⁴⁰⁵. Causality is not required for risk prediction and if a biomarker measured earlier in the life course is predictive of adult bone health, it is not required that the same associations should persist if the same biomarker is measured again, later in the life course. However, it would be interesting to investigate this further in an animal model, and in skeletal tissue, and to determine whether there are long last changes to the epigenome in response to a maternal vitamin D deficient diet during pregnancy and whether external stimuli, such as mechanical loading, can alter DNA methylation.

7.1.1 Hypothesis

Prenatal vitamin D deficiency is associated with altered DNA methylation of the CpG loci of interest in tibial tissue. DNA methylation within tibial tissue will be altered in response to mechanical stimuli to better adapt the skeleton to external stimuli.

7.1.2 Aims

1. To determine whether prenatal vitamin D depletion alters DNA methylation in mouse tibiae.
2. To determine whether mechanical loading alters DNA methylation in mouse tibiae.
3. To determine whether DNA methylation is associated with bone strength in mouse tibiae.

7.1.3 Methods

The mouse experiment was designed and carried out by Dr Steph Borg, University of Sheffield, as described in **section** Error! Reference source not found.. Briefly, C57BL6 mice were placed on a vitamin D replete diet (1000 IU/kg chow) or a deplete diet (0 IU/kg chow) 6 weeks prior to mating until weaning at 3 weeks (prenatal diet). After weaning, offspring were fed a postnatal vitamin D replete diet. At 8 and 16 weeks of age mice underwent mechanical loading of their left tibia for 2 weeks, prior to culling and collection of tibiae. Within this chapter, tibiae has been collected from 18 week old mice that were fed a control diet (prenatal and postnatal replete) or a prenatal vitamin D deficient diet (prenatal deplete and postnatal replete). DNA was extracted from tibiae using the DNeasy Blood and Tissue kit using user defined instructions as described in **section** Error! Reference source not found.. DNA methylation of 4 genes (*RXRA*, *VDR*, *Runx2* and *Osterix*) (**Figure 7.1**) were measured using sodium bisulfite pyrosequencing as described in **section 2.2.4**.

To determine whether maternal vitamin D deficiency alters DNA methylation, DNA methylation of specific CpGs upstream of the promoters of *RXRA*, *VDR*, *Runx2* and *Osterix* were measured in both the non-loaded and loaded tibiae of 18 week old mice and independent t-tests compared DNA methylation between the prenatal vitamin D deficient group and control group (**Section 7.2.2**). To determine the effect of mechanical loading on DNA methylation, independent t-tests compared DNA methylation between the non-loaded and loaded limbs of mice exposed to a control or prenatal vitamin D deficient diet (**Section 7.2.3**). To determine whether there were any associations between DNA methylation and tibial stiffness and ultimate force, linear regression analyses were adjusted for treatment group and for mechanical loading (**Section 7.2.4**).

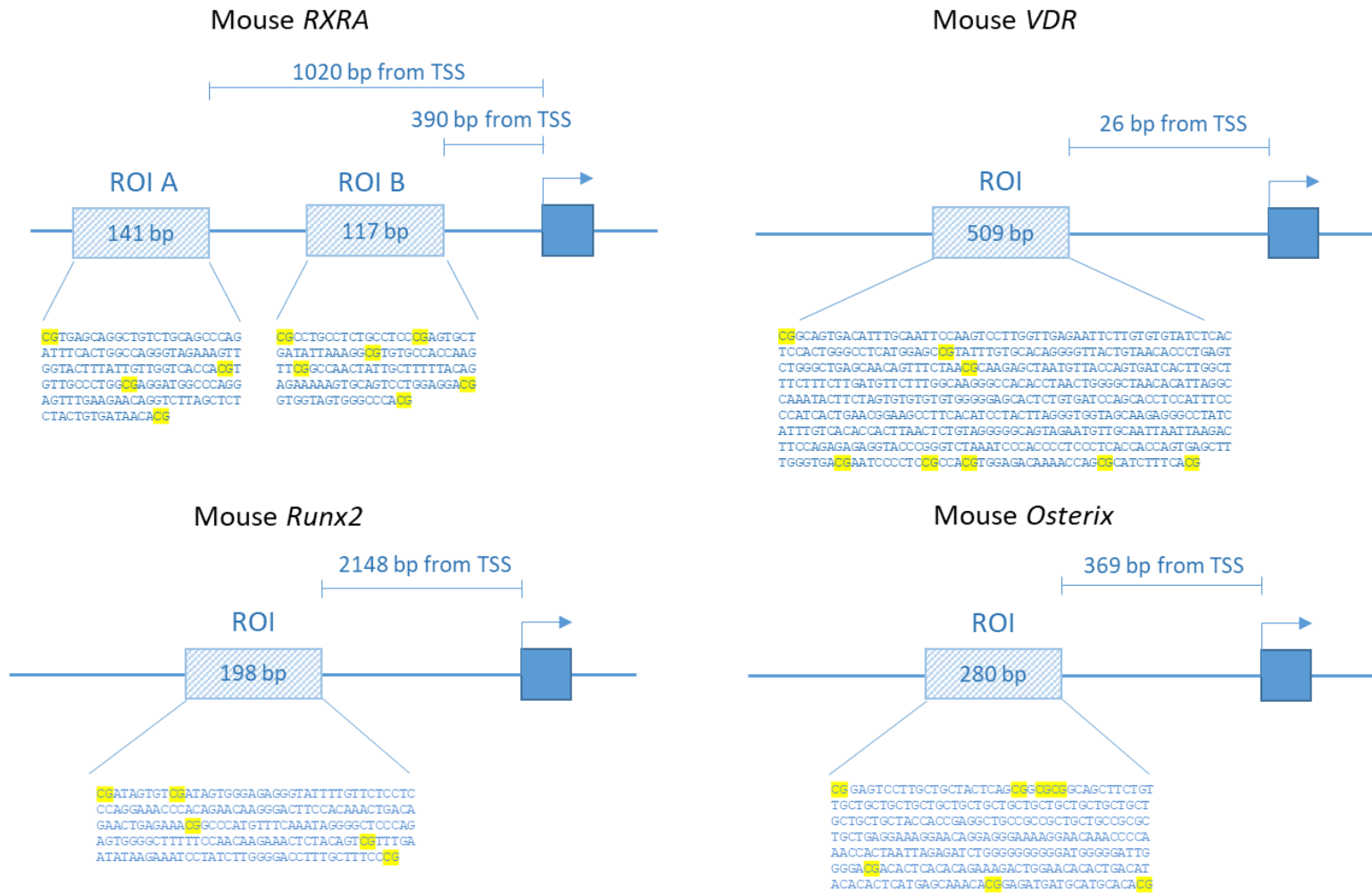


Figure 7.1 Location of the CpGs of interest with respect to the gene transcriptional start site.

CpGs of interest are highlighted in yellow. ROI = region of interest, TSS = transcriptional start site.

7.2 Results

7.2.1 Selection of regions of potential differential methylation in the candidate genes of interest

DNA methylation was measured upstream of the transcriptional start site of four genes: *RXRA*, *VDR*, *Runx2* and *Osterix*. *RXRA* and *VDR* play an important role within the vitamin D pathway regulating transcription of target genes, whereas *Runx2* and *Osterix* are two transcription factors which play a vital role in osteoblast differentiation. There is limited homology between the promoter regions of these genes in humans and mice, so we could not analyse the same regions that were investigated in humans within the MAVIDOS trial. The regions of interest were selected in a similar manner to the selection process involved in designing the human *Runx2* and *Osterix* primers. First, the transcriptional start site, promoter region, location of CpG islands and DNase 1 hypersensitive regions were mapped on the genomic DNA sequence. MatInspector analyses were further used to determine putative transcription factor binding sites of nuclear receptors to the genomic region. Pyrosequencing primers for *RXRA*, *VDR* and *Osterix* were designed upstream of the TSS, within the promoter region within CpG shore regions. Conversely, Wakitani *et al.*, sequenced the mouse *Runx2* promoter in a range of tissues including bone tissue and identified a differentially methylated region -2484 bp to -2148 bp upstream of the *Runx2* promoter⁴⁰⁶ therefore, pyrosequencing primers for DNA methylation measurement of *Runx2* were designed within this region.

7.2.2 Vitamin D deficiency during pregnancy is associated with altered offspring DNA methylation in tibial tissue

In the non-loaded tibiae, mice exposed to a prenatal vitamin D deficient diet had lower *Osterix* CpG 11 methylation compared to the control diet ($p = 0.031$, mean difference = 1.5 %, 95 % CI: 0.12, 2.96) and there were no significant differences in methylation at individual CpGs upstream of the *RXRA*, *VDR* or *Runx2* promoters (**Figure 7.2**). In the loaded tibiae, mice exposed to a prenatal vitamin D deplete diet had lower *Runx2* CpG 24 methylation compared to the control diet ($p = 0.036$, mean difference = 3.4 %, 95 % CI: 0.27, 6.61) and there were no significant differences in DNA methylation of *RXRA*, *VDR* or *Osterix* between the two treatment groups.

A

Control diet vs prenatal vitamin D deficient diet										
Non-loaded limb						Loaded limb				
Gene	CpG	n	Mean diff. (%)	(95 % CI)	p	n	Mean diff. (%)	(95 % CI)	p	
<i>RXRA A</i>	1	12	-1.7	(-5.193, 1.883)	0.322	11	-0.4	(-4.119, 3.285)	0.805	
	2	10	-0.9	(-7.616, 5.836)	0.726	10	-1.1	(-5.995, 3.833)	0.626	
	3	10	-0.5	(-3.695, 2.637)	0.710	9	-0.1	(-4.613, 4.326)	0.942	
	4	12	0.4	(-1.954, 2.811)	0.697	11	-0.7	(-2.856, 1.446)	0.477	
<i>RXRA B</i>	1	10	8.4	(-3.461, 20.240)	0.141	11	-0.2	(-8.300, 7.932)	0.960	
	2	10	6.6	(-2.906, 16.126)	0.148	11	1.6	(-5.984, 9.232)	0.641	
	3	12	2.6	(-4.586, 9.789)	0.439	12	-0.2	(-4.303, 3.906)	0.916	
	4	12	2.4	(-3.289, 8.095)	0.369	12	0.4	(-2.052, 2.822)	0.732	
	5	12	5.9	(-4.437, 16.151)	0.234	12	2.8	(-3.312, 8.942)	0.330	
	6	12	4.8	(-2.118, 11.698)	0.153	12	0.4	(-3.594, 4.411)	0.825	
<i>VDR</i>	1	11	-2.8	(-10.408, 4.906)	0.437	12	1.7	(-4.785, 8.219)	0.569	
	2	11	-2.5	(-10.599, 5.689)	0.512	12	2.3	(-2.768, 7.348)	0.337	
	3	12	-0.4	(-6.120, 5.387)	0.890	12	2.5	(-1.196, 6.136)	0.164	
	4	12	-2.2	(-6.968, 2.668)	0.344	12	0.9	(-2.814, 4.667)	0.593	
	5	12	-0.7	(-5.504, 4.104)	0.752	12	1.6	(-2.283, 5.436)	0.384	
	8	12	0.7	(-4.535, 5.972)	0.767	12	-3.0	(-8.582, 2.669)	0.269	
	9	12	-1.1	(-5.566, 3.403)	0.603	12	-0.6	(-4.399, 3.206)	0.734	
	10	12	-1.1	(-3.556, 1.276)	0.318	12	-2.5	(-6.404, 1.431)	0.188	
	<i>Runx2</i>	24	12	2.6	(-4.272, 9.482)	0.418	12	3.4	(0.269, 6.614)	0.036*
		25	12	0.6	(-7.714, 8.914)	0.875	12	0.2	(-4.564, 4.927)	0.934
26		12	-0.2	(-7.206, 6.820)	0.952	12	0.7	(-3.906, 5.353)	0.735	
27		10	2.0	(-0.339, 4.277)	0.085	11	0.1	(-2.814, 2.934)	0.963	
28		12	0.7	(-2.491, 3.824)	0.648	12	-0.6	(-3.573, 2.313)	0.644	
<i>Osterix</i>	8	11	-0.2	(-0.982, 0.637)	0.641	12	-0.4	(-2.757, 1.900)	0.691	
	9	12	0.1	(-1.287, 1.503)	0.866	12	-0.7	(-2.497, 1.047)	0.383	
	10	12	0.0	(-1.079, 1.006)	0.939	12	0.5	(-1.000, 2.033)	0.465	
	11	12	1.5	(0.117, 2.957)	0.037*	12	0.8	(-0.478, 2.035)	0.197	
	17	9	-0.4	(-1.065, 0.267)	0.199	10	-2.0	(-4.418, 0.442)	0.087	
	18	10	1.2	(-1.627, 4.025)	0.356	9	1.7	(-4.006, 7.361)	0.508	
19	10	-0.9	(-2.674, 0.948)	0.304	11	-1.0	(-3.617, 1.536)	0.347		

B

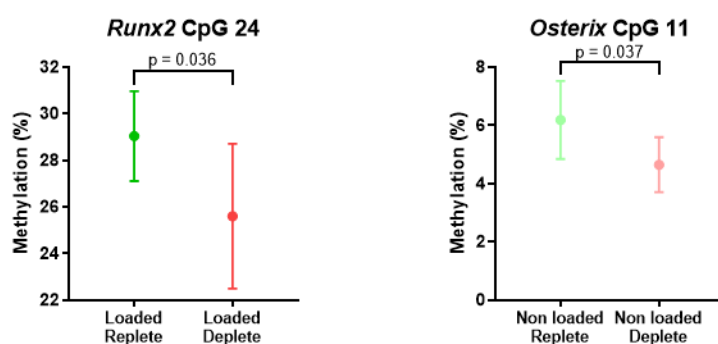


Figure 7.2 Tibial DNA methylation in mice fed a control diet and prenatal vitamin D deficient diet.

Independent t-tests compared DNA methylation between the control diet (replete) and the prenatal vitamin D deficient diet (deplete) within non-loaded and loaded tibiae of 18 week old mice. Graphs represent mean and 95 % confidence intervals.

7.2.3 Mechanical loading is associated with altered tibial DNA methylation in mice exposed to a prenatal vitamin D deficient diet

In the control group, there were no significant differences in DNA methylation of *RXRA*, *VDR*, *Osterix* or *Runx2* between the loaded and non-loaded limb (**Figure 7.3**). In the prenatal vitamin D deficient group, DNA methylation of *RXRA* B CpG 6 was significantly lower in the non-loaded limb compared to the loaded limb ($p = 0.026$, mean difference = -4.7 %, 95 % CI: -8.80, -0.69); there were no significant differences in DNA methylation of *VDR*, *Runx2* or *Osterix* between the non-loaded and loaded limbs.

A

		Non-loaded vs loaded limb								
		Control diet				Prenatal vitamin D deficient diet				
Gene	CpG	n	Mean diff. (%)	(95 % CI)	p	n	Mean diff. (%)	(95 % CI)	p	
<i>RXRA A</i>	1	11	-3.1	(-7.213, 1.067)	0.127	12	-1.8	(-4.964, 1.294)	0.221	
	2	8	-1.0	(-7.806, 5.761)	0.686	12	-1.2	(-5.270, 2.843)	0.520	
	3	8	-0.6	(-5.660, 4.380)	0.766	11	-0.3	(-3.187, 2.679)	0.849	
	4	11	1.0	(-1.935, 4.011)	0.450	12	-0.1	(-1.622, 1.432)	0.893	
<i>RXRA B</i>	1	9	7.5	(-3.565, 18.584)	0.153	12	-1.1	(-9.992, 7.866)	0.796	
	2	9	4.1	(-5.593, 13.891)	0.347	12	-0.8	(-8.344, 6.670)	0.809	
	3	12	0.8	(-5.249, 6.786)	0.782	12	-2.0	(-7.715, 3.651)	0.444	
	4	12	-0.6	(-4.460, 3.223)	0.727	12	-2.6	(-7.492, 2.219)	0.254	
	5	12	-0.1	(-9.863, 9.633)	0.980	12	-3.2	(-10.119, 3.806)	0.336	
	6	12	-0.4	(-7.241, 6.514)	0.909	12	-4.7	(-8.800, -0.690)	0.026*	
<i>VDR</i>	1	12	-2.7	(-9.615, 4.155)	0.398	11	1.7	(-5.486, 8.960)	0.600	
	2	12	-2.6	(-9.904, 4.614)	0.436	11	2.1	(-3.572, 7.772)	0.424	
	3	12	-3.2	(-8.656, 2.289)	0.218	12	-0.3	(-4.607, 3.914)	0.860	
	4	12	-1.8	(-5.848, 2.265)	0.348	12	1.3	(-3.270, 5.840)	0.544	
	5	12	-1.3	(-6.273, 3.757)	0.588	12	1.0	(-2.564, 4.600)	0.541	
	8	12	0.0	(-4.458, 4.518)	0.988	12	-3.6	(-9.899, 2.609)	0.223	
	9	12	-2.8	(-7.751, 2.184)	0.240	12	-2.3	(-5.444, 0.847)	0.135	
	10	12	-1.4	(-4.508, 1.731)	0.345	12	-2.7	(-6.119, 0.649)	0.102	
	<i>Runx2</i>	24	12	0.9	(-5.374, 7.167)	0.757	12	1.7	(-2.514, 5.980)	0.385
		25	12	-0.9	(-8.753, 6.883)	0.789	12	-1.4	(-7.252, 4.545)	0.620
26		12	-0.3	(-7.182, 6.585)	0.920	12	0.6	(-4.818, 6.054)	0.805	
27		12	0.1	(-1.484, 1.647)	0.910	9	-1.8	(-5.807, 2.152)	0.313	
28		12	0.2	(-2.589, 2.929)	0.894	12	-1.1	(-4.445, 2.192)	0.467	
<i>Osterix</i>	8	11	-0.2	(-1.110, 0.675)	0.595	12	-0.5	(-2.778, 1.831)	0.657	
	9	12	0.0	(-1.355, 1.442)	0.946	12	-0.8	(-2.559, 0.979)	0.343	
	10	12	-0.8	(-2.431, 0.855)	0.310	12	-0.2	(-1.065, 0.595)	0.542	
	11	12	1.2	(-0.348, 2.738)	0.115	12	0.4	(-0.666, 1.539)	0.398	
	17	9	-0.3	(-0.940, 0.362)	0.328	10	-1.9	(-4.306, 0.550)	0.100	
	18	11	-1.8	(-6.371, 2.704)	0.385	8	-1.4	(-4.509, 1.799)	0.334	
	19	12	-0.7	(-1.930, 0.457)	0.213	9	-0.9	(-3.848, 2.050)	0.494	

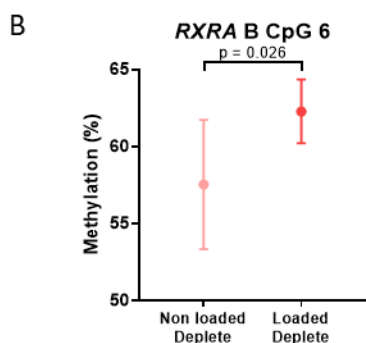


Figure 7.3 Tibial DNA methylation in the non-loaded and loaded tibiae of mice fed a control or prenatal vitamin D deficient diet.

Independent t-tests compared DNA methylation between the non-loaded and loaded limb within 18 week old mice fed a control diet (replete) or prenatal vitamin D deficient diet (deplete). Graphs represent mean and 95 % confidence intervals.

7.2.4 DNA methylation is associated with tibial stiffness in 18 week old mice

The results showed that there was a positive association between tibial stiffness and DNA methylation of *VDR* CpG 4 ($b = 0.315$ (95 % CI: 0.269, 1.555), $p = 0.008$) and CpG 5 ($b = 0.261$ (95 % CI: 0.075, 1.450), $p = 0.031$) (Table 7.1). There were no significant associations between tibial stiffness and DNA methylation of *RXRA*, *Runx2* or *Osterix*. There were no significant associations between ultimate force and DNA methylation of *RXRA*, *VDR*, *Runx2* or *Osterix*. There was a trend towards a positive association between ultimate force and *Osterix* CpG 19 methylation however this did not reach statistical significance $b = 0.216$ (95 % CI: -0.005, 0.711), $p = 0.053$).

Table 7.1 Associations between DNA methylation and stiffness or ultimate force.

	CpG	Stiffness				Ultimate Force			
		n	B (95% CI)		p	n	B (95% CI)		p
<i>RXRA A</i>	1	22	0.019	(-0.946, 1.073)	0.897	22	-0.136	(-0.281, 0.055)	0.174
	2	19	-0.013	(-1.019, 0.935)	0.929	19	-0.019	(-0.186, 0.156)	0.855
	3	18	0.073	(-0.990, 1.653)	0.601	18	-0.064	(-0.301, 0.166)	0.549
	4	22	-0.152	(-2.409, 0.645)	0.242	22	-0.055	(-0.355, 0.193)	0.544
<i>RXRA B</i>	1	20	-0.018	(-0.435, 0.385)	0.900	20	0.068	(-0.049, 0.094)	0.512
	2	20	-0.012	(-0.511, 0.473)	0.935	20	0.021	(-0.078, 0.095)	0.844
	3	23	-0.049	(-0.682, 0.469)	0.704	23	0.098	(-0.047, 0.153)	0.284
	4	23	-0.092	(-1.019, 0.509)	0.494	23	0.029	(-0.118, 0.158)	0.766
	5	23	-0.044	(-0.463, 0.338)	0.747	23	0.024	(-0.063, 0.080)	0.809
	6	23	-0.163	(-0.895, 0.236)	0.238	23	-0.029	(-0.119, 0.090)	0.773
<i>VDR</i>	1	22	0.242	(-0.024, 0.907)	0.062	22	0.110	(-0.036, 0.140)	0.231
	2	22	0.171	(-0.186, 0.849)	0.196	22	0.132	(-0.026, 0.157)	0.149
	3	23	0.141	(-0.320, 1.032)	0.286	23	0.136	(-0.032, 0.204)	0.143
	4	23	0.315	(0.269, 1.555)	0.008*	23	0.142	(-0.025, 0.233)	0.109
	5	23	0.261	(0.075, 1.450)	0.031*	23	0.129	(-0.036, 0.226)	0.147
	8	23	-0.200	(-1.348, 0.213)	0.145	23	0.005	(-0.144, 0.151)	0.961
	9	23	0.021	(-0.970, 1.114)	0.887	23	0.017	(-0.172, 0.201)	0.872
	10	22	-0.190	(-3.312, 0.555)	0.152	22	-0.025	(-0.410, 0.320)	0.800
<i>Osterix</i>	8	23	-0.123	(-3.027, 1.107)	0.344	23	0.090	(-0.192, 0.547)	0.328
	9	23	0.039	(-2.236, 2.963)	0.774	23	0.057	(-0.326, 0.598)	0.546
	10	23	0.094	(-1.764, 3.207)	0.552	23	0.083	(-0.283, 0.603)	0.459
	11	23	0.722	(-1.764, 3.207)	0.552	23	0.160	(-0.283, 0.603)	0.459
	17	18	-1.644	(-4.439, 1.150)	0.229	18	-0.295	(-0.785, 0.195)	0.218
	18	18	-0.125	(-1.555, 0.629)	0.380	18	0.008	(-0.179, 0.192)	0.938
	19	20	0.093	(-1.465, 2.740)	0.531	20	0.216	(-0.005, 0.711)	0.053
<i>Runx2</i>	24	23	0.081	(-0.454, 0.813)	0.561	23	-0.031	(-0.132, 0.097)	0.753
	25	23	0.101	(-0.306, 0.691)	0.430	23	0.074	(-0.054, 0.124)	0.419
	26	23	0.085	(-0.386, 0.754)	0.508	23	0.064	(-0.067, 0.137)	0.481
	27	20	-0.220	(-2.658, 0.403)	0.138	20	0.051	(-0.212, 0.345)	0.620
	28	23	0.056	(-0.874, 1.338)	0.666	23	-0.001	(-0.200, 0.197)	0.988

Linear regression analyses adjusted for prenatal diet and mechanical loading.

7.3 Discussion

Many animal studies have investigated the effect of a vitamin D deficient diet during pregnancy on offspring skeletal health. Borg *et al.* found that mechanical loading in both the control mice and mice exposed to prenatal vitamin D deficiency promoted an anabolic response in cortical and trabecular bone (**Table 7.2**) however, control mice were intrinsically stronger and responded more effectively to mechanical stimulation than mice which were exposed to prenatal vitamin D deficiency²⁴⁵. Within this chapter, we have shown that as well as the phenotypic changes arising from a maternal vitamin D deficient diet, the epigenome is altered in the skeleton of adult offspring. This suggests that an adverse early life environment can have long term consequences that persist into adulthood and that this is reflected both in altered phenotype and altered epigenome. Within the MAVIDOS trial, *RXRA* and *CDKN2A* DNA methylation in umbilical cord tissue was shown to be altered in response to maternal cholecalciferol supplementation during pregnancy and there were no associations between DNA methylation and bone measures at birth, despite studies in the SWS showing that DNA methylation of these two genes were inversely associated with bone measures in later childhood^{299,323}. This suggests that DNA methylation of these genes may be predictive of later bone health and not reflective of the current bone state, or that there are other factors that occur in-between these two time points, such as learning to walk which puts stress on the skeleton. This external stimulus may alter DNA methylation, or it is possible that after this stimulus, the skeleton adapts and at this time point the bone measures are reflective of the DNA methylation profile however, this is unknown. Within this chapter we have shown that a maternal vitamin D deficient diet during pregnancy alters DNA methylation in adult mice and that mechanical loading alters DNA methylation.

In the non-loaded limb, a prenatal vitamin D deficient diet was associated with lower *Osterix* CpG 11 methylation compared to the control diet. The *Osterix* CpGs of interest are located 369 bp upstream of the *Osterix* TSS within the promoter region. The functional importance of these CpGs has not been investigated previously however, often methylation in promoter regions is associated with gene repression. If this is the case, lower *Osterix* methylation in prenatal vitamin D deficient mice may be associated with increased *Osterix* expression which would be expected to promote osteoblast differentiation and an increase in the number of osteocytes. Borg *et al.*, found that a vitamin D deficient diet did not alter trabecular parameters in non-loaded bones but there was an increase in the ratio of mineralisation surface to tibial bone surface at the medial and lateral areas of the tibia and increased cortical porosity compared to the control mice²⁴⁵. With an increased mineralisation area, perhaps due to increased resorption by osteoclasts, there is greater demand for osteocytes to be embedded in the matrix to allow adequate mineralisation to occur. This could be part of a compensatory mechanism in response to low maternal vitamin D during pregnancy to

Chapter 7

maintain skeletal homeostasis. Conversely, an increase in cortical porosity has been shown to be associated with bone loss and an increased risk of developing osteoporosis⁴⁰⁷. It would therefore be interesting to follow up these mice at later time points to determine bone health in later life and whether there are features typical of osteoporosis. This suggests that maternal vitamin D deficiency resulting in fetal vitamin D depletion may have long term consequences and can increase the risk of developing osteoporosis in later life.

Table 7.2 Trabecular, cortical and bone formation parameters of mouse tibiae²⁴⁵.

		Control			Prenatal vitamin D deficiency			p for non loaded ^a	p for loaded ^b
		Non loaded	Loaded	p	Non loaded	Loaded	p		
Trabecular parameters	TbBV/TV	8.28 (0.95)	12.63 (0.84)	0.0013*	9.07 (1.99)	12.94 (2.60)	0.0005*	0.4102	0.7940
	TbTh	0.048 (0.002)	0.069 (0.005)	<0.0001*	0.049 (0.002)	0.067 (0.003)	0.0002*	0.3194	0.5362
	TbSp	0.249 (0.02)	0.235 (0.01)	0.1294	0.255 (0.031)	0.243 (0.021)	0.1075	0.6998	0.4012
	TbN	1.85 (0.46)	1.83 (0.16)	0.3679	1.73 (0.21)	1.91 (0.34)	0.4646	0.5701	0.6415
Cortical parameters	CtBV	0.560 (0.03)	0.839 (0.03)	<0.0001*	0.587 (0.044)	0.770 (0.044)	0.0002*	0.7959	0.0105*
	CtTV	0.952 (0.04)	1.277 (0.03)	<0.0001*	0.995 (0.072)	1.243 (0.056)	0.0010*	0.2299	0.2258
	CtBV/TV	58.8 (0.02)	65.7 (0.01)	<0.0001*	59.1 (0.026)	61.9 (0.010)	0.0093*	0.2076	<0.0001*
	MA	0.392 (0.02)	0.438 (0.02)	0.0077*	0.407 (0.043)	0.473 (0.016)	0.0150*	0.4550	0.0034*
	CtPo	0.467 (0.16)	1.292 (0.29)	0.0010*	0.688 (0.234)	1.385 (0.492)	0.0298*	0.0494	0.7063
	CtTh	0.209 (0.005)	0.288 (0.01)	<0.0001*	0.218 (0.008)	0.286 (0.011)	0.0002*	0.0883	0.1429
MS/BS	Medial	0.353 (0.129)	0.647 (0.238)	0.0776	0.637 (0.067)	0.638 (0.171)	0.9821	0.0017	0.946
	Lateral	0.707 (0.241)	0.767 (0.216)	0.6252	0.987 (0.066)	0.725 (0.191)	0.0184*	0.0351	0.7306
	Trabecular	0.453 (0.264)	0.432 (0.165)	0.8576	0.375 (0.086)	0.442 (0.074)	0.1815	0.5158	0.8961
MAR	Medial	0.528 (0.523)	0.302 (0.134)	0.3409	0.628 (0.841)	0.600 (0.321)	0.9499	0.8106	0.0779
	Lateral	0.732 (0.524)	0.772 (0.592)	0.9962	1.053 (0.618)	0.673 (0.217)	0.2037	0.3547	0.7385
	Trabecular	0.777 (0.628)	0.866 (0.379)	0.8714	0.742 (0.396)	0.792 (0.209)	0.7917	0.9108	0.7089
BFR	Medial	0.183 (0.158)	0.208 (0.106)	0.8885	0.433 (0.628)	0.383 (0.258)	0.8802	0.3832	0.1739
	Lateral	0.568 (0.533)	0.630 (0.496)	0.9437	1.063 (0.694)	0.485 (0.208)	0.0991	0.1979	0.5675
	Trabecular	0.307 (0.171)	0.448 (0.315)	0.6594	0.297 (0.206)	0.338 (0.059)	0.6516	0.9290	0.4831
3 point bending	Stiffness	38.9 (4.5)	57.4 (8.8)	0.0016*	38.6 (6.3)	45.2 (5.6)	0.0807	0.9239	0.0195*
	Ultimate Force	10.60 (1.25)	15.35 (0.95)	<0.0001*	10.18 (0.46)	11.88 (0.91)	0.0042*	0.4613	<0.0001*

^a = p value for non-loaded; control vs prenatal vitamin D deficiency, ^b = p value for loaded; control vs prenatal vitamin D deficiency. TbBV/TV = trabecular bone volume / tissue volume, TbTh = trabecular thickness, TbSp = trabecular separation, TbN = trabecular number, CtBV = cortical bone volume, CtTV = cortical tissue volume, CtBV/TV = cortical bone volume / tissue volume, MA = mineralisation area, CtPo = cortical porosity, CtTh = cortical thickness, MS/BS = mineralisation surface/ bone surface, MAR = mineralisation apposition rate, BFR = bone formation rate.

In the loaded limbs, mice exposed to a prenatal vitamin D deficient diet had lower *Runx2* CpG 24 methylation compared to control mice. Wakitani *et al.*, identified this region as differentially methylated in bone tissue⁴⁰⁶ so it would be interesting to determine the functional importance of these CpG loci on *Runx2* promoter activity. The *Runx2* CpGs are located over 2000 bp upstream of the *Runx2* TSS and Ensembl maps this region as part of the *Runx2* promoter. Wakitani *et al.*, found that there was an inverse association between DNA methylation of *Runx2* CpG -2101 and *Runx2* gene expression⁴⁰⁶. This CpG site is 40 bp away from our CpGs of interest so it is likely that similar associations would be shown. This would suggest that lower methylation is likely be associated with increased *Runx2* gene expression. There were no significant differences in the ratio of mineralisation surface to bone surface, mineralisation apposition rate, bone formation rate or trabecular parameters in loaded bones between the control mice and prenatal vitamin D deficient mice²⁴⁵ which suggests that osteoblast function has not been altered in mice exposed to a prenatal vitamin D deficient diet, and there is adequate mineralisation and bone formation. Amongst loaded bones of prenatal vitamin D deficient mice there was decreased cortical bone volume, decreased ratio of cortical bone volume to tissue volume and increased mineralisation area compared to loaded bones in the control mice²⁴⁵. The increased mineralisation area could be due to increased resorption of osteoclasts, and without altered osteoblast performance it would take longer for the bone formation to be completed. This could result in temporary decreased bone strength following loading compared to mice fed a control diet. Studies in mice have shown that *Runx2* overexpression can promote osteoclast differentiation through *RANKL* and *Osteoprotogerin*. Therefore, a decrease in *Runx2* methylation could be linked to an increase in *Runx2* expression, which is associated with increased osteoblast differentiation and stimulation of osteoclast differentiation through *RANKL* and *Osteoprotogerin*. Conversely, *Runx2* overexpression was also shown to inhibit β -*catenin* levels, which plays an important role in *WNT* signalling and bone formation^{408,409}. This may be part of a negative feedback loop to control osteoblast numbers and osteoblast differentiation.

The results showed that in the control group, there were no differences in DNA methylation between the loaded and non-loaded limbs whereas in mice exposed to a prenatal vitamin D deficient diet, mechanical loading was linked to higher *RXRA* B CpG 6 methylation compared to the non-loaded limb. These *RXRA* CpGs are located 390 bp upstream of the *RXRA* TSS, within the promoter region, of which DNA methylation is often associated with gene repression. In the mice exposed to prenatal vitamin D deficiency, mechanical loading significantly improved trabecular and cortical parameters but there was a decrease in the ratio of mineralisation surface to bone surface at the lateral part of the tibia²⁴⁵. The decreased mineralisation to bone surface ratio following mechanical load could be due to osteoclasts resorbing a smaller surface area. *RXRA* has been shown to play a role in osteoclast differentiation, and a study in the loss of *RXRA* function in hematopoietic

cells resulted in giant non-resorbing osteoclasts and increased bone mass⁴¹⁰ which suggests that there may be a mechanism between *RXRA* expression and altered osteoclast function and resorption. In the MAVIDOS trial we have shown that maternal cholecalciferol supplementation during pregnancy is associated with lower *RXRA* CpG methylation in umbilical cord tissue compared to cord tissue from placebo supplemented mothers. Unfortunately, the *RXRA* CpGs of interest in humans do not seem to be conserved across humans and mice, as assessed by comparing the genomic regions of DNA to determine sequence similarity. Nonetheless, a decrease in *RXRA* methylation following vitamin D supplementation, and an increase in *RXRA* methylation following vitamin D deficiency is to be expected, despite the species differences. Moreover, studies within the SWS cohort have shown that there is an inverse association between *RXRA* CpG methylation and bone measures in childhood²⁹⁹. Therefore, in mice exposed to prenatal vitamin D deficiency, an increase in *RXRA* methylation would be associated with decreased bone measures in later life.

These results show a novel finding where mechanical loading is associated with altered *RXRA* methylation in tibial tissue. The altered response suggests that in tibial tissue this is a dynamic response which allows the skeleton to adapt to mechanical stress. It would be interesting to investigate this further and to investigate methylation changes with respect to mechanical loading in real time, such as following a time course experiment. Comparison of DNA methylation in loaded and non-loaded bones also showed that loading altered DNA methylation, this is the first time that this has been shown. It suggests that DNA methylation may play a role in the mechanism by which loading affects bone strength, either initiating a change in expression or consolidating a change in expression mediated by a change in histone modification. Moreover as DNA methylation is a relatively stable mark this also suggests a mechanism by which bone loading in early life may induce persistent effects at later time points through the life course. Understanding the full extent of the methylation changes and the timing of the events will be very important in understanding the basic mechanism by which loading improves bone strength. This could be investigated further. To do this, mice could undergo mechanical loading for two weeks and DNA methylation as well as gene expression and histone modifications could be measured at different time points such as at 0, 1, 2, 4 and 6 weeks after initial loading. This could provide insight into the timing surrounding altered methylation and if it is associated with altered gene expression and histone modifications. Altered gene expression would also provide insight into whether altered methylation of the CpGs of interest is associated with gene expression or repression and could provide insight into the mechanism involved and how that is associated with changes to bone strength.

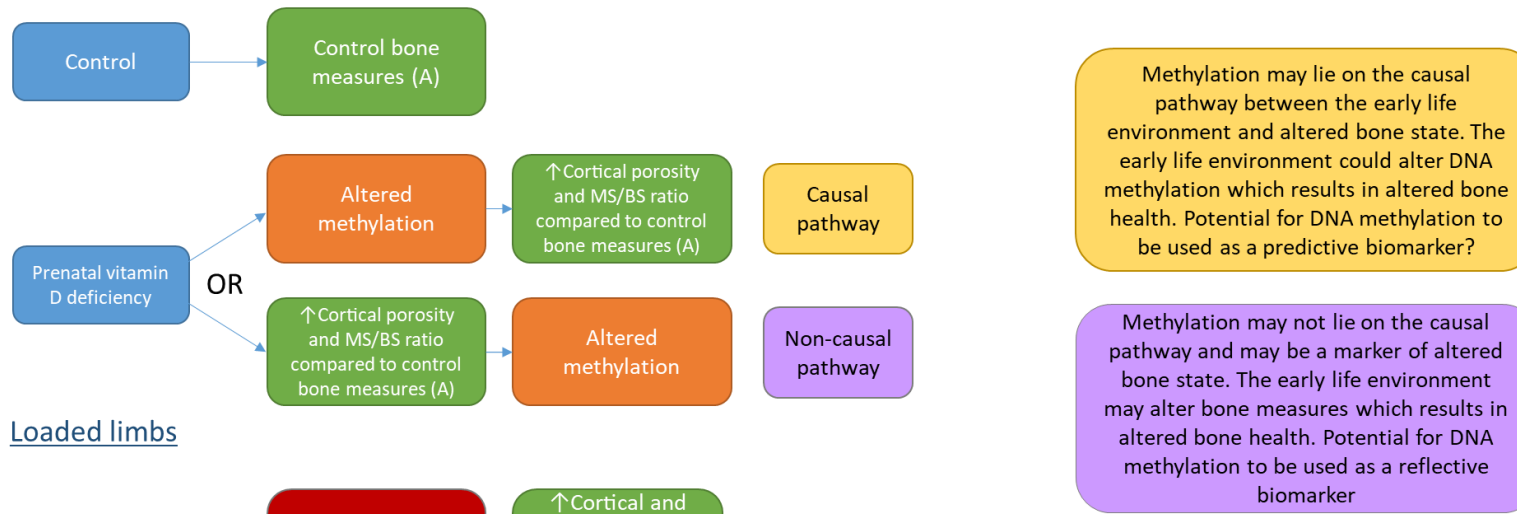
Mechanical loading has been shown to result in increased stiffness and ultimate force, whereas in prenatal vitamin D deficient mice there was only an increase in ultimate force and not stiffness²⁴⁵. Furthermore, mechanical loading in control mice resulted in greater stiffness and ultimate force

compared to loading in prenatal vitamin D deficient mice. This suggests that vitamin D supplementation may not alter skeletal strength, however it may influence how the bone responds to pressure and mechanical loading. If a smaller load is required to fracture the bones, this suggests that the bones are weaker and are more susceptible to becoming osteoporotic in later life. Furthermore, Main *et al.*, have shown that tibial stiffness and the ability of the skeleton to adapt to mechanical load decreases with age⁴¹¹. The results showed that DNA methylation of *VDR* was positively associated with tibial stiffness when adjusting for treatment group and loading as covariates. The *VDR* CpGs are located 26 bp from the *VDR* TSS, within the promoter region and methylation of the promoter region of a gene is typically associated with gene repression. A positive association between *VDR* methylation and stiffness would likely be linked to a decrease in *VDR* expression, resulting in less coupling with *RXR α* and decreased regulation of target genes so you would expect a decrease in activation of genes and pathways that play a positive role in bone development. Conversely, altered methylation may prevent the binding of an inhibitory transcription factor, which could be associated with increased *VDR* expression, increased coupling with *RXR α* and binding to VDREs in target genes such as *Osteocalcin* which is involved in mineralisation of the bone matrix. 1,25(OH)₂D₃ can act independently of *VDR* by binding to membrane bound G-protein coupled receptors which activate the *MAPK* pathways resulting in cross talk with *RXR α* :*VDR* bound to VDREs which could act as a compensatory mechanism. DNA methylation in peripheral tissues has been shown to be stable, however DNA methylation in tibiae may change in response to external stimuli. This would allow the tibiae to better respond to the stimulus in the future to prevent detrimental effects. For instance, after a great mechanical load or a fracture, bone remodelling occurs which involves the coupling of osteoclasts to resorb old bone and osteoblasts to form new bone matrix, which needs to be mineralised. Therefore, these genes need to be actively transcribed which could be consolidated through the lack of methylation in individual cell types within the bone.

Limitations to these experiments include the low sample size. Following DNA methylation pyrosequencing, some methylation values had to be discarded due to failing internal controls resulting in a lower sample size at some CpG loci. Another limitation is that the Osterix CpGs of interest were lowly methylated, with average values around 5 % which may be too low to result in significant phenotypic differences. To overcome this, a mouse methylation array would be used to highlight suitable DMRs however, no such arrays are available. To compensate for this, CpGs further upstream of the promoter would be investigated to identify greater methylation values. This could be through manually sequencing upstream of the TSS by bisulfite pyrosequencing, although this can be time consuming and costly. There is evidence to show that human arrays can be used for mouse models and 13,715 probes from the Illumina Infinium Human Methylation

(HM)450 BeadChip was shown to uniquely match the mouse genome⁴¹². This could highlight differentially methylated regions within the mouse genome which are altered in response to prenatal vitamin D deficiency and/or mechanical loading and could be investigated further through bisulfite pyrosequencing. Furthermore, pathway analysis could identify which pathways are altered providing insight into the mechanism between vitamin D deficiency, DNA methylation and altered bone outcomes. A third limitation is that there is no cell type correction data available. Tibial bone consists of many cell types and methylation patterns are known to be tissue and cell type specific. A fourth limitation is that the mice were loaded twice, during their pubertal growth between weeks 8-10 and during adult growth in weeks 16-18. Ideally, DNA methylation would have been measured in mice that were only loaded in adulthood. Furthermore, no other studies have looked at the effects of two periods of loading. Currently, DNA methylation has not been measured in 10 week old mice and it would be interesting to see how the results compare. It would also be interesting to determine the timings of altered methylation, gene expression and histone modifications in response to mechanical loading and/or prenatal vitamin D deficiency. This could be through a time course experiment where mice undergo mechanical loading and parameters are measured at different time points.

Non-loaded limbs



Loaded limbs

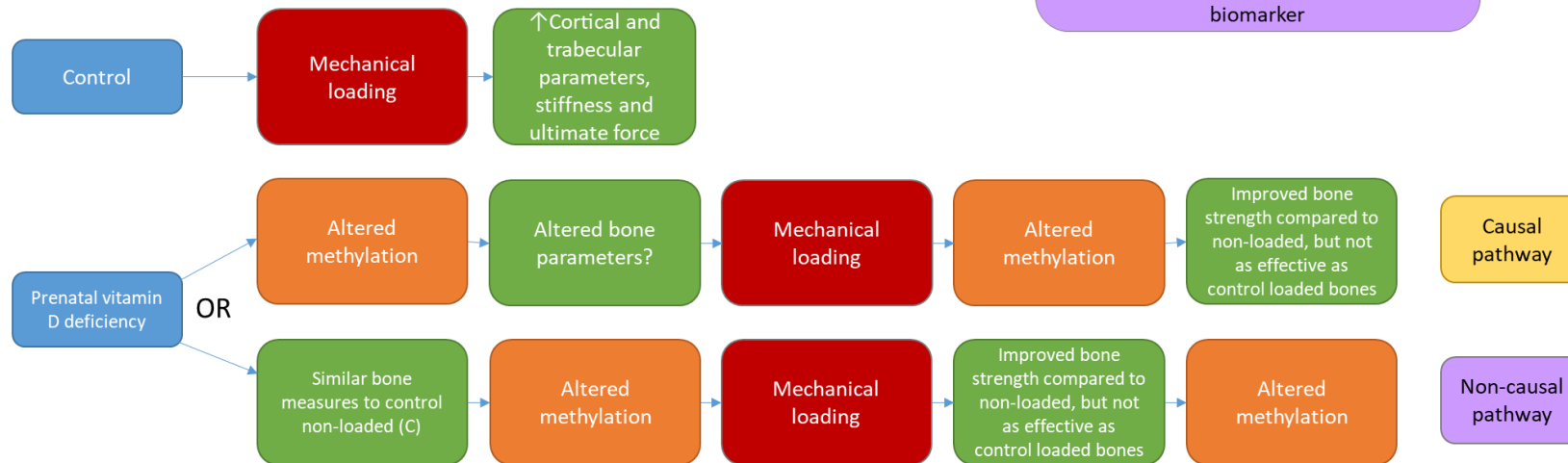


Figure 7.4 Possible relationship linking prenatal vitamin D deficient diet with altered methylation and bone measures.

In conclusion, we have shown that prenatal vitamin D deficiency is associated with altered DNA methylation of the *RXRA* CpGs of interest. This provides supporting evidence that the early life environment, with respect to vitamin D status, is associated with altered DNA methylation and altered phenotype in adult life. It is unclear whether altered DNA methylation is causally involved in bone phenotype in response to a maternal vitamin D deficient diet during pregnancy or whether the methylation profile is simply a marker of the altered bone phenotype (figure). If the biomarker is predictive, this could identify individuals at risk of not achieving peak bone mass in adulthood. Whereas if the marker is reflective, this could help in following up the patients during their life course and assessing whether the interventions are beneficial or whether a different approach should be considered. Currently, it is unknown how epigenetic marks at birth, such as in umbilical cord tissue or in peripheral blood, compare to the epigenetic marks in adult tibial tissue and whether they could be used to predict the adult phenotype. In the future, it would be interesting to measure DNA methylation in proxy tissues, such as blood or umbilical cord tissue, at birth and to determine associations with bone measures and tibial DNA methylation in adulthood. It would also be interesting to determine whether there are similar findings to what has been shown in the MAVIDOS and SWS cohorts, where DNA methylation of *RXRA* is not associated with bone measures at birth but has been shown to be associated with bone measures in childhood. Within this chapter, we have shown that mechanical loading altered DNA methylation amongst mice exposed to a maternal vitamin D deficient diet during early life. Nonetheless, there are some caveats such as only a few CpG loci have been sequenced and CpG loci were predominantly unmethylated (~5 %) which suggests that methylation changes detected may be too small to have a significant effect on phenotype. Nonetheless, this provides preliminary evidence which has scope to be expanded further such as through the use of human methylation arrays which have shown overlap with the mouse genome⁴¹². Furthermore, the functional relevance of the CpG loci could be investigated through site directed mutagenesis in a luciferase reporter system which could provide insight into the effect that altered methylation of these CpG loci has on gene promoter activity.

Chapter 8 Final Discussion

8.1 Final discussion

Osteoporosis can be a debilitating condition due to the associated morbidity and mortality arising as a consequence to the increased risk of fracture⁷. To date, prevention strategies are very limited, and often patients remain undiagnosed for long periods of time¹¹. Furthermore, patients with osteoporosis remain untreated and/or compliance with treatment is low which increases the susceptibility to fractures following a fall^{2,7}. Epidemiological studies have highlighted that the early life environment, particularly during pregnancy and early infancy, is associated with the risk of developing diseases such as osteoporosis in later adulthood^{215,217}. Furthermore, the early life environment has been shown to be associated with altered DNA methylation²⁸⁶, which may be used as a biomarker for later health. It is unclear whether altered DNA methylation lies on the causal pathway between the early life environment and altered bone health or whether the early life environment results in altered bone health which is consolidated by changes to the epigenome. Causality is not required for risk prediction, and a suitable predictive biomarker would help to identify at risk individuals in need of additional interventions during early infancy to improve bone health and reduce the risk of developing osteoporosis in later life. A predictive biomarker could also be used to determine the effectiveness of early life intervention studies on improving later bone outcomes. Conversely, a reflective biomarker could provide insight into the current bone state and could be used to assess the effectiveness of interventions and identify changes to the intervention / treatment strategy if needed. Studies within the SWS cohort have identified two candidate biomarkers, *RXRA* and *CDKN2A*, of which DNA methylation in umbilical cord tissue has been shown to be associated with bone outcomes at 4 and 6 years of age^{299,323}. Randomised control trials provide an opportunity to investigate these observations and associations further. Within the MAVIDOS trial, maternal cholecalciferol supplementation during pregnancy was shown to improve bone outcomes in infants born during the winter months²³⁶. Further investigation into the MAVIDOS trial will provide valuable insight into whether DNA methylation of these candidate genes can be used as a predictive biomarker for later bone health and could aid in the direction of future interventions that may have a positive effect on the bone health trajectory and thus play a role in decreasing the risk of developing osteoporosis in later adulthood.

8.2 Summary of main findings

Within the MAVIDOS trial, infants born to a maternal cholecalciferol supplemented diet had lower methylation of *RXRA* and *Osterix*, higher *CDKN2A* methylation and unaltered *Runx2* methylation compared to the placebo group (**Figure 8.1**). When the analyses were stratified by season of birth, *RXRA* methylation was lower amongst infants born in summer and autumn to cholecalciferol

supplemented mothers, *CDKN2A* methylation was higher amongst infants born in autumn, *Osterix* methylation was lower amongst infants born in spring and there were no seasonal differences in *Runx2* between the two maternal treatment groups. With intervention as a covariate, there were positive associations between *Osterix* and *Runx2* methylation at birth and bone outcomes at birth, but there were no associations between *RXRA* or *CDKN2A* methylation at birth and bone outcomes at birth. Within the placebo group, there were positive and inverse associations between *Osterix* and *Runx2* methylation at birth and bone measures at birth, but there were no associations between *RXRA* or *CDKN2A* methylation at birth and bone measures at birth. Whereas within the cholecalciferol supplemented group there was an inverse association between *RXRA* methylation at birth and bone measures at birth and no associations between methylation at birth of *CDKN2A*, *Osterix* or *Runx2* and bone measures at birth. When the analyses were stratified by season of birth, methylation levels at *Osterix* and *Runx2* were positively and inversely associated with bone measures amongst infants born in all four seasons, *RXRA* methylation at birth were inversely and positively associated with bone measures amongst infants born in the summer and autumn months respectively, whereas there were no associations between *CDKN2A* methylation at birth and bone measures at birth within any of the four seasons.

Functional *in vitro* studies have shown that mutation of the *RXRA* CpGs of interest, which have been shown to be associated with bone mass during childhood within the SWS cohort²⁹⁹, significantly decreases *RXRA* promoter activity in a luciferase construct in two osteosarcoma cell lines. *In silico* analyses have identified that the region containing the core *RXRA* CpGs of interest lie within a DNase 1 hypersensitive region with histone mark enrichment suggesting that it may be part of an enhancer which has a regulatory effect on expression. Excision of this region of interest and cloning into a minimal promoter vector is able to elicit a luciferase response despite the lack of a promoter. Furthermore, exclusion of different core *RXRA* CpGs has a differential effect on luciferase expression. Radiolabelled EMSAs have identified specific transcription factor binding across the *RXRA* CpGs of interest, which could be investigated further.

Measurement of DNA methylation in tibiae of adult mice exposed to prenatal vitamin D deficiency highlighted altered DNA methylation at *RXRA*, *Osterix* and *Runx2*. Furthermore, there is evidence of interaction between prenatal vitamin D deficiency, DNA methylation, mechanical loading and bone strength in adulthood.

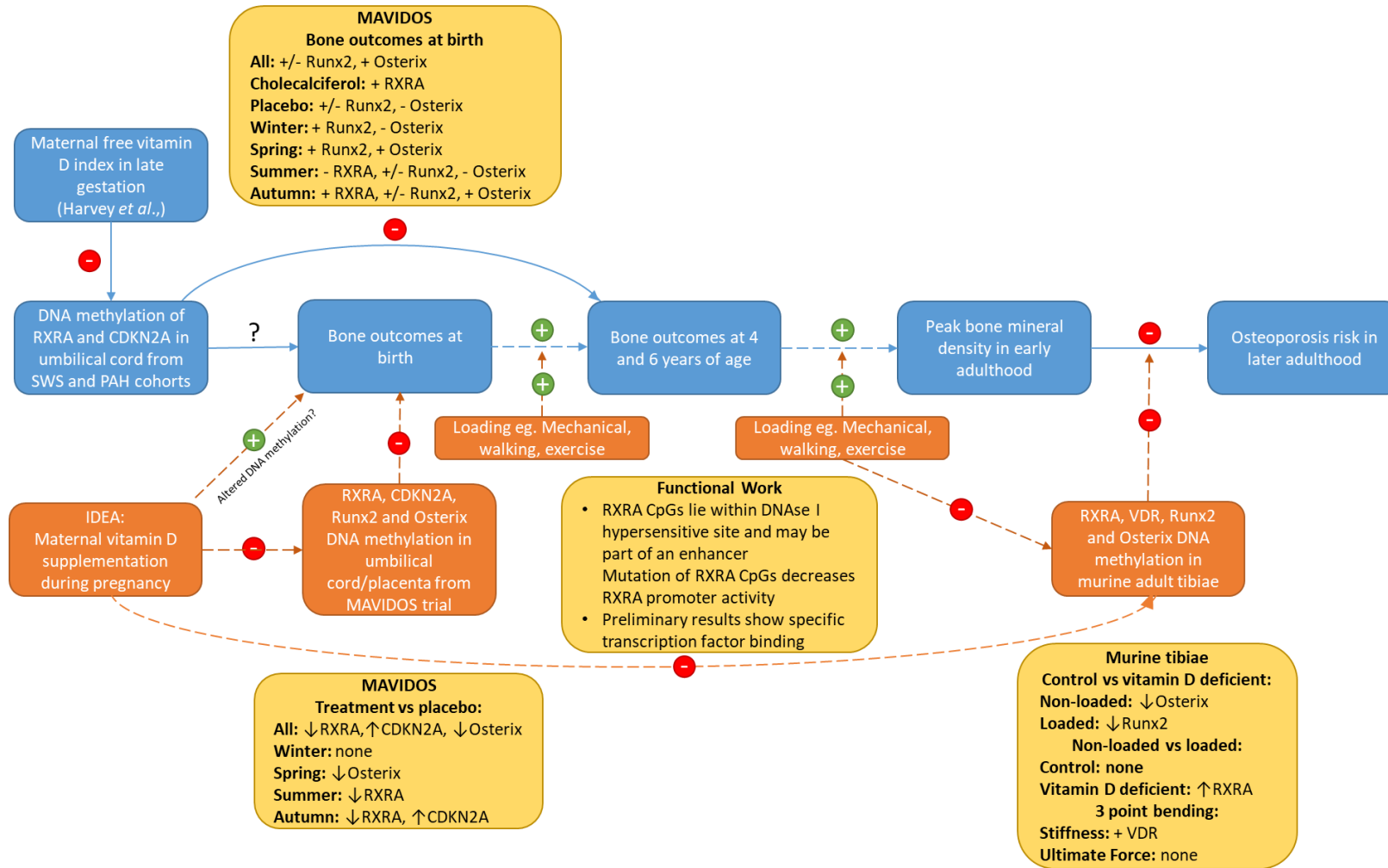


Figure 8.1 Summary of main findings.

+ = positive associations, - = inverse associations

8.3 Discussion of main findings

8.3.1 DNA methylation of *RXRA* may be used as a predictive biomarker of later bone health

Within the MAVIDOS trial, we have shown that maternal cholecalciferol supplementation is associated with altered *RXRA* methylation in umbilical cord tissue. The direction of effect suggests that with vitamin D supplementation there is a decrease in *RXRA* methylation which is likely associated with an increase in *RXRA* expression. *RXRA* is able to form dimers with VDR, as well as other nuclear receptors such as TR and PPAR, which can have downstream effects associated with bone measures^{326–328}. With an increase in *RXRA* expression, there could be increased binding to VDREs in target genes such as *osteocalcin* which is involved in mineralisation of bone matrix. The MAVIDOS trial has shown that infants born in the winter months to cholecalciferol supplemented mothers had improved bone measures at birth compared to the placebo group²³⁶ however, these phenotypic changes were not reflected in methylation of *RXRA* amongst infants born in the winter months. Instead, *RXRA* methylation was associated with bone measures amongst infants born in the summer and autumn months. This could be due to DNA methylation of *RXRA* not being reflective of the current bone state, but instead it may be predictive of bone health later in childhood. It would be interesting to determine associations at 4 and 6 years of age as these become available. The associations amongst the summer and autumn months may be due to increased maternal exposure to UVB during pregnancy, coupled together with maternal vitamin D supplementation. This could result in increased maternal serum 25(OH)D₃ concentrations and increased transfer to the fetus, altering *RXRA* methylation at birth. Conversely, the phenotypic differences in winter may be as a result of low vitamin D in the placebo group negatively impacting fetal skeletal development compared to the cholecalciferol supplemented group. Within the placebo group, the maternal vitamin D status of mothers that delivered in the winter and spring months decreased from 14 to 34 weeks gestation whereas amongst mothers that delivered in the summer and autumn, maternal vitamin D status increased from early to late pregnancy. It would be interesting to determine whether infants born to cholecalciferol supplemented mothers in summer and autumn have improved bone measures at ages 4 and 6 compared to the placebo group.

Functional investigation into these CpGs of interest in **Chapter 6** has shown that site directed mutagenesis of individual CpG loci decreases *RXRA* promoter activity, which suggests that these CpG sequences are important for *RXRA* promoter activity. The DMR containing the *RXRA* CpGs of interest showed properties typical of an enhancer region, as shown by H3K4Me1 enrichment and the DNase 1 hypersensitive sites, and cloning of this region into a minimal promoter vector, which

is used to test regulatory regions, demonstrated that this region has enhancer properties in osteosarcoma cell lines. This suggests that the *RXRA* CpGs identified maybe be important for *RXRA* transcriptional activity. Using EMSAs we have shown that GR binds over *RXRA* CpGs 4 (-2649) and 5 (-2642), both of which were shown to be altered by maternal cholecalciferol supplementation. The consensus binding sequence recognised by GR is a symmetric repeat of 'AGAACA (n=3) TGTCT' whereas the consensus sequence for VDR is a direct repeat of 'AGGTCA (n=3) AGGTCA'³⁵⁷. There is evidence to suggest that VDR can bind as a homodimer as well as a heterodimer and that VDR can bind to half sites, although there is preferential binding as a dimer with *RXRA*³⁵⁷. It is possible that VDR could partially bind to this hexameric half site or that other nuclear receptors may bind such as TR or PPAR which could be investigated through EMSAs. This could alter transcription factor binding and histone modifications which could result in altered chromatin structure and changes to gene expression, such as in genes related to bone formation and bone mineralisation. As DNA methylation across the response elements of many transcription factors, although not all, has been shown to block transcription factor binding⁴¹³, methylation across these sites may affect nuclear receptor binding and the transcriptional activity of *RXRA*. This could be investigated further through the use of methylated probes which would further determine whether altered methylation of these CpG loci alters transcription factor binding, such as that of GR.

Within the MAVIDOS trial, *RXRA* methylation at birth was not associated with bone measures at birth with intervention as a covariate. However, altered methylation may be associated with bone measures in later childhood so it would be interesting to determine associations at 4 and 6 years of age. It is unclear whether methylation of *RXRA* lies on the causal pathway or is simply a marker of later bone health (**Figure 8.2**). Causality is not required for risk prediction however, if *RXRA* methylation is causally involved in bone health and also predictive of later bone health, targeted interventions could be used to try to specifically alter *RXRA* methylation. It is possible that maternal vitamin D supplementation alters *RXRA* methylation at birth, which is associated with bone measures in later childhood. Conversely, maternal vitamin D supplementation during pregnancy may improve fetal skeletal development amongst infants born in the winter months, and may be associated with improved skeletal growth during early childhood and this may be consolidated with methylation marks on these *RXRA* CpG loci.

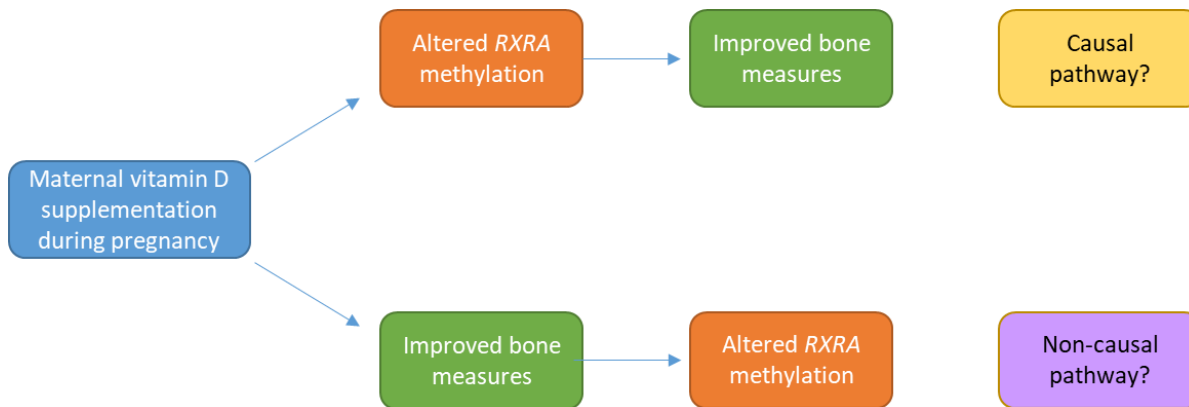


Figure 8.2 Possible relationship between maternal cholecalciferol supplementation, altered *RXRA* methylation and improved bone measures.

8.3.2 Maternal cholecalciferol supplementation is associated with altered methylation of *CDKN2A* and *Osterix* and methylation of *Runx2* and *Osterix* were associated with bone measures at birth within the MAVIDOS trial

To identify further biomarkers of later bone health with respect to maternal vitamin D supplementation we also examined the methylation status of *CDKN2A* (**Chapter 4**), which has been shown to be inversely associated with bone measures in later childhood within the SWS cohort³²³, and we investigated the methylation status of two transcription factors, *Runx2* and *Osterix* (**Chapter 5**), that play a vital role in osteoblast differentiation and bone formation (**Figure 1.5**).

Maternal cholecalciferol supplementation during pregnancy was associated with increased *CDKN2A* methylation at birth although there were no significant associations between *CDKN2A* methylation and bone measures at birth with intervention as a covariate (**Figure 8.3**). These findings are similar to what was observed with the methylation status of *RXRA*. The functional relevance of the *CDKN2A* CpGs of interest have been investigated by Lillycrop *et al.*, which showed that site directed mutation has a negative effect on *ANRIL* promoter activity³²². An increase in *CDKN2A* methylation is likely associated with a decrease in *CDKN2A* expression which could be linked to a decrease in *p14^{INK4A}* and *p16^{ARF}* production, decreased inhibition of *CDK4/6*, and phosphorylation of *Rb* resulting in cell cycle progression and cell proliferation (**Figure 4.4**). This could result in an increased number of proliferating mesenchymal stem cells with the potential to differentiate into osteoblasts which would be associated with increased bone formation. Associations between *CDKN2A* methylation at birth and bone measures at 4 and 6 years of age should be investigated further when these bone measures become available.

Interestingly, we have shown altered methylation and associations between methylation and bone measures in bone related genes, especially amongst infants born in the winter months. The functional relevance of the *Osterix* CpGs of interest has not been investigated however, methylation within the promoter region is often associated with decreased promoter activity. A decrease in *Osterix* methylation could be linked to increased *Osterix* expression and an increase in differentiation into mature osteoblasts which could have a positive effect on bone formation. This is further supported by the inverse association between *Osterix* CpG 3 methylation and BMD at birth amongst infants born in the winter months. Maternal cholecalciferol supplementation during pregnancy was not associated with altered *Runx2* CpG methylation, however only a few CpG loci were sequenced. Conversely, it could be argued that as *Runx2* plays a role in early osteoblast differentiation, the differentiation capacity has not been altered which could be a control mechanism. Maternal vitamin D deficiency during pregnancy is common⁴¹⁴, so if low vitamin D was causally involved in altered *Runx2* methylation this could affect the differentiation capacity of mesenchymal stem cells into osteoblasts which would have a detrimental affect in many infants.

A genome wide approach, such as through an EPIC array, may be useful to identify further epigenetic marks predictive of bone outcomes. This would need to be replicated further across many different cohorts. Together, a panel of biomarkers could be used as an indicator of predicted bone measures in childhood which could influence bone health in later life and the risk of developing osteoporosis.

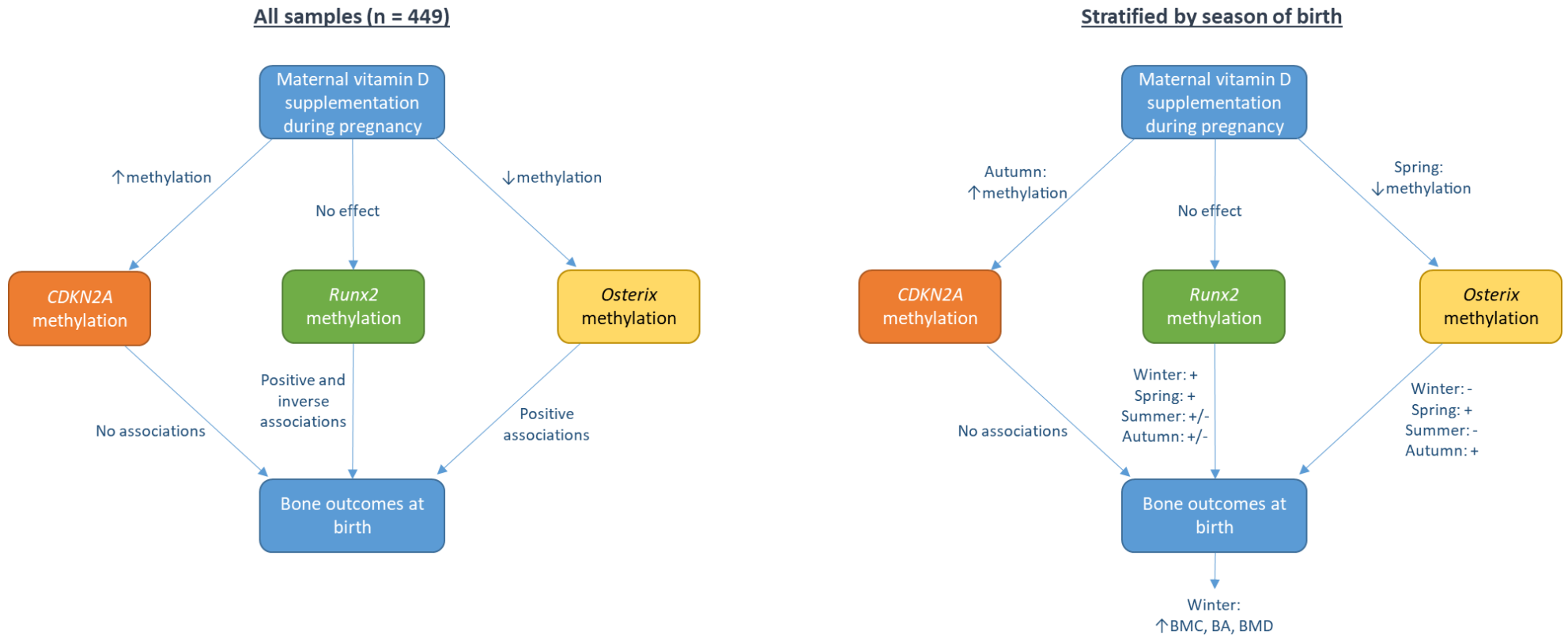


Figure 8.3 Summary of main *CDKN2A*, *Runx2* and *Osterix* findings within the MAVIDOS trial.

+ = positive associations, - = inverse associations.

8.3.3 A prenatal vitamin D deficient diet is associated with altered DNA methylation in tibiae from adult mice

Within this thesis, the relationship between maternal vitamin D supplementation during pregnancy, altered DNA methylation and bone measures at birth have been investigated. However, associations between DNA methylation and bone measures in later childhood or adulthood have not been investigated as these are not available within the MAVIDOS trial. Using a mouse model in collaboration with Dr S Borg, University of Sheffield, we were able to investigate the relationship between maternal vitamin D status during pregnancy, DNA methylation in adult tibial tissue and adult bone health. The results showed that prenatal vitamin D deficiency was associated with altered methylation in adult tibiae. Furthermore, we have shown a novel finding of altered DNA methylation in tibiae of prenatal vitamin D deficient mice in response to mechanical loading. Further investigation could provide insight into the mechanism behind how mechanical loading improves bone strength. Using a time course experiment, mice could undergo mechanical loading and DNA methylation, gene expression and histone modifications could be measured. This could provide insight into the timings of altered epigenetic modifications and gene expression. It would also provide insight into whether altered DNA methylation may be causally involved in altered gene expression and altered phenotype, or simply be a marker to consolidate the changes in gene expression and histone modifications (Error! Reference source not found.). Borg *et al.*, found that mechanical loading in both the control mice and mice exposed to prenatal vitamin D deficiency promoted an anabolic response in cortical and trabecular bone however, control mice were intrinsically stronger and responded more effectively to mechanical stimulation than mice which were exposed to prenatal vitamin D deficiency²⁴⁵. Furthermore, we have shown that there is altered DNA methylation in mice exposed to a prenatal vitamin D deficient diet, and following mechanical loading there is altered methylation in mice exposed to a prenatal vitamin D deficient diet and not amongst those in the control group. This could be an adaptive response to mechanical stress to try and better adapt the skeleton. It would be interesting to follow these mice further into old age and to investigate the timing of onset of osteoporosis. For instance, if mechanical loading during childhood and adulthood in mice exposed to a prenatal vitamin D deficient diet is able to delay the onset of developing osteoporosis, this could be used as a preventative measure in humans in individuals that are known to be at an increased risk of developing osteoporosis. Furthermore, the type of exercise may prove to be more beneficial such as swimming vs running which could be investigated further and could be used as a targeted intervention.

8.4 Future work

Currently, within the MAVIDOS trial bone measurements are being recorded in children aged 4 and 6. It would be interesting to determine any differences in bone measures between the two maternal treatment groups, as well as within each season of birth, and to determine associations between DNA methylation at birth of *RXRA*, *CDKN2A*, *Osterix* and *Runx2* and bone measures in childhood with intervention as a covariate. The MAVIDOS trial is a mainly Caucasian population so associations should be determined in other trials and ethnicities, especially in randomised control trials which are following children through early childhood. However, whether DNA methylation is part of a causal pathway is undetermined and further exploration into key mechanisms could be investigated. A selection of the MAVIDOS DNA samples are undergoing an 850k array which could identify differentially methylated regions between the two maternal treatment groups. This could be investigated further and DNA methylation could be measured in these potentially altered genes.

The functional importance of the *RXRA* CpGs of interest have been investigated in two osteosarcoma cell lines, but this could be investigated further, such as in primary cells. Transcription factor binding could be investigated further, with EMSAs or with CHIP and pathway analysis could be used to identify key signalling pathways that may be altered. Preliminary work has shown that excision of genomic regions of the *RXRA* gene has a differential effect on luciferase expression so we could investigate transcription factor binding within the DMR or DNA methylation of flanking CpGs could also be measured to provide greater insight into this region. The functional relevance of the *RXRA* CpGs of interest could also be investigated in other primary cells or cell lines, such as HUVECS, which could be used to reflect the use of umbilical cords within the MAVIDOS trial.

DNA methylation was measured in murine tibiae from Dr Borg's study however, this could be investigated further. Currently, DNA methylation was measured in tibiae from 18 week old mice that were exposed to prenatal vitamin D deficiency. DNA could additionally be measured in the 10 week old mice exposed to the same diet to investigate DNA methylation during the growth period. Similarly, the regions of interest could be expanded to provide a greater insight into the relationship between the early life environment, vitamin D deficiency, DNA methylation and skeletal growth. This could be through bisulfite sequencing and measurement of DNA methylation, or it could be through the use of a human methylation array, such as the Illumina HM450 BeadChip array of which 13,715 probes have been shown to match with the bisulfite converted mouse genome⁴¹². A time course experiment combining prenatal vitamin D deficiency and mechanical loading could be investigated with respect to DNA methylation, gene expression and histone modifications which can provide insight into the dynamic response and provide insight into the mechanism and related pathways. Furthermore, DNA methylation could be measured in umbilical cord and blood samples

could be taken at several intervals during the life course to investigate how they compare to DNA methylation in tibial tissue. Also, additional measurement in blood would allow measurement at several time points whereas tibial tissue can only be investigated once.

8.5 Implications for human health

Osteoporosis is a debilitating disease that affects the ageing population. Peak bone mineral density in adulthood has been shown to be causally related to osteoporosis risk³⁴⁹ and it has been shown that a 10 % increase in peak bone mineral density is able to delay the development of osteoporosis by up to 13 years²⁹. Currently, many individuals with osteoporosis remain undiagnosed or are not receiving treatment^{2,7,11}, so it would be beneficial to intervene earlier in the life course and to delay the onset of this disease. Many studies have shown that the early life environment can influence bone health in adulthood²¹⁵ and studies have shown that the early life environment can alter the epigenome resulting in altered phenotype²⁸⁶. DNA methylation is easily measured and can be used as a biomarker to predict individuals that are at risk of not achieving their peak bone mineral density in early adulthood and are more susceptible to suffering from osteoporosis in later life. Furthermore, targeted interventions during the early life period and during development could aim to alter DNA methylation of genes directly involved in altered bone phenotype. Within the MAVIDOS trial, we have shown that maternal cholecalciferol supplemented was associated with altered DNA methylation of *RXRA*, *CDKN2A* and *Osterix* but not *Runx2*; with evidence of associations between DNA methylation at *RXRA*, *Osterix* and *Runx2* and bone measures at birth. Follow up investigation at 4 and 6 years of age will determine associations between DNA methylation of these candidate genes at birth and bone measures in early childhood. This will provide evidence as to whether these are suitable predictive biomarkers and will help to assess whether maternal vitamin D supplementation during pregnancy is a suitable intervention that can benefit bone health through the life course.

List of References

List of References

1. Consensus development conference: diagnosis, prophylaxis, and treatment of osteoporosis. *Am. J. Med.* **94**, 646–50 (1993).
2. Hernlund, E. *et al.* Osteoporosis in the European Union: medical management, epidemiology and economic burden. *Arch. Osteoporos.* **8**, 136 (2013).
3. Kanis, J. A. Diagnosis and Clinical Aspects of Osteoporosis. in *Pocket Reference to Osteoporosis* 11–20 (Springer International Publishing, 2019). doi:10.1007/978-3-319-26757-9_2
4. Kanis, J. A. *et al.* The Burden of Osteoporotic Fractures: A Method for Setting Intervention Thresholds. *Osteoporos. Int.* **12**, 417–427 (2001).
5. Delgado-Calle, J., Garmilla, P. & Riancho, J. A. Do epigenetic marks govern bone mass and homeostasis? *Curr. Genomics* **13**, 252–63 (2012).
6. Cummings, S. R. *et al.* Risk Factors for Hip Fracture in White Women. *N. Engl. J. Med.* **332**, 767–774 (1995).
7. Kanis, J. A., Cooper, C., Rizzoli, R., Reginster, J.-Y. & (IOF), on behalf of the S. A. B. of the E. S. for C. and E. A. of O. (ESCEO) and the C. of S. A. and N. S. of the I. O. F. European guidance for the diagnosis and management of osteoporosis in postmenopausal women. *Osteoporos. Int.* **30**, 3–44 (2019).
8. Elliot-Gibson, V., Bogoch, E. R., Jamal, S. A. & Beaton, D. E. Practice patterns in the diagnosis and treatment of osteoporosis after a fragility fracture: a systematic review. *Osteoporos. Int.* **15**, 767–778 (2004).
9. Giangregorio, L., Papaioannou, A., Cranney, A., Zytaruk, N. & Adachi, J. D. Fragility Fractures and the Osteoporosis Care Gap: An International Phenomenon. *Semin. Arthritis Rheum.* **35**, 293–305 (2006).
10. Haaland, D. A. *et al.* Closing the osteoporosis care gap: increased osteoporosis awareness among geriatrics and rehabilitation teams. *BMC Geriatr.* **9**, 28 (2009).
11. Barton, D. W., Behrend, C. J. & Carmouche, J. J. Rates of osteoporosis screening and treatment following vertebral fracture. *Spine J.* **19**, 411–417 (2019).
12. Bliuc, D. *et al.* Mortality Risk Associated With Low-Trauma Osteoporotic Fracture and Subsequent Fracture in Men and Women. *JAMA* **301**, 513 (2009).
13. Von Friesendorff, M. *et al.* Hip fracture, mortality risk, and cause of death over two decades.

doi:10.1007/s00198-016-3616-5

14. Kanis, J. A. *et al.* The components of excess mortality after hip fracture. *Bone* **32**, 468–473 (2003).
15. Papaioannou, A. *et al.* Mortality, Independence in Living, and Re-fracture, One Year Following Hip Fracture in Canadians. *J. SOGC* **22**, 591–597 (2000).
16. Kanis, J. A. & Kanis, J. A. Assessment of fracture risk and its application to screening for postmenopausal osteoporosis: Synopsis of a WHO report. *Osteoporos. Int.* **4**, 368–381 (1994).
17. Kanis, J. A., Johnell, O., Oden, A., Johansson, H. & McCloskey, E. FRAX™ and the assessment of fracture probability in men and women from the UK. *Osteoporos. Int.* **19**, 385–397 (2008).
18. Kanis, J. A., Cooper, · C, Rizzoli, · R & Reginster, J.-Y. Executive summary of European guidance for the diagnosis and management of osteoporosis in postmenopausal women. (2019). doi:10.1007/s40520-018-1109-4
19. Adachi, J. D. *et al.* Predictors of imminent non-vertebral fracture in elderly women with osteoporosis, low bone mass, or a history of fracture, based on data from the population-based Canadian Multicentre Osteoporosis Study (CaMos). *Arch. Osteoporos.* **14**, 53 (2019).
20. Juby, A. G. & De Geus-Wenceslau, C. M. Evaluation of Osteoporosis Treatment in Seniors after Hip Fracture. *Osteoporos. Int.* **13**, 205–210 (2002).
21. Hajcsar, E. E., Hawker, G. & Bogoch, E. R. Investigation and treatment of osteoporosis in patients with fragility fractures. *CMAJ* **163**, 819–22 (2000).
22. Cree, M. W., Juby, A. G. & Carriere, K. C. Mortality and morbidity associated with osteoporosis drug treatment following hip fracture. *Osteoporos. Int.* **14**, 722–727 (2003).
23. Raisz, L. G. Pathogenesis of osteoporosis: concepts, conflicts, and prospects. *J. Clin. Invest.* **115**, 3318–3325 (2005).
24. Bonjour, J. P., Theintz, G., Law, F., Slosman, D. & Rizzoli, R. Peak bone mass. *Osteoporos. Int.* **4 Suppl 1**, 7–13 (1994).
25. Weaver, C. M. *et al.* The National Osteoporosis Foundation’s position statement on peak bone mass development and lifestyle factors: a systematic review and implementation recommendations. *Osteoporos. Int.* **27**, 1281–1386 (2016).

List of References

26. Chew, C. K. & Clarke, B. L. Causes of low peak bone mass in women. *Maturitas* **111**, 61–68 (2018).
27. Matkovic, V. *et al.* Timing of peak bone mass in Caucasian females and its implication for the prevention of osteoporosis. Inference from a cross-sectional model. *J. Clin. Invest.* **93**, 799–808 (1994).
28. Recker, R. R. *et al.* Bone gain in young adult women. *JAMA* **268**, 2403–8 (1992).
29. Hernandez, C. J., Beaupre, G. S. & Carter, D. R. A theoretical analysis of the relative influences of peak BMD, age-related bone loss and menopause on the development of osteoporosis. *Osteoporos. Int.* **14**, 843–847 (2003).
30. McVeigh, J. A., Howie, E. K., Zhu, K., Walsh, J. P. & Straker, L. Organized Sport Participation From Childhood to Adolescence Is Associated With Bone Mass in Young Adults From the Raine Study. *J. Bone Miner. Res.* **34**, 67–74 (2019).
31. Slemenda, C. W. *et al.* Bone mass and anthropometric measurements in adult females. *Bone Miner.* **11**, 101–9 (1990).
32. Jeddi, M. *et al.* Relative Importance of Lean and Fat Mass on Bone Mineral Density in Iranian Children and Adolescents. *Int. J. Endocrinol. Metab.* **13**, e25542 (2015).
33. Arabi, A. *et al.* Sex differences in the effect of body-composition variables on bone mass in healthy children and adolescents. *Am. J. Clin. Nutr.* **80**, 1428–1435 (2004).
34. Harris, M., Nguyen, T. ., Howard, G. ., Kelly, P. . & Eisman, J. . Genetic and Environmental Correlations Between Bone Formation and Bone Mineral Density: A Twin Study. *Bone* **22**, 141–145 (1998).
35. Nguyen, T. V, Howard, G. M., Kelly, P. J. & Eisman, J. A. Bone mass, lean mass, and fat mass: same genes or same environments? *Am. J. Epidemiol.* **147**, 3–16 (1998).
36. Seeman, E. *et al.* Do genetic factors explain associations between muscle strength, lean mass, and bone density? A twin study. *Am. J. Physiol. Metab.* **270**, E320–E327 (1996).
37. Arden, N. K. & Spector, T. D. Genetic Influences on Muscle Strength, Lean Body Mass, and Bone Mineral Density: A Twin Study. *J. Bone Miner. Res.* **12**, 2076–2081 (1997).
38. Flicker, L. *et al.* Bone density determinants in elderly women: A twin study. *J. Bone Miner. Res.* **10**, 1607–1613 (2009).

39. Krall, E. A. & Dawson-Hughes, B. Heritable and life-style determinants of bone mineral density. *J. Bone Miner. Res.* **8**, 1–9 (2009).
40. Kulak, MD, C. A. M. *et al.* OSTEOPOROSIS AND LOW BONE MASS IN PREMENOPAUSAL AND PERIMENOPAUSAL WOMEN. *Endocr. Pract.* **6**, 296–304 (2000).
41. Seeman, E. *et al.* Reduced Bone Mass in Daughters of Women with Osteoporosis. *N. Engl. J. Med.* **320**, 554–558 (1989).
42. Garnero, P., Sornay-Rendu, E., Chapuy, M.-C. & Delmas, P. D. Increased bone turnover in late postmenopausal women is a major determinant of osteoporosis. *J. Bone Miner. Res.* **11**, 337–349 (2009).
43. Christiansen, C., Riis, B. J. & Rødbro, P. Screening procedure for women at risk of developing postmenopausal osteoporosis. *Osteoporos. Int.* **1**, 35–40 (1990).
44. Christiansen, C., Riis, B. J. & Rødbro, P. PREDICTION OF RAPID BONE LOSS IN POSTMENOPAUSAL WOMEN. *Lancet* **329**, 1105–1108 (1987).
45. Prestwood, K. M. *et al.* The short-term effects of conjugated estrogen on bone turnover in older women. *J. Clin. Endocrinol. Metab.* **79**, 366–371 (1994).
46. Gilbert, S. F. *Developmental biology*. (Sinauer Associates, 2000).
47. Kronenberg, H. M. Developmental regulation of the growth plate. *Nature* **423**, 332–336 (2003).
48. Olsen, B. R., Reginato, A. M. & Wang, W. Bone Development. *Annu. Rev. Cell Dev. Biol.* **16**, 191–220 (2000).
49. Ducy, P., Zhang, R., Geoffroy, V., Ridall, A. L. & Karsenty, G. *Osf2/Cbfa1*: a transcriptional activator of osteoblast differentiation. *Cell* **89**, 747–54 (1997).
50. Marieb, E. N. & Hoehn, K. *Human anatomy & physiology*. (Pearson Benjamin Cummings, 2007).
51. Šošić, D., Brand-Saberi, B., Schmidt, C., Christ, B. & Olson, E. N. Regulation of paraxis Expression and Somite Formation by Ectoderm- and Neural Tube-Derived Signals. *Dev. Biol.* **185**, 229–243 (1997).
52. Cserjesi, P. *et al.* Scleraxis: a basic helix-loop-helix protein that prefigures skeletal formation during mouse embryogenesis. *Development* **121**, 1099–110 (1995).

List of References

53. Oberlender, S. A. & Tuan, R. S. Expression and functional involvement of N-cadherin in embryonic limb chondrogenesis. *Development* **120**, 177–87 (1994).
54. Hall, B. K. & Miyake, T. Divide, accumulate, differentiate: cell condensation in skeletal development revisited. *Int. J. Dev. Biol.* **39**, 881–93 (1995).
55. OpenStax. Anatomy and Physiology. (1362).
56. Chen, Q., Johnson, D. M., Haudenschild, D. R. & Goetinck, P. F. Progression and Recapitulation of the Chondrocyte Differentiation Program: Cartilage Matrix Protein Is a Marker for Cartilage Maturation. *Dev. Biol.* **172**, 293–306 (1995).
57. Kovacs, C. S. Bone Development in the Fetus and Neonate: Role of the Calcitropic Hormones. *Curr. Osteoporos. Rep.* **9**, 274–283 (2011).
58. Maxhimer, J. B., Bradley, J. P. & Lee, J. C. Signaling pathways in osteogenesis and osteoclastogenesis: Lessons from cranial sutures and applications to regenerative medicine. *Genes Dis.* **2**, 57–68 (2015).
59. Li, H. *et al.* miR-17-5p and miR-106a are involved in the balance between osteogenic and adipogenic differentiation of adipose-derived mesenchymal stem cells. *Stem Cell Res.* **10**, 313–324 (2013).
60. Imai, Y. *et al.* Nuclear Receptors in Bone Physiology and Diseases. *Physiol. Rev.* **93**, 481–523 (2013).
61. Robling, A. G., Castillo, A. B. & Turner, C. H. BIOMECHANICAL AND MOLECULAR REGULATION OF BONE REMODELING. *Annu. Rev. Biomed. Eng.* **8**, 455–498 (2006).
62. Cianferotti, L. & Brandi, M. L. Pathogenesis of osteoporosis. in *Osteoporosis* 6–21 (Future Medicine Ltd, 2013). doi:10.2217/ebo.12.159
63. Hedgecock, N. L. *et al.* Quantitative regional associations between remodeling, modeling, and osteocyte apoptosis and density in rabbit tibial midshafts. *Bone* **40**, 627–637 (2007).
64. Burger, E. H. & Klein-Nulend, J. Mechanotransduction in bone--role of the lacuno-canalicular network. *FASEB J.* **13 Suppl**, S101-12 (1999).
65. Crockett, J. C., Rogers, M. J., Coxon, F. P., Hocking, L. J. & Helfrich, M. H. Bone remodelling at a glance. *J. Cell Sci.* **124**, 991–998 (2011).
66. Bruderer, M., Richards, R., Alini, M. & Stoddart, M. Role and regulation of RUNX2 in

- osteogenesis. *Eur. Cells Mater.* **28**, 269–286 (2014).
67. Akiyama, H. *et al.* Osteo-chondroprogenitor cells are derived from Sox9 expressing precursors. *Proc. Natl. Acad. Sci. U. S. A.* **102**, 14665–70 (2005).
 68. Kern, B., Shen, J., Starbuck, M. & Karsenty, G. Cbfa1 Contributes to the Osteoblast-specific Expression of *type I collagen* Genes. *J. Biol. Chem.* **276**, 7101–7107 (2001).
 69. Ducky, P. *et al.* A Cbfa1-dependent genetic pathway controls bone formation beyond embryonic development. *Genes Dev.* **13**, 1025–1036 (1999).
 70. Karsenty, G., Kronenberg, H. M. & Settembre, C. Genetic Control of Bone Formation. *Annu. Rev. Cell Dev. Biol.* **25**, 629–648 (2009).
 71. Komori, T. *et al.* Targeted disruption of Cbfa1 results in a complete lack of bone formation owing to maturational arrest of osteoblasts. *Cell* **89**, 755–64 (1997).
 72. Lee, B. *et al.* Missense mutations abolishing DNA binding of the osteoblast-specific transcription factor OSF2/CBFA1 in cleidocranial dysplasia. *Nat. Genet.* **16**, 307–310 (1997).
 73. Mundlos, S. *et al.* Mutations involving the transcription factor CBFA1 cause cleidocranial dysplasia. *Cell* **89**, 773–9 (1997).
 74. Nakashima, K. *et al.* The novel zinc finger-containing transcription factor osterix is required for osteoblast differentiation and bone formation. *Cell* **108**, 17–29 (2002).
 75. Wang, X. *et al.* p53 functions as a negative regulator of osteoblastogenesis, osteoblast-dependent osteoclastogenesis, and bone remodeling. *J. Cell Biol.* **172**, 115–125 (2006).
 76. Day, T. F., Guo, X., Garrett-Beal, L. & Yang, Y. Wnt/ β -Catenin Signaling in Mesenchymal Progenitors Controls Osteoblast and Chondrocyte Differentiation during Vertebrate Skeletogenesis. *Dev. Cell* **8**, 739–750 (2005).
 77. Hill, T. P., Später, D., Taketo, M. M., Birchmeier, W. & Hartmann, C. Canonical Wnt/ β -Catenin Signaling Prevents Osteoblasts from Differentiating into Chondrocytes. *Dev. Cell* **8**, 727–738 (2005).
 78. Long, F. Building strong bones: molecular regulation of the osteoblast lineage. *Nat. Rev. Mol. Cell Biol.* **13**, 27–38 (2012).
 79. Zhao, Q., Eberspaecher, H., Lefebvre, V. & de Crombrughe, B. Parallel expression of Sox9 and Col2a1 in cells undergoing chondrogenesis. *Dev. Dyn.* **209**, 377–386 (1997).

List of References

80. Akiyama, H., Chaboissier, M.-C., Martin, J. F., Schedl, A. & de Crombrughe, B. The transcription factor Sox9 has essential roles in successive steps of the chondrocyte differentiation pathway and is required for expression of Sox5 and Sox6. *Genes Dev.* **16**, 2813–28 (2002).
81. Lefebvre, V., Huang, W., Harley, V. R., Goodfellow, P. N. & de Crombrughe, B. SOX9 is a potent activator of the chondrocyte-specific enhancer of the pro alpha1(II) collagen gene. *Mol. Cell. Biol.* **17**, 2336–46 (1997).
82. Sekiya, I. *et al.* SOX9 Enhances Aggrecan Gene Promoter/Enhancer Activity and Is Up-regulated by Retinoic Acid in a Cartilage-derived Cell Line, TC6. *J. Biol. Chem.* **275**, 10738–10744 (2000).
83. Bridgewater, L. C., Lefebvre, V. & de Crombrughe, B. Chondrocyte-specific Enhancer Elements in the *Col11a2* Gene Resemble the *Col2a1* Tissue-specific Enhancer. *J. Biol. Chem.* **273**, 14998–15006 (1998).
84. Dy, P. *et al.* Sox9 Directs Hypertrophic Maturation and Blocks Osteoblast Differentiation of Growth Plate Chondrocytes. *Dev. Cell* **22**, 597–609 (2012).
85. Rodda, S. J. & McMahon, A. P. Distinct roles for Hedgehog and canonical Wnt signaling in specification, differentiation and maintenance of osteoblast progenitors. *Development* **133**, 3231–3244 (2006).
86. St-Jacques, B., Hammerschmidt, M. & McMahon, A. P. Indian hedgehog signaling regulates proliferation and differentiation of chondrocytes and is essential for bone formation. *Genes Dev.* **13**, 2072–2086 (1999).
87. Ingham, P. W. & McMahon, A. P. Hedgehog signaling in animal development: paradigms and principles. *Genes Dev.* **15**, 3059–3087 (2001).
88. Tu, X., Joeng, K. S. & Long, F. Indian hedgehog requires additional effectors besides Runx2 to induce osteoblast differentiation. *Dev. Biol.* **362**, 76–82 (2012).
89. Schroeter, E. H., Kisslinger, J. A. & Kopan, R. Notch-1 signalling requires ligand-induced proteolytic release of intracellular domain. *Nature* **393**, 382–386 (1998).
90. Honjo, T. The shortest path from the surface to the nucleus: RBP-J kappa/Su(H) transcription factor. *Genes Cells* **1**, 1–9 (1996).
91. Hilton, M. J. *et al.* Notch signaling maintains bone marrow mesenchymal progenitors by

- suppressing osteoblast differentiation. *Nat. Med.* **14**, 306–314 (2008).
92. Cadigan, K. M. & Peifer, M. Wnt Signaling from Development to Disease: Insights from Model Systems. *Cold Spring Harb. Perspect. Biol.* **1**, a002881–a002881 (2009).
93. Jenny, A. Planar Cell Polarity Signaling in the Drosophila Eye. in *Current topics in developmental biology* **93**, 189–227 (2010).
94. Kohn, A. D. & Moon, R. T. Wnt and calcium signaling: β -Catenin-independent pathways. *Cell Calcium* **38**, 439–446 (2005).
95. Baron, R. & Kneissel, M. WNT signaling in bone homeostasis and disease: from human mutations to treatments. *Nat. Med.* **19**, 179–192 (2013).
96. Gong, Y. *et al.* LDL receptor-related protein 5 (LRP5) affects bone accrual and eye development. *Cell* **107**, 513–23 (2001).
97. Little, R. D. *et al.* A Mutation in the LDL Receptor–Related Protein 5 Gene Results in the Autosomal Dominant High–Bone-Mass Trait. *Am. J. Hum. Genet.* **70**, 11–19 (2002).
98. Boyden, L. M. *et al.* High Bone Density Due to a Mutation in LDL-Receptor–Related Protein 5. *N. Engl. J. Med.* **346**, 1513–1521 (2002).
99. Gaur, T. *et al.* Canonical WNT Signaling Promotes Osteogenesis by Directly Stimulating *Runx2* Gene Expression. *J. Biol. Chem.* **280**, 33132–33140 (2005).
100. Poole, K. E. S. *et al.* Sclerostin is a delayed secreted product of osteocytes that inhibits bone formation. *FASEB J.* **19**, 1842–1844 (2005).
101. van Bezooijen, R. L. *et al.* Sclerostin Is an Osteocyte-expressed Negative Regulator of Bone Formation, But Not a Classical BMP Antagonist. *J. Exp. Med.* **199**, 805–814 (2004).
102. Delgado-Calle, J. *et al.* Epigenetic regulation of alkaline phosphatase in human cells of the osteoblastic lineage. *Bone* **49**, 830–838 (2011).
103. Brunkow, M. E. *et al.* Bone Dysplasia Sclerosteosis Results from Loss of the SOST Gene Product, a Novel Cystine Knot–Containing Protein. *Am. J. Hum. Genet.* **68**, 577–589 (2001).
104. Balemans, W. *et al.* Identification of a 52 kb deletion downstream of the SOST gene in patients with van Buchem disease. *J. Med. Genet.* **39**, 91–97 (2002).
105. Tu, X. *et al.* Noncanonical Wnt Signaling through G Protein-Linked PKC δ Activation Promotes Bone Formation. *Dev. Cell* **12**, 113–127 (2007).

List of References

106. Pizette, S. & Niswander, L. BMPs Are Required at Two Steps of Limb Chondrogenesis: Formation of Prechondrogenic Condensations and Their Differentiation into Chondrocytes. *Dev. Biol.* **219**, 237–249 (2000).
107. Bandyopadhyay, A. *et al.* Genetic Analysis of the Roles of BMP2, BMP4, and BMP7 in Limb Patterning and Skeletogenesis. *PLoS Genet.* **2**, e216 (2006).
108. Wu, M., Chen, G. & Li, Y.-P. TGF- β and BMP signaling in osteoblast, skeletal development, and bone formation, homeostasis and disease. *Bone Res.* **4**, 16009 (2016).
109. Devlin, R. D. *et al.* Skeletal Overexpression of Noggin Results in Osteopenia and Reduced Bone Formation. *Endocrinology* **144**, 1972–1978 (2003).
110. Wozney, J. *et al.* Novel regulators of bone formation: molecular clones and activities. *Science (80-)*. **242**, 1528–1534 (1988).
111. Reddi, A. H. & Huggins, C. Biochemical Sequences in the Transformation of Normal Fibroblasts in Adolescent Rats. *Proc. Natl. Acad. Sci.* **69**, 1601–1605 (1972).
112. Tsuji, K. *et al.* BMP2 activity, although dispensable for bone formation, is required for the initiation of fracture healing. *Nat. Genet.* **38**, 1424–1429 (2006).
113. Tan, X. *et al.* Smad4 is required for maintaining normal murine postnatal bone homeostasis. *J. Cell Sci.* **120**, 2162–70 (2007).
114. Capdevila, J. & Johnson, R. L. Endogenous and Ectopic Expression ofnogginSuggests a Conserved Mechanism for Regulation of BMP Function during Limb and Somite Patterning. *Dev. Biol.* **197**, 205–217 (1998).
115. Valverde-Franco, G. *et al.* Defective bone mineralization and osteopenia in young adult FGFR3^{-/-} mice. *Hum. Mol. Genet.* **13**, 271–284 (2003).
116. Montero, A. *et al.* Disruption of the fibroblast growth factor-2 gene results in decreased bone mass and bone formation. *J. Clin. Invest.* **105**, (2000).
117. Liu, Z., Lavine, K. J., Hung, I. H. & Ornitz, D. M. FGF18 is required for early chondrocyte proliferation, hypertrophy and vascular invasion of the growth plate. *Dev. Biol.* **302**, 80–91 (2007).
118. Ohbayashi, N. *et al.* FGF18 is required for normal cell proliferation and differentiation during osteogenesis and chondrogenesis. *Genes Dev.* **16**, 870–879 (2002).

119. Jacob, A. L., Smith, C., Partanen, J. & Ornitz, D. M. Fibroblast growth factor receptor 1 signaling in the osteo-chondrogenic cell lineage regulates sequential steps of osteoblast maturation. *Dev. Biol.* **296**, 315–328 (2006).
120. Sabbieti, M. G. *et al.* Endogenous FGF-2 is critically important in PTH anabolic effects on bone. *J. Cell. Physiol.* **219**, 143–151 (2009).
121. Yang, D., Guo, J., Divieti, P. & Bringhurst, F. R. Parathyroid hormone activates PKC- δ and regulates osteoblastic differentiation via a PLC-independent pathway. *Bone* **38**, 485–496 (2006).
122. Jilka, R. L. *et al.* Increased bone formation by prevention of osteoblast apoptosis with parathyroid hormone. *J. Clin. Invest.* **104**, 439–446 (1999).
123. McCauley, L. K., Koh, A. J., Beecher, C. A. & Rosol, T. J. Proto-Oncogene *c-fos* Is Transcriptionally Regulated by Parathyroid Hormone (PTH) and PTH-Related Protein in a Cyclic Adenosine Monophosphate-Dependent Manner in Osteoblastic Cells¹. *Endocrinology* **138**, 5427–5433 (1997).
124. Xian, L. *et al.* Matrix IGF-1 maintains bone mass by activation of mTOR in mesenchymal stem cells. *Nat. Med.* **18**, 1095–1101 (2012).
125. Zhang, M. *et al.* Osteoblast-specific Knockout of the Insulin-like Growth Factor (IGF) Receptor Gene Reveals an Essential Role of IGF Signaling in Bone Matrix Mineralization. *J. Biol. Chem.* **277**, 44005–44012 (2002).
126. Sutton, A. L. M. & MacDonald, P. N. Vitamin D: More Than a “Bone-a-Fide” Hormone. *Mol. Endocrinol.* **17**, 777–791 (2003).
127. Fu, G. K. *et al.* Cloning of Human 25-Hydroxyvitamin D-1 α -Hydroxylase and Mutations Causing Vitamin D-Dependent Rickets Type 1. *Mol. Endocrinol.* **11**, 1961–1970 (1997).
128. Nagpal, S., Na, S. & Rathnachalam, R. Noncalcemic Actions of Vitamin D Receptor Ligands. *Endocr. Rev.* **26**, 662–687 (2005).
129. Haussler, M. R. *et al.* The vitamin D hormone and its nuclear receptor: molecular actions and disease states. *J. Endocrinol.* **154 Suppl**, S57-73 (1997).
130. Matsumoto, T. *et al.* Stimulation by 1,25-dihydroxyvitamin D₃ of in vitro mineralization induced by osteoblast-like MC3T3-E1 cells. *Bone* **12**, 27–32 (1991).
131. Drissi, H. *et al.* 1,25-(OH)₂-Vitamin D₃ Suppresses the Bone-Related Runx2/Cbfa1 Gene

List of References

- Promoter. *Exp. Cell Res.* **274**, 323–333 (2002).
132. Viereck, V. *et al.* Differential regulation of Cbfa1/Runx2 and osteocalcin gene expression by vitamin-D3, dexamethasone, and local growth factors in primary human osteoblasts. *J. Cell. Biochem.* **86**, 348–356 (2002).
133. Javed, A. *et al.* Multiple Cbfa/AML sites in the rat osteocalcin promoter are required for basal and vitamin D-responsive transcription and contribute to chromatin organization. *Mol. Cell. Biol.* **19**, 7491–500 (1999).
134. Sierra, J. *et al.* Regulation of the bone-specific osteocalcin gene by p300 requires Runx2/Cbfa1 and the vitamin D3 receptor but not p300 intrinsic histone acetyltransferase activity. *Mol. Cell. Biol.* **23**, 3339–51 (2003).
135. Lian, J. B. *et al.* Species-Specific Glucocorticoid and 1,25-Dihydroxyvitamin D Responsiveness in Mouse MC3T3-E1 Osteoblasts: Dexamethasone Inhibits Osteoblast Differentiation and Vitamin D Down-Regulates Osteocalcin Gene Expression*. *Endocrinology* **138**, 2117–2127 (1997).
136. Klaus, G. *et al.* Interaction of IGF-I and 1 α ,25(OH)₂D₃ on receptor expression and growth stimulation in rat growth plate chondrocytes. *Kidney Int.* **53**, 1152–1161 (1998).
137. Krohn, K. *et al.* 1,25(OH)₂D₃ and Dihydrotestosterone Interact to Regulate Proliferation and Differentiation of Epiphyseal Chondrocytes. *Calcif. Tissue Int.* **73**, 400–410 (2003).
138. Schwartz, Z., Schlader, D. L., Ramirez, V., Kennedy, M. B. & Boyan, B. D. Effects of vitamin D metabolites on collagen production and cell proliferation of growth zone and resting zone cartilage cells in vitro. *J. Bone Miner. Res.* **4**, 199–207 (2009).
139. Donohue, M. M. & Demay, M. B. Rickets in VDR Null Mice Is Secondary to Decreased Apoptosis of Hypertrophic Chondrocytes. *Endocrinology* **143**, 3691–3691 (2002).
140. Baylink, D., Stauffer, M., Wergedal, J. & Rich, C. Formation, mineralization, and resorption of bone in vitamin D—deficient rats. *J. Clin. Invest.* **49**, 1122–1134 (1970).
141. DeLuca, H. F. The vitamin D story: a collaborative effort of basic science and clinical medicine. *FASEB J.* **2**, 224–36 (1988).
142. Christakos, S., Ajibade, D. V., Dhawan, P., Fechner, A. J. & Mady, L. J. Vitamin D: metabolism. *Endocrinol. Metab. Clin. North Am.* **39**, 243–53, table of contents (2010).
143. Bikle, D. D. Vitamin D Metabolism, Mechanism of Action, and Clinical Applications. *Chem.*

- Biol.* **21**, 319–329 (2014).
144. WEBB, A. R., DECOSTA, B. R. & HOLICK, M. F. Sunlight Regulates the Cutaneous Production of Vitamin D₃ by Causing Its Photodegradation*. *J. Clin. Endocrinol. Metab.* **68**, 882–887 (1989).
 145. MATSUOKA, L. Y., IDE, L., WORTSMAN, J., MACLAUGHLIN, J. A. & HOLICK, M. F. Sunscreens Suppress Cutaneous Vitamin D₃ Synthesis*. *J. Clin. Endocrinol. Metab.* **64**, 1165–1168 (1987).
 146. Matsuoka, L. Y. *et al.* Clothing prevents ultraviolet-B radiation-dependent photosynthesis of vitamin D₃. *J. Clin. Endocrinol. Metab.* **75**, 1099–1103 (1992).
 147. WEBB, A. R., KLINE, L. & HOLICK, M. F. Influence of Season and Latitude on the Cutaneous Synthesis of Vitamin D₃: Exposure to Winter Sunlight in Boston and Edmonton Will Not Promote Vitamin D₃ Synthesis in Human Skin*. *J. Clin. Endocrinol. Metab.* **67**, 373–378 (1988).
 148. Holick, M. F. *et al.* Photosynthesis of previtamin D₃ in human skin and the physiologic consequences. *Science* **210**, 203–5 (1980).
 149. Armbrecht, H. J. *et al.* Characterization and regulation of the vitamin D hydroxylases. *J. Steroid Biochem. Mol. Biol.* **43**, 1073–1081 (1992).
 150. Nykjaer, A. *et al.* An endocytic pathway essential for renal uptake and activation of the steroid 25-(OH) vitamin D₃. *Cell* **96**, 507–15 (1999).
 151. Pike, J. W. & Meyer, M. B. The vitamin D receptor: new paradigms for the regulation of gene expression by 1,25-dihydroxyvitamin D(3). *Endocrinol. Metab. Clin. North Am.* **39**, 255–69, table of contents (2010).
 152. Deeb, K. K., Trump, D. L. & Johnson, C. S. Vitamin D signalling pathways in cancer: potential for anticancer therapeutics. *Nat. Rev. Cancer* **7**, 684–700 (2007).
 153. Garabedian, M., Holick, M. F., Deluca, H. F. & Boyle, I. T. Control of 25-hydroxycholecalciferol metabolism by parathyroid glands. *Proc. Natl. Acad. Sci. U. S. A.* **69**, 1673–6 (1972).
 154. Boyle, I. T., Gray, R. W. & DeLuca, H. F. Regulation by calcium of in vivo synthesis of 1,25-dihydroxycholecalciferol and 21,25-dihydroxycholecalciferol. *Proc. Natl. Acad. Sci. U. S. A.* **68**, 2131–4 (1971).
 155. Tanaka, Y. & Deluca, H. F. The control of 25-hydroxyvitamin D metabolism by inorganic

List of References

- phosphorus. *Arch. Biochem. Biophys.* **154**, 566–74 (1973).
156. Tanaka, Y. & Deluca, H. F. The control of 25-hydroxyvitamin D metabolism by inorganic phosphorus. *Arch. Biochem. Biophys.* **154**, 566–74 (1973).
157. Zierold, C., Reinholz, G. G., Mings, J. A., Prah, J. M. & DeLuca, H. F. Regulation of the porcine 1,25-dihydroxyvitamin D₃-24-hydroxylase (CYP24) by 1,25-dihydroxyvitamin D₃ and parathyroid hormone in AOK-B50 cells. *Arch. Biochem. Biophys.* **381**, 323–7 (2000).
158. Perwad, F. *et al.* Dietary and Serum Phosphorus Regulate Fibroblast Growth Factor 23 Expression and 1,25-Dihydroxyvitamin D Metabolism in Mice. *Endocrinology* **146**, 5358–5364 (2005).
159. Holick, M. F. Resurrection of vitamin D deficiency and rickets. *J. Clin. Invest.* **116**, 2062–72 (2006).
160. Bar-Shavit, Z. The osteoclast: A multinucleated, hematopoietic-origin, bone-resorbing osteoimmune cell. *J. Cell. Biochem.* **102**, 1130–1139 (2007).
161. Crockett, J. C., Mellis, D. J., Scott, D. I. & Helfrich, M. H. New knowledge on critical osteoclast formation and activation pathways from study of rare genetic diseases of osteoclasts: focus on the RANK/RANKL axis. *Osteoporos. Int.* **22**, 1–20 (2011).
162. Leibbrandt, A. & Penninger, J. M. Novel Functions of RANK(L) Signaling in the Immune System. in *Advances in experimental medicine and biology* **658**, 77–94 (2009).
163. Asagiri, M. & Takayanagi, H. The molecular understanding of osteoclast differentiation. *Bone* **40**, 251–264 (2007).
164. Aoki, S. *et al.* Function of OPG as a traffic regulator for RANKL is crucial for controlled osteoclastogenesis. *J. Bone Miner. Res.* **25**, 1907–1921 (2010).
165. Boyce, B. F. & Xing, L. Functions of RANKL/RANK/OPG in bone modeling and remodeling. *Arch. Biochem. Biophys.* **473**, 139–146 (2008).
166. Hill, P. A. Bone Remodelling: <https://doi.org/10.1093/ortho.25.2.101> (2019). doi:10.1093/ORTHO.25.2.101
167. Richards, J. B., Zheng, H.-F. & Spector, T. D. Genetics of osteoporosis from genome-wide association studies: advances and challenges. *Nat. Rev. Genet.* **13**, 576–588 (2012).
168. Richards, J. *et al.* Bone mineral density, osteoporosis, and osteoporotic fractures: a genome-

- wide association study. *Lancet* **371**, 1505–1512 (2008).
169. Styrkarsdottir, U. *et al.* Multiple Genetic Loci for Bone Mineral Density and Fractures. *N. Engl. J. Med.* **358**, 2355–2365 (2008).
170. Estrada, K. *et al.* Genome-wide meta-analysis identifies 56 bone mineral density loci and reveals 14 loci associated with risk of fracture. *Nat. Genet.* **44**, 491–501 (2012).
171. Styrkarsdottir, U. *et al.* New sequence variants associated with bone mineral density. *Nat. Genet.* **41**, 15–17 (2009).
172. Timpson, N. J. *et al.* Common variants in the region around Osterix are associated with bone mineral density and growth in childhood. *Hum. Mol. Genet.* **18**, 1510–1517 (2009).
173. Rivadeneira, F. *et al.* Twenty bone-mineral-density loci identified by large-scale meta-analysis of genome-wide association studies. *Nat. Genet.* **41**, 1199–1206 (2009).
174. Kiel, D. P. *et al.* Genome-wide association with bone mass and geometry in the Framingham Heart Study. *BMC Med. Genet.* **8**, S14 (2007).
175. Ioannidis, J. P. A. *et al.* Association of Polymorphisms of the Estrogen Receptor α Gene With Bone Mineral Density and Fracture Risk in Women: A Meta-Analysis. *J. Bone Miner. Res.* **17**, 2048–2060 (2002).
176. Mann, V. & Ralston, S. H. Meta-analysis of COL1A1 Sp1 polymorphism in relation to bone mineral density and osteoporotic fracture. *Bone* **32**, 711–7 (2003).
177. Riancho, J. A., Valero, C. & Zarrabeitia, M. T. MTHFR Polymorphism and Bone Mineral Density: Meta-Analysis of Published Studies. *Calcif. Tissue Int.* **79**, 289–293 (2006).
178. Uitterlinden, A. G. *et al.* The Association between Common Vitamin D Receptor Gene Variations and Osteoporosis: A Participant-Level Meta-Analysis. *Ann. Intern. Med.* **145**, 255 (2006).
179. Trenkman, M. GWAS cracks fracture risk. *Nat. Rev. Rheumatol.* **15**, 126–126 (2019).
180. Morris, J. A. *et al.* An atlas of genetic influences on osteoporosis in humans and mice. *Nat. Genet.* **51**, 258–266 (2019).
181. Manolagas, S. C. Birth and Death of Bone Cells: Basic Regulatory Mechanisms and Implications for the Pathogenesis and Treatment of Osteoporosis*. *Endocr. Rev.* **21**, 115–137 (2000).

List of References

182. Lane, N. E. Epidemiology, etiology, and diagnosis of osteoporosis. *Am. J. Obstet. Gynecol.* **194**, S3–S11 (2006).
183. Manolagas, S. C. & Weinstein, R. S. New Developments in the Pathogenesis and Treatment of Steroid-Induced Osteoporosis. *J. Bone Miner. Res.* **14**, 1061–1066 (1999).
184. Jilka, R. L., Weinstein, R. S., Takahashi, K., Parfitt, A. M. & Manolagas, S. C. *Linkage of Decreased Bone Mass with Impaired Osteoblastogenesis in a Murine Model of Accelerated Senescence osteoporosis • aging • remodel-ing • bone formation • osteoclast formation. The Journal of Clinical Investigation* **97**, (1996).
185. D'Ippolito, G., Schiller, P. C., Ricordi, C., Roos, B. A. & Howard, G. A. Age-Related Osteogenic Potential of Mesenchymal Stromal Stem Cells from Human Vertebral Bone Marrow. *J. Bone Miner. Res.* **14**, 1115–1122 (1999).
186. Lips, P., Courpron, P. & Meunier, P. J. Mean wall thickness of trabecular bone packets in the human iliac crest: Changes with age. *Calcif. Tissue Res.* **26**, 13–17 (1978).
187. Parfitt, A. M., Villanueva, A. R., Foldes, J. & Rao, D. S. Relations between histologic indices of bone formation: Implications for the pathogenesis of spinal osteoporosis. *J. Bone Miner. Res.* **10**, 466–473 (2009).
188. Schenk, R. K., Merz, W. A. & Müller, J. A quantitative histological study on bone resorption in human cancellous bone. *Cells Tissues Organs* **74**, 44–53 (1969).
189. Jilka, R. *et al.* Increased osteoclast development after estrogen loss: mediation by interleukin-6. *Science (80-.).* **257**, 88–91 (1992).
190. Lei, Z., Xiaoying, Z. & Xingguo, L. Ovariectomy-associated changes in bone mineral density and bone marrow haematopoiesis in rats. *Int. J. Exp. Pathol.* **90**, 512–9 (2009).
191. Eriksen, E. F., Langdahl, B., Vesterby, A., Rungby, J. & Kassem, M. Hormone Replacement Therapy Prevents Osteoclastic Hyperactivity: A Histomorphometric Study in Early Postmenopausal Women. *J. Bone Miner. Res.* **14**, 1217–1221 (1999).
192. Lips, P. Vitamin D Deficiency and Secondary Hyperparathyroidism in the Elderly: Consequences for Bone Loss and Fractures and Therapeutic Implications. *Endocr. Rev.* **22**, 477–501 (2001).
193. Bischoff-Ferrari, H. A. *et al.* Effect of Vitamin D on Falls. *JAMA* **291**, 1999 (2004).
194. Sambrook, P. N. *et al.* Serum Parathyroid Hormone Predicts Time to Fall Independent of

- Vitamin D Status in a Frail Elderly Population. *J. Clin. Endocrinol. Metab.* **89**, 1572–1576 (2004).
195. Barker, D. J. & Osmond, C. Infant mortality, childhood nutrition, and ischaemic heart disease in England and Wales. *Lancet (London, England)* **1**, 1077–81 (1986).
196. Syddall, H. *et al.* Cohort Profile: The Hertfordshire Cohort Study. *Int. J. Epidemiol.* **34**, 1234–1242 (2005).
197. Barker, D. J., Winter, P. D., Osmond, C., Margetts, B. & Simmonds, S. J. Weight in infancy and death from ischaemic heart disease. *Lancet (London, England)* **2**, 577–80 (1989).
198. Fall, C. H. *et al.* Fetal and infant growth and cardiovascular risk factors in women. *BMJ* **310**, 428–32 (1995).
199. Osmond, C., Barker, D. J., Winter, P. D., Fall, C. H. & Simmonds, S. J. Early growth and death from cardiovascular disease in women. *BMJ* **307**, 1519–24 (1993).
200. Hales, C. N. *et al.* Fetal and infant growth and impaired glucose tolerance at age 64. *BMJ* **303**, 1019–1022 (1991).
201. Barker, D. J. *et al.* Type 2 (non-insulin-dependent) diabetes mellitus, hypertension and hyperlipidaemia (syndrome X): relation to reduced fetal growth. *Diabetologia* **36**, 62–7 (1993).
202. Sayer, A. A., Syddall, H. E., Gilbody, H. J., Dennison, E. M. & Cooper, C. Does sarcopenia originate in early life? Findings from the Hertfordshire cohort study. *J. Gerontol. A. Biol. Sci. Med. Sci.* **59**, M930-4 (2004).
203. SAYER, A. A. *et al.* Are rates of ageing determined *in utero* ? *Age Ageing* **27**, 579–583 (1998).
204. Lumey, L. H. *et al.* Cohort Profile: the Dutch Hunger Winter Families Study. doi:10.1093/ije/dym126
205. Stein, A. D., Ravelli, A. C. & Lumey, L. H. Famine, third-trimester pregnancy weight gain, and intrauterine growth: the Dutch Famine Birth Cohort Study. *Hum. Biol.* **67**, 135–50 (1995).
206. Stein, A. D., Zybert, P. A., van der Pal-de Bruin, K. & Lumey, L. H. Exposure to famine during gestation, size at birth, and blood pressure at age 59 y: evidence from the dutch famine. *Eur. J. Epidemiol.* **21**, 759–765 (2006).
207. Painter, R. C. *et al.* Blood pressure response to psychological stressors in adults after

List of References

- prenatal exposure to the Dutch famine. *J. Hypertens.* **24**, 1771–1778 (2006).
208. Roseboom, T. J. *et al.* Coronary heart disease after prenatal exposure to the Dutch famine, 1944-45. *Heart* **84**, 595–8 (2000).
209. Stein, A. D. *et al.* Anthropometric measures in middle age after exposure to famine during gestation: evidence from the Dutch famine. *Am. J. Clin. Nutr.* **85**, 869–876 (2007).
210. Ravelli, A. C. *et al.* Glucose tolerance in adults after prenatal exposure to famine. *Lancet (London, England)* **351**, 173–7 (1998).
211. Roseboom, T., De Rooij, S. & Painter, R. The Dutch famine and its long-term consequences for adult health. doi:10.1016/j.earlhumdev.2006.07.001
212. Cleal, J. K. *et al.* Mismatched pre- and postnatal nutrition leads to cardiovascular dysfunction and altered renal function in adulthood. *Proc. Natl. Acad. Sci. U. S. A.* **104**, 9529–33 (2007).
213. Desai, M. *et al.* Maternal obesity and high-fat diet program offspring metabolic syndrome. *Am. J. Obstet. Gynecol.* **211**, 237.e1-237.e13 (2014).
214. Howie, G. J., Sloboda, D. M., Reynolds, C. M. & Vickers, M. H. Timing of maternal exposure to a high fat diet and development of obesity and hyperinsulinemia in male rat offspring: same metabolic phenotype, different developmental pathways? *J. Nutr. Metab.* **2013**, 517384 (2013).
215. Dennison, E. M., Syddall, H. E., Sayer, A. A., Gilbody, H. J. & Cooper, C. Birth Weight and Weight at 1 Year Are Independent Determinants of Bone Mass in the Seventh Decade: The Hertfordshire Cohort Study. *Pediatr. Res.* **57**, 582–586 (2005).
216. Oliver, H., Jameson, K. A., Sayer, A. A., Cooper, C. & Dennison, E. M. Growth in early life predicts bone strength in late adulthood: The Hertfordshire Cohort Study. *Bone* **41**, 400–405 (2007).
217. Antoniadou, L., MacGregor, A. J., Andrew, T. & Spector, T. D. Association of birth weight with osteoporosis and osteoarthritis in adult twins. *Rheumatology* **42**, 791–796 (2003).
218. Gale, C. R., Martyn, C. N., Kellingray, S., Eastell, R. & Cooper, C. Intrauterine Programming of Adult Body Composition¹. *J. Clin. Endocrinol. Metab.* **86**, 267–272 (2001).
219. Yarbrough, D. E., Barrett-Connor, E. & Morton, D. J. Birth Weight as a Predictor of Adult Bone Mass in Postmenopausal Women: The Rancho Bernardo Study. *Osteoporos. Int.* **11**, 626–630 (2000).

220. Cooper, C. *et al.* Growth in infancy and bone mass in later life. *Ann. Rheum. Dis.* **56**, 17–21 (1997).
221. Cooper, C. *et al.* Childhood growth, physical activity, and peak bone mass in women. *J. Bone Miner. Res.* **10**, 940–947 (2009).
222. Cooper, C. *et al.* Maternal Height, Childhood Growth and Risk of Hip Fracture in Later Life: A Longitudinal Study. *Osteoporos. Int.* **12**, 623–629 (2001).
223. Moinuddin, M. M. *et al.* Cigarette smoking, birthweight and osteoporosis in adulthood: results from the hertfordshire cohort study. *Open Rheumatol. J.* **2**, 33–7 (2008).
224. Oreffo, R. O. C., Lashbrooke, B., Roach, H. I., Clarke, N. M. P. & Cooper, C. Maternal protein deficiency affects mesenchymal stem cell activity in the developing offspring. *Bone* **33**, 100–7 (2003).
225. Lanham, S. A., Roberts, C., Cooper, C. & Oreffo, R. O. C. Intrauterine programming of bone. Part 1: Alteration of the osteogenic environment. *Osteoporos. Int.* **19**, 147–156 (2008).
226. Lanham, S. A., Roberts, C., Perry, M. J., Cooper, C. & Oreffo, R. O. C. Intrauterine programming of bone. Part 2: Alteration of skeletal structure. *Osteoporos. Int.* **19**, 157–167 (2008).
227. Lanham, S. *et al.* Altered vertebral and femoral bone structure in juvenile offspring of microswine subject to maternal low protein nutritional challenge. (2019).
228. Lanham, S. A. *et al.* Maternal high-fat diet: effects on offspring bone structure. *Osteoporos. Int.* **21**, 1703–1714 (2010).
229. Wharton, B. & Bishop, N. Rickets. *Lancet* **362**, 1389–1400 (2003).
230. Kovacs, C. S. Fetal Mineral Homeostasis. *Pediatr. Bone* 247–275 (2012). doi:10.1016/B978-0-12-382040-2.10011-5
231. Mahon, P. *et al.* Low maternal vitamin D status and fetal bone development: Cohort study. *J. Bone Miner. Res.* **25**, 14–19 (2010).
232. Viljakainen, H. T. *et al.* Maternal Vitamin D Status Determines Bone Variables in the Newborn. *J. Clin. Endocrinol. Metab.* **95**, 1749–1757 (2010).
233. Brunvand, L., Quigstad, E., Urdal, P. & Haug, E. Vitamin D deficiency and fetal growth. *Early Hum. Dev.* **45**, 27–33 (1996).

List of References

234. Congdon, P., Horsman, A., Kirby, P. A., Dibble, J. & Bashir, T. Mineral content of the forearms of babies born to Asian and white mothers. *BMJ* **286**, 1233–1235 (1983).
235. Harvey, N. C. *et al.* MAVIDOS Maternal Vitamin D Osteoporosis Study: study protocol for a randomized controlled trial. The MAVIDOS Study Group. *Trials* **13**, 13 (2012).
236. Harvey, N. C. *et al.* O16 Maternal Gestational Vitamin D Supplementation Results in Greater Bone Mass for Offspring Born During Winter Months: The Mavidos Multicentre Randomized, Double-Blind, Placebo-Controlled Trial. *Rheumatology* **55**, i41–i41 (2016).
237. Brooke, O. G. *et al.* Vitamin D supplements in pregnant Asian women: effects on calcium status and fetal growth. *Br. Med. J.* **280**, 751–4 (1980).
238. Brooke, O. G., Butters, F. & Wood, C. Intrauterine vitamin D nutrition and postnatal growth in Asian infants. *Br. Med. J. (Clin. Res. Ed)*. **283**, 1024 (1981).
239. Javaid, M. *et al.* Maternal vitamin D status during pregnancy and childhood bone mass at age 9 years: a longitudinal study. *Lancet* **367**, 36–43 (2006).
240. Morley, R., Carlin, J. B., Pasco, J. A. & Wark, J. D. Maternal 25-Hydroxyvitamin D and Parathyroid Hormone Concentrations and Offspring Birth Size. *J. Clin. Endocrinol. Metab.* **91**, 906–912 (2006).
241. Miller, S. C., Halloran, B. P., DeLuca, H. F. & Jee, W. S. Studies on the role of vitamin D in early skeletal development, mineralization, and growth in rats. *Calcif. Tissue Int.* **35**, 455–60 (1983).
242. Lanham, S. A. *et al.* Effect of vitamin D deficiency during pregnancy on offspring bone structure, composition and quality in later life. *J. Dev. Orig. Health Dis.* **4**, 49–55 (2013).
243. Glazier, J. D., Mawer, E. B. & Sibley, C. P. Calbindin-D9K Gene Expression in Rat Chorionallantoic Placenta Is Not Regulated by 1,25-Dihydroxyvitamin D₃. *Pediatr. Res.* **37**, 720–725 (1995).
244. Halloran, B. P. & De Luca, H. F. Effect of vitamin D deficiency on skeletal development during early growth in the rat. *Arch. Biochem. Biophys.* **209**, 7–14 (1981).
245. Borg, S. A. *et al.* Early life vitamin D depletion alters the postnatal response to skeletal loading in growing and mature bone. *PLoS One* **13**, e0190675 (2018).
246. Kovacs, C. S., Woodland, M. L., Fudge, N. J. & Friel, J. K. The vitamin D receptor is not required for fetal mineral homeostasis or for the regulation of placental calcium transfer in mice. *Am.*

- J. Physiol. Metab.* **289**, E133–E144 (2005).
247. Kato, S. *et al.* In vivo function of VDR in gene expression-VDR knock-out mice. *J. Steroid Biochem. Mol. Biol.* **69**, 247–251 (1999).
248. Johnson, L. E. & DeLuca, H. F. Vitamin D Receptor Null Mutant Mice Fed High Levels of Calcium Are Fertile. *J. Nutr.* **131**, 1787–1791 (2001).
249. Dardenne, O., Prud'homme, J., Arabian, A., Glorieux, F. H. & St-Arnaud, R. Targeted Inactivation of the 25-Hydroxyvitamin D3-1 α -Hydroxylase Gene (CYP27B1) Creates an Animal Model of Pseudovitamin D-Deficiency Rickets*. *Endocrinology* **142**, 3135–3141 (2001).
250. Panda, D. K. *et al.* Targeted ablation of the 25-hydroxyvitamin D 1-hydroxylase enzyme: Evidence for skeletal, reproductive, and immune dysfunction. *Proc. Natl. Acad. Sci.* **98**, 7498–7503 (2001).
251. Ryan, B. A. *et al.* Mineral Homeostasis in Murine Fetuses Is Sensitive to Maternal Calcitriol but Not to Absence of Fetal Calcitriol. *J. Bone Miner. Res.* **34**, 669–680 (2019).
252. Godfrey, K. M., Costello, P. M. & Lillycrop, K. A. The developmental environment, epigenetic biomarkers and long-term health. *J. Dev. Orig. Health Dis.* **6**, 399–406 (2015).
253. BIRD, A. & MACLEOD, D. Reading the DNA Methylation Signal. *Cold Spring Harb. Symp. Quant. Biol.* **69**, 113–118 (2004).
254. Kumar, S. *et al.* The DNA (cytosine-5) methyltransferases. *Nucleic Acids Res.* **22**, 1–10 (1994).
255. Bocheva, G. & Boyadjieva, N. Epigenetic regulation of fetal bone development and placental transfer of nutrients: progress for osteoporosis. *Interdiscip. Toxicol.* **4**, (2011).
256. Robertson, K. D. DNA methylation and human disease. *Nat. Rev. Genet.* **6**, 597–610 (2005).
257. Kim, J. K., Samaranyake, M. & Pradhan, S. Epigenetic mechanisms in mammals. *Cell. Mol. Life Sci.* **66**, 596–612 (2009).
258. Adcock, I. M., Ford, P., Ito, K. & Barnes, P. J. Epigenetics and airways disease. *Respir. Res.* **7**, 21 (2006).
259. Barter, M. J., Bui, C. & Young, D. A. Epigenetic mechanisms in cartilage and osteoarthritis: DNA methylation, histone modifications and microRNAs. *Osteoarthr. Cartil.* **20**, 339–349 (2012).

List of References

260. Gruenbaum, Y., Stein, R., Cedar, H. & Razin, A. Methylation of CpG sequences in eukaryotic DNA. *FEBS Lett.* **124**, 67–71 (1981).
261. Song, F. *et al.* Association of tissue-specific differentially methylated regions (TDMs) with differential gene expression. *Proc. Natl. Acad. Sci. U. S. A.* **102**, 3336–41 (2005).
262. Ko, Y.-G. *et al.* Stage-by-stage change in DNA methylation status of Dnmt1 locus during mouse early development. *J. Biol. Chem.* **280**, 9627–34 (2005).
263. Burdge, G. C. & Lillycrop, K. a. Nutrition, epigenetics, and developmental plasticity: implications for understanding human disease. *Annu. Rev. Nutr.* **30**, 315–39 (2010).
264. Okano, M., Bell, D. W., Haber, D. A. & Li, E. DNA methyltransferases Dnmt3a and Dnmt3b are essential for de novo methylation and mammalian development. *Cell* **99**, 247–57 (1999).
265. Hata, K., Okano, M., Lei, H. & Li, E. Dnmt3L cooperates with the Dnmt3 family of de novo DNA methyltransferases to establish maternal imprints in mice. *Development* **129**, 1983–93 (2002).
266. Nan, X. *et al.* Transcriptional repression by the methyl-CpG-binding protein MeCP2 involves a histone deacetylase complex. *Nature* **393**, 386–389 (1998).
267. Hanson, M., Godfrey, K. M., Lillycrop, K. A., Burdge, G. C. & Gluckman, P. D. Developmental plasticity and developmental origins of non-communicable disease: Theoretical considerations and epigenetic mechanisms. *Prog. Biophys. Mol. Biol.* **106**, 272–280 (2011).
268. Bird, A. DNA methylation patterns and epigenetic memory. *Genes Dev.* **16**, 6–21 (2002).
269. Burdge, G. C., Lillycrop, K. a & Jackson, A. a. Nutrition in early life, and risk of cancer and metabolic disease: alternative endings in an epigenetic tale? *Br. J. Nutr.* **101**, 619–630 (2009).
270. Li, E., Beard, C. & Jaenisch, R. Role for DNA methylation in genomic imprinting. *Nature* **366**, 362–365 (1993).
271. Temple, I. K. Imprinting in Human Disease with Special Reference to Transient Neonatal Diabetes and Beckwith-Wiedemann Syndrome. in *Development of the Pancreas and Neonatal Diabetes* **12**, 113–123 (KARGER, 2007).
272. Tycko, B. & Morison, I. M. Physiological functions of imprinted genes. *J. Cell. Physiol.* **192**, 245–58 (2002).

273. Ciesielski, P., Jóźwiak, P. & Krześlak, A. [TET proteins and epigenetic modifications in cancers]. *Postepy Hig. Med. Dosw. (Online)* **69**, 1371–83 (2015).
274. Venkatesh, S. & Workman, J. L. Histone exchange, chromatin structure and the regulation of transcription. *Nat. Rev. Mol. Cell Biol.* **16**, 178–189 (2015).
275. Fuks, F. *et al.* The Methyl-CpG-binding Protein MeCP2 Links DNA Methylation to Histone Methylation. *J. Biol. Chem.* **278**, 4035–4040 (2003).
276. Burdge, G. C. & Lillycrop, K. a. Fatty acids and epigenetics. *Curr. Opin. Clin. Nutr. Metab. Care* **17**, 156–61 (2014).
277. Bartel, D. P. MicroRNAs: genomics, biogenesis, mechanism, and function. *Cell* **116**, 281–97 (2004).
278. Shomron, N. & Levy, C. MicroRNA-Biogenesis and Pre-mRNA Splicing Crosstalk. *J. Biomed. Biotechnol.* **2009**, 1–6 (2009).
279. Yi, R., Qin, Y., Macara, I. G. & Cullen, B. R. Exportin-5 mediates the nuclear export of pre-microRNAs and short hairpin RNAs. *Genes Dev.* **17**, 3011–6 (2003).
280. Kusenda, B., Mraz, M., Mayer, J. & Pospisilova, S. MicroRNA biogenesis, functionality and cancer relevance. *Biomed. Pap. Med. Fac. Univ. Palacky. Olomouc. Czech. Repub.* **150**, 205–15 (2006).
281. Gibb, E. A., Brown, C. J. & Lam, W. L. The functional role of long non-coding RNA in human carcinomas. *Mol. Cancer* **10**, 38 (2011).
282. Mercer, T. R., Dinger, M. E. & Mattick, J. S. Long non-coding RNAs: insights into functions. *Nat. Rev. Genet.* **10**, 155–159 (2009).
283. Ravasi, T. *et al.* Experimental validation of the regulated expression of large numbers of non-coding RNAs from the mouse genome. *Genome Res.* **16**, 11–9 (2006).
284. Gluckman, P. D., Hanson, M. A. & Spencer, H. G. Predictive adaptive responses and human evolution. *Trends Ecol. Evol.* **20**, 527–533 (2005).
285. Burdge, G. C. *et al.* Progressive, Transgenerational Changes in Offspring Phenotype and Epigenotype following Nutritional Transition. *PLoS One* **6**, e28282 (2011).
286. Waterland, R. A. & Michels, K. B. Epigenetic Epidemiology of the Developmental Origins Hypothesis. *Annu. Rev. Nutr.* **27**, 363–388 (2007).

List of References

287. Gluckman, P. D. & Hanson, M. A. *Mismatch : why our world no longer fits our bodies*. (Oxford University Press, 2006).
288. Godfrey, K. M., Lillycrop, K. A., Burdge, G. C., Gluckman, P. D. & Hanson, M. A. Epigenetic Mechanisms and the Mismatch Concept of the Developmental Origins of Health and Disease. *Pediatr. Res.* **61**, 5R-10R (2007).
289. Gluckman, P. D. & Hanson, M. A. Living with the past: evolution, development, and patterns of disease. *Science* **305**, 1733–6 (2004).
290. Heijmans, B. T. *et al.* Persistent epigenetic differences associated with prenatal exposure to famine in humans. *Proc. Natl. Acad. Sci.* **105**, 17046–17049 (2008).
291. Tobi, E. W. *et al.* DNA methylation differences after exposure to prenatal famine are common and timing- and sex-specific. *Hum. Mol. Genet.* **18**, 4046–53 (2009).
292. Waterland, R. A. & Jirtle, R. L. Early nutrition, epigenetic changes at transposons and imprinted genes, and enhanced susceptibility to adult chronic diseases. *Nutrition* **20**, 63–8 (2004).
293. Gluckman, P. D., Hanson, M. A., Buklijas, T., Low, F. M. & Beedle, A. S. Epigenetic mechanisms that underpin metabolic and cardiovascular diseases. *Nat. Rev. Endocrinol.* **5**, 401–408 (2009).
294. Waterland, R. A. & Jirtle, R. L. Transposable elements: targets for early nutritional effects on epigenetic gene regulation. *Mol. Cell. Biol.* **23**, 5293–300 (2003).
295. Whitelaw, E., Morgan, H. D., Sutherland, H. G. E. & Martin, D. I. K. Epigenetic inheritance at the agouti locus in the mouse. *Nat. Genet.* **23**, 314–318 (1999).
296. Lillycrop, K. A. *et al.* Induction of altered epigenetic regulation of the hepatic glucocorticoid receptor in the offspring of rats fed a protein-restricted diet during pregnancy suggests that reduced DNA methyltransferase-1 expression is involved in impaired DNA methylation and changes in histone modifications Europe PMC Funders Group. *Br J Nutr* **97**, 1064–1073 (2007).
297. Lillycrop, K. A., Phillips, E. S., Jackson, A. A., Hanson, M. A. & Burdge, G. C. Dietary Protein Restriction of Pregnant Rats Induces and Folic Acid Supplementation Prevents Epigenetic Modification of Hepatic Gene Expression in the Offspring. *J. Nutr.* **135**, 1382–1386 (2005).
298. Lillycrop, K. A. *et al.* Feeding pregnant rats a protein-restricted diet persistently alters the

- methylation of specific cytosines in the hepatic PPAR α promoter of the offspring. *Br. J. Nutr.* **100**, 278–282 (2008).
299. Harvey, N. C. *et al.* Childhood Bone Mineral Content Is Associated With Methylation Status of the RXRA Promoter at Birth. *J. Bone Miner. Res.* **29**, 600–607 (2014).
300. Fetahu, I. S., HÅ¶lbaus, J. & KÅ¶llay, E. Vitamin D and the epigenome. *Front. Physiol.* **5**, 164 (2014).
301. Novakovic, B. *et al.* Placenta-specific Methylation of the Vitamin D 24-Hydroxylase Gene. *J. Biol. Chem.* **284**, 14838–14848 (2009).
302. Wjst, M., Heimbeck, I., Kutschke, D. & Pukelsheim, K. Epigenetic regulation of vitamin D converting enzymes. *J. Steroid Biochem. Mol. Biol.* **121**, 80–83 (2010).
303. Ollikainen, M. *et al.* DNA methylation analysis of multiple tissues from newborn twins reveals both genetic and intrauterine components to variation in the human neonatal epigenome. *Hum. Mol. Genet.* **19**, 4176–4188 (2010).
304. Zhu, H. *et al.* A Genome-Wide Methylation Study of Severe Vitamin D Deficiency in African American Adolescents. *J. Pediatr.* **162**, 1004-1009.e1 (2013).
305. Zhou, Y. *et al.* DNA methylation levels of CYP2R1 and CYP24A1 predict vitamin D response variation. *Journal of Steroid Biochemistry and Molecular Biology* **144**, 207–214 (2014).
306. Rawson, J. B. *et al.* Vitamin D intake is negatively associated with promoter methylation of the Wnt antagonist gene DKK1 in a large group of colorectal cancer patients. *Nutr. Cancer* **64**, 919 (2012).
307. Doig, C. L. *et al.* Recruitment of NCOR1 to VDR target genes is enhanced in prostate cancer cells and associates with altered DNA methylation patterns. *Carcinogenesis* **34**, 248–256 (2013).
308. Villagra, A. *et al.* Reduced CpG methylation is associated with transcriptional activation of the bone-specific rat osteocalcin gene in osteoblasts. *J. Cell. Biochem.* **85**, 112–22 (2002).
309. Hassan, M. Q. *et al.* HOXA10 controls osteoblastogenesis by directly activating bone regulatory and phenotypic genes. *Mol. Cell. Biol.* **27**, 3337–52 (2007).
310. Hemming, S. *et al.* EZH2 and KDM6A Act as an Epigenetic Switch to Regulate Mesenchymal Stem Cell Lineage Specification. *Stem Cells* **32**, 802–815 (2014).

List of References

311. Huang, S. *et al.* Upregulation of miR-22 Promotes Osteogenic Differentiation and Inhibits Adipogenic Differentiation of Human Adipose Tissue-Derived Mesenchymal Stem Cells by Repressing *HDAC6* Protein Expression. *Stem Cells Dev.* **21**, 2531–2540 (2012).
312. ZUO, C. *et al.* Expression profiling of lncRNAs in C3H10T1/2 mesenchymal stem cells undergoing early osteoblast differentiation. *Mol. Med. Rep.* **8**, 463–467 (2013).
313. Zhu, L. & Xu, P.-C. Downregulated lncRNA-ANCR promotes osteoblast differentiation by targeting EZH2 and regulating Runx2 expression. *Biochem. Biophys. Res. Commun.* **432**, 612–617 (2013).
314. Jain, K. K. (Kewal K. . *The handbook of biomarkers.* (Springer, 2010).
315. Clarke-Harris, R. *et al.* PGC1 Promoter Methylation in Blood at 5-7 Years Predicts Adiposity From 9 to 14 Years (EarlyBird 50). *Diabetes* **63**, 2528–2537 (2014).
316. Barrès, R. *et al.* Acute Exercise Remodels Promoter Methylation in Human Skeletal Muscle. *Cell Metab.* **15**, 405–411 (2012).
317. Wong, C. C. Y. *et al.* A longitudinal study of epigenetic variation in twins. *Epigenetics* **5**, 516–26 (2010).
318. Woodfine, K., Huddleston, J. E. & Murrell, A. Quantitative analysis of DNA methylation at all human imprinted regions reveals preservation of epigenetic stability in adult somatic tissue. *Epigenetics Chromatin* **4**, 1 (2011).
319. Lu, T.-P. *et al.* Identification of Genes with Consistent Methylation Levels across Different Human Tissues. *Sci. Rep.* **4**, 4351 (2015).
320. Murphy, S. K., Huang, Z. & Hoyo, C. Differentially methylated regions of imprinted genes in prenatal, perinatal and postnatal human tissues. *PLoS One* **7**, e40924 (2012).
321. Godfrey, K. M. *et al.* Epigenetic Gene Promoter Methylation at Birth Is Associated With Child's Later Adiposity. *Diabetes* **60**, 1528–1534 (2011).
322. Lillycrop, K. *et al.* ANRIL Promoter DNA Methylation: A Perinatal Marker for Later Adiposity. *EBioMedicine* **19**, 60–72 (2017).
323. Curtis, E. M. *et al.* Perinatal DNA Methylation at *CDKN2A* Is Associated With Offspring Bone Mass: Findings From the Southampton Women's Survey. *J. Bone Miner. Res.* (2017). doi:10.1002/jbmr.3153

324. Chambon, P. The retinoid signaling pathway: molecular and genetic analyses. *Semin. Cell Biol.* **5**, 115–125 (1994).
325. Mangelsdorf, D. J. *et al.* Characterization of three RXR genes that mediate the action of 9-cis retinoic acid. *Genes Dev.* **6**, 329–344 (1992).
326. Kliewer, S. A., Umesono, K., Mangelsdorf, D. J. & Evans, R. M. Retinoid X receptor interacts with nuclear receptors in retinoic acid, thyroid hormone and vitamin D3 signalling. *Nature* **355**, 446–449 (1992).
327. Kliewer, S. A., Umesono, K., Noonan, D. J., Heyman, R. A. & Evans, R. M. Convergence of 9-cis retinoic acid and peroxisome proliferator signalling pathways through heterodimer formation of their receptors. *Nature* **358**, 771–4 (1992).
328. TAKEYAMA, K. & KATO, S. The Vitamin D3 1alpha-Hydroxylase Gene and Its Regulation by Active Vitamin D3. *Biosci. Biotechnol. Biochem.* **75**, 208–213 (2011).
329. Bourguet, W., Ruff, M., Chambon, P., Gronemeyer, H. & Moras, D. Crystal structure of the ligand-binding domain of the human nuclear receptor RXR- α . *Nature* **375**, 377–382 (1995).
330. Mangelsdorf, D. J. & Evans, R. M. The RXR heterodimers and orphan receptors. *Cell* **83**, 841–850 (1995).
331. MacDonald, P. N. *et al.* Retinoid X receptors stimulate and 9-cis retinoic acid inhibits 1,25-dihydroxyvitamin D3-activated expression of the rat osteocalcin gene. *Mol. Cell. Biol.* **13**, 5907 (1993).
332. Haussler, M. R. *et al.* The Nuclear Vitamin D Receptor: Biological and Molecular Regulatory Properties Revealed. *J. Bone Miner. Res.* **13**, 325–349 (1998).
333. Staal, A. *et al.* Distinct conformations of vitamin D receptor/retinoid X receptor-alpha heterodimers are specified by dinucleotide differences in the vitamin D-responsive elements of the osteocalcin and osteopontin genes. *Mol. Endocrinol.* **10**, 1444–1456 (1996).
334. Kim, K. *et al.* MafB negatively regulates RANKL-mediated osteoclast differentiation. *Blood* **109**, 3253–9 (2007).
335. Menéndez-Gutiérrez, M. P. *et al.* Retinoid X receptors orchestrate osteoclast differentiation and postnatal bone remodeling. *J. Clin. Invest.* **125**, 809–823 (2015).
336. Kim, W. Y. & Sharpless, N. E. The Regulation of INK4/ARF in Cancer and Aging. *Cell* **127**, 265–275 (2006).

List of References

337. Matheu, A. *et al.* Anti-aging activity of the *Ink4/Arf* locus. *Aging Cell* **8**, 152–161 (2009).
338. Nilsson, K. & Landberg, G. Subcellular localization, modification and protein complex formation of the cdk-inhibitor p16 in Rb-functional and Rb-inactivated tumor cells. *Int. J. Cancer* **118**, 1120–1125 (2006).
339. Jin, X., Nguyen, D., Zhang, W. W., Kyritsis, A. P. & Roth, J. A. Cell cycle arrest and inhibition of tumor cell proliferation by the p16INK4 gene mediated by an adenovirus vector. *Cancer Res.* **55**, 3250–3 (1995).
340. Jacobs, J. J. L., Kieboom, K., Marino, S., DePinho, R. A. & van Lohuizen, M. The oncogene and Polycomb-group gene *bmi-1* regulates cell proliferation and senescence through the *ink4a* locus. *Nature* **397**, 164–168 (1999).
341. Abella, A. *et al.* Cdk4 promotes adipogenesis through PPAR γ activation. *Cell Metab.* **2**, 239–249 (2005).
342. Pomerantz, J. *et al.* The *Ink4a* tumor suppressor gene product, p19Arf, interacts with MDM2 and neutralizes MDM2's inhibition of p53. *Cell* **92**, 713–23 (1998).
343. Zhang, Y., Xiong, Y. & Yarbrough, W. G. ARF promotes MDM2 degradation and stabilizes p53: ARF-INK4a locus deletion impairs both the Rb and p53 tumor suppression pathways. *Cell* **92**, 725–34 (1998).
344. Congrains, A. *et al.* Genetic variants at the 9p21 locus contribute to atherosclerosis through modulation of ANRIL and CDKN2A/B. *Atherosclerosis* **220**, 449–455 (2012).
345. Cheng, S. *et al.* Long non-coding RNA ANRIL promotes the proliferation, migration and invasion of human osteosarcoma cells. *Exp. Ther. Med.* **14**, 5121–5125 (2017).
346. Conceição, A. L. G. *et al.* Differential Expression of *ADAM23*, *CDKN2A (P16)*, *MMP14* and *VIM* Associated with Giant Cell Tumor of Bone. *J. Cancer* **6**, 593–603 (2015).
347. Mohseny, A. B. *et al.* Small deletions but not methylation underlie CDKN2A/p16 loss of expression in conventional osteosarcoma. *Genes, Chromosom. Cancer* **49**, 1095–1103 (2010).
348. Nielsen, G. P., Burns, K. L., Rosenberg, A. E. & Louis, D. N. CDKN2A Gene Deletions and Loss of p16 Expression Occur in Osteosarcomas That Lack RB Alterations. *Am. J. Pathol.* **153**, 159–163 (1998).
349. Trajanoska, K. *et al.* Assessment of the genetic and clinical determinants of fracture risk:

- Genome wide association and mendelian randomisation study. *BMJ* **362**, (2018).
350. Wang, Y. & Zhao, S. *Vascular Biology of the Placenta*. *Vascular Biology of the Placenta* (Morgan & Claypool Life Sciences, 2010).
351. Rogenhofer, N. *et al.* Correlation of Vitamin D3 (Calcitriol) Serum Concentrations with Vitamin B12 and Folic Acid in Women Undergoing in vitro Fertilisation/Intracytoplasmatic Sperm Injection. *Gynecol. Obstet. Invest.* **84**, 136–144 (2019).
352. Wegler, C., Wikvall, K. & Norlin, M. Effects of Osteoporosis-Inducing Drugs on Vitamin D-Related Gene Transcription and Mineralization in MG-63 and Saos-2 Cells. *Basic Clin. Pharmacol. Toxicol.* **119**, 436–442 (2016).
353. Shull, S., Tracy, R. P. & Mann, K. G. Identification of a vitamin D-responsive protein on the surface of human osteosarcoma cells. *Proc. Natl. Acad. Sci. U. S. A.* **86**, 5405–9 (1989).
354. Thompson, L. *et al.* Effect of 25-hydroxyvitamin D3 and 1 α ,25 dihydroxyvitamin D3 on differentiation and apoptosis of human osteosarcoma cell lines. *J. Orthop. Res.* **30**, 831–844 (2012).
355. Ochiai, E. *et al.* Molecular Mechanism of the Vitamin D Antagonistic Actions of (23S)-25-Dehydro-1 α -Hydroxyvitamin D3-26,23-Lactone Depends on the Primary Structure of the Carboxyl-Terminal Region of the Vitamin D Receptor. *Mol. Endocrinol.* **19**, 1147–1157 (2005).
356. Willie, B. M. *et al.* Diminished response to in vivo mechanical loading in trabecular and not cortical bone in adulthood of female C57Bl/6 mice coincides with a reduction in deformation to load. *Bone* **55**, 335–346 (2013).
357. Khorasanizadeh, S. & Rastinejad, F. Nuclear-receptor interactions on DNA-response elements. *Trends Biochem. Sci.* **26**, 384–90 (2001).
358. Gude, N. M., Roberts, C. T., Kalionis, B. & King, R. G. Growth and function of the normal human placenta. *Thromb. Res.* **114**, 397–407 (2004).
359. Cooper, C. *et al.* Maternal gestational vitamin D supplementation and offspring bone health (MAVIDOS): a multicentre, double-blind, randomised placebo-controlled trial. *Lancet Diabetes Endocrinol.* **4**, 393–402 (2016).
360. Tobi, E. W. *et al.* DNA methylation signatures link prenatal famine exposure to growth and metabolism. *Nat. Commun.* **5**, 1–14 (2014).

List of References

361. Salle, B. L., Rauch, F., Travers, R., Bouvier, R. & Glorieux, F. H. Human fetal bone development: histomorphometric evaluation of the proximal femoral metaphysis. *Bone* **30**, 823–828 (2002).
362. Beckett, E. L. *et al.* Relationship between methylation status of vitamin D-related genes, vitamin D levels, and methyl-donor biochemistry. *J. Nutr. Intermed. Metab.* **6**, 8–15 (2016).
363. Cundy, T., Reid, I. R. & Grey, A. Metabolic bone disease. *Clin. Biochem. Metab. Clin. Asp.* 604–635 (2014). doi:10.1016/B978-0-7020-5140-1.00031-6
364. Williams, G. R. Actions of thyroid hormones in bone. *Endokrynol. Pol.* **60**, 380–8
365. Nomura, Y. *et al.* Global methylation in the placenta and umbilical cord blood from pregnancies with maternal gestational diabetes, preeclampsia, and obesity. *Reprod. Sci.* **21**, 131–7 (2014).
366. Saleh, R. & Reza, H. M. Short review on human umbilical cord lining epithelial cells and their potential clinical applications. *Stem Cell Research and Therapy* **8**, (2017).
367. Maillacheruvu, P. F., Engel, L. M., Crum, I. T., Agrawal, D. K. & Peebles, E. S. From cord to caudate: Characterizing umbilical cord blood stem cells and their paracrine interactions with the injured brain. *Pediatric Research* **83**, 205–213 (2018).
368. Miki, T., Lehmann, T., Cai, H., Stolz, D. B. & Strom, S. C. Stem Cell Characteristics of Amniotic Epithelial Cells. *Stem Cells* **23**, 1549–1559 (2005).
369. Vascular Biology of the Placenta - NCBI Bookshelf. Available at: <https://www.ncbi.nlm.nih.gov/books/NBK53247/>. (Accessed: 24th October 2019)
370. Wu, M. *et al.* Comparison of the Biological Characteristics of Mesenchymal Stem Cells Derived from the Human Placenta and Umbilical Cord. doi:10.1038/s41598-018-23396-1
371. Ogasawara, T. *et al.* Role of cyclin-dependent kinase (Cdk)6 in osteoblast, osteoclast, and chondrocyte differentiation and its potential as a target of bone regenerative medicine. *Oral Sci. Int.* **8**, 2–6 (2011).
372. Gluckman, P. D., Hanson, M. A., Cooper, C. & Thornburg, K. L. Effect of in utero and early-life conditions on adult health and disease. *N. Engl. J. Med.* **359**, 61–73 (2008).
373. VanArsdale, T., Boshoff, C., Arndt, K. T. & Abraham, R. T. Molecular Pathways: Targeting the Cyclin D-CDK4/6 Axis for Cancer Treatment. *Clin. Cancer Res.* **21**, 2905–2910 (2015).

374. Purnell, B. A. DNA methylation in hematopoietic cascade. *Science* **355**, 258–259 (2017).
375. Kawane, T. *et al.* Runx2 is required for the proliferation of osteoblast progenitors and induces proliferation by regulating Fgfr2 and Fgfr3. *Sci. Rep.* **8**, 13551 (2018).
376. Takahashi, A. *et al.* DNA methylation of the RUNX2 P1 promoter mediates MMP13 transcription in chondrocytes. *Sci. Rep.* **7**, 7771 (2017).
377. Farshdousti Hagh, M. *et al.* Different Methylation Patterns of RUNX2, OSX, DLX5 and BSP in Osteoblastic Differentiation of Mesenchymal Stem Cells. *Cell J.* **17**, 71–82 (2015).
378. Jonason, J. H., Xiao, G., Zhang, M., Xing, L. & Chen, D. Post-translational Regulation of Runx2 in Bone and Cartilage. *J. Dent. Res.* **88**, 693–703 (2009).
379. Sullivan, A. M., Bubb, K. L., Sandstrom, R., Stamatoyannopoulos, J. A. & Queitsch, C. DNase I hypersensitivity mapping, genomic footprinting, and transcription factor networks in plants. *Curr. Plant Biol.* **3–4**, 40–47 (2015).
380. Local, A. *et al.* Identification of H3K4me1-associated proteins at mammalian enhancers. *Nat. Genet.* **50**, 73–82 (2018).
381. Shlyueva, D., Stampfel, G. & Stark, A. Transcriptional enhancers: from properties to genome-wide predictions. *Nat. Rev. Genet.* **15**, 272–286 (2014).
382. Calo, E. & Wysocka, J. Modification of enhancer chromatin: what, how, and why? *Mol. Cell* **49**, 825–37 (2013).
383. Guenther, M. G., Levine, S. S., Boyer, L. A., Jaenisch, R. & Young, R. A. A chromatin landmark and transcription initiation at most promoters in human cells. *Cell* **130**, 77–88 (2007).
384. Yang, Y. & Cvekl, A. Large Maf Transcription Factors: Cousins of AP-1 Proteins and Important Regulators of Cellular Differentiation. *Einstein J. Biol. Med.* **23**, 2–11 (2007).
385. John, S. *et al.* Interaction of the Glucocorticoid Receptor with the Chromatin Landscape. *Mol. Cell* **29**, 611–624 (2008).
386. Rodan, S. B. *et al.* Characterization of a Human Osteosarcoma Cell Line (Saos-2) with Osteoblastic Properties. *CANCER RESEARCH* **47**, (1987).
387. Franceschi, R. T., James, W. M. & Zerlauth, G. 1?, 25-Dihydroxyvitamin D3 specific regulation of growth, morphology, and fibronectin in a human osteosarcoma cell line. *J. Cell. Physiol.* **123**, 401–409 (1985).

List of References

388. Zou, B. *et al.* Correlation Between the Single-Site CpG Methylation and Expression Silencing of the XAF1 Gene in Human Gastric and Colon Cancers. *Gastroenterology* **131**, 1835–1843 (2006).
389. Heintzman, N. D. *et al.* Distinct and predictive chromatin signatures of transcriptional promoters and enhancers in the human genome. *Nat. Genet.* **39**, 311–318 (2007).
390. Creighton, M. P. *et al.* Histone H3K27ac separates active from poised enhancers and predicts developmental state. *Proc. Natl. Acad. Sci. U. S. A.* **107**, 21931–6 (2010).
391. Heinz, S., Romanoski, C. E., Benner, C. & Glass, C. K. The selection and function of cell type-specific enhancers. *Nat. Rev. Mol. Cell Biol.* **16**, 144–154 (2015).
392. Serfling, E., Jasin, M. & Schaffner, W. Enhancers and eukaryotic gene transcription. *Trends Genet.* **1**, 224–230 (1985).
393. McDowell, I. C. *et al.* Glucocorticoid receptor recruits to enhancers and drives activation by motif-directed binding. *Genome Res.* **28**, 1272–1284 (2018).
394. Moutsatsou, P., Kassi, E. & Papavassiliou, A. G. Glucocorticoid receptor signaling in bone cells. *Trends in Molecular Medicine* **18**, 348–359 (2012).
395. Steineger, H. H., Arntsen, B. M., Spydevold & Sørensen, H. N. Retinoid X receptor (RXR α) gene expression is regulated by fatty acids and dexamethasone in hepatic cells. *Biochimie* **79**, 107–110 (1997).
396. Song, L.-N. Demonstration of vitamin D receptor expression in a human megakaryoblastic leukemia cell line: Regulation of vitamin D receptor mRNA expression and responsiveness by forskolin. *J. Steroid Biochem. Mol. Biol.* **57**, 265–274 (1996).
397. Prideaux, M. *et al.* SaOS2 Osteosarcoma Cells as an In Vitro Model for Studying the Transition of Human Osteoblasts to Osteocytes. *Calcif. Tissue Int.* **95**, 183–193 (2014).
398. Bilbe, G., Roberts, E., Birch, M. & Evans, D. B. PCR phenotyping of cytokines, growth factors and their receptors and bone matrix proteins in human osteoblast-like cell lines. *Bone* **19**, 437–445 (1996).
399. Pautke, C. *et al.* Characterization of osteosarcoma cell lines MG-63, Saos-2 and U-2 OS in comparison to human osteoblasts. *Anticancer Res.* **24**, 3743–8
400. Bouillon, R. *et al.* Vitamin D and Human Health: Lessons from Vitamin D Receptor Null Mice. *Endocr. Rev.* **29**, 726–776 (2008).

401. Yoshizawa, T. *et al.* Mice lacking the vitamin D receptor exhibit impaired bone formation, uterine hypoplasia and growth retardation after weaning. *Nat. Genet.* **16**, 391–6 (1997).
402. Seldeen, K. L. *et al.* Chronic vitamin D insufficiency impairs physical performance in C57BL/6J mice. *Aging (Albany. NY).* **10**, 1338–1355 (2018).
403. Seldeen, K. L. *et al.* A mouse model of vitamin D insufficiency: is there a relationship between 25(OH) vitamin D levels and obesity? *Nutr. Metab. (Lond).* **14**, 26 (2017).
404. Belenchia, A. M., Johnson, S. A., Kieschnick, A. C., Rosenfeld, C. S. & Peterson, C. A. Time Course of Vitamin D Depletion and Repletion in Reproductive-age Female C57BL/6 Mice. *Comp. Med.* **67**, 483–490 (2017).
405. Sinha, K. M. & Zhou, X. Genetic and molecular control of osterix in skeletal formation. *J. Cell. Biochem.* **114**, 975–84 (2013).
406. Wakitani, S., Yokoi, D., Hidaka, Y. & Nishino, K. The differentially DNA-methylated region responsible for expression of runt-related transcription factor 2. *J. Vet. Med. Sci.* **79**, 230–237 (2017).
407. Cooper, D. M. L., Kawalilak, C. E., Harrison, K., Johnston, B. D. & Johnston, J. D. Cortical Bone Porosity: What Is It, Why Is It Important, and How Can We Detect It? *Curr. Osteoporos. Rep.* **14**, 187–198 (2016).
408. Enomoto, H. *et al.* Induction of Osteoclast Differentiation by Runx2 through Receptor Activator of Nuclear Factor- κ B Ligand (RANKL) and Osteoprotegerin Regulation and Partial Rescue of Osteoclastogenesis in Runx2^{-/-} Mice by RANKL Transgene. *J. Biol. Chem.* **278**, 23971–23977 (2003).
409. Haxaire, C., Haÿ, E. & Geoffroy, V. Runx2 Controls Bone Resorption through the Down-Regulation of the Wnt Pathway in Osteoblasts. *Am. J. Pathol.* **186**, 1598–1609 (2016).
410. Menéndez-Gutiérrez, M. P. *et al.* Retinoid X receptors orchestrate osteoclast differentiation and postnatal bone remodeling. *J. Clin. Invest.* **125**, 809–23 (2015).
411. Main, R. P., Lynch, M. E. & van der Meulen, M. C. H. Load-induced changes in bone stiffness and cancellous and cortical bone mass following tibial compression diminish with age in female mice. *J. Exp. Biol.* **217**, 1775–83 (2014).
412. Wong, N. C. *et al.* Exploring the utility of human DNA methylation arrays for profiling mouse genomic DNA. *Genomics* **102**, 38–46 (2013).

List of References

413. Yin, Y. *et al.* Impact of cytosine methylation on DNA binding specificities of human transcription factors. *Science* (80-.). **356**, (2017).
414. Mulligan, M. L., Felton, S. K., Riek, A. E. & Bernal-Mizrachi, C. Implications of vitamin D deficiency in pregnancy and lactation. *Am. J. Obstet. Gynecol.* **202**, 429.e1-429.e9 (2010).

